ISBN 978-5-6042418-2-0

ION TRANSPORT IN ORGANIC AND INORGANIC MEMBRENES

CONFERENCE PROCEEDING

RUSSIAN ACADEMY OF SCIENCES

RUSSIAN MEMBRANE SOCIETY

MINISTRY OF SCIENCE AND HIGHER EDUCATION OF THE RUSSIAN FEDERATION

RAS SCIENTIFIC COUNCIL ON PHYSICAL CHEMISTRY

RUSSIAN MEMBRANE NETWORK

KUBAN STATE UNIVERSITY

KURNAKOV INSTITUTE OF GENERAL AND INORGANIC CHEMISTRY RAS

«MEMBRANE TECHNOLOGY» INNOVATION ENTERPRISE

INTERNATIONAL CONFERENCE

Ion transport in organic and inorganic membranes-2019

Conference Proceedings

20 – 25 May 2019

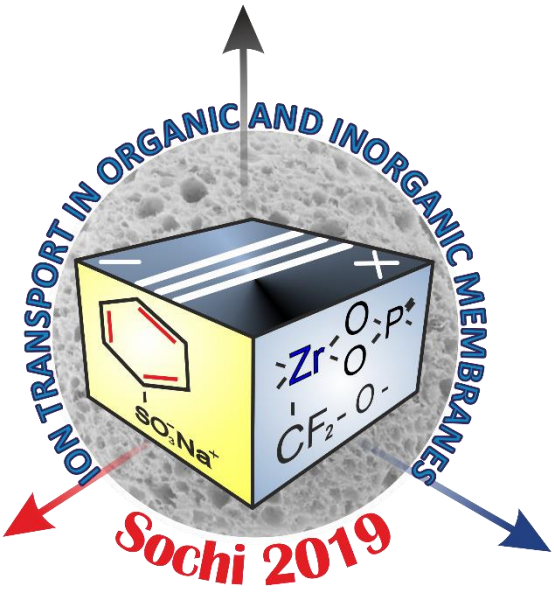

SCIENTIFIC/ORGANIZING COMMITTEE

Chairman	**YAROSLAVTSEV A.B.** *(Russia)*
Co-chairmen	**ZABOLOTSKIY V.I.** *(Russia)*
	POURCELLY G. *(France)*
	NIKONENKO V.V. *(Russia)*
Scientific secretary	**KONONENKO N.A.** *(Russia)*
	SHKIRSKAYA S.A. *(Russia)*

AGEEV E.P. *(Russia)*	**RUBINSTEIN I.** *(Israel)*
BAZINET L. *(Canada)*	**SHAPOSHNIK V.A.** *(Russia)*
BILDYUKEVICH A.V. (*Belarus)*	**SHELDESHOV N.V.** *(Russia)*
CRETIN M. *(France)*	**STAROV V.M.** *(UK)*
DAMMAK L. *(France)*	**TSKHAY A.A.** *(Kazakhstan)*
FILIPPOV A.N. *(Russia)*	**VASIL'EVA V.I.** *(Russia)*
KHOHLOV A.R. *(Russia)*	**VOLFKOVICH Yu.M.** *(Russia)*
NOVAK L. *(Czech Republic)*	**VOLKOV V.V.** *(Russia)*
OZERIN A.N. *(Russia)*	**VOROTYNTSEV M.A.** *(Russia)*
PISMENSKAYA N.D. *(Russia),*	**XU T.** *(China)*

Local organizing committee *(Krasnodar, Russia)*

ACHOH A.R.	**KUDASHOVA D.S.**
ANDREEVA M.A.	**LOZA N.V.**
BUTYLSKII D.Yu.	**LOZA S.A.**
ETEREVSKOVA S.I.	**MAREEV S.A.**
FALINA I.V.	**MELNIKOV S.S.**
GIL V.V.	**POROZHNYY M.**
KOZMAI A.E.	**RYBALKINA O.A.**

Sponsors:

Ministry of Science and Higher Education of the Russian Federation

«MEMBRANE TECHNOLOGY» INNOVATION ENTERPRISE

Preface

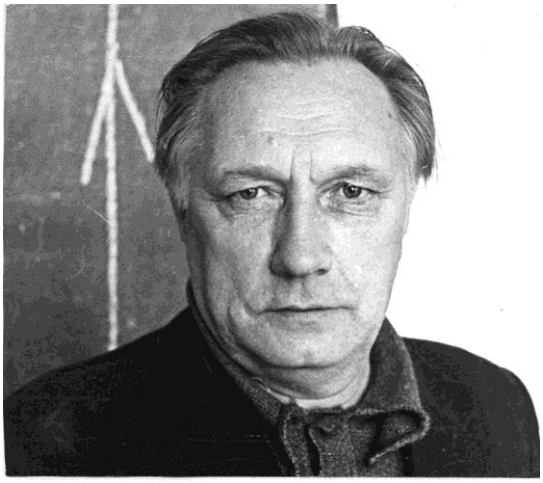

This year, Nikolai Petrovich Gnusin would have turned 100 years old; he was born on November 19, 1919.

He actively participated in the Great Patriotic (Second World) War and was awarded an order and multiple medals. So, he began to study at a university (at the Leningrad Technological Institute) only after the War. In 1953, he obtained his PhD degree. Due to his talents and energy, he obtained the title of professor as early as in 1960. He worked in several republics of the former Soviet Union: in Gomel (Belarus), Novosibirsk (Russia) and Kiev (Ukrane). In 1970, he became the head of the Physical Chemistry Department at the Kuban State University in Krasnodar. In Krasnodar, there was the longest period of his active life. He worked at the university up to 2010.

Even before Krasnodar, Nikolai Petrovich was a world-known scientist. He has published a considerable number of articles and several books. He developed a solid background in experimental methods for studying electrochemical properties of ion-exchange materials and membranes. His famous three-wire conduction model for calculation the conductivity of ion-exchange columns has already appeared. However, the main research and technological results were obtained in Krasnodar. Here, Nikolai Petrovich created a well balanced collective, which included chemists, physicians, mathematicians and technologists. His scientific heritage incudes 5 books, about 400 articles and conference abstracts, 30 patents. He prepared over 300 professionals in the field of electro-membrane processes, among them 5 doctors of science and 20 candidates.

Nikolai Petrovich is considered as the Russian father of electrochemistry of ion-exchange resins and membranes. He developed the principles of actual electro-membrane separation processes; he was one of the first scientists who have seen the huge potential of these processes because of increasing gravity of environmental issues, closely associated with the need in low-waste technologies.

He founded our annual Conferences on ion-exchange membranes. The first Conference was organized under powerful leadership of Nikolai Petrovich Gnusin in 1975, Goryachi Klyuch, near Krasnodar. Later on, all the Conferences were held on the Black Sea shore. And now, in 2019, there is the 45th Conference.

The whole life of Nikolai Petrovich was devoted to the construction of a membrane electrochemistry building, which we are trying to continue to build and improve now. We remember and honor the founder of this building.

Organizing committee

В этом году Николаю Петровичу Гнусину исполнилось бы 100 лет. Вклад Николая Петровича в мембранную науку и технологии трудно переоценить. Уже до своего появления в Краснодаре в 1970 г., он был ученым с мировым именем. Им было издано несколько монографий, создан задел в экспериментальных методах изучения электрохимических свойств ионообменных материалов и мембран; уже появилась знаменитая трехпроводная модель проводимости. Но основные результаты были получены Николаем Петровичем в Краснодаре. Он выкристаллизовал здесь коллектив так, как это умеют делать химики, выращивая кристаллы нужной структуры. По его плану, в эту структуру должны были входить и химики, и физики, и математики, и технологи. Николай Петрович тщательно отбирал каждую категорию сотрудников. С Виктором Ивановичем Заболоцким он познакомился в Ленинграде, Нинель Петровна Березина приехала из Новосибирска, Александр Иванович Мешечков и Виктор Васильевич Никоненко – из Майкопа. Одними из первых его аспирантов были выпускники престижных московских вузов Владимир Федорович Письменский (МИФИ) и Николай Петрович Борисов (МАИ). Не менее ценные ученики были выращены и в Краснодаре: Геннадий Николаевич Истошин, Николай Викторович Шельдешов, Наталья Анатольевна Кононенко, Наталия Дмитриевна Письменская. Цементировали коллектив Нина Васильевна Витульская и Елена Вячеславовна Верижская. Фактически в 80-е годы в Краснодаре появился небольшой НИИ Мембран с вполне сбалансированным составом, способный успешно решать как фундаментальные, так и прикладные задачи в области ионообменных мембран.

Приятно сознавать, что дело Николая Петровича продолжает успешно развиваться. Теперь в Краснодаре имеется полноценный Институт Мембран, имеющий несколько лабораторий и насчитывающий более 30 сотрудников. Виктору Ивановичу Заболоцкому, руководителю института, удалось сохранить мультифункциональную структуру коллектива и его эффективность. Постепенно происходит смена поколений при сохранении основных принципов сотрудничества и традиций. Сейчас мы вышли на рубеж, когда сразу несколько молодых ученых приблизились к защите своих докторских диссертаций. Это Светлана Шкирская, Станислав Мельников, Ирина Фалина, Семен Мареев, Антон Козмай. Хотя тематика готовящихся диссертаций по-прежнему вращается вокруг ионообменных мембран, каждый их этих молодых людей вносит свою изюминку, каждый из них своеобразен и оригинален. И у каждого из них уже есть свои, еще более молодые ученики. Думается, Николай Петрович, наблюдая за развитием своего детища, был бы доволен его сегодняшним состоянием. Мы остаемся благодарны Николаю Петровичу за его энергию и прозорливость, за его уроки − как надо относиться к делу, которому ты служишь, за его доброту и справедливость.

Организационный комитет

Харизма профессора Николая Петровича Гнусина

Греческое слово харизма (χάρισμα) переводится как дар. Это слово представляется до сих пор загадочным и даже мистическим. Обладающие харизмой таинственным образом притягивают к себе людей и заряжают их энергией. Николай Петрович Гнусин был, несомненно, харизматической личностью. Можно ли проникнуть в загадку его харизмы? В 1967 г. в Москве проходила Всесоюзная научно-техническая конференция по синтезу и применению ионообменных мембран. Организатор этой конференции, профессор, лауреат Государственной премии Кирилл Максимович Салдадзе в загадочном стиле Лайнуса Полинга рассказал о необыкновенном электродиализаторе, созданным коллективом НИИ Пластмасс, но при этом скрыл все его детали. Это надо так уметь. Самым внимательным слушателем конференции был Николай Петрович Гнусин. Ему в это время было 48 лет. Он был в расцвете сил и полон энергии. В заключительный день конференции Николай Петрович предложил раскрыть все секреты таинственного аппарата. Он сумел извлечь из докладов сотрудников особенности конструкции, свойства мембран и режимы, объединить их так, что они восстали из пепла подобно птице Фениксу. Эффект его выступления был ошеломляющим как для создателей, так и обычных слушателей. Я был свидетелем этого чуда, но уверен, что и раньше он демонстрировал не меньшей силы харизматические поступки. Это очень напоминает известное описание жизни знаменитого ученого Н.В. Тимофеева-Ресовского писателем Д. Граниным в романе «Зубр». К Николаю Петровичу люди подходили на конференциях не только поздороваться, но и как бы за благословлением на добрые дела. С такими же намерениями я приехал к нему в 1973 г. в Краснодар и он, узнав, что у меня многотысячная картотека литературы на перфокартах, пригласил прочитать лекции. Встречи в Краснодаре и Воронеже стали ежегодными. Они оказали на меня такое воздействие, что, несмотря на различные подходы к большинству проблем, полагаю, что, если мне и удалось что-то сделать полезное, то больше всего обязан этим Николаю Петровичу. С Николаем Петровичем мы встречались не только на конференциях, лекциях и защитах диссертаций. Особую роль играли неформальные контакты. С Николаем Петровичем мы плавали по воронежским рекам на байдарке, собирали грибы. Особенно поражало то, что черные грузди он мог видеть даже под землей.

Знаете ли вы еще хотя бы одного крупного ученого, который, как Николай Петрович, мог придти к концу футбольной встречи, в которой играл Виктор Иванович Заболоцкий, Николай Петрович Борисов и я, с авоськой пива и потом по-дружески с нами беседовать? Однако это отнюдь не значит, что Николай Петрович был мягкотелым. Он мог жестко разговаривать и с директором предприятия, и с ректором университета, а главное, отстаивать интересы своего коллектива. Николай Петрович не был членом правящей КПСС и был предан истинным идеям народовластия.

У каждого из нас своя информация о Великой Отечественной войне. Молодое поколение чаще всего её получало от уставших ветеранов, в глазах которых потух блеск глаз, еще недавно бывший столь ярким. Великий закон сохранения энергии имеет еще одно малоизвестное следствие. Энергия лидера не исчезает, а сохраняется в его учениках. Глядя на дела его многочисленных учеников можно сделать вывод, что энергия даже умножается во времени вопреки стандартным законам природы. Николай Петрович был на передовой всю блокаду Ленинграда, и он неоднократно рассказывал о событиях того трудного времени. Во время последней беседы с ним незадолго до кончины мне удалось найти вопрос, который больше, чем обычные рассказы о баталиях, позволил живо представить реальность событий. Я спросил его: «Где Вы зимой в холода спали, если не было блиндажа?». Он ответил, что снимали с орудия чехол, клали его на снег и ложились. На вопрос болели ли солдаты, он ответил, что из первого набора расчета орудия он остался один в живых. От этого ответа страшное военное время приблизилось и осталось навечно в памяти. Его жена, Бела Яковлевна, с которой он тогда еще не был знаком, отказалась от эвакуации и работала вблизи операционной медсестрой. Она не могла забыть сотни, а может быть и больше, отломанных отмороженных пальцев, отпиленных ног. Для того чтобы понять их жизни, как и других истинных героев войны, это знать совершенно необходимо.

В пьесе лауреата Нобелевской премии Мориса Метерлинка «Синяя птица» внуки встретили умерших дедушку и бабушку, удивились, что им удалось так сохраниться после смерти. На что они ответили: «Это потому что вы помните о нас». Мы помним Николая Петровича, о чем свидетельствует эта конференция, посвященная столетию его рождения. Если открыть алфавитный указатель РИНЦ, то мы увидим, что индекс Хирша Николая Петровича Гнусина в настоящее время равен 20, а число ссылок на его работы за последние пять лет, когда его уже не было с нами, составило 604. Это значит, что он живет не только в нашей памяти, но и в делах большого множества ученых. Всю жизнь буду гордиться тем, что однажды он меня назвал своим другом. Большей почести для меня быть не может.

Владимир Алексеевич Шапошник
Воронежский государственный университет,
г. Воронеж,
E-mail: v.a.shaposhnik@gmail.com

К 100-летию со дня рождения Николая Петровича Гнусина

Николай Петрович Гнусин – выдающийся электрохимик. В 1965 г. на Всероссийской конференции по электрохимии в г. Тбилиси он впервые сделал доклад об электрохимии ионитов как новом научном направлении. И с тех пор посвятил свое творчество именно ему.

Основной вклад Николая Петровича и его школы в науку электрохимию состоит в формировании фундаментальных представлений об электропроводности ионообменных материалов. Сформулирована и математически описана трехпроводная модель ионного переноса тока. На ее основе реализованы промышленные установки для обессоливания воды, удаления, извлечения, концентрирования, конверсии веществ.

Он создал крупную научную школу, создал кафедру физической химии в Кубанском государственном университете, объединил ежегодными международными научными конференциями заинтересованных специалистов многих стран. В моей жизни Николай Петрович сыграл большую роль. Неоднократно выступал оппонентом, поддерживая исследования по металл-ионообменным нанокомпозитам в Воронежском государственном университете. Был оппонентом по моей докторской диссертации, защита которой проходила в Ленинградском государственном университете. И спустя много лет, мне предоставилась честь оппонировать математическую трехпроводную модель в диссертации, руководителем которой был Николай Петрович.

Я глубоко признательна заведующему кафедрой физической химии Кубанского государственного университета Виктору Ивановичу Заболоцкому и всем сотрудникам этой замечательной кафедры за плодотворное продолжение дела, начатого великим Николаем Петровичем Гнусиным, добрую память о нашем общем учителе.

Тамара Александровна Кравченко
Заслуженный деятель науки РФ,
доктор химических наук,
профессор кафедры физической химии
Воронежского государственного университета

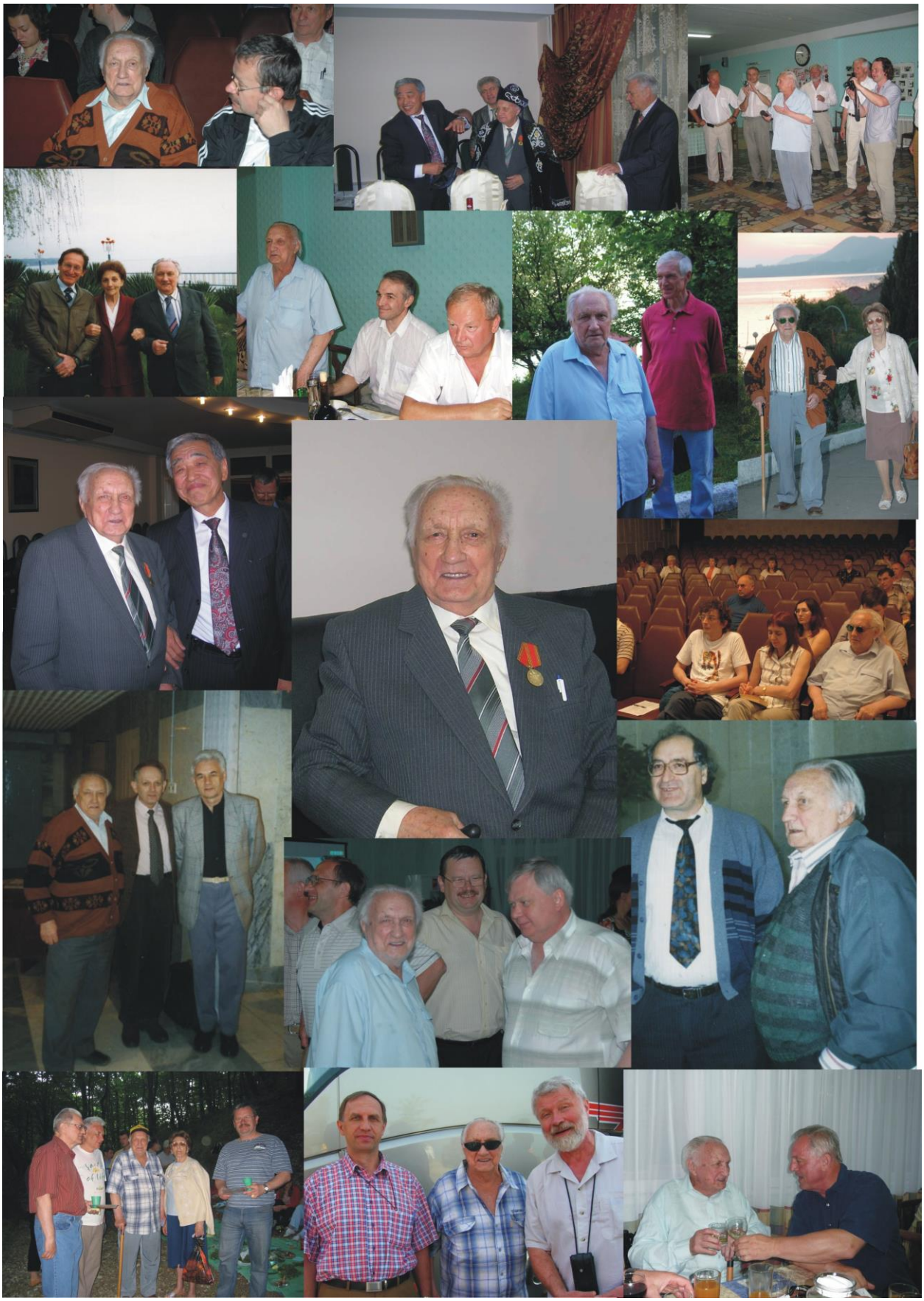

Contents

1. **Emil Abdrashitov, Dina Kritskaya, Veslav Bokun, Ardalion Ponomarev, Ksenia Novikova, Evgeny Sanginov, Yury Dobrovolsky** Synthesis and properties of ion-exchange membranes based on ultra high-molecular weight polyethylene (*Chernogolovka, Russia*) 21
2. **Emil Abdrashitov, Dina Kritskaya, Veslav Bokun, Ardalion Ponomarev, Ksenia Novikova, Evgeny Sanginov, Yury Dobrovolsky** Synthesis and transport properties of ion exchange mem-branes based on porous polytetrafluoroethylene films and sulphonated polystyrene (*Chernogolovka, Russia*) 24
3. **Aslan Achoh, Stanislav Melnikov, Konstantin Lebedev, Victor Zabolotskiy** Electrochemical characteristics and specific selectivity of bilayer ion-exchange membranes in ternary (sulfate/nitrate) solutions *(Krasnodar, Russia)* 27
4. **Elmara Akberova, Vera Vasil'eva, Elena Goleva, Denis Kostylev** SEM-diagnostics of changes in the microstructure of the heterogeneous anion-exchange membrane MA-40 after electrodialysis reversal of mineralized natural water *(Voronezh, Russia)* 30
5. **Rihab Belhadj Ammar, Takoua Ounissi, Lasâad Dammak, Emna Selmane Bel Hadj Hmida** Novel nitrate selective anion-exchange membranes: synthesis and tests dialysis *(Tunis El Manar, Tunisie; Thiais, France)* 33
6. **Marina Andreeva, Natalia Kutenko, Natalia Loza** Correlation between polyaniline synthesis conditions into MK-40 membrane and current-voltage curves of composites *(Krasnodar, Russia)* 34
7. **Marina Andreeva, Natalia Loza, Natalia Kononenko, Sergej Timofeev** Influence of polymerization time during polyaniline synthesis into MF-4SK membrane on current-voltage curves of obtained composites *(Krasnodar, Russia)* 36
8. **Anatoly Antipov, Mikhail Vorotyntsev** Multielectron oxidizer redox-mediated autocatalysis for hydrogen-bromate redox flow batteries *(Moscow, Russia; Dijon, France)* 38
9. **Artem Bagishev, Ivan Kovalev, Mikhail Popov, Alexander Nemudry** Development of microtubular solid oxide fuel cells *(Novosibirsk, Russia)* 41
10. **Irina Bagryantseva, Valentina Ponomareva, Anna Gaydamaka** Proton conductor electrolytes based on cesium dihydrogen phosphate and thermally stable polymers *(Novosibirsk, Russia)* 42
11. **Victor Bayandin, Nina Shaglaeva** New ion-exchange materials based on copolymers of divinylsulfide *(Irkutsk, Russia)* 43
12. **Stepan Bazhenov, Margarita Kostyanaya, Vladimir Vasilevsky, Alexey Nikitin, Igor Sedov, Alexey Volkov** Membrane absorption of ethylene from hydrocarbon gaseous media *(Moscow, Chernogolovka, Russia)* 45
13. **Stepan Bazhenov, Maryam Madumarova, Margarita Kostyanaya, Eduard Novitsky** Gas-liquid hollow fiber membrane contactors for CO_2 desorption from monoethanolamine solutions *(Moscow, Russia)* 48

14. **Myriam Bdiri, Asma Ben Sghaier, Lobna Chaabane, Christian Larchet, Lasâad Dammak** Enzymatic cleaning of fouled cation-exchange membranes used in electrodialysis of beverages in food industry *(Thiais, France)* 51
15. **Tomáš Belloň, Petr Polezhaev, Zdeněk Slouka** Experimental observation of phenomena developing on anion-exchange membrane during current-voltage measurement *(Praha, Pilsen, Czech Republic)* 53
16. **Tomáš Belloň, Petr Polezhaev, Zdeněk Slouka** Investigation of behavior of a heterogeneous anion-exchange membrane and single anion-exchange resin particle in the presence of ssdna using optical measurements *(Praha, Pilsen, Czech Republic)* 54
17. **Tomáš Belloň, Petr Polezhaev, Zdeněk Slouka** The influence of size and charge of counterions on the behavior of a cation-exchange system *(Praha, Pilsen, Czech Republic)* 55
18. **Tomáš Belloň, Petr Polezhaev, Lucie Vobecká, Zdeněk Slouka** Micro and milifluidic systems as tools for studying electrokinetics and ion transport in ion-exchange systems *(Praha, Czech Republic)* 56
19. **Olga Belobrovaya, Victor Galushka, Igor Galushka, Andrei Karagaichev, Anton Mantsurov, Valentina Polyanskaya, Denis Terin** The influence in situ gamma rays of chemical processes fabrication nanoscale porous silicon and its perspectives applications *(Saratov, Russia)* 59
20. **Vladimir Berezkin, Sergey Bedin, Alexander Vasiliev, Yuriy Grigoriev, Vladimir Nazmov** Regular track membranes – production and application prospects *(Moscow, Novosibirsk, Russia)* 61
21. **Denis Bondarev, Alexander Bespalov, Victor Zabolotskiy, Svetlana Eterevskova** The study of electrochemical stability of the anion-exchange membranes MA-41 modified by poly- N,N –diallylmorpholinium *(Krasnodar, Russia)* 64
22. **Katsiaryna Burts, Tatiana Plisko, Alexandr Bildyukevich, Guoqiang Li, Joanna Kujawa, Wojciech Kujawski** Preparation of thin film composite membranes for peRvaporation via interfacial polymerization technique *(Minsk, Belarus; Torun, Poland)* 66
23. **Anastasia But, Victor Zabolotskiy, Anna Kovalenko, Makhamet Urtenov, Vera Vasil'eva** Heterogeneous membrane with dominant electroconvection at work under intensive current conditions *(Krasnodar, Voronezh, Russia)* 69
24. **Dmitrii Butylskii, Semyon Mareev, Christian Larchet, Lasâad Dammak, Victor Nikonenko** Experimental study of surface morphology of ion-exchange membranes and its impact on the membrane electrochemical characteristics *(Krasnodar, Russia; Thiais, France)* 72
25. **Dmitrii Butylskii, Daria Chuprynina, Tongwen Xu, Natalia Pismenskaya** Membrane specific permselectivity in mixed solutions *(Krasnodar, Russia; Hefei, China)* 74
26. **Sergey Bychkov, Elena Shubnikova, Mikhail Popov, Stanislav Chizhik, Alexander Nemudry** Modeling of oxygen transport in hollow fiber membranes *(Novosibirsk, Russia)* 75

27. **Ladislav Čopák, Anastasia Bocharova** Treatment of acidic wastewater using membrane technologies *(Stráž pod Ralskem, Czech Republic; Krasnodar, Russia)* 76
28. **Ekaterina Dankovtseva, Irina Falina** Diffusion permeability of ion-exchange membranes in solutions of sulfuric acid and chromium sulfate (*Krasnodar, Russia)* 79
29. **Yuliya Dzyazko, Vladimir Ogenko, Yury Volfkovich, Valentin Sosenkin, Katerina Kudelko, Tatiana Yatsenko** Multifuctional composite adsorbent based on hydrated zirconium dioxide containing nanoparticles of oxidized graphene *(Kyiv, Ukraine; Moscow, Russia)* 81
30. **Irina Falina, Vera Kolenkevich, Natalia Loza** Diffusion permeability of the modified ion-exchange membranes in sodium, calcium and magnesium chloride solutions *(Krasnodar, Russia)* 84
31. **Irina Falina, Irina Myakinchenko, Olga Demina** Asymmetry of diffusion permeability of bilayer ion exchange membranes, modified by polyaniline *(Krasnodar, Russia)* 86
32. **Ilia Faykov, Vera Nesterova, Alexandra Pulyalina, Irina Podeshvo, Galina Polotskaya** Thermally rearranged polymer membranes for bioalcohol purification *(St. Petersburg, Russia)* 88
33. **Anatoly Filippov, Tamara Philippova** Impact of external electric field on hydrodynamic permeability of a charged porous layer (membrane) *(Moscow, Russia)* 91
34. **Anatoly Filippov, Svetlana Shkirskaya** Simultaneous verification of the cell model for electroosmotic permeability and electrical conductivity of cation-exchange membrane *(Moscow, Krasnodar, Russia)* 94
35. **Igor Gainutdinov, Igor Zilberberg, Alexander Nemudry** The ionic motion and structure features of modified cobaltites at different temperatures – *ab initio* molecular dynamic simulation *(Novosibirsk, Russia)* 97
36. **Georgy Ganchenko, Natalya Ganchenko, Evgeny Demekhin** About features of electroconvection near non perfectselective ionexchange membranes *(Krasnodar, Russia)* 98
37. **Natalya Ganchenko, Maria Repina, Dmitri Oksuz'an** Mathematical modeling of how gravitational effects influence overlimiting current regime *(Krasnodar, Rostov-on-Don, Russia)* 100
38. **Violetta Gil, Mikhail Porozhnyy** Effect of water splitting rate on the intensity of electroconvection and space charge region characteristics *(Krasnodar, Russia)* 102
39. **Daniel Golubenko, Andrey Yaroslavtsev** Development of anion-exchange membrane based on grafted copylimer of polystyrene and uv-irradiated polymethylpentene *(Moscow, Chernogolovka, Russia)* 105
40. **Georgy Golubev, Ilya Eremeev, Ilya Borisov, Vladimir Vasilevsky, Alexey Volkov** Porous condenser for thermo-membrane separation processes of aqueous media *(Moscow, Russia)* 107
41. **Georgy Golubev, Ivan Podtynnikov, Stepan Bazhenov, Ilya Borisov** Regeneration of triethylene glycol by thermopervaporation with porous condenser *(Moscow, Russia)* 110

42. **Andrey Gorobchenko, Semyon Mareev** Impact of current density distribution in electrodialysis system on transition time of chronopotentiograms *(Krasnodar, Russia)* 113
43. **Vitaly Gudza, Natalja Chubyr, Anna Kovalenko, Makhamet Urtenov** Mathematical modeling of the influence of dissociation/recombination reaction of water molecules on the binary salt ions transport taking into account thermal effects *(Krasnodar, Russia)* 116
44. **Vladimir Gursky, Sergey Timofeev** Self-oscillation process during the diffusion of co-ions through ion-exchange membranes *(Sosnovy Bor, Saint-Petersburg, Russia)* 119
45. **Evgenia Grushevenko, Ivan Podtynnikov, Olga Scharova, Alina Knyazeva, Ilya Borisov** Polydecylmethylsiloxane-based thin film composite membrane with enhanced organic selectivity *(Moscow, Russia)* 120
46. **Tatsiana Hliavitskaya, Alexandr Bildyukevich, Lyudmila Rozhdestvenska, Yuliya Dzyazko** Effect of kollidon on the structure and properties of PES membranes *(Minsk, Belarus; Kyiv, Ukraine)* 123
47. **Tatyana Karpenko, Anastasya Boyarishcheva, Nikita Kovalev, Alina Shpak, Nikolay Sheldeshov, Victor Zabolotskiy** Investigation of the transport of ions and molecules of organic acids and bases through bipolar membranes *(Krasnodar, Russia)* 125
48. **Natalia Kartashova, Dmitriy Konev, Pavel Loktionov, Anatoly Antipov, Pavel Chukanov, Kseniya Kolobkova, Olga Goncharova, Mikhail Vorotyntsev** Investigation of the charge-discharge characteristics of a hydrogen-bromate flow-battery in various modes *(Moscow, Chernogolovka, Russia; Dijon, France)* 128
49. **Victor Kasperchik, Ala Yaskevich, Alexandr Bildyukevich** Applying of hybrid membrane-coagulation methods for surface water treatment *(Minsk, Belarus)* 130
50. **Ruslan Kayumov, Evgeny Sanginov, Alexander Karelin, Yury Dobrovolsky** Physico-chemical properties of protonated and salt forms of the Nafion membranes plasticized with aprotic solvents *(Chernogolovka, Russia)* 132
51. **Daria Khanukaeva, Anatoly Filippov, Pramod Kumar Yadav, Ashish Tiwari** Hydrodynamic permeability of a fibrous membrane modelled as a package of composite solid-porous cylindrical cells in micropolar flow *(Moscow, Russia; Uttar-Pradesh, Rajasthan, India)* 135
52. **Anastasiia Kharina, Tatiana Eliseeva, Alexandra Tikhaya** The peculiarities in electrodialysis of tryptophan - mineral salt solution *(Voronezh, Russia)* 138
53. **Kseniya Kim, Olga Kozaderova, Sabukhi Niftaliev** Degradation of ion-exchange membranes in electrodialysis wastewater production of mineral fertilizers *(Voronezh, Russia)* 140
54. **Evgenia Kirillova, Anna Kovalenko** Mathematical modeling, numerical and asymptotic solution of the boundary problems of membrane systems taking into account the water splitting in intensive current modes *(Wiesbaden, Germany; Krasnodar, Russia)* 141

55. **Sofia Kleinikova, Konstantin Gor'kov, Ekaterina Zolotukhina** Acetaldehyde electro-oxidation on silver catalysts in aqueous ethanol solutions *(Chernogolovka, Moscow, Russia)* 144
56. **Anastasia Klevtsova, Yuliya Yakovleva, Natalia Pismenskaya** The effect of the pH of the desorbing NaCl solution on the degree of extraction of anthocyanins from cation- and anion exchange resin *(Krasnodar, Russia)* 146
57. **Tatyana Kolganova, Anastasia Yelnikova, Ekaterina Lapshina, Anna Parshina, Ekaterina Safronova, Olga Bobreshova** Potentiometric multisensory systems with hybrid materials based on perfluorosulfonic cation-exchange membranes for determination of drugs in pharmaceuticals *(Voronezh, Moscow, Russia)* 148
58. **Denis Kolot, Aslan Achoh** Study of transport characteristics of perfluorinated MF-4SK membrane in sulfate / nitrate solutions *(Krasnodar, Russia)* 149
59. **Natalia Kononenko, Anatoly Filippov, Sergey Dolgopolov, Mariya Salaschenko** Asymmetry of current-voltage characteristics of bi-layer hybrid perfluorinated membranes in sodium chloride solution *(Krasnodar, Moscow, Russia)* 152
60. **Andrey Kononov, Victor Nikonenko** Evaluation of applicability of the teorell-meyer-sievers model to describe the sorption and kinetic properties of ion-exchange membranes *(Krasnodar, Russia)* 154
61. **Andrey Kononov, Veronika Sarapulova, Semyon Mareev** Influence of ion transport in ion-exchange membrane bulk on the shape of chronopotentiometric curves *(Krasnodar, Russia)* 155
62. **Alexander Korzhov, Anastasia But, Victor Zabolotskiy** Study of the decarbonization process in an electrodializer with bipolar membranes *(Krasnodar, Russia)* 157
63. **Alexander Korzhov, Sergey Loza, Kristina Dmitrieva, Ilya Bondarenko, Victor Zabolotskiy** Electrochemical wastewaters treatment in metallurgical enterprises by the example electrodialysis of sulphate-vanadium solusion *(Krasnodar, Russia)* 159
64. **Margarita Kostyanaya, Danila Bakhtin, Viktoria Ignatenko, Stepan Bazhenov, Tatiana Anokhina** Gas-liquid contactors based on cellulose for desorption of CO_2 from industrial physical absorbant *(Moscow, Russia)* 161
65. **Diana Kotova, Svetlana Vasil'eva, Tatiana Krysanova, Anna Sokruykina** The role of solvent during adsorption of α - tocopherol on clinoptilolite *(Voronezh, Russia)* 164
66. **Anna Kovalenko, Makhamet Urtenov** Problems of sustainable calculation of theoretical current-voltage characteristics, chronopotentiograms and chronogalvanograms for a membrane channel with forced convection, reactions of water dissociation/recombination and electroconvection *(Krasnodar, Russia)* 167
67. **Anna Kovalenko, Makhamet Urtenov, Alexander Pismenskiy, Natalia Seidova, Konstantin Sobchenko, Natalja Chubyr** Software package for the analysis of time series in electro-membrane systems *(Krasnodar, Russia)* 170

68. **Ivan Kovalev, Mikhail Popov, Marat Sharafutdinov, Alexander Titkov, Sergey Bychkov, Alexander Nemudry** Direct AC/DC heating of hollow fiber membranes *(Novosibirsk, Russia)* 173
69. **Nikita Kovalev, Tatyana Karpenko, Nikolay Sheldeshov, Victor Zabolotskiy** Influence of type of bipolar cation-exchange and anion-exchange membranes on the characteristics of the process of producing sulfurate acid and sodium hydroxide from sodium sulfate *(Krasnodar, Russia)* 174
70. **Tatyana Kovrigina, Tulegen Chalov, Edil Ergozhin** Synthesis of anion- and cation-exchange membranes by chemical modification of films-matrix *(Krasnodar, Russia)* 177
71. **Olga Kozaderova, Oleg Kozaderov, Kseniya Kim, Sabukhi Niftaliev** Electrodialysis of ammonia-containing aqueous solutions *(Voronezh, Russia)* 180
72. **Anton Kozmai, Svetlana Zyryanova, Victor Nikonenko** Modelling of anion-exchange membrane transport properties with taking into account the change in exchange capacity and swelling when varying bathing solution concenration and pH *(Krasnodar, Russia)* 183
73. **Tamara Kravchenko, Lev Polyanskii, Dmitrii Konev, Dmitrii Vakhnin** Theory and practice of water deoxygenation by metal-ion exchange nanocomposites *(Voronezh, Russia)* 186
74. **Vitalii Kravtsov, Irina Kulikova, Artem Bessonov, Ivan Evdokimov** Study of membrane fouling during acid whey bipolar electrodialysis *(Stavropol', Russia)* 189
75. **Vyacheslav Krysanov, Natalia Plotnikova, Anastasia Okushko** Role of ion exchange matrix in process of reducing sorption of molecular oxygen by metalcontaining nanocomposites *(Voronezh, Russia)* 192
76. **Darya Kudashova, Irina Falina, Natalia Kononenko** Influence of stabilizers on the morphology of platinum dispersion on the surface of perfluorinated membrane *(Krasnodar, Russia)* 195
77. **Mukesh Kumar** Fluid flow through membrane: An analytical approach for Navier-Stokes equation by Lie symmetry analysis *(Prayagraj, India)* 197
78. **Alexandra Kuriganova, Nikita Faddeev, Igor Leontyev, Nina Smirnova** Pulse alternating current synthesis of Pd/C catalysts and their application in PEM fuel cells thechnologies *(Novocherkassk, Rostov-on-Don, Russia)* 198
79. **Anastasiia Kuznetsova, Lyudmila Ermakova, Anna Volkova, Tatiana Antropova** Transport characteristics of porous glass membranes in electrolyte solutions *(St. Petersburg, Russia)* 199
80. **Sergey Lakeev, Ann Korneychuk, Polina Semina, Nina Kozlova, Alexander Khorokhorin, Alexander Smolyanskii** Properties of interference patterns in the transmission spectra of nuclear filters prepared from the polyethylenerephthalate films irradiated by xenon ions *(Moscow, Krasnoyarsk, Russia)* 202
81. **Alyona Larkina, Alexandra Pulyalina, Galina Polotskaya, Ludmila Vinogradova** Purification of n-butanol from aqueous solutions using novel pervaporation membranes based on polymer composites *(Saint Petersburg, Russia)* 205

82. **Denis Lebedev, Maksim Novomlinsky, Vladimir Kochemirovsky, Tatiana Antropova, Irina Anfimova** Study of mechanisms of the ions tranosport in active nanofiltrational membranes containing gold nanoparticles *(St. Petersburg, Russia)* 208
83. **Sergey Loza, Kristina Dmitrieva, Alexander Korzhov, Nikita Smyshliaev, Nazar Romanyuk, Ilya Bondarenko, Natalia Loza** Obtaining electric energy by reverse electrodialysis *(Krasnodar, Russia)* 210
84. **Sergey Loza, Stanislav Utin, Natalia Loza, Victor Dotsenko** Transport characteristics of bilayered profiled membranes modified by superbranched polymers *(Krasnodar, Russia)* 212
85. **Aleksandr Lysenko, Olga Astashkina, Nadezhda Diankina** Sorption active carbon membranes *(Saint Petersburg, Russia)* 214
86. **Anna Lysova, Andrey Yaroslavtsev** Proton-conducting hybrid membranes based on polybenzimidazoles and silica with imidazoline-functionalized surface *(Moscow, Russia)* 215
87. **Aleksandra Lytkina, Natalia Zhilyaeva, Natalia Orekhova, Margarita Ermilova, Nina Shevlyakova, Vladimir Tverskoy, Andrey Yaroslavtsev** C4 hydrocarbons seporation through the polyethylene-graft-sulfonated polystyrene membranes *(Moscow, Russia)* 217
88. **Mariia Makhonina, Kseniia Otvagina, Nail Yanbikov, Andrey Vorotyntsev, Alla Mochalova, Ilya Vorotyntsev** Utilization of gasseparation membranes based on polyelectrolytes *(Nizhniy Novgorod, Russia)* 220
89. **Alexander Malakhov, Stepan Bazhenov** Gas separation in a membrane contactor with a reversible reaction of a gas with an absorbent: experiment and model *(Moscow, Russia)* 223
90. **Semyon Mareev, Dmitrii Butylskii** Effect of surface charge of ion-exchange membrane on its electrochemical characteristics *(Krasnodar, Russia)* 226
91. **Semyon Mareev, Svetlana Zyryanova, Christian Larchet, Lasâad Dammak, Victor Nikonenko** Chronopotentiometry of ion-exchange membranes with hydrophobic areas on the surface: 2D simulation and experiment *(Krasnodar, Russia, Thiais, France)* 228
92. **Natalia Matushkina, Nadezda Strusovskaya, Eugene Ageev** Peculiarities of behavior of pervoporation membranes from isotactic polypropylene *(Moscow, Russia)* 229
93. **Dmitrii Matveev, Tatyana Plisko, Anton Shustikov, Alexander Bildyukevich, Vladimir Volkov** Formation, structure and performance of porous membranes based on acrylonitrile copolymers *(Moscow, Russia; Minsk, Belarus)* 232
94. **Stanislav Melnikov, Elena Nosova, Anastasia But** Wastewater treatment from organic compounds by the example of acetic acid electrodialysis *(Krasnodar, Russia)* 235
95. **Stanislav Melnikov, Svetlana Shkirskaya** Current-voltage characteristics of bilayered ion-exchange membranes in sodium chloride solution *(Krasnodar, Russia)* 238

96. **Vladislav Menshikov, Sergey Belenov, Leonid Polevoj** The activity of trimetallic catalysts with different gold content for methanol electrooxidation *(Rostov-on-Don, Russia)* 241
97. **Arthur Merkel, Martin Ondrušek** An integrated process developed for whey demineralization *(Stráž pod Ralskem, Czech Republic)* 243
98. **Elizaveta Moguchikh, Anastasia Alekseenko, Kirill Paperzh, Angelina Pavlets, Vladimir Guterman** The effect of post-processing on the stability of platinum copper electrocatalysts *(Rostov-on-Don, Russia)* 246
99. **Ilya Moroz, Aleksey Rogov, Dmitrii Butylskii, Semyon Mareev, Natalia Pismenskaya** Vizualization of electroconvection during electrodialysis of strong electrolyte and ampholyte solutions *(Krasnodar, Russia)* 248
100. **Kamila Mugtasimova, Alexey Melnikov, Alexey Kashin, Vitaliy Sinitsyn** Structure – proton transport correlations in perfluorinated sulfopolymer membranes with shorter side chains *(Moscow, Russia)* 250
101. **Andrey Naumov, Pavel Apel, Sergey Kulik, Ivan Eremchev, Dmitry Zagorskiy** Optical visualization of filtration process of colloidal particles in track-etched membranes at nano-scale *(Troitsk, Dubna, Moscow, Russia)* 252
102. **Ekaterina Nazyrova, Svetlana Shkirskaya, Anastasiya Norenko, Ekaterina Dankovtseva** Selectivity of heterogeneous cation-exchange membranes modified by polyaniline *(Krasnodar, Russia)* 253
103. **Vera Nesterova, Alexandra Pulyalina, Galina Polotskaya** Aromatic polyamide membranes for organophilic pervaporation *(Saint Petersburg, Russia)* 256
104. **Vladlen Nichka, Michail Porozhnyy, Svetlana Shkirskaya, Natalia Pismenskaya, Victor Nikonenko** Modified microheterogeneous model for describing the electrical conductivity of membranes in diluted electrolyte solutions *(Krasnodar, Russia)* 259
105. **Natalya Niftalieva, Mikhail Popov, Alexander Nemudry** Conversion of hydrocarbons using hollow fiber oxygen-permeable membranes *(Novosibirsk, Russia)* 260
106. **Victor Nikonenko, Anna Kovalenko, Elizaveta Evdochenko, Matthias Wessling, Gerald Pourcelly** Relationships between electroconvection and water splitting in membrane systems in intensive current regimes *(Krasnodar, Russia; Aachen, Germany; Montpellier, France)* 261
107. **Ksenia Novikova, Nina Smirnova, Yury Dobrovolsky** Influence of carbon support on catalytic layer performance of fuel cells *(Chernogolovka, Novocherkassk, Russia)* 264
108. **Eduard Novitsky, Evgenia Grushevenko, Vladimir Vasilevsky, Alexey Volkov** The effect of absorbent feeding conditions on the parameters of reverse electrodialysis *(Moscow, Russia)* 266
109. **Ivan Novomlinskiy, Irina Gerasimova, Vadim Volotchaev, Vladimir Guterman** Platinum electrocatalysts based on oxide and oxide carbon carriers for fuel cell *(Rostov-on-Don, Russia)* 269
110. **Maksim Novomlinsky, Denis Lebedev, Alena Fogel, Vladimir Kochemirovsky** Synthesis of nanoporous membranes with gold nanoparticles by laser-induced deposition *(St. Petersburg, Russia)* 271
111. **Takoua Ounissi, Lasâad Dammak, Christian Larchet, Jean-François Fauvarque, Emna Selmane Bel Hadj Hmida** Lithium extraction by 274

diffusion dialysis using novel composite *membranes (Tunis El Manar, Tunisie; Thiais, France)*

112. **Iliya Petriev, Ivan Lucenko, Kirill Voronin, Polina Pushankina, Mikhail Baryshev** Gas transroptation parameters of membranes modified by star-like palladium nanocrystallites *(Krasnodar, Russia)* 276
113. **Natalia Pismenskaya, Olesya Rybalkina, Kseniia Tsygurina, Ekaterina Melnikova** Coupling between mass transfer and proton generation during electrodialysis of ampholyte-containing solutions *(Krasnodar, Russia)* 278
114. **Alexander Pismenskiy, Mahamet Urtenov, Anna Kovalenko** Mathematical modeling of mass and heat transfer during electrodialysis of sodium dihydrophosphate *(Krasnodar, Russia)* 281
115. **Petr Polezhaev, Tomáš Belloň, Lucie Vobecká, Zdeněk Slouka** Selectivity of ion-exchange resin particles – the factor of internal structure *(Praha, Plzeň, Czechia)* 284
116. **Valentina Ponomareva, Irina Bagryantseva, Anna Gaydamaka** Study of phase composition and electrotransport properties of systems based on mono and disubstituted phosphates of cesium and rubidium *(Novosibirsk, Russia)* 287
117. **Valentina Ponomareva, Konstantin Kovalenko, Elena Shutova, Anastasia Cheplakova, Danil Dybtsev, Vladimir Fedin** Study of new proton-conducting materials based on metal organic polymers *(Novosibirsk, Russia)* 288
118. **Alla Reshetnikova, Vladimir Shaposhnik** The main role of equipolar contacts ion-exchangers grans in the electrodeionization *(Voronezh, Russia)* 290
119. **Nazar Romanyuk, Sergey Loza, Natalia Loza** Competitive transfer of sodium and calcium ions through ion exchange membranes modified by polyaniline *(Krasnodar, Russia)* 292
120. **Olesya Rybalkina, Kseniia Tsygurina, Ekaterina Melnikova, Anton Kozmai, Natalia Pismenskaya** Study of protonation-deprotonation reactions in the system anion-exchange membrane / KHT solution using impedance spectroscopy *(Krasnodar, Russia)* 295
121. **Ilya Ryzhkov, Anton Vyatkin, Anastasia Bortsova, Mikhail Simunin, Sofia Kozlova, Valerij Kucheryavyj** Switchable ionic selectivity in conductive nanoporous membranes: 1D and 2D mathematical models *vs* experimental data *(Krasnoyarsk, Russia)* 298
122. **Valentin Sedelkin, Larisa Potekhina, Olga Lebedeva, Marina Schneider, Elmira Ulyanova** Research of kinetic transformations of the chemical supremolecular structure in the system: the original raw material - forming solution - filter membrane *(Engels, Russia)* 301
123. **Maxim Shalygin, Alina Kozlova, Alexander Netrusov, Vladimir Teplyakov** Vapor-phase membrane method for recovery and concentration of bioalcohols from fermentation broths *(Moscow, Russia)* 304
124. **Vladimir Shaposhnik** Conjugate transport of mass and energy in ion exchange membranes by electrodialyse *(Voronezh, Russia)* 305
125. **Nikolay Sheldeshov, Victor Zabolotskiy, Konstantin Lebedev** Transfer processes in membrane systems used for production acids and bases from their salts by bipolar electrodialysis *(Krasnodar, Russia)* 307

126. **Vladimir Shelistov, Elizaveta Frants, Georgy Ganchenko** On the features of electrophoresis of charge-selective particles *(Krasnodar, Russia)* 308
127. **Svetlana Shkirskaya, Viktoria Soloshko** Water transport in modified ion exchange membranes *(Krasnodar, Russia)* 309
128. **Inna Shkorkina, Veronika Sarapulova, Olesya Rybalkina** Study of electrochemical characteristics of Fuji Type – X anion exchange membranes produced via electrospinning method *(Krasnodar, Russia)* 311
129. **Ekaterina Skolotneva, Daria Mareeva, Semyon Mareev, Christian Larchet, Lasâad Dammak, Victor Nikonenko** Applicability of approximate equations for calculation of the chronopotentiometric transition time in membrane systems with a diffusion layer of finite length *(Krasnodar, Russia)* 313
130. **Ilya Strylets, Denis Terin, Marina Kardash, Tamara Druzhinina** Influence of the fiber filler on the sorption characteristics of polymer composites "POLIKON A" *(Saratov, Moscow, Russia)* 315
131. **Valentina Titorova, Veronika Sarapulova, Natalia Pismenskaya, Victor Nikonenko** Diffusion pearmability of commercial homogeneous and heterogeneous ion-exchange membranes in NaCl, $CaCl_2$ and Na_2SO_4 solutions *(Krasnodar, Russia)* 317
132. **Ekaterina Titskaya, Maria Timchenko, Irina Falina, Anastasia Alekseenko** The effect of catalyst composition on characteristics of membrane-electrode assemble of hydrogen-air fuel cell *(Krasnodar, Russia)* 320
133. **Sergey Tsipliaev, Denis Terin, Marina Kardash, Igor Galushka, Larisa Karpenko-Jereb, Timur Turaev** The investigations of the structure and properties of ion-exchange materials "POLIKON CA" with mosaic-lateral morphology (*Saratov, Russia; Graz, Austria)* 323
134. **Alexandr Tskhay, Yelena Pryatko, Konstantin Kudelya** Combined electric baromembrane technology for desalination of the caspian sea water *(Almaty, Republic of Kazakhstan)* 326
135. **Kseniia Tsygurina, Olesya Rybalkina, Ekaterina Melnikova, Gerald Pourcelly, Natalia Pismenskaya** Influence of the «facilitated» diffusion NH_3 through the anion-exchange membrane on the rate of water splitting in electrodialysis process *(Krasnodar, Russia; Montpellier, France)* 327
136. **Valery Ugrozov** Gas diffusion through structurally inhomogeneous bilayer membrane *(Moscow, Russia)* 330
137. **Artem Ulihin, Nikolay Uvarov, Valentina Ponomareva, Konstantin Kovalenko, Vladimir Fedin** Nanocomposites based on lithium perchlorate in the metal-organic framework matrix *(Novosibirsk, Russia)* 332
138. **Makhamet Urtenov, Victor Nikonenko, Anna Kovalenko, Elizaveta Evdochenko** Analysis of the theoretical current-voltage characteristics of a membrane channel (*Krasnodar, Russia)* 333
139. **Aminat Uzdenova, Makhamet Urtenov, Victor Nikonenko** Effect of potential of pulsed electric field on average current density in electrodialysis cell: numerical experiment *(Krasnodar, Karachaevsk, Russia)* 336
140. **Dmitrii Vakhnin, Natalya Zheltoukhova, Alina Tregubova, Tamara Kravchenko** Oxygen electroredox – sorption by metal ion-exchange nanocomposites. The current effect *(Voronezh, Russia)* 339

141. **Vera Vasil'eva, Elmara Akberova** Electroconvective instability in systems with heterogeneous membranes ralex with different content of ion-exchanger *(Voronezh, Russia)* 342
142. **Vera Vasil'eva, Mikhail Smagin, Elena Goleva** A comparative analysis of the effect of phenylalanine on physicochemical, structural and transport characteristics of profiled heterogeneous ion-exchange membranes MK-40 and MA-40 *(Voronezh, Russia)* 344
143. **Lucie Vobecká, Zdeněk Slouka** Water splitting at ion-exchnage resin particles and the heterogeneous ion-exchange membranes *(Prague, Czech Republic)* 347
144. **Yury Volfkovich** Activated carbons as nanoporous electron-ion exchangers with hydrophilic - hydrophobic properties *(Moscow, Russia)* 350
145. **Yury Volfkovich, Alexey Mikhalin, Alexey Rychagov, Valentin Sosenkin, Marina Kardash, Natalya Kononenko, Sergei Tsipliaev, Svetlana Shkirskaya** Influence of the manufacturing method of mosaic cation – anion - exchange membranes on the characteristics of capacitive deionization of water *(Moscow, Engels, Krasnodar, Russia)* 353
146. **Vitaly Volkov, Alexander Chernyak, Olga Yarmolenko, Vladimir Tverskoy, Daniel Golubenko** Hydration and ionic transport in ion exchange membranes on NMR data *(Chernogolovka, Moscow, Russia)* 356
147. **Bogdan Voloshin, Sergey Bychkov, Stanislav Chizhik, Alexander Nemudry** Study of oxygen transport in grossly nonstoichiometric oxides via oxygen partial pressure relaxation technique *(Novosibirsk, Russia)* 359
148. **Bogdan Voloshin, Mikhail Popov, Sergey Bychkov, Stanislav Chizhik, Alexander Nemudry** Analysis of kinetic and thermodynamic properties of non-stoichiometric oxides in reaction with oxygen using the conception of continuous homologuos series *(Novosibirsk, Russia)* 360
149. **Daria Voropaeva, Daniel Golubenko, Ardalion Ponomarev, Andrey Yaroslavtsev** Plastisized polymer electrolytes based on sulfonated polystyrene: solvation and Li^+/Na^+ conductivity *(Moscow, Russia)* 361
150. **Mikhail Vorotyntsev, Anatoly Antipov, Dmitry Konev** Surprising dependence of the current density of bromate electroreduction on the microelectrode radius *(Moscow, Chernogolovka, Russia; Dijon, France)* 363
151. **Anton Vyatkin, Anastasia Bortsova, Mikhail Simunin, Maksim Mishnev, Ilya Ryzhkov** Experimental study of switchable ion transport in carbon coated nanoporous alumina membranes *(Krasnoyarsk, Russia)* 366
152. **Pramod Kumar Yadav** Motion through non-homogeneous porous medium: hydrodynamic permeability of membrane composed by cylindrical particles *(Prayagraj, India)* 369
153. **Nail Yanbikov, Kseniia Otvagina, Tatyana Sazanova, Alexandr Logunov, Ilya Vorotyntsev** Gas separation properties of silica-organic polymer membranes modified by plasma and ozone exposure *(Nizhniy Novgorod, Russia)* 370
154. **Andrey Yaroslavtsev** Membrane materials in modern energy *(Moscow, Chernogolovka, Russia)* 372
155. **Polina Yurova, Irina Stenina, Andrey Yaroslavtsev** Homogeneous cation exchange membranes modified by pedot: synthesis and properties *(Moscow, Russia)* 375

156. **Yana Yutskevich, Sergey Mikhaylin, Anton Kozmai, Natalia Pismenskaya** Application of continuous-flow electrophoresis to separate b-lactoglobulin hydrolysate *(Krasnodar, Russia; Québec, Canada)* 377
157. **Dmitry Zagorskiy, Sergei Kruglikov, Sergei Bedin, Ilia Doludenko, Alexandr Shatalov, Dmitry Cherkasov, Dmitry Panov** Features of galvanic deposition of multicomponent metallic nanowires in porous of track etched membranes *(Moscow, Russia)* 380
158. **Vladimir Zhdanov, Alexander Larin** Effect of surface diffusion on separation of gas mixtures in nanosized porous membranes *(Moscow, Russia)* 383
159. **Umirzak Zhusipbekov, Gulzipa Nurgalieva, Zamira Bayakhmetova, Aynur Shakirova, Dulat Duysenbay** Sorption of toxic compounds of iron and cobalt from solutions of humine substances *(Almaty, Kazakhstan)* 386
160. **Svetlana Zyryanova, Natalya Terikhova, Lasâad Dammak, Victor Nikonenko** Effect of surface morphology on electrochemical characteristics of a homogeneous anion-exchange membrane AMX modified with an inert hydrophobic material *(Krasnodar, Russia; Thiais, France)* 389
161. **Libor Šeda, Ladislav Čopák** Heavy metal sulphate salts removal from sulphuric acid solution via diffusion dialysis: pilot scale validation *(Stráž pod Ralskem, Czech Republic)* 398

SYNTHESIS AND PROPERTIES OF ION-EXCHANGE MEMBRANES BASED ON ULTRA HIGH-MOLECULAR WEIGHT POLYETHYLENE

[1]Emil Abdrashitov, [1,2]Dina Kritskaya, [1]Veslav Bokun, [1,2]Ardalion Ponomarev, [2]Ksenia Novikova, [2]Evgeny Sanginov, [2]Yury Dobrovolsky

[1] Chernogolovka Branch of the N.N, Semenov Federal Research Center for Chemical Physics, RAS, Russia, *E-mail:dinak@binep.ac.ru*

[2]Institute of Problems of Chemical Physics of RAS, Chernogolovka, Russia, *E-mail:kcenia-4@mail.ru*

Introduction

Ultra high molecular weight polyethylene (UHMWPE) is a promising polymer matrix for preparation of composite ion-exchange membranes due to its excellent mechanical properties, good chemical and thermal stability. In recent years, we have realized the synthesis of a series of polystyrene (PS) based composites, precursors of ion-exchange membranes, using the styrene ability to both efficient sorption from a solution by certain polymer films and efficient thermal polymerization at elevated temperatures [1]. However, during the synthesis by this method the films should be kept in the styrene solution that causes a side styrene polymerization on the film surface and in the bulk of the solution. All this requires thorough washing of the resulting composites films and leads to high reagent consumptions. In this regard, it seems more promising to carry out the composite synthesis by gas phase styrene polymerization keeping the polymer matrix in the saturated monomer vapor.

Such approach was realized in our previous work [2] allowed successfully modifying of polyvinylidene fluoride (PVDF) film by polystyrene through the vapor phase polymerization, that provide considerably simplifying the synthesis conditions, and reducing procedure time and reagent consumption. By sulfonation of the developed composites the PVDF-sulfonated PS membranes with an ion exchange capacity (IEC) of up to 2.7 mmol g-1 and high proton conductivity were prepared [2].

The aim of this work was to apply the developed method for the preparation of composite membranes based on a UHMWPE matrix and to study their properties.

Experiments

UHMWPE film (SVMPE-1000 grade, by LLC Formoplast, St. Petersburg) with a thickness of 50-100 microns was used as a polymer matrix. The samples fixed in the holder-cartridge were preliminarily kept in the "styrene – polymerization initiator - divinylbenzene" solution. Then the swollen samples were located in the reactor above the level of styrene containing an inhibitor. The reactor with the loaded samples was purged with argon, sealed and thermostated at 110 °C for 1 - 5 hours to conduct styrene polymerization. When finished the composite films were removed from the reactor and thoroughly washed with toluene. The content of PS formed in the matrix (wt.%, rel. to the initial film weight) was determined by the weight gain of the dried samples.

The PS content in the surface layer of the prepared composites was analyzed by ATR-FTIR. Ion-exchange membranes were obtained by sulfonation of the composite using sulfuric acid. The proton conductivity of the membranes was measured by impedance spectroscopy. For testing the membranes as electrolyte of a hydrogen-air fuel cell (FC) the following conditions were used: T = 25 °C; $RH_{H2} = RH_{air} = 100$; gas flow: 0.1 l/min (H_2), 0.4 l/min (air); p (H_2) = p (air) = 1 atm.

Results and Discussion

It was shown that keeping the UHMWPE films in the styrene vapor during 1–5 h under described conditions leads to the formation of PS inside of the films up to 60 wt. %. The modification of the films was accompanied by a mainly increase in the film thickness and a slight increase in their length and width.

Fig. 1 shows the data on the PS accumulation in the UHMWPE films during the styrene gas phase polymerization at 110 ° C. As can be seen, there is a noticeable the PS content spread, which is associated, possibly, with uncontrolled evaporation of the sorbed monomer during the samples loading into the reactor and outputting the reaction to a steady-state conditions. Nevertheless, it

can be concluded that the PS accumulation is almost linearly dependent on the reaction time and is approximately 6 wt.% per h at 110 °C.

DSC data of the UHMWPE-PS composites showed that the PS formation did not change the content of the crystallinity samples. So, it can be conclude, that the styrene polymerization proceeds in the amorphous phase of the polymer matrix.

The PS content in the surface layer of the composites was estimated by ATR-FTIR. For this purpose, the characteristic polystyrene band at 697 cm^{-1}, the out-of-plane deformation vibrations of C–H bonds of the aromatic ring, which does not overlapped by the matrix bands, was used. It was found that the PS content in the surface layer is slightly higher than the average PS content in the bulk composite.

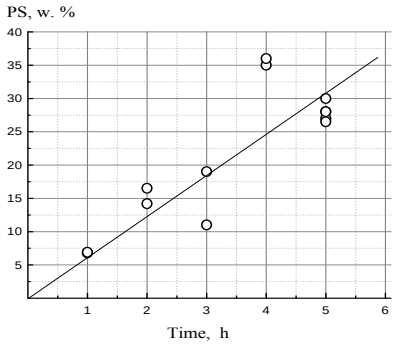

Figure 1. Kinetics of PS accumulation in the UHMWPE films (50 μm) during sorption of styrene from saturated vapor at 110°C.

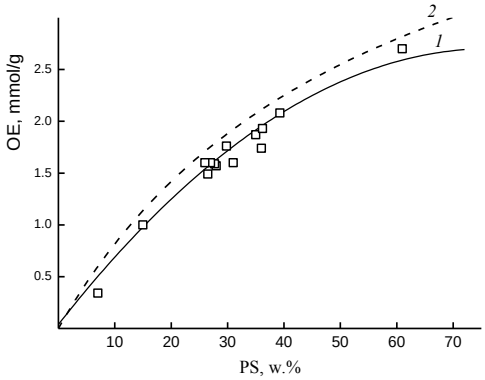

Figure 2. Dependencies of the experimental (1) and calculated (2) IECs of the UHMWPE-sPS membranes on the PS content.

Fig. 2 presents the results of the UHMWPE-PS composites sulfonation. The UHMWPE-sulfonated PS membranes (UHMWPE-sPS) with IEC up to 2.6 mmol/g were obtained. According to IR data (Fig. 3) the sulfonation lead to appearance new absorption bands at 1008 and 1040 cm^{-1}, which were referred to the symmetric stretching vibrations of the $–SO_3^-$ and C-S vibrations of the aromatic ring of the sulfonated PS. The intensity of these bands increases with increase in the PS content.

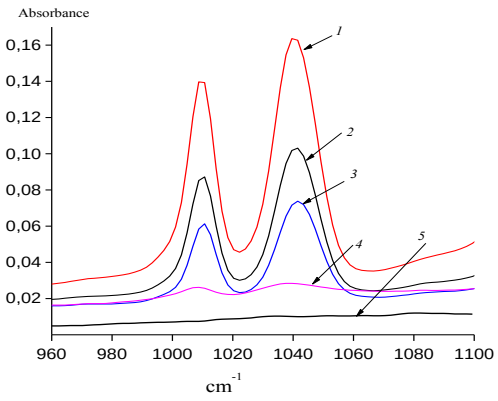

Figure 3. ATR-FTIR-spectra of UHMWPE-sPS membranes in the Na+ form. The PS content in the composites are 36 (1), 27 (2), 15 (3), and 7 (4) wt. %. 5 – the initial UHMWPE film.

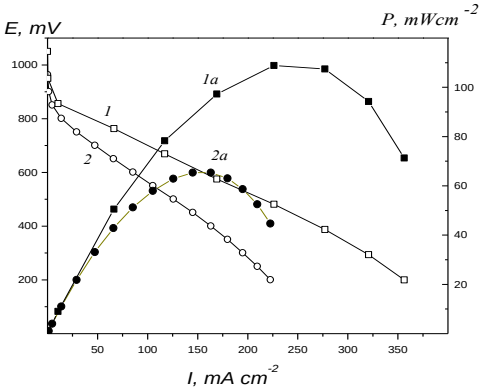

Figure 4. The current-voltage (1, 2) and power (1a, 2a) characteristics of the FC based on the UHMWPE-sPS (1, 1a) and Nafion-115 (2, 2a) membranes.

It was established that the dependence of the water uptake of the UHMWPE-sPS membranes on their IEC values at room temperature is described by the linear ratio of 16 mol H_2O/mol SO_3^-. The maximum value of 60 mS/cm at room temperature for proton conductivity of the UHMWPE-sPS membranes was reaches. The results of the comparative tests of the synthesized membrane UHMWPE-sPS (IEC~ 2.6 mmol g^{-1}) and the Nafion-115 membrane (IEC~ 0.9 mmol g^{-1}) in FC are presented in Fig. 4. As can be seen, the current-voltage and power characteristics of FC based on the developed membranes significantly exceed those for the Nafion-115.

This research was supported by the Russian Science Foundation, Project №17-79-30054.

References

1. *PonomarevA. N., AbdrashitovE. F., KritskayaD. A., BokunV. Ch., SanginovE. A., and Dobrovol'skii Yu. A.,* Synthesis of polymer nanocomposite ion-exchange membranes from sulfonated polystyrene and study of their properties, Russ. J. Electrochem. 2017. V. 53. P.589.
2. *Ardalion N. Ponomarev, Dina A. Kritskaya, Emil F. Abdrashitov, Veslav C. Bokun, Ksenia S. Novikova, Evgeny A. Sanginov, Yury A. Dobrovolsky,* Thermal polymerization of sorbed in polymer films from the gas phase styrene as a method for creating a precursor of ion-exchange membranes, Russ. J. Electrochem. 2019. V. 55. in press.

SYNTHESIS AND TRANSPORT PROPERTIES OF ION EXCHANGE MEMBRANES BASED ON POROUS POLYTETRAFLUOROETHYLENE FILMS AND SULPHONATED POLYSTYRENE

[1]Emil Abdrashitov, [1,2]Dina Kritskaya, [1]Veslav Bokun, [1,2]Ardalion Ponomarev, [2]Ksenia Novikova, [2]Evgeny Sanginov, [2]Yury Dobrovolsky

[1] Chernogolovka Branch of the N.N, Semenov Federal Research Center for Chemical Physics, RAS, Russia, E-mail: *dinak@binep.ac.ru*

[2]Institute of Problems of Chemical Physics of RAS, Chernogolovka, Russia, E-mail: *kcenia-4@mail.ru*

Introduction

Previously, we have developed a new method for the synthesis of polymer "stretched polytetrafluoroethylene (PTFE) - polystyrene"composites by stretching a PTFE film in a liquid monomer followed by thermal polymerization of styrene sorbed from a solution into the forming porous PTFE structure [1, 2]. It was shown that protonconducting membranes, obtained by sulfonation of the synthesized "stretched PTFE - polystyrene"composites, have excellent transport properties [3]. It seemed promising to investigate the possibility of creating a PTFE-PS composite (a precursor of ion-exchange membranes) by polymerizationof styrene sorbed into industrial porous teflon, and to study the transport properties of the membranes synthesized on its basis.

On the example of a polyvinylidene fluoridefilm it was established [4]that the thermal styrene polymerization can be effectively carried out inside of this film not only during styrene sorption from the liquidphase, but also from the vapor. The vapor-phase synthesis method of the «polymer matrix-PS» precursor is more convenient in comparison with the liquid-phase one. The essence of this approach is preliminary swelling of the polymer film in the monomer solution with the initiator with following keepingthe swollen film over the liquid styrene in a reactor thermostated at 110 °C. This new method significantly shortens the stage of homopolymerwashing, reduces the consumption of working solutions (monomers and solvents) and the total synthesis time.

The aim of this work was the development of liquid and vapor-phase styrene polymerization methods to obtain PTFE-PS composites based on a commercial porous PTFE film (por-PTFE) produced by LLC Formoplast (St. Petersburg) as well as the study of the properties of membranes obtained by the sulfonation of por-PTFE-PS composites.

Experiments

Figure 1 shows a micrograph of thepor-PTFE film taken with an optical microscope (transmission mode) at a 100-fold magnification. The thickness of the por-PTFE film is 100 μm. Through pores with a size of 7 × 60 microns are clearly visible. Their geometrical dimensions do not practically change when the por-PTFE film is heated in air at 120 – 130°C for 2 - 3 h. The density is about 0.7 g/cm^3, i.e. the polymer fills only 0.35 part of the volume of the porous film. When filling the film free volume with a liquid with a density of about 1 g/cm^3, the liquid/polymer weight ratio should be about 0.9.

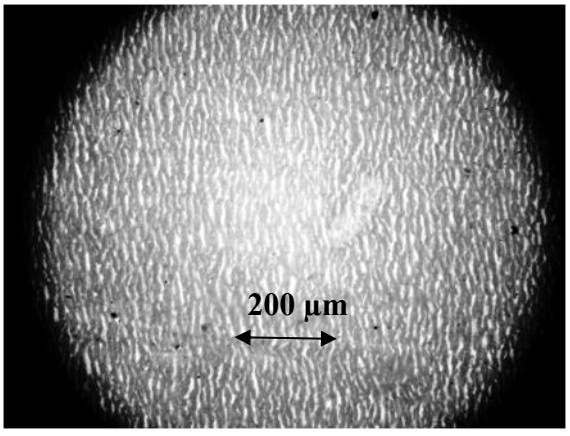

Figure 1. Micrograph of the por-PTFE film by Biomed 6optical microscope.

Study of the por-PTFE film swelling in a liquid styrene, toluene, or a solution of them showed that the film absorbs up to 60 - 80 wt.%of liquid at room temperature. As can be estimated, almost the whole part of the film free volume is available for sorption.

To realize a vapor-phase synthesis of a composite precursor, a por-PTFE film, previously swollen in a styrene-initiator-divinylbenzenesolution, was locatedin a reactor over a solution of inhibited monomer. Then the reactor was kept in an air thermostat for 1 to 3 hours at 110 °C. In the case of liquid-phase synthesis, a pore-PTFE film fixed in a cartridge was immersed in a reactor with a styrene-initiator-divinylbenzene solution and the reactor was placed in a thermostat at 90 °C. The accumulation of polystyrene in the porous film was carried out in 2 - 3 stages. The time of each stage (~ 2 hours) was limited by the gelation of the reaction solution and replacing with a fresh solution.

Results and Discussion

Figure 2 and 3 show the kinetics of the accumulation of polystyrene in the por-PTFE film during the polymerization using the vapor-and liquid-phase methods.

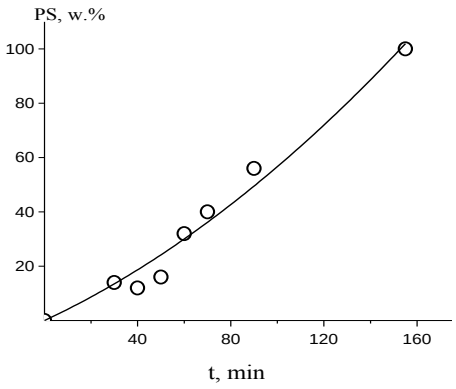

Figure 2. The PS accumulation bythepor-PTFE film during the polymerization of styrene sorbedby the film from the vapor at 110 °C.

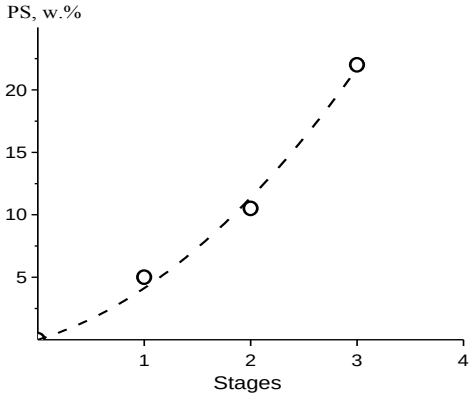

Figure 3. The PS accumulation by thepor-PTFE film during the polymerization of styrene sorbedby the film from a liquid at 90 °C.

As can be seen, during the vapor phase synthesis the amount of polystyrene implanted in PTFE reaches 100 wt.% (relative to the matrix) for 2.5 hours (Fig. 2). Following keeping the synthesized por-PTFE-PS samples in toluene at room temperature leads to only partial leaching of the PS. The por-PTFE-PS composites containing up to 60 wt.%of PS were obtained. In the case of liquid-phase synthesis (Fig. 3), the PS accumulation rate increases markedly from one stage to another, but it is noticeably lower than that in the vapor phase method at 110 °C (Fig. 2).

Study of the por-PTFE-PS composite swelling in toluene at room temperature showed that the swelling is determined by the sorption of toluene into the implanted PS (Fig. 4). Even with a low PS content (about 10 wt.%), the amount of the sorbed toluene is noticeably less than that for the initial porous film at room temperature. As can be seen, the polymerization of styrene inside of the film pores at 90 and 110 °C is accompanied by a gradual film shrinkage and filling of the pores with polystyrene.

Figure 5 shows the ATR IR spectra of the surface of theinitial porous PTFE film (curve 3) and the por-PTFE-PS composites with different PS contents (curves 1 and 2). As can be seen, effective absorption is observed in the region of 700 $cm^{-1}$of the IR spectra of composites, which is attributed to the characteristic absorption of polystyrene (697 cm^{-1}). This is indicate the PS formation in the pores of the film-matrix. The intensity of the absorption increases markedly with increasing content of PS in the composite.

By sulfonation of the por-PTFE-PS composites with different PS content,new proton exchange por-PTFE-sulfonated PS membranes with ion exchange capacity of up to 1.6 mmol/g and proton conductivity in water at room temperature up to 100 mS/cm were prepared.

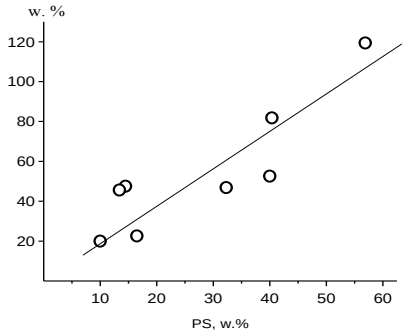

Figure 4. Dependence of the swelling of porous composite films in toluene on the implanted PS content. T = 25 °C.

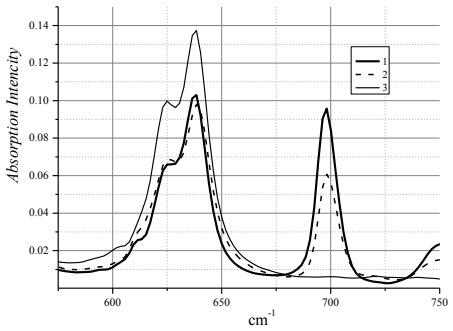

Figure 5. ATR IR spectra of the surface of the por-PTFE-PS composites with 33 (1) and 18 (2) wt.% of PS and the surface of the commercial porous PTFE film (3).

This research was supported by the Russian Science Foundation, Project №17-79-30054.

References

1. *E.F. Abdrashitov, D.A. Kritskaya, V.C. Bokun, A.N. Ponomarev*, Restructuring of polytetrafluoroethylene films during crazing in liquid media as an effective sorption method // Russian Journal of Physical Chemistry B. 2016. V. 10. № 5.P. 820-824.
2. *E.F. Abdrashitov, D.A. Kritskaya, V.C. Bokun, A.N. Ponomarev*, Kinetics of the thermal polymerization of styrene in stretched polytetrafluoroethylene films // Russian Journal of Physical Chemistry B. 2017. V. 11. № 1.P. 167-172.
3. *EmilF. Abdrashitov, DinaA. Kritskaya, VeslavC. Bokun, ArdalionN. Ponomarev, KseniaS. Novikova,EvgenyA. Sanginov, YuryA. Dobrovolsky*, Synthesis and properties of stretched polytetrafluoroethylene–sulfonated polystyrene nanocomposite membranes//SolidStateIonics. 2016. V. 286. P.135.
4. *Ardalion N. Ponomarev, Dina A. Kritskaya, Emil F. Abdrashitov, Veslav C. Bokun, Ksenia S. Novikova, Evgeny A. Sanginov, Yury A. Dobrovolsky,* Thermal polymerization of sorbed in polymer films from the gas phase styrene as a method for creating a precursor of ion-exchange membranes, Russ. J. Electrochem. 2019. V. 55. in press.

ELECTROCHEMICAL CHARACTERISTICS AND SPECIFIC SELECTIVITY OF BILAYER ION-EXCHANGE MEMBRANES IN TERNARY (SULFATE/NITRATE) SOLUTIONS

Aslan Achoh, Stanislav Melnikov, Konstantin Lebedev, Victor Zabolotskiy
Kuban State University, Krasnodar, Russia, E-mail: *achoh-aslan@mail.ru*

Introduction

At present, it has been established that many properties of membranes are controlled by phenomena determined by the structure and properties of the thin surface layer of membranes. According to many researchers, modification of membranes surface or volume are possible to expand their range and improve physico-chemical and technical-economical characteristics [1, 2]. In this regard, a new direction in membrane electrochemistry has emerged, associated with the creation and research of modified ion-exchange membranes (bilayer, multilayer, composite, etc.) and the evaluation of the effect of modification on their electrotransport characteristics. These studies are of great scientific and practical importance and provide an opportunity to obtain membranes with unique properties.

It is important to note that despite the large number of works in the field of modification of ion-exchange membranes, the mechanism for improving membrane properties, which is due to modification, the effect of modifying layers on the transfer of ions and molecules in these electro-membrane systems is not fully understood.

The aim of this work is to study the transport and electrochemical characteristics of surface-modified heterogeneous anion-exchange membranes MA-41, in sulfate-nitrate solutions of electrolytes, in comparison with the initial membrane MA-41.

Experiments

Measurements of the current-voltage characteristics (CVC) of the membranes were carried out on a rotating membrane disk. The current-voltage characteristics of the membranes were recorded in galvanostatic mode, with a stepwise increase in current density. The working solution consisted of a mixture of sodium sulfate of 0.015 mol eq / l and sodium nitrate of 0.015 mol eq / l. At the same time, the ratio of concentrations of sodium sulfate to sodium nitrate changed, but the total concentration remained constant at 0.03 mol eq / l. The composition of the solution in the lower chamber (cathodic) was kept constant. The rotational speed of the membrane disk ranged from 100 to 500 rpm. The feed rate of the solution into the anode chamber was 7.5 ± 0.1 ml / min. The temperature in the experiments was kept constant and was equal to 25 ± 0.1 ° C.

Results and discussion

It is known that modification of an anion-exchange membrane with a cation-exchange film significantly reduces the value of the limiting current. In order to evaluate the effect of the thickness of the modifying film, the CVC of the membranes under investigation were recorded at 100 rpm in a mixture of solutions of 0.015 mol eq / l of sodium sulfate and 0.015 mol eq / l of sodium nitrate. The thickness of the diffusion layer was kept constant.

The experiments performed show that the deposition of a cation-exchange film on an anion-exchange membrane leads to an decrease in the limiting current of the initial membrane by an order of magnitude (Fig. 1).

A comparative analysis of the dependences of the limiting current of the initial and modified membrane shows that the deposition of a cation-exchange film on the heterogeneous membrane leads to a multiple decrease in the limiting current and the limiting current does not depend on the thickness of the diffusion layer (Fig. 2).

The limiting currents for the initial membrane MA-41 from different disk rotation speeds, found by the method of tangents, coincide with those calculated by the Levich theory, which is depicted by the dotted line in Figure 2b. It should be noted that for a modified membrane, with a film thickness of 15 μm, the limiting current does not change with the speed of rotation of revolutions. This can be explained by the fact that the limiting state occurs on the border of the modifying film

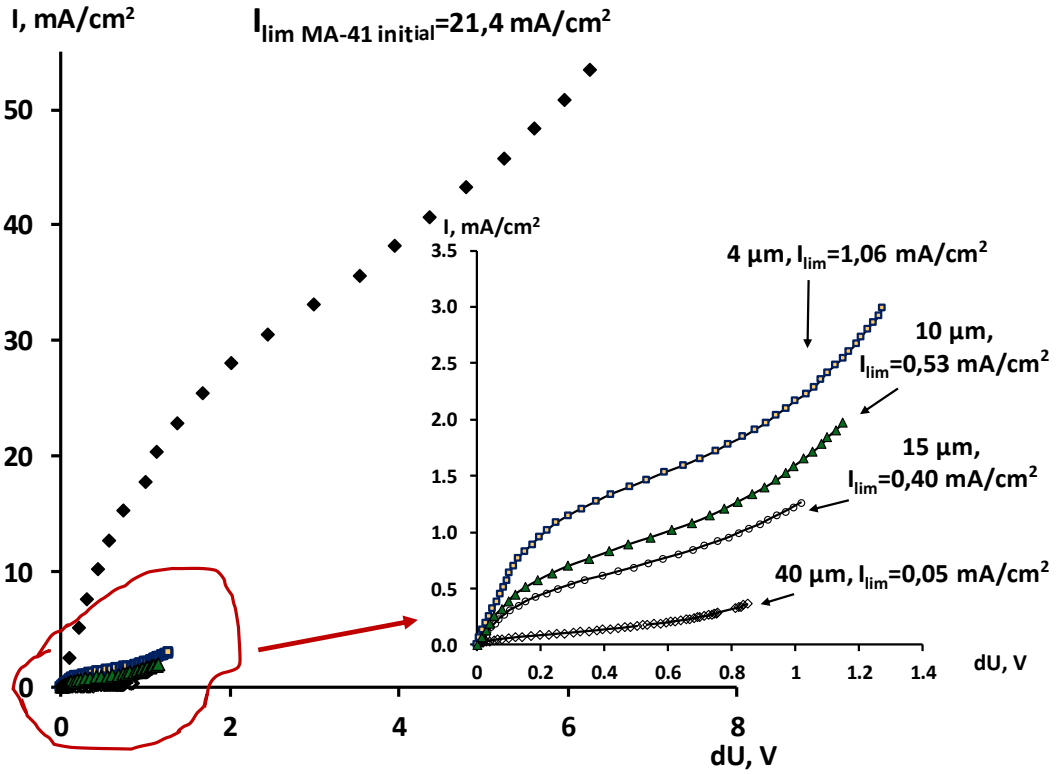

Figure 1. Current-voltage characteristics of the original and modified membranes with different thicknesses of the modifying film, at 100 rpm.

This can be explained by the fact that the limiting state occurs on the border of the modifying film and membrane. In the modifying film, sulfate and nitrate ions are Co-ions, therefore their transport is limited due to charge selectivity.

The selective properties of the membrane with a modifying film are influenced by such factors as: thickness and charge (concentration of fixed groups) of the film, that is confirmed by experimental data (Fig. 3). In this case, the dependence of the selectivity coefficient on the dimensionless current density nonlinearly depends on the thickness of the modifying film, which is confirmed by experimental data and numerical calculations (Fig. 4).

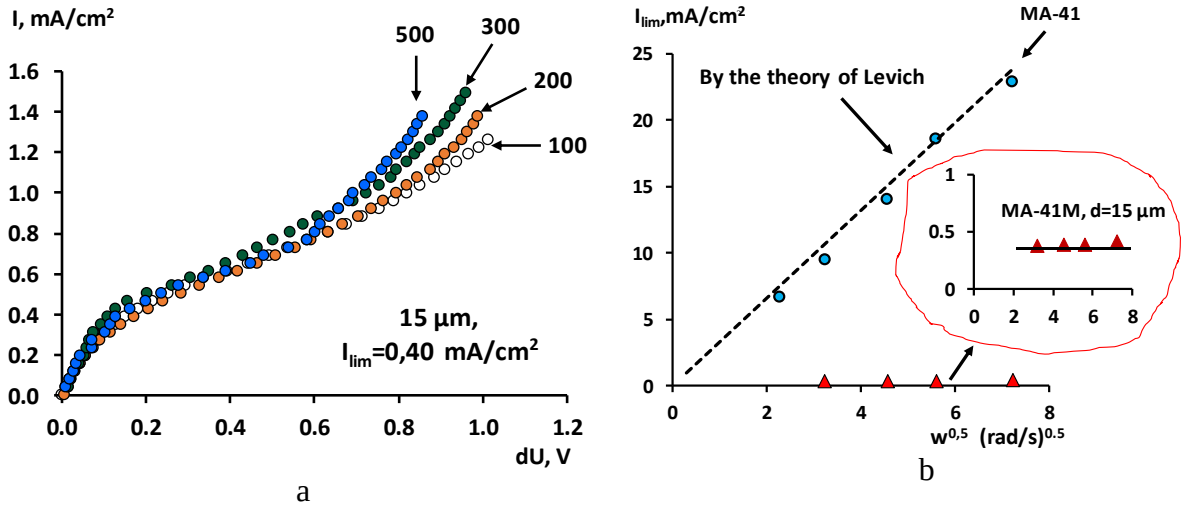

Figure 2. The dependence of the CVC of the modified MA-41 membrane at different speeds of rotation of the AMD (a), the dependence of the limiting current on the square root of the angular velocity of rotation of the AMD (b).

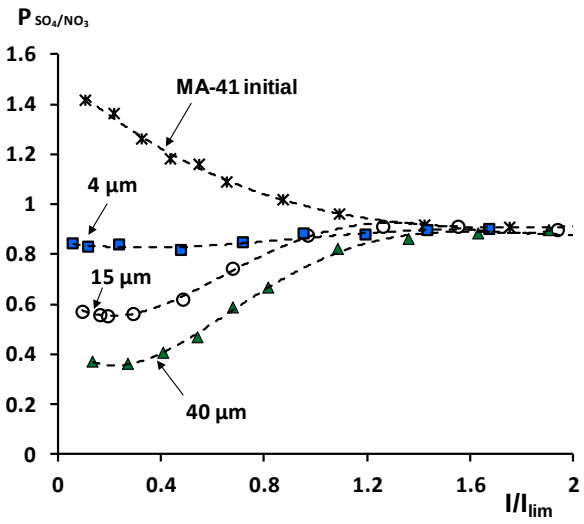

Figure 3 Dependence of the selectivity coefficients of the initial and modified membranes on the dimensionless density.

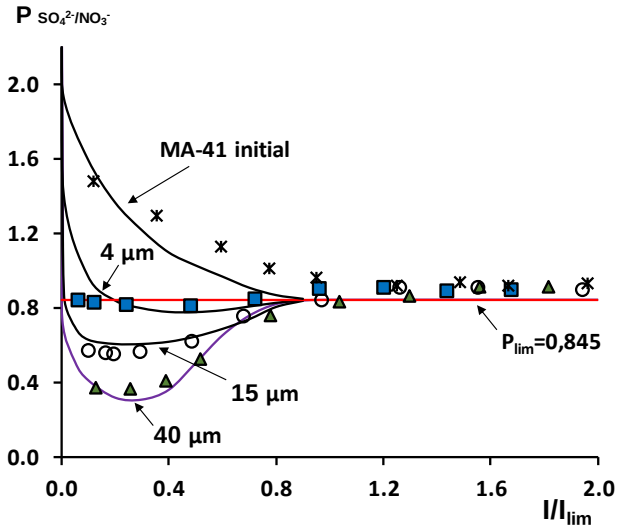

Figure 4. Dependence of membrane selectivity coefficients on dimensionless current: line - calculation by model, markers - experimental data.

A comparison of numerical calculations with experimental data shows that the effect of electrodiffusion of singly charged Co-ions through a modifying layer and, as a result, through a two-layer membrane increases with increasing thickness of the modifying layer. Numerical calculations also qualitatively describe the experimental data. The discrepancy at low currents is not particularly surprising since the real object does not correspond to what is incorporated in the model [3]. In the model, the thickness is close to zero on a real object it is quite concrete.

Acknowledgement

This research was financially supported by Russian Foundation of Basic Research project № 18-38-00773 mol_a.

References

1. *Mulyati, S., Takagi R., Fujii A., Ohmukai Y., Matsuyama H.* // J. Membr. Sci. 2013. V. 431., P. 113.
2. *Luo T., Abdu S., Wessling M.//* J. Membr. Sci. 2018. V. 555., P. 429.
3. *Achoh A.R., Zabolotsky V.I., Melnikov S.S., Lebedev K.A.//* International Conference Proceedings "Ion transport in organic and inorganic membranes" 21 – 26 May Krasnodar 2018. P. 23 – 25.

SEM-DIAGNOSTICS OF CHANGES IN THE MICROSTRUCTURE OF THE HETEROGENEOUS ANION-EXCHANGE MEMBRANE MA-40 AFTER ELECTRODIALYSIS REVERSAL OF MINERALIZED NATURAL WATER

Elmara Akberova, Vera Vasil'eva, Elena Goleva, Denis Kostylev
Voronezh State University, Voronezh, Russia, E-mail: *elmara_09@inbox.ru*

Introduction

The operational efficiency of electromembrane water treatment systems is limited mainly by a decrease in the electrochemical activity of membranes under the influence of polarization and temperature effects, as well as precipitation. The purpose of this work is to study the changes in the structural properties of the anion-exchange membrane MA-40 during long-term operation in an electrodialysis apparatus during desalination of mineralized natural waters.

Experiments

It was studied a sample of MA-40 membrane from the anode chamber of the reverse electrodialysis unit after its 1000-h operation during desalination of the natural waters of the Aral region. The treated water was with a high value of hardness and a high content of chlorides and sulfates [1]. Membrane samples after electrodialysis of natural waters were provided by LLP «Membrane Technologies, S.A.», Almaty, Kazakhstan Republic.

Results and Discussion

The SEM images of the sides of the MA-40 membrane surface facing the electrode (side *1*) and adjacent (side *2*) sections of the electrodialyzer are shown in fig. 1. On both sides of the membrane surface, the formation of a precipitate is visualized, which is localized not only on areas with good electrical conductivity, where the ion exchanger particles are located, and covers almost the entire surface with a film.

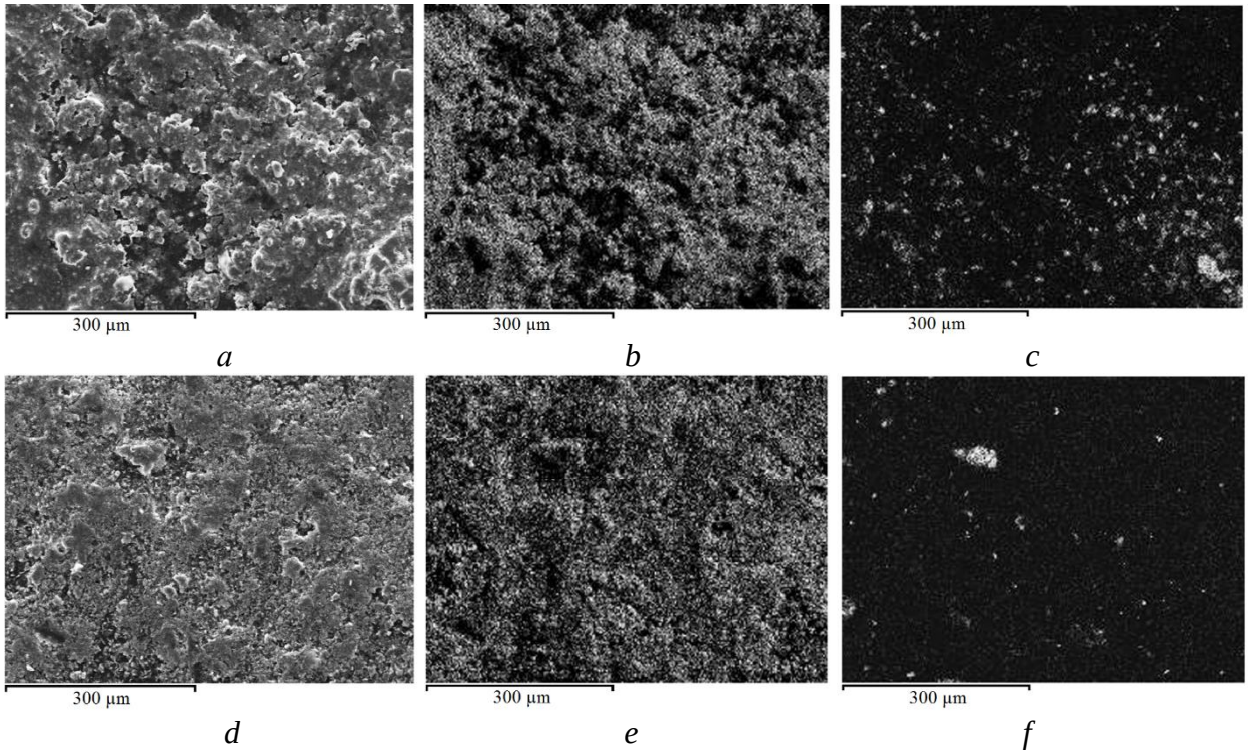

Figure 1. The SEM image (a, d) and the corresponding distribution maps of Mg (b, e) and Ca (c, f) on the side 1 (a-c) and 2 (d-f) of the surface of dry samples of MA-40 membrane from a reversal electrodialysis apparatus. The distribution of the elements is indicated in white.

The nature of the precipitate on the ion-exchange membrane depends on the pH value and the rate of ion migration through the membrane. The distribution maps of the elements (Fig. 1) and

the results of X-ray microanalysis of the composition of the sediment on the surface revealed the preferential Mg content and the presence of the Ca, Fe, and Si elements.

Under reversing of the electrodialysis electrode polarity, the functions of its electrode and working chambers simultaneously change. The electrode section alternately becomes either anodic or cathodic. Schemes of the precipitate formation by different mechanisms during the operation of the electrodialysis reversal are shown in Fig. 2.

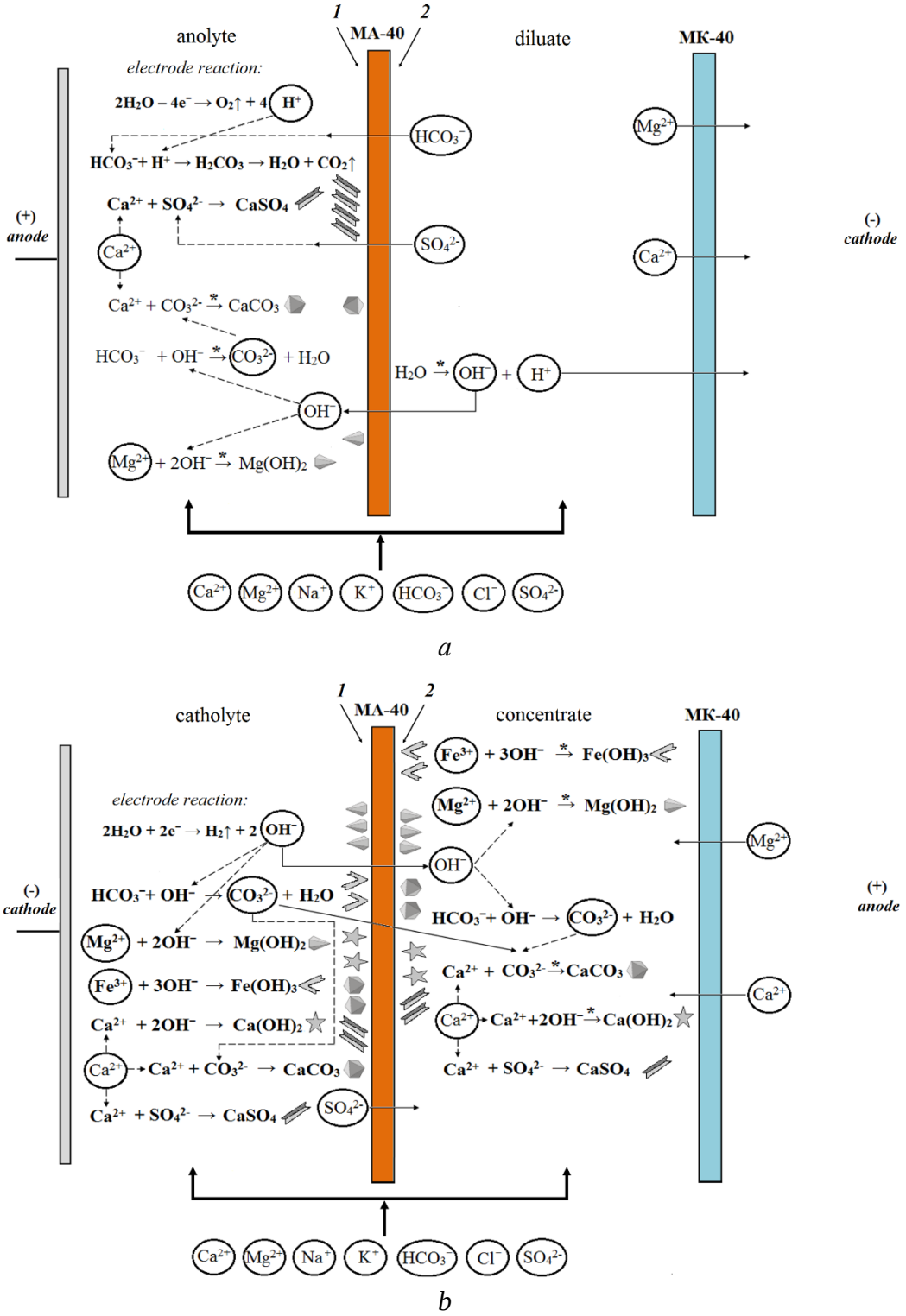

*Figure 2. The general scheme of the precipitate formation during operation of the electrodialyzer in the modes of direct (a) and reverse (b) current. * - reactions occurring at the solution – membrane interface. The numbers 1 and 2 show the designation of the membrane sides.*

It should be noted that the MA-40 membrane is characterized by a high catalytic activity of ionic groups in the heterolytic reaction of the water dissociation in solution at the interface. In case of accidental incorrect of the current mode or excess of the local limiting current density in the desalination section near the surface (side *2*) of the anion-exchange membrane, hydroxyl ions are formed, which migrate to the electrode section (Fig. 2a). On the one hand, the transfer of hydroxyl ions through the membrane can shift the balance of weakly acidic anions. For example, with a local increase in pH in the solution at the interface and in the membrane pore space, the balance shifts towards the formation of carbonate ions, which leads to the precipitation of carbonates. On the other hand, the migration of hydroxyl ions through an anion-exchange membrane can lead to the precipitation of hydroxides of multiply charged cations due to a local increase in the pH of the solution near the membrane.

When the polarity of the electrodes changes, the probability of hydroxide precipitation on the surface facing the electrode (side *1*) of MA-40 membrane increases significantly, which is a consequence of an increase pH in the diluate solution due to the electrode reaction (Fig. 2b). In this case, alkalization of the solution also occurs at the surface membrane (side *2*) facing the adjacent section of concentrating. The elemental composition of the surface corresponds to $Mg(OH)_2$ crystals, the quantitative content of which is predominant on both sides of the membrane surface. A significant increase in the pH of the treated water is accompanied by precipitation of poorly soluble calcium carbonate. The presence of iron ions in the composition of the precipitates on the surface of the investigated membrane MA-40 according to the results of X-ray microanalysis indicates the formation of a dense stable precipitate of iron hydroxide.

It was found that sedimentation occurs not only on the membrane surface but also in its bulk. The precipitation is promoted by an increase in the pH of the internal pore solution due to the migration of hydroxyl ions into the membrane phase. Comparison of data on the elemental composition of the cross section and the distribution map of the elements allows us to conclude about the different content and different localization of sediment over the cross sectional area of the MA-40 membrane. If insoluble compounds with Mg are predominantly formed on the membrane surface, the formation of a mixture of $CaCO_3$ and $Ca(OH)_2$ is established on both sides of the membrane phase.

Acknowledgements

The work is supported by the grant of the President of the Russian Federation MK-925.2018.3.

Microphotographs of the membrane surface and cross-section were obtained on the equipment of the Collective Use Center of Voronezh State University. URL: http://ckp.vsu.ru.

References

1. *Vasil'eva V.I., Akberova E.M., Goleva E.A., Yatsev A.M., Tzkhai A.A.* // Journal of Surface Investigation: X-ray, Synchrotron and Neutron Techniques. 2017. V. 11. No. 2. P. 429-436.

NOVEL NITRATE SELECTIVE ANION-EXCHANGE MEMBRANES: SYNTHESIS AND TESTS DIALYSIS

[1]Rihab Belhadj Ammar, [1]Takoua Ounissi, [2]Lasâad Dammak, [1]Emna Selmane Bel Hadj Hmida

[1]Laboratoire de Chimie Analytique et d'Électrochimie, Département de chimie, Faculté des Sciences de Tunis, Campus Universitaire, 2092 Tunis El Manar, Tunisie

[2]Institut de Chimie et des Matériaux Paris-Est (ICMPE), UMR 7182 CNRS, Université Paris-Est, 2 Rue Henri Dunant, 94320 Thiais, France

Introduction

The methemoglobinemia, the formation of nitrosamines as well as the eutrophication are the most important consequences of the presence of the nitrate ions in a higher amount than the norm defined by OMS in drinkable water, medical products, agriculture and food processing effluents. Eliminating the chemical species has become a major stake against these risks. Because of this, many biologic and physico-chemical procedures were applied for treating these ions [1]. The aim of this study is the synthesis of novel anionic exchange membranes based on polyepichlorhydrin (PECH) quaternized by 1,4-diazabicyclo- [2,2,2]-octane (DABCO) which shows a highly performance in fuel cells and electrodialysis [2].

Experiments

The originality of this work is the incorporation of a nitrate selective complexing (NC) in the PECH/DABCO matrix. Morphological and thermal properties of these membranes were determined. The water uptake, exchange capacities, conductivities and transport number of these membranes were also measured. Dialysis tests were carried out using our novel membranes by a diffusion cell.

Results and Discussion

Different compositions were tested with varying the PECH-DABCO / Complexing agent (See Table 1). We tried to fabricate a membrane with 30% $^{wt.}$ of the complexing agent, but unfortunately the obtained membranes crumble and are nonhomogeneous.

The characterization of Membranes M1-M3 shows that the surface of our membranes is homogenous and they are thermally stables.

Table 1: Main characteristics of membranes used in the experiments

Membrane (composition in %wt.)	Water Uptake (%)	Exchange Capacity (meq.g^{-1})	Conductivity (mS.cm^{-1})
M1: PECH/DABCO ; NC (90; 10)	12.05	0.67	2.03
M2: PECH/DABCO ; NC (85; 15)	17.28	0.69	3.52
M3: PECH/DABCO ; NC (80; 20)	11.11	0.62	2.61

The performance of these composite membranes was tested in diffusion dialysis of binary solutions containing a mixture of nitrates and interferant ions. We observed a remarkable selectivity for NO_3^- which we attribute to the effect of the complexing agent. The evaluation of the efficiency of eliminating these ions is maintained by the variation of a quantity known as the removal rate as a function of certain parameters such as dialysis duration, the initial concentration of the solution and coexistences ions.

References

1. *Kikhavani T., Ashrafizadeh S. N., Van der Bruggen B.* Nitrate selectivity and transport properties of a novel anion exchange membrane in electrodialysis // Electrochim. Acta. 2014. V. 144. P. 341-351.
2. *Hmida E. S. B. H., Ouejhani A., Lalléve G., Fauvarque J. F., Dachraoui M.* A novel anionic electrodialysis membrane can be used to remove nitrate and nitrite from wastewater // Desalin. Water Treat. 2010. V. 23. P. 13-19.

CORRELATION BETWEEN POLYANILINE SYNTHESIS CONDITIONS INTO MK-40 MEMBRANE AND CURRENT-VOLTAGE CURVES OF COMPOSITES

Marina Andreeva, Natalia Kutenko, Natalia Loza
Kuban State University, Krasnodar, Russia, E-mail: *andreeva_marina_90@bk.ru*

Introduction

Nowadays the development of ion-exchange membranes selective to the singly charged ions is one of the interesting challenges in membrane electrochemistry [1]. Selective extraction of ions has many applications [2]. It is reported that polymerization of polyaniline (PANI) on the cation-exchange membrane (CEM) surface results in the appearance of permselectivity towards the transfer of singly charged ions [1]. The properties of composites are significantly influenced by the content and structural organization of PANI in the membrane phase. Thus, the aim of this work is to study the polarization behavior of anisotropic composites based on heterogeneous CEM and PANI depending on the amount of injected PANI.

Experiments

The base CEM used for modification was heterogeneous MK-40 membrane. The MK-40/PANI membranes were obtained under the conditions of electrodiffusion of monomer and oxidant in 4-chamber electrodialysis cell [3]. A 0.01 M aniline solution in 0.05 M HCl and 0.002 M $K_2Cr_2O_7$ in 0.05 M HCl were fed into the cell chambers next to the test membrane on the anode and cathode sides, respectively. A 0.05 M HCl solution was circulated through the electrode chambers. Polymerization of PANI was carried out by passing different current density i = 20, 30, 40 and 50 mA/cm^2. Polymerization time was 60 min. The membrane area was 7.1 cm^2. PANI layer on the MK-40 membrane surface was formed on the side of concentration chamber. The measurements of I-V curves of obtained membranes were made in the same cell for the membrane modification. Cyclic voltammetry was carried out at a scan rate of $1*10^{-4}$ A/s. All chambers were pumped with 0.05 M HCl solution at a flow rate of 14 ml/min.

Results and Discussion

I-V curves of obtained composite MK-40/PANI membranes are measured for both membrane orientations: modified and non-modified surface layers are placed towards the desalination chamber (Fig. 1). The values of limiting current density, slope of ohmic and plateau regions are determined. The specificity of such type of membranes is in formation of an internal bipolar boundary between the cation- and anion-exchange layers. Pristine MK-40 membrane is selective to the transfer of positively charged ions, PANI has anion-exchange properties. So, these membranes can be like bipolar membrane in the electric field.

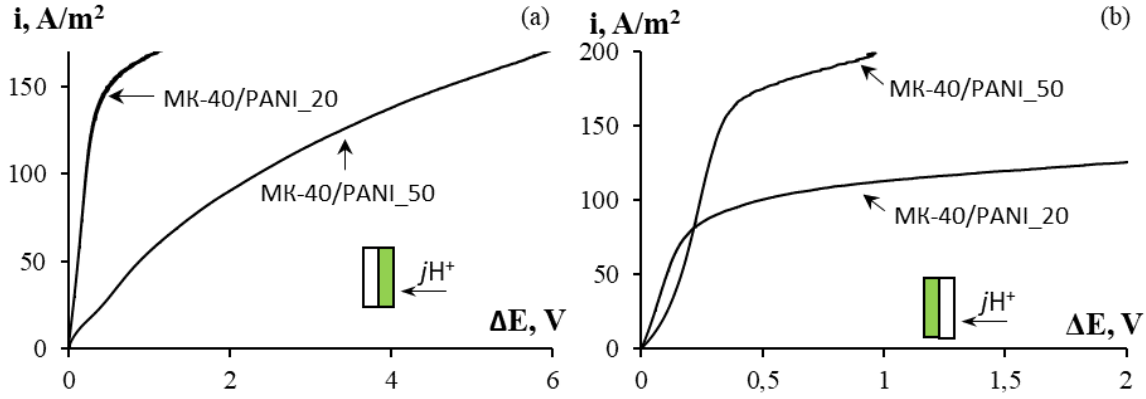

Figure 1. I-V curves of membranes synthesized at 20 (MK-40/PANI_20) and 50 (MK-40/PANI_50) mA/cm^2: modified (a) and non-modified (b) surface layer are placed towards desalination chamber.

Asymmetric I-V characteristics are observed for all composites. The slope of the ohmic region and the conductivity of the membrane are higher for the case when non-modified surface layer is

placed towards the desalination chamber. The slope of the ohmic region on the I-V curve decreases with the rise of *i* during PANI synthesis due to the increase of membrane resistance.

The values of limiting current density, i_{lim}, and membrane potential at which the limiting state occurs increase for composites obtained at $i > 30$ mA/cm^2 in the case when non-modified surface layer is placed towards the desalination chamber. Also, a change in the shape of the ohmic region on I-V curve is observed for these composites. The increase in i_{lim} can be attributed to a range of factors. PANI chains generated on the gel-phase of ion-exchange resin block the flux of H^+ ions through the membrane/solution interface. It leads to a local increase in concentration of H^+ ion inside the membrane. As a result, an inverse diffusion occurs. It might be one cause of the limiting current increase. Another reason could be an increase in the concentration of current carriers in the depleted diffusion layer due to the co-ion flux. The more the macropores in the membrane and the more PANI on its surface, the more significant the effect.

Now consider the case when the modified side of the composite is oriented toward the desalination chamber. The increase of i_{lim} at the membrane/solution interface is observed for MK-40/PANI_20 membrane. Two local maxima on the derivative of I-V curve are appeared for composite membrane obtained at $i > 30$ mA/cm^2 (Fig. 2a). The first i_{lim} into the region of low membrane potential, called pseudo-limiting current, is due to the formation of depleted (in relation to mobile ions) layer at the bipolar junction within the membrane. The second one, which is higher than pseudo-limiting current and close to the i_{lim} of the non-modified membrane is due to saturation of the diffusion across the depleted diffusion layer in the solution. Similar effects are observed for MF-4SK membranes modified by PANI [3]. The bigger the current applied during the PANI synthesis, the more pronounced the pseudo-limiting current as shown in Fig. 2a. Consequently, internal bipolar junction in the composite membrane plays a major role.

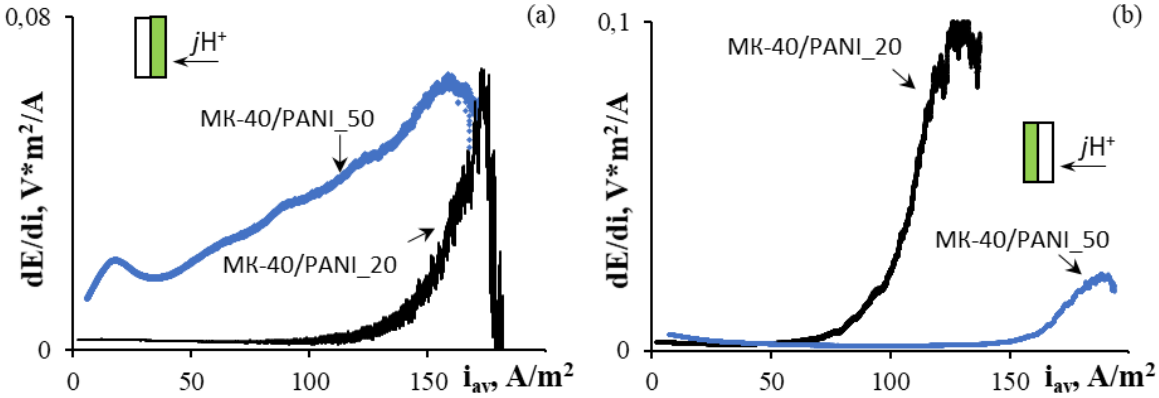

Figure 2. Derivative of I-V curve, dE/di vs i_{av}, for membranes synthesized at i=20 (MK-40/PANI_20) and 50 (MK-40/PANI _50) mA/cm^2: modified (a) and non-modified (b) surface layers are placed towards desalination chamber.

Thus, the analysis of I-V curves of the composite membranes allows us to find the conditions for obtaining materials with the most pronounced asymmetry effect of transport properties.

The present work is supported by the Russian Foundation for Basic Research (project № 18-38-20069 mol_a_ved).

References

1. *Luo T., Abdu S., Wessling M.* Selectivity of ion exchange membranes: A review // J. Membr. Sci. 2018. V. 555. P. 429-454.
2. *Ge L., Wu B., Yu D., Mondal A. N., Hou L., Ul Afsar N., Li Q., Xu T., Miao J., Xu T.* Monovalent cation perm-selective membranes (MCPMs): New developments and perspectives // Chinese J. Chem. Eng. 2017. V. 25. P. 1606-1615.
3. *Loza N. V., Dolgopolov S. V., Kononenko N. A., Andreeva M. A., Korshikova Yu. S.* Effect of surface modification of perfluorinated membranes with polyaniline on their polarization behavior // Russ. J. Electrochem. 2015. V. 51. P. 538-545.

INFLUENCE OF POLYMERIZATION TIME DURING POLYANILINE SYNTHESIS INTO MF-4SK MEMBRANE ON CURRENT-VOLTAGE CURVES OF OBTAINED COMPOSITES

[1]Marina Andreeva, [1]Natalia Loza, [1]Natalia Kononenko, [2]Sergej Timofeev
[1]Kuban State University, Krasnodar, Russia, E-mail: *andreeva_marina_90@bk.ru*
[2]Plastpolymer OJSC, St. Petersburg, Russia

Introduction

Enhancing the effectiveness of the electrodialysis is currently achieved by modification of ion-exchange membranes [1, 2]. Characteristics of these new membranes depend heavily on the modifier quantity. Polyaniline (PANI) is one of the perspective modifying agents [1]. The possibility of controlling the process of PANI layer formation on the membrane surface in external electric field by means of chronopotentiometry is shown in previous studies [3]. However, the polarization behavior of these composites has not been analyzed. Therefore, the purpose of the study is to investigate the impact of the modifier on the I-V curve and estimate the asymmetry effect of obtained membranes.

Experiments

Homogeneous perfluorinated membrane was used as the cation exchange membrane for modification. Polymerization of aniline on the surface of the base membrane was carried out in a four-compartment cell. Membrane orientation is presented in Fig. 1. Constant current density supplied to the polarizing electrodes (Fig. 1, No. 1) was 20 mA/cm^2. The membrane area was 7.1 cm^2. Polymerization time was varied from 5 to 60 min. The modified surface layer of the composite membrane was formed on the concentration compartment side. Ten composites were obtained. Registration of I-V curve of composite membranes were made in the same experimental set-up for the membrane modification (Fig. 1). The difference is that a solution of 0.05 M HCl was pumped through all the compartments (Fig. 1, No. 2-4) at a flow rate of 14 ml/min. I-V curves of pristine as well as composite membranes were carried out at a scan rate 1*10^{-4} A/s. Membrane potential was measured using Ag/AgCl electrodes inserted into Luggin-Haber capillaries (Fig. 1, No. 6).

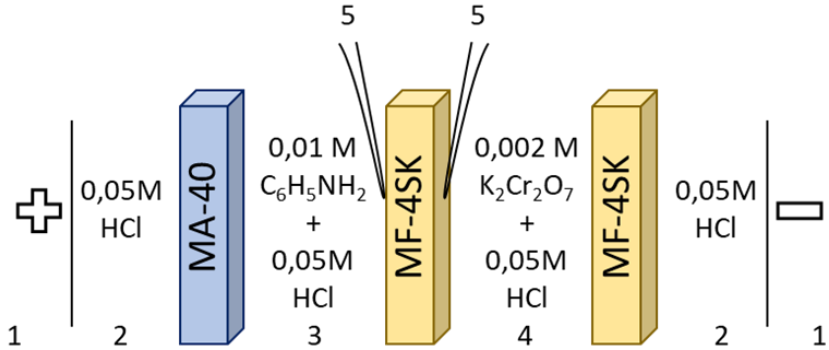

Figure 1. Scheme of four-compartment cell: 1 – polarizing electrodes; 2 – electrode compartments; 3 – desalination compartment; 4 – concentration compartment; 5 – Luggin-Haber capillaries.

Results and Discussion

Representative I-V curves of the pristine MF-4SK membrane and composite membranes modified for 30 and 60 min, respectively, are shown in Fig. 2. The first membrane orientation when the unmodified membrane surface layer was placed towards the desalination compartment is presented in Fig. 2a. The second case when the modified membrane surface layer was placed towards the desalination compartment is presented in Fig. 2b. An analysis of I-V curves has been made. It is found that the introduction of PANI into the near-surface layer of the pristine MF-4SK membrane leads to a decrease in the limiting current. Also, it is shown that the increase of

polymerization time results in membrane resistance growth, complemented by reduction of the slope of the ohmic region.

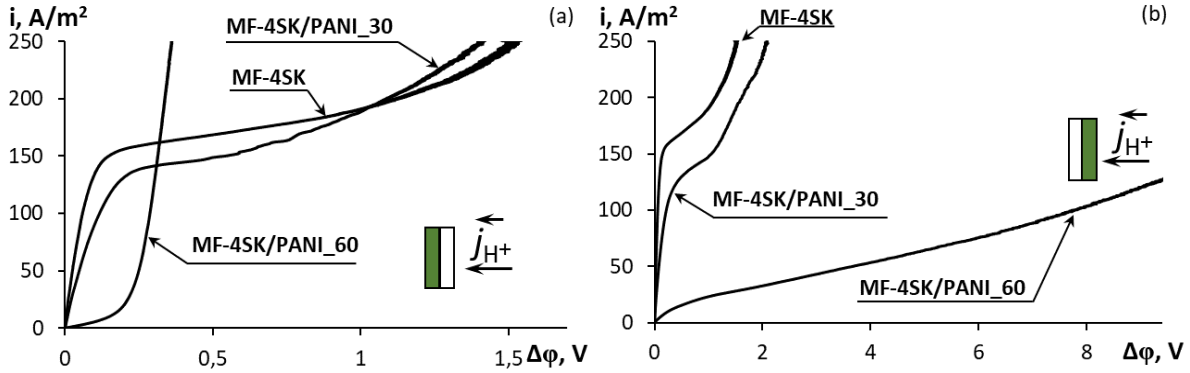

Figure 2. I-V curves of pristine MF-4SK membrane and membranes synthesized during 30 (MF-4SK/PANI_30) and 60 (MF-4SK/PANI_60) min: unmodified (a) and modified (b) surface layer was placed towards the desalination compartment.

The asymmetry of I-V curves of obtained composites has been established. It is found that the longer the polymerization time, the greater the asymmetry effect. The higher values of limiting current, slope of the ohmic region, plateau length are observed in the case when the unmodified membrane surface layer is placed towards the desalination compartment compared with reverse orientation.

I-V curves for both membrane orientations are considered abnormal for the composites obtained during polymerization time more than 30 min. There is no «plateau» region on the I-V curve when the unmodified membrane surface layer is placed towards the desalination compartment. However, oscillations of membrane potential typical for over-limiting region are observed at low current densities above 10 A/m^2. Two local maxima on the differential I-V curve are found when the modified membrane surface layer is placed towards the desalination compartment. The first maximum in the region of low membrane potentials is associated with depletion of the bipolar boundary inside the composite membrane formed by PANI and pristine membrane. The second maximum corresponds to the depletion of the membrane/solution interface, as in the case of a monopolar membrane. However, this limiting current is significantly lower compared with the pristine membrane. Similar results were obtained in [4]. The paper studies I-V curves of composite membranes obtained at different current densities.

Thus, the polarization behavior of obtained composites was studied. We can make a conclusion that the introduction of PANI into the near-surface layer of the pristine MF-4SK membrane leads to reduction of characteristic points on the I-V curve. An increase of the polymerization time also results in more pronounced asymmetric I-V curves.

Acknowledgments

The present work is supported by the Russian Foundation for Basic Research (project № 18-08-00771 A).

References

1. *Ran J., Wu L., He Y., Yang Z., Wang Y., Jiang C., Ge L., Bakangura E., Xu T.* Ion exchange membranes: new developments and applications // J. Membr. Sci. 2017. V. 522. P. 267-291.
2. *Luo T., Abdu S., Wessling M.* Selectivity of ion exchange membranes: A review // J. Membr. Sci. 2018. V. 555. P. 429-454.
3. *Andreeva M., Kutenko N., Loza N., Kononenko N.* Oxidative polymerization of aniline on MF-4SK membrane surface under external electric field by chronopotentiometry // Ion transport in organic and inorganic membranes. Intern. Conf. Proc. 2018. P. 36-38.
4. *Loza N. V., Dolgopolov S. V., Kononenko N. A., Andreeva M. A., Korshikova Yu. S.* Effect of surface modification of perfluorinated membranes with polyaniline on their polarization behavior // Russ. J. Electrochem. 2015. V. 51. P. 538-545.

MULTIELECTRON OXIDIZER REDOX-MEDIATED AUTOCATALYSIS FOR HYDROGEN-BROMATE REDOX FLOW BATTERIES

[1,2,3] *Anatoly Antipov, [1-4,] ** Mikhail Vorotyntsev

[1]D. I. Mendeleev University of Chemical Technology of Russia, Moscow, Russia
[2]M. V. Lomonosov Moscow State University, Moscow, Russia
[3]Institute of Problems of Chemical Physics, Russian Academy of Sciences, Chernogolovka, Russia
[4]ICMUB, UMR 6302 CNRS-Université de Bourgogne, Dijon, France
*e-mail: *89636941963antipov@gmail.com*, **e-mail: *mivo2010@yandex.com*

Currently, the prerequisites for the transition to a decentralized (distributed) energy model have been formed on the territory of the Russian Federation. Such a model offers efficient accumulation and storage of electricity within the local power grid in the vicinity of a potential consumer, which significantly reduces the need in high-power transmission lines usage. A promising solution to the electricity accumulation and storaging problem in distributed networks is the use of redox flow batteries (RFB). These systems are structurally divided into two parts: (a) a membrane electrode assembly (MEA) and (b) a system of tanks for liquid reagent storage. Such a separation provides the ability to independently scale the system power density (by increasing the area of the MEA electrodes) and energy capacity (by increasing the volume of reagent tanks), which gives the RFB an important advantage in stationary power storage applications.

Modern studies of the RFB, in particular, this study, are primarily aimed to overcome two fundamental barriers that significantly hinder the development of this direction: (a) insufficient specific power due to small values of standard exchange currents for the RFB heterogeneous redox reactions and (b) low energy density compared with other chemical energy sources due to insufficient energy capacity of the reagents per volume or mass unit for a known value of the redox potential.

The progress in creation of hybrid redox flow batteries, in particular, hydrogen-bromine batteries, implementing an oxidation reaction of hydrogen at the anode and the reduction reaction of molecular bromine at the cathode, made a significant contribution to overcome the first of the above barriers: led to an increase in specific power density for such devices.

However, the problem of insufficient energy density in modern RFB has not yet been solved.

An opportunity to handle this problem is to use salts of bromine oxoacids as new multielectron aqueous oxidizers. As a promising example one can point out lithium bromate or (significantly cheaper sodium bromate) aqueous solutions, that give outstanding theoretical estimates for the voluminous charge and energy densities of the cathodic process, eg. 1400 A h / L and 2000 W h / L at 25 °C while 1600 A h / L and 2300 W h / L at 60 °C [1], since the density of the saturated $LiBrO_3$ solution is about 1.8 g/cm^3 [2].

Nevertheless, all these attractive features of the bromate anion as an oxidant for the cathode are counterbalanced by the lack of its electroactivity within the potential range positive with respect to the hydrogen electrode, for all tested electrode materials including noble metals. Such an inconsolable situation has drastically changed after the recent proposition of new electrochemical redox-mediated autocatalysis EC" mechanism, that theoretically justifies the bromate electroreduction process to be performed in acidic media in the presence of trace amount of bromine, that serves as a mediating redox agent, implementing the ***autocatalytical*** features for such a system [1,3].

The present study offers a wide extension of the promising concepts above, both offers a variety of analytical models and an experimental verification of the fact that the problem of bromate anions insufficient electrochemical activity can be solved by redox mediator autocatalysis (EC" mechanism). The main fundamental purpose of this study is to develop theoretical foundations and to create an integrated methodology (combining analytical, numerical and experimental methods) that establishes the relationship between the mass transfer processes of the main reagents and characteristics of a hydrogen-bromate redox flow battery, based on the new mediated redox autocatalytic mechanism that allows one to use perspective multielectron aqueous solutions as oxidizers.

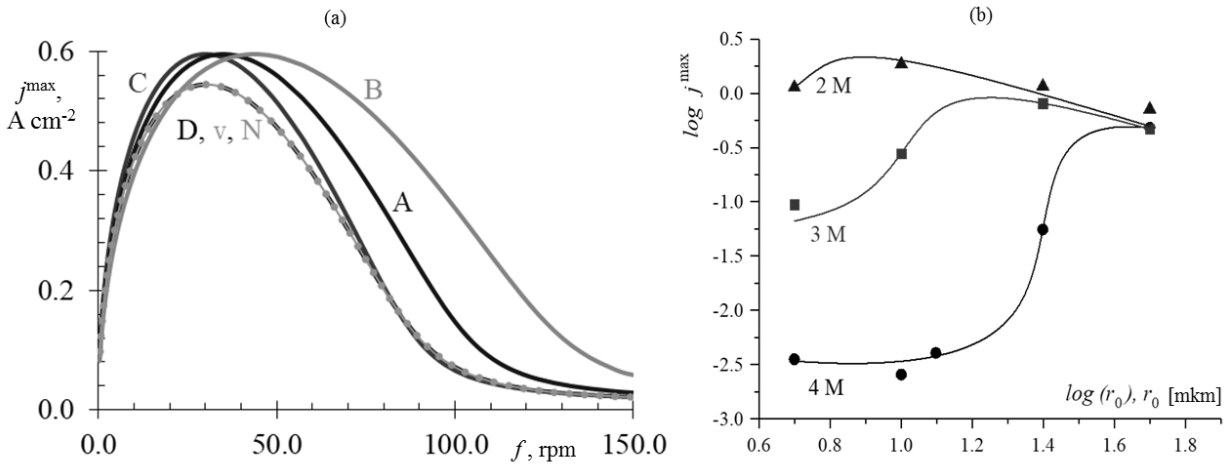

Figure 1. (a) An example of the non-monotonic dependence of the maximum cathodic current density j^{max} in A · cm^{-2} on the the intensity of convection mixing, governed by the rotating disc electrode (RDE) frequency in rpm. The A, B, C curves correspond to the Nernst stagnant layer model, D curve responds to the Generalized Nernst layer model, V curve and N set of points match the convective-diffusion model analytical and numerical solutions, correspondingly [1]. (b) An example of the non-monotonic dependence of the maximum cathodic current density j^{max} in A · cm^{-2} on the magnitude of the microelectrode radius r_0 in bilogarithmic coordinates. For three different concentrations of acid the set of points corresponds to the experimental data, solid lines represent predictions of the analytical theory.

The main fundamental conclusions of the study are:

- The process of bromate anions electroreduction in an acidic media (the concentration of bromate anion and acid is about mol / L) in the presence of a trace amount of molecular bromine (the concentration about mmol / L) shows a significant value of the specific cathodic current density (of the order of A · cm^{-2}) achievable in spite of the the lack of bromate electroactivity at the electrode surface but due to autocatalytic effects of the system. Such features are demonstrated both for a variety of model systems with controlled hydrodynamics (rotating disc electrode, microelectrode), and for real prototype of a hydrogen-bromate redox flow battery.

- For the case of rotating disk electrode in stationary conditions the presence of the nonmonotonic dependence predicted in the framework of the analytical theory, in particular, the area of sharp rapid ***increase*** for the cathodic current density (by several orders of magnitude) while the intensity of convection mixing ***decreases***, has been proved both experimentally and using numerical simulation methods.

- For the case of a disk microelectrode the mentioned above non-monotonic behavior, in particular, a sharp ***increase*** in cathode current density while the radius of the electrode ***decreases*** has been predicted analytically and confirmed experimentally.

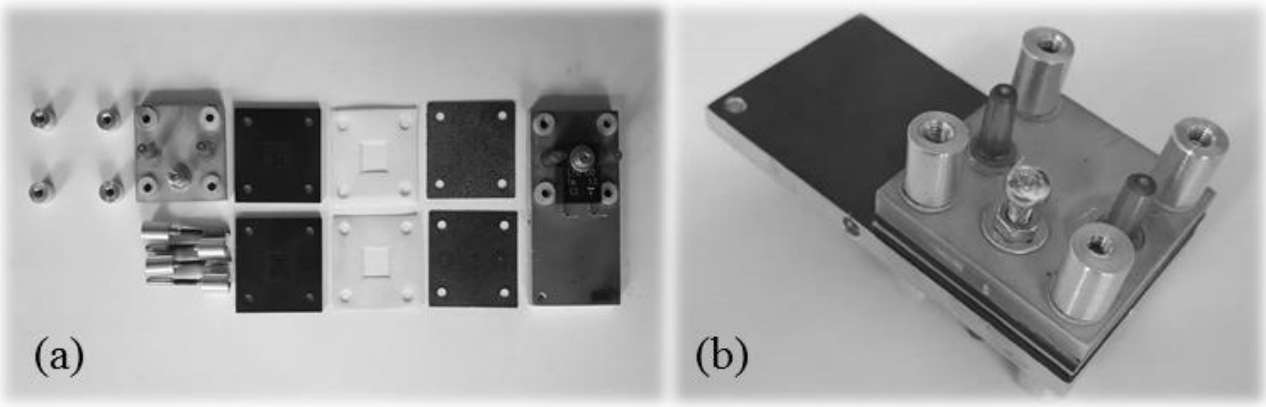

Figure 2. Experimental sample of a hydrogen-bromate redox flow battery membrane-electrode assembly: (a) disassemled and (b) assembled.

The applied objective of the present work is to implement the hybrid principle of power sources design to create on the basis of the fuel cell and redox flow battery concepts a fundamentally new hybrid electrochemical generator that utilizes bromate anions as a multielectron aqueous oxidizer. Therefore an experimental sample of a hydrogen-bromate redox flow battery MEA, operating on the basis of the principles proposed in the study, has been shown to demonstrate high electrochemical performance of specific current density (up to $\boldsymbol{1.5\ A \cdot cm^2}$) and power (up to $\boldsymbol{0.9\ W \cdot cm^2}$) [4].

Acknowledgements.

The reported study was funded by RFBR according to the research project № 18-03-00574.

References

1. *Vorotyntsev M. A., Antipov A. E., Konev D. V.* Bromate anion reduction: novel autocatalytic (EC″) mechanism of electrochemical processes. Its implication for redox flow batteries of high energy and power densities // Pure Appl. Chem. 2017. V. 89. P. 1429-1448.
2. *Bruno T. J., Lide D. R.* CRC Handbook of Chemistry and Physics, 97th ed., (W. M. Haynes, ed.). CRC Press, Boca Raton, FL, 2015.
3. *Vorotyntsev M. A., Konev D. V., Tolmachev Y. V.* Electroreduction of halogen oxoanions via autocatalytic redox mediation by halide anions: novel EC" mechanism. Theory for stationary 1D regime. Electrochim. Acta. 2015. Vol. 173. P. 779–795.
4. *Modestov A. D., Konev D. V., Antipov A. E., Tripachev O. V. et al.* A hydrogen–bromate flow battery for air- deficient environments // Energy Tech. 2017.Vol. 6. P. 242-245.

DEVELOPMENT OF MICROTUBULAR SOLID OXIDE FUEL CELLS

[1]Artem Bagishev, [1,2]Ivan Kovalev, [1]Mikhail Popov, [1]Alexander Nemudry
[1]Institute of Solid State Chemistry and Mechanochemistry SB RAS, Novosibirsk, Russia
E-mail: *popov@solid.nsc.ru*
[2]Novosibirsk State Technical University, Novosibirsk, Russia

Introduction

Alternative methods of power generation attract more attention in recent years. This interest is caused, from one side, by reduction of mineral fuels, from other - by economic efficiency of the innovative approaches in the production of electric power and strict ecological requirements for new technologies.

One of directions of alternative energy development are the high temperature electrochemical devices (ECD). Such devices allows to a) effectively (efficiency 60-70%) transform an organic fuel and hydrogen, in electric power with the use of solid-oxide fuel cells (SOFC) and b) process carbon dioxide and aquatic steam in a synthesis gas ($CO + 2H_2$), utilizing the extrass of greenhouse gases, effectively stocking energy of cheap energy sources, with the use of high temperature solid-oxide electrolyzers (SOE). As known, hydrogen is not only basis of ecofriendly hydrogen energy but also feedstock for the various hydroprocessing technologies, multi-tonnage production of ammonia and methanol and subsequent chemical products

Structurally SOE/SOFC can be divided into planar and tubular shape. A planar design is widely used in stationary devices, by power from a megawatt and higher, as provides good heat and mass transfer, compactness of assembling and allows to use the standard methods of ceramic treatment. The substantial lack of planar configuration is high requirements to absence of considerable temperature gradients along a membrane, that can result in device destruction during thermal cycling and dramatic changes of temperature. This results in a slow startup speed.

The problem can be solved using microtubular (mt) membranes [1-2], the advantages of which are improved thermal and mechanical stability, ease of sealing. The rapid launch of high-temperature ECD opens the possibility of developing a promising niche of compact, mobile devices in transport, in the military field and in household appliances.

Results and Discussion

This paper presents the results of measuring medium-temperature microtubular solid oxide fuel cell with cathode composition $SrCo_{1-x}Ta_xO_{3-\delta}$. As part of the work, the methodology for obtaining mt-SOFC was worked out. Functional layers were obtained by dip-coating. The results obtained suggest that cathode composition $SrCo_{1-x}Ta_xO_{3-\delta}$ is greatly promising for SOFC development.

Acknowledgements

The research was funded within the state assignment to ISSCM SB RAS (project No. AAAA-A17-117030310277-6).

References

1. *Mikhail P. Popov, Daniel V. Maslennikov, Igor I. Gainutdinov, Igor P. Gulyaev, Andrey N. Zagoruiko, Alexander P. Nemudry* // Catalysis Today, https://doi.org/10.1016/j.cattod.2018.11.009
2. *Mikhail P. Popov, Igor I. Gainutdinov, Sergey F. Bychkov, Alexander P. Nemudry*, New approaches for enhancement of oxygen fluxes on hollow fiber membranes // Materials Today: Proceedings 4 (2017) 11381–11384.

PROTON CONDUCTOR ELECTROLYTES BASED ON CESIUM DIHYDROGEN PHOSPHATE AND THERMALLY STABLE POLYMERS

[1,2]Irina Bagryantseva, [1,2]Valentina Ponomareva, [1,2] Anna Gaydamaka

[1]Institute of Solid State Chemistry and Mechanochemistry SB RAS, Novosibirsk, Russia

[2]Novosibirsk State University, Novosibirsk, Russia

E-mail: *ponomareva@solid.nsc.ru*

Introduction

The family of acid salts of alkali metals with the common formula $M_nH_m(AO_4)_p$ (A = P, S, Se) presents an important class of proton conductors with high proton conductivity ~10^{-2} S/cm in the medium temperature range 130-250°C due to the superprotonic phase. Among them CsH_2PO_4 and its composites undoubtedly have a great potential for use as a proton-conducting membrane in fuel cells (FCs) [1]. Recently, the systems based on CsH_2PO_4 and polymer additive have been intensively studied [2-4]. The thin-film flexible membranes are preferable for improving the electrochemical characteristics of FCs. Such systems combine high proton conductivity of the acid salt with the flexibility, hydrophobicity, mechanical stability and flexibility of the polymer. Mechanically strong membranes with the thickness less than100 μm can be obtained by the solvent casting technique. Due to the pure solubility of CsH_2PO_4 in common solvents such membranes are a physical dispersion of acid salt particles in the polymer matrix. For this purpose the fine salt particles should be obtained. The conductivity of CsH_2PO_4-based polymer systems is determined by the morphology and the nature of the distribution of salt particles in the volume of the membrane depending on the energy of adhesion similarly to the composites based on acid salts and highly dispersed inorganic oxide (SiO_2, TiO_2 etc.) [5].

Results and Discussion

This work is devoted to the investigation of the mechanism of formation of new high-conductive polymer membranes based on CsH_2PO_4 and thermally stable polymers of different composition such as fluoropolymers and butyral. The synthesis conditions were studied and optimized. The investigation of electrotransport, structural, thermal properties and the mechanism of proton conductivity of the polymer composites were carried out. The proton conductivity and changes in structural properties of «CsH_2PO_4-polymer» systems with varying polymer matrix were examined. The small content of the polymer results in the conductivity remaining at the level of the initial salt in the superionic phase. But the high polymer concentrations lead to the percolation threshold of the "conductor-insulator" type with the further decrease in the electrotransport characteristics. The different ways of particle size reduction was examined. The range of different water partial pressure on the proton conductivity was studied for the suppression of CsH_2PO_4 dehydration and extension of superionic phase stability. The changes of structural characteristics of the salt in the polymer matrices were studied by XRD. The addition of a polymer matrix results in a partial amorphization of the CsH_2PO_4. The particle size and its distribution in the volume of the membrane have been characterized by electron microscopy. The addition of appropriate amount of polymer matrix also provides the flexibility of the membrane, increasing of hydrolytic stability, sufficient mechanical strength and gas permeability while maintaining high proton conductivity.

This work was carried out with a partial financial support from RFBR grant 18-08-01279.

References

1. *Uda T., Haile S.M.* // Solid-State Lett. 2005. V.8. A245–A246.
2. *Qing G., Kikuchi R., Takagaki A., Sugawara T. et al.* // J. Electrochem. Soc. 2014. V.161. F451–F457.
3. *Qing G., Kikuchi R., Takagaki A. et al.*// Electrochim. Acta 169 (2015) 219–226.
4. *Oh S.-Y., Kawamura G., Muto H., Matsuda A.* // SSI 225 (2012) 223–227.
5. *Ponomareva V.G., Lavrova G.V., Simonova L.G.* // SSI 1999. V.118. P. 317-323.

NEW ION-EXCHANGE MATERIALS BASED ON COPOLYMERS OF DIVINYLSULFIDE

Victor Bayandin, Nina Shaglaeva
Irkutsk National Research Technical University, Russia, E-mail: *bayandinvv @yandex.ru*

Introduction

Ion exchange materials are widely used in water treatment, hydrometallurgy and other industries for the extraction of metals from diluted solutions, the separation of the individual components of the mixture and purification of waste water, etc. Ion exchange materials are widely used in water treatment, hydrometallurgy and other industries for the extraction of metals from diluted solutions, the separation of the individual components of the mixture and purification of waste water, etc. At the moment, as cross-linking agent in the synthesis of ion exchangers used divinylbenzene. The main drawback of these ion exchange resins is a multistage obtain divinylbenzene and the use of readily available starting materials.

In the Irkutsk scientific center developed a one-step synthesis technology divinylsulfide (DVS) reaction of acetylene with hydrogen sulfide or sodium sulfide and effected its production of pilot batches [1]. The main advantage of this method of obtaining divinylsulfide is the availability and low cost of raw materials.

Experiments

Insoluble copolymers were obtained by radical copolymerization of divinylsulfide with 4-vinylpyridine (VP), which are yellow powders and have high mechanical strength and osmotic stability, resistant to salts, dilute acids and alkalis (boiling samples for 6 hours in 10% saline, sulfuric, nitric acid and sodium hydroxide does not cause the destruction of the framework). Copolymers swell well in organic solvents: in acetone - by 500%, in hexane - by 300%. The swelling capacity of copolymers in an aqueous solution of acid and alkali is much lower and amounts to 100% and 60%, respectively. Table 1 presents the results of copolymerization DVS-VP.

Table 1: Copolymerization DVS and VP

NO EXPERIMENT	THE COMPOSITION OF THE INITIAL MIXTURE, MOL. %		CONTENT NITROGEN AND SULFUR, MASS. %		THE COMPOSITION OF THE COPOLYMER, MOL. %		OUTPUT, %
	VP	DVS	N	S	VP	DVS	
1	**20.0**	**80.0**	**5.01**	**23.42**	**32.11**	**67.89**	**65**
2	**40.1**	**59.9**	**7.90**	**16.83**	**54.36**	**45.64**	**75**
3	**50.0**	**50.0**	**8.78**	**12.67**	**61.23**	**38.77**	**92**
4	**80.0**	**20.0**	**12.11**	**3.45**	**88.75**	**11.25**	**80**

Results and Discussion

The study of silver ion adsorption by the considered ICE-VP copolymer was carried out in solutions of nitric acid, where this metal is present in the form of the Ag + cation. Extraction of Pt, Pd and Au ions was studied in hydrochloric and sulfuric acid solutions, in which these metals exist in the form of acid complexes of different composition. For acid complexes Pt, Pd, Au, with an increase in the concentration of acids, there is a slight decrease in the degree of extraction of metal ions with the exception of the gold tetrachloride complex in a sulfate medium (Figure 1). To a greater extent, a decrease in the degree of extraction of metal ions is manifested for chlorine complexes of platinum and gold in a solution of hydrochloric acid (Figure 1).

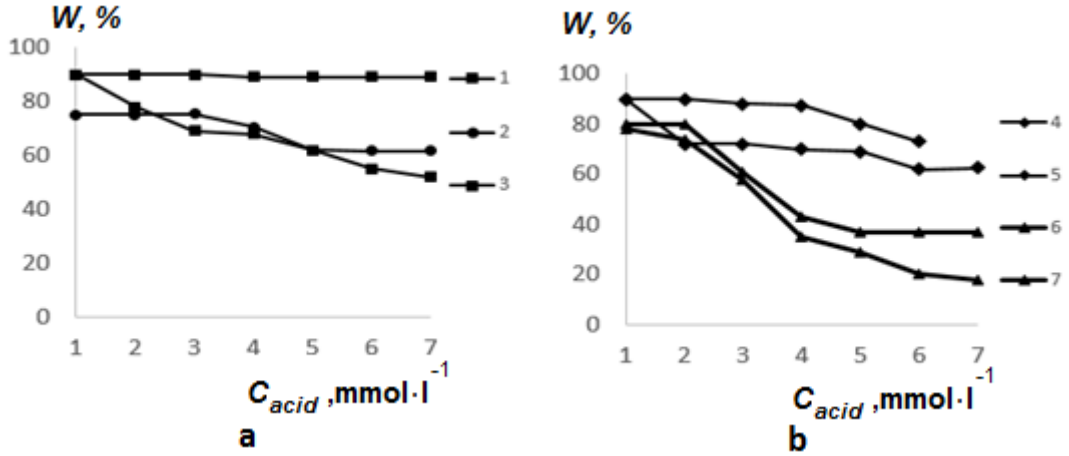

Figure1. Influence of the nature and concentration of acids on the degree of extraction of Au (III) ions in H_2SO_4 (1) and HCl (3), Ag (I) in HNO_3 (2), Pd (II) in H_2SO_4 (4) and HCl (5), Pt (IV) in H_2SO_4 (6) and HCl (7).

The given character of the dependence is in favor of the anion exchange at the pyridine nitrogen atom and the manifestation of the competing effect of acid anions, taking into account their size and mobility. Coordination interaction of metal ions by nitrogen and sulfur atoms is not excluded, which is more characteristic of the cationic form of silver.

Acknowledgments

The results reported in this communication were obtained under the State assignment from the Ministry of Education and Science of Russia no. 4.5867.2017/8.9. The study was supported by the RFBR (grant no. 19-08-00342).

References

1. *Trofimov B.A., Amosova S.V.* Divinyl sulfide. Patent Britich № 1369280. 1974. C.A. 1975. V.83. 27563.

MEMBRANE ABSORPTION OF ETHYLENE FROM HYDROCARBON GASEOUS MEDIA

[1]Stepan Bazhenov, [1]Margarita Kostyanaya, [1]Vladimir Vasilevsky, [2]Alexey Nikitin, [2]Igor Sedov, [1]Alexey Volkov

[1]A.V.Topchiev Institute of Petrochemical Synthesis (TIPS RAS), Moscow, Russia

E-mail: *sbazhenov@ips.ac.ru*

[2] Institute of Problems of Chemical Physics (IPCP RAS), Chernogolovka, Russia

Introduction

The method of the selective continuous single-stage membrane absorption process of olefins separation proposed in the work is based on a synergistic combination of membrane gas-separation process [1] and absorption capture of unsaturated hydrocarbons from gas mixtures [2]. In this case, absorption/desorption processes take place in a membrane gas-liquid module (contactor). This is an apparatus where the membrane acts as the interface between gas and liquid phases. Such a configuration of the module has the following advantages: the high specific surface area, compactness of the equipment, the independent control of gas and liquid flows [3]. Furthermore, the cyclic absorption/desorption process is carried out via well-defined phase interface provided by the membrane. Thus the mass transfer surface area is constant which leads to the fact that all equipment works with the same efficiency even if the process conditions or fluid characteristics change in a wide range. In addition, the absence of direct interaction of gas and liquid leads to low energy losses. There is no need to separate the two phases at the outlet of the apparatus, and there is no droplet entrainment and foaming of the liquid absorbent.

In the present work, it is proposed to carry out the process of ethylene separation from a model mixture with ethane using an aqueous solution of silver nitrate as an absorbent.

The driving force of the process is the difference in the partial pressure of ethylene from different sides of the membrane. High selectivity of ethylene separation is provided by its chemical interaction with the active component of the liquid absorbent. In contrast to conventional olefin distillation extraction at high pressures and low temperatures, this direct interaction also determines the single-stage nature of ethylene separation. The great advantage of this method is increased energy efficiency because in this case the leading role belongs to the reversible chemical interaction between the ethylene and the silver ions in the liquid absorbent, which occurs at room temperatures (above 0°C) and relatively low pressures.

Experiments

Figure 1 shows the principle of a highly selective continuous single-stage membrane-absorption process for the separation of olefins from hydrocarbon gas media.

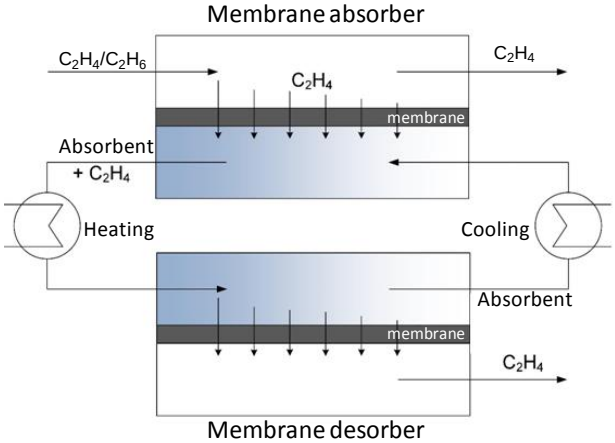

Figure 1. Principle of selective continuous single-stage membrane-absorption process for the separation of olefins from hydrocarbon gas media.

The main working elements of the process are membrane modules operating in absorption and desorption mode. In the present work, the attention is focused on the absorption stage. Hydrocarbon with ethylene enters the membrane module operating in the absorption mode, where the ethylene penetrates through the membrane, then dissolves and interacts with the active component of the liquid absorbent (aqueous solution of transition metal - silver).

The membrane applied in this process should provide barrier properties toward the olefin absorbent. This is critically important since the penetration of liquid absorbent into the structure of the membrane and the filling of transport pores negatively affect the efficiency of the olefin mass transfer [4]. From this point of view, the composite membranes with a thin non-porous selective layer are the best choise. Following these considerations, we used commercial flat-sheet composite gas separation membrane MDK-3 (ZAO NTC Vladipor) with thin non-porous selective layer made from organosilicon polymer material.

Table 1 lists the parameters of the membrane module and the conditions of the absorption process.

Table 1: Data on hollow fiber membrane contactor and absorption conditions

Parameter	Value
Gas mixture	19% (C_2H_4) / 81% (C_2H_6)
Volume of gas mixture (mL)	400
Absorption temperature (˚C)	20
Type of membrane module	Flat-sheet
Surface area of membrane (cm^2)	189
Absorbent	3,5 M aqueous $AgNO_3$
Volume of absorbent (mL)	500
Gas linear velocity (cm/s)	1
Liquid linear velocity (cm/s)	0 - 4

Gas mixture composition during the experiments was analyzed using gas chromatograph Chromatec "Gazochrom-2000" which is equipped with a thermal conductivity detector. Gas chromatography parameters were as follows: detector temperature was 160 °C, column temperature was 50 °C. The sample volume was 0.5 mL.

Results and Discussion

Figure 2 shows the dependence of the decrease in the ethylene content in the closed gas loop with studied gas mixture during the experiment in the membrane absorber at different liquid linear velocities. The zero solvent velocity corresponds to the stagnant liquid layer within the liquid channel of the membrane module.

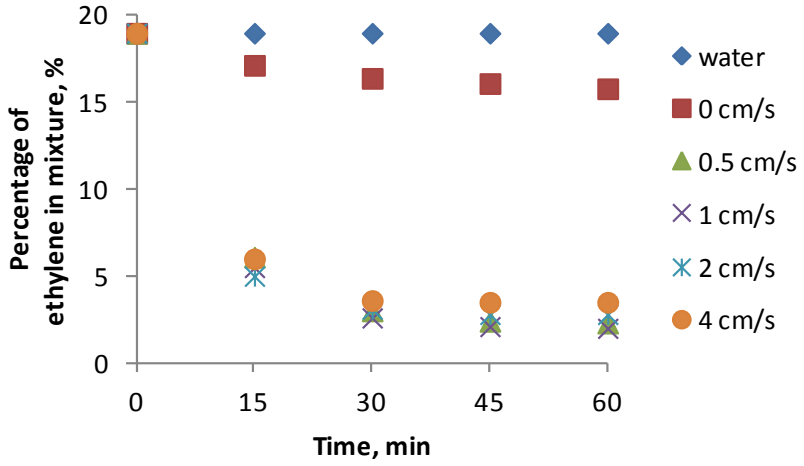

Figure 2. Ethylene content in the gas mixture vs. time of experiment.

The influence of the liquid absorbent linear velocity on the efficiency of the ethylene absorption process can be seen more clearly in Figure 3, where the final contents of ethylene within the closed gas loop with studied gas mixture after 1 h of experiment are presented.

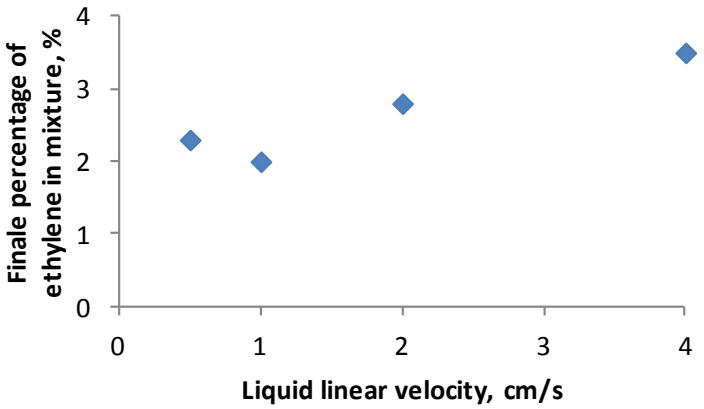

Figure 3. Ethylene content in the gas mixture after 1 h of absorption experiment vs. linear velocity of the liquid absorbent.

The ethylene absorption process is most efficient at the absorbent linear velocity of 1 cm/s. The achieved ethylene recovery is more than 90%.

Acknowledgments

This work was supported by the Ministry of Science and Higher education of the Russian Federation, project 14.607.21.0171 (unique project identifier RFMEFI60717X0171).

References

1. *Bessarabov D.G., Jacobs E.P., Sanderson R.D., Beckman I.N.* Use of nonporous polymeric flat-sheet gas-separation membranes in a membrane-liquid contactor: experimental studies // J. Membr. Sci. 1996. V. 113. P. 275-284.
2. *Keller G.E., Marcinkowsky A.E., Verma S.K., Williamson K.D.* Olefin Recovery and Purification via Silver Complexation // Separation and Purification Technology. 1992. V. 1.
3. *Roizard D.* Gas–Liquid Membrane Contactor. Encyclopedia of Membranes. 2016.
4. *Mosadegh-Sedghi S., Rodrigue D., Brisson J. Iliuta M.* // J. Membr. Sci. 2014. Vol. 452. P. 332-353.

GAS-LIQUID HOLLOW FIBER MEMBRANE CONTACTORS FOR CO_2 DESORPTION FROM MONOETHANOLAMINE SOLUTIONS

Stepan Bazhenov, Maryam Madumarova, Margarita Kostyanaya, Eduard Novitsky
A.V.Topchiev Institute of Petrochemical Synthesis (TIPS RAS), Moscow, Russia
E-mail: *sbazhenov@ips.ac.ru*

Introduction

Monoethanolamine (MEA) is the primary alkanolamine which is applied to achieve a high carbon dioxide (CO_2) recovery degree (80-99%) from gas streams. MEA provides fast CO_2 absorption kinetics, relatively high CO_2 sorption capacity and selectivity. The combination of MEA-based solvents with hollow fiber membranes in compact, low-weight and modular gas-liquid contactors is a perspective way to provide the CO_2 absorption [1]. At present, attempts are being made to optimize MEA-based solvents for their use in membrane contactors. The vast majority of works are devoted to membrane CO_2 absorption 30% wt. aqueous MEA. Some researchers propose to increase the MEA content up to 90%wt. [2], thus increasing the sorption capacity of the solvent. However, this approach seems to be unfavorable if the solvent regeneration (CO_2 desorption) is considered. Traditionally, the CO_2 desorption from MEA is carried out at temperatures of 110–140 ºC, which provide efficient desorption of CO_2, but lead to the thermochemical degradation of MEA, especially in the presence of dissolved unbound oxygen. A. Bello with coworkers [3] found out that the MEA degradation grows both with an increase in the desorption temperature and in the MEA content in the solvent. As a result, a wide range of products is formed: oxazolidone-2, MEA dimers and trimers, amides, amines, aldehydes, ammonia, carboxylic acids, etc. The latter form heat stable MEA salts (HSS) that stimulate corrosion of equipment and pipelines, catalyze further destruction of MEA [4], reduce CO_2 fluxes and mass transfer coefficients during CO_2 absorption in membrane contactors [5]. Alternative CO_2 solvents with higher stability (solutions of sterically hindered amines, ammonia, amino acid salts, ionic liquids [1]) are still less competitive compared to MEA because of their higher costs and other physicochemical properties.

In contrast to the above, our previous experimental results showed that the MEA desorption process can be effectively carried out at temperatures of 70-90°C in case of reduced MEA concentration in the solution (10-14%wt.) and increased CO_2-loading (0.55-0.7 mol CO_2/mol IEA) [6]. Thus the aim of present work is the development of hollow fiber membrane contactors for the desorption of CO_2 from the MEA solution with unconventional properties.

Experiments

1. Hollow fiber membranes

The porous asymmetric hollow fiber membranes made from polysulfone (PSf) was prepared according via dry-wet phase inversion technique described in details elsewhere [10]. The composite membranes with a thin protective layer from poly(trimethylsilyl)propyne (PTMSP) was fabricated according to the modified procedure developed earlier [7]: the impregnation step was avoided and the PTMSP casting solution was forced into the lumen side of the membranes from the both ends sequentially. The gas permeances of the CO_2, N_2 and He were evaluated using constant pressure/variable volume gas permeation method at 23±2°C.

2. Membrane contactor

The gas-liquid membrane contactors were prepared using both porous and composite membranes. The glass modules were used as shells. The ends of contactors were sealed with epoxy resin (EDP universal). The effective length of membranes was 18 cm. The number of membranes in porous contactor was 8, specific surface area – 454 m^2/m^3; the number of membranes in composite contactor was 3, specific surface area – 172 m^2/m^3.

3. CO_2 desorption experiment

CO_2 desorption experiment was carried out on the lab-scale set-up, which simplified scheme and overall view is presented in Figure 1.

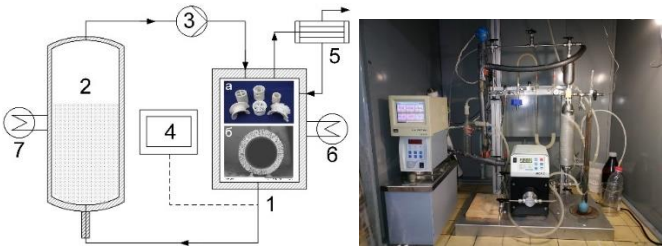

Figure 1. Lab-scale set-up for CO_2 desorption from MEA solution: 1- desorption unit (a - small stripping column with Rashig rings (∅6 mm); b - membrane gas-liquid contactor with hollow fibers); 2 - solvent tank with CO_2-rich MEA solution; 3- solvent gear pump; 4 - temperature control unit; 5 - condenser; 6 - heater (thermostate); 7- cooler (tap water).

Results and discussion

1. Porous hollow fiber membranes and contactor based on them

The properties of porous membranes are given in Table 1.

Table 1: Geometrical and transport properties of porous membranes

Inner diameter d_i, mm	1,16
Outer diameter d_o, mm	1,61
He permeance, m^3 (STP)/(m^2·h·bar)	350±20
N_2 permeance, m^3 (STP)/(m^2·h·bar)	150±5
CO_2 permeance, m^3 (STP)/(m^2·h·bar)	123±6
He/CO_2 ideal selectivity	2,8
CO_2/N_2 ideal selectivity	0,8

The porous membranes have a fine-porous structure (mesoporous level) of the inner skin layer. This is evidenced by the values of gas permeance and ideal selectivity for the studied gases (see Table 1). For example, the ideal He/CO_2 selectivity pair is 2.8 that is close to the ideal selectivity in the case of gas transport by the Knudsen diffusion mechanism (3.3), which is realized in pores 2-50 nm.

The results of CO_2 desorption from MEA solvent are presented in Figure 2. The experiment is carried out under the following conditions: solvent – aqueous MEA, 12% wt. with initial CO_2-loading 0.6 mole/mole; solvent volume – 400 ml; desorption temperature – 90°C; pressure – 1 bar; solvent flowrate – 10 ml/min.

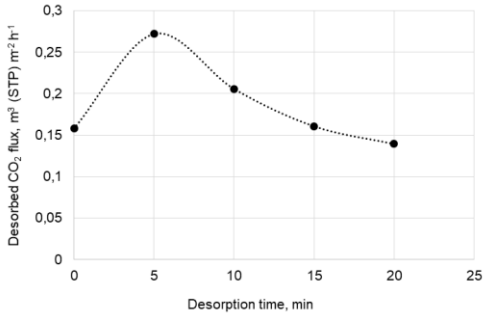

Figure 2. The flux of CO_2 desorbed in porous membrane contactor vs. time of desorption experiment.

Results show that the desorption process can be efficiently carried out at 90°C with a relatively high flux of desorbed CO_2. The transition time period of 5 min can be detected at the beginning of the process when the CO_2 flux rises up to 2 times. Then one can observe the decline of CO_2 flux due to depletion of CO_2 in the closed solvent loop. However, at the 20^{th} minute of process the intensive solvent droplet appearance in the contactor shell was observed. This was the result of the wetting effect of membrane pores which was enhanced with decreasing of solvent surface tension at high desorption temperature. The solvent CO_2-loading after 20 min of experiment was only 0.49 mole/mole.

2. Composite hollow fiber membranes

The main reason for the application of composite membranes is the protective function of thin selective layer that allows withstanding the deterioration effect of wetting phenomenon. The transport properties of fabricated composite membranes are given in Table 2.

Table 2: Transport properties of composite membranes

He permeance, m^3 (STP)/(m^2·h·bar)	5.7±1.0
N_2 permeance, m^3 (STP)/(m^2·h·bar)	4.0±1.8
CO_2 permeance, m^3 (STP)/(m^2·h·bar)	16.7±7.3
He/CO_2 ideal selectivity	0.3–0.5
CO_2/N_2 ideal selectivity	4.1–4.2

Comparison of the results in Tables 1 and 2 clearly shows that the deposition of a thin PTMSP layer changes the membrane properties. The permeance of all gases decreases by an order of magnitude, while the permeance of the target component (CO_2) decreases from 123 to 16.7 m^3 (STP)/(m^2·h·bar). The ideal selectivity for the CO_2/N_2 pair increases from 0.8 to 4.1-4.2. This proves that the formation of a thin non-porous layer of PTMSP on the inner surface of the PSf hollow fiber supports occurs. The value CO_2/N_2 ideal selectivity close to that for pure PTMSP material (3.5-6.5, depending on the method of obtaining the polymer and its microstructure), indicates that the thin layer PTMSP is non-defective. The used technique allows to obtain composite membranes with the best transport properties among the known similar works published earlier [8-9]. Thus, the fabricated membranes are very perspective for the application in gas-liquid membrane contactor for the CO_2 desorption from aqueous MEA solutions.

Acknowledgments

The reported study was funded by RFBR according to the research project № 18-08-00886 A.

References

1. *Bazhenov S., Lyubimova E.* Gas–liquid membrane contactors for carbon dioxide capture from gaseous streams //Petrol. Chem. 2016. V. 56. P. 889-914.
2. *Chabanon E., Bonaceur R., Castel C., Rode S., Roizard D., Favre E.* Pushing the limits of intensified CO_2 post-combustion capture by gas–liquid absorption through a membrane contactor //Chem. Eng. Proc.: Process Intensif. 2015. V. 91. P. 7-22.
3. *Bello A., Idem R.* Pathways for the Formation of Products of the Oxidative Degradation of CO_2-Loaded Concentrated Aqueous Monoethanolamine Solutions during CO_2 Absorption from Flue Gases//Ind. Eng. Chem. Res. 2005. V. 44. P. 945-969.
4. *Bazhenov S., Rieder A., Schallert B., Vasilevsky V., Unterberger S., Grushevenko E., Volkov V., Volkov A.* Reclaiming of degraded MEA solutions by electrodialysis: Results of ED pilot campaign at post-combustion CO_2 capture pilot plant //Int.J.Greenh.Gas Control. 2015. V. 42. P. 593-601.
5. *Franco J., deMontigny D., Kentish S., Perera J., Stevens G.* Effect of amine degradation products on the membrane gas absorption process //Chem. Eng. Sci. 2009. V. 64. P. 4016-4023.
6. *Novitsky E., Vasilevsky V., Grushevenko E., Volkov A., Volkov V., Bazhenov S.* Method for carbon dioxide removal from gas mixtures. Patent RF №2656661, 04.05.2017.
7. *Ovcharova A., Vasilevsky V., Borisov I., Bazhenov S., Volkov A., Bildyukevich A., Volkov V.* Polysulfone porous hollow fiber membranes for ethylene-ethane separation in gas-liquid membrane contactor //Sep. Purif. Technol. 2017. V. 183. P. 162-172.
8. *Malakhov A., Bazhenov S., Vasilevsky V., Borisov I., Ovcharova A., Bildyukevich A., Volkov V., Giorno L., Volkov A.* Thin-film composite hollow fiber membranes for ethylene/ethane separation in gas-liquid membrane contactor //Sep. Purif. Technol. 2019. V. 219. P. 64-73.
9. *Borisov I., Ovcharova A., Bakhtin D., Bazhenov S., Volkov A., Ibragimov R., Gallyamov R., Bondarenko G., Mozhchil R., Bildyukevich A., Volkov V.* Development of polysulfone hollow fiber porous supports for high flux composite membranes: air plasma and piranha etching //Fibers. 2017. V. 5. P. 6.

ENZYMATIC CLEANING OF FOULED CATION- EXCHANGE MEMBRANES USED IN ELECTRODIALYSIS OF BEVERAGES IN FOOD INDUSTRY

Myriam Bdiri, Asma Ben Sghaier, Lobna Chaabane, Christian Larchet, Lasâad Dammak
Institut de Chimie et des Matériaux Paris-Est (ICMPE), UMR 7182 CNRS, Université Paris-Est, 2 Rue Henri Dunant, 94320 Thiais, France

Introduction

Enzymatic agents, especially protease, were experimented as cleaning solutions for fouled polymer based membranes for filtration (UF and MF) used in dairy industry and their efficiency was proved in numerous studies [1]. The use of enzymes as biological solutions for the cleaning of ion-exchange membranes (IEMs) fouled by organic compounds could be an interesting alternative to chemical cleanings [2, 3]. In this work enzymatic cleanings were tested for the first time as biological solutions to clean cation-exchange membranes (CEMs) constituted from poly(styrene-co-divinylbenzene) (PS-DVB) copolymer with sulfonic groups reinforced by PVC cloth fouled by organic compounds during electrodialysis treatments of beverages in food industry –*confidential subject*- [4].

Experiments

Three classes of enzymes (β-glucanase, protease and polyphenol axidase) were experimented as an alternative solution to chemical cleanings for environmental purpose, for their inertness towards polymer matrix and their specific actions [5] on polysaccharides, proteins and phenolic compounds, respectively, which represent abundant fouling agents in treated beverages.

First, operating conditions were optimized using each enzyme solution separately with two concentrations (0.1 and 1.0 $g.L^{-1}$) at three temperatures (30, 40 and 50 °C). The evolution of the CEMs parameters; electrical conductivity (κ_m), ion-exchange capacity (IEC) and contact angle (θ) was determined during the cleanings. Then, cleaning with three successive enzyme solutions or the use of two enzymes simultaneously were tested taking into account the optimal conditions of enzymatic activity (concentration, T (°C) and pH).

Results and Discussion

This preliminary study showed an internal and external efficiency that is reflected in the evolution of studied parameters as presented for « Tyrosinase® : a polyphenol oxidase » enzyme in Fig. 1.

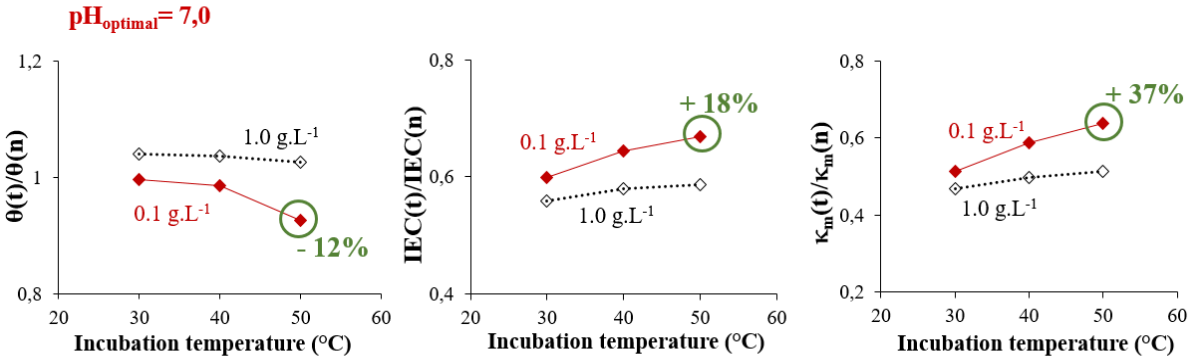

Figure 1. Evolution of the contact angle, the ion-exchange capacity and the electrical conductivity of the treated(t) CEM vs. incubation temperatures and concentrations of Tyrosinase during optimization of its operating conditions.

The use of successive cleanings with the three kind of enzymes demonstrated the enhancement of the global cleaning efficiency and showed that their actions could be complementary towards differents substrats (foulants). The cleaning durations could also be optimized using enzymes mixture after studying their operating compatibility.

Acknowledgement: The authors thank AB Enzymes GmbH, Germany for providing us free samples of liquid enzymes solutions conditioned in their specific buffers.

References

1. *Rudolph G., Schagerlöf H., Morkeberg Krogh K. B., Jönsson A.-S., Lipnizki F.* Investigations of Alkaline and Enzymatic Membrane Cleaning of Ultrafiltration Membranes Fouled by Thermomechanical Pulping Process Water // Membranes. 2018. V. 8. P. 91.
2. *Garcia-Vasquez W., Dammak L., Larchet C., Nikonenko V., Grande D.* Effects of acid–base cleaning procedure on structure and properties of anion-exchange membranes used in electrodialysis // J. Membr. Sci. 2016. V. 507. P. 12–23.
3. *Doi S., Yasukawa M., Kakihana Y., Higa M.* Alkali attack on anion exchange membranes with PVC backing and binder: Effect on performance and correlation between them // J. Membr. Sci. 2019. V. 573. P. 85–96.
4. *Bdiri M., Dammak L., Chaabane L., Larchet C., Hellal F., Nikonenko V., Pismenskaya N. D.* Cleaning of cation-exchange membranes used in electrodialysis for food industry by chemical solutions // Sep. Purif. Technol. 2018. V. 199. P. 114–123.
5. *Fersht A.* Enzyme structure and mechanism, 2nd ed, W.H. Freeman, New York, 1985.

EXPERIMENTAL OBSERVATION OF PHENOMENA DEVELOPING ON ANION-EXCHANGE MEMBRANE DURING CURRENT-VOLTAGE MEASUREMENT

[1]Tomáš Belloň, [1]Petr Polezhaev, [1,2]Zdeněk Slouka

[1]University of Chemistry and Technology, Prague, Chemical Engineering Dep., Technická 5, 166 28 Praha 6, Czech Republic

[2]University of West Bohemia, New Technologies Research Centre, Univerzitní 8, 306 14, Pilsen, Czech Republic

Abstract

Ion-exchange systems represented, for example, by ion-exchange membranes on ion-exchange resin particles exhibit nonlinear current-voltage curves, on which one finds three distinct regions. These regions are referred to as underlimiting, limiting and overlimiting ones. Each of these regions reflects proceeding phenomena responsible for the ion transport. It is known that all important transport processes take place on the depletion side of the ion-exchange systems. We capture the situation at the interface between a cation-exchange system and an electrolyte on the depletion side as it develops during the measurement of a current-voltage curve by using fluorescent and optical observations. Our observations allow to describe qualitatively transport phenomena occurring in ion-exchange systems and to assign their onset to the particular points on the current-voltage curve. We show that current voltage-curve for the studied systems, namely a single cation-exchange particle and a heterogeneous cation-exchange membrane, have a shape typical for ion-exchange systems, i.e. we can clearly recognize underlimiting, limiting and overlimiting region. Interestingly, the overlimiting region of both systems can be divided into two parts based on the slope of the current-voltage curve in this region. We show that there is a qualitative and quantitative change in the developed electroconvection as the major mechanism governing the overlimiting current when the system transitions from the first part of the overlimiting region to the second one. This transition of electroconvection causes its mixing effect to change from local to global. Figure 1 shows measured CVC curve and corresponding images displayed at given points on CVC curve.

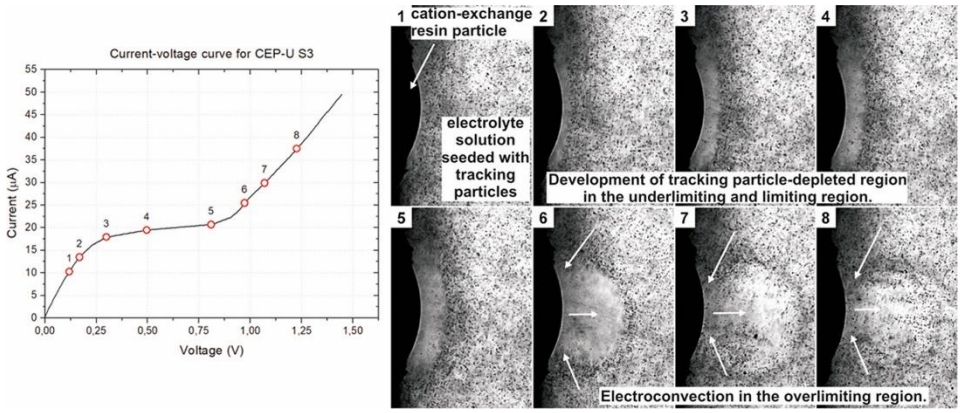

Figure 1 Measured current-voltage curve with corresponding images from optical microscope displayed at given point marked on CVC curve.

Acknowledgements

This work was supported by the Czech science foundation (grant number 18-13491S) and by specific university research funds MSMT no. 20-SVV/2018.

INVESTIGATION OF BEHAVIOR OF A HETEROGENEOUS ANION-EXCHANGE MEMBRANE AND SINGLE ANION-EXCHANGE RESIN PARTICLE IN THE PRESENCE OF SSDNA USING OPTICAL MEASUREMENTS

[1]Tomáš Belloň, [1]Petr Polezhaev, [1,2]Zdeněk Slouka

[1]University of Chemistry and Technology, Prague, Chemical Engineering Dep., Technická 5, 166 28 Praha 6, Czech Republic

[2]University of West Bohemia, New Technologies Research Centre, Univerzitní 8, 306 14, Pilsen, Czech Republic

Abstract

Electrostatic interactions between the charge fixed in ion-exchange membranes and the charge borne by large ions present in the desalted electrolyte can significantly promote fouling of the ion-exchange membranes in the case the two charges are opposite. We investigate the effect of DNA on both systems by measuring current-voltage curves in the solutions having different concentration of mobile DNA. Direct observation of the depletion side of the pristine heterogeneous anion-exchange membrane using visual observations using optical microscope and camera attached directly to the microscope showed that the polarization of the membrane leads to formation of intensive chaotic vortex localized to the membrane surface on which two large counter-rotating vortices superimpose later further polarization. The addition of DNA does not affect the formation of two large vortices however our data strongly indicate that there is an effect on the local vortex, which is responsible for the large changes in the current-voltage curves. Surprisingly, the observation of the anion-exchange particle revealed that DNA strongly affects the electrokinetic around the particle although this is not manifested in the measured current-voltage curves. On this system the DNA changes the electrokinetic picture completely and very likely creates bipolar junction capable of water splitting. Figure 1a shows current-voltage curves with marked points having corresponding images from the optical microscope on the right side of the graph. Figure 1b shows lab-on-a-chip solution used for electrochemical and electrokinetic measurement.

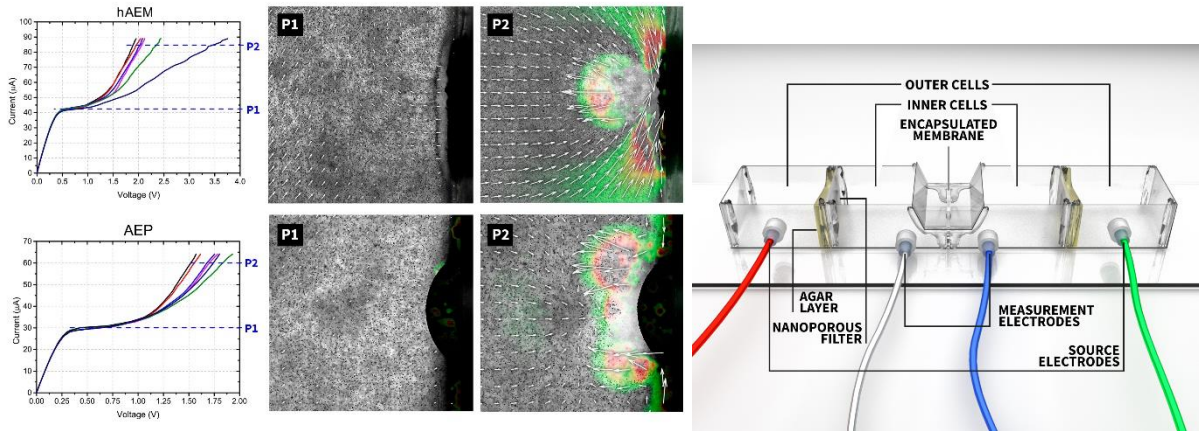

Figure 1. a) Current-voltage curves and images from optical microscope b) Lab-on-a-chip solution.

Acknowledgements

This work was supported by the Czech science foundation (grant number 18-13491S), specific university research funds MSMT no. 20-SVV/2018 and by internal grant number 409 88 1807 provided by UCT Prague.

THE INFLUENCE OF SIZE AND CHARGE OF COUNTERIONS ON THE BEHAVIOR OF A CATION-EXCHANGE SYSTEM

[1]Tomáš Belloň, [1]Petr Polezhaev, [1,2]Zdeněk Slouka

[1]University of Chemistry and Technology, Prague, Chemical Engineering Dep., Technická 5, 166 28 Praha 6, Czech Republic

[2]University of West Bohemia, New Technologies Research Centre, Univerzitní 8, 306 14, Pilsen, Czech Republic

Abstract

Electrodialysis and electrodeionisation are membrane separation processes industrially used to purify water and to separate ions from ionic solutions. These processes are based on the use of a system of several membranes with high selectivity toward particular ionic components contained in the solution so that one can achieve high separation performance.

The main goal of this work is to elucidate the influence of size and charge of counterions on the electrochemical and electrokinetic behavior of studied ion-exchange membranes. In our experiments, we use a heterogeneous cation-exchange membrane and homogeneous cation-exchange particle encapsulated in plastic glue and placed into a "lab-on-a-chip" type system. We study experimentally the behavior of the systems in 6 ionic solutions: HCl, LiCl, NaCl, KCl as solutions containing monovalent cations and CaCl2 and MgCl2 as solutions containing divalent cation. The following experiments with aforementioned solutions have been performed: (i) measurement of current-voltage curves, (ii) measurement of chronopotentiometric curves and (iii) simultaneous measurement of chronoamperometric curves and optical observation of particle motion in solution using Particle image velocimetry method.

We evaluated several parameters such as the limiting current density, transition time as a time required to create a depletion layer and compare the experimental results with predictions of Sand equation, the intensity of the vortices and the corresponding flow rates of the solution in the vicinity of the membrane. The results are then discussed with respect to the differences between the cations that have been measured. The final aim of this work is to find the relation between the behavior of the ion-exchange membrane and the composition of the electrolyte.

Figure 1 shows typical PIV vector velocity map for given values of inserted voltage of external electric field.

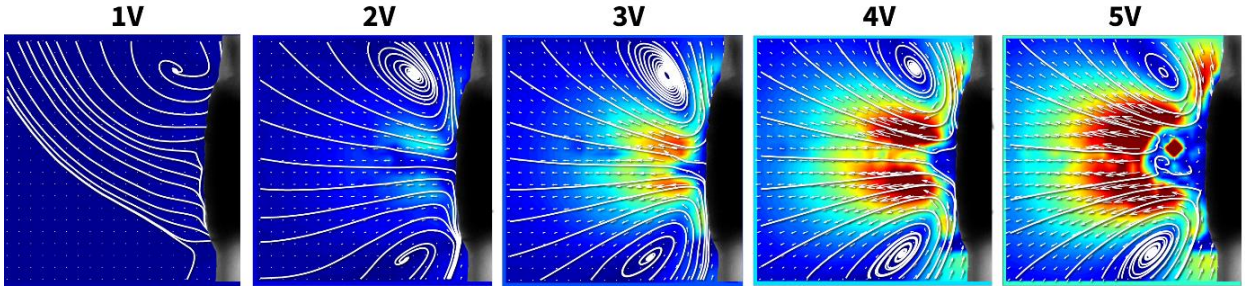

Figure 1 Calculated vector velocity map for given values of voltage. The red color reffers to the highest velocity, blue color reffers to the lowest velocity of the liquid.

Acknowledgements

This work was supported by the Czech science foundation (grant number 18-13491S).

MICRO AND MILIFLUIDIC SYSTEMS AS TOOLS FOR STUDYING ELECTROKINETICS AND ION TRANSPORT IN ION-EXCHANGE SYSTEMS

[1]Tomáš Belloň, [1]Petr Polezhaev, [1]Lucie Vobecká, [1]Zdeněk Slouka

[1]University of Chemistry and Technology, Dept. of Chemical Engineering, Prague, 16628, Czech republic, E-mail: *bellonto@vscht.cz, lucie.vobecka@vscht.c, sloukaz @vscht.cz*

Introduction

Ion-exchange based technologies are inherent part of many industrial applications that are today not only used for desalination of water but also for cleaning of specialty chemicals, desalination of diary and other food products or processing of waste waters. Although the principles and underlying mechanisms of these electromembrane technologies have been studied for more than six decades, there are many open questions to which the scientists and engineers are looking for answers. These questions can be related to understanding fundamental science behind ion-exchange processes such as appearance of electroconvection, water splitting and other reaction-transport characteristics of these systems or to the properties and behavior influencing performance of electromembrane units such as the effect of fouling, ion selectivity and many others. In the Laboratory of microchemical engineering at UCT Prague, we strive for better understanding of the behavior of ion-exchange systems by performing experiments in a non-standard format. These experiments are conducted in systems that not only allow to carry out electrochemical characterization of studied systems and to analyze the system behavior based on the differences between the input and output streams but also direct observation of processes that occur at the interface between ion-exchange systems and desalted electrolyte or reconstruct spatial patterns of concentration or potential profiles.

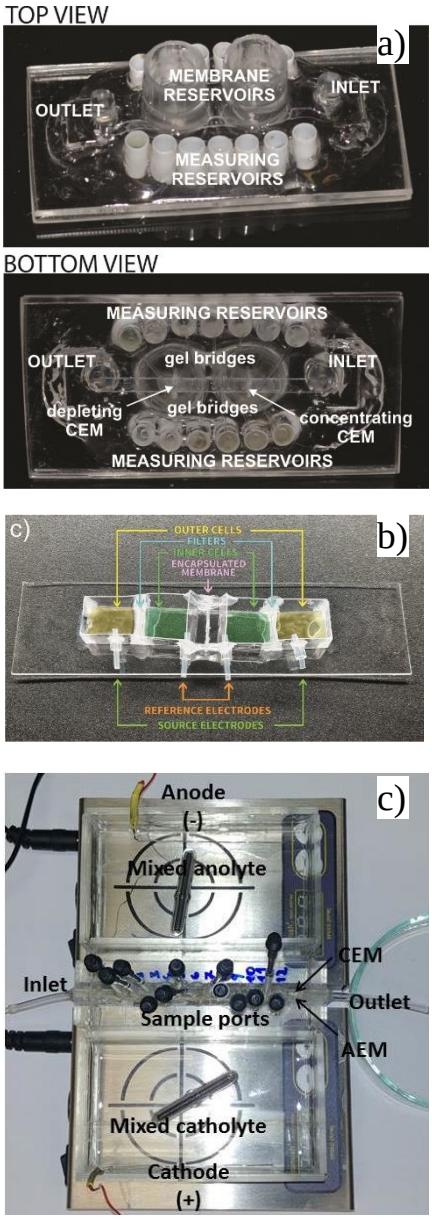

Figure 2. Various mili and microfluidic systems used in our research: a) chip for measurement of electric potential profiles in an ICP based chip, b) chip for characterization of ion-exchange systems under static conditions, c) chip for investigation of desalination under forced convection.

Experiments

Figure 1 show three representative mili- and microfluidic systems that have been used in our experiments to analyze ion-exchange systems in detail. Figure 1a shows a chip used for reconstruction of electric potential profile in a system with two cation-exchange membranes used for ion-concentration polarization based desalination. Figure 1b shows a four-chamber chip allowing to study single or multiple ion-exchange systems and small pieces of ion-exchange membranes under various conditions (imaging of electrokinetics, quantification of water splitting, investiagtion of fouling) and Figure 1c shows flow-through electrodialysis channel allowing to study separation of ions on ion-exchange membranes in a flow format.

Results and Discussion

In this contribution we will present some representative experiments we conduct in our laboratory.

The experimental activity aims at finding answers to two basic questions and these are: (i) how does structure (both geometry and composition) of ion-exchange systems affect their behavior and performance, and (ii) how does desalted electrolyte influence the efficiency of electrodialysis.

The structure of the systems is usually investigated by the use of optical microscopy and microcomputed tomography which also allows to reconstruct the internal structure of heterogeneous ion-exchange membranes [1]. Recently, we also embarked on analysis of ion-exchange resin particles by atomic force microscopy. The structure of these systems is further investigated indirectly by using solutions containing counterions of various sizes which then provide information about characteristic dimensions of the ion-exchange systems. Another technique we use for this purpose is energy dispersive analysis (EDS) which can provide information on elemental composition on a surface.

Most of the electrochemical and electrokinetic experiments are carried out in the chip depicted in Figure 1b. As mentioned above, the experiments in this chip are performed under static conditions, i. e. no forced flow is applied. The investigation in this chip allows one to investigate the electrokinetics at the interface between the studied system and the surrounding electrolyte, water splitting reaction, the manifestation of fouling [2], or simply the study of the basic characteristics of the system [3] such as measurement of transport number or the resistance of the system. Figure 2 depicts one of the experiments carried out in such a cell focused on imaging of phenomena occurring at the ion-exchange system and a water electrolyte interface during the measurement of current-voltage curves [4].

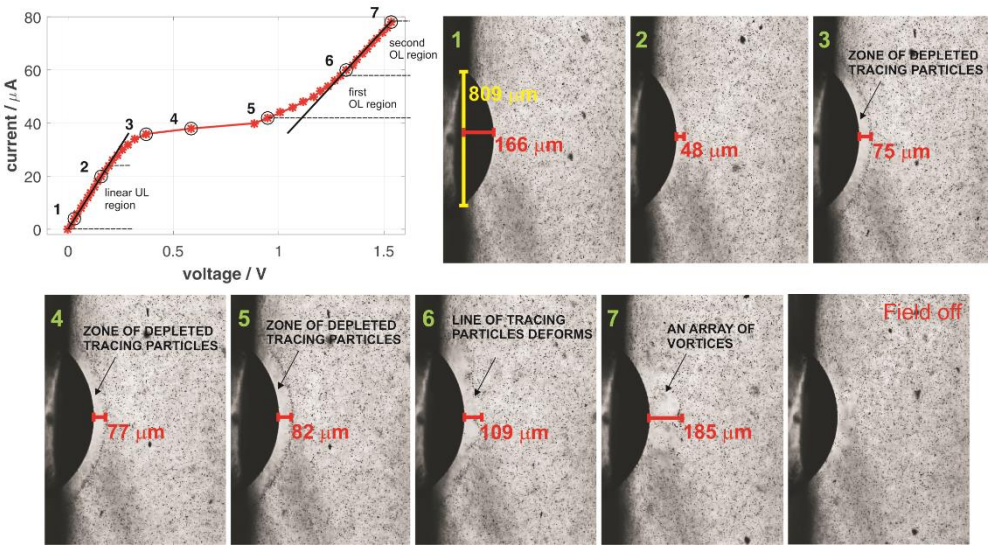

Figure 3. Imaging of depletion side of a cation exchange particle during it polarization. Melamine-based 2 μm particles were used as tracking markers.

The flow-through systems (Figs. 1a and c) are used in experiments with forced flow. The main attention is devoted to the reconstruction of electric potential and concentration profiles established under various condition in systems with ion-exchange membranes. An example of such a measurement can be seen in Figure 3. It shows experimentally obtained profile of electric potential in a flow through system in which two cation-exchange membranes were integrated on a single channel and connected in series. This arrangement of membranes creates depletion and concentration regions in the channel simultaneously and creates suitable conditions for ion concentration polarization desalination or an analyte pre-concentration. Our experimental data show, that one can clearly distinguish the depletion and concentration regions and calculate local values of electric field which may be two orders of magnitude higher in the depletion zone than those in the concentration zone [5].

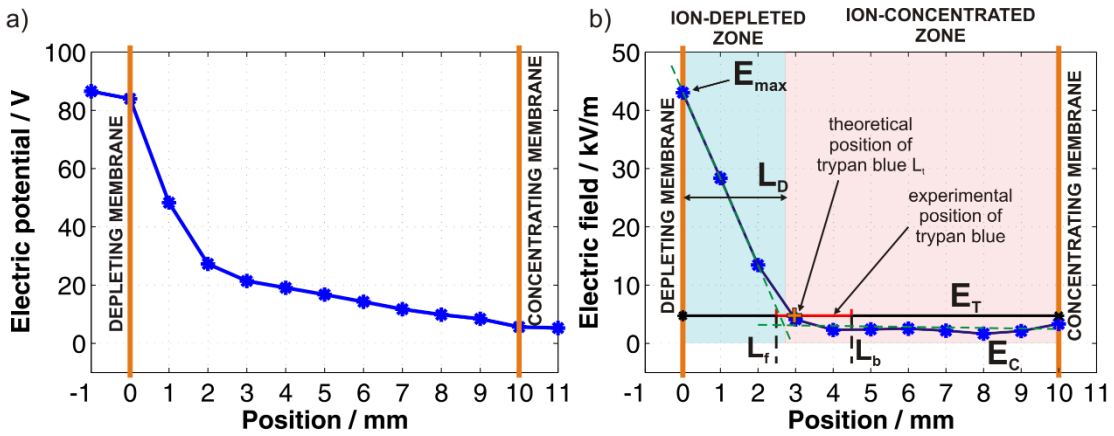

Figure 4. a) Electric potential profile measured in a flow-through channel with two integrated cation exchange membranes with applied DC bias of 100 V, and b) numerically evaluated values of local electric field strength.

References

1. *Svoboda, M., et al.*, Swelling induced structural changes of a heterogeneous cation-exchange membrane analyzed by micro-computed tomography. Journal of Membrane Science, 2017. **525**: p. 195-201.
2. *Tomáš Belloň, P.P., Lucie Vobecká, Zdeněk Slouka*, Fouling of a heterogeneous anion-exchange membrane and single anion-exchange resin particle by ssDNA manifests differently. Journal of Membrane Science, 2019. **572**: p. 619 - 631.
3. *Vobecka, L., et al.*, Heterogeneity of heterogeneous ion-exchange membranes investigated by chronopotentiometry and X-ray computed microtomography. Journal of Membrane Science, 2018. **559**: p. 127-137.
4. *Tomáš Belloň, P.P., Lucie Vobecká, Miloš Svoboda, Zdeněk Slouka.* Experimental observation of phenomena developing on ion-exchange systems during current-voltage curve measurement. Journal of Membrane Science 2019 [cited 572; 607-618].
5. *Slouka, Z., et al.*, Integrated, DC voltage-driven nucleic acid diagnostic platform for real sample analysis: Detection of oral cancer. Talanta, 2015. **145**: p. 35-42.

THE INFLUENCE IN SITU GAMMA RAYS OF CHEMICAL PROCESSES FABRICATION NANOSCALE POROUS SILICON AND ITS PERSPECTIVES APPLICATIONS

[1]Olga Belobrovaya, [1]Victor Galushka, [1]Igor Galushka, [2]Andrei Karagaichev, [1]Anton Mantsurov, [1]Valentina Polyanskaya, [1,3]Denis Terin

[1]Saratov State University, Saratov, E-mail: *terinden@mail.ru*

[2]Regional Clinical Oncology Center, Saratov

[3]Yuri Gagarin State Technical University of Saratov

Introduction

Lithium-ion batteries (LIB) typically consist of an anode, a cathode, and an electrolyte, with a separator electronically separating the anode and cathode [1]. Upon charging of the battery, lithium ions are extracted from the cathode and stored in the anode. When the battery is being discharged, the Li ions are extracted from the anode and stored in the cathode. Nanostructured Si has been investigated as a possible solution to the pulverization of Si upon Li insertion and extraction. One method of fabricating nanostructured Si is metal-assisted chemical etching (MAC) [2], which creates Si nanowires (NWs) from a top-down process on a Si wafer. The NWs formed by MAC etching depend on parameters such as the orientation of the Si, the doping density of the Si, and the etching conditions under which the NWs are formed. The performance of Si anodes for LIBs was shown to improve with the addition of carbon and other elements. This paper presents experimental studies of the formation of silicon porous structures upon in situ irradiation, their optical and structural properties.

Experiments

By the method of water non-electrolytic etching (MAC) or metal-stimulated chemical etching, porous silicon was obtained. The MAC method is based on the substitution of silicon for the reduction of $Ag^+ \rightarrow Ag^0$ on the surface of a silicon substrate. Porous silicon structures formed a two-step MAC method on gamma-quanta irradiated and unirradiated silicon substrates KDB 4.5 <111>. Porous silicon structures were also obtained on irradiated and non-irradiated substrates when irradiated in situ by a bremsstrahlung gamma — radiation from a Varian Unique medical linear electron accelerator at the Saratov Regional Oncology Center with an electron energy of 6 MeV. The accelerator is calibrated according to the absorbed dose at the maximum of ionization and the total dose of radiation was 24 kP when receiving the samples within an hour. The distance from the target to the surface of the plate is 100 cm, in order for the samples to be in the region of the maximum ionization. Structural and optical properties were studied using a MIRA 2 LMU scanning electron microscope, on a DRON-4 diffractometer using an X-ray tube with a copper anode (Cu-Kα). Raman spectra (RS) were recorded on a Renishaw inVia spectrometer with a laser wavelength of 532 nm. The photoluminescence (PL) spectra were recorded simultaneously on the equipment for measuring cattle.

Results and Discussion

Figure 1 shows the surface morphology and cleavage of a sample of porous silicon obtained by the MAC method on a substrate irradiated with a dose of 30 kP, and the etching time is 60 minutes. With increasing time of etching the surface structure of the samples revealed more. While the size of the diameter of porous silicon in their array demonstrates a wide distribution of diameters from about 40 to 200 nm, for each individual structure the diameter does not change significantly along the nanowire. The X-ray structural analysis of substrates and samples without irradiation and after exposure to gamma radiation allowed us to establish a number of interesting phenomena. X-ray diffraction analysis of porous silicon samples revealed the removal of microstresses not only in the substrate, but also partially in the layer upon irradiation in the process of preparation. The interplanar distances in the samples studied are different. Moreover, the greatest interplanar distance in the unirradiated sample and the smallest of the samples obtained in situ during irradiation on the irradiated substrate.

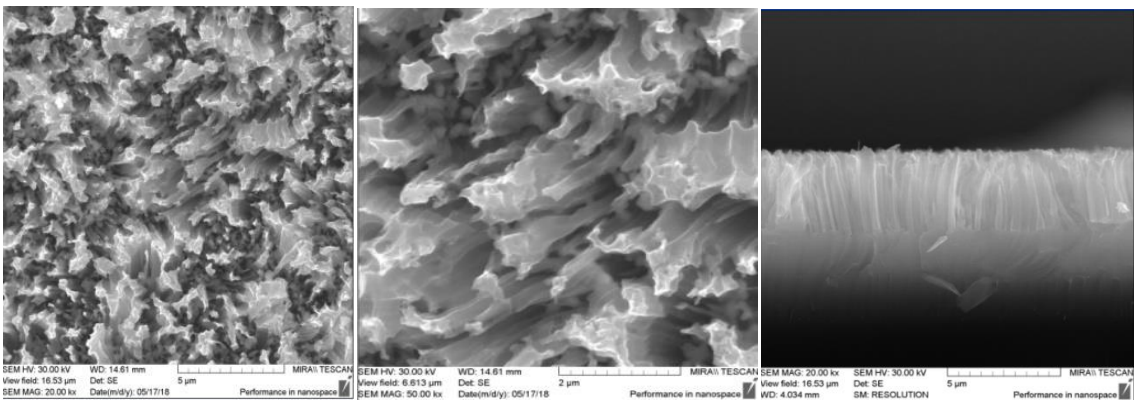

Figure 1. Surface morphology and of the end face of a porous silicon sample, etching time 60 minutes.

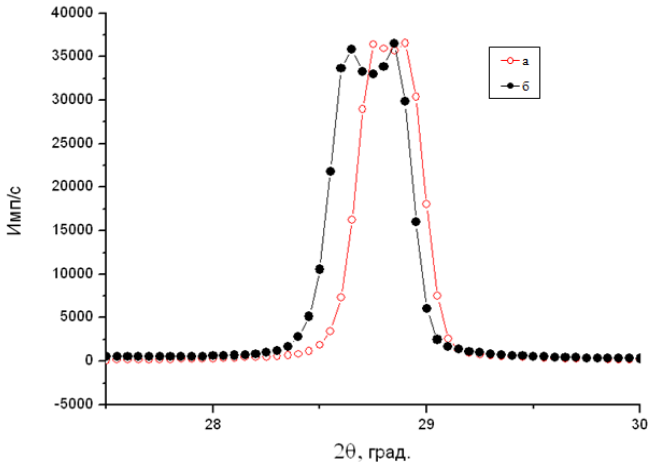

Figure 2. Diffraction pattern of samples of porous silicon of the <111> plane, obtained in situ on the irradiated substrate (a) and unirradiated substrate (b).

Raman spectra in the presence of silver are characterized by the effect of surface amplification of SERS. A large Raman scattering signal and the presence of a metal — Ag suppresses PL, however, we observe it on samples obtained in situ on previously irradiated substrates. The appearance of photoluminescence in samples irradiated at the time of preparation on irradiated substrates indicates ordering of the growing layer when it is obtained on the irradiated substrate, which is confirmed by X-ray diffraction studies.

The obtained data allow us to conclude about the controllability of the process of chemical synthesis and the promise of the method of metal-stimulated chemical etching to obtain promising nanoporous silicon structures.

The reported study was funded by RFBR according to the research project №18-07-00752 A.

References

1. *McSweeney W., Geaney H., O'Dwyer C.* Nano Res. 2015, 8(5), P. 1395-1442.
2. *Huang Z.* Materials Views. 2011. № 23. P. 285-308.

REGULAR TRACK MEMBRANES – PRODUCTION AND APPLICATION PROSPECTS

[1]Vladimir Berezkin, [2]Sergey Bedin, [1]Alexander Vasiliev, [1]Yuriy Grigoriev, [3]Vladimir Nazmov

[1]Shubnikov Institute of Crystallography of Federal Research Center "Crystallography and Photonics" of Russian Academy of Sciences. Moscow. Russia. Email: *berezkin38@mail.ru*

[2]Moscow state education university. Moscow. Russia

[3]Budker Institute of nuclear physics SB RAS. Novosibirsk. Russia

Introduction

The regular and oriented structures may be used in systems meant for control of irradiation in optical and infrared ranges and as elements of data storage equipments. The template synthesis on track membrane (TM) with regularly located pores is considered as prospect method of these structures production. Moreover, regular TM can be used as optical diffraction elements.

Experiments

X-ray band of synchrotron irradiation was used to produce regular TM. To generate pores, polyethylene terephtalate (PET) film was irradiated perpendicularly to ones surface through template. The one was bidimensional array of regular through micropores in tantalum plate of 2 μm thickness [1]. Pore diameter was 1 μm and pore surface density was 10^6 cm^{-2}. Pore formation was realized with chemical etching of irradiated film in 10 % NaOH aqueous solution under temperature of 60 C^0 pending 30 min. Then regular TM formed in etching was flushed in distilled water.

The experimental investigations on light diffraction with regular pore system were carried. He-Ne laser was applied as light source. The transparent scheme of diffraction was used. The distance between membrane and screen was of 0.5 m.

The Fe microstructures were formed in dead-end pores of regular TM by metal electrodeposition method.

Results and discussion

Optical micrographs of irradiated PET film (a) and generated regular TM (b) are shown in Fig.1.

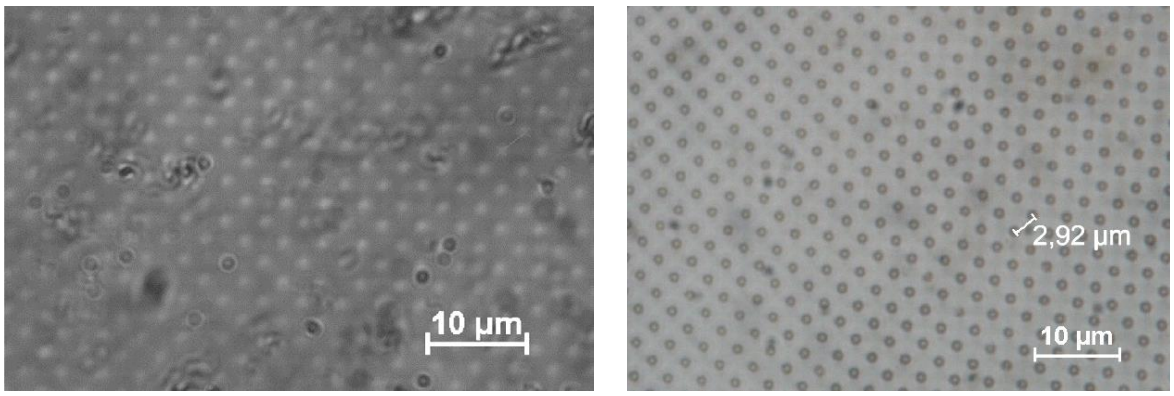

a *b*

Figure 1. Optical micrographs of irradiated PET film (a) and generated regular TM (b).

The micrographs were produced on optical polarized microscope Nikon LV100 with objective Planachromat 100X in transparent regime. The SEM micrographs of surface (a) and cleavage (b, c) produced at electron microscope FEI Scios 30 kB are presented in Fig. 2. The TM sample was irradiated previously with UF radiation The one crisps the sample and enables preparing of smooth cleavage at pore center [2].

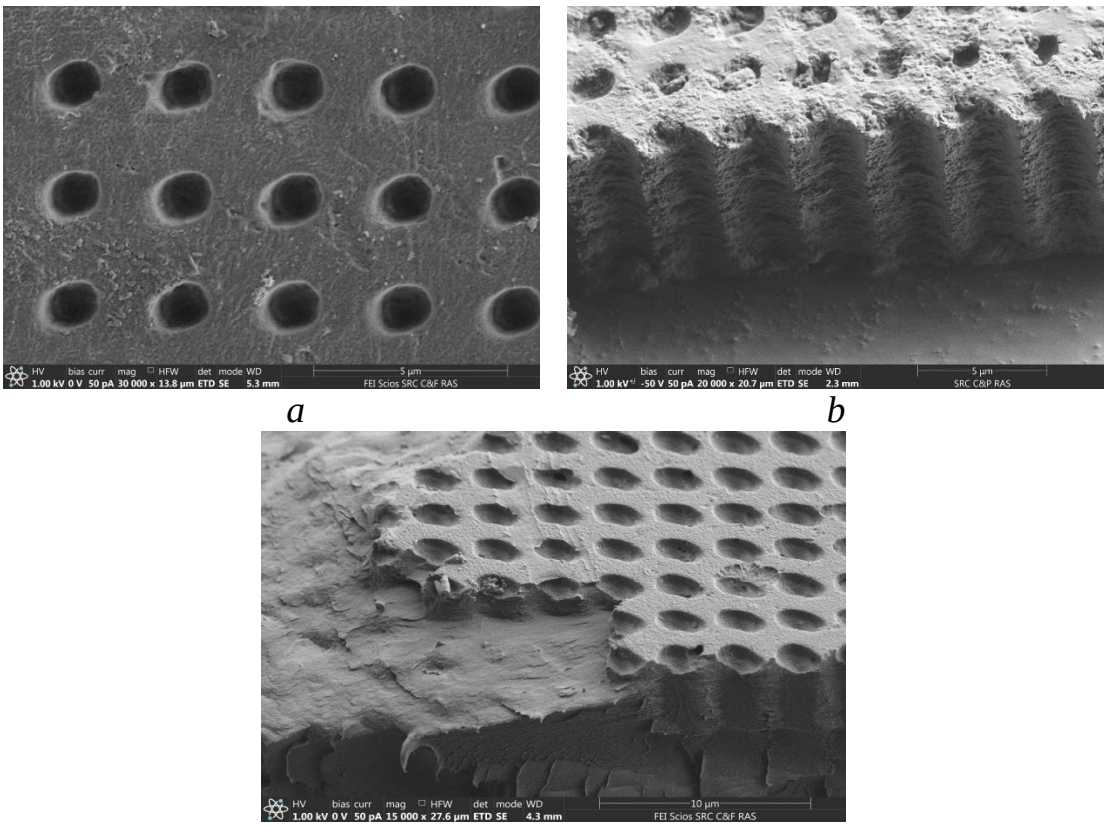

Figure 2. The SEM micrographs of surface (a) and cleavage (b, c) produced at electron microscope FEI Scios 30 kB.

Diffraction picture obtained with regular pore system presents ensemble of light spots (reflections) (Fig.3). The ones maximum location corresponds to diffraction picture generated with bidimensional grating. Reflections are located at system of horizontal and vertical lines crossings.

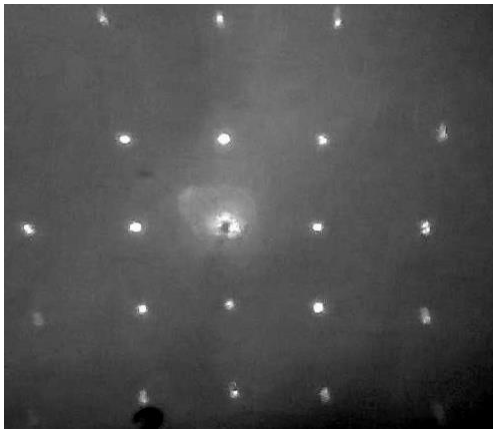

Figure 3. Diffraction picture obtained with regular pore system.

The well known condition is satisfied for every line:

$$d \sin\theta = m\lambda \ (m = 1,2,3,\ldots),$$

d – distance between pores; θ – diffraction angle; m – diffraction order, λ - wavelength.

This result supports ability of regular TM application as diffraction elements.

The Fe microstructures were formed in dead end pores of regular PET TM with electrodeposition method (Fig4).

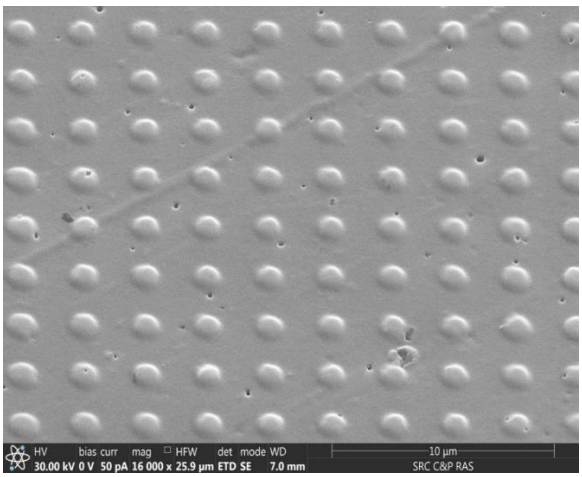

Figure 4. The Fe microstructures formed in dead end pores of regular PET TM with electrodeposition method.

Metallic microstructures formed on polymer films basis are prospective in creation of magnetic memory systems with high information density. Application of thin nonmagnetic metal films and through pores in magnetic structures deposition enables magnetic isolation of every functional element. Application of dead-end pores enables supplementary advantages associated with element size decrease.

References

1. *Goldenberg B.G., Lemzyakov A.G., Nazmov V.P., Pindyurin V.F.//* Physics Procedia, 2016, V. 84, P. 205.
2. *Orelovitch O.L., Apel P.Yu., Surtovska B.//* Materials Chemistry and Physics, 2003, V. 81, № 2, P. 349.

THE STUDY OF ELECTROCHEMICAL STABILITY OF THE ANION-EXCHANGE MEMBRANES MA-41 MODIFIED BY POLY-N,N-DIALLYLMORPHOLINIUM

Denis Bondarev, Alexander Bespalov, Victor Zabolotskiy, Svetlana Eterevskova
Kuban State University, Krasnodar, Russia, E-mail: *bondarew.denis1992@gmail.com*

Introduction

It was previously shown that modification of anion-exchange membranes MA-41 with poly-N, N-diallylmorpholinium bromide leads to a decrease in the intensity of water dissociation at the membrane / solution interface and an increase in mass transfer [1]. To introduce the obtained modified membrane into industrial devices for electrodialysis, it is necessary to investigate its electrochemical and thermal stability [2,3]. Studying the stability of the MA-41 membrane modified by poly-N,N-diallylmorpholinium bromide is advisable to carry out with method of electrochemical impedance [4]. This method allows us to accurately estimate the intensity of the dissociation of water on the modified membranes.

Experiments

The stability tests of MA-41 membranes modified by poly-N,N-diallylmorpholinium bomide (hereinafter MA-41M) were performed in a semi-industrial electrodialysis cell at a current density of $i = 2i_{lim}$. The spectra of the electrochemical impedance were recorded in a flow-through 4-chamber cell, the concentration of the model sodium chloride solution was 0.01 M. The range of frequencies under study was from 1 MHz to 0.005 Hz. The obtained spectra of the electrochemical impedance were processed by the method of equivalent circuits. Using mathematical processing of the spectra, we determined the frequency of the maximum for the semicircle of the Gerischer impedance and calculated the effective dissociation constant of water using equation (1).

$$\chi = \frac{2\pi f_{G\max}}{\sqrt{3}} \tag{1}$$

where: f_{Gmax} - frequency at the point of maximum of Gerischer impedance, Hz.

Results and discussion

Figure 1 shows the MA-41M membrane spectrum processed by the method equivalent circuit.

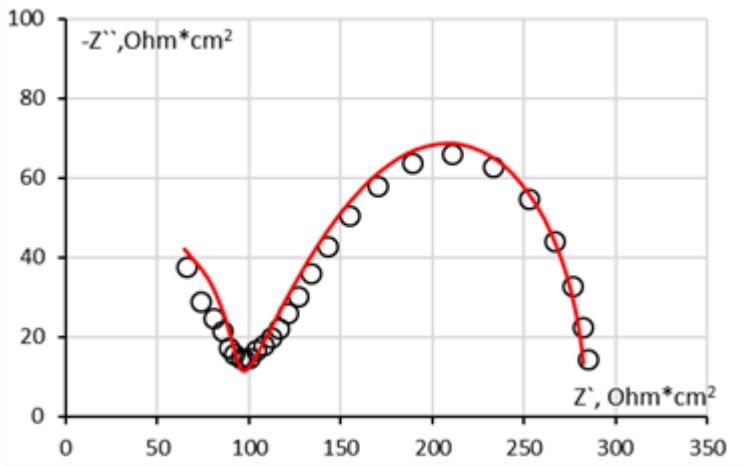

Figure 1. The spectrum of the electrochemical impedance of the MA-41M membrane. The dots indicate the experimental values, the solid line calculated values by the method of equivalent circuits.

Figure 2 shows the dependence of the effective water dissociation constant of dimensionless current density for the original modified MA-41M membrane and for MA-41M membranes after conducting stability tests at a current density of $i = 2i_{lim}$.

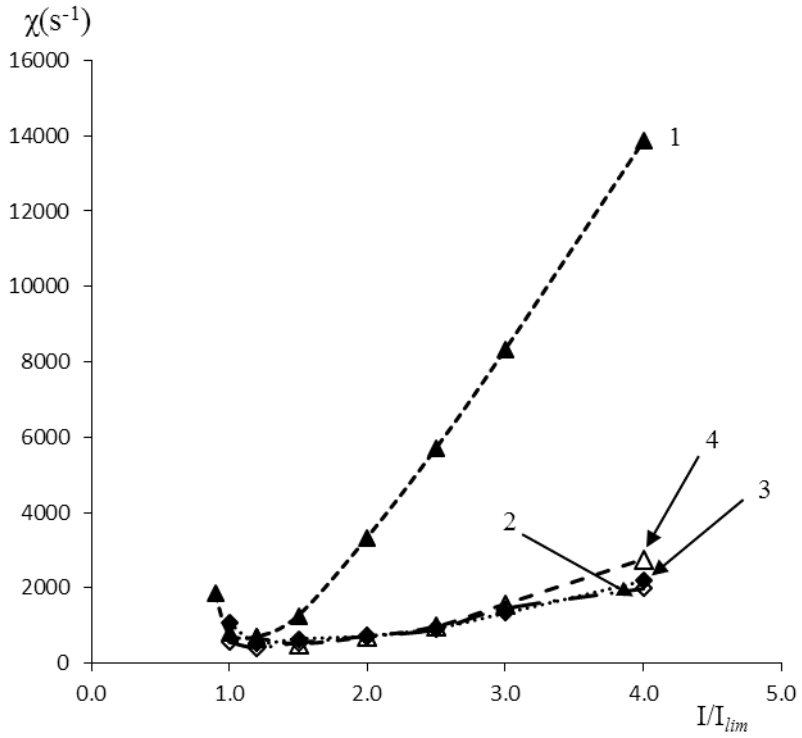

Figure 2. The dependence of the effective dissociation constant of water of dimensionless current density, where: 1 - the initial membrane MA-41, 2 - the modified membrane MA-41M, 3 - the modified membrane MA-41 M after 10 hours of stability tests, 4 - the modified membrane MA - 41M after 25 hours of stability tests.

Thus, it was shown that the rate of water dissociation on the modified MA-41M membrane is 7.5–8 times less than on the initial MA-41 membrane. At the same time, the value of the effective dissociation constant of water for the membrane MA-41M is much less than for the initial membrane as before the endurance tests so and after 25 hours of work in the electrodialysis apparatus. This indicates a high electrochemical and thermal stability of the modified anion-exchange membrane MA-41M.

References

1. *Zabolotskiy, V.I., Bondarev, D.A., Bespalov, A.V. //* Electrochemistry. 2018. V. 54, № 11. P. 963-969.
2. *Zabolotskiy V.I., But A.Yu., Vasil`eva V.I., Akberova E.M., Melnikov S.S. //* J. Membr. Sci. 2017. V. 526. P. 60-72.
3. *Kniaginicheva E., Pismenskaya N., Melnikov S., Belashova E., Nikonenko V., Sistat P., Cretin M.//* J. Membr. Sci. 2015. V. 496. P. 78-83.
4. *Zabolotskiy V.I., Ganych V.V., Sheldeshov N.V. // Electrochemistry. 1991. V. 27, № 10. P. 1245-1249.*

PREPARATION OF THIN FILM COMPOSITE MEMBRANES FOR PERVAPORATION VIA INTERFACIAL POLYMERIZATION TECHNIQUE

Katsiaryna Burts[1], Tatiana Plisko[1], Alexandr Bildyukevich[1], Guoqiang Li[2], Joanna Kujawa[2], Wojciech Kujawski[2]

[1]Institute of Physical Organic Chemistry, National Academy of Sciences of Belarus, Minsk, Belarus
E-mail: *katyaburt@gmail.com*

[2]Nicolaus Copernicus University in Toruń, Faculty of Chemistry, Torun, Poland
E-mail: *wkujawski@umk.pl*

Introduction

Pervaporation is an important membrane process in biofuel and chemical industries. Dehydration of alcohol azeotropic mixtures is a well-known application of pervaporation. In order to increase permeation flux of polyamide membranes without sacrificing the selectivity, the membrane morphology must be converted from a dense thick film to asymmetric or composite type morphology. Composite membrane consists of a top selective layer formed on a chemically different asymmetric porous substrate. The advantage of composite membranes is the possibility to combine the benefits of the independent polymeric layers to obtain the desired membrane performance. Interfacial polymerization is an effective technique to prepare the composite membrane with the thin interfacially polymerized selective layer [1]. Polyamide (PA) is one of polymers that can be obtained via interfacial polymerization. PAs feature high selectivity in the separation of alcohol/water mixtures [2]. In this work the effect of the amine nature and the ratio of amine and acyl component upon the formation of thin selective layer via interfacial polymerization technique on the structure, performance and hydrophilic-hydrophobic properties of thin film composite PA/polyacrylonitrile (PAN) membranes were studied.

Experiments

Ultrafiltration PAN (poly (acrylonitrile-co-methyl acrylate) (92: 8), VNIISV, Russia, Mw=107 kDa) membranes were used as porous supports for thin film composite membrane (TFC) preparation. They were fabricated via a non-solvent induced phase inversion technique using distilled water as a coagulant. Two types of porous supports were prepared for TFC membranes formation: in order to study the effect of amine and acyl component PAN membranes were prepared from 17 wt.% PAN casting solutions in dimethylformamide and to study the effect of amine nature 13 wt.% PAN casting solutions in dimethyl sulfoxide were used. A thin selective layer was formed via interfacial polymerization on the surface of the selective layer of PAN ultrafiltration membranes. The selective layer of PAN membrane was brought into contact with amine (diethylenetetramine (DETA), triethylenetetramine (TETA), polyethylene imine (PEI, hyperbranched, M=10000 $g \cdot mol^{-1}$) and piperazine (PZ) aqueous solution for 15 s. The excess of the amine solution was removed using blotting paper. Thereafter the top of the membrane was brought into the contact with trimesoyl chloride (TMC)/hexane solution for 15 s. The prepared membranes were immersed in the ethanol to remove the excess of unreacted reagents and dried for 24 hours at room temperature.

The membrane structure was studied by scanning electron microscopy (LEO 1430 VP microscope, Leo Electron Microscopy Lrd., Cambridge, UK) at 30 keV. Water contact angle was determined via the sessile drop method (Goniometer Attention Theta from Biolin Scientific, Gothenburg, Sweden). Pervaporation performance of composite membranes was studied during separation of ethanol/water mixture with 90 wt.% ethanol content (the temperature of the feed solution was equal to 35°C, downstream pressure ≤1 mbar). The composition of feed and permeate solution were analyzed using gas chromatograph Varian 3300 with TCD detector (Varian Inc., USA) and with Porapak Q packed column.

Results and Discussion

According to SEM microphotographs analysis it was found that the selective layer thickness depends on the TETA/TMC ratio (Figure 1, Table 1). The highest thickness, 290 nm, was observed

for the membranes obtained in the case of the maximum TMC/TETA ratio (Figure 1 b). When the TETA concentration by weight was higher than TMC one, membranes feature the thinnest selective layer (c.a 60-70 nm) (Figure 1 c). Membranes with an equal by weight TETA and TMC content in water and organic solutions respectively had an intermediate value of selective layer thickness — 90 nm (Figure 1 c).

Table 1: PA/PAN composite membrane properties and pervaporation performance

TETA concentration, wt.%	TMC concentration, wt.%	Flux, $kg \cdot m^{-2} \cdot h^{-1}$	Water content in permeate, wt.%	Contact angle, °	Selective layer thickness, nm
0.1	0.05	0.580	87	45±2	60-70
0.1	0.1	0.270	90	94±2	90
0.05	0.1	0.187	81	86±2	290

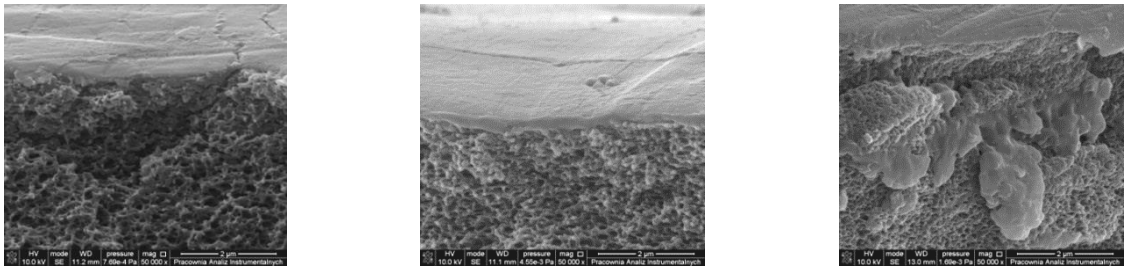

a *b* *c*

Figure 1. SEM images of the cross section of PA/PAN flat-sheet membranes with different TETA and TMC content in water and organic phase: a – 0.1 wt.% TETA, 0.1 wt.% TMC; b – 0.05 wt.% TETA, 0.1 wt.% TMC;c - 0.1 wt.% TETA, 0.05 wt.% TMC.

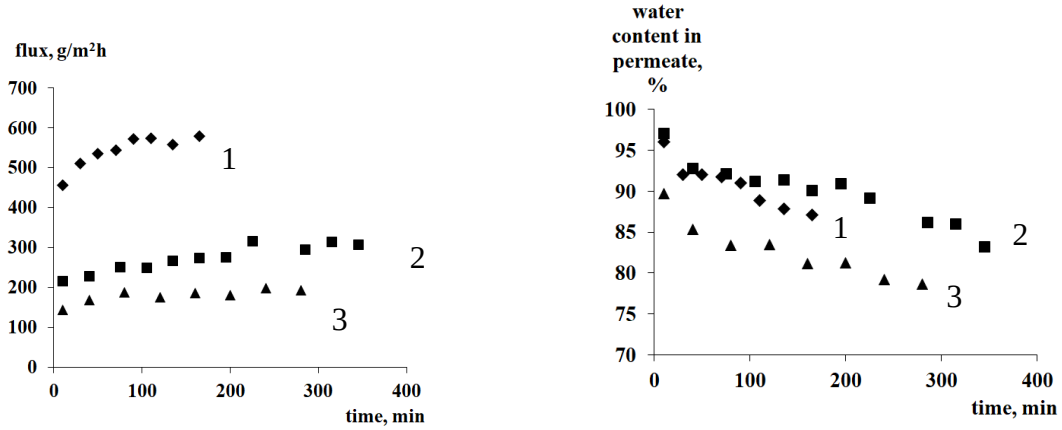

a *b*

Figure 2. Time dependence of flux and water content in permeate for PA/PAN composite membranes: 1 – 0.1 wt.% TETA, 0.05 wt.% TMC; 2 – 0.1 wt.% TETA, 0.1 wt.% TMC; 3 – 0.05 wt.% TETA, 0.1 wt.% TMC.

It was revealed that membrane water contact angle is dependent on the TETA/TMC ratio. Membrane surface with TMC excess was found to be hydrophobic, and water contact angle was from 86 to 94°.

It was shown that all developed membranes feature decrease in the water content in permeate and increase the flux upon pervaporation which is due to the selective layer swelling. Composite membranes obtained from 0.1 wt.% aqueous TETA solution and 0.05 wt.% TMC in hexane solution had the highest flux. It is known that the membrane flux is inversely proportional to the selective layer thickness. Data obtained are consistent with this statement.

The effect of amine type on the PA/PAN composite membrane structure and performance was also studied. It was found that thickness and structure of the selective layer depends on the amine nature. It is due to the different amine solubility in organic phase, i.e. the different distribution

coefficient of amine between aqueous and organic phases. It was found that thickness of the selective layer for the composite membranes with DETA was 60 nm, and for membranes with TETA — 245 nm.

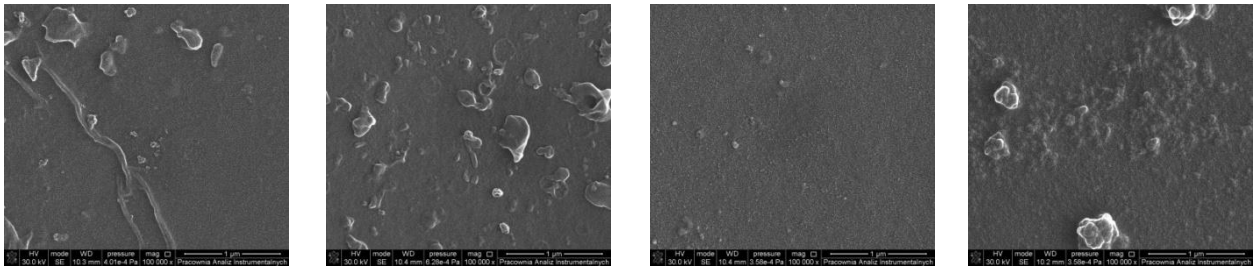

a *b* *c* *d*

Figure 3. SEM-images of the selective layer of PA/PAN flat-sheet membranes (0.15 wt.% amine aqueous solution, 0.075 wt.% TMC solution in hexane): a –DETA, b –TETA, c – PEI, d – PZ.

According to the SEM images (Figure 3), the obtained irregular nodular structures of polyamide were formed on the surface of the membrane selective layer for membranes obtained with DETA, TETA and PZ. Nodular structures were almost absent for the membranes with PEI (Figure 3 c). It should be noticed that membranes obtained with PEI feature the lowest flux and the highest water content in permeate.

Table 2: Composite membranes performance in pervaporation of 90 wt.% ethanol/10 wt.% water mixture at 30°C (selective layer is formed using 0,15 wt.% amine aqueous solution and 0,075 wt.% TMC solution in hexane)

AMINE NATURE	J, $KG \cdot M^{-2} \cdot H^{-1}$	WATER CONTENT IN PERMEATE, %
DETA	**0.125**	**22**
TETA	**0.111**	**45**
PEI	**0.076**	**83**
PZ	**0.338**	**27**

It was found that the membranes obtained with PEI have the most uniform surface of the selective layer without nodular structures which were observed for membranes with DETA, TETA, PZ. It may be due to the polymeric nature of PEI and its hyperbranched structure which results in lower rate of PEI diffusion to the organic phase compared to low molecular weight amines which leads to the higher TMC concentration at the interphase between aqueous and organic solutions and thicker PA selective layer formation. The highest flux observed for the membranes obtained from PZ. It occurs due to the lowest cross-linking of the selective layer because of PZ low functionality and rigid structure.

Acknowledgments

This work was carried out with a financial support from Belarussian Republican Foundation for Fundamental Research (project №X19PM-052) and using statutory funds of Nicolaus Copernicus University in Torun (Faculty of Chemistry, T-109 "Membranes and membrane separation processes - fundamental and applied research").

References

1. *Huang S., Hsu C., Liaw D., Hu C., Lee K., Lai J.* Effect of chemical structures of amines on physicochemical properties of active layers and dehydration of isopropanol through interfacially polymerized thin-film composite membranes // J. Membr. Sci. 2008. V. 307. P. 73-81.
2. *Li C., Huang S., Liaw D., Lee K., Lai J.* Interfacial polymerized thin-film composite membranes for pervaporation separation of aqueous isopropanol solution // Sep. Purif. Technol. 2008. V. 62. P. 694-701.

HETEROGENEOUS MEMBRANE WITH DOMINANT ELECTROCONVECTION AT WORK UNDER INTENSIVE CURRENT CONDITIONS

Anastasia But[1], Victor Zabolotskiy[1], Anna Kovalenko[1], Makhamet Urtenov[1], Vera Vasil'eva[2]

[1]Kuban State University, Krasnodar, Russia, E-mail: *nastya310392@mail.ru*

[2]Voronezh State University, Voronezh, Russia

Introduction

Progress in the development of electromembrane technologies is associated with the intensification of electromembrane processes and the transition to the over-limit current modes of electrodialysis. Under these conditions, the dominant mechanism of ion transfer is electroconvection [1]. The foundations of the theory of electroconvection have been laid down in the works of Dukhin and Mishchuk [2], Rubinstein and co-authors [3]. It is known that electroconvection depends on the morphology of the surface of ion-exchange membranes and their chemical composition. According to the theoretical estimates, in Rubinshtein's paper, a ten percent curvature of the plane membrane surface leads to a 30% acceleration of the onset of superconductivity, and a small increase in the current limit on a "wave-shaped" membrane is associated with an increase in surface area compared to a flat membrane.

Changes in the chemical composition of ion-exchange membranes can be achieved by modifying its surface. The modification allows to suppress the catalytic activity of anion-exchange membranes with respect to the water dissociation reaction. Reduction of the water splitting rate can be achieved by replacing the ionic groups in the thin surface layer with equipolar ionic groups with low catalytic activity towards water dissociation reaction [4].

The aim of the work is to evaluate the influence of the change in the fraction of a non-conducting surface, as well as the different degree of dispersion of an ion exchanger in the manufacture of heterogeneous membranes on their properties. Investigate experimental heterogeneous and modified anion-exchange membranes by the method of a rotating membrane disk.

Experiments

To assess the effect of the share of a non-conductive surface on the total mass transfer the objects of study were selected experimental heterogeneous sulfo-cation-exchange membranes Ralex CM Pes (MEGA as, Czech Republic). The volume fraction of the ion exchange resin in the mixture used in the manufacture of CM Pes membranes is 58%. The membranes were obtained by rolling the homogenized mixture of milled ion-exchanger with varying time of its milling with polyethylene.

In order to evaluate the effect of water dissociation on electroconvection, highly basic anion-exchange membranes were used: homogeneous AMX ("Tokuyama Soda", Japan) and modified heterogeneous membrane MA-41-M (OOO IP Shchekinoazot, Russia).

The electroconvection is investigated under conditions of forced hydrodynamic convection when the linear velocity of flow of an electroconvection-unperturbed solution is nonzero.

Membranes were investigated by the method of a rotating membrane disk. The working solution was used 0.01 M solution of NaCl. The current-voltage characteristics (CVC), the limiting current density at different speeds of rotation of RMD were calculated.

Results and Discussion

Figure 1 shows CVC calculated for heterogeneous anion-exchange membranes with different ratios of nonconducting (l) and conducting ($\bar{l}$) areas and, hence, different surface fractions of inert areas $\theta = \frac{l}{l+\bar{l}}$. For comparison, the CVC of a homogeneous anion-exchange membrane is shown in the same figure. The ohmic potential jump $\Delta\varphi_{ohm}$ is excluded from the potential $\Delta\varphi$ of the membrane/solution system.

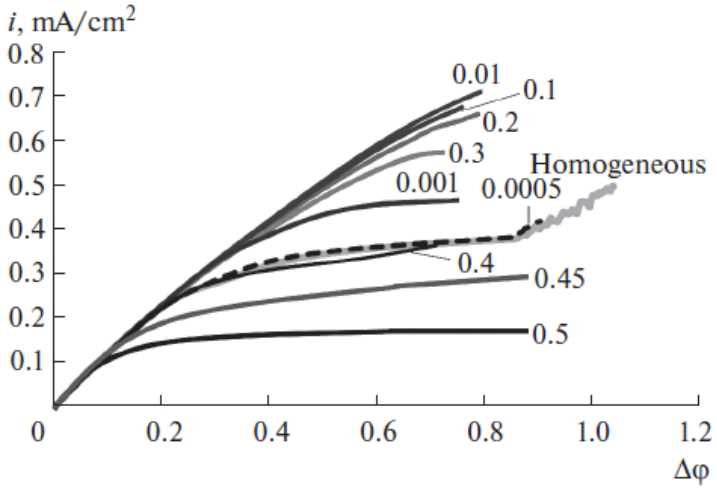

Figure 1. Current–voltage characteristics of a homogeneous anion-exchange membrane and heterogeneous anionexchange membranes with different surface fractions of inert regions $\theta = \frac{l}{l+\bar{l}}$ *Values of θ for the membranes are given at the CVC curves. The ohmic potential jump* $\Delta\varphi_{ohm}$ *of the membrane is excluded from the potential jump* $\Delta\varphi$.

As can be seen from figure the CVC curve for the homogeneous membrane has three segments. In contrast to the homogeneous membrane, on the current-voltage characteristics of the heterogeneous membrane, the plateau of limiting current is absent. As can be seen from fig. 1, electroconvective vortices appear on heterogeneous membranes even before the onset of the limiting state.

At a large value of θ > 0.3, mass transfer through the homogeneous membrane is higher than through the heterogeneous membranes. In this case, the effect of shielding the heterogeneous membranes by inert areas (polyethylene) is higher than the contribution of heteroelectroconvection. At a 40:60 percentage ratio of the nonconducting and conductive areas (θ = 0.4), the mass transfer through the homogeneous and heterogeneous membranes is almost the same. At θ < 0.3, mass transfer through the heterogeneous membrane exceeds that through the homogeneous membrane as a result of the development of heteroelectroconvection.

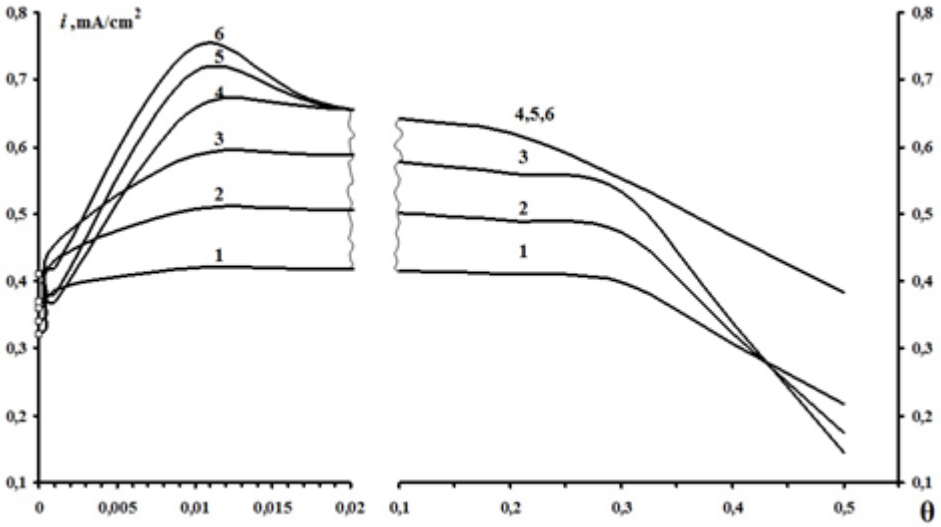

Figure 2. Dependence of the current density in terms of salt ions on the fraction of inert regions on the membrane surface for different values of electric potential jump Δϕ: (1) 0.4, (2) 0.5, (3) 0.6, (4) 0.7, (5) 0.8, and (6) 0.9 V.
The data points on the y axis refer to the current density for the homogeneous membrane at different voltages.

The dependence of the current density on the surface fraction of the nonconducting portions θ for different values of the electric potential jump Δφ is shown in Figure 2. The maximum transfer of salt ions at this step size is observed for the heterogeneous membranes with a polyethylene surface fraction of θ = 0.01. With a change in the degree of dispersion of the ion exchange resin and polyethylene, the value of θ corresponding to the maximum mass transfer through the heterogeneous membrane will be different.

We can conclude that the optimal proportion of conductive areas should be more than 70% by analyzing the data obtained.

As is known, the water spliting influences strongly on electroconvection, which flows in an electro-membrane system under ultra-limiting current conditions simultaneously with electroconvection.

In Figure 3, the experimental CVCs are summarized in Levich coordinates. The solid line shows the dependence of the limiting current on the speed of rotation of the membrane disk for a homogeneous membrane (AMX), and the dotted and dash-dotted lines show, respectively, for the heterogeneous MA-41 and MA-41M membranes. The dots represent i_{lim}, found from the experimental CVC tangent method.

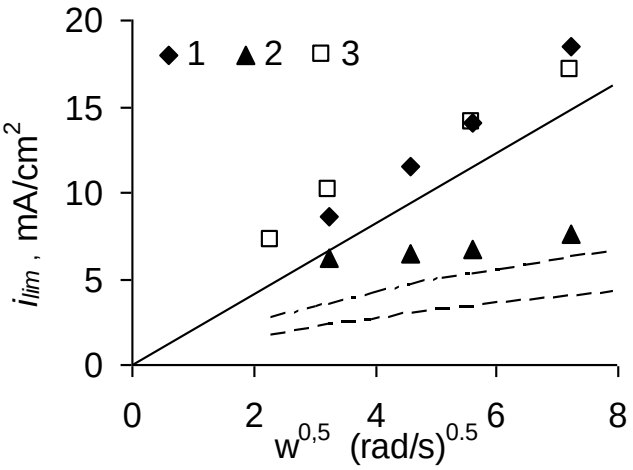

Figure 3. Limiting current vs. the square root of the rotation angular velocity (Levich coordinates) for different membranes. The points are the experimental values of the limiting current for the membranes: 1 – AMX; 2 – MA-41; 3 – MA-41M.

A comparison of experimental limit currents and calculated electrodiffusion limit currents shows that electroconvective transfer of ions in dilute solutions is already observed at $i = i_{\text{lim}}$. For the modified heterogeneous membrane, i = ilim electroconvection ion transport is more than three times greater than the electrodiffusion transport of ions.

Acknowledgements

This research was financially supported by Fund for Promoting Innovation contract №12667GU/2017.

References

1. *Zabolotsky V.I., Novak L., Kovalenko A.V., Nikonenko V.V., Urtenov M.H., Lebedev K.A., But A.Y. //* Petroleum Chemistry. 2017. V. 57. Iss. 9. P. 779.
2. *Dukhin S. S., Mishchuk N.A.* // J. Membr. Sci. 1993. V. 79. P. 199.
3. *Rubinstein B. Zaltzman J. Pretz C. Linder* // Rus. J. Electrochem. 2002. V. 38. P. 864
4. *Zabolotsky V.I., Sharafan M.V., Chermit R. Kh.* RF Patent No 2013133028 dated 2015

EXPERIMENTAL STUDY OF SURFACE MORPHOLOGY OF ION-EXCHANGE MEMBRANES AND ITS IMPACT ON THE MEMBRANE ELECTROCHEMICAL CHARACTERISTICS

[1]Dmitrii Butylskii, [1]Semyon Mareev, [2]Christian Larchet, [2]Lasaad Dammak, [1]Victor Nikonenko

[1]Membrane Institute, Kuban State University, Krasnodar, Russia, E-mail: *dmitrybutylsky@mail.ru*

[2]Institut de Chimie et des Matériaux Paris-Est, UMR 7182, 2 Rue Henri Dunant, 94320 Thiais, France

Introduction

The influence of the surface morphology of ion-exchange membranes (IEMs) on mass transfer rate is a fundamental and practical important issue in all applications. It is known that the IEM surface can be geometrically or electrically heterogeneous [1, 2].

The geometric surface heterogeneity can be expressed as waviness or roughness. Furthermore, some methods for IEM profiling are known in the industry to make geometric surface heterogeneity. The undulated or profiled membrane surface results in an essential gain in mass transfer rate [3, 4, 5] due to several effects: an increase in active membrane area available for mass transfer; an increase in contribution of the forced convection due to better hydrodynamic conditions.

The electrical surface heterogeneity can be expressed as the presence of conductive and non-conductive regions on the membrane surface. Experimental studies have shown that inhomogeneities of IEM surface in some conditions cause a decrease [6] and in the others an increase [7] in mass transport in membrane system.

Our work displays the application of Scanning Electrochemical Microscopy (SECM) method for investigation of geometrical and electrical surface heterogeneity of IEMs.

Experiments

Developed scanning electrochemical microscope consisted of an electrodialysis (ED) cell, hydraulic and instrumentation systems. The design of the ED cell 2 allows for the in situ SECM measurement of the potential distribution near the surface of ion-exchange membrane during electrodialysis.

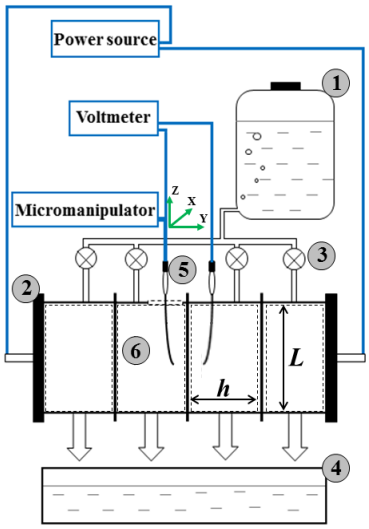

Figure 1. Schematic Representation of the Scanning Electrochemical Microscope. h is the distance between the membranes in the cell, L is the channel length. 1 – sealed container, 2 – electrodialysis cell, 3 – valves, 4 – common tank, 5 – mobile capillary, 6 – desalination compartment.

The compartments of the flow cell are formed by membranes and Plexiglas frames with a square hole of a 2 × 2 cm^2 area. Solution inlets and outlets of the Plexiglas frames ensured plane-parallel flow of the solution between the membranes.

The tips of Luggin glass capillaries are installed from both sides of the studied membrane. Mobile capillary 5 is placed in desalination compartment 6 of the ED cell through a hole in the upper part of the compartment. Such an arrangement allows moving the capillary by the micromanipulator in three directions. A fixed capillary in the concentration compartment is fasten in the frame adjacent to the surface of the studied membrane.

All measurements were conducted in 0.02 M NaCl solution at current density of 0.5 j_{lim}.

Potential drops were measured between a mobile capillary which moves towards the membrane surface and a fixed capillary connected to the reference electrodes (Ag/AgCl) as a function of distance.

Results and Discussion

The surfaces of undulated IEMs were visualized using the SECM method. In the case of Neosepta CMX membrane a significant correlation between the average value of amplitude excursion, *b*, of swollen membrane determined *in situ* by SECM (45 ± 5 μm) and by optical microscopy (55 ± 10 μm) (Fig. 2) was found. We attribute this undulation to non-uniform swelling of the membrane, which is caused by the presence of reinforcing net and non-uniform distribution of ion-exchange material.

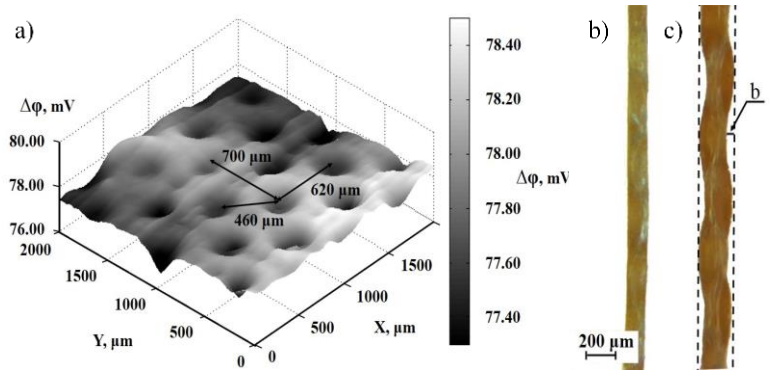

Figure 2. Potential Drop Distribution Near the Surface of the CMX Membrane (a), Optical Cross Section Images of the Dry (b) and Swollen (c) CMX Membrane.

The presence of conductive and non-conductive regions on the IEMs was visualized using the SECM method. It was found for the M1 and M2 membranes that the data obtained by SECM method correlates with optical images (Fig. 3) and theoretical conceptions [2].

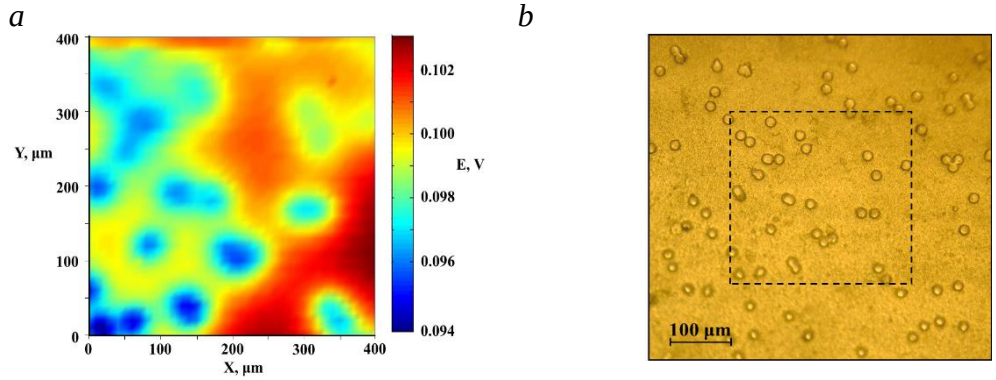

Figure 3. Potential Drop Distribution Near the Surface of the M2 Membrane (a) and an Optical Image of This Membrane (b).

In addition there is an interest in the electrochemical characteristics investigation of studied membranes having different electric and geometric surface heterogeneity.

Acknowledgments

We are grateful to the RFBR (17-08-01538 A) for financial support.

References

1. *Butylskii D. Y. et al.* // Electrochimica Acta. 2018. Vol. 273. P. 289-299.
2. *Butylskii D. Y. et al.* // Petroleum Chemistry. 2016. Vol. 56. №. 11. P. 1006-1013.
3. *Balster J. et al.* // J. Phys. Chem. 2007. Vol. 111. P. 2152–2165.
4. *Zabolotskii V. I. et al.* // Russ. J. Electrochem. 2005. Vol. 41. P. 1053–1060.
5. *Vermaas D. A. et al.* // J. Membr. Sci. 2014 Vol. 453. P. 312–319.
6. *Rubinstein I. et al.* // Physical review E. 2002. Vol. 65. №. 4. P. 041507.
7. *Davidson S. M. et al.* // Sci. Rep. 2016. Vol. 6. P. 22505.

MEMBRANE SPECIFIC PERMSELECTIVITY IN MIXED SOLUTIONS

[1]Dmitrii Butylskii, [2]Daria Chuprynina, [3]Tongwen Xu, [1]Natalia Pismenskaya

[1]Membrane Institute, Kuban State University, Krasnodar, Russia, E-mail: *dmitrybutylsky@mail.ru*

[2]Department of Analytical Chemistry, Kuban State University, Krasnodar, Russia

[3]CAS Key Laboratory of Soft Matter Chemistry, Collaborative Innovation Center of Chemistry for Energy Materials, University of Science and Technology of China, Hefei, China

Introduction

Ion exchange membranes (IEM) are main component in numerous engineering applications, such as dialysis, electrodialysis, fuel cells etc. Creation of specific permselective membranes is one of the most important tasks for modern membrane science [1]. Another no less important problem is the creation of precise techniques to determine the specific permselectivity. The verification of the method for membrane permselectivity estimation in mixed solutions during electrodialysis is reported here.

Experiments

Neosepta CMX (Japan), CJMC-3 and CJMC-5 (China) cation-exchange membranes were used to verify the method for membrane specific permselectivity estimation in mixed solutions during electrodialysis. The measurements were carried out in a four-chamber electrodialysis cell. A 0.02 eq/dm^3 mixed NaCl − $CaCl_2$ (1:1) solution circulated through the desalting chamber. In the remaining chambers, a 0.02 M NaCl solution was pumped. The Na^+ and Ca^{2+} concentrations were found using Dionex ICS-3000 ion-chromatograph with conductometric detector.

Results and Discussion

It is found that when the current density increases, the specific permselectivity of the membrane system declines. This effect is explained by the fact that at low current densities, the specific permselectivity is controled by the transport in the membrane, and at high current densities close to the limiting current density, this property is mainly determined by the transport through the depleted diffusion boundary layer [2].

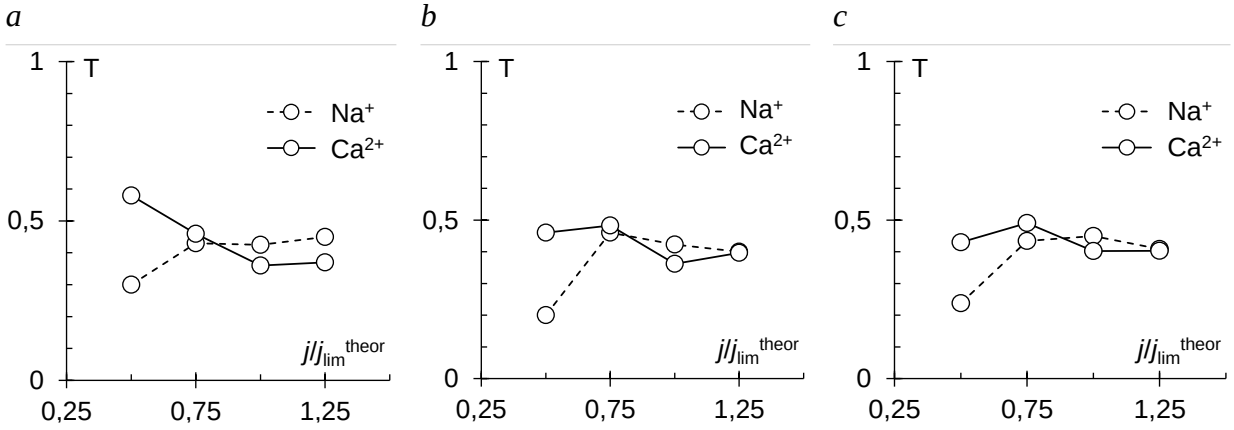

Figure 1. Counterions transport numbers in cation-exchange membranes: Neosepta CMX (a), CJMC-3 (b) and CJMC-5 (c).

Acknowledgments

We are grateful to the Russian Science Foundation (19-19-00381) for financial support.

References

1. *Luo T., Abdu S., Wessling M.* Selectivity of ion exchange membranes: A review// J. Membr. Sci. 2018. V. 555. P. 429.
2. *Nikonenko V. V., Zabolotskii V. I., Lebedev K. A.* Model for the competitive transport of ions through ion exchange membranes // Russ. J. Electrochem. 1996. V. 32. P. 234-236.

MODELING OF OXYGEN TRANSPORT IN HOLLOW FIBER MEMBRANES

[1]Sergey Bychkov, [1]Elena Shubnikova, [1]Mikhail Popov, [1,2]Stanislav Chizhik, [1]Alexander Nemudry

[1]Institute of Solid State Chemistry and Mechanochemistry SB RAS, Novosibirsk, Russia
[2]Novosibirsk State University, Novosibirsk, Russia, E-mail: *csagbox@gmail.com*

Introduction

Oxygen transport membranes (OTMs) made of the mixed ionic-electronic conducting (MIEC) oxides can be used in such innovative technologies as partial oxidation of light hydrocarbons and oxy-fuel combustion [1–2]. A significant drawback of planar and tubular membranes is the high requirements for the absence of significant temperature gradients along the membrane, which can result in the destruction of OTM during thermal cycling and abrupt temperature changes. The advantages of hollow fiber (HF) membranes are not only improved mechanical stability but also higher oxygen fluxes due to small thickness of gas-tight layer sandwiched between porous layers. In addition to technological advantages, (HF) are convenient as an object of study of the mechanism of oxygen exchange of oxides with the gas phase. However, such works are still few in comparison with the number of studies on the oxygen permeability of planar membranes.

Experiments

$Ba_{0.5}Sr_{0.5}Co_{0.8}Fe_{0.2}O_{3-\delta}$ (BSCF), $Ba_{0.5}Sr_{0.5}Co_{0.78}W_{0.02}Fe_{0.2}O_{3-\delta}$ (BSCFW2) and $Ba_{0.5}Sr_{0.5}Co_{0.75}Mo_{0.05}Fe_{0.2}O_{3-\delta}$ (BSCFM5) materials were synthesized by ceramic method described in [3, 4]. The obtained precursors were calcined at 900°C for 6 h in air. The powders were then pressed into green disks at 300 MPa followed by sintering at 1100–1160°C in air for about 6 h to get dense samples. The crystal structure of BSCF/ BSCFW2/ BSCFM5 samples was examined by X-ray powder diffraction using D8 Advance diffractometer (Bruker, Germany).

Results and Discussion

This work presents the results of an experimental study and computer simulation of oxygen transport in HF membranes made of $Ba_{0.5}Sr_{0.5}Co_{0.8}Fe_{0.2}O_{3-\delta}$ (BSCF) material and its derivatives: $Ba_{0.5}Sr_{0.5}Co_{0.78}W_{0.02}Fe_{0.2}O_{3-\delta}$ (BSCFW2) and $Ba_{0.5}Sr_{0.5}Co_{0.75}M_{0.05}Fe_{0.2}O_{3-\delta}$ (BSCFM5) which demonstrate high and stable oxygen fluxes, thermal and mechanical stability during thermal cycling. Computer simulation of oxygen fluxes in membranes were based on a semi-empirical dependence of the oxygen flux on the partial pressures of oxygen (pO_2) which is widely used in the case of flat membranes and was rationalized by the oxygen transport model presented in:

$$J = \frac{pO_{2,1}{}^{n} - pO_{2,2}{}^{n}}{\frac{h}{DK} + \frac{2}{k_{ads}}} = \gamma(T)(pO_{2,1}{}^{n} - pO_{2,2}{}^{n}) \quad (1)$$

Acknowledgements

The research was funded within the state assignment to ISSCM SB RAS (project No. AAAA-A17-117030310277-6).

References

1. *J. E. ten Elshof, B. A. van Hassel, H. J. M. Bouwmeester,* Activation of methane using solid oxide membranes // Catal. Today. 25 (1995) 397–402.
2. *F. M. B. Marques, V. V. Kharton, E. N. Naumovich, A. L. Shaula, A. V. Kovalevsky, A. A. Yaremchenko* // Solid State Ionics 177 (2006) 1697–1703.
3. *M. P. Popov, S. F. Bychkov, A. P. Nemudry*, Direct AC heating of oxygen transport membranes // Solid State Ionics 312 (2017) 73–79.
4. *E. V. Shubnikova, O. A. Bragina, A. P. Nemudry*, Mixed conducting molybdenum doped BSCF materials // J. Ind. Eng. Chem. 59 (2018 [R2.2]) 242–250.

TREATMENT OF ACIDIC WASTEWATER USING MEMBRANE TECHNOLOGIES

[1]Ladislav Čopák, [2]Anastasia Bocharova
[1]MemBrain s.r.o., Pod Vinicí 87, 471 27, Stráž pod Ralskem, Czech Republic
E-mail: *ladislav.copak@membrain.cz*
[2]Kuban State University, Krasnodar, Stavropolskaya Street 149, Russia

Introduction

The concept of diffusion dialysis (DD) followed by electrodialysis (ED) was applied to process technological wastewater containing ca 12 wt. % of sulphuric acid, metal sulphate ions and undefined organic substances. DD parameters like acid recovery ratio and metal ions rejection factors and purity of outlet streams were evaluated in the presented work. The ED was applied on the dialysate stream leaving DD process. The ED process was evaluated regarding the flux of salt, feed capacity, current efficiency and specific energy consumption. Similar concept for processing of acidic waste water was recently proposed by Zou et al. (2018). This study results show big potential for processing the acidic wastewater by membrane technologies while bringing ecological and economical benefits.

Experiments

The experiments were carried out with real waste water sample. The wastewater was provided by a customer who is interested in decreasing the costs for disposal of the spent acidic solution. Table 1 presents feed water composition measured by inductively coupled plasma (ICP), ion chromatography (IC), titration and thermal methods.

Table 1: Feed Water Quality Analysis Results

Parameter	Value	Method
Na (mg l^{-1})	55500	ICP
Zn (mg l^{-1})	258	
K (mg l^{-1})	50.5	
Ca (mg l^{-1})	44.6	
Fe (mg l^{-1})	27.3	
Si (mg l^{-1})	20.8	
Mg (mg l^{-1})	9.18	
Al (mg l^{-1})	4.14	
Sulphates (mg l^{-1})	289000	IC
H_2SO_4 (g l^{-1})	148.591	titration
TOC (mg l^{-1})	953	thermal combustion
Density (kg l^{-1})	1.2242	

Figure 1 shows the scheme of the wastewater processing. In most cases, processing of technological wastewater requires pre-treatment. The solution was mixed with activated carbon to remove as much organic compounds as possible, filtration followed.

Recovery of the acid proceeded in the DD step in single-pass, continuous regime. For this purpose, innovative spiral wound membrane module (Spiraltec GmbH) with anion exchange membrane FAD (Fumatech, active area ca 5 m^2) was employed. Flowrate of water and the acidic feed was kept at 9 l h^{-1}. Under the driving force of concentration gradient, acid is transported from the feed into water. The metal cations are repulsed by the positively charged anion exchange membrane. The metal cations thus diffuse significantly slower than the acid anions and hydrogen cations which have very high mobility compared to other ions. In this experiment, deionized water was used as a stripping medium. There are two streams leaving the module: diffusate (water enriched by acid) and dialysate (wastewater containing majority of salts after the dialysis). The desired product is diffusate containing significantly lower concentrations of the metal ions than dialysate. Obtained acid can be reused in the production process. Further, the obtained dialysate was neutralized with NaOH and stabilized against iron oxidation and precipitation by the addition of $Na_2S_2O_5$. This solution was further processed with electrodialysis in batch regime. The ion

exchange membranes Ralex^{TM} of the manufacturer Mega a.s. were used. The aim of the ED step was to demineralise dialysate.

All samples from the DD step were taken during the steady state which was indicated by steady value of conductivity measured in time, as well as flow rate of the dialysate and the diffusate.

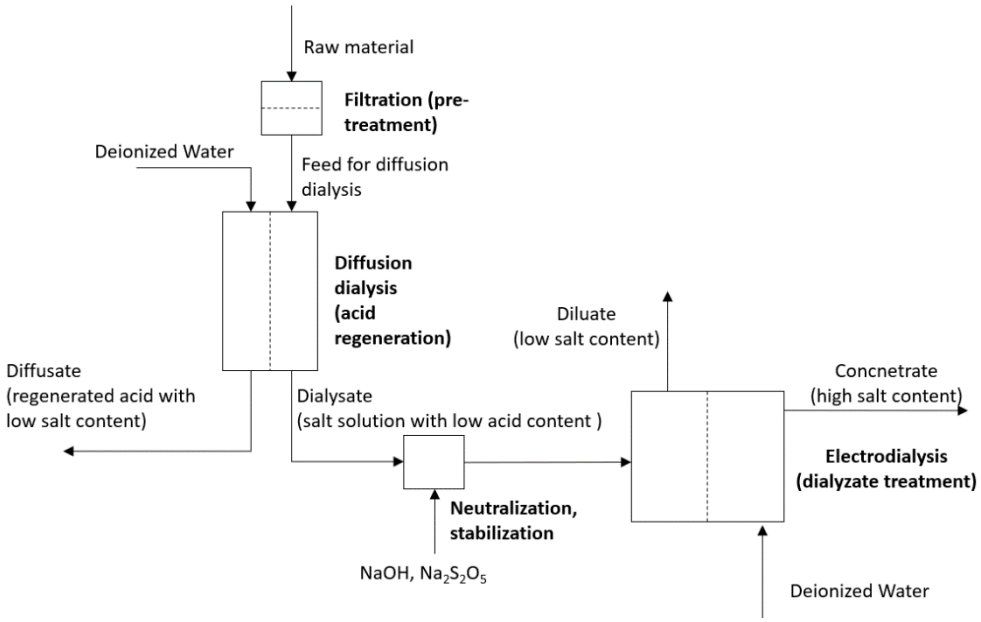

Figure 1. Process flow diagram of the acid regeneration and salt concentration.

Results and Discussion

Results of the DD step are shown in Table 2. Flow rates of the dialysate and the diffusate were 165 ml min^{-1} and 150 ml min^{-1}, respectively.

Table 2: Feed Water Quality Analysis Results

REJECTION FACTOR (%)	NA	82
	ZN	96
	K	88
	CA	91
	FE	86
	SI	61
	MG	94
	AL	92
	TOC	81
RECOVERY RATIO (%)	H_2SO_4	87

The rejection factor R_i of each metal ion i, acid recovery fraction Y and purity P_j of outlet stream j were calculated from the equations 1 - 3

$$R_{\mathrm{I}} = 1 - \frac{\dot{m}_{\mathrm{I,DIF}}}{\dot{m}_{\mathrm{I,FEED}}} \quad (1)$$

$$Y = \frac{\dot{m}_{\mathrm{H_2SO_4,DIF}}}{\dot{m}_{\mathrm{H_2SO_4,FEED}}} \quad (2)$$

$$P_j = \frac{c_{\mathrm{H^+,J}}}{\sum_i c_{\mathrm{I,J}}} \quad (3)$$

where $\dot{m}_{i,\mathrm{DIF}}$ represents mass flow of component i (Na, Zn, … , Al) in the diffusate in kg s^{-1}, $\dot{m}_{i,\mathrm{FEED}}$ represents mass flow of component i in the feed in kg s^{-1} and $c_{i,j}$ represents concentration of component i in stream j (feed, diffusate or dialysate) in mol l^{-1}.

We can see that the rejection factors of the monovalent metal ions (Na, K) are lower than the rejection factors of the multivalent ions such as Mg^{2+} or Al^{3+}. Low value of the Si rejection factor can be caused by the fact that Si is in the form of uncharged species which diffuse through the anion exchange membrane.

In total, 6 ED tests were carried out. Table 3 contains results of the third test. Usage of $Na_2S_2O_5$ was 1 g/l to maintain reduction environment. To decrease the precipitation potential, also small amount of antiscalant (Ropur 6000A) was added into the concentrate solution (C). Compositions of C and diluate (D) are also in Table 3. Concentration of organic matter was not determined.

Table 3: Quality Analysis Results of ED feed and products

	C	D
CA (MG L^{-1})	**35.6**	**3.06**
FE (MG L^{-1})	**14.1**	**1.91**
K (MG L^{-1})	**128**	**1.74**
MG (MG L^{-1})	**5.62**	**0.413**
NA (MG L^{-1})	**31100**	**2010**
ZN (MG L^{-1})	**40.6**	**1.91**
SULPHATES (MG L^{-1})	**55575.0**	**3945.0**
TDS (MG L^{-1})	**98400**	**6850**

	D	C	E
INITIAL WEIGHT (KG)	**1.01**	**0.41**	**0.251**
FINAL WEIGHT (KG)	**0.63**	**0.69**	**0.229**
STACK VOLTAGE (V)	**10**	CURRENT RESTRICTION (A)	**1.54**
FLUX OF SALT (G M^{-2} H^{-1})	**573**	FEED CAPACITY (KG M^{-2} H^{-1})	**7.63**
CURRENT EFFICIENCY (%)	**96**	SPECIFIC ENERGY CONSUMPTION, (WH KG_{F}^{-1})	**28**

The value of TDS of concentrate stream is not high compared to the feed solution. Due to small amount of the feed sample for the ED step, tests with maximum achievable concentration approach were not performed. For such a case bigger volume of feed per one test would be needed. Instead of performing one test with achieving high sulphate concentration, we decided to perform several tests to check the effect of the solution on the membranes. There were no effects on the ED performance nor visual damage of the membranes observed.

We have proven the applicability of the diffusion dialysis followed by electrodialysis concept for highly acidic waste water treatment in the laboratory scale. The free acid can be regenerated from the solution and reused in the production process while the salt solution can be treated with electrodialysis. There is evident environmental (less emissions into nature) and economic impacts with utilization of the membrane separation methods. The capital and operating costs for the pre-treatment, DD and ED technologies should be compared by the cost benefits brought by utilization of DD and ED. The benefits are as follows:

- chemical cost saving due to recovered sulphuric acid,
- chemical cost savings due to saving of the neutralizing agent (Na_2CO_3),
- savings of the penalty fee for high TDS content in the waste water,
- ideally earning money by selling of the salts.

In the presented process example, the savings for H_2SO_4 and Na_2CO_3 for 1 ton of processed waste (12 % H_2SO_4) water are 5 $ and 29 $ (40$ t^{-1} H_2SO_4, 210 $ t^{-1} Na_2CO_3), respectively. The other factors (fees) are individual for each company but can be in the similar range as saved money for buying of the fresh chemicals.

Acknowledgements

This work was carried out in the frame of the IP project (Decision Nr. 6/2018) supported by the Czech Ministry of industry and trade and in the frame of project LO1418 supported by the Czech Ministry of education, youth and sports. The project utilizes Membrane innovation centre infrastructure.

References

1. *Zou L., Wu Y., Zhang G.* Separation of acidic HCl/glyphosate liquor through diffusion dialysis and electrodialysis // Desalination and Water Treatment 2018. V. 105. P. 199-208.

DIFFUSION PERMEABILITY OF ION-EXCHANGE MEMBRANES IN SOLUTIONS OF SULFURIC ACID AND CHROMIUM SULFATE

Ekaterina Dankovtseva, Irina Falina
Kuban State University, Krasnodar, Russia, E-mail: *irina_falina@mail.ru*

Introduction

The electroplating industry is one of the largest consumers of water and the most dangerous source of environmental pollution of heavy metals. Partial treatment of wastewater from pollution with the purpose of their reuse in the same production is much cheaper than their full treatment. Electromembrane technologies allow creating closed water circulation systems and returning valuable components to the production cycle. The limiting electrodialysis concentration is restricted by back diffusion of the ions from the concentration chamber to desalination one. To increase the content of the target component in the solution, it is necessary to change the membrane properties in order to obtain materials with low diffusion permeability, for example, by their modification by conjugated polymers [1]. The purpose of this work is the comparative study of the diffusion permeability of ion-exchange membranes and composites with polyaniline on their basis in solutions containing H^+ and Cr^{3+}-ions.

Experimental

The objects of study were homogeneous perfluorinated membrane MF-4SK, heterogeneous membrane MK-40, as well as composite with polyaniline on the base of MK-40, obtained in an electrodialysis apparatus [2]. The value of the integral diffusion permeability coefficient (P, m^2/s) was determined from the diffusion rate of the electrolyte H_2SO_4, $Cr_2(SO_4)_3$ and their equivalent mixture of various concentrations into pure water. The experimental error didn't exceed 5%.

Results and Discussion

Figure 1 shows the concentration dependences of the integral diffusion permeability coefficient of the investigated membranes in solutions of sulfuric acid. It can be seen from the Fig. 1 that the diffusion permeability of the MK-40 membrane after modification is 3 - 4 times lower in comparison with the initial sample. In addition, for a modified sample, the diffusion permeability is almost independent of the electrolyte concentration.

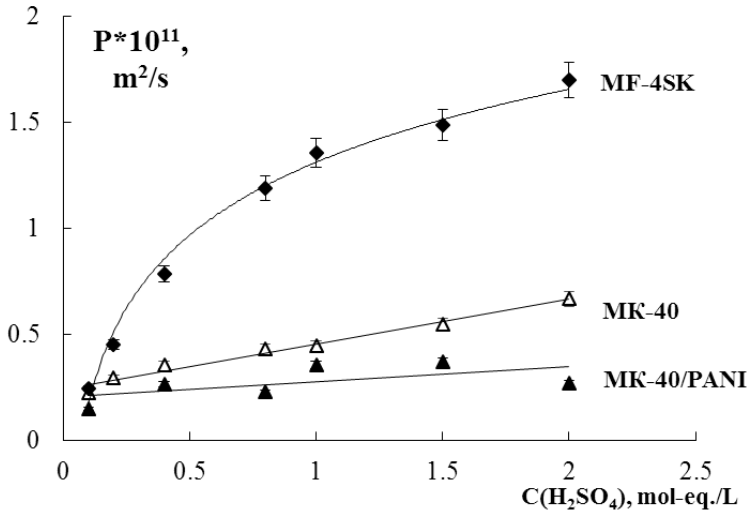

Figure 1. Concentration dependences of diffusion permeability of the MK-40, MF-4SK and MK-40/PANI membranes in sulfuric acid solutions.

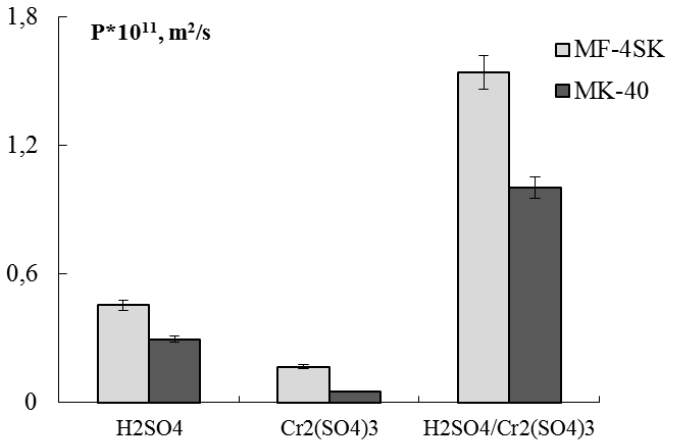

Figure 2. Diffusion permeability of the MK-40, MF-4SK membranes in different solutions with concentration 0.2 mol-eq./L.

Figure 2 shows the diffusion permeability of the membrane MF-4SK and MK-40 in 0.2 mol-eq./L solutions of H_2SO_4, $Cr_2(SO_4)_3$ and their equivalent mixture. One can see that the diffusion permeability of the membranes is significantly lower in the chromium sulfate solution than in the sulfuric acid solution. This is due to the influence of the counterion on the diffusion transfer, since co-ions are identical in these electrolytes. An increase in diffusion permeability of both membranes in the equivalent mixture of $Cr_2(SO_4)_3$ and H_2SO_4 is observed. It could be caused by blocking of fixed ions by the triply-charged cations, which facilitates the transport of co-ions and leads to an increase in the diffusion permeability of the membranes in the mixed solution.

Acknowledgements

The work was funded by Russian Foundation for Basic Research (project No 18-38-20069 mol_a_ved).

References

1. *Sata T., Sata T., Yang W.* Studies on cation-exchange membranes having permselectivity between cations in electrodialysis // Journal of Membrane Science, Volume 206, Issues 1–2, 31 August 2002, Pages 31-60.
2. *Loza N.V., Loza S.A., Kononenko N.A., Magalyanov A.V.* Ion transport in sulfuric acid solution through anisotropic composites based on heterogeneous membranes and polyaniline // Petroleum Chemistry. 2015. Vol. 55. № 9. P. 724-729.

MULTIFUCTIONAL COMPOSITE ADSORBENT BASED ON HYDRATED ZIRCONIUM DIOXIDE CONTAINING NANOPARTICLES OF OXIDIZED GRAPHENE

[1]Yuliya Dzyazko, [1]Vladimir Ogenko, [2]Yury Volfkovich, [2]Valentin Sosenkin, [1]Katerina Kudelko, [1]Tatiana Yatsenko

[1] V.I. Vernadskii Institute of General & Inorganic Chemistry of the NAS of Ukraine, Kyiv, Ukraine
E-mail: *dzyazko@gmai.com*

[2]A.N. Frumkin institute of Physical Chemistry & Electrochemistry of the RAS, Moscow, Russia
E-mail: *yuvolf40@mail.ru*

Introduction

Graphene oxide (GO, one graphite sheet) and GO-like materials (several sheets) are attractive adsorbents of inorganic ions [1] and organic molecules [2]. Ion exchange ability is due to carboxyl groups, which are located along perimeter of nanoparticles. Phenolic groups make also their contribution to ion exchange. These groups provide hydrophilicity of some GO regions. GO contains also hydrophobic regions [3, 4] that are responsible for adsorption of neutral organic molecules. Both hydrophilic and hydrophobic pores can be recognized with a method of standard contact porosimetry (MSCP) that is suitable not only for carbon [3, 4] but also for any other materials, for instance, ion exchange polymers [5, 6].

Unfortunately practical application of GO materials in adsorption columns is difficult due to their small particle size, since such particles provide high hydrodynamical resistance. Other important limitation is good dispersibility. It means difficult separation of solid and liquid: baromembrane methods are required for this purpose. The solution of this problem is to develop GO-containing composites. Hydrated zirconium dioxide (HZD) has been proposed, since oxides of multivalent metals possess not only cation exchange, but also anion exchange ability.

Experimental

GO has been obtained from graphite using the modified Hammer's method. [7]. The composite was synthesized by dispersion of GO in sol of insoluble zirconium hydroxocomplexes followed by ultrasonic activation and precipitation. The composite contained ≈2% of GO. The material as well as its constituents were investigated with MSCP and TEM. The isotherms of Pb^{2+} and $HCrO_4^-$ adsorption from one-component solutions have been obtained, adsorption of phenol from water was also investigated.

Results and discussion

HZD primary particles formed elliptic splices (up to 150 nm) with uneven edges (Fig. 1a). GO nanoparticles are distributed on the HZD surface. Carbon is evaporated under the action of accelerated electrons. Chains of fused spherical and elliptic HZD nanoparticles (≈20 nm) have been also found (Fig. 1b). Their surface is free from GO. The material includes also GO aggregates (50-150 nm), which are not associated with HZD surface. Their traces are seen in Fig. 1c. Thus, the HZD-FO sample consists of HZD particles, which are partially covered with GO, and GO aggregates.

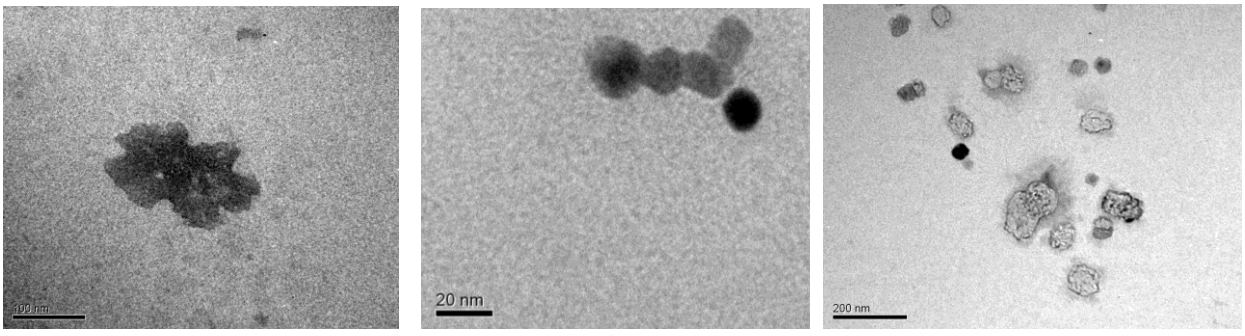

a *b* *c*

Figure 1. TEM images of HZD-GO composite.

Integral pore volume distributions, which were obtained both in water and octane media, are plotted in Fig. 2 as dependencies of pore volume (V) on logarithm of effective pore radius (r^*) [3]. The r^* term is applied to the materials containing both hydrophilic and hydrophobic pores. HZD is characterized by compact structure: this adsorbent is practically non-porous within the r^* interval of 1 nm - 2 μm: only a small build-up is visible at r^*=1.5 nm. Only micropores and macropores ($r^* > 2$ μm) contribute to porosity. At $r^* > 15$ μm , the effect of voides between granules is observed, this interval is outside the focus of our attention.

As opposed to completely hydrophilic HZD, GO contains both hydrophilic and hydrophobic regions. In contrast to ordinary carbon materials [3], the $V - r^*$ distribution for water medium is shifted towards lower r^* values relatively the curve obtained in octane (r^*<2 μm). It is typical for ion exchange membranes [5], which demonstrate strong swelling in water like ion exchange resins [6]. This "superhydrophilicity" is caused for hydration of functional groups. Micropores, which are evidently attributed to the voids between primary nanoparticles, are mainly hydrophilic. The region at 10-100 nm is related to hydrophilic pores caused by the interstices between aggregates. These pores are rather regular in octane medium. Hydration of the GO surface results in smoother build-up.

Starting at r^*=2 μm, hydrophobic pores dominate in GO. These macropores are attributed to agglomerates of micron size, curing of sheets etc. Thus, the pores caused by nanosized fragments and their aggregates are hydrophilic. At the same time, the voids between agglomerates are hydrophobic. It means, aggregation is due to formation of hydrogen bonds between functional groups along the particles On the contrary, agglomerates are formed by hydrophobic regions. This is probably due to involvement of hydrophilic regions in aggregate formation.

As opposed to HZD, the HZD-GO sample is characterized by developed pores in the interval of r^*=3 nm-1.5 μm. The integral distributions, which were obtained in different media, are rather close to each other due to the effect of hydrophilic inorganic matrix. However, the volume of hydrophilic pores is higher than that obtained in octane. This is observed within the interval of r^* =1 nm - 100 μm. In other words, this interval is much wider comparing with GO. The regular peaks at 20 (water) and irregular maximum at 50 (octane) nm are evidently due to GO.

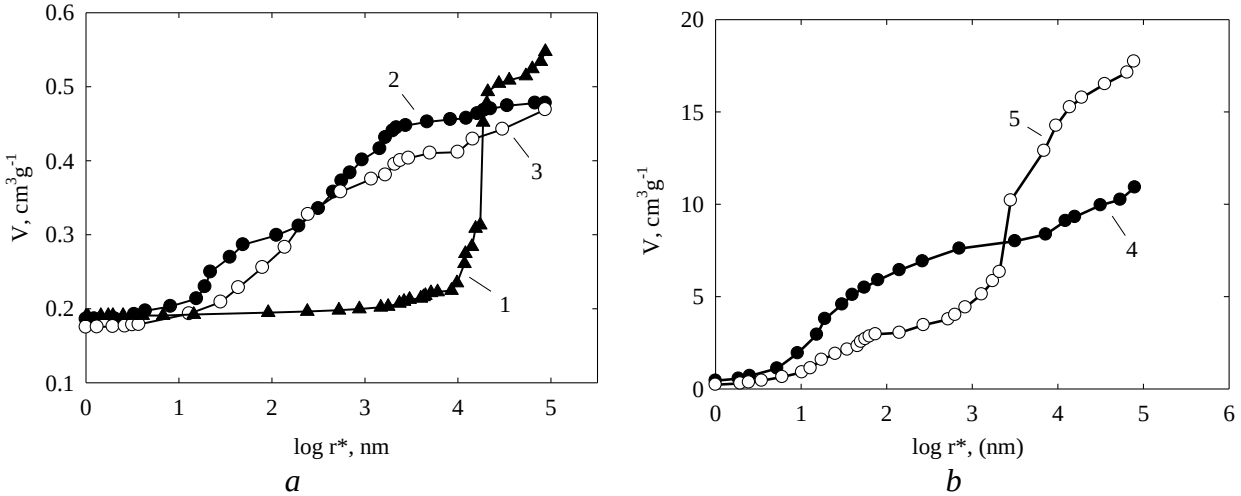

a *b*

Figure 2. Integral pore size distributions obtained for HZD (1), composite (2, 3) and GO (4, 5). Working liquid is water (1, 2, 4) or octane (3, 5).

The isotherm of Pb^{2+} adsorption on GO is characterized by a rapid build-up in the field of low equilibrium concentrations (C) followed by plateau (Fig. 3). In the case of HZD, the growth of adsorption capacity (A) is much slower. In comparison with HZD, the isotherm for HZD-GO shows a steeper ascent. GO in the composite depresses $HCrO_4^-$ adsorption: this is caused by screening of adsorption centers on the HZD surface.

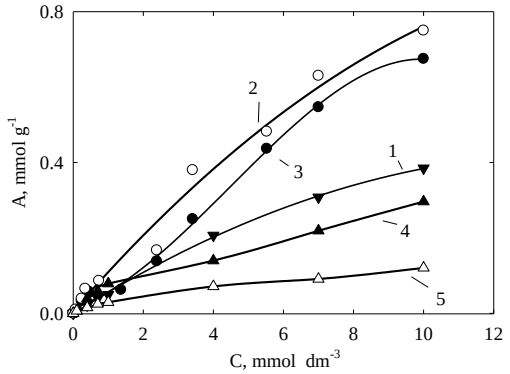

FIGURE 3. ISOTHERMS OF PB^{2+} (1-3) AND $HCRO_4^-$ (4, 5) ADSORPTION ON HZD (1, 4), GO (2) AND HZD-GO (3, 5).

TABLE 1: ADSORPTION OF PHENOL

SAMPLE	CONCENTRATION, MG DM^{-3}		REMOVAL DEGREE, %
	INITIAL	FINAL	
HZD	**5**	**4.7**	**6**
	21	**20.5**	**2**
	70	**69**	**1**
GO	**5**	**<0.001**	**100**
	21	**<0.001**	**100**
	70	**0.004**	**99**
HZD-GO	**5**	**<0.001**	**100**
	21	**0.03**	**99**
	70	**0.42**	**99**

Despite depressed anion exchange properties, the composite adsorbs phenol that is a weak acid (Table 1). When the initial concentration of this component is 5 mg dm^{-3}, the HZD-GO sample removes it down to maximal allowable concentration for tap water (1 μg dm^{-3}). Adsorption is due to hydrophobic regions of GO sheets. Indeed, pure GO sorbs phenol very efficiently. In the case of one-component HZD, adsorption of phenol is inconsiderable.

Conclusions

As opposed to BET method, the MSCP gives high specific surface area of GO in octane: this solvent wets ideally the sheet penetrating between them. Much higher value of surface area for water medium is caused by hydration of functional groups followed by swelling of GO. This behavior is similar to ion exchange polymers. The filler provides loosening of HZD within a wide interval of pore size. The filler improves adsorption of Pb^{2+} ions increasing the capacity in 1.7 times due to its expressed cation exchange properties. Contrary, GO depresses adsorption of $HCrO_4^-$ anions. The composite is effective towards weakly acidic phenol.

References

1. *Wu M., Kempaiah R., Huang P.-J.J., Maheshwari V., Liu J.* Adsorption and Desorption of DNA on Graphene Oxide Studied by Fluorescently Labeled Oligonucleotides // Langmuir. 2011. V. 27. N 6. P. 2731-2738.
2. *Sitko R., Turek E., Zawisza B., Malicka E., Talik E., Heimann J., Gagor A., Feist B., Wrzalik R.* Adsorption of divalent metal ions from aqueous solutions using graphene oxide // Dalton Trans. 2013. V. 42. N 16. P. 5682-5689.
3. *Shulga Y.M.. Baskakov S.A., Baskakova Y.V.. Lobach A.S., Kabachkov E.N., Volfkovich Y.M., Sosenkin V.E., Shulga N.Y., Nefedkin S.I., Kumar Y., Michtchenko A.* Preparation of graphene oxide-humic acid composite-based ink for printing thin film electrodes for micro-supercapacitors // J. Alloys Compounds. 2018. V. 730. P. 88-95.
4. *Volfkovich Y.M., Rychagov A.Y., Sosenkin V.E., Efimov O.N., Os'makov M.I.* Measuring the specific surface area of carbon nanomaterials by different methods // Russ. J. Electrochem. 2014. V.50. N 11. P.1099-1101.
5. *Kononenko N.A., Berezina N.P., Vol'fkovich Y.M., Shkol'nikov E.I., Blinov I.A.* Investigation of ion-exchange materials structure by standard porosimetry method. J. Appl. Chem. USSR. 1985. V. 58. N 10: P. 2029-2033.
6. *Dzyazko Y.S., Perlova O.V., Perlova N.A., Volfkovich Y.M., Sosenkin V.E., Trachevskii V.V., Sazonova V.F., Palchik A.V.* Composite cation-exchange resins containing zirconium hydrophosphate for purification of water from U(VI) cations // Desalination and Water Treatment. 2017. V. 169. P. 142-152.

7. *Marcano D.C., Kosynkin D.V., Berlin J.M., Sinitskii A., Sun Z., Slesarev A., Alemany L.B., Lu W., Tour J.M.* Improved synthesis of graphene oxide // ACS Nano. 2010. V. 4. N 8. P. 4806-4814.

DIFFUSION PERMEABILITY OF THE MODIFIED ION-EXCHANGE MEMBRANES IN SODIUM, CALCIUM AND MAGNESIUM CHLORIDE SOLUTIONS

Irina Falina, Vera Kolenkevich, Natalia Loza
Kuban State University, Krasnodar, Russia, E-mail: *irina_falina@mail.ru*

Introduction

Electromembrane technologies are widely used for separation and concentration of substances in the processing of raw materials in the dairy industry. In order to prevent the fouling on the membrane surface by the whey components, a thin layer of oppositely charged modifier covers the membrane surface [1]. The modification of the cation exchange membrane by polyaniline is the prospective for this purpose, but it may change the transport properties of the membrane towards the ionic components of the whey. The aim of the work was to study the influence of the surface modification of heterogeneous MK-40 cation exchange membrane by polyaniline on the diffusion transfer of sodium, calcium and magnesium chlorides solutions.

Experiments

The modification of the heterogeneous MK-40 cation-exchange membrane was performed by successive diffusion of the monomer (anilinium chloride) and oxidant (ammonium peroxydisulfate) solutions through the membrane to water. After modification the membrane was washed with water and immersed in electrolyte solution. Diffusion permeability was determined by the diffusion of the electrolyte through the membrane to water.

Results and Discussion

The concentration dependencies of the initial and modified membranes diffusion permeability are shown on Fig. One can see, that for NaCl solution the diffusion permeability increases as the concentration rise while for $CaCl_2$ and $MgCl_2$ solutions it reduces, that is typical for electrolytes containing divalent ions [2].

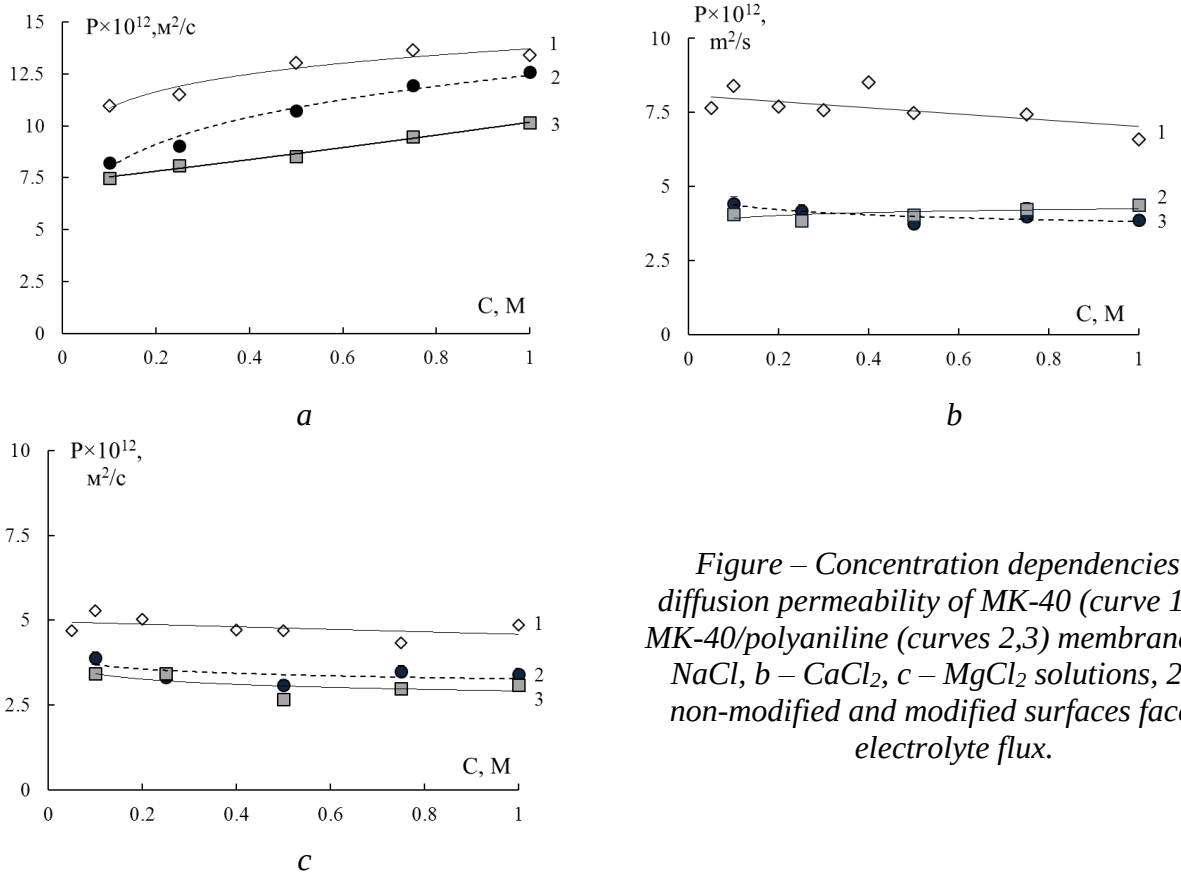

Figure – Concentration dependencies of diffusion permeability of MK-40 (curve 1) and MK-40/polyaniline (curves 2,3) membranes: a – NaCl, b – $CaCl_2$, c – $MgCl_2$ solutions, 2, 3 – non-modified and modified surfaces face the electrolyte flux.

The modification by polyaniline causes the decrease in diffusion permeability of the membrane in 1.2 – 2 times depending on the electrolyte nature. It should be noted, that diffusion permeability curves for modified membrane retain increasing type in NaCl solutions, but becomes almost independent on the concentration in $CaCl_2$ and $MgCl_2$ solutions.

The diffusion permeability was measured for different orientation of the modified membrane in the experimental cell – by modified and non-modified surfaces towards the electrolyte flux (P_s and P_w respectively). The asymmetry of diffusion permeability is most pronounced for sodium chloride solutions, and asymmetry coefficient (P_s/P_w) achieves 0.73. In solutions of divalent cations the asymmetry coefficient is about 0.9, that is comparable with the experimental error. The peculiarities in diffusion transport of mono- and divalent cations chlorides, which are the components of the whey, through MK-40 membrane modified by polyaniline is revealed.

Acknowledgements

The work was supported by the Russian Foundation for Basic Research and Krasnodar Region Administration (project No 19-48-230040).

References

1. *Persico, M., Bazinet, L.* Fouling prevention of peptides from a tryptic whey hydrolysate during electromembrane processes by use of monovalent ion permselective membranes // J. Membr. Sci. 2018. V. 549. P. 486-494.
2. *Demina, O.A., Kononenko, N.A., Falina, I.V., Demin, A.V.* Theoretical estimation of differential coefficients of ion-exchange membrane diffusion permeability // Colloid J. 2017. V. 79, No 3. P. 317-327.

ASYMMETRY EFFECT OF DIFFUSION PERMEABILITY OF BILAYER ION EXCHANGE MEMBRANES, MODIFIED BY POLYANILINE

Irina Falina, Irina Myakinchenko, Olga Demina
Kuban State University, Krasnodar, Russia

Nowadays the membrane materials with asymmetric properties attract the interest of researches. Polyaniline is the prospective modifier to form the barrier layer on the surface of ion-exchange membrane [1]. The literature presents a large number of experimental results on asymmetry of the transport properties of anisotropic ion-exchange membranes, including diffusion permeability. However, the theoretical investigations in this field are not sufficient. The aim of the work was the description of diffusion flux in bi-layer MF-4SK membrane modified by polyaniline in sodium chloride solutions.

Experimental

The object of research was perfluorinated membrane MF-4SK and MF-4SK, modified by polyaniline on the surface and in the bulk. The surface modification by polyaniline was performed by successive diffusion of monomer (anilinium chloride) and oxidant (ammonium peroxidisulfate) through the membrane to water. The bulk-modified sample was obtained by modifying both sides of the membrane. After modification, the samples were washed with water and equilibrated with NaCl solutions.

Results and Discussion

Fig. 1 presents the concentration dependencies of diffusion permeability for initial MF-4SK and surface and bulk modified composites MF-4SK/PANI. As can be seen that modification the membrane by polyaniline leads to essential decrease in diffusion permeability. The diffusion permeability of the surface modified membrane changes within 10% with different orientation in diffusion cell: by modified and non-modified surfaces towards the electrolyte flux.

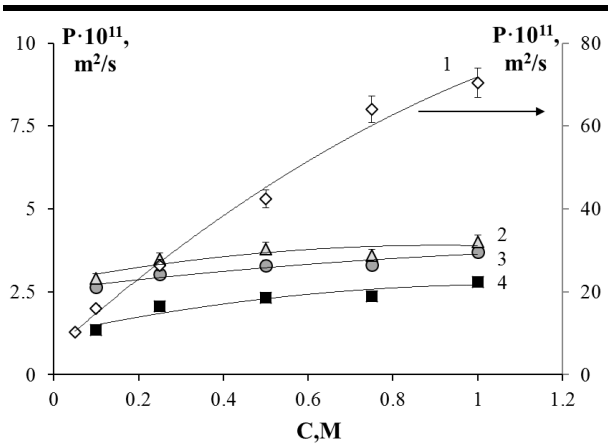

FIGURE 1. CONCENTRATION DEPENDENCIES OF THE MEMBRANE DIFFUSION PERMEABILITY IN NACL SOLUTIONS. 1 – MF-4SK, 2, 3 – NON-MODIFIED AND MODIFIED SURFACES OF MF-4SK/PANI MEMBRANE FACES THE ELECTROLYTE FLUX, 4 – BULK-MODIFIED SAMPLE.

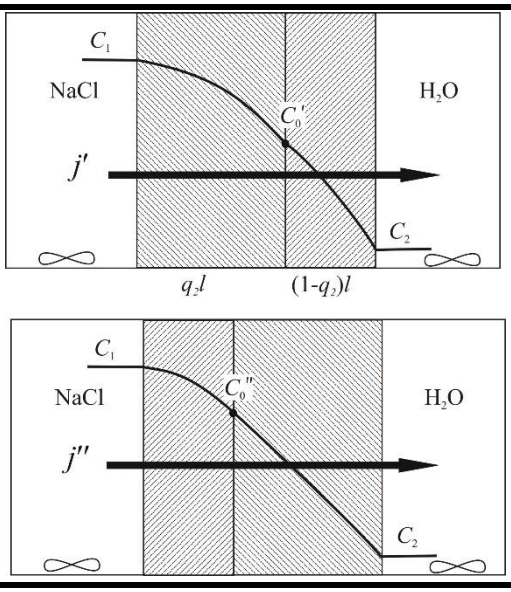

FIGURE 2. SCHEMATIC PRESENTATION OF THE SYSTEM "BI-LAYER MEMBRANE – NACL" SOLUTION WITH CONSIDERING THE DIFFERENT ORIENTATION OF THE MEMBRANE TOWARDS THE ELECTROLYTE FLUX.

The authors [2] proposed the approach to description of the diffusion properties of bilayer membranes based on presentation of the diffusion flux as the power function

$$j = bC^{\beta},$$

where β is the parameter, describing the shape of the concentration profile inside the membrane, b is the empirical coefficient. In [2] it was supposed that surface-modified membrane consist of two clearly defined layers (Fig. 2). At the boundary between the layers, there is a continuity of concentration of the virtual solution (C_0', C_0''), which makes it possible to write down the equations for flows through separate layers of the membrane. Under the stationary diffusion transfer, the flows passing through the membrane and the individual layers are equal. The assessment of diffusion flux through the modified membranes within the framework of this approach does not accurately describe the diffusion behavior of the membrane due to disregarding the thicknesses of the layers. In present work, we accounted the thickness of the layers by entering the fraction of the modified layer of the total thickness of the membrane q. The resulting equations have the form

$$j' = d_2 q l(C_2^{\beta_2} - {C_0}'^{\beta 2}); \qquad j' = d_1(1-q)l({C_0}'^{\beta 1} - {C_1}^{\beta 1});$$
$$j'' = d_1(1-q)l({C_2}^{\beta 1} - {C_0}''^{\beta 1}); \qquad j'' = d_2 q l({C_0}''^{\beta 2} - {C_1}^{\beta 2}),$$

where l is the membrane thickness, d_2, d_1 are the empirical coefficient, which indicates the degree of reduction in diffusion flux when passing through a unit of the membrane thickness, $b_1 = d_1(1-q)l$, $b_2 = d_2 q l$.

The diffusion flux calculation results accounting the layers thickness is presented on Fig. 3. One can see that the diffusion flux depends on the layers thickness, and for the investigated bi-layer MF-4SK/PANI membrane the fraction of the modified layer is about 0.5 on total thickness of the sample. Changing the membrane orientation towards the electrolyte flux varies the layer thickness within 10% error.

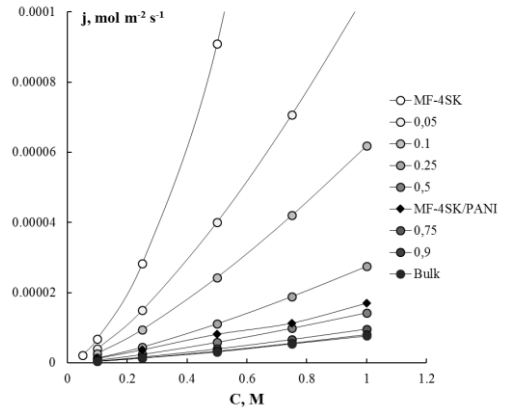

FIGURE 3 – CONCENTRATION DEPENDENCIES OF THE DIFFUSION FLUX IN NACL SOLUTIONS. 0.05, 0.1, 0.25, 0.5, 0.75, 0.9 – CALCULATION RESULTS (CURVE NUMBER DEFINES THE Q_2 VALUE), MF-4SK, MF-4SK/PANI AND BULK – EXPERIMENTAL DATA FOR INITIAL, SURFACE- AND BULK-MODIFIED SAMPLES CORRESPONDINGLY.

Berezina and al. in [3] investigated the images of the surface-modified membranes, obtained under similar conditions, and shown that the thickness of the modified layer varies from 30 to 65% depending on the properties of the basic matrix. The obtained results are in a good agreement with the data, presented in [3].

In present work, we proposed the method of the estimation of diffusion permeability of bi-layer membranes accounting not only concentration of the virtual solution on the inner interfacial bound but also the thicknesses of the layers.

Acknowledgements

The work was supported by the Russian Foundation for basic Research (project No 18-38-20069 mol_a_ved).

References

1. *Kononenko N.A., Loza N.V., Shkirskaya S.A., Falina I.V., Khanukaeva D.Yu.* // J. Solid State Electrochem. 2015. Vol. 19, Iss. 9. P. 2623-2631.
2. Kononenko, N.A., Gnusin, N.P., Berezina, N.P., Parshikov, S.B. // Rus. J. Electrochem., Volume 38, Issue 8, August 2002, Pages 828-833.

3. *Berezina N.P., Shkirskaya S.A., Kolechko M.V., Popova O.V., Senchikhin I.N., Roldugin V.I. //* Rus. J. Electrochem. 2011. T. 47. № 9. C. 995-1005.

THERMALLY REARRANGED POLYMER MEMBRANES FOR BIOALCOHOL PURIFICATION

[1]Ilia Faykov, [1]Vera Nesterova, [1]Alexandra Pulyalina, [2]Irina Podeshvo, [1,2]Galina Polotskaya

[1]St. Petersburg State University, St. Petersburg, Russia

[2]Institute of Macromolecular Compounds of Russian Academy of Sciences, St. Petersburg, Russia

E-mail: *ifaykov@gmail.com*

Introduction

Pervaporation as a membrane-based technology is a promising technique for purification of liquid mixtures and can be applied to solve different tasks, such as separation of azeotropic and thermally unstable mixtures, dehydration of solvents, and recovery of specific organic compounds. Pervaporation has several advantages over conventional separation techniques (e.g. distillation), including feasible scale-up, low energy consumption and environmental friendliness. In view of the limited range of industrial membranes, the search for novel membrane materials with high exploitative characteristics is of primary task. In the present work, there were obtained novel polymer membranes based on thermally rearranged polymer (TRP) and its prepolymer polyamic acid (PAA), which have high thermal and chemical stability.

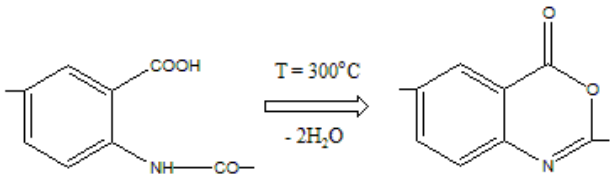

Figure 1. Formation of benzoxazinone fragments.

The aim of present work was the research of physico-chemical characteristics and transport properties of novel membranes based on heteroatomic polymers in separation of water – n-butanol mixture. The problem of separation of n-butanol – water mixture is of current importance due to wide use of n-butanol as new generation biofuel base and industrial solvent.

Experiments

TRP was produced by stepwise heating of PAA. The process of n-butanol dehydration was investigated by membrane method of separation with the use of vacuum pervaporation. The main physico-chemical parameters of the membranes such as contact angles, surface tension, membrane density, and sorption characteristics were studied. Contact angles were measured by sessile drop method at room temperature and atmospheric pressure. Membrane density was measured via flotation method using solutions of isopropanol and CCl_4, at 20 °C. Thermogravimetric analysis, differential scanning calorimetry and scanning electron microscopy were used to investigate heat resistance and structure of the membranes. Transport properties of the membranes were studied for water – n-butanol mixture in a wide range of concentrations at 20 °C.

Results and discussion

Some physical characteristics of the researched membranes are presented in Table 1. According to the data, thermal treatment of PAA leads to more dense structure and to higher value of glass transition temperature T_g. This probably indicates a restructuring of the membrane as a result of thermal transformation, which leads to the formation of a more rigid-chain polymer with less chain flexibility. The fractional free volume decreases as a result of thermal transformation of PAA to the TRP, which could be explained by densification of the membrane structure. This fact significantly affects the transport characteristics of the membranes in pervaporation experiments.

Table 1: Physical characteristics of the membranes

Membrane	T_g,°C	Density, g/sm^3	Fractional free volume	Contact angles, °	
				Water	Ethanol
PAA	121	1.310	0.114	67.4	20.1
TRP	258	1.333	0.096	73.1	28.4

For TRP membranes there were obtained higher values of contact angles up to water and ethanol compared to PAA, which indicates an increase in the hydrophobicity of the membrane surface during the thermal transformation of PAA to TRP.

Pervaporation tests have shown that the membrane based on TRP could selectively extract water from water – n-butanol mixture. The correlations between concentrations of water in the permeate and in the feed are presented on Figure 2. The membrane based on TRP produces the permeate enriched with water while the membrane based on PAA passes both water and alcohol. This phenomenon can be explained by higher value of fractional free volume and by the existence of carboxylic groups in PAA which have high affinity to water and alcohol. The liquid-vapor equilibrium curve for the water – n-butanol system makes it possible to evaluate the effectivity of pervaporation technique. The permeate content for both TRP and PAA membranes is located above the liquid-vapor equilibrium curve. Thus, membrane separation is more effective compared to the conventional methods such as distillation and rectification.

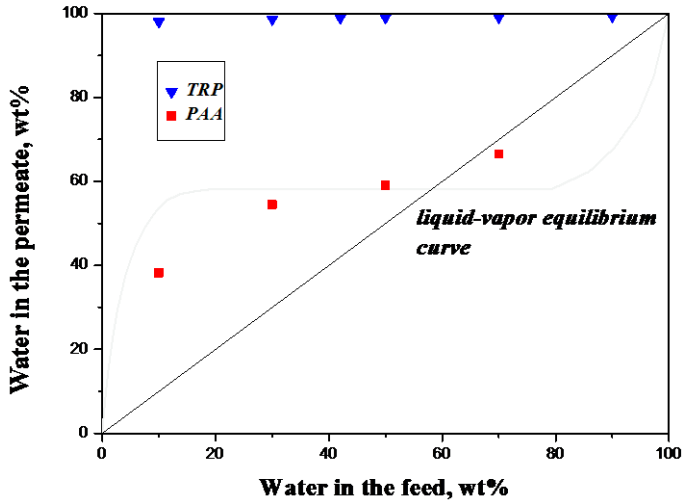

Figure 2. Dependence of water content in the permeate on water content in the feed in pervaporation of water– n-butanol mixture using PAA and TRP membranes. The liquid-vapor equilibrium curve for n-butanol-water mixture at 20°C.

Figure 3 shows the main transport characteristics of the membranes: total flux and separation factor of water - n-butanol mixture for PAA and TRP membranes. As it can be seen from Fig. 3a, total flux for PAA and TRP membranes increases with increasing water concentration in the feed. At the same time, the permeate flow through PAA membrane is higher than through TRP membrane, while TRP membrane has a higher separation factor than PAA in all the range of feed

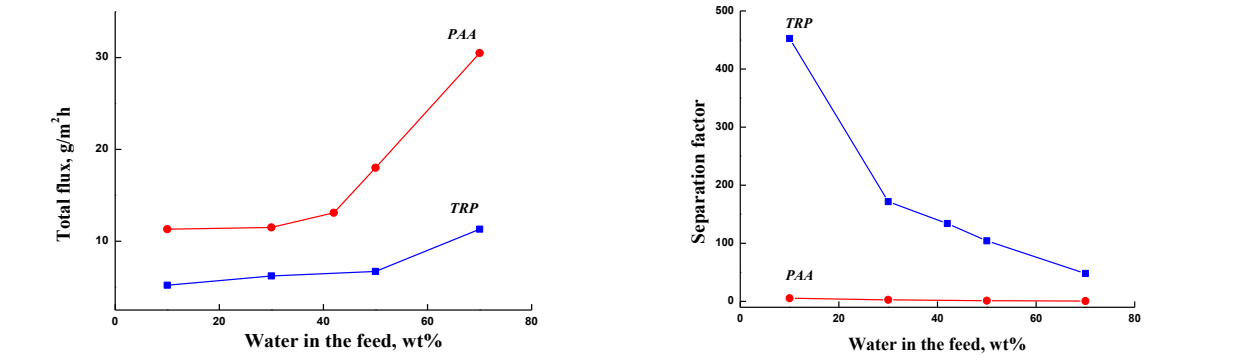

Figure 3. Dependence of (a) total flux and (b) separation factor on water content in the feed in pervaporation of water – n-butanol mixture using PAA and TRP membranes, 20°C.

composition. The separation factor decreases with increasing water content in the feed for both the membranes. The maximum value of separation factor was obtained for mixture containing 10% water, 452 and 5.5 for membranes based on TRP and PAA, respectively.

Conclusion

In summary, the novel polymer membranes based on thermally rearranged polymer were developed and investigated in pervaporation of water – n-butanol mixture. Thermal transformation of PAA to TRP lead to more compact membrane structure and to change in the physical parameters of the researched membranes. It was found that the membrane based on TRP was more effective than its prepolymer PAA and could be used as a dense layer in composite membranes for purification of n-butanol as biofuel base.

Acknowledgement

This work was carried out with financial support of Russian Science Foundation (RSF) (grant 18-79-10116).

IMPACT OF EXTERNAL ELECTRIC FIELD ON HYDRODYNAMIC PERMEABILITY OF A CHARGED POROUS LAYER (MEMBRANE)

Anatoly Filippov, Tamara Philippova
Gubkin University, Moscow, Russia, E-mail: *filippova.tam@yandex.ru*

Introduction

In [1], in the framework of thermodynamics of nonequilibrium processes, based on the previously proposed cell model of a charged membrane [2], the electroosmotic permeability and electrical conductivity of the ion-exchange membrane (layer), considered as the kinetic coefficients of the Onsager matrix, were calculated. Here we will use the results of the mentioned works and apply them to the calculation of the transfer of solvent (water) and electric current through a charged porous layer of oil-bearing rock, which is in equilibrium with an aqueous solution of 1:1 binary electrolyte. In this study, as in [1, 2], as independent thermodynamic forces specified in the course of the experiment, we choose pressure and electric potential gradients (there is no gradient of electrolyte concentration), respectively: $\nabla p = \left(p_{20} - p_{10}\right)/h$, $\nabla\varphi = \left(\varphi_{20} - \varphi_{10}\right)/h$. Here h is the thickness of the porous layer, and the indices "1" and "2" indicate the left and right sides of the layer (reservoir), which are in contact with the equilibrium solution of the binary 1:1 electrolyte of constant concentration C_0 (Fig. 1a).

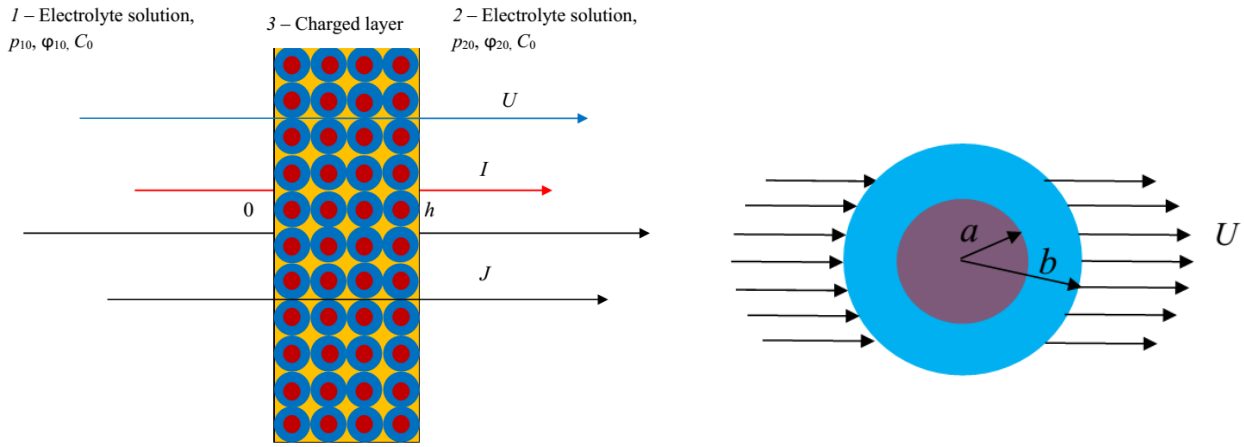

(a) *(b)*

Figure 1. Graphical Presentation of the Cell Model of a Charged Layer (a) and Single Cell (b).

As the dependent thermodynamic parameters determined in the experiment, we take the flux densities of: U - solvent (water), I - mobile charges (electric current density). As for the flux of the solute (salt), which can also occur when pressure and electric potential gradients are applied, for simplicity we do not consider it here. Then the phenomenological transport equations in the case of isothermal processes can be written as the following system of equations:

$$\begin{cases} U = -\left(L_{11}\nabla p + L_{12}\nabla\varphi\right), \\ I = -\left(L_{12}\nabla p + L_{22}\nabla\varphi\right). \end{cases} \qquad (1)$$

Theoretical Part

We will model the charged rock layer of a cellular-globular structure with a periodic lattice (Fig. 1a) of porous charged spherical particles of the same radius a enclosed in spherical liquid shells of radius b (Fig. 1b), which is chosen so that the ratio of the particle volume to the cell volume is equal to the volume fraction of particles in the dispersed system (porous layer): $\gamma^3 = \left(a/b\right)^3 = 1 - m_0$, where m_0 is macroscopic porosity (active porosity, available for filtration). The cell method makes it possible to reduce the problem of determining the kinetic coefficients of a whole layer to a boundary problem for a single cell. The mathematical formulation of the problem for a single cell (Fig. 1b) is given in [1, 2] and is not presented here for brevity. The designations

of variables and parameters completely coincide with those in the articles [1-3]. The hydrodynamic permeability L_{11} of the negatively charged porous layer (reservoir) applying an aqueous solution of 1:1 electrolyte was determined by the cell model in [2]. In the simplest for calculations case of excluded co-ions (the co-ions in the pores of the reservoir are neglected), it is equal to:

$$L_{11}=\frac{a^2}{45\mu^{o}\left(1-m_0\right)}\left[\begin{array}{l}-18\sqrt[3]{1-m_0}-\dfrac{5m\left(6+s^2\left[1-2\left(s/\tanh s-1\right)^{-1}\right]\right)m_0^2}{\left[2\left(1-m\right)\left(s/\tanh s-1\right)^{-1}+m\right]s^2-6\left(1-m\right)}+\\ +15+3\left(1-m_0\right)^2+\dfrac{45}{ms^2\left(1+\dfrac{\bar{\rho}}{\bar{\rho}_0}\dfrac{\left(\bar{\rho}-C_0\right)D_{+}}{\bar{\rho}D_{m+}+\left(3/m_0-1\right)C_0D_{+}}\right)}\end{array}\right], \qquad (2)$$

The formula for electroosmotic permeability L_{12}, obtained in the same limiting case of excluded co-ions and 1:1 electrolyte is correspondingly as follows,

$$L_{12}=3\frac{F_0D_{+}}{RT}\frac{\left(1+\dfrac{m_0}{3-m_0}\dfrac{D_{m+}}{D_{+}}\right)\dfrac{C_0}{\bar{\rho}}}{m_0\left(\dfrac{D_{m+}}{D_{+}}\dfrac{\bar{\rho}_0}{\bar{\rho}}+1\right)+\left(\left(3-m_0\right)\dfrac{\bar{\rho}_0}{\bar{\rho}}-m_0\right)\dfrac{C_0}{\bar{\rho}}}, \qquad (3)$$

Here $m=\mu^{i}/\mu^{o}$, $s^2=a^2/\left(mk_{D}\right)=s_0^2/m$, $D_{\pm}$ – diffusion coefficients of electrolyte ions in a dilute solution, D_{m+} – diffusion coefficient of the counterion (cation) in the layer, $\bar{\rho}=\rho_{V}/F$ – layer exchange capacity (ρ_{V} – fixed charge volume density), $\bar{\rho}_0=\mu^{o}D_{+}/\left(k_{D}RT\right)$ – characteristic exchange capacity of the problem (estimates show that $\bar{\rho}_0>>\bar{\rho}$), $R_{b}=\sqrt{k_D}$ – characteristic thickness of the filtration layer (Brinkman radius), k_{D} – specific (Darcy) hydrodynamic permeability of the ionite grain (gel), μ^{o}, μ^{i} – viscosities of the fluid in the liquid shell surrounding cationic grain and in the grain itself, R – the universal gas constant, T – the absolute temperature. By virtue of ideality, formulas (1) – (2) do not include the diffusion coefficient of a co-ion D_{m-} in the porous layer and the coefficient of equilibrium distribution γ_{m} of electrolyte molecules in the pores [1, 2]. Despite the approximate formulas (2) – (3), they work well for real membranes.

Results of Calculations

Using formulas (2) – (3) and the first of the Onsager relations (1), one can calculate the solvent flux density (linear velocity U) at any values of pressure gradients and electric potential. This means that it is possible to regulate the flux of solvent passing through the reservoir, changing the external electric field at a constant pressure gradient. To assess the relative influence of the external electric field on the linear velocity of the solvent (water) through the stratum, we will use the ratio $U/U^{*}=1+\chi\nabla\bar{\varphi}/\nabla\bar{p}$, where U^{*} is the linear flow rate only in the presence of a pressure gradient on the reservoir, U is the flow rate due to pressure and electric potential gradients, $\bar{\varphi}=\varphi F/\left(RT\right)$ is the dimensionless electric potential, $\bar{p}=pa^2/\left(\mu^{o}D_{+}\right)$ is the dimensionless pressure. The calculations were performed using the Mathematica-11 application package and are shown in Fig. 2 for $\chi\left(C_0/\bar{\rho}\right)$ and $\chi\left(m_0;\bar{\rho}_0/\bar{\rho}\right)$.The coefficient of proportionality in the case of coinciding viscosity values $\left(m=1\right)$ is easily determined from relations (1), (2) and (3):

$$\chi = \frac{135(1-m_0)\left(1+\dfrac{m_0}{3-m_0}\dfrac{D_{m+}}{D_+}\right)\dfrac{C_0}{\bar{\rho}}}{\left[-\dfrac{45}{s_0^2}m_0\left(1-\dfrac{C_0}{\bar{\rho}}\right)+\left(m_0\left(\dfrac{D_{m+}}{D_+}\dfrac{\bar{\rho}_0}{\bar{\rho}}+1\right)+\left((3-m_0)\dfrac{\bar{\rho}_0}{\bar{\rho}}-m_0\right)\dfrac{C_0}{\bar{\rho}}\right)\times\right.}$$
$$\left.\times\left(18\left[1-\sqrt[3]{1-m_0}\right]+2m_0\left[5\left(\left(\frac{s_0}{\operatorname{th} s_0}-1\right)^{-1}-1\right)m_0-3\right]+\frac{15}{s_0^2}\left[3-2m_0^2\right]\right)\right]. \quad (4)$$

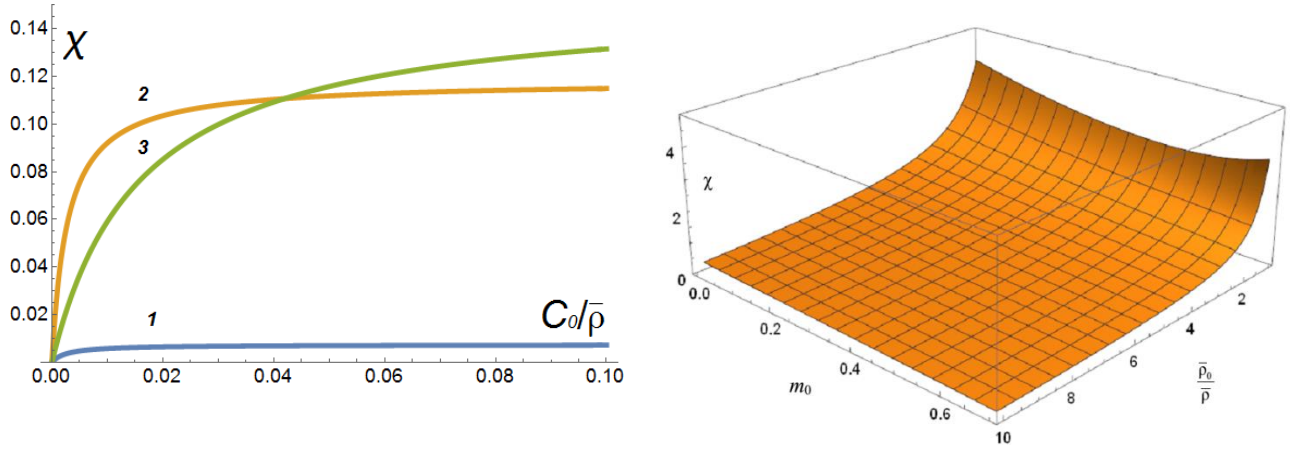

(a) *(b)*

Figure 2. The dependences of the dimensionless coefficient χ *on the relative concentration (a) of electrolyte HCl (m=1):* $m_0 = 9.5\%$, $s_0 = 1$ *(1),* $m_0 = 9.5\%$, $s_0 = 4$ *(2),* $m_0 = 50\%$, $s_0 = 4$ *(3);* $D_+ = 9610$, $D_{m+} = 838\,\mu m^2/s$; $\bar{\rho}$=1.22, $\bar{\rho}_0 = 158$ mol/dm^3 *and on the porosity* m_0 *of the layer and the ratio of exchange capacities* $\bar{\rho}_0/\bar{\rho}$ *(b) under* $s_0 = 2$, $C_0/\bar{\rho} = 0.1$, $D_+/D_{m+} = 11.5$.

Thus, the imposition of an external electric field on a negatively charged stratum, whose intensity vector is co-directed with the barofiltration velocity, leads to an increase in the rate of fluid transfer through the charged porous layer due to the addition of the electroosmotic component to the convective flow. Under the action of an electric field in the opposite direction, a slower flow of solvent occurs.

Conclusion

Based on the cell model and the thermodynamics of irreversible processes (Onsager's approach), a new method for calculating the solvent flow (water) and an electric current flowing through a charged porous layer (membrane) is proposed with the simultaneous action of an external pressure gradient and an electric potential gradient. It is shown that with the increase in the electrolyte concentration, the total permeability of the porous structure also increases due to both barofiltration and electroosmotic transfer of the solvent.

This study was supported by RFBR (project No.17-08-01287).

References

1. *Filippov A.* A Cell Model of an Ion-Exchange Membrane. Electrical Conductivity and Electroosmotic Permeability // Colloid J. 2018. V. 80. P. 728-738.
2. *Filippov A.* A Cell Model of an Ion-Exchange Membrane. Hydrodynamic Permeability // Colloid J. 2018. V. 80. P. 716-727.
3. *Filippov A.N., Philippova T.S., Kalinin V.V.* Influence of an External Electric Field on Permeability of a Charged Porous Layer // Proceedings of Gubkin Russian State University of Oil and Gas. 2018. No. 3(292). P. 207-220.

SIMULTANEOUS VERIFICATION OF THE CELL MODEL FOR ELECTROOSMOTIC PERMEABILITY AND ELECTRICAL CONDUCTIVITY OF CATION-EXCHANGE MEMBRANE

[1]Anatoly Filippov, [2]Svetlana Shkirskaya
[1]Gubkin University, Moscow, Russia, E-mail: *filippov.a@gubkin.ru*
[2]Kuban State University, Krasnodar, Russia

Introduction

Electroosmotic permeability (EOP) of ion-exchange membranes is an important factor that significantly affects their use, for example, in fuel cells (FC). Excessive loss of water by such a membrane leads to its destruction and possible overheating of the fuel cell itself. Therefore, for effective operation of ion-exchange membranes in FC, it is necessary, preferably before the experiment, to know how their electroosmotic permeability will change with varying moisture content and concentration of the background electrolyte, as well as the geometric and physico-chemical characteristics of the ion exchangers. However, the existing theories for the calculation of EOP do not fully answer the questions posed. This motivated us to build a closed cell model of the ion-exchange membrane, considering the transfer of water or other solvent in the hydration/solvation shells of ions [1]. Within this model, exact and approximate formulas were obtained for the electroosmotic permeability L_{12} and the specific electrical conductivity (SEC) L_{22} of the charged porous layer (membrane) [2]. In this work, we applied the developed cell model to the characterization of MF-4SC cation-exchange membranes previously made in the pristine (pure) state, as well as halloysite modified with nanotubes, functionalized with Pt or Fe nanoparticles [3] and placed in different concentrations of HCl. Electroosmotic permeability of the membrane at a constant current density, $D_I = L_{12}/L_{22}$ (m^3/C), was determined by the volumetric method in a two-chamber cell with polarizing silver chloride electrodes. The conductivity L_{22} (S/m) of the membrane was calculated based on the measurement of its active resistance.

Theoretical Part

The formulas for L_{12} and L_{22}, obtained in the general case of a non-ideal membrane in [2], are rather cumbersome expressions. Therefore, we present here only the formulas for L_{22} and $D_I = L_{12}/L_{22}$ in the limiting case of an ideally selective cation-exchange membrane (case of excluded co-ions) and 1:1 electrolyte:

$$L_{22} = C_0 D_+ \frac{F^2}{RT}\left(\frac{2m_0}{3-m_0}\left(1+\frac{D_-}{D_+}\right) + \frac{9\left(1-m_0\right)}{3-m_0} \frac{\left(\frac{D_{m+}}{D_+}+\frac{\bar{\rho}}{\bar{\rho}_0}\right)\bar{\rho}}{m_0\bar{\rho}\left(\frac{D_{m+}}{D_+}+\frac{\bar{\rho}}{\bar{\rho}_0}\right)+\left(3-m_0\left(1+\frac{\bar{\rho}}{\bar{\rho}_0}\right)\right)C_0} \right), \quad (1)$$

$$D_I = \frac{3}{F\bar{\rho}_0} \frac{3-m_0\left(1-\frac{D_{m+}}{D_+}\right)}{\left(\frac{D_{m+}}{D_+}+\frac{\bar{\rho}}{\bar{\rho}_0}\right)\left(9\left(1-m_0\right)+2m_0^2\left(1+\frac{D_-}{D_+}\right)\right)+2m_0\left(1+\frac{D_-}{D_+}\right)\left(\frac{3-m_0}{\bar{\rho}}-\frac{m_0}{\bar{\rho}_0}\right)C_0}. \quad (2)$$

Here m_0 – macroscopic porosity (active porosity) of the membrane, $D_\pm$ – diffusion coefficients of electrolyte ions in a dilute solution, D_{m+} – diffusion coefficient of the counterion (cation) in the membrane, $\bar{\rho}=\rho_V/F$ – membrane exchange capacity (ρ_V – fixed charge volume density), $\bar{\rho}_0 = \mu^o D_+/\left(k_D RT\right)$ – characteristic exchange capacity of the problem (estimates show that $\bar{\rho}_0 >> \bar{\rho}$), k_D – specific (Darcy) hydrodynamic permeability of the ionite grain (gel), μ^o – dynamic viscosity of the solution, R – the universal gas constant, T – the absolute temperature, C_0 – equivalent concentration of the electrolyte solution in equilibrium with the membrane. By virtue of ideality, formulas (1) – (2) do not include the diffusion coefficient of a co-ion D_{m-} in the membrane and the

coefficient of equilibrium distribution γ_m of electrolyte molecules in the pores of the membrane [1, 2].

Despite the approximate formulas (1) – (2), they work well for real membranes. It is seen that the dependence (2) of electroosmotic permeability D_I at constant current density on the concentration C_0 of a 1:1 electrolyte solution is hyperbolic one and decreases monotonically to zero with increasing C_0.

Comparison Between Theory and Experiment

The parameters of the cell model $(D_{m+}, m_0, \bar{\rho}_0)$ were determined based on experimental dependencies $D_I(C_0)$ and $L_{22}(C_0)$, minimizing the deviation error of a specially constructed target function from its experimental values at different electrolyte concentrations,

$$f(C_0) = D_I(C_0)\cdot H(C_1 - C_0) + L_{22}(C_0 + C_1)\cdot H(C_0 - C_1)\cdot H(C_2 - C_0). \quad (3)$$

Here *H(x)* is the Heaviside unit function, and the selected concentration values C_1, C_2 depend on the experimental data range so that the electroosmotic permeability and electrical conductivity do not overlap each other. In our case, when using the experimental data of work [3], we assumed C_1=1, C_2=2 mol/L and formulas (1) – (2) for an ideally selective cation-exchange membrane were applied. The results of simultaneous optimization of electrical conductivity (1) and electroosmotic permeability (2) for the unmodified (pristine) perfluorinated membrane MF-4SC are shown for example in Fig. 1 and 2, which demonstrates satisfactory agreement between theory and experiment.

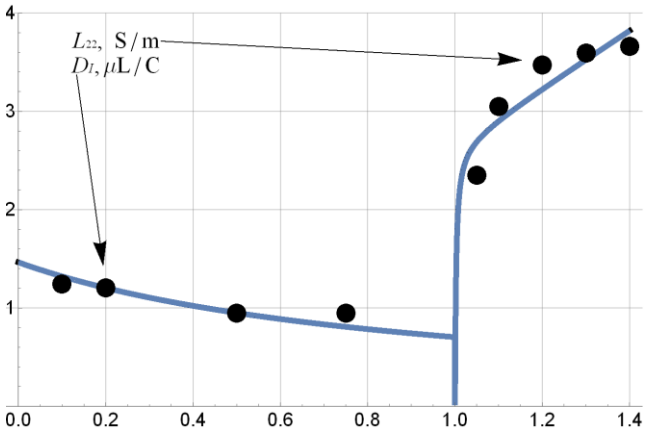

Figure 1. Graphical Results of Simultaneous Optimization of EOP and SEC for Pristine Membrane MF-4SC.

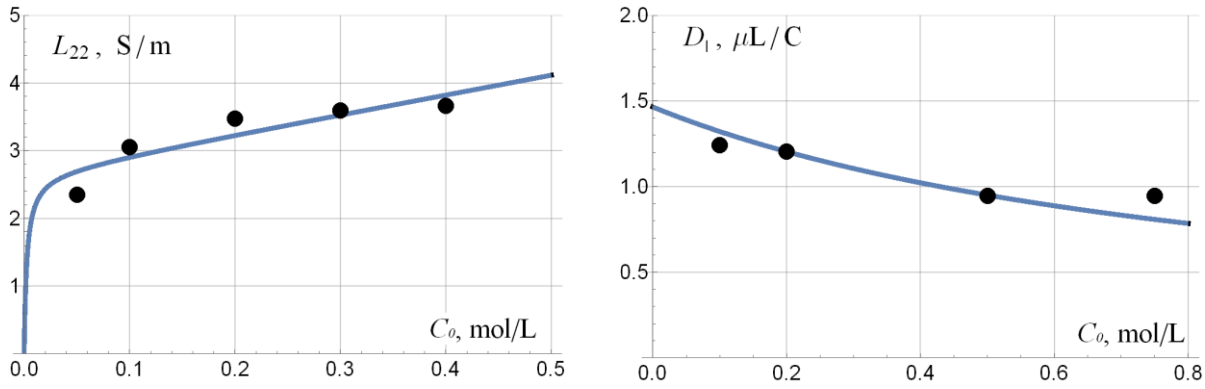

(a) (b)

Figure 2. Comparison of Experimental (Points) and Theoretical Dependencies for SEC (a) and EOP (b) in Case of Pristine Membrane MF-4SC.

The magnitudes of the model physicochemical parameters $(D_{m+}, m_0, \bar{\rho}_0)$, obtained from optimization procedure written for Mathematica software, are listed in Table 1. The values of

exchange capacity $\bar{\rho}$ were measured in independent experiments for all membranes used. Specific hydrodynamic permeability of a cationite grain (gel) was evaluated using relation $k_D = \mu^o D_+ / (\bar{\rho}_0 RT)$ (last column of Table 1). It is seen from Table 1 that k_D decreases from pristine to modified membranes. It may mean compaction of the ionite grains (gel) due to their modification by halloysite nanotubes with metal nanoparticles. It should be noted that the macroporosity m_0 is within the limits of the values obtained by the standard contact porosimetry method [4] and proton diffusivity in tested membranes is less approximately from 10 to 15 times than in a dilute electrolyte solution.

Table 1: Physicochemical Parameters Obtained by Simultaneous Optimization Using Approximate Formulas (1)-(2) for Ideal Cation-Exchange Membrane

Membrane	D_{m+}, μm²/s	m_0, %	$\bar{\rho}$, mol/dm³	$\bar{\rho}_0$, mol/dm³	k_D, $\left(\text{Å}^o\right)^2$
MF-4SC pristine	586	9.6	1.08	106	3.64
MF-4SC/Hall+Pt	838	10.1	1.22	158	2.45
MF-4SC/Hall+Fe	674	8.9	1.16	167	2.32

Conclusion

In this work, within the framework of the thermodynamics of nonequilibrium processes based on the cell model of the ion-exchange membrane (porous charged layer), two electrokinetic coefficients of the Onsager matrix are determined: electroosmotic permeability and electrical conductivity. The membrane is considered as an ordered assemblage of porous charged particles of spherical shape, placed in spherical shells filled with a solution of a binary electrolyte. Based on the results obtained by the least squares method and specially developed optimization procedure, the physicochemical parameters of the cell model were found, which allowed acceptably describing the available experimental results for pure and modified cation-exchange membranes MF-4SC modified by halloysite nanotubes which are functionalized with platinum or iron nanoparticles.

This study was supported by RFBR (project No.17-08-01287) and the Ministry of Education and Science of the Russian Federation (Grant No.14.Z50.31.0035).

References

1. *Filippov A.* A Cell Model of an Ion-Exchange Membrane. Hydrodynamic Permeability // Colloid J. 2018. V. 80. P. 716-727.
2. *Filippov A.* A Cell Model of an Ion-Exchange Membrane. Electrical Conductivity and Electroosmotic Permeability // Colloid J. 2018. V. 80. P. 728-738.
3. *Filippov A., Afonin D., Kononenko N., Lvov Y., Vinokurov V.* New approach to characterization of hybrid nanocomposites // Colloids and Surfaces A. Physicochemical and Engineering Aspects. 2017. V. 521. P. 251-259.
4. *Petrova D.A., Filippov A.N., Kononenko N.A., Shkirskaya S.A., Timchenko M.O., Ivanov E.V., Vinokurov V.A., Lvov Yu.M.* Perfluorinated hybrid membranes modified by metal decorated clay nanotubes // J. Membr. Sci. 2019 (in press).

THE IONIC MOTION AND STRUCTURE FEATURES OF MODIFIED COBALTITES AT DIFFERENT TEMPERATURES – *AB INITIO* MOLECULAR DYNAMIC SIMULATION

[1]Igor Gainutdinov*, [2]Igor Zilberberg, [1]Alexander Nemudry
[1]Institute of Solid State Chemistry and Mechanochemistry SB RAS, Novosibirsk, Russia
E-mail: *ur1742@gmail.com*
[2]Boreskov Institute of Catalysis SB RAS, Novosibirsk, Russia

Introduction

Oxides with perovskite structure Sr(Ba,La,..)Co(Fe,..)O_{3-x} are ancestors of wide range of technologically important substances, used as oxide ionic conductors. Nevertheless, these compounds are not stable enough at low partial pressures of oxygen and in the CO_2 atmosphere. Also, various structural phase transitions observed in these materials, what hamper their technological applications. In addition, low-temperature structural modifications usually have low ionic conductivity. Recently we reported results of influence of Mo doping on properties of $Ba_{0.5}Sr_{0.5}Co_{0.8}Fe_{0.2}O_{3-x}$ and $SrFeO_{3-x}$ system [1-2] that increased stability of substances in various atmospheres, suppressed phase transitions etc.

Despite the progress in the experimental study of these materials, the mechanisms providing high mobility of oxygen ions are still not clear in many aspects. The microscopic picture of the dynamic processes in these materials can be studied using the molecular dynamics method.

Experiments

We performed ab initio molecular dynamic simulations for $SrCoMoO_{1-x}$ and $SrCo_{0.875}Mo_{0.125}O_{1-x}$ (x=0, 0.125, 0.25) compounds with VASP package. The system contained of 2x2x2 elementary cells (40-38 ions) was calculated with PAW PBE pseudopotentials in gamma point only approach in periodic boundary conditions. The thermal expansion, velocity autocorrelation function, vibrational spectra, effective charges of ions, oxygen motion and typical oxygen configurations of B-cations neighborhood was studied in temperature range 800-1350K.

Results and Discussion

It was shown that thermal expansion coefficients are close to reported previously by other authors and are about 20-40e-6 K^{-1}. The Mo doping cause "contraction" of structure with lowering the volume of studied system and lowering the thermal expansion up to 2 times.

The velocity autocorrelation function (VAF) was used for vibrational spectra calculation. Analysis of inner ionic motions was performed for various temperatures and it showed in particular that vacancies may move both to B-cation neighbor and Mo neighbor despite the Mo effective charge calculated by Bader procedure is about +2.6 elementary charges. The effective charges of ions during vacancy motion vary by a small amount.

Acknowledgements

This work was performed under the Russian Scientific Foundation (grant No. 18-13-00059).

References

1. *E.V. Shubnikova, O.A. Bragina, A.P. Nemudry*, Journal of Industrial and Engineering Chemistry 59 (2018) 242–250.
2. *O.A. Savinskaya, A.P. Nemudry, A.N. Nadeev, S.V. Tsybulya*, Solid State Ionics 179 (2008) 1076–1079.

ABOUT FEATURES OF ELECTROCONVECTION NEAR NON PERFECTSELECTIVE IONEXCHANGE MEMBRANES

[1]Georgy Ganchenko, [2]Natalya Ganchenko, [1]Evgeny Demekhin

[1]Laboratory of micro- and nanoscale electro- and hydrodynamic, Financial University, Krasnodar, Russia, E-mail: *gancgenko.ru@gmail.com*

[2]Kuban State University, Krasnodar, Russia, E-mail: *nataly.ganchenko@gmail.com*

Introduction

The report is dedicated to the study of electroconvection and transition to overlimiting current regime near ion-selective surfaces under external direct electric field. It is generally believed that the electrokinetic instability, which was theoretically predicted by B. Zalzman and I. Rubinstein [1], is the key mechanism leading to the overlimiting currents in the membrane systems. Later, the electrokinetic instability was observed during the experiments [2,3]. Initially, the electrokinetic instability was predicted theoretically using the model of ideally selective electric membrane, which implies the total absence of co-ion flux through the membrane. It was also shown within this model that the electrokinetic instability may only occur from the limiting current regime (nonequilibrium electrokinetic instability), when the extended space charge region forms [4]. But as it was reported in the recent work of B. Zalzman and I. Rubinstein [5], through the dismissing of the ideally selective membrane model and assuming of a little co-ion flux through the membrane, the electrokinetic instability may arise directly from the Ohmic current regime (equilibrium electrokinetic instability), which gives a new insight into electroconvection and overlimiting current regimes in the membrane systems.

Mathematical model

Within our theoretical investigation we used the standard model of binary monovalent electrolyte, which is mathematically described by the Nernst-Planck-Poisson-Stockes (NPPS) system of nonlinear equations in partial derivatives along with the corresponding border and initial conditions. Let us focus on the setup geometry. There are three domains, each of which is being simulated simultaneously. Two filled with the electrolyte domains are separated by the ion selective membrane of a finite width (Fig. 1). Two oppositely charged electrodes are situated on the either side of the domains with electrolyte in order to create a potential difference in the system. The pumping of the electrolyte along the membrane is absent, so in the one-dimensional case there is no movement of the electrolyte. The domain of the ion-selective membrane is simulated by the uniform density of the space charge, N, in the Poisson equation, and it is N that defines the ion-selectivity degree of the membrane (The higher is the value of N, the more ideal is the ion-selective membrane). Thus, the ion transport inside the membrane is described by the NPPS system of equations taking into account the coefficient of the membrane selectivity. A similar model was scrutinized in [5].

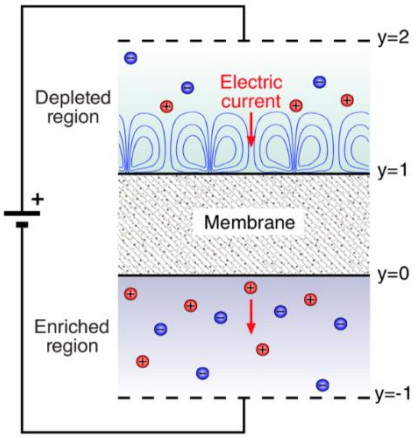

Figure 1. Scheme of the electrodialysis cell, taken as a computation domain.

Results

The investigation of the mathematical model was conducted as by the analysis of the linear stability of the one dimensional solution, as by direct numerical simulation of the full non stationary two-dimensional system in case of white noise perturbations being superimposed on the initially distributions of functions.

Research [6, 7] indicated that three regimes of electrokinetic instability may realize depending on the value of the space charge in the membrane, N. For large enough N (for close to ideal membranes), the classical non-equilibrium electroconvection arises. With decreasing of N, the electroconvection becomes equilibrium, right as it was predicted in [5], the critical value of the potential drop, meanwhile, increases. If the value of N declines close to such values that the charge density of the membrane consists about 10% of the charge of co-ions in the equilibrium electroneutral solution, then large enough potential drop leads to the arising of a new type of oscillating electrokinetic instability, the frequency of oscillations is about 50-300 Hz. During the investigation, the critical values of the governing parameters were obtained, as well as the sophisticated nonlinear structures arising after stability loss were described.

This work was supported, in part, by the Russian Foundation for Basic Research (Project Nos. 18-08-01158-a and 18-58-15004) and by the Grant Board under the President of Russian Federation (Project No. MK-5302.2018.1) The research was carried out using the equipment of the shared research facilities of the HPC computing resources at Lomonosov Moscow State University.

References

1. *Rubinstein I. and Zaltzman B.* Electro-osmotically induced convection at a permselective membrane // Phys. Rev. E 2000. V. 62. P. 2238.
2. *Rubinstein S.M. et al.* Direct observation of a nonequilibrium electro-osmotic instability // Physical Review Letters. 2008. Vol. 101, № 23. P. 236101.
3. *Nikonenko V.V. et al.* Intensive current transfer in membrane systems: Modelling, mechanisms and application in electrodialysis // Advances in Colloid and Interface Science. 2010. Vol. 160, № 1-2. Pp. 101–123.
4. *Zholkovskij E.K., Vorotyntsev M.A., Staude E.* Electrokinetic Instability of Solution in a Plane-Parallel Electrochemical Cell // Journal of Colloid and Interface Science. 1996. Vol. 181, № 1. Pp. 28–33.
5. *Rubinstein I., Zaltzman B.* Equilibrium Electroconvective Instability // Physical Review Letters. 2015. Vol. 114, № 11. P. 114502.
6. *Ganchenko G.S. et al.* Modes of electrokinetic instability for imperfect electric membranes // Phys. Rev. E. 2016. Vol. 94, № 6. P. 063106.
7. *Demekhin E.A., Ganchenko G.S., Kalaydin E.N.* Transition to electrokinetic instability near imperfect charge-selective membranes // Physics of Fluids. 2018. Vol. 30, № 8. P. 082006.

MATHEMATICAL MODELING OF HOW GRAVITATIONAL EFFECTS INFLUENCE OVERLIMITING CURRENT REGIME

[1]Natalya Ganchenko, [2]Maria Repina, [3]Dmitri Oksuz'an
[1]Kuban State University, Krasnodar, Russia, E-mail: *nataly.ganchenko@gmail.com*
[2]Southern Federal University, Rostov-on-Don, Russia.
[3]Kuban State Technological University, Krasnodar, Russia

Introduction

Study aims to theoretically evaluate the influence of the gravitational effects on the occurrence and development of overlimiting current regime near the ion-selective membranes. It is generally accepted that electrokinetic instability is the most probable mechanism of transition to overlimiting currents in the membrane systems [1]. However, additional factors become to play a crucial role in the stability loss by shifting the critical values of governing parameters of the system, if some special circumstances are taken into account in the mathematical model. Among such factors are the hydrophobic properties of the membrane surface [2] and the high enough salt concentration of the electrolyte solution [3]. The influence of the gravitational effects also belongs to such factors; the density, moreover, can change as due to non uniformity of the electrolyte temperature [4,5], as due to non homogenous distribution of salt ions in the electrolyte solution [6].

Mathematical model

Our theoretical investigation is based on the standard model of binary monovalent electrolyte solution, mathematically described by Nernst—Planck—Poisson—Stockes system of equations. Electrolyte is situated horizontally between two ion-selective surfaces, which are under external direct electric field. The model also takes into account the Joule heating by using Bousinesq approximation in energy equation with corresponding border conditions for the temperature function. The membrane surfaces are assumed to be partly thermoisolated, and there is no outer heating. Besides, it is assumed that the electrolyte density depends on the salt concentration (Fig.1).

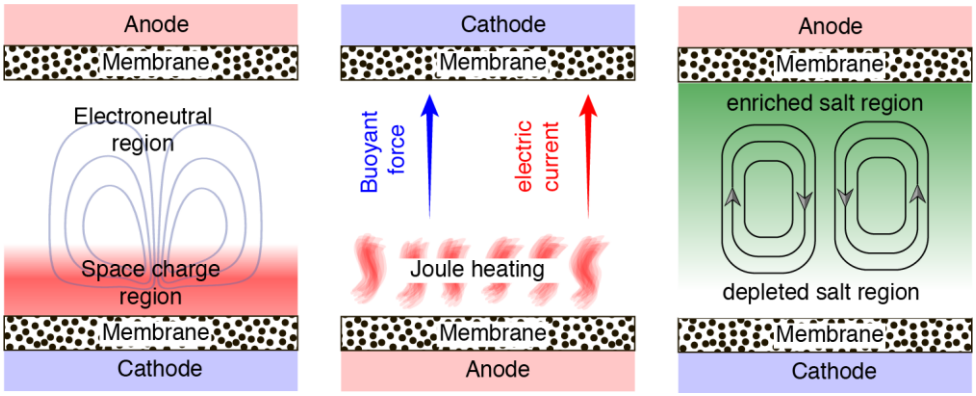

Figure 1. Electrokinetic instability and gravitation effects.

Results

The investigation showed that for good enough thermoisolation in the system the thermoelectrokinetic instability arises [3, 4]. This is a principally new type of microscale instability which is totally different from the widely known Rayleigh–Benard heat instability. Moreover, it was proved during the numerical experiments that the Rayleigh—Benard convection without outer heating is physically impossible in the membrane systems with microchannels, in contrast to thermoelectroconvection, the circumstances for which manifestation are physically real. The increasing of salt concentration in the electrolyte leads to occurrence of gravitational instability due to non homogeneous distribution of salt concentration in the electrolyte. This mechanism competes for playing a key role in the instability and, hence, in the overlimiting regime occurrence with the mechanism of thermoelectrokinetic convection. Which type of instability will be realized

depends on the set of physical parameters. Unstable stratifications occur for the channel orientation opposite to the vector of gravity acceleration.

Depending on the relation between concentration and heat Rayleigh numbers, one of the two aforementioned instability types prevails. The analysis of the linear stability of the one dimensional solution provided the critical values of the governing parameters, and the direct numerical simulation of full two- and three-dimensional NPPS system of equations allowed to observe and describe the sophisticated coherent structures arising for different parameters of the system.

This work was supported, in part, by the Russian Foundation for Basic Research (Project Nos. 18-38-00611-mol_a). The research was carried out using the equipment of the shared research facilities of the HPC computing resources at Lomonosov Moscow State University.

References

1. *Rubinstein I. and Zaltzman B.* Electro-osmotically induced convection at a permselective membrane // Phys. Rev. E 2000. V. 62. P. 2238.
2. *Shelistov V.S., Demekhin E.A., Ganchenko G.S.* Electrokinetic instability near charge-selective hydrophobic surfaces // Phys. Rev. E. 2014. Vol. 90, № 1. P. 013001.
3. *Pismenskiy A. et al.* Mathematical modelling of gravitational convection in electrodialysis processes // Desalination. 2006. Vol. 192, № 1-3. Pp. 374–379.
4. *Demekhin E.A. et al.* Thermoelectroconvection near charge-selective surfaces // Phys. Rev. E. 2015. Vol. 91, № 6. P. 063006.
5. *Kalaydin E.N. et al.* Thermoelectrokinetic instability and salt superconcentration near permselective electric membranes // Phys. Rev. Fluids. 2017. Vol. 2, № 11. P. 917.
6. *Karatay E. et al.* Coupling between Buoyancy Forces and Electroconvective Instability near Ion-Selective Surfaces // Physical Review Letters. 2016. Vol. 116, № 19. P. 194501.

EFFECT OF WATER SPLITTING RATE ON THE INTENSITY OF ELECTROCONVECTION AND SPACE CHARGE REGION CHARACTERISTICS

Violetta Gil, Mikhail Porozhnyy
Institute of Membranes, Kuban State University, Krasnodar, Russia, E-mail: *violetta_gil@mail.ru*

Introduction

Electrochemical separation processes with ion-exchange membranes, in particular under condition of high concentration polarization, are often complicated by sedimentation on the surface and in the bulk of the membrane. Concentration polarization phenomenon and membrane scaling remain common problems that alter irreversibly the membrane integrity and decrease the process performance.

A number of experimental studies [1,2], concerning electrodialysis (ED) treatment of the solutions whose mineral composition imitates concentrated milk or whey, show that scale is formed on both cation-exchange and anion-exchange membranes surfaces facing the diluate compartment of the cell. While the ED process proceeds the ion concentration near the diluate side of the membrane becomes zero causing water splitting, consequently, the pH changes, which lead to scaling of minerals (multivalent ions) on the membranes.

In order to better understand the sequence of events leading to scaling and to give theoretically reasonable and clear recommendations for the practice of fighting this phenomenon, it is necessary to establish a relationship between the water splitting rate and the characteristics of the space charge region (SCR) of the depleted diffusion boundary layer (DBL), as well as the intensity of electroconvection. As is known, the latter can reduce membrane scaling. Although it has been suggested in the literature that the reason for the decrease in electroconvection intensity with the increase in the water splitting rate is reduction of space charge density [3], this effect remains unproven.

The objective of this work is the processing of experimental data using a model based on Nernst-Planck and Poisson equations in condition of water splitting. In addition to calculating the thicknesses of different zones of the DBL, the space charge density will be calculated as a function of the rate of water splitting reaction at the membrane/depleted solution interface. Such calculations will be performed to process of the experimental data obtained for two types of membranes characterized by high and low water splitting rates.

Theory

Consider an ion-exchange membrane separating two identical 1:1 electrolyte solutions. A direct current of density I flows normally to the membrane surface. The fluxes J_i of salt cations (+) and anions (–), H^+ and OH^- ions in the DBL are described by the Nernst-Planck equations:

$$J_i = -D_i\left(\frac{dC_i}{dX} - z_i C_i \frac{FE}{RT}\right), \qquad i = \text{"+", "–", "H", "OH"} \tag{1}$$

where D_i, z_i, and C_i are the diffusion coefficient, charge and concentration of ions i, E is the electric field, the notations F, R and T are as usual; the normal coordinate X for the cation-exchange membrane (that will be considered here) takes its zero value in the bulk and $X=\delta$ at the membrane interface; $z_+=1$, $z_-=-1$.

The space electric charge, which is due to unbalance of the total amounts of cations and anions in a volume element, is connected with the electric field by the Poisson equation:

$$\varepsilon_0 \varepsilon \frac{dE}{dX} = F\left(C_+ - C_- + C_H - C_{OH}\right) \tag{2}$$

where ε_0 is the permittivity of the vacuum, ε is the relative dielectric permeability.

The current density I is summed of the ionic fluxes:

$$I=F(J_+ - J_- + J_H - J_{OH}) \tag{3}$$

In steady state the salt ions fluxes do not vary with the coordinate X. The fluxes of H^+ and OH^- ions are variable due to the generation or recombination of these ions, however, the sum $J_W=J_H -$

J_{OH} remains constant because the amount of H^+ ions appearing or disappearing at a point X is equal to the corresponding amount of OH^- ions.

DBL is a region beyond the water splitting reaction zone, the total flux of water ions ($J_W=J_H-J_{OH}$) is assumed to be known there. As well, the total current density I is given.

The problem is solved by the method developed in the case of a binary electrolyte without water splitting [4]. As earlier [4], it is supposed that the DBL lying between X=0 and $X=\delta$ consists of three zones: the electroneutral zone of thickness δ_1; the electromigration zone of space charge region (SCR) of thickness δ_2; and the quasi-equilibrium part of the SCR adjacent to the membrane surface (quasi-equilibrium electric double layer) of thickness δ_3. The electromigration and quasi-equilibrium zones are separated by a point X_s where $dC_+/dX=0$ and the concentration of the salt counter-ions reaches its minimum (noted as C_{+s}). For calculation of the minimum salt cation concentration in the DBL, C_{+s}, the following equation is obtained:

$$\frac{2D_+}{J}\left(C_+^0-C_{+s}\right)+\frac{\varepsilon\varepsilon_0 RT}{2F^2D_+C_{+s}^2}\frac{J_+^2}{J}+\sqrt{\frac{2\varepsilon\varepsilon_0 RT}{F^2C_{+s}}}=\delta\,, \qquad J=J_++\frac{D_+}{D_{OH}}J_{OH} \tag{4}$$

The three terms in the left-hand side of Eq. (4) are the thicknesses of the three zones of the DBL: δ_1, δ_2 and δ_3, respectively.

Results and Discussion

The calculation of the total DBL thickness and its different zones thicknesses starting from the experimental data presented in Fig. 1 should be considered as an example of application of the developed method to describe ion-transfer phenomena in the cases of membranes characterized by low (Fig. 1a) and high (Fig. 1b) water splitting rates. To find the desired characteristics it is sufficient to know the partial current densities of Na^+ and H^+ ions through the cation-exchange membrane and the partial current densities of Cl^- and OH^- ions through the anion-exchange membrane.

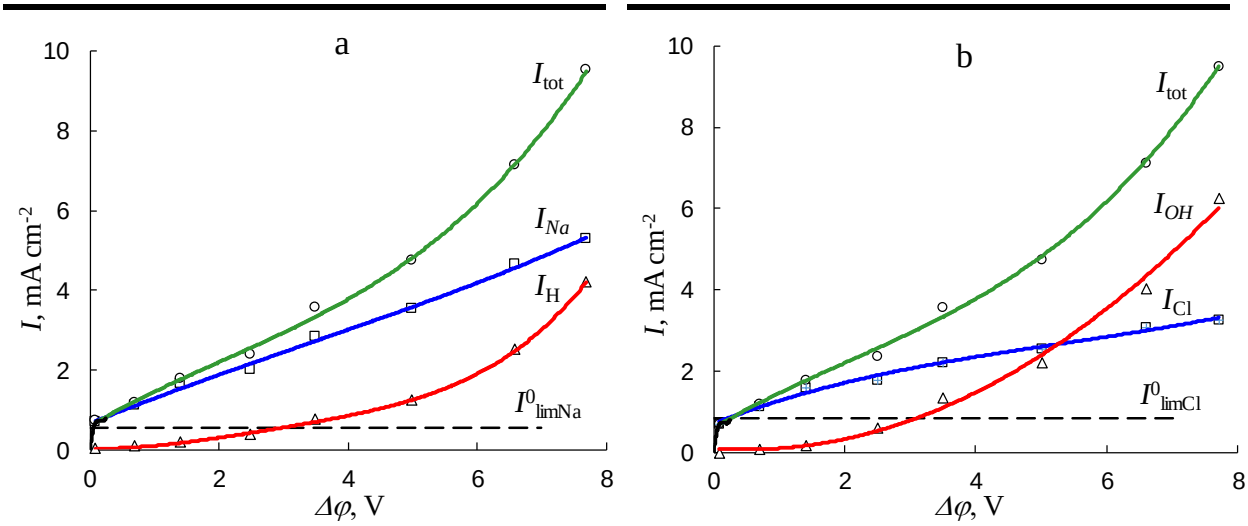

Figure 1. Current-Voltage Curves for the Diluate Compartment Formed of the Cation-Exchange Membrane MK-40 and the Anion-Exchange Membrane MA-40 in 0.002 M NaCl Solution. The total current and partial currents of Na^+ and H^+ ions through the MK-40 membrane (a) and partial currents of Cl^- and OH^- ions through the MA-40 membrane (b) are shown. The data are taken from [5].

The algorithm includes the calculation of the theoretical value of the potential drop (PD), which is compared with the experimental value for the given current density. To calculate the PD between the tips of two measuring capillaries, one should evaluate the PD across the anion- and cation-exchange membranes, including the Donnan PD at the interfaces and the PD across the DBLs

adjoining these membranes, as well as the PD across the bulk solution layer between the external edges of the DBLs in the diluate compartment.

The results of calculation show that increasing water splitting rate reduces the space charge density. This reduction is due to the H^+ (or OH^-) ions, the products of water splitting, which enter the SCR at the depleted membrane surface as co-ions. Reducing the space charge density, in turn, leads to a decrease in the intensity of electroconvection. Thus, to increase electroconvection, it is necessary to reduce water splitting, which together can help to decrease the membrane scaling.

Acknowledgment

The authors are grateful to the RFBR, Russia (grant 17-08-01442).

References

1. *Andreeva M. A., Gil V. V., Pismenskaya N. D., Dammak L., Kononenko N. A., Larchet C., Grande D., Nikonenko V. V.* Mitigation of membrane scaling in electrodialysis by electroconvection enhancement, pH adjustment and pulsed electric field application // J. Membr. Sci. 2018. V. 549. P. 129-140.
2. *Merkel A, Ashrafi A. M.* An investigation on the application of pulsed electrodialysis reversal in whey desalination // International Journal of Molecular Sciences. In press.
3. *Mishchuk N. A.* Concentration polarization of interface and non-linear electrokinetic phenomena // Adv. Colloid Interface Sci. 2010. V. 160. P. 16-39.
4. *Nikonenko V. V., Zabolotsky V. I., Gnusin N. P.* Electrotransport of ions through a diffusion layer where is a deviation from the local electroneutrality // Electrochimiya. 1989. V. 25. P. 301.
5. *Zabolotsky V. I., Nikonenko V. V., Pismenskaya N. D., Laktionov E. V., Urtenov M. Kh., Strathmann H., Wessling M., Koops G.H.* Coupled transport phenomena in overlimiting current electrodialysis // Sep. Purif. Technol. 1998. V. 14. P. 255-267.

DEVELOPMENT OF ANION-EXCHANGE MEMBRANE BASED ON GRAFTED COPYLIMER OF POLYSTYRENE AND UV-IRRADIATED POLYMETHYLPENTENE

[1,2]Daniel Golubenko, [1,2]Andrey Yaroslavtsev

[1]N.S. Kurnakov Institute of General and Inorganic Chemistry, Russian Academy of Sciences, 119991 Moscow, Russian Federation, E-mail: *golubenkodaniel@yandex.ru*

[2]Institute of Problems of Chemical Physics, Russian Academy of Sciences, 142432 Chernogolovka, Moscow Region, Russian Federation

Introduction

Ion exchange membranes are used in many membrane processes, for example, electrodialysis, electrodeionization, fuel cells, diffusion dialysis. Radiation-grafting copolymerization of monomers onto ready polymer films is a promising method for membranes fabrication, which allows to simplify the formation of the film as much as possible and to fine-tune the transport properties of the membranes [1]. We have showed [2] that instead of X-rays, more available UV radiation can be used to activate the film. From the obtained graft copolymers of polystyrene and UV-activated polymethylpentene, we synthesized cation-exchange membranes whose transport properties were on par with the best homogeneous ion-exchange membranes available on the market [3]. The next important step is to obtain anion-exchange membranes, which are used in tandem with cation-exchange membranes in most membrane processes.

Experiments

In this work, we consider the opportunity to obtaine anion-exchange membranes based on graft copolymers of PS and UV-oxidized PMP in two stages (Fig. 1). At first, polystyrene is chloromethylated with chloromethyl methyl ether in the presence of Lewis acid $SnCl_4$. At the second stage, quaternary ammonium functional groups are obtained by treating the chloromethylated polymer with trimethylamine.

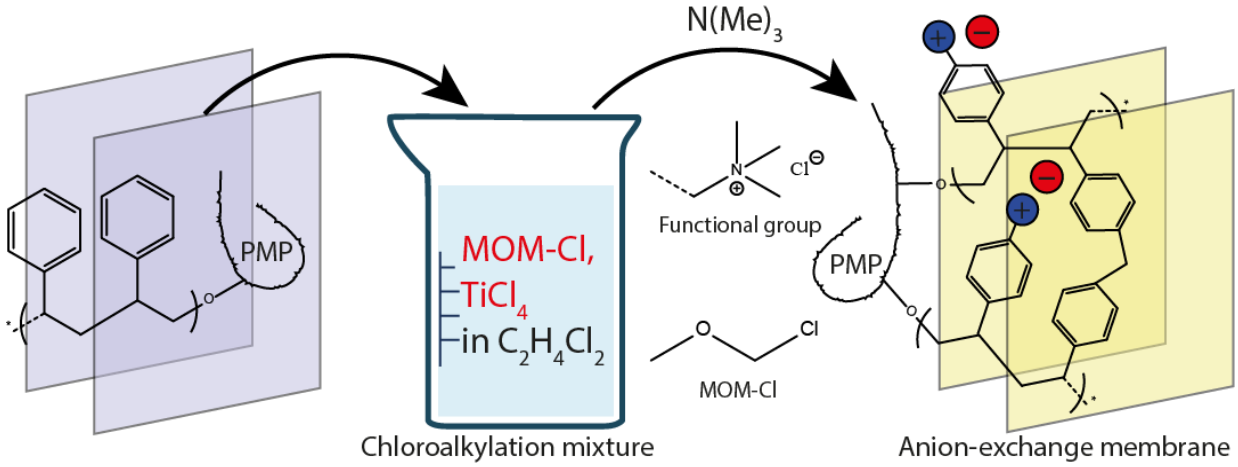

Figure 1. Synthesis scheme of anion-exchange membranes from graft copolymer.

Results and Discussion

The resulting anion-exchange membranes have an ionic conductivity (in 0.5M NaCl) in the range of 5–25 mS cm^{-1} and an ion-exchange capacity in the range of 1.3–2.9 mmol g^{-1}. The properties of anion-exchange membranes depend not only on the content of polystyrene and its degree of crosslinking in the initial film, as in the case of cation-exchange membranes, but also on the conditions of the chloromethylation reaction. Thus, increasing the concentration of halogen-ether in the alkylating mixture leads to an increase in the yield of ionic groups and the degree of membrane swelling. An increase in the concentration of Lewis acid on the contrary reduces the degree of swelling of the membrane. It was shown that there is an optimal time for chloroalkylation, which allows to obtain membranes with the best combination of conductivity

and selectivity. For the considered copolymer it is 30-90 min, depending on the degree of PS crosslinking in the initial copolymer film. The resulting anion-exchange membranes have an excellent combination of selectivity and specific ionic conductivity, which, together with a small thickness, gives them a significant advantage over commercial membranes in applications that require low ionic resistance: reverse electrodialysis, Red-Ox flow batteries and power supplies. The membranes with high graft levels (GD> 100%) and optimal chloroalkylation time have the best combination of conductivity and selectivity.

This work was supported by the Russian Science Foundation (project no. 17-79-30054).

References

1. *Mahmoud Nasef M., Saidi H.* Preparation of crosslinked cation exchange membranes by radiation grafting of styrene/divinylbenzene mixtures onto PFA films // J. Memb. Sci. 2003. V. 216. P. 27.
2. *Golubenko D.V., Yaroslavtsev A.B.* New approach to the preparation of grafted ion exchange membranes based on UV-oxidized polymer films and sulfonated polystyrene // Mendeleev. Commun. 2017. V. 27. P. 572.
3. *Golubenko D.V., Pourcelly G., Yaroslavtsev A.B.* Permselectivity and ion-conductivity of grafted cation-exchange membranes based on UV-oxidized polymethylpenten and sulfonated polystyrene// Sep. Purif. Technol. 2017. V. 207. P. 329.

POROUS CONDENSER FOR THERMO-MEMBRANE SEPARATION PROCESSES OF AQUEOUS MEDIA

Georgy Golubev, Ilya Eremeev, Ilya Borisov, Vladimir Vasilevsky, Alexey Volkov
A.V. Topchiev Institute of Petrochemical Synthesis, Moscow, Russia, E-mail: *GolubevGS@ips.ac.ru*

Introduction

Thermo-membrane processes are the processes of membrane separation, with a temperature gradient as a driving force. These processes include, in particular, membrane distillation process of separation water solutions of organic and non-organic substances, which flows with change of the phase state of the initial solution, followed by the separation of the steam phase with the porous hydrophobic membrane [1]. This process can be successfully applied in seawater desalination, treatment of the wastewater etc. In comparison with another processes of the MD separation, this process possesses unique properties, for instance: 100% (theoretical) retention of the non-volatile components of separated mixtures, moderate exploitation parameters, lack of sensitivity to concentration of the mixture to be separated and chemical resistance to various impurities and pollutants [2]. The most widely used configurations of MD are the direct contact membrane distillation, where the both sides of membrane are in direct contact with the feed and permeate solutions, respectively, and the air gap membrane distillation, where the membrane inlet side is contacted with the hot feed solution and the cold surface of condenser is separated from the membrane outlet side by the air layer. The last configurations of MD can be successfully operated only in the vertical position since the condensed liquid permeate is evacuated from the module by the gravity force. Membrane processes with the air gap configuration have certain limits in the design and orientation.

The novel module configuration was proposed in which one of the air gap walls is made of a porous material that increases the efficiency of the condensate outlet from the module [3]. With this process organization, the permeate does not accumulate in the air gap, that allows to reduce the thickness of the air gap and thus maximize the driving force of the process. Other advantages of the new process are the simplicity of the module design and the ability to work with any module orientation.

This work describes a study of the process of concentration the model solutions of sodium chloride imitators of the waste water of reverse osmosis, using apparatus with porous condenser.

Experiments

Membrane distillation set-up with porous metal surface permeate condensation is shown schematically in Figure 1.

In this study, MFFK-1 (Vladipor, Russia) commercial flat sheet membranes were used. Total active area of membrane amounts to 14.7×10^{-3} m^2. Porous condenser based on a sintered stainless steel (VMZ-Techno, Russian Federation; thickness 200 μm; porosity 30%).

Membrane distillation with porous condenser (MD-PC) process proceeds as follows: feed was continuously circulated between hot part of the membrane module and feed tank. The membrane was in direct and continuous contact with the feed. The permeate passes through the membrane, evaporates in the air gap 2.5 mm and then condensed on the porous cooling plate. The condensate wets the condensation surface, penetrates the pores and flows into with coolant chamber. It should be noted that the pressure in coolant chamber is lower than in the condensation chamber, by the fact that the pump providing a coolant circulation system is located after the module. Held in the coolant chamber permeate is used as refrigerant. MD-PC experiments were performed in contact with binary aqueous mixtures of salt. Water sodium chloride solution were prepared using weight method, utilizing sodium of "CP" quality and distilled water. The content of sodium chloride in the concentrate and in the condensate was determined using conductometric method, diluting the concentrate with distilled water in advance. Quantity of the separated products was determined using weight method.

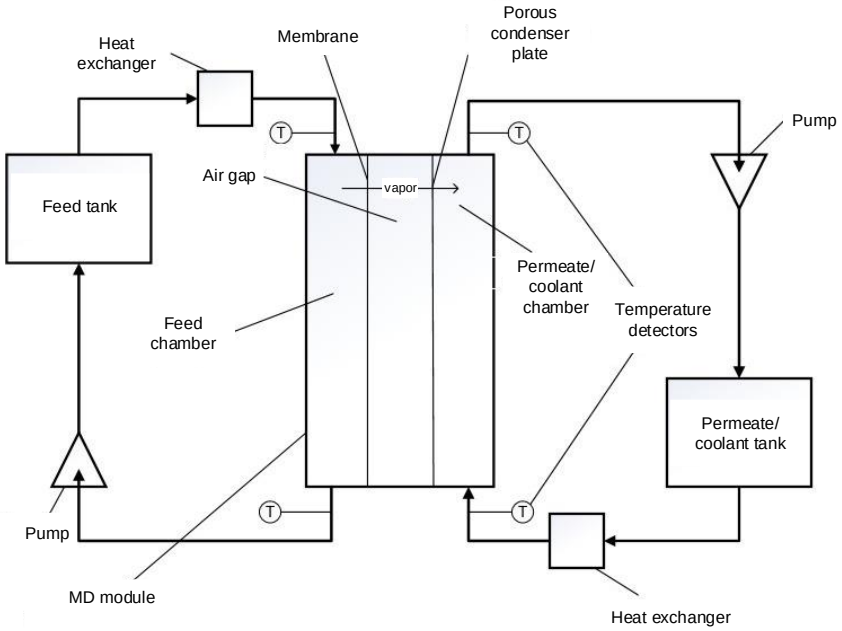

Figure 1. Scheme of membrane distillation set-up with porous cooling plate used in experiments.

Results and Discussion

Figure 2 shows the temperature dependences of the permeate flux under the MD-PC separation of aqueous solution of sodium chloride concentration of 50 g/l. The increase of the feed temperature from 40 up to 80 °C at constant coolant circuit temperature of 20 °C and an air gap of 2.5 mm led to more than 3-fold higher permeate fluxes. At the maximum temperature difference of 60 °C tested in this study, it was possible to achieve the water flux of 6.8 kg/m^2·h.

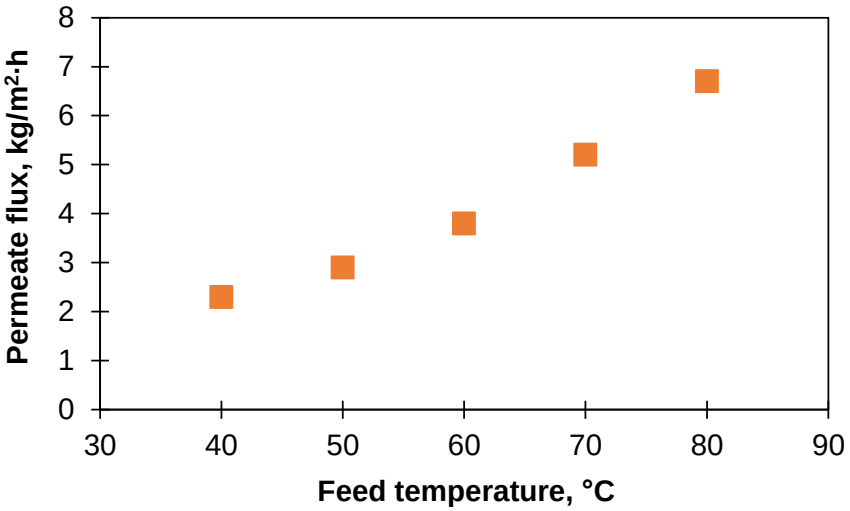

Figure 2. Dependences of permeate flux on feed temperature for 50 g/l NaCl solution, T_c = 20˚C, $l_{air\ gap}$ = 2.5 mm.

Figure 3 shows the concentration NaCl in feed dependences of permeate flux. Pure water, brackish water, Baltic and Caspian sea, Red sea and waste water of reverse osmosis with NaCl concentrations of 0, 5, 10, 40, 50 g/l, respectively, were studied as model solutions. As the salt concentration increases, a certain decline in the permeate flux was observed. Flux decline might be caused via the concentration polarization phenomenon which occurs at high permeate fluxes. Concentration polarization leads to an increase of the salt content in the liquid boundary layer near the membrane, which in turn reduces the driving force of the MD process [4].

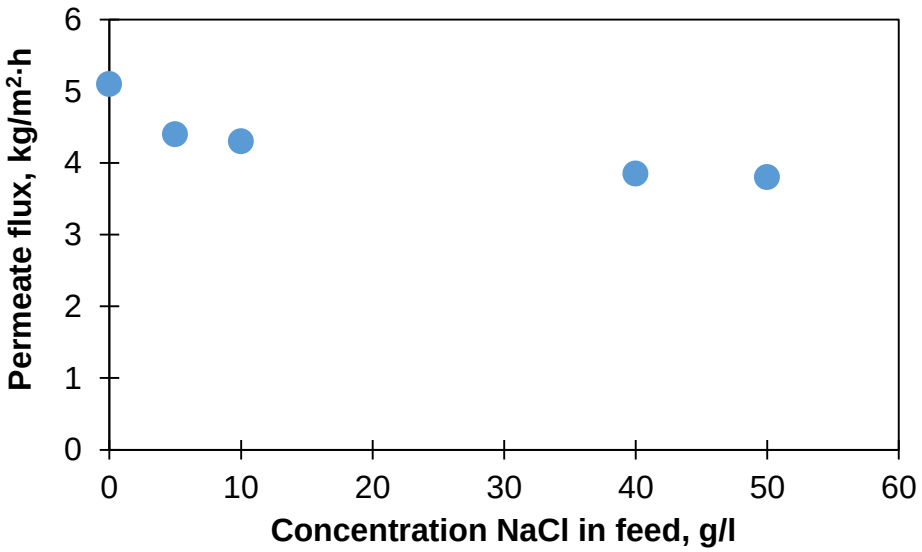

Figure 3. Dependences of permeate flux on concentration NaCl in feed, T_f = 60 °C, T_c = 20°C, $l_{air\ gap}$ = 2.5 mm.

Acknowledgements

The reported study was funded by RFBR according to the research project № 18-58-80031.

References

1. *Driolli A.A., Macedonio F.* Membrane distillation: recent development and perspectives // Desalination. 2015. V. 356. P. 56
2. *Wang P., Chung T.S.* Recent advances in membrane distillation processes: Membrane development, configuration design and application exploring // J. Membr. Sci. 2015. V. 474. P. 39.
3. *Volkov A.V., Novitsky E.G., Borisov I.L., Vasilevsky V.P., Volkov V.V.* Porous condenser for thermally driven membrane processes: Gravity independent operation // Sep. Pur. 2016. V. 171. P. 191.
4. *Martınez-Dıez L., Vazquez-Gonzalez M.I.* Temperature and concentration polarization in membrane distillation of aqueous salt solutions // J. Membr. Sci. 1999 V. 156. P. 265.

REGENERATION OF TRIETHYLENE GLYCOL BY THERMOPERVAPORATION WITH POROUS CONDENSER

Georgy Golubev, Ivan Podtynnikov, Stepan Bazhenov, Ilya Borisov
A.V. Topchiev Institute of Petrochemical Synthesis, Moscow, Russia, *E-mail: GolubevGS@ips.ac.ru*

Introduction

Russian Federation is a leading international gas producer. Both natural and associated petroleum gases produced always contain moisture. Therefore, the key stage in gas treatment is dehydration performed via absorption of water by triethylene glycol (TEG), regeneration of the latter being an essential step. In industry, absorbent regeneration is most often carried out using distillation [1], but high energy consumption and large scale characteristics of distillation columns contribute to the search and development of compact and alternative approaches, such as membrane separation methods (primarily, pervaporation) due to their compactness, high degree of modularity and universality [2].

There are three different ways to implement the pervaporation process: vacuum pervaporation, pervaporation with gas striping and thermopervaporation (TPV). The use of vacuum pervaporation is the most common method in experimental research and commercial use. It should be noted that the main industrial application of vacuum pervaporation is the dehydration of organic solvents. As membranes, primarily non-porous membranes or composite membranes with a thin non-porous layer of polydimethylsiloxane or polyvinyl alcohol are used. The use of pervaporation for TEG regeneration in combination with the dehydration of natural gas was patented in 2006 [3]. At the same time, the main focus in the literature is on the dehydration of monoethylene glycol (MEG) [4, 5], whose widespread use in industry may be limited due to its higher volatility compared to TEG. Gas-liquid membrane contactors are also considered as promising approaches for the implementation of the stage of absorption of water vapor from natural gas under conditions of subsea production [6].

Recently, thermopervaporation has attracted more and more attention of researchers, because in this process, unlike vacuum pervaporation, the separation proceeds at atmospheric pressure using low-grade heat, and at the same time has high separation characteristics [7]. Dehydration of TEG by thermopervaporation was not previously studied. The essence of the thermopervaporation method is that in the separation module the selective membrane is separated by a small air gap from the cooled surface (metal plate), on which the pairs (permeate) that have passed through the membrane condense. In the development of this approach, a new version of the TPV module configuration was recently proposed, where a porous metal partition [8] is used as a cold plate (condensation surface of permeate vapor). The porous condensation surface allows to solve the problem of blocking the air gap with a liquid permeate, reduce the air gap size and thus achieve maximum compactness of the separation device and process performance compared to traditional thermopervaporation.

This work describes a study of the process of dehydration the model solutions of TEG-water, using thermopervaporation with porous condenser (TPV-PC).

Experiments

Thermopervaporation pilot scale with a porous metal surface permeate condensation is shown schematically in Figure 1. MDK-I (diffusion composition membrane – Isogel) (Vladipor, Russia) commercial flat sheet membranes were used. Porous condenser based on a sintered stainless steel (VMZ-Techno, Russian Federation; thickness 200 μm; porosity 30%). The module is equipped with 2 membranes, total active area of which amounts to 255 cm^2.

TPV-PC process proceeds as follows: feed was continuously circulated between hot part of the membrane module (4) and feed tank (1). The membrane selective layer was in direct and continuous contact with the feed. The permeate passes through the membrane (5), evaporates in the air gap 2.0 mm (6) and then condensed on the porous cooling plate (7). The condensate wets the condensation surface, penetrates the pores and flows into with coolant chamber. It should be noted that the pressure in coolant chamber is lower than in the condensation chamber, by the fact

that the pump (10) providing a coolant circulation system is located after the TPV-PC module. Held in the coolant chamber permeate is used as refrigerant. Accumulated during the experiment condensed permeate is discharged from the coolant tank (11) and analyzed. Thermopervaporation experiments were performed in contact with model solutions of TEG-water. The concentration of water in the TEG varied in the range of 30-5 wt.%.

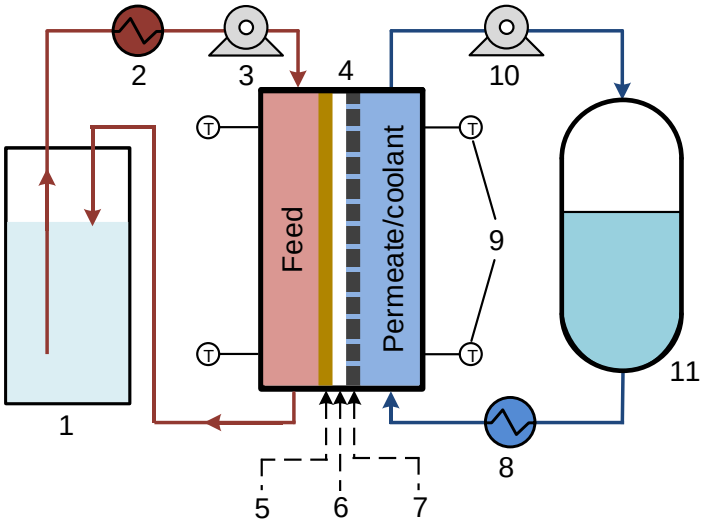

Figure 1. Scheme of pilot thermopervaporation set-up with porous cooling plate used in experiments.

Results and Discussion

Figure 2 shows the results of TPV-PC experimental studies of the total permeate flux through the MDK-I membrane and the separation factor from the TEG concentration in the feed. The total permeate flux with an increase in TEG in the feed decreases linearly from 0.8 to 0.38 kg/m^2·h, and the separation factor is almost independent of the concentration of TEG in the feed and corresponds to a value of 7.2. Separation factor is calculated as

$$\alpha_{ij} = \frac{C_i^p \cdot C_j^f}{C_j^p \cdot C_i^f}$$

where C^p and C^f stand for the weight fractions of the component in the permeate and feed mixtures, respectively. Then, mass fluxes of the component in the permeate are defined as $J_i = J \cdot C_i^p$.

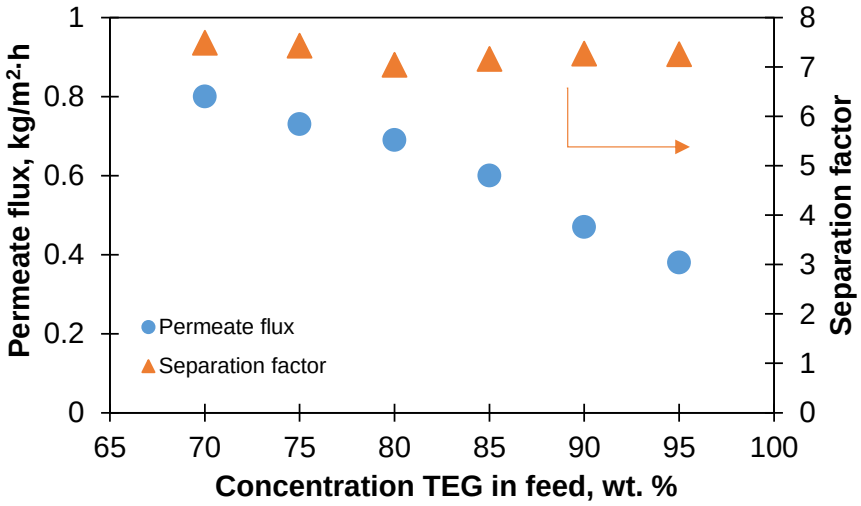

Figure 2. Dependences of permeate flux and separation factor on concentration TEG in feed, T_f = 60 °C, T_c = 10 °C, $l_{air\ gap}$ = 2.0 mm.

Figure 3 shows the dependence of the TEG flux and water through the membrane on the concentration of TEG in the feed. The flux of water through the membrane with increasing TEG in the feed decreases close to a linear relationship.

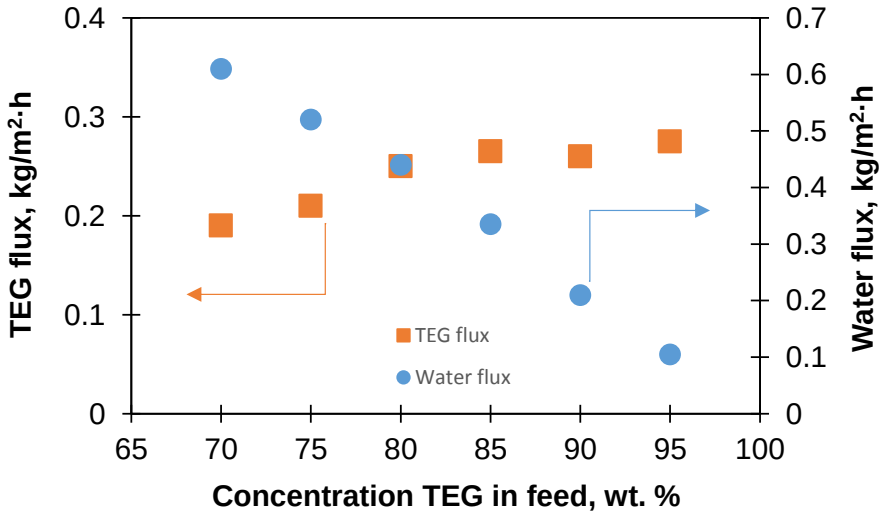

Figure 3. Dependences of TEG flux and water flux on concentration TEG in feed, T_f = 60 °C, T_c = 10 °C, $l_{air\ gap}$ = 2.0 mm.

Acknowledgements

The reported study was funded by RFBR according to the research project № 19-08-01217.

References

1. *Piemonte V., Maschietti M., Gironi F.* A Triethylene Glycol–Water System: A study of the TEG regeneration processes in natural gas dehydration plants // Energ. Sources Part A. 2012. V. 34. P. 456.
2. *Lin H., Thompson S.M., Serbanescu-Martin A., Wijmans J.G., Amo K.D., Lokhandwala K.A., Merkel T.C.* Dehydration of natural gas using membranes. Part I: Composite membranes. // J. Membr. Sci. 2012. V. 413. P.70.
3. *Wijmans J.G., Ng A., Mairal A.P.* Natural gas dehydration apparatus. // U.S. Patent No. 7,132,008. 2006. Washington, DC: U.S. Patent and Trademark Office.
4. *Guo R., Hu C., Li B., Jiang Z.* Pervaporation separation of ethylene glycol/water mixtures through surface crosslinked PVA membranes: coupling effect and separation performance analysis // J. Membr. Sci. 2007. V. 289. P. 191.
5. *Yu C., Zhong C., Liu Y., Gu X., Yang G., Xing W., Xu N.* Pervaporation dehydration of ethylene glycol by NaA zeolite membranes // Chem. Eng. Res. Des. 2012. V. 90. P. 1372.
6. *Dalane K., Svendsen H.F., Hillestad M., Deng L.* Membrane contactor for subsea natural gas dehydration: Model development and sensitivity study // J. Membr. Sci. 2018. V. 556. P. 263.
7. *Borisov I.L., Volkov V.V.* Thermopervaporation concept for biobutanol recovery: The effect of process parameters // Sep. Pur. Technol. 2015. V. 146. P. 33.
8. *Borisov I.L., Golubev G.S., Vasilevsky V.P., Volkov A.V., Volkov V.V.* Novel hybrid process for bio-butanol recovery: Thermopervaporation with porous condenser assisted by phase separation // J. Membr. Sci. 2017. V. 523. P. 291.

IMPACT OF CURRENT DENSITY DISTRIBUTION IN ELECTRODIALYSIS SYSTEM ON TRANSITION TIME OF CHRONOPOTENTIOGRAMS

Andrey Gorobchenko, Semyon Mareev
Membrane Institute, Kuban State University, Krasnodar, Russia, *E-mail: gorobchenkoandrey@mail.ru*

Introduction

Significant progress in understanding of membrane behavior in electrodialysis systems was recently achieved due to developing of 2D first principles models based on the coupled Nernst–Planck–Poisson–Navier–Stokes (NPP-NS) equations and electric current stream function. These models allow computation of concentration and electric field in overlimiting current regime, analysis of the EC modes, the role of surface properties and others. In this paper, we propose a mathematical model, which allows to describe the development of electroconvection at overlimiting currents and to assess the impact of current density distribution on transition time of chronopotentiograms.

Theoretical

The system under study is half of the desalination flow-through channel of an electrodialyzer at the side of the cation-exchange membrane (CEM) [1]. 2D non-stationary ion transfer in the system under study is described by the NPP-NS and electric current stream function equation system. The membrane is considered as fully homogeneous with constant fixed charge. A non-slip condition is applied at membrane/solution interface. The system parameters are as follows: channel length (L) are 2, 3, 4, 6, 8, 10, 12, 15, 20 and 30 mm, width is H=0.25L, average current density in the channel is $i_{av}=2i_{lim}$, average velocity is $V_0=4$ mm/s, concentration of NaCl solution is 20 mM. Numerical solution of the problem was obtained using Comsol Multiphysics software package.

Results and Discussion

Results of the calculations are presented in Table 1, where i_{av} – average current density, τ_s – the Sand transition time, τ_m – model transition time.

Table 1: Results of Calculation

L, MM	2	3	4	6	8	10	12	15	20	30
I_{AV} , A/M^2	**204.39**	**155.98**	**128.76**	**98.26**	**81.11**	**69.90**	**61.90**	**53.35**	**44.04**	**33.61**
T_S , S	**0.3077**	**0.5283**	**0.7753**	**1.3312**	**1.9536**	**2.6306**	**3.3545**	**4.5169**	**6.6286**	**11.3820**
T_M , S	**0.3668**	**0.6107**	**0.8807**	**1.4803**	**2.1451**	**2.8673**	**3.6363**	**4.8692**	**7.0926**	**12.0870**
T_M/T_S, %	**19.2**	**15.6**	**13.6**	**11.2**	**9.8**	**9**	**8.4**	**7.8**	**7**	**6.2**

It is shown, that the model transition time (τ_m) does not coincide with the Sand transition time (τ_s). The fact is that, over time, the current density in the modeling system diverge from the specified average value (Figure 1).

Current density distribution at membrane/solution interface and in the solution layer (Figure 2) shows that the diverge of current density from the specified average value decreases with increasing channel length, which explains the decrease in relative error between model transition time (τ_m) and Sand transition time (τ_s) of chronopotentiograms.

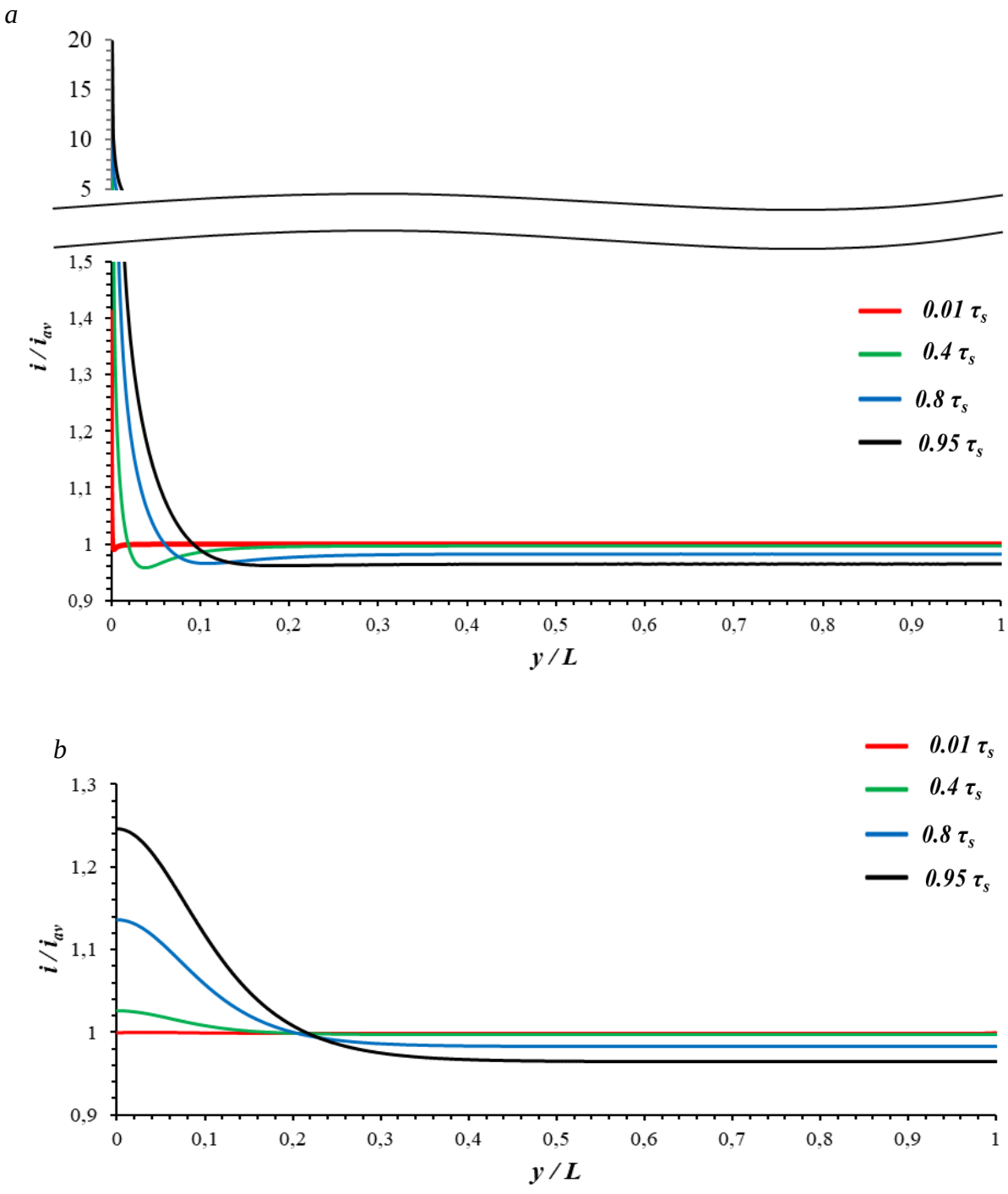

Figure 1. Current Density Distribution along the Channel Length (L=2 mm) at CEM/Solution Interface(a) and in the Solution Layer (b) Depending on the Time

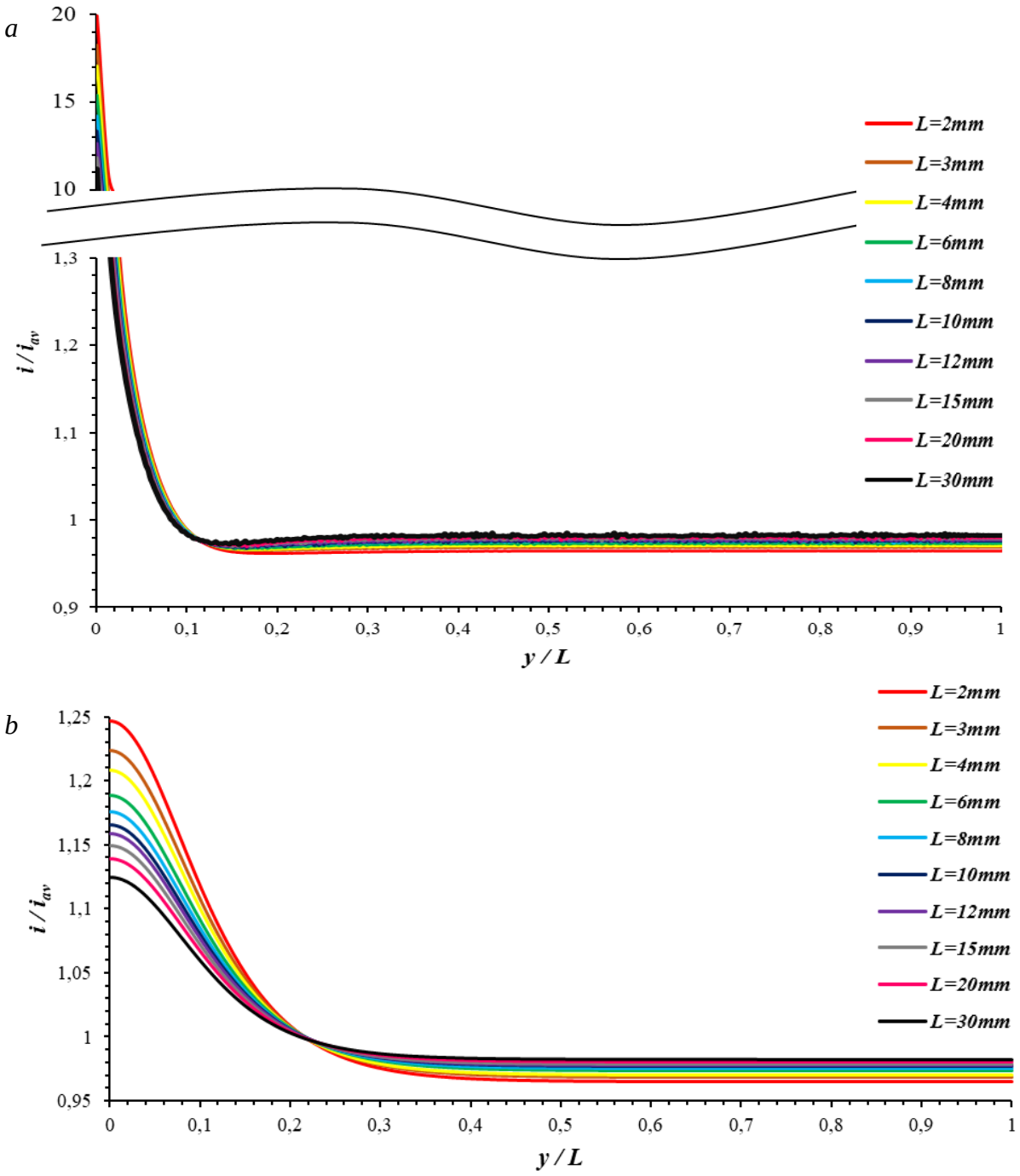

Figure 2. Current Density Distribution at CEM/Solution Interface (a) and in the Solution Layer (b) at $\tau=0.95\tau_s$, Depending on the Length of Channel

Thus, we can conclude that the disposition of current density distribution along the channel has a significant effect on the transition time of chronopotentiograms.

Acknowledgments

The study is realized with the financial support of the Russian Foundation of Basic Research, project № 17-08-01538.

References

1. *Uzdenova A.* 2D mathematical modelling of overlimiting transfer enhanced by electroconvection in flow-through electrodialysis membrane cells in galvanodynamic mode // Membranes. 2019. V. 9 (3). P. 1-19.

MATHEMATICAL MODELING OF THE INFLUENCE OF DISSOCIATION/RECOMBINATION REACTION OF WATER MOLECULES ON THE BINARY SALT IONS TRANSPORT TAKING INTO ACCOUNT THERMAL EFFECTS

[1]Vitaly Gudza, [2]Natalja Chubyr, [1]Anna Kovalenko, [1]Makhamet Urtenov

[1]Kuban State University, 149 Stavropolskaya Street, 350040, Krasnodar, Russia,
E-mail: *vitaliy.gudza@gmail.com*

[2]Kuban State Technology University, 2 Moskovskaya Street, 350042, Krasnodar, Russia
E-mail: *chubyr-natalja@mail.ru*

Introducion

Taking into account the influence of the reaction of dissociation/recombination of water molecules is important for understanding of transport processes in electro-membrane systems, because some authors consider that the emergence of new charge carriers H^+ and OH^- may lead to reduction or even disappearance of space charge, which is the basis for other mechanisms of transport of, for example, electroconvective. The dissociation reaction of water molecules is endothermic, and the recombination is exothermic, with the centers of the reaction areas separated in space, which causes an uneven temperature distribution. And this affects all the physical properties of water, for example, the dissociation coefficient, the heat capacity of water, etc., and some significantly, and others slightly. In addition, uneven temperature distribution can cause gravitational convection. Thus, the study of temperature effects associated with the reactions of dissociation and recombination of water molecules is an actual problem. In this work, we will restrict ourselves to the consideration of the influence of the uneven distribution of temperature on the coefficient of dissociation of water molecules.

Problem definition

The paper uses a mathematical model of electrodiffusion of ions H^+ and OH^-, as well as two salt ions in the diffusion layer in electromembrane systems with a perfectly selective membrane taking into account the heat equation. The transition to the dimensionless form of the system of equations is carried out, trivial and nontrivial similarity criteria are calculated, a numerical study is carried out and the basic laws of heat and mass transport are established.

Dimensionless form of differential equations and similarity criteria

Differential equations [1], modeling of one-dimensional stationary process migration for singly charged ions of salt in the Nernst diffusion layer, taking into account the reactions of dissociation/recombination of water and temperature effects associated with Joule heating of the solution and reaction of the dissociation/recombination of water for the convenience of the numerical solution was brought to a dimensionless form:

$$\frac{dC_1}{dx} = C_1E - j_1\,, \tag{1}$$

$$\frac{dC_2}{dx} = -C_2E - j_2\,, \tag{2}$$

$$\frac{dC_3}{dx} = C_3E - j_3\,, \tag{3}$$

$$\varepsilon D_3 \frac{d}{dx} j_3 = a(\gamma e^{b(T-1)} - C_3C_4)\,, \tag{4}$$

$$\frac{dC_4}{dx} = -C_4E - j_4\,, \tag{5}$$

$$\varepsilon D_4 \frac{d}{dx} j_4 = a(\gamma e^{b(T-1)} - C_3C_4)\,, \tag{6}$$

$$\varepsilon \frac{dE}{dx} = C_1 - C_2 + C_3 - C_4 . \quad (7)$$

$$Le \cdot \frac{\varepsilon}{\mu} \cdot \frac{d^2T}{dx^2} + \varepsilon E \cdot I + Arn \cdot a \cdot (C_3 C_4 - \gamma e^{b(T-1)}) = 0 \quad (8)$$

In these equations: $Le = \frac{Sc}{\Pr} = \frac{a}{D} = 88.6$ - Lewis number, $Arn = \frac{q}{RT_0} = 22.8$ - thermal analogue Arrhenius criterion, $\mu = \frac{C_{10} R}{\rho_0 c_p}$ - constant having a meaning of relative specific volume heat capacity.

The system of equations contains three small parameters ε, μ and γ moreover, the parameter ε enters the equations singularly, i.e. as a coefficient at derivatives, and the parameters μ and γ are regular, so the system of equations is both singularly and regularly perturbed. It is shown that the parameters ε, μ and γ are related by similarity criteria $\varepsilon\mu = n_{a,1}$, $\gamma = n_{a,2}\varepsilon^2$, где $n_{a,1}$, $n_{a,2}$, where, some universal constants.

The parameter $a = 14$ is the square of the ratio of the Debye length to the width of the recombination region and therefore the width of the recombination region is approximately 37% of the width of the quasi-equilibrium region of the space charge (Debye length).

Results and Discussion

To analyze the results of the numerical solution, along with the graphs of the desired functions [2] C_i, E, j_3, j_4, T, the plots of the functions $\rho(x) = C_1 - C_2 + C_3 - C_4$, $p(x) = C_3 C_4 - \gamma e^{b(T-1)}$ were also considered. The function $\rho(x)$ characterizes the charge density distribution, and $p(x)$ - deviation from the equilibrium of the dissociation/recombination reaction.

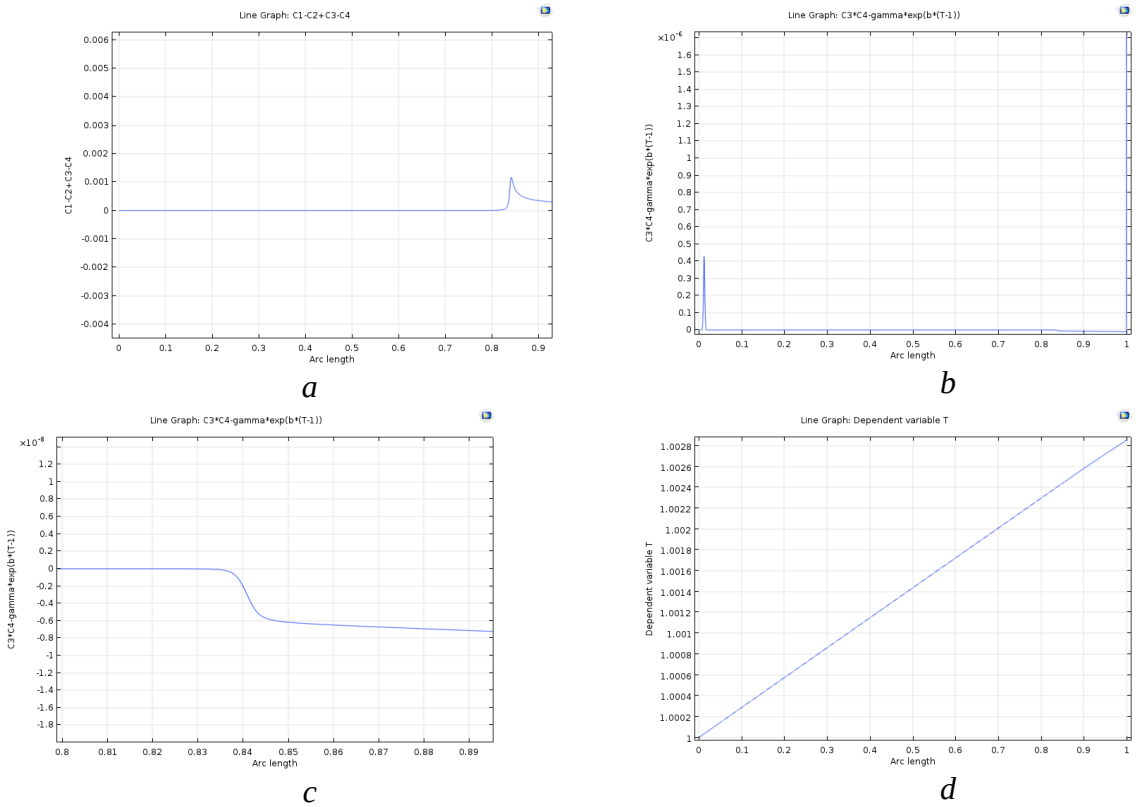

a *b* *c* *d*

Figure 1. a) the plot of the function $\rho(x) = C_1 - C_2 + C_3 - C_4$ ([0, 0.93]) , b) the plot of the function $p(x) = C_3 C_4 - \gamma e^{b(T-1)}$, c) the plot of the function $p(x) = C_3 C_4 - \gamma e^{b(T-1)}$ in the space charge region, d) temperature plot.

It follows from figure 1 (a) that the diffusion layer is divided into three regions: the first region of electroneutrality (ER), where $\rho(x) = 0$, the second region of the space charge (SCR, $\rho(x) > 0$) and the intermediate layer between them , where the charge distribution density has a pronounced local maximum.

The SCR itself can be divided into extended SCR and quasi-equilibrium part of the SCR (having very small dimensions and adjacent to the interface). In the quasi-equilibrium part of the SCR, the charge density distribution obeys the exponential law (not shown in the figure).

The general view of the $p(x)$ function graph (fig.1b) shows that the deviation from the equilibrium occurs in a narrow recombination region, which is located inside the ER and in the space charge region (fig.1c), and in the first case $p(x) > 0$, that is, recombination prevails over dissociation $C_3C_4 >> \gamma e^{b(T-1)}$. In the second case – on the contrary, and dissociation prevails over recombination everywhere in OPZ, as well as in the intermediate layer. The temperature (fig.1d) increases linearly by 0.0028 in dimensionless form or $0.0028 \cdot 298 = 0.83$ degree.

This increase depends on the total current density or potential jump applied in the diffusion layer and can range from several degrees to tens. The evaluation of the terms of equation (8) shows that all the terms of the equation are small in comparison with the first, that is, the second derivative $\frac{d^2T}{dx^2} \approx 0$, from which it follows that the temperature is linear and determined by the boundary conditions.

Conclusion

In this paper, we propose a mathematical model of binary salt ion transport through the diffusion layer of the cation-exchange membrane, taking into account the dissociation/recombination reaction of water molecules and the temperature effects associated with them, as well as with Joule heating in solution. Established the basic laws of migration of ions of the salt with the light of the reactions of dissociation/recombination of water molecules and temperature effects.

The reported study was funded by RFBR according to the research project:
19-08-00252 A «Theoretical and experimental study of current-voltage characteristics of electromembrane systems»

References

1. *Kovalenko A.V., Urtenov M.A.Kh., Chubyr N.O., Gudza V.A.* Matematicheskoye modelirovaniye vliyaniya osnovnykh temperaturnykh effektov na statsionarnyy perenos ionov soli v diffuzionnom sloye [Mathematical modeling of the influence of the main temperature effects on the stationary transport of salt ions in the diffusion layer] // Ekologicheskiy vestnik nauchnykh tsentrov chernomorskogo ekonomicheskogo sotrudnichestva [Ecological Bulletin of Scientific Centers of the Black Sea Economic Cooperation], 2018, vol.15, no.3, pp.76–86
2. *Kovalenko A.V., Urtenov M.A.Kh., Pismensky A.V., Uzdenova A.M., Gudza V.A., Chubyr N.O.* Numerical study of the temperature effects associated with the dissociation/recombination reaction of water molecules and joule heating membrane systems // Ion Transport in Organic and Inorganic Membranes Conference Proceedings. 2018. pp. 291-293.

SELF-OSCILLATION PROCESS DURING THE DIFFUSION OF CO-IONS THROUGH ION-EXCHANGE MEMBRANES

[1]Vladimir Gursky, [2]Sergey Timofeev

[1]«A.P. Aleksandrov Research Institute of Technology» (NITI), Sosnovy Bor, Leningrad region, Russia E-mail: *gurskyvs@yandex.ru*

[2]JSC «Plastpolimer», Saint-Petersburg, Russia, E-mail: *svtimof@mail.ru*

The Donnan dialysis – is a common method of reducing the level of background signal, caused by high eluate conductivity in ion chromatography. During the research of membrane suppression systems for ion chromatography, it was discovered that in some cases suppression of background conductivity leads to the sinusoidal base line. Oscillation amplitude in most cases is 0,5% from background conductivity level and practically doesn't lower the metrological characteristics of analyte determination.

Further research has shown that such oscillations of the eluate electrical conductivity are observed during co-ions diffusion through ion-exchange membranes without process of The Donnan dialysis.

It was found that during the diffusion of acids through cation-exchange capillaries (ТФ4СК of different water capacity) type of co-ion (sulfate, nitrate, phosphate, oxalate) and its concentration $(0,5\text{-}20)^{-2}$ mol/l effects the oscillation range of conductivity. Similar conductivity self-oscillations were detected during the research of sodium-ions diffusion from hydroxide solution through anion-exchange membrane Fumasep FAA.

Probable reasons of oscillations are discussed.

POLYDECYLMETHYLSILOXANE-BASED THIN FILM COMPOSITE MEMBRANE WITH ENHANCED ORGANIC SELECTIVITY

Evgenia Grushevenko, Ivan Podtynnikov, Olga Scharova, Alina Knyazeva, Ilya Borisov
A.V. Topchiev Institute of Petrochemical Synthesis, Moscow, Russia
E-mail: *evgrushevenko@ips.ac.ru*

Introduction

The environmental situation today requires an integrated approach to the processing of raw materials and the creation of non-waste production. Membrane technologies have already proven to be a worthy alternative to the traditional method of separation of gas and liquid mixtures. One of the most difficult task for traditional methods is organic removal from the liquid mixture. An example of such a problem is to recover oxygenates from wastewater. Membrane materials based on silicone rubbers are characterized with such important properties as stability to hydrocarbons and other organic solvents exposure, as well as the stability of transport characteristics in time. It allowed them to find real industrial application as selective layer materials for membranes, despite their lesser selectivity values in comparison with high-permeable glassy polymers [1].

In our previous work, three different silicone rubbers with alkyl side groups were synthesized by using the recently proposed in-situ technique that combines two hydrosilylation reactions: the introduction of side alkyl group followed by polymer chains cross-linking in the same reaction mixture [2]. As a result, dense membranes made of polyhexylmethylsiloxane (PHexMS), polyoctylmethylsiloxane (POMS) or polydecylmethylsiloxane (PDecMS) were fabricated for further investigation of their mechanical, structural and gas transport properties.

The goal of this work was to develop composite membranes with a selective layer based on the polydecylmethylsiloxanes and study them in the process of gas separation and hydrophobic pervaporation.

Experiments

Membrane materials with high selectivity to organic vapors and with the stability of separation characteristics over time were created from cross-linkable polymers based on polymethylsiloxane modified by alkyl hydrocarbon radicals. Polyalkylmethylsiloxane membranes were synthesized by novel technique via the hydrosilylation reaction using polymethylhydrosiloxane, 1-alkene (such as 1-decene (PDecMS)), and 1,7-octadiene, over Karstedt's catalyst. The technique involves in situ modification and cross-linking [3]. Dense film membrane poly(dimethylsiloxane) (PDMS) and poly(decylmethylsiloxane) (PDecMS) were investigated in hydrophobic pervaporation.

In this work, we developed a composite membrane based on PDecMS on microfiltration (MFFK-1, Vladipor, Russia) porous support. The selective layer was cast on a porous support by dip-coating. As PDMS-based composite membrane, several commercial samples were selected: Pervap 4060 (Sulzer Chemtech, Switzerland), Pervatech PDMS, (Pervatech, Holland), PolyAn POL_OR_M2 (PolyAn GmbH, Germany) and MDK-3 (JSC NTC “Vladipor”, Russia). Vacuum pervaporation experiments were carried out on the laboratory scale setup, described in detail in [4]. The model mixture was a 1 wt. % solution of n-butanol in water.

Results and Discussion

Pervaporation characteristics of PDMS and PDecMS are presented in Table 1. PDMS is a more highly permeable material than PDecMS, as evidenced by the higher permeate flux through the membrane of this polymer. This phenomenon is explained by the greater mobility of the PDMS chain (Tg = -123°C) in comparison with PDecMS (Tg = -68°C). However, the membrane based on PDecMS is characterized by a higher selectivity for butanol, which is expressed by a separating factor (α) of 2 greater than the separation factor compared to PDMS. The task of wastewater treatment from 1-butanol (taking into account the need for its recovery) suggests a high selectivity of the process. Otherwise, the concentration of 1-butanol in the permeate will be small with a sufficiently large volume, which will require an increase in the number of purification steps. Thus,

the high separation factor makes it possible to call PDecMS a promising material for creating composite pervaporation membranes.

Table 1: Pervaporation properties of dense film PDMS and PDecMS membrane

Material	J (BuOH), g/(m²·h)	J (H_2O), g/(m²·h)	α (BuOH/H_2O)
PDMS	8.1	20	38
PDecMS	3.5	5.3	69

Since for use in industrial membrane modules, membranes with high productivity are required, in this work, for the first time, a composite membrane with a selective layer based on polydecylmethylsiloxane on a microfiltration substrate MFFK-1 was obtained. The choice of the microfiltration substrate was because the permeability of the polyalkylmethylsiloxane membrane material is not high enough, and the high performance of the substrate will make it possible to obtain an acceptable membrane performance for the target component. The cross-section of the PDecMS membrane is shown in Fig. 1.

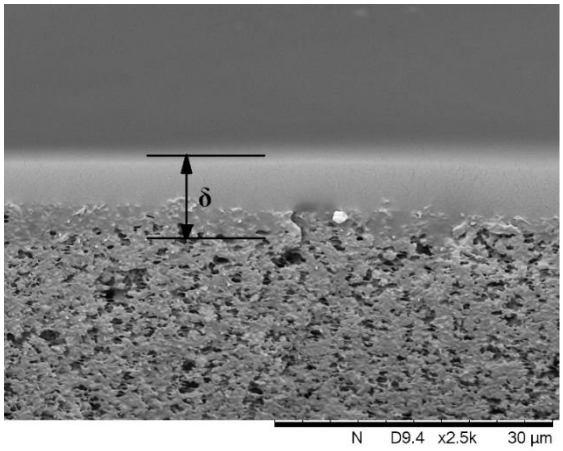

Figure 1. A cross-section of the obtained composite membrane.

The thickness of the selective layer of PDecMS was 9 μm, which is confirmed by the gas permeability of the resulting membrane (P/l (CO_2) = 0.25 $m^3/(m^2 \cdot atm \cdot h)$. According to the work [2], the gas permeability coefficient for CO_2 PDMS is 780 Barrer. Thus, it can be calculated that the effective thickness of the selective layer of the membrane is 9 μm.

For the obtained composite membrane, the separation characteristics of a binary mixture (1% wt. 1-butanol in water) were studied. For comparison, the following commercially available membrane samples with a selective layer based on siloxane polymers were investigated: Pervap 4060 (Sulzer Chemtech, Switzerland), Pervatech PDMS, (Pervatech, Holland), PolyAn (PolyAn GmbH, Germany) and MDK-3 (NTC " Vladipor ", Russia). Table 2 presents the main pervaporation properties of membranes. The studied commercial membranes are characterized by high fluxes (both the general and the target component — 1-butanol) while having low separation factors. PDecMS membrane showed almost three times greater separation factor (60) than MDK-3 membrane (24) and other commercial membranes which were studied.

The total membrane flow of PDecMS is significantly lower than that of the commercial analogs MDK-3. If we go to the value of permeability, it can be noted that the permeability of n-butanol for the resulting membrane PDecMS (2.6 $mol/(m^2 \cdot h \cdot kPa)$) is, on average, 2 times lower than that of commercial samples (6.4 $mol/(m^2 \cdot h \cdot kPa)$). Having estimated the permeability of the PDecMS membrane with a selective layer thickness of 4.5 μm, we can say that the permeability of the composite membrane in n-butanol becomes comparable with the permeability values for commercial samples (5.2 $mol/(m^2 \cdot h \cdot kPa)$). As a whole, with 3 times greater selectivity and, accordingly, the separation factor of the n-butanol / water mixture, this suggests the potential of using a PDecMS membrane in the pervaporation process of separating oxygenates from water effluents.

Table 2: Main pervaporation characteristics of membranes (t = 30°C, feed rate 120 ml/min)

Membrane	J, kg/(m²·h)	J_{BuOH}, kg/(m²*h)	α
Pervap 4060	0.59	0.11	23
PolyAn	1.70	0.14	10
Pervatech BV	0.85	0.10	13
MDK-3	0.65	0.12	24
PDecMS	0.12	0.05	60

Thus, the membrane demonstrated the greatest efficiency of the separation of 1-butanol from water compared with the best commercial polysiloxane-based membranes.

Acknowledgments

This work was performed at the A.V. Topchiev Institute of Petrochemical Synthesis and supported by the Russian Science Foundation, project no. 17-79-20296.

References

1. *Bernardo P., Drioli E., Golemme G.* Membrane gas separation: a review/state of the art // Ind. Eng. Chem. Res. 2009. V. 48. P. 4638-4663.
2. *Grushevenko E.A., Borisov I.L., Bakhtin D.S., Bondarenko G.N., Levin I.S., Volkov A.V.* Silicone rubbers with alkyl side groups for C_{3+} hydrocarbon separation // React. Funct. Polym. 2019. V. 134. P. 156-165.
3. *Grushevenko E.A., Borisov I.L., Bakhtin D.S., Legkov S.A., Bondarenko G.N., Volkov A.V.* Membrane material based on octyl-substituted polymethylsiloxane for separation of C_3/C_1 hydrocarbons // Petroleum Chemistry. 2017. V. 57. N. 4. P. 334-340.
4. *I.L.Borisov, E.A.Grushevenko, I.A.Podtynnikov, D.S.Bakhtin, G.N.Bondarenko.* Novel Membrane Material Based on Polybutadiene and Polydimethylsiloxane for Gas Separation and Hydrophobic Pervaporation // Petroleum Chemistry. 2018. V. 58. P. 1113-1122.

EFFECT OF KOLLIDON ON THE STRUCTURE AND PROPERTIES OF PES MEMBRANES

[1]Tatsiana Hliavitskaya, [1]Alexandr Bildyukevich, [2]Lyudmila Rozhdestvenska, [2]Yuliya Dzyazko

[1]Institute of Physical Organic Chemistry National Academy of Sciences of Belarus, Minsk, Belarus
E-mail: *hlyavitskaya1706@gmail.com*

[2] Institute of General and Inorganic Chemistry, Ukrainian National Academy of Sciences, Kyiv, Ukraine

Introduction

Membrane modification is used to improve membrane performance and reduce membrane fouling. Common membrane modification method is introduction of hydrophilic additives to polymer casting solution. The following additives are introduced to the casting solution: polyethylene glycol (PEG), polyvinylpyrrolidone (PVP), Pluronic, Tetronic and others polymers [1-3].

The aim of this research is to study the effect of Kollidone addition in the casting solution on the structure and permeability of polyethersulfone (PES) flat sheet ultrafiltration membranes. Because of its solubility in water and its high binding power, Kollidon is a very valuable product for the pharmaceutical industry. BASF Corporation have wide range of Kollidon grades. Generally, Kollidon is a mixture of polyvinyl acetate (PVA) and PVP. As it was mentioned above, PVP is known to be widely used as hydrophilizing additive in casting solution, but literature review has not any information about using PVA as hidrophilic additive. Firstly, PVA is not soluble in a number of organic solvents, including those, which are commonly used for membrane preparation: N,N-dimethylacetamide (DMAc), N-methyl-2-pyrrolidone and N,N-dimethylformamide. However, the introduction of lithium chloride (LiCl) into the PVA-DMAc system leads to the formation of a homogeneous solution [4]. In this regard, the membrane formation was carried out from the polymer system PES-Kollidon -glycerol-PEG-400-DMAc-LiCl. The influence of Kollidone in the casting solution on the structure and properties of PES membranes was discussed at first time.

Experiments

Firstly, Kollidone (Sigma-Aldrich Chemie, Germany) and LiCl (Reahim, Russia) were dissolved in appropriate amount of DMAc (EKOS-1, Russia). PES (Ultrason E 6020P, BASF, Germany) glycerol (EKOS-1, Russia), polyethylene glycol with molecular weight 400 (PEG-400, BASF, Germany) were dissolved at 90^{o}C with stirring in mixture DMAc- Kollidon-LiCl. Content of PES, Glycerol and PEG-400 were constant – 22; 10 and 10 wt % respectively. Amount of Kollidon in the casting solution was changed from 0,1 up to 1,0 wt %. The weight ratio of Kollidone to LiCl was constant 1:1. Polymer solutions were uniformly cast on glass plate with casting knife at room temperature. The glass plate was immediately immersed into the coagulation bath with distilled water. After immersion membranes were washed to remove residues of solvent and subjected to research.

Results and Discussion

Studies on the effect of Kollidon concentration in the casting solution on the viscosity show that increase in concentration of this mixture leads to increase in viscosity of casting solution. It was revealed, that the maximum concentration of Kollidon in casting solution (at which it was possible to get a stable solution) was 1,0 wt %. Increase in Kollidon concentration also led to increase in the turbidity of the solutions. For example, turbidity rise from 4,12 NTU (for 0 wt % Kollidon addition) up to 3190 NTU (for 1,0 wt % Kollidon addition).

Characteristics and performance of PES membranes were improved by addition of Kollidon to the casting solution. Studies on the effect of the Kollidon concentration in the polymeric solution show that membranes prepared by using 0-0,9 wt % Kollidon are characterized by higher pure water flux (PWF), but their rejection (PVP, K-30) was just the same. When the casting solution contains 0,9 wt % Kollidon the PWF increase from 55 $l \cdot m^{-2}h^{-1}bar^{-1}$ (for initial) to 106 $l \cdot m^{-2}h^{-1}bar^{-}$

[1] and the rejection was 95,0 % and 93,6 % respectively. Introduction of 1,0 wt % Kollidon resulted to decrease in PWF. Antifouling experiment upon BSA filtration allow the conclusion that adjunction Kollidon to polymer solution lead to the best antifouling performance. Flux recovery ratio (FRR) increased from 40 % for initial membranes up to 63 % for 1,0 wt % Kollidon membranes. Higher FRR values for modified membranes were provided by higher hydrophobicity of selective layer. The FTIR-spectra studies reveal the presence of PVP and PVA on the selective layer of the modified membranes. The SEM analysis (fig.1) showed that all prepared membranes were characterized by a typical asymmetric structure, but in case of modified membranes the thickness of the interjacent layer decreased. The shape and size of the macrovoids in the supporting layer changed too.

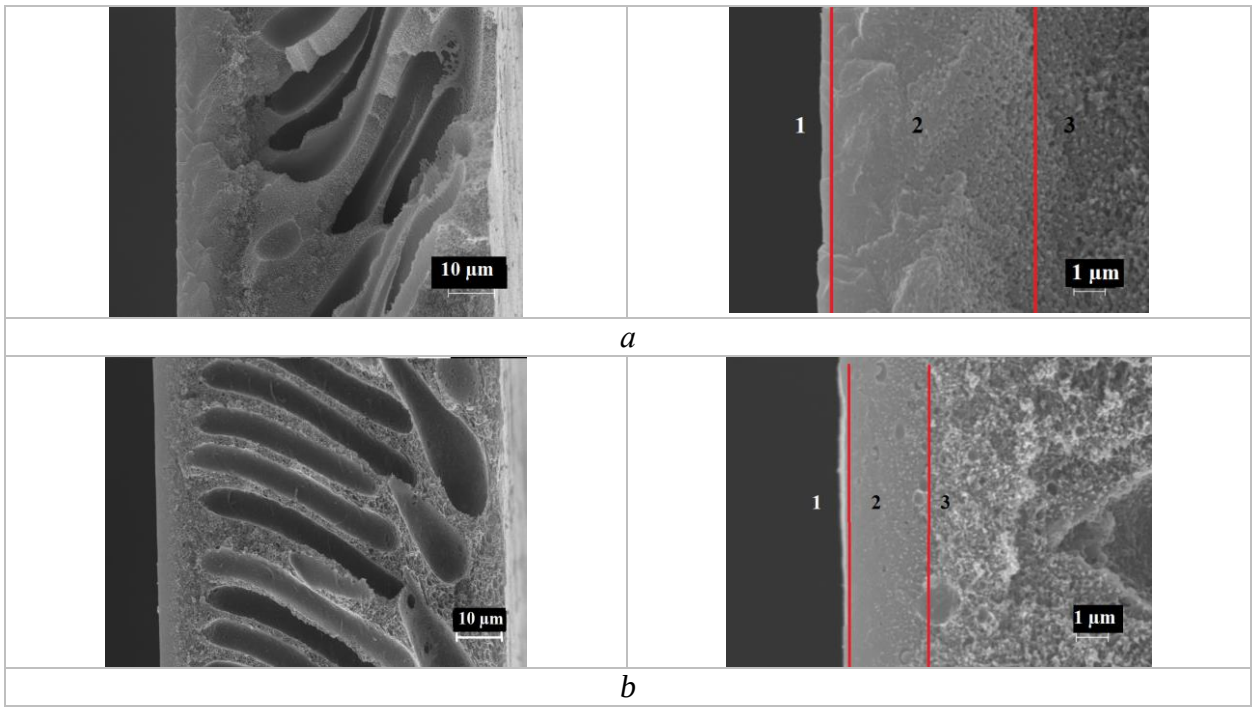

Figure 1. SEM images of the cross-section and skin layer of membranes. Concentration of Kollidon in the casting solution: (a) – 0 wt%, (b) – 0,9 wt%. (1) – skin layer, (2) – interjacent layer, (3) – supporting layer.

Acknowledgments

This research was supported by the Belarusian Republican Foundation for fundamental research (Project № X18-УКА-021).

References

1. *Idris A., Norashikin M.J., Noordin M.Y.* Synthesis, characterization and performance of asymmetric polyethersulfone (PES) ultrafiltration membranes with polyethylene glycol of different molecular weights as additives // Desalination. 2007. V. 207 P. 324-339
2. *Zhao Ch., Xue J., Ran F., Sun Sh.* Modification of polyethersulfone membranes – A review of methods // Progr. in Mat. Sci. 2013. V. 58. P. 76-150
3. *Zhao W., Su Y., Li Ch., Shi Q., Ning X., Jiang Z.* Fabrication of antifouling polyethersulfone ultrafiltration membranes using Pluronic F127 as both surface modifier and pore-forming agent // J. Membr. Sci. 2008. V. 318. P. 405-412
4. *Tosh B., Saikia C., Dass N.* Development of a Nonaqueous solvent system for PVA and its characterization // J. Appl. Pol. Sci. 1999 V. 74. P. 663–669

INVESTIGATION OF THE TRANSPORT OF IONS AND MOLECULES OF ORGANIC ACIDS AND BASES THROUGH BIPOLAR MEMBRANES

Tatyana Karpenko, Anastasya Boyarishcheva, Nikita Kovalev, Alina Shpak, Nikolay Sheldeshov, Victor Zabolotskiy

Kuban State University, Krasnodar, Russia, E-mail: *tany1328@mail.ru*

Introduction

Due to the high demand for bipolar membranes in various areas of the chemical industry, it has become necessary to create and study new processes using such membranes. However, process costs are determined by the properties of the membranes. The electrochemical characteristics of the bipolar membrane are mainly determined by its resistance and the transport numbers of ions through the membrane. However, if the resistance and the potential difference at the membrane affects mainly the energy consumption of the electrodialysis process, the transport number of ion through the membrane also determine the qualitative and quantitative composition of the resulting solutions [1]. The aim of this work is to develop a method for measuring the effective transport numbers and flows of ions and molecules through an individual bipolar membrane.

Experiments

The proposed method is based on the use of filtration membranes to exclude the interfering effect of the processes occurring on the membranes located to the left and right of the analyzing membrane [2]. The possibilities of the proposed method are shown by the example of the system "sodium hydroxide solution | bipolar ion exchange membrane | solution containing citric acid and sodium citrate» (Figure 1).

A modified bipolar membrane made of Ralex CMH-PES cation exchange membrane and Ralex AMH-PES anion exchange membrane was used as a bipolar membrane. A catalytic phosphoric acid additive was added to the bipolar region of the membrane to reduce the voltage drop on the membrane. Ultrafiltration hydrophobic membranes of the type UFFK, ZAO STC "Vladipor", Vladimir were used as the filtration membrane the.

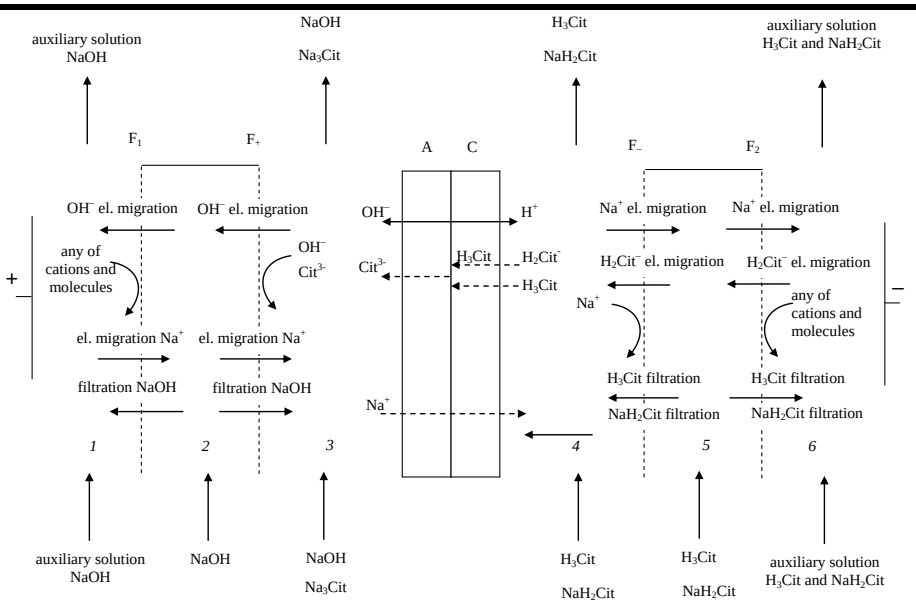

FIGURE 1. SCHEME OF IONS AND MOLECULES TRANSFER PROCESSES THROUGH THE INVESTIGATED BIPOLAR MEMBRANE IN THE SYSTEM "ALKALI SOLUTION – SOLUTION OF CITRIC ACID AND SODIUM CITRATE».

The formulas for the calculation of ion flows transferred through the investigated bipolar membrane follow from the equations of the balance of flows through this membrane and the rate of ion accumulation in alkaline solutions and in mixture of citric acid and sodium citrate. For example, for the rate of accumulation of anion of organic acid in alkali solution:

$$\frac{dn_{A,3}}{d\tau} = J_{A,b,bm}, \quad (1)$$

where $n_{A,3}$ is the quantity of anion of an organic acid in alkali solution; $J_{A,b,bm}$ is the flow of anion of the organic acid from bipolar membrane to the alkaline chamber.

For the rate of accumulation of hydroxyl ions in alkali solution:

$$\frac{dn_{OH,3}}{d\tau} = J_{NaOH,F+} - J_{OH,m,F+} + J_{OH,b,bm} \quad (2)$$

where $n_{OH,3}$ is the quantity of hydroxyl ions in alkali solution; $J_{NaOH,F+}$ is the convective flow of sodium hydroxide into alkaline chamber through filtration membrane F^+; $J_{OH,m,F+}$ is the electromigration flow of hydroxyl ion through the filtration membrane from alkaline chamber; $J_{OH,b,bm}$ is the flow of hydroxyl ion in the alkaline chamber from the bipolar membrane.

Results and Discussion

The analysis of ion transport numbers through the bipolar membrane in the asymmetric system "organic acid, organic acid salt – sodium hydroxide" shows that in the system with citric acid, the transport number of coion is lower than in the system with acetic acid (Figure 2, 3). It may be due to the lower diffusion coefficient of citric acid through the cation exchange layer of the bipolar membrane, compared with acetic acid, due to the greater molar mass, as well as a large charge of the anion of citric acid.

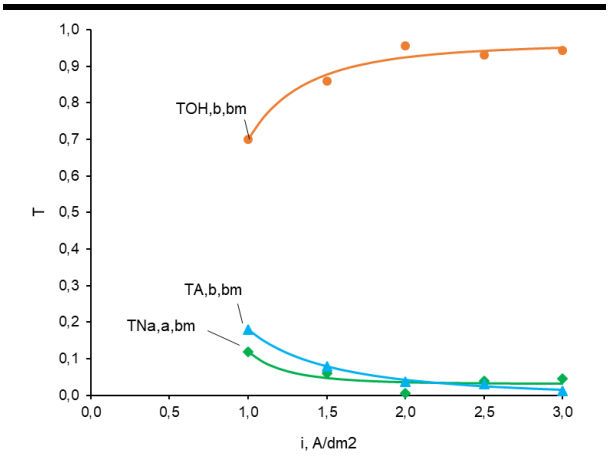

FIGURE 2. THE DEPENDENCE OF THE EFFECTIVE TRANSPORT NUMBERS OF IONS THROUGH THE BIPOLAR MEMBRANE ON THE ELECTRIC CURRENT DENSITY IN THE SYSTEM "ACETIC ACID, SODIUM ACETATE – NAOH».

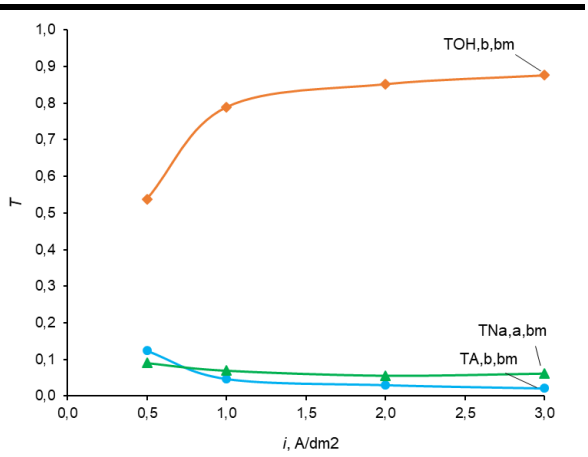

FIGURE 3. THE DEPENDENCE OF THE EFFECTIVE TRANSPORT NUMBERS OF IONS THROUGH THE BIPOLAR MEMBRANE ON THE ELECTRIC CURRENT DENSITY IN THE SYSTEM "CITRIC ACID, SODIUM CITRATE – NAOH».

The analysis of the transport numbers of ions through the bipolar membrane in the system "amine, amine-sulfuric acid", allows to do the following conclusions:

1) with increase in the molar mass of the molecule (the transition from system with dimethylamine to system with diethylamine), the transport number of hydrogen ions through the cation exchange layer of the bipolar membrane slightly increases and the transport number of organic base cation decreases (Figure 4, 5). This effect may be associated with lower diffusion coefficient of diethylamine compared to dimethylamine through the anion exchange layer of the bipolar membrane;

2) with increase in the charge of the base cation (ethylenediamine), its transfer is somewhat reduced, probably due to the large interaction energy with oppositely charged fixed groups in the cation exchange layer of the bipolar membrane (Figure 6).

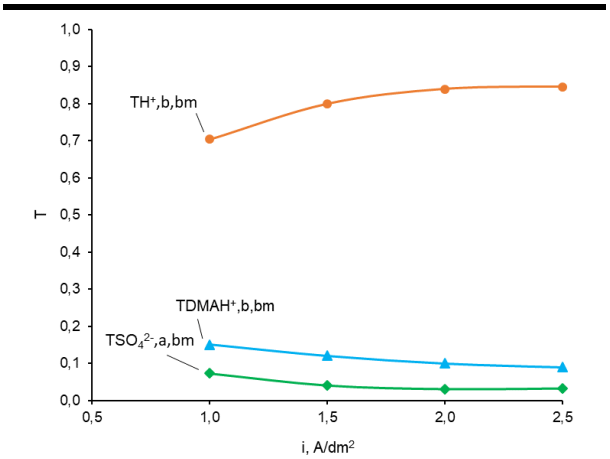

FIGURE 4. THE DEPENDENCE OF THE EFFECTIVE TRANSPORT NUMBERS OF ION THROUGH THE BIPOLAR MEMBRANE DEPENDING ON THE ELECTRIC CURRENT DENSITY IN THE SYSTEM " DIMETHYLAMINE, DIMETHYLAMINE SULFATE–H_2SO_4».

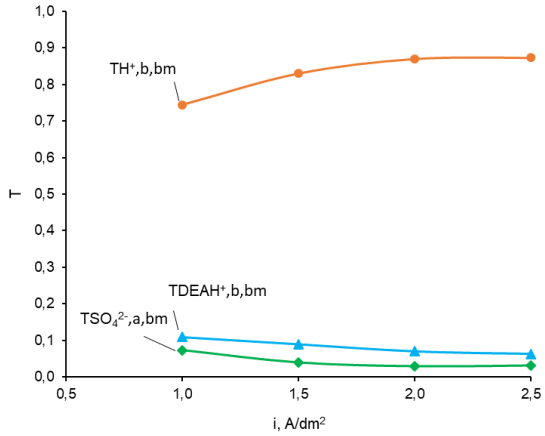

FIGURE 5. THE DEPENDENCE OF THE EFFECTIVE TRANSPORT NUMBERS OF ION THROUGH THE BIPOLAR MEMBRANE DEPENDING ON THE ELECTRIC CURRENT DENSITY IN THE SYSTEM " DIETHYLAMINE, DIETHYLAMINE SULFATE–H_2SO_4».

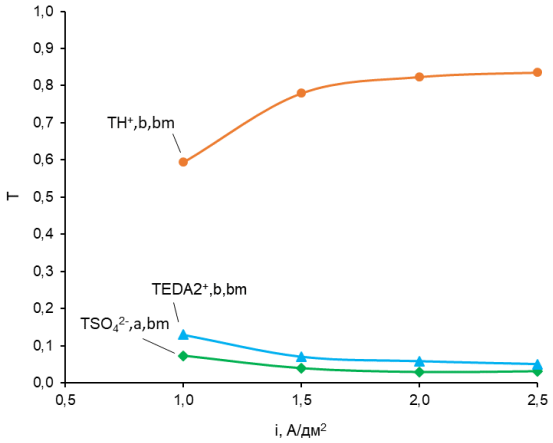

FIGURE 6. THE DEPENDENCE OF THE EFFECTIVE TRANSPORT NUMBERS OF ION THROUGH THE BIPOLAR MEMBRANE ON THE ELECTRIC CURRENT DENSITY IN THE SYSTEM "ETHYLENEDIAMINE, ETHYLENEDIAMINE SULFATE – H_2SO_4».

Therefore, the method of hydrodynamic isolation of the investigated membrane allows to measure the flows and the transport number of ion through the individual bipolar membrane in membrane systems containing organic substances such as acids, bases and their salts.

The present work is supported by Russian Foundation for Basic Research, research project № 17-08-01689.

References

1. *Shel'deshov, N.V., Zabolotskii, V.I.* Bipolar ion exchange membranes. Synthesis. Properties. Application, in Membranes and membrane technologies // Yaroslavtsev, A.B., Ed. Moscow: Nauchniy mir. 2013. P. 70-125. (in Russian)
2. *Zabolotskii, V.I., Shel'deshov, N.V., Orel, I.V., Lebedev, K.A.* Determining the ion transport numbers through a membrane by its hydrodynamic isolation // *Russ. J. Electrochem*. 1997. Vol. 33. P. 1066-1071.

INVESTIGATION OF THE CHARGE-DISCHARGE CHARACTERISTICS OF A HYDROGEN-BROMATE FLOW-BATTERY IN VARIOUS MODES

[1,2,3] *Natalia Kartashova, [1,3]Dmitriy Konev, [1]Pavel Loktionov, [1,2,3] *Anatoly Antipov, [1]Pavel Chukanov, [1]Kseniya Kolobkova, [2]Olga Goncharova, [1-4]Mikhail Vorotyntsev

[1]D. I. Mendeleev University of Chemical Technology of Russia, Moscow, Russia
[2]M. V. Lomonosov Moscow State University, Moscow, Russia
[3]Institute of Problems of Chemical Physics, Russian Academy of Sciences, Chernogolovka, Russia
[4]ICMUB, UMR 6302 CNRS-Université de Bourgogne, Dijon, France
*E-mail: *kartashova9natali@gmail.com*

Introduction

Recently flow-batteries became a very promising technology in the field of energy storage. They allow to generate electricity during the electrochemical reaction of liquid reagents. In the article [1] it was demonstrated that it is possible to carry out the electroreduction of bromate anions in acidic solution on autocatalytically weakly active electrodes (for example, carbon electrodes) due to the presence of bromine trace. In this case, a catalytic cycle consists of a heterogeneous reaction on the electrode surface for a reversible redox pair of Br_2/Br^- and an irreversible homogeneous reaction of the BrO_3^-/Br_2 proportionation. Using of bromates as energy-intensive substances is a promising idea because it allows to increases energy storage of the flow-batteries from tens to hundreds of W*h/kg.

Experiments

The main purpose of the research was to investigate the process of electrooxidation of a bromide-anion and the electroreduction of the bromate-anion in a hydrogen-bromate flow-battery. Two modes for device testing were used - acidic and alkaline solution. Also, different methods such as spectrophotometry and electrospray ionization-mass spectrometry (ESI-MS) were used to control the composition of solutions. The energy efficiency of the bromide anion into the bromate anion was analyzed in different modes.

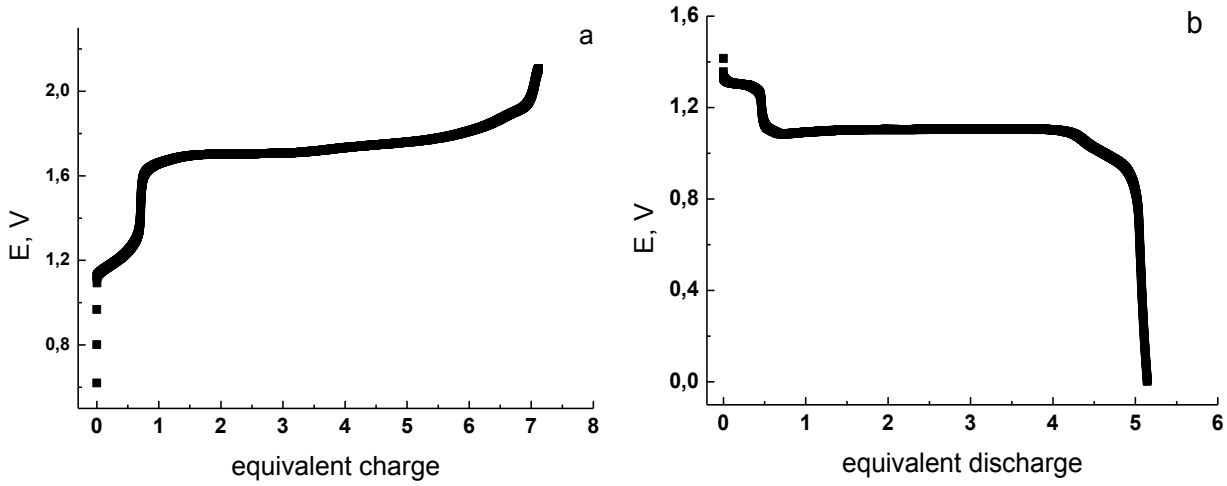

Figure 1. Charge-discharge curves of H_2/BrO_3^- flow-battery. Membrane electrode unit design: positive electrode - carbon paper Toray EC-TP1-120, negative electrode - carbon paper Freudenberg H23C8 (loading Pt / C 1 mg/cm^2), membrane - Nafion 117. a) galvanostatic mode:1 A, positive electrode - 0.5 M NaBr 1 M H_2SO_4, 50 ml/min, the negative electrode is open to the atmosphere; b) galvanostatic mode:-1 A, positive electrode -product of the conversion solution (a) after passing 7 equivalents of charge, negative electrode - hydrogen, 10 ml / min.

Results and Discussion

As a result, an energy efficiency exceeding 72% was achieved in both acidic and alkaline solutions. The best result was obtained for sulfuric acid. The experimental energy efficiency of bromide to bromate for acidic solution was more 1,5 times higher than alkaline. An example of a charge-discharge cycle based on a hydrogen-bromate "chemistry" was successfully demonstrated.

This research was supported by the Russian Ministry of Education and Research (Grant № 14.574.21.0150, UIN RFMEFI57417X0150).

References

1. *Modestov A.D. Konev D.V., Tripachev O.V, Antipov A.E., Tolmachev Y.V., Vorotyntsev M.A.* A hydrogen-bromate flow battery for air-deficient enviroments. // Energy technology. 2018. V. 6. № 2. P.242-245.

APPLYING OF HYBRID MEMBRANE-COAGULATION METHODS FOR SURFACE WATER TREATMENT

Victor Kasperchik, Ala Yaskevich, Alexandr Bildyukevich
Institute of physical organic chemistry NASB, Minsk, Belarus, E-mail: *ufm@ifoch.bas-net.by*

Introduction

Now for the purification of the surface waters the membrane technologies in particular the low-pressure dead-end ultrafiltration are increasingly applied instead of the traditional coagulation methods. At the same time carrying out the ultrafiltration in the dead-end mode leads to significantly greater membrane fouling compared to the cross-flow ultrafiltration [1]. For improving of the membrane transport characteristics various coagulants are used as additional utility reagents [2]. The main aim of this work was to determine optimal type of the applied coagulant (organic, inorganic or its mixtures) for purification of the surface water from the dissolved organic substances of the different nature by ultrafiltration.

Experiments

Commercial ultrafiltration Multibore® membranes (Inge GmbH, Germany) were used for the surface water treatment. The surface water from Svisloch river (Minsk region) was used for the investigation of the membrane purification. Low and high basic aluminium polyoxychlorides (AQUAM-18 and AQUAM-15, Ksant-Invest Ltd, Belarus), poly- [N,N - dimethyl - N,N - diallyl ammonium chloride] (PDMDAAC, Magnafloc LT-37, BASF, Germany) and poly- [epichlorohydrin - dimethylamine] (polyamine, Magnafloc LT-32, BASF, Germany) were used as inorganic and organic coagulants. Total organic carbon (TOC) was controlled before and after purification of the water samples. Transmembrane flux was measured by standard methods.

Results and Discussion

The main results of the membrane water purification from dissolved organic substances are presented in the Table. Ultrafiltration without coagulant also can be used for the surface water treatment. However in this case degree of water purification is lower than for all types of coagulants investigated in this paper. It should be noted that transmembrane fluxes for the untreated by coagulants samples of the surface water is always lower than these ones for the treated water samples (Figure). When we applied individual inorganic or organic coagulants in combination with ultrafiltration the quality of the water purification from organic substances was improved. But this improving was not significant compared to uncoagulated samples of the surface water. The best results were obtained when the mixtures of organic and inorganic coagulants were applied.

Table: Results of membrane water purification from dissolved organic substances

Coagulant type	C_1/C_2, mg/dm^3, inorganic/organic coagulant	TOC, mg/dm^3
Initial water	0/0	4,18
Ultrafiltration without coagulant	0/0	2,66
Magnafloc LT-32	0/5	2,16
Magnafloc LT-37	0/5	2,32
AQUAM-18	5,4/0	2,25
AQUAM-15	4,5/0	2,23
AQUAM-18/Magnafloc LT-32	5,4/1,5	1,31
AQUAM-15/Magnafloc LT-32	4,5/1,5	1,86
AQUAM-18/Magnafloc LT-37	5,4/1,5	2,16
AQUAM-15/Magnafloc LT-37	4,5/1,5	1,33

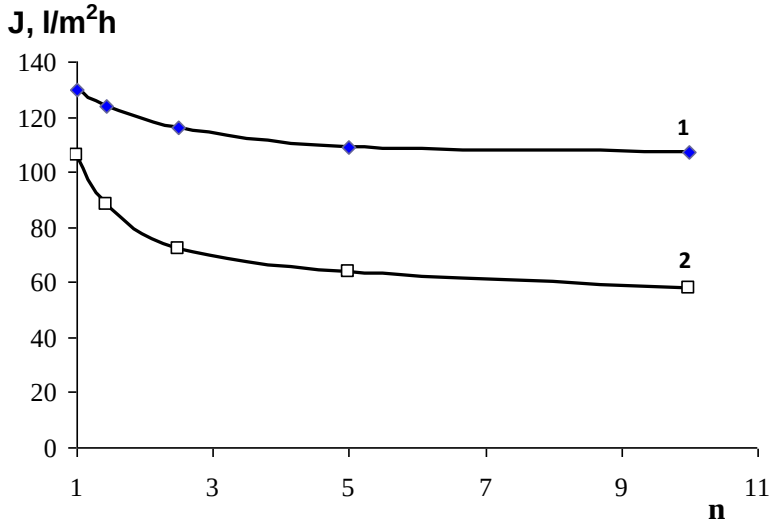

Figure. Typical dependence of transmembrane flux (J) vs. degree of concentration (n): 1 – ultrafiltration with mixture high basic aluminium polyoxychloride/PDMDAAC, 2 – ultrafiltration without coagulant.

It is interesting that the most significant organic content decline in the water purified by ultrafiltration was observed for two completely different coagulant mixtures: low basic aluminium polyoxychloride – polyamine and high basic aluminium polyoxychloride – PDMDAAC. Probably it can be explained by more complicated impurity capture mechanism during formation of the colloid particles leading to increase of the efficiency of surface water purification from organic substances of the different nature.

Thus it was found that the use of the hybrid membrane-coagulation methods is much more effective than the use of ultrafiltration and coagulation methods separately. It is preferable to use the mixture of organic and inorganic coagulants. This allows to obtain the best results for the surface water purification from dissolved organic substances.

References

1. *Fane A.G., Fell C.J.D.*//Desalination.1987. V.62,N2. P.117-136.
2. *Shenglei Sun et al*//J. Hazardous Materials. 2016.V.307. P. 108-118.

PHYSICO-CHEMICAL PROPERTIES OF PROTONATED AND SALT FORMS OF THE NAFION MEMBRANES PLASTICIZED WITH APROTIC SOLVENTS

[1,2]Ruslan Kayumov, [1,2]Evgeny Sanginov, [1]Alexander Karelin, [1,2]Yury Dobrovolsky

[1]Institute of Problems of Chemical Physics of Russian Academy of Sciences, Chernogolovka, Russia,
[2]Competence Center of National Technology Initiative in IPCP RAS, Chernogolovka, Russia
E-mail: *kayumov@icp.ac.ru*

Introduction

The creation of new electrochemical systems with high energy density, improved dynamic characteristics, an extended range of operating temperatures and increased fire and explosion safety is a key direction in the development of electrochemical energy. Much attention is attracted to metal-ion batteries, the most famous representatives of which are lithium-ion batteries commercialized in 1991. The prospects for improving their safety and extending the operating temperature range are associated with the replacement of currently used liquid and gel electrolytes by polymeric electrolytes, which simultaneously serve as a separator.

The best-known representative of this class of materials is the Nafion perfluorinated ionomeric membrane in protonated form. It has excellent mechanical, chemical, electrochemical, and thermal stability, and is widely used as an electrolyte/separator in the production of hydrogen fuel cells and other electrochemical devices. It is known that the proton in the Nafion membrane is rather easily replaced by other cations (Li^+, Na^+, K^+, Mg^{2+}, etc.). The introduction of specially selected dipolar aprotic solvents into such modified membranes makes it possible to obtain polyelectrolytes with unipolar conductivity with a metal cation of the order of 10^{-5}–10^{-3} S/cm [1], which are close in conductivity to liquid Li^+-conducting electrolytes used in modern batteries, which are suitable for use in metal-ion electrochemical systems.

The aim of the work was to establish the general laws of the formation of the physicochemical and transport properties of polymer electrolytes based on the salt forms of the Nafion® 115 membrane with one- and two-charge cations of the different nature plasticized by polarized aprotic solvents.

Experiments

Nafion®115 polymer membrane in the form of a film with a thickness of 125 μm was purified according to a known method; to remove water, the membrane was first dried at 130 °C in a vacuum oven for 3 hours, and then kept in a desiccator over P2O5 for a week.

The replacement of mobile protons with an alkali metal cation in Nafion-M^{z+} samples (where M^{z+} = H^+, NH_4^+, Li^+, Na^+, K^+, Rb^+, Cs^+, Ba^{2+}, Sr^{2+}, Ca^{2+}, Mg^{2+}) was performed by keeping the samples in water-alcohol (1:1 by volume) with 2 M alkali solution at 60–80 °C for 2 hours, followed by thorough washing with bidistilled water.

To obtain plasticized samples, dried Nafion membranes in salt form were kept for 2 days at room temperature in an aprotic solvent in the presence of activated molecular sieves. To obtain films with different DMSO content, the samples were briefly placed in a solvent, dried with filter paper, and kept for two days to achieve a uniform distribution of the plasticizer in the sample. The degree of swelling of the membrane in the solvent was determined as the ratio of the amount of absorbed solvent to the weight of the dry membrane. All experiments with aprotic solvents were carried out in a dry box.

The physico-chemical properties of the obtained samples were studied by the methods of synchronous thermal analysis, IR spectroscopy, voltamperometric and impedancemetry.

Results and Discussion

Among dipolar aprotic solvents acetonitrile (AN), propylene carbonate (PC), ethylene carbonate (EC), N, N- dimethylformamide (DMF) and dimethyl sulfoxide (DMSO), the best plasticizer for salt forms of the Nafion membrane is dimethyl sulfoxide.

Table 1: Physical properties of solvents used as plasticizers for Nafion-Li$^+$, and characteristics of polymer electrolyte samples at room temperature

Solvent	t_{melt}, °C	μ, D	η, mPa·s	Swelling degree, wt %	n**	σ, S/cm
AN	-44	3.924	0.38 (25 °C)	10	2.7	$1.2\cdot10^{-5}$
DMSO	18.5	3.960	1.99 (25 °C)	130	18.3	$2.0\cdot10^{-3}$
DMF	-60	3.820	0.80 (25 °C)	150	22.5	$6.0\cdot10^{-3}$
PC	-48.8	5.000	2.53 (25 °C)	60	6.5	$1.0\cdot10^{-5}$
EC	36.4	4.900	2.56 (25 °C)*	40*	5.0	$1.6\cdot10^{-5}$*

* supercooled

** n is the number of moles of solvent per mole of lithium

In general, the dependence of some physicochemical characteristics (ionic conductivity, activation energy of conductivity, heat of evaporation and melting of DMSO) of polymer electrolytes in the series Na^+–Cs^+ correlates with the radius of the cation, with which its interaction energy decreases with the solvent and anion (Fig. 1). In the case of double charged cations, the conductivity is 0.17–0.42 mS/cm, and the activation energy of conductivity decreases with the cation radius increase (Fig. 1).

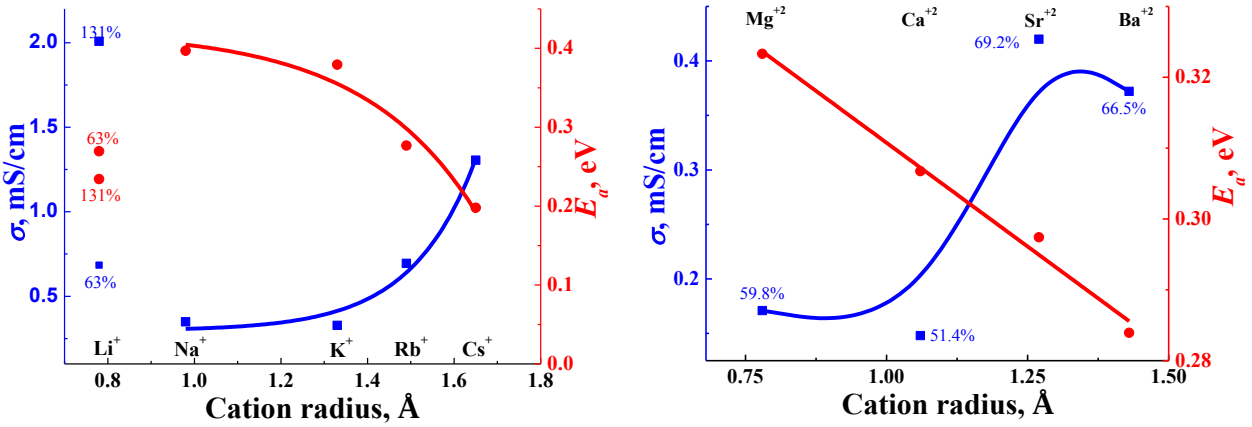

Figure 1. Dependence of conductivity and activation energy of conductivity of Nafion-M^{Z+} membranes plasticized by DMSO on cation radius. Percent show the swelling degree.

The report will show that with an increase in DMSO content in Nafion-M^+ membranes (M = H, Li, NH_4), the conductivity increases to 1–10 mS/cm. The percolation threshold for such systems was found to be n = 2, 4, and 6 mol of DMSO per mole of H^+, Li^+, and NH_4^+, respectively, which is associated with the formation of cationic solvate complexes of Li^+ $(DMSO)_4$, $H^+(DMSO)_2$ and $NH_4^+(DMSO)_4$.

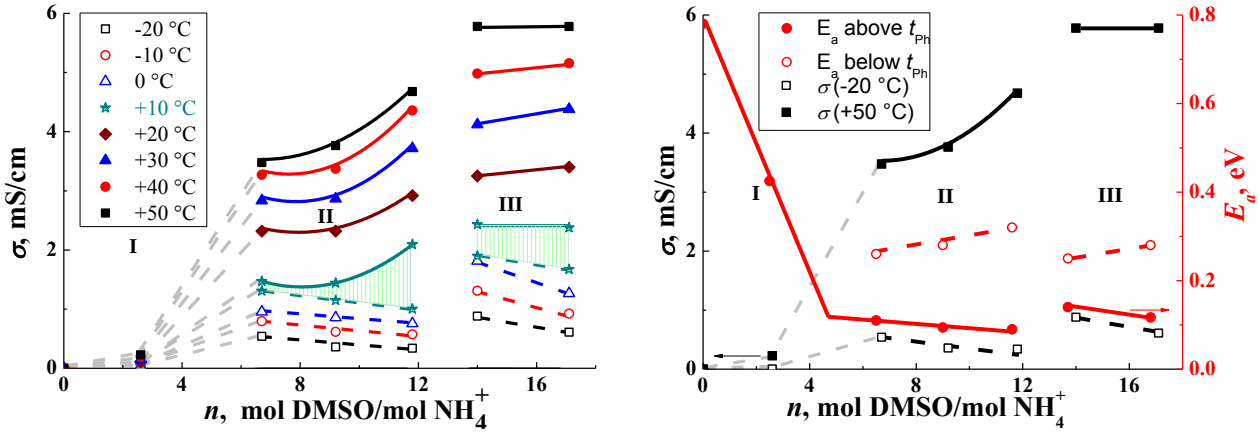

Figure 2. Ionic conductivity and activation energy of conductivity above and below the phase transition temperature t_{Ph}, depending on the content of DMSO in ammonium substituted membranes.

In the case of Nafion- NH_4^+, a step change in the ionic conductivity and the activation energy of conductivity from the plasticizer content (DMSO) was detected (Fig. 2). A strong solvation is observed in the region of $n \leq 6$, after which the ionic transport is sharply intensified. The change in conductivity at $n = 12–14$ is due to the swelling of the polymer matrix with a change in the geometry of the conducting channels.

This work was supported by Russian Scientific Foundation (Contract No. 17-79-30054).

References

1. *Doyle C.M., Lewittes M.E., Roelofs M.G., Perusich S.A., Lowrey R.E.* Relationship between ionic conductivity of perfluorinated ionomeric membranes and nonaqueous solvent properties // J. Membrane Sci. 2001. V. 184. No. 2. P. 257–273.

HYDRODYNAMIC PERMEABILITY OF A FIBROUS MEMBRANE MODELLED AS A PACKAGE OF COMPOSITE SOLID-POROUS CYLINDRICAL CELLS IN MICROPOLAR FLOW

[1]Daria Khanukaeva, [1]Anatoly Filippov, [2]Pramod Kumar Yadav, [3]Ashish Tiwari

[1]Gubkin University, Moscow, Russia, E-mail: *khanuk@yandex.ru*

[2]Motilal Nehru National Institute of Technology, Allahabad-211004, Uttar-Pradesh, India

[3]Birla Institute of Technology & Science, Pilani-333031, Rajasthan, India

Introduction

The cell-model technique, offered by Happel and Brenner, is being actively developed during the last decades and applied to the modeling of filtration flows in various porous media, in particular, in membranes. The original idea consists in the representation of a membrane material as a package of identical cells, most often, cylindrical or spherical. Each cell may contain solid core, porous layer and the region of free flow or a combination of two mentioned regions. The flow is considered inside a separate cell, the influence of the others being taken into account via boundary conditions on its outer surface. Substantial progress was achieved in modeling of Newtonian liquids flows in various types of cells. If the flow is described by the Brinkman equations in porous region and by the Stokes equations in non-porous region, analytical solutions of the problem were obtained and used for the calculation of hydrodynamic permeability of the membrane as a whole. The review of these results can be found in [1].

Meanwhile, many filtrating media, for example, suspensions and physiological liquids exhibit non-Newtonian properties and can be modeled as micropolar liquids, mathematically described by Eringen in the 1960s. Microrotation and couple stresses are taken into account for modeling of micropolar liquids flows, which are described by the system of continuity, momentum and moments of momentum equations. Up to the knowledge of the authors, only few applications of micropolar theory in cell models were published, and combined solid-porous particle in the cell has not been considered anywhere, except for the authors' work [2]. The present paper is the second part of the mentioned study of micropolar flow through the assemblage of cylindrical particles. It considers the flow directed perpendicular to the cell axis and investigates the hydrodynamic permeability of a fibrous membrane.

Statement of the problem

The scheme of the cell is shown in Fig.1. The cell consists of three coaxial layers: the inner layer is a solid core of radius *a*, the intermittent layer $a < r < b$ (region 1) is porous, and the outer layer $b < r < c$ (region 2) is occupied by the free micropolar liquid. Uniform flow of velocity **U** is directed perpendicular to the symmetry axis of the cell and corresponds to $\theta = 0$ of the cylindrical coordinate system (r, θ, z). The components of linear and angular velocity vectors are $\mathbf{v}\{U(r,\theta); V(r,\theta); 0\}$, $\boldsymbol{\omega}\{0; 0; \Omega(r,\theta)\}$ respectively.

The field equations of creeping flow in absence of external forces and couples in region 2 are

$$\begin{aligned} &\nabla \cdot \mathbf{v}_2 = 0, \\ &-(\mu + \kappa)\nabla \times \nabla \times \mathbf{v}_2 + 2\kappa \nabla \times \boldsymbol{\omega}_2 = \nabla P_2, \\ &-(\delta + \varsigma)\nabla \times \nabla \times \boldsymbol{\omega}_2 + 2\kappa \nabla \times \mathbf{v}_2 - 4\kappa \boldsymbol{\omega}_2 = 0, \end{aligned} \qquad (1)$$

where subscript 2 corresponds to the second region, $\mathbf{v}, \boldsymbol{\omega}$ are linear and angular velocity vectors respectively, P is the pressure, ρ is the liquid density, $\mu, \kappa, \alpha, \delta, \varsigma$ are the viscosity coefficients of the micropolar medium. Detailed discussion of viscosity coefficients definitions and the form of system (1) representation can be found in [3]. It is worth noting here the property of the non-dimensional governing equations for micropolar flows to involve all the viscosities and characteristic scales in the form of two non-dimensional parameters: the number of micropolarity $N^2 = \kappa/(\mu + \kappa)$ and the scale factor $L^2 = (\delta + \varsigma)/(4\mu b^2)$. These two values totally define the properties of the micropolar creeping flow.

The governing equations for porous region $a < r < b$ are written in the same form, as in [2], and include the porosity ε and the permeability *k* of the porous medium

$$\begin{aligned} &\nabla \cdot \mathbf{v}_1 = 0, \\ &-\left(\frac{\mu}{\varepsilon}+\frac{\kappa}{\varepsilon}\right)\nabla\times\nabla\times\mathbf{v}_1+\frac{2\kappa}{\varepsilon}\nabla\times\boldsymbol{\omega}_1-\frac{\mu+\kappa}{k}\mathbf{v}_1=\nabla P_1, \\ &-(\delta+\varsigma)\nabla\times\nabla\times\boldsymbol{\omega}_1+2\kappa\nabla\times\mathbf{v}_1-4\kappa\boldsymbol{\omega}_1=0, \end{aligned} \tag{2}$$

where subscript 1 is used for the notation of the first region. Apart from parameters *N* and *L* the non-dimensional form of equations (2) includes the porosity ε and parameter $\sigma = b/\sqrt{k}$, which represents the relation of macro scale of the cell *b* and the micro scale of porous medium $\sqrt{k}$.

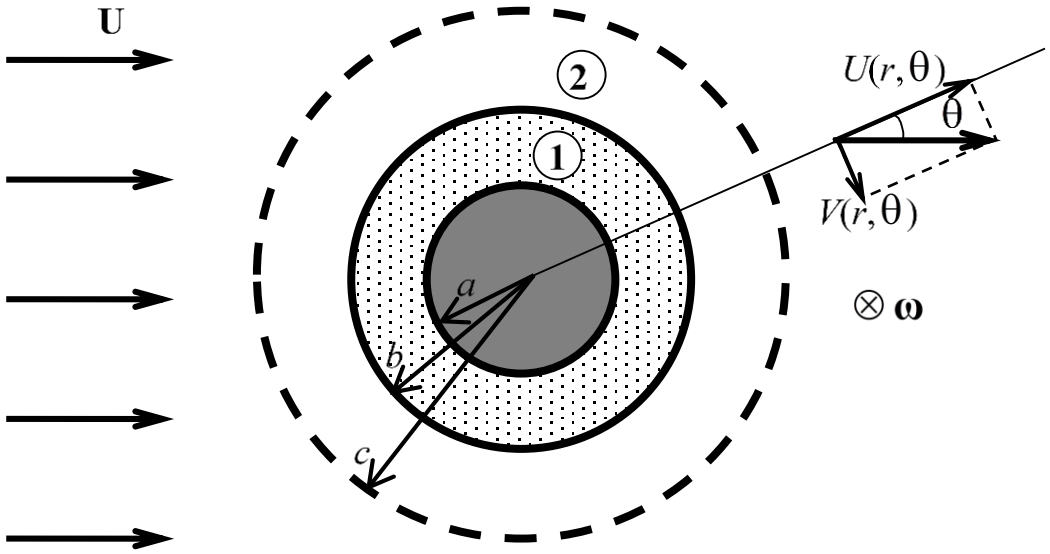

Figure 1. The scheme of the flow.

Systems (1) and (2) allow separate general solutions of the form $\mathbf{v}_i(r,\theta)=\{u_i(r)\cos\theta; v_i(r)\sin\theta; 0\}$, $\boldsymbol{\omega}_i(r,\theta)=\{0; 0; \omega_i(r)\sin\theta\}$, $P_i(r,\theta)=p_i(r)\cos\theta$, $i=1,2$ due to the symmetry of the flow.

Boundary conditions for the closure of the boundary value problem (BVP) are the following: at the solid surface $r=a$ no-slip and no-spin conditions are allowed only

$$u_1(a)=0,\quad v_1(a)=0,\quad \omega_1(a)=0. \tag{3}$$

At the liquid-porous interface $r=b$ there were applied the continuity of all velocities components

$$u_1(b-0)=u_2(b+0),\quad v_1(b-0)=v_2(b+0),\quad \omega_1(b-0)=\omega_2(b+0) \tag{4}$$

and the continuity of the stress and couple stress tensor components, normal and tangential to the boundary surface,

$$t_{rr1}(b-0)=t_{rr2}(b+0),\quad t_{r\theta1}(b-0)=t_{r\theta2}(b+0),\quad m_{rz1}(b-0)=m_{rz2}(b+0). \tag{5}$$

At the boundary $r=c$ there were used the continuity of linear velocity normal component, Happel's no-stress condition and no-couple stress condition respectively

$$u_2(c)=U,\ t_{r\theta2}(c)=0,\ m_{rz2}(c)=0. \tag{6}$$

No-spin condition $\omega_2(c)=0$ was used instead of the no-couple stress condition at this surface as the alternative BVP in our paper [2]. It was found that the difference in the hydrodynamic permeability of the membrane for these two statements does not exceed several percents of the

overall variation of this characteristics. So, in the present work there are shown the results only for one BVP (1-6). The discussion of various variants of BVP statements can be found in [3].

Results and discussion

It was found the dimensionless hydrodynamic permeability L_{11} of a membrane as a function of parameters N, L, σ, intrinsic cell porosity ε and the overall porosity of the membrane $\gamma \approx 1-b^2/c^2$. The dependency of L_{11} on the characteristics of porous medium for the micropolar flow exhibits the same properties as those, known for the Newtonian flow: a decay with the growths of the permeability parameter σ and an increase with the growth of both types of porosity. In all cases the hydrodynamic permeability for a micropolar flow is less than for the non-polar liquid due to the additional degrees of freedom and types of viscosity, which are necessary to be overcame by the flow.

The most interesting is the dependencies of the hydrodynamic permeability on the micropolar parameters N and L. The corresponding curves are shown in Fig.2 for the cases of flow directed perpendicular to the axis of the cell, investigated in the present study; parallel to the axis of the cell, studied in [2]; and for the case of chaotic orientation of the cylindrical cells with respect to the flow direction, which is the most natural for real membranes. The latter was calculated as the weighted sum of the former two with the coefficients 2/3 and 1/3 respectively.

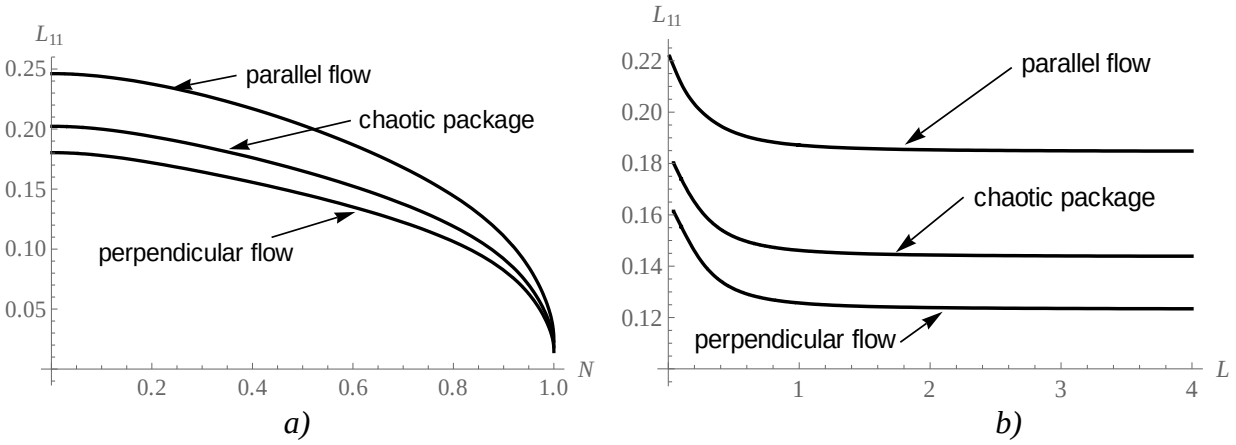

Figure 2. Variation of the dimensionless hydrodynamic permeability L_{11} of a membrane with the parameters N (a) and L (b) for $\sigma = 3;\ \varepsilon = 0.75;\ a/b = 0.5;\ \ c/b = 1.5$.

Fig.2a, plotted for the average meaning of L = 0.2 demonstrates several times drop down of the value of L_{11} with the variation of N in its allowed range, which corresponds to the change of microrotaion viscosity κ. Fig.2b, plotted for the average micropolarity number N = 0.5, indicates an asymptotic behavior of the hydrodynamic permeability as a function of the micropolar scale factor L. The initial position of the asymptotic behavior has occurred to be defined by the value of N, but the value of asymptote depends on the orientation of the cell (parallel/perpendicular).

This work is supported by RFBR (project N 19-08-00058).

References

1. *Deo S., Filippov A.N., Tiwari A., Vasin S.I. and Starov V. M.* Hydrodynamic permeability of aggregates of porous particles with an impermeable core // Adv. Coll. Interface Sci. 2011. V.164(1), P.21-37.
2. *Khanukaeva D.Yu., Filippov A.N., Yadav P.K., Tiwari A.* Creeping flow of micropolar fluid parallel to the axis of cylindrical cells with porous layer // Eur. J. Mech. / B Fluids 2019. V.76, P.73-80.
3. *Khanukaeva D.Yu., Filippov A.N.* Isothermal Flows of Micropolar Liquids: Formulation of Problems and Analytical Solutions // Colloid J. 2018. V.80(1), P.14-36.

THE PECULIARITIES IN ELECTRODIALYSIS OF TRYPTOPHAN - MINERAL SALT SOLUTION

Anastasiia Kharina, Tatiana Eliseeva, Alexandra Tikhaya
Voronezh State University, Voronezh, Russia, E-mail: *aukharina@gmail.com*

Introduction

Recovery of heterocyclic essential amino acids from solutions of their microbiological synthesis is an actual applied task. The modern electromembrane method - electrodialysis allows to solve the problem of isolation and purification of amino acids, claimed as pure compounds in medical, pharmaceutical industry and biotechnology.

At the same time, the regularities and peculiarities of current-voltage curves as well as transport characteristics of ion-exchange membranes in electrodialysis of mixed solutions of amino acid and mineral salt are practically not studied despite they are necessary for the development of ideas about electromembrane separation of organic ampholytes and strong electrolytes by electrodialysis.

Experiments

The objective of this study is to reveal the peculiarities of current-voltage curves and transport characteristics of ion-exchange membranes in electrodialysis of model solutions containing heterocyclic essential amino acid L-tryptophan 0.02M and sodium chloride 0.01M.
Electrodialysis has been carried out in a seven-compartment electrodialysis stack (ED) with alternating cation- and anion-exchange membranes. There have been used heterogeneous anion-exchange membranes MA-41 and cation-exchange membranes MC-40 manufactured by NPO "Shchekinoazot", Russia. ED stack has AgCl electrodes placed from the both sides of the studied ion-exchange membrane at the distance of 0.2 mm to obtain the current-voltage curve (CVC).

Results and Discussion

In electrodialysis before exceeding the limiting current density (i_{lim}) the most part of amino acid at pH value of solution close to isoelectric point exists in bipolar form. This type of ions does not take part in current transfer through the membranes. Therefore the presence of tryptophan in salt's solution does not affect significantly the value of limiting current density for cation-exchange memebrane.The presence of heterocyclic amino acid in mineral salt solution influences on the shape of current-voltage curves in the overlimiting conditions of electrodialysis. In particular, in the cation-exchange membrane phase bipolar ions can be recharged into cations that are able to migrate through the membrane in the course of facilitated electromigration [1]. It leads to lower values of membrane voltage at the same current density in the system including tryptophan in comparison with an individual sodium chloride solution [2]. The reduction of plateau length and increase of slope angle of this CVC plot for cation-exchange membrane in a solution containing tryptophan along with mineral salt is detected. It is caused by grow of the membrane surface hydrophobicity in such solution [3] and, accordingly, the contribution of electroconvection.

The presence of tryptophan in the initial solution leads to decrease in the value of i_{lim} and plateau length increase of CVC of anion-exchange membrane containing fixed quaternary ammonium groups in comparison with the individual solution of NaCl. The low mobility of tryptophan, as well as the possibility of intermolecular interactions of the heterocyclic amino acid with the membrane matrix, reduces the conductive properties of the membrane. The amino acid fills the pores, the conductive membrane channels. As a result, the mass transfer of ions of the mineral salt through the ion-exchange membrane is complicated due to the competitive transport of tryptophan and mineral salt ions. In addition, the catalytic activity of the amino group of the indole cycle of tryptophan is greater than that of the ionogenic groups of the membrane MA-41 [4]. Intensive dissociation of water at the interface suppresses electroconvection. This fact is confirmed by the larger values of the current efficiency for hydroxyl ions, which are formed during the water

splitting at the interface of the anion-exchange membrane – mineral salt solution containing tryptophan under overlimiting conditions of electrodialysis.

At the same time, the size factor is also significant. Namely, the volume of the side radical of tryptophan is the reason for the decrease in mass transfer of strong electrolyte ions through membranes.

The heterocyclic amino acid flux through MA-41 and MC-40 membrane has a conventional shape for ampholite with a maximum at the limiting current density and further decrease in mass transfer due to the barrier effect [5] that corresponds to the limiting diffusion current density at the ion-exchange membrane CVC. Facilitated electromigration of amino acids is observed at the intensive overlimiting conditions [1]. Moreover, the tryptophan flux through the MA-41 from solution containing sodium cloride is higher than that through the MC-40 at the overlimiting conditions of electrodialysis.

The inability of amino acid bipolar ions to migrate under an electric field determines the approach to the procedures of their separation, conditions for retention of ampholyte ions in electrodialyzer deionization sections and provides maximum mass transfer of charged impurities. The revealed features of CVCs and mass transfer in the studied solutions show that it is very important to take into account the nature of amino acids as well as membrane type for the forecast of amino acid electromembrane demineralization results.

References

1. *Shaposhnik V.A., Eliseeva T.V., Tekuchev A.Yu., Lushchik I.G.* Assisted electromigration of bipolar ions through ion-selective membranes in glycine solutions // Russ. J. Electrochem. 2001. V. 37. № 2. P. 170-175.
2. *Bukhovets A., Eliseeva T., Dalthrope N., Oren Y.* The influence of current density on the electrochemical properties of anion-exchange membranes in electrodialysis of phenylalanine solution // Electrochim. Acta. 2011. V. 56. P. 10283-10287.
3. *Pismenskaya N.D., Nikonenko V.V., Melnik N.A., Shevtsova K.A., Belova E.I., Pourcelly G., Cot, D., Dammak L., Larchet* C. Evolution with time of hydrophobicity and microrelief of a cation-exchange membrane surface and its impact on overlimiting mass transfer // J. Phys. Chem. 2012. V. 116. P. 2145-2161.
4. *Zabolotsky V.I., Sheldeshov N.V., Gnusin N.P.* Dissociation of water molecules in systems with ion-exchange membranes // Advances in Chemistry. 1988. V.57. №8. P. 1403-1414.
5. *Eliseeva T.V., Shaposhnik V.A.* Effects of circulation and facilitated electromigration of amino acids in electrodialysis with ion-exchange membranes // Russ. J. Electrochem. V.36. №1. 2000. P. 64–67.

DEGRADATION OF ION-EXCHANGE MEMBRANES IN ELECTRODIALYSIS WASTEWATER PRODUCTION OF MINERAL FERTILIZERS

Kseniya Kim, Olga Kozaderova, Sabukhi Niftaliev
Voronezh State University of Engineering Technologies, Voronezh, Russia
E-mail: *kmkseniya@yandex.ru*

The purpose of the work is to investigate the physicochemical and transport characteristics of heterogeneous cation-exchange (Ralex CM (H)-Pes) and anion-exchange (Ralex AM (H)-Pes) membranes differing in time of using in an industrial electrodialysis vessel under desalting and concentration of waste ammonium and nitrate-containing water (conditioned membranes, membranes after one and six years of use).

Experiments

The estimation of the conducting properties of membranes was carried out by the contact-difference method for solutions of ammonium nitrate in the concentration range 0.01-0.3 mol/dm^3 at 1 kHz frequency of an alternating current. Diffusion permeability of the ion-exchange membranes under study was measured in a flow cell for system sodium chloride / membrane / water.

Results and Discussion

Electroconductivity of the gel phase for cation-exchange membranes changed from 0.023 Ohm^{-1}cm^{-1} to 0.030 Ohm^{-1}cm^{-1}, and for anion-exchange membranes - from 0.011 Ohm^{-1}cm^{-1} to 0.031 Ohm^{-1}cm^{-1}. Analysis of the results showed that with long-term use of heterogeneous ion-exchange membranes in the electrodialyzer, their partial destruction is observed, and the diffusion permeability increases from $2.1\cdot10^{-12}$ m/s to $6.4\cdot10^{-12}$ m/s for cation-exchange membranes and $0.8\cdot10^{-12}$ m/s to $6.1\cdot10^{-12}$ m/s for anion-exchange membranes. At the same time, their total exchange capacity for cation-exchange membranes is reduced from 1.14 mmol/g to 1.08 mmol/g, and for anion-exchange membranes from 1.12 mmol/g to 0.98 mmol/g.

Table 1: Characteristics of ion exchange membranes

Parameter	RC0*	RC1	RC6	RA0	RA1	RA6
Diffusion permeability (NaCl 0,5 mol/dm^3), 10^{-12} м^2/с	2.1	2.2	6.4	0.8	0.8	6.1
Total exchange capacity (NaOH/HCl), mmol/g	1.14	1.11	1.08	1.12	1.04	0.98
Electroconductivity of the gel phase, Ohm^{-1}cm^{-1}	0.023	0.026	0.030	0.011	0.019	0.031

*The number equals to the use duration in years.

In the electrodialysis of the ammonium nitrate solution with the concentration of 0.01 mol/dm^3, the fluxes through the anion exchange membrane are much less than fluxes through the cation exchange membrane, since insoluble precipitate is formed in the anion exchange membrane. Electrodialysis with a current density exceeding the limiting value is accompanied by irreversible dissociation of water molecules at the interface with the solution, and the ion-exchange membrane starts to be freed from precipitate, as a result of which its electrochemical regeneration takes place. The obtained results testify insignificant deterioration of operational characteristics of ion-exchange membranes in the course of electrodialysis, which proves the prospects of its use for purification of waste nitrogen-containing water produced during the production of mineral fertilizers.

MATHEMATICAL MODELING, NUMERICAL AND ASYMPTOTIC SOLUTION OF THE BOUNDARY PROBLEMS OF MEMBRANE SYSTEMS TAKING INTO ACCOUNT THE WATER SPLITTING IN INTENSIVE CURRENT MODES

[1]Evgenia Kirillova, [2] Anna Kovalenko

[1]RheinMain University of Applied Sciences, Wiesbaden, Germany, E-mail: *kirillova@web.de*

[2]Kuban State University, Krasnodar, Russia, E-mail:*Savanna-05@mail.ru*

Introduction

Water is indispensable for life. However, drinking water is a scarce resource as most water on earth is of salty nature, polluted with industrial wastes, or contaminated with pathogenic agents. Today, clean drinking water is not accessible for about one billion people in the developing countries. Besides, it is expected that the human population will grow by further two billion people within the next three decades, including a doubling of the human population on the African continent. The human population is growing and water consumption per capita is increasing , both happening especially in developing countries. While safe drinking water supply is limited, global water scarcity becomes the number one challenge for the global human society [1]. In our opinion, the future of desalination processes will be based on the smart integration of various desalination techniques into optimized hybrid process superstructures with the membrane processes operating outside of today's process conditions. In the case of electrodialytic desalination this will be the case for operation at higher current densities as compared to today's traditional operation once the governing phenomena are comprehensibly understood.

The processes that run in electromembrane systems are very complex. The mass transfer in dilute solutions is characterized by a large number of different phenomena: the flow in the solution, the electric current transmitted through the ions, water dissociation, electrical and thermal convection, etc.

The aim is the investigation of the processes that occur in the solution near the membrane, in the so-called boundary layer. The mass transfer in this diffusion layer is described by the electrodiffusion equation system, which consists of Nernst-Planck-Poisson equations and the equation of current flow.

The boundary value problem corresponding to this mathematical model contains two small parameters, one of which is singular (as a factor in the derivative), and the second is regular (continuous). Thus, this problem belongs to the class of mixed or singularly regularly perturbed problems and is poorly amenable to numerical solution (hard problems [2]). Due to the presence of two small parameters, standard methods of a small parameter are not applicable without significant modification. These problems are characteristic of almost all boundary-value problems simulating the transport of salt ions in membrane systems. Thus, the development of numerical and analytical methods for solving such problems is an urgent problem.

Research results

Researches on this topic has been conducted since the mid-70s by scientists of the Kuban State University under the direction of Babeshko V.A., Urtenov M.Kh., Nikonenko V.V., members of the departments of physical chemistry and applied mathematics.

Babeshko V.A. and Urtenov M.Kh. developed an original method for solving one-dimensional boundary value problems of electrochemistry, which consists in decomposing the Nernst-Planck-Poisson system into equations that allow to calculate the electric field intensity and concentration [3]. It was called the decomposition method (splitting) and was used to obtain a numerical solution of boundary value problems simulating the transport of ions of an arbitrary salt [4]. In combination with the factorization method developed by them, the theory of ion transport of arbitrary salt, for example, binary and ternary salt was actually created [5-6].

In the future, the decomposition method was distributed by Urtenov M.Kh., Seyidova N.M., Kirillova E.V. on boundary problems taking into account the dissociation of water [7-8].

A nontrivial generalization of the decomposition method into two-dimensional and three-dimensional problems was obtained by authors of this study under the guidance of prof. Urtenov

M.Kh. [9–10] . Using this method, boundary-value problems were formulated and solved that simulate the phenomenon of electroconvection in the desalination channel [11], namely the occurrence of vortices as a result of the electric force in the space charge region on the electrolyte solution (electroconvection).

For the first time, such problems with the use of various simplifications were studied in [12–17]. In contrast to these works, a 2D model was first developed in [18–20], based on the Nernst-Planck-Poisson equations interconnected with the Navier – Stokes equations, which does not contain fitting parameters and allows finding hydrodynamic, electric, and concentration fields in the desalination channel, including membrane / solution boundary. The current-voltage characteristics calculated using this model for the first time qualitatively corresponded to those observed in real electromembrane systems. They have an initial linear section, an inclined plateau corresponding to the attainment of the limiting state in electromembrane systems, and a "over-limit" section characterized by a rapid increase in current, which is accompanied by an increase in fluctuations of the potential jump.

However, this model does not take into account the dissociation of water, although the emergence of new current carriers may lead to the disappearance of the expanded space charge region and, accordingly, to the cessation of electroconvection. Consequently, the modeling of the effect of the dissociation / recombination reaction on the main processes occurring in membrane systems, the development of methods for the numerical and asymptotic solution of boundary problems of the corresponding models is an actual problem.

We have developed an asymptotic method for solving the boundary-value problem of a one-dimensional model of transfer of ions of a binary salt with allowance for the dissociation reaction of water molecules, which generalizes the method used in [20]. In method [20], to the left of the center of the recombination region, the concentration of hydroxyl ions is assumed to be zero, and to the right, the concentration of hydrogen ions is assumed to be zero. Thus, the equilibrium condition is not satisfied. In our method, there are no zero concentrations, and the equilibrium condition is satisfied everywhere except for the recombination region (where the recombination significantly exceeds dissociation) and the space charge region (where the dissociation greatly exceeds the recombination). In addition, for the asymptotic solution of the problem in the space charge region, the decomposition method is used.

Conclusion

In this paper, we propose a new method for the asymptotic solution of a boundary value problem corresponding to a mathematical model of the transport salt ions in a diffusion layer, taking into account the reaction of water dissociation / recombination. This method, after appropriate modifications, can be applied, for almost all boundary-value problems simulating the transport salt ions in membrane systems, taking into account the dissociation / recombination of water, in our opinion.

The reported study was funded by RFBR according to the research project № 19-08-00252 "Theoretical and experimental research of current-voltage characteristics of electromembrane systems"

References

1. *Edward J.et al.*The state of desalination and brine production: A global outlook // The Science of the total environment. 2019. V.657, P. 1343-1356.
2. *Doolan E.P., Miller J. J. H., Schilders W. H. A.* Uniform Numerical Methods for Problems with Initial and Boundary Layers. Dublin, Boole Press 1980. 340 p.
3. *Babeshko V.A., Zabolotskij V.I., Kirillova E.V., Urtenov M.Kh.* Decomposition of Nernst-Planck-Poisson equation// Doklady Akademii nauk SSSR. 1995. V. 343(3), P. 485-486
4. *Babeshko V.A., Zabolotskii V.I., Seidov R.R., Urtenov M.Kh.* Decomposition equations for a unidimensional steady-state transfer of electrolyte ions // Russian Journal of Electrochemistry. 1997. V. 33(8). P. 785-792

5. *Babeshko V.A., Zabolotskii V.I., Korzhenko N.M., Seidov R.R., Urtenov M.Kh.* Stationary transport theory of ternary electrolyte in the Nernst layer // Doklady Physical Chemistry. 1998. V. 361(1-3). P. 215-218,
6. *Babeshko V.A., Zabolotskii V.I., Korzhenko N.M., Seidov R.R., Urtenov M.Kh.* Theory of steady-stay transfer of ternary electrolyte in nernst layer //Doklady Akademii Nauk. V. 1998361(2). P. 208-211
7. *Zabolotskii V.I., Nikonenko V.V., Korzhenko N.M., Seidov R.R., Urtenov M.Kh.* Mass transfer of salt ions in an electromembrane system with violated electroneutrality in the diffusion layer: The effect of a heterolytic dissociation of water // Russian Journal of Electrochemistry 2002. V. 38(8). P. 810-818,
8. *Urtenov M.A.-Kh., Kirillova E.V., Seidova N.M., Nikonenko V.V.* Decoupling of the Nernst-Planck and Poisson equations. Application to a membrane system at overlimiting currents // Journal of Physical Chemistry B. 2007. V. 111(51). P. 14208-14222
9. *Kovalenko A.V., Khromykh A.A., Urtenov M.K.* Decomposition of the two-dimensional Nernst-Planck-Poisson equations for a ternary electrolyte // Doklady Mathematics 2014. 90(2). P. 635-636,
10. *Kovalenko A.V., Khromykh A.A., Urtenov M.K.* Asymptotic solutions of boundary value problems of two-dimensional transport models for a ternary electrolyte // Doklady Mathematics. 2015. V. 92(2). P. 622-623
11. *Pismenskiy A., Urtenov M., Kovalenko A., Mareev S.* Electrodialysis desalination process in conditions of mixed convection // Desalination and Water Treatment. 2015. V. 56(12), P. 3211-3213
12. *Rubinstein I. and Zaltzman B.* Electro-Osmotic Slip of the Second Kind and Instability in Concentration Polarization at Electrodialysis Membranes // Mathematical Models and Methods in Applied Sciences. 2001. V. 11(02) P. 263-300,
13. *Rubinstein I. et al.* Experimental Verification of the Electroosmotic Mechanism of Overlimiting Conductance Through a Cation Exchange Electrodialysis Membrane // Russian Journal of Electrochemistry 2002. V. 38(8) P. 853-863.,
14. *Zaltzman B. and Rubinstein I.* Electro-osmotic slip and electroconvective instability //Journal of Fluid Mechanics 2007. V. 579. P. 173.,
15. *Yoshinobu Tanaka.* Water dissociation reaction generated in an ion exchange membrane // Journal of Membrane Science. 2010. V. 350 (1-2). P. 347-360.,
16. *Wessling M., Garrigos Morcillo L., and Abdu S.* Nanometer-thick lateral polyelectrolyte micropatterns induce macrosopic electro-osmotic chaotic fluid instabilities // Scientific reports 2014. V.4. P. 4294.
17. *Scott M. Davidson, Matthias Wessling, and Ali Mani.* On the Dynamical Regimes of Pattern-Accelerated Electroconvection // Scientific reports. 2016. V.6. P. 22505.
18. *Urtenov M.K., Uzdenova A.M., Kovalenko A.V., Nikonenko V.V., Pismenskaya N.D., Vasil'eva V.I., Sistat P., Pourcelly G.* Basic mathematical model of overlimiting transfer enhanced by electroconvection in flow-through electrodialysis membrane cells // Journal of Membrane Science. 2013. V. 447. P. 190-202,
19. *Nikonenko V.V., Kovalenko A.V., Urtenov M.K., Pismenskaya N.D., Han J., Sistat P., Pourcelly G.* Desalination at overlimiting currents: State-of-the-art and perspectives // Desalination. 2014.V. 342. P. 85-106
20. *Kovalenko A.V., Urtenov M.K., Seidova N.M., Pismenskiy A.V.,* The influence of reaction of dissociation / recombination of molecules of water on transporting electrolyte 1: 1 in the membrane systems in the diffusion layer. Part 2. Asymptotic analysis. Scientific Journal of KubSAU, 2016. V. 122(08). P. 241- 254. http://ej.kubagro.ru/2016/08/pdf/17.pdf

ACETALDEHYDE ELECTRO-OXIDATION ON SILVER CATALYSTS IN AQUEOUS ETHANOL SOLUTIONS

[1,2]Sofia Kleinikova, [1]Konstantin Gor'kov, [1]Ekaterina Zolotukhina

[1]IPCP RAS, Chernogolovka, Russia, E-mail: *zolek@icp.ac.ru*

[2]M.V. Lomonosov MSU, Moscow, Russia, E-mail: *ksofi3003@gmail.com*

Introduction

Curretly the problem of acetaldehyde extraction from corresponding monohydric alcohols is resolved by extraction and sorption methods, but the selective aldehydes determination, particularly acetaldehyde, is possible only using the chromatography [1], although many papers are dedicated to electrochemical acetaldehyde oxidation in aqueous media. There are only separate information that the electrochemical determination in the presence of ethanol is possible.

Earlier our group carried out researches that revealed the possibility to use silver composites for selective acetaldehyde (ethanal) oxidation in the oxygen atmosphere [3]. In order to define the mechanism of this process and to evaluate the possibility of the selective acetaldehyde determination in ethanol in this work, there are studied the regularities of the process of acetaldehyde electro-oxidation on a silver catalyst in the presence of ethanol.

Table 1: Acetaledehyde sorption α from ethanol solution by the ion-exchange matrix or/and its oxidation during 5h

Matrix type (ionic form)	α, %	
	Ethanal sorption	Ethanal oxidation
GCE (Na^+)	15±2	10±2
GAE (OH^-)	49±2	65±5
PAE (OH^-)	58±3	97±3

Experiments

The electro-oxidation process was performed in the three-electrode electrochemical cell in aqueous and aqueous-ethanol media using the stationary disk electrode from polycrystalline silver (d = 1 mm). The electrochemical methods were chronoamperometry and cyclic voltammetry.

Results and Discussion

The experiments in media with different acidity allowed to conclude, that the hydroxide ions play the important role in the electro-oxidation process. Its presence in solution facilitates the electro-oxidation of acetaldehyde on Ag-electrode, the oxidation peak on CV is observed at potential -0,1 V (Fig.1). Besides, there were revealed the linear dependence between the acetaldehyde concentration (1-30 mM) and the positive charge of cycle in alkaline media (Fig.2). In this case, the intensity of oxidation significantly depends on the state of the silver surface. Pre-oxidation of the silver surface at potentials of $Ag(OH)_{ads}$ formation [4] provides larger current responses compared to the non-oxidized silver surface (Fig.2), that correlate with data [3]. This effect can be related with formation of more developed silver surface at its serial oxidation/reduction.

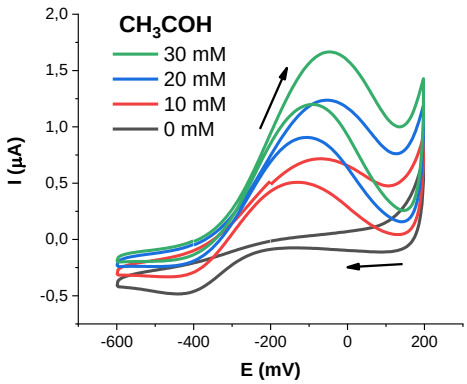

Figure 1. Cyclic voltammogram plots of Ag in 0.1 M NaOH with various concentration of acetaledehyde. Scan rate of 50 mV/s.

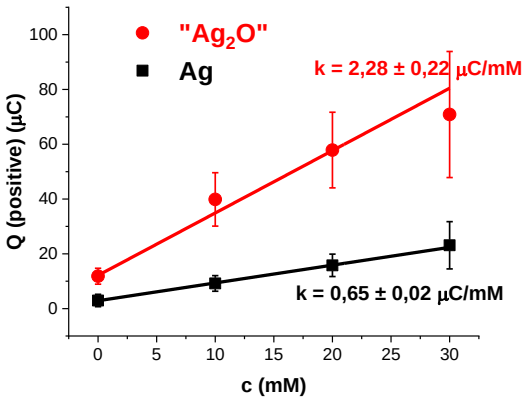

Figure 2. Linear dependence between the positive charge and acetaledehyde concentration for Ag and Ag-pretreated electrodes.

Carrying out the acetaldehyde oxidation in the oxigen atmosphere provides larger current responses compared to the inert argon atmosphere that demonstrate the influence of adsorbed oxygen on the electro-oxidation process.

There is shown, that in aqueous-ethanol medium the current responses of ethanol oxidation are not observed, while after acetaldehyde injection in 1 M ethanol solution it is kept the linear dependence between the acetaldehyde concentration (1-30 mM) and the positive charge of cycle with less sensitivity (Fig.3).

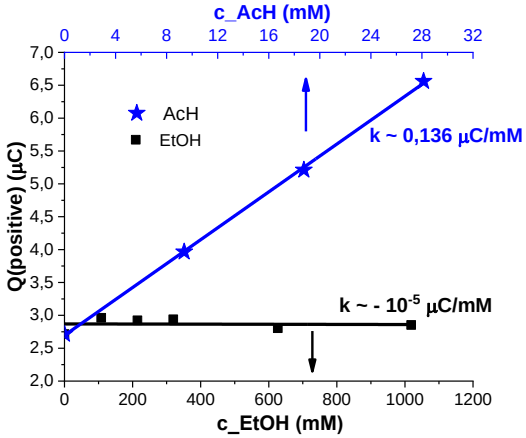

Figure 3. Linear dependence between the positive charge and acetaledehyde/ethanol concentraion for Ag.

References

1. *Santos A.L., Takeuchi R.M., Munoz R.A.A. et al.* Electrochemical Determination of Organic Compounds in Automotive Fuels // Electroanalysis. 2014, №26. p. 233–242.
2. *Shereema R.M., Nambiar S.R., Shankar S.S. et al.* CeO_2–MWCNT nanocomposite based electrochemical sensor for acetaldehyde // Analytical methods. 2015, № 7, p. 4912–4918.
3. *Sakardina E.A., Kravchenko T.A., Zolotukhina E.V. et al.* Silver/ion exchanger nanocomposites as low-temperature redox-catalysts for methanal oxidation // Electrochimica Acta. 2015, №179. p. 364–371.
4. *Lesnikh N.N., Tutukina N.M., Marshakov I.K.* Conditions for the occurrence of pitting lesions of silver in alkaline media // Bulletin of VSU, series: chemistry, biology, pharmacy. 2008, № 2, p. 41–47.

THE EFFECT OF THE pH OF THE DESORBING NaCl SOLUTION ON THE DEGREE OF EXTRACTION OF ANTHOCYANINS FROM CATION- AND ANION EXCHANGE RESIN

Anastasia Klevtsova, Yuliya Yakovleva, Natalia Pismenskaya
Kuban State University, Krasnodar, Russia, E-mail: *nastya_k1314@mail.ru*

Introduction

Anthocyanins are valuable food coloring. Besides, they are used in medicine and cosmetic industries. Only recently, researches have begun to consider the recovering of anthocyanins, as high value compounds, transforming some food effluents to raw material with high potential economic value. Now ion exchange resins are considered as effective materials for the preliminary separation of anthocyanins from plant materials [1]. The aim of the work is to test the possibility of desorbing anthocyanins from ion exchange resins using aqueous salt solutions with different pH values.

Experiments

We study the process of desorption of anthocyanins from cation exchange (KU-2-8) and anion exchange (AV-17-8) resins using 1 M NaCl aqueous solution with pH values of 3,0±0,1 and 11,0±0,1.

First of all, we started with the sorption process of anthocyanins by ion exchange resins. The aqueous solution of anthocyanins was used with pH values of 3,0±0,1 and 9,0±0,1. Ten samples (1,0±0,1 g) of each ion exchange resin were placed into tubes containing aqueous solution of anthocyanins (V=20 cm^3). The range of anthocyanins concentrations, C_{Ant}, was from 5±1 mg/dm^3 to 50±1 mg/dm^3. The conccentration of anthocyanins in the solution equilibrated with ion-exchange resins was calculated by the standard method using spectrophotometry [2]. In this preliminary experiment, it was shown that the highest largest amount of anthocyanins was sorbed by the resin, if the pH of the solution was equal to 3,0±0,1 (KU-2-8) or 9,0±0,1 (AV-17-8). These samples were used in anthocyanin extraction experiments. Ten samples of each ion exchange resin (1,0±0,1 g) were placed into tubes containing aqueous solution of 1 M NaCl (V=20 cm^3) with a pH value of 3,0±0,1 and 11,0±0,1. After a defined period of time (ranging from 10 to 180 min) two aliquots (1 cm^3) were taken from each tube and brought up to 10 cm^3 by buffer solutions (pH = 1,0 or pH = 4,5). The concentration of desorbate in the solution (m_{Ant}) was determined using spectrophotometry method [2].

It is known that anthocyanins change their structure and charge depending on the pH value of the medium. For example, their charge becomes positive, and the color is red if pH is less than 3. Their charge becomes negative, and the color is blue, green or yellow if pH is more than 7 [3]. This property of anthocyanins was used to determine their charge in the resin and solution using the previously obtained dependence of the color of anthocyanins vs the pH of the medium.

Results and Discussion

It was shown that desorption of anthocyanins from resin KU-2-8 was more intense if the pH value of the salt solution was 11,0 compared to 3,0 (Fig. 1). The cause is electrostatic repulsion of negatively charged anthocyanins and negatively charged fixed groups of KU-2-8 resin if the pH of the salt solution was 11,0 as well as electrostatic interactions of positively charged anthocyanins and negatively charged fixed groups of KU-2-8 resin if the pH of the salt solution was 3,0.

In the case of pH of the solution equal to 3,0 anthocyanins acquire a positive charge in the AV-17-8. They become co-ions and are pushed out of the anion exchange resin due to the effect of Donnan exclusion. If the salt solution is 11,0, the anthocyanins become counterions, and this makes it difficult to extract them from the anion exchange resin. (Fig. 2).

The results can be useful for developing a method for the extraction of anthocyanins from ion exchange resins.

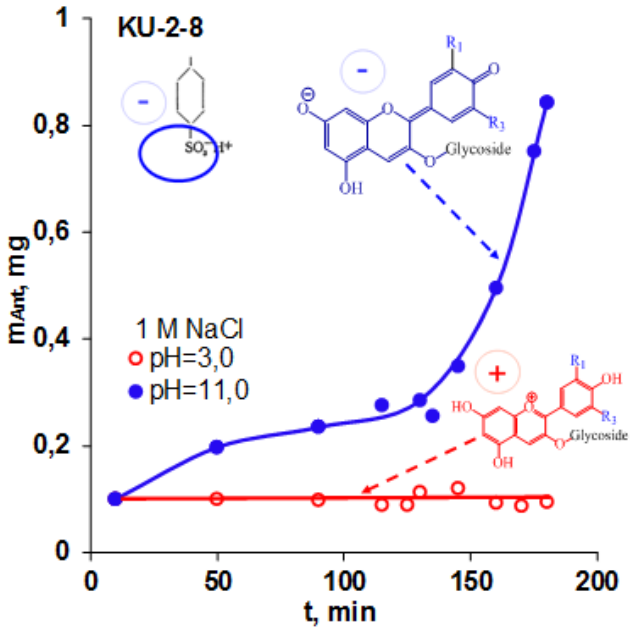

Figure 1. The Kinetics of Anthocyanins Desorption from KU-2-8 Using 1M NaCl Aqueous Solution with pH Value 3,0 and 11,0.

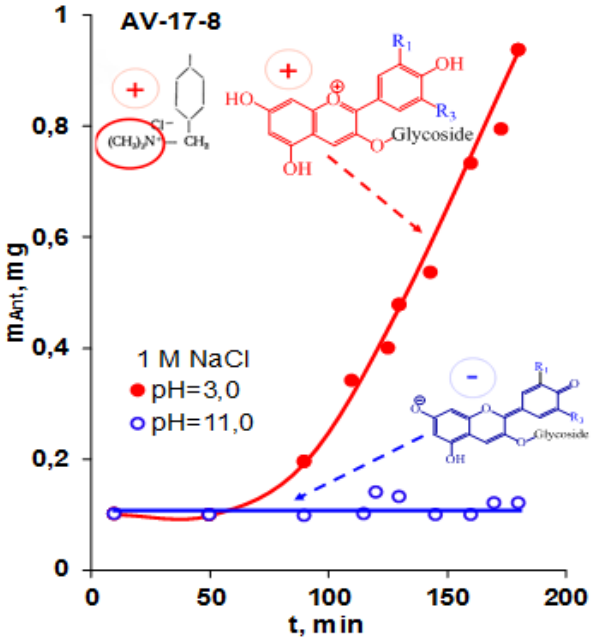

Figure 2. The Kinetics of Anthocyanins Desorption from AV-17-8 Using 1M NaCl Aqueous Solution with pH value 3,0 and 11,0.

Acknowledgements

The study is realized with the financial support of the Russian Foundation for Basic Research and Krasnodar Region Administration, project № 19-48-230024 reg_a.

References

1. *Maria R., Kosseva V. K., Joshi P. S.* Science and Technology of Fruit Wine Production 2017, Academic Press is an imprint of Elsevier, P.1-758.
2. Juice products. Methods for the determination of anthocyanins: MGS GOST ISO 32709-2014.
3. *Ribéreau-Gayon P., Glories Y., Maujean A., Dubourdieu D.* Handbook of Enology: The Chemistry of Wine, Stabilization and Treatments, 2nd ed. Dunod: Paris, 2006. V. 2.

POTENTIOMETRIC MULTISENSORY SYSTEMS WITH HYBRID MATERIALS BASED ON PERFLUOROSULFONIC CATION-EXCHANGE MEMBRANES FOR DETERMINATION OF DRUGS IN PHARMACEUTICALS

[1]Tatyana Kolganova, [1]Anastasia Yelnikova, [1]Ekaterina Lapshina, [1]Anna Parshina, [2]Ekaterina Safronova, [1]Olga Bobreshova

[1]Voronezh State University, Voronezh, Russia, E-mail: *tanyadenisova@list.ru*

[2]Kurnakov Institute of General and Inorganic Chemistry RAS, Moscow, Russia

Introduction

Pharmaceuticals based on amino- and sulfur-compounds are widely used. Alkali and/or alkaline-earth metal cations are part of such pharmaceuticals too. Since the composition of these media is complex, the application of a multisensory approach is effective. The prospects of using potentiometric sensors and multisensory systems based on hybrid membranes for the determination of organic and inorganic ions are discussed in [1]. The aim of this work is a development of potentiometric multisensory systems with DP (Donnan potential)-sensors based on hybrid perfluoromembranes for the determination of amino- and sulfur-containing drugs in pharmaceuticals.

Experiments

Aqueous solutions of procaine, lidocaine, bupivacaine hydrochlorides, cysteine, as well as aqueous solutions of glutamic and aspartic acids, taurine, sulfacetamide containing KOH or NaOH were investigated. Moreover, aqueous solutions containing CH_3COCOO^-, HS^-, NH_4^+, K^+, OH^- ions were investigated too. The composition of test solutions and the ranges of components concentrations (from $1.0\cdot10^{-4}$ to $1.0\cdot10^{-2}$ M or $1.0\cdot10^{-1}$ M) were chosen taking into account the composition of pharmaceuticals based on them. The hybrid materials based on Nafion and MF-4SC membranes and hydrated zirconia and silica nanoparticles modified by amine-containing groups (3-aminopropil-, 3-(2-imidazol-1-yl) propyl-), sulfo groups ($-SO_3H$, $-(CH_2)_3-SO_3H$)), acid salt of heteropolyacid ($K_xH_{3-x}PW_{12}O_{40}$); acid salts of heteropolyacids ($Cs_xH_{3-x}PW_{12}O_{40}$, $Cs_xH_{4-x}SiW_{12}O_{40}$); carbon nanotubes; poly-3,4-ethylenedioxythiophene (PEDOT) were investigated as electrode active materials in DP-sensors. The initial membranes were prepared by casting or extrusion and the hybrid materials were prepared by casting or *in situ*.

Results and Discussion

The multisensory systems based on perfluoromembranes for simultaneous determination of drugs anions and the alkaline metal cations, including drugs anions with similar chemical properties, in pharmaceuticals are developed. A variation of DP-sensors characteristics was achieved by the introducing dopants nanoparticles with different surface properties into membranes, as well as by treatment of membranes with physicochemical methods. This allows increasing a number of sorption centers and optimizing the interstitial space size for analytes, depending on their charge sign, size, and nature of the functional groups [2, 3]. It is shown that the size of interstitial membrane space influences not only on the concentration of definable and interfering ions in membrane, but also on the conformation of organic ions in the pores and on the mechanisms of their interaction with membrane components [3]. The criterions for the selection of membranes compositions for DP-sensors arrays based on the study of dependences the DP-sensors characteristics on the equilibrium and transport properties of membranes are proposed.

This work was supported by the Russian Foundation of Basic Research (projects no. 19-48-363008 r_mol_a).

References

1. *Apel P.Yu., Bobreshova O.V., Volkov A.V., Volkov V.V., Nikonenko V.V., Stenina I.A., Filippov A.N., Yampolskii Yu.P., Yaroslavtsev A.B.* // Membranes and Membrane Technologies. 2019. V. 1. № 2. P. 45-63.
2. *Parshina A.V., Denisova T.S., Safronova E.Y., Karavanova Y.A., Safronov D.V., Bobreshova O.V., Yaroslavtsev A.B.* // Journal of analytical chemistry. 2017. V. 72. №12. P. 1243-1250.
3. *Safronova E., Parshina A., Kolganova T., Bobreshova O., Pourcelly G., Yaroslavtsev A.* // Journal of Electroanalytical Chemistry. 2018. V. 816. P. 21-29.

STUDY OF TRANSPORT CHARACTERISTICS OF PERFLUORINATED MF-4SK MEMBRANE IN SULFATE / NITRATE SOLUTIONS

Denis Kolot, Aslan Achoh
Kuban State University, Krasnodar, Russia

Introduction

Ion exchange membranes with a modified layer are of great use in electrodialysis technologies. The development of ion-exchange membranes with increased selectivity to individual sorts of ions of the same charge sign, but differing in its size, will allow to expand the use of electrodialysis in the field of membrane technology. The development of perfluorinated membranes, their modifications, research and growth, membrane technologies based on them are promising and developing directions of modern science.

The idea of producing two-layer and anisotropic membranes intended for separating multi-ion electrolyte solutions is fruitfully used for a long time in the creation of industrial reverse osmosis, nanofiltration, ultrafiltration, gas separation membranes. As a rule, these membranes are composed of a thin selective layer (several micrometers thick). The properties of the selective layer determine the characteristics of the membranes.

Mechanisms of specific selectivity are of considerable interest for studying the charge selectivity of membranes. The competing transfer of singly and doubly charged ions that are in solution through a surface-modified layer occurs due to the strong electrostatic repulsion of doubly charged ions as compared to single-charged ones. This separation of ions occurs due to kinetic, and than thermodynamic properties. However, the transport properties of such systems are not fully understood and are of great interest to researchers.

The aim of this work is to study the transport characteristics of a homogeneous perfluorinated membrane MF-4SK in sulphate-nitrate solutions of electrolytes.

Experiments

The object of the study was the perfluorinated MF-4SK membrane obtained by a watering method from a 10% solution of perfluorosulfopolymer dissolved in isopropanol.

The membrane was obtained with a reinforcing mesh of nylon for impart mechanical strength. The thickness of the membrane was 150 ± 5 microns.

The electrical resistance of the membranes was determined by analyzing the frequency spectrum of the electrochemical impedance in the mercury-contact cell. The frequency spectra of the electrochemical impedance were obtained using a "Parstat 4000" potentiostat-galvanostat-impedance meter in the frequency range of 1 Hz - 500 kHz. Diffusion permeability was studied on two chamber cells in mono-ionic forms of sulfate and sodium nitrate, as well as in a mixed solution of sulfate and sodium nitrate. According to the standard method, an electrolyte solution was poured into one of the chambers and distilled water was poured into the other [1, 2]. In mixed solutions, the diffusion permeability was determined by the increase in concentration in a chamber with distilled water using an ion chromatograph. A sample of 0.25 ml was taken for analysis. The integral permeability coefficients were determined separately for sulfate ions and nitrate ions. Also the exchange capacity of the experimental samples was determined by the standard method. The temperature in the experiments was kept constant and was equal to 25 ± 0.1 ° C.

Results and discussion

The greatest interest for the study of ion transport in electrodialysis processes with surface modified membranes is the surface layer in which, due to the strong electrostatic repulsion of doubly charged ions as compared to singly charged ones, separation occurs. The conductive characteristics of the modifier determine the transport properties of the entire membrane system. In this regard, the specific conductivity of the membrane MF-4SK in sulfate and sodium nitrate was investigated (Fig. 1).

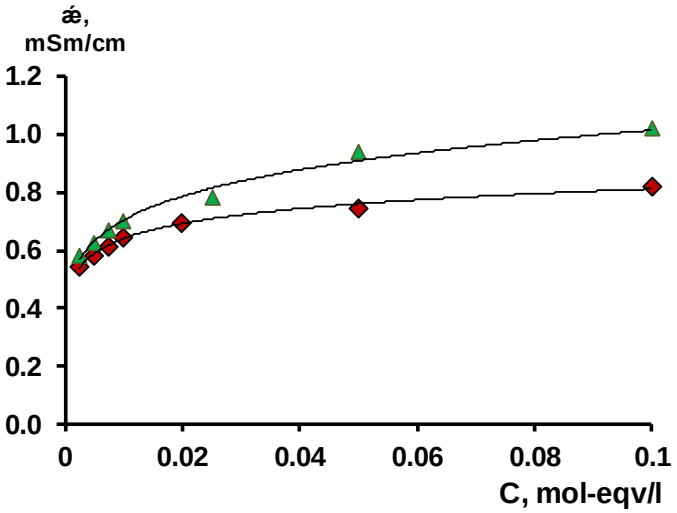

Figure 1. Conductivity of MF-4SK membrane depending on electrolyte concentration.

Studies show that the electrical conductivity of the membrane in the test solutions are close. This is explained by the fact that in the cation-exchange membrane of MF-4SK sodium ions are counter-ions and determine the conductive properties. However, the electrical conductivity in sodium nitrate increases by 20% with an increase in concentration. Using a three-wire model, the proportion of gel and intergel in the test solutions was calculated. In sodium nitrate, the gel fraction is $f_1 = 0.167$, the intergel phase is $f_2 = 0.833$. In a solution of sodium sulfate, the gel fraction is $f_1 = 0.123$, the intergel phase is $f_2 = 0.867$.

In the process of separation of sulfate and nitrate of ions of limiting is the stage of diffusion of anions through the cation-exchange membrane MF-4SK, which are co-ions. Figure 2 shows the diffusion flow of salts through the MF-4SK cation-exchange membrane. The solid line shows the flows in pure sulphate and sodium nitrate. The dotted line is the flow of a mixture of salts of sulfate and sodium nitrate, while the dashed line shows the flows in a mixture of salts.

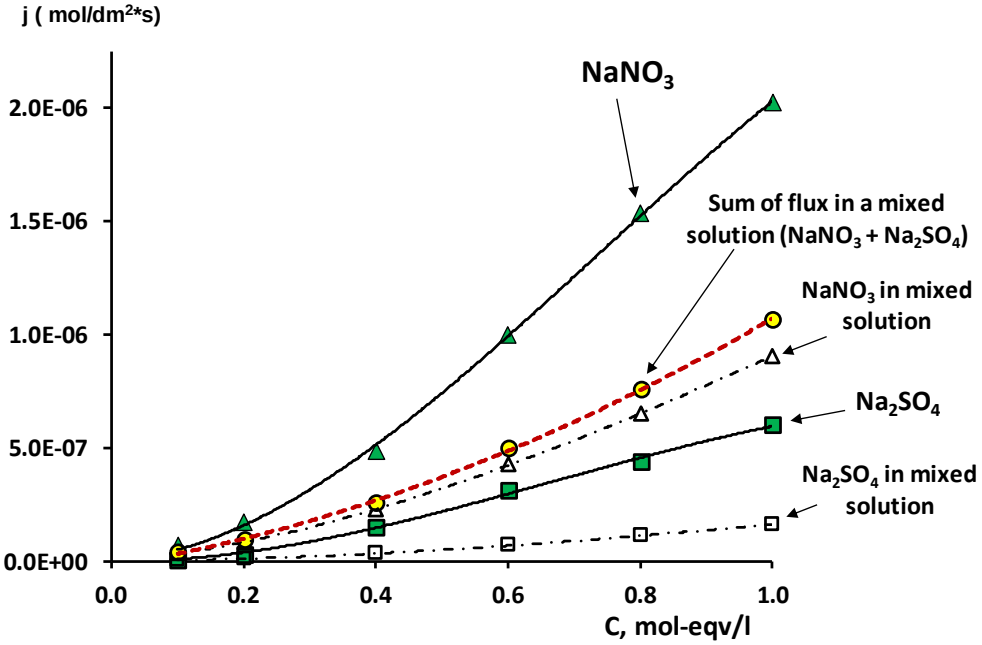

Figure 2. Dependence of the diffusion flow of salt through the membrane of MF-4SK on the concentration of salt.

Studies show that in a pure sodium nitrate diffusion flow in comparison with sulfate is much higher. In this case, in a mixed solution, the ratio of sodium nitrate to sulfate flows is maintained in favor of sodium nitrate, and it is equal to 9.4. The diffusion permeability coefficients P * m

(mol/dm^2·s) were calculated. In a solution of sodium nitrate, about a concentration of 0.1 mol/l, the diffusion permeability coefficient is 3.86 × 10-11 mol/dm^2·sec. In sodium sulfate at the same concentration of 3.41 × 10-12 mol/dm^2·sec. Such a difference in diffusion permeability coefficients can be explained by charge selectivity and high degree of hydrogenation of sulfate ions, which makes it difficult to transport through the cation-exchange membrane. The membrane exchange capacity was determined according to the standard procedure, which amounted to 0.81 mmol/g-swollen membrane. These data are consistent with the literature data and may be useful in further work on modeling the transport processes of membrane ions modified by the MF-4SK cation-exchange film.

Acknowledgement

This research was financially supported by Russian Foundation of Basic Research project № 18-38-00773 mol_a.

References

1. *Berezina N.P., Kononenko N.A., Dvorkina G.A., Sheldeshov N.V.* Physico-chemical properties of ion-exchange materials. Krasnodar, 1999. P. 82
2. *Zabolotskii V.I., Gnusin N.P., Sheretova G.M.* The account of structural heterogeneity of ion exchanger in describing the equilibrium distribution of electrolyte in ion exchange systems. J. physical chemistry 1985. V. 59. P. 2467.

ASYMMETRY OF CURRENT-VOLTAGE CHARACTERISTICS OF BI-LAYER HYBRID PERFLUORINATED MEMBRANES IN SODIUM CHLORIDE SOLUTION

[1]Natalia Kononenko, [2]Anatoly Filippov, [3]Sergey Dolgopolov, [1]Mariya Salaschenko

[1]Kuban State University, Krasnodar, Russia, *E-mail: kononenk@chem.kubsu.ru*

[2]Gubkin University, Moscow, Russia

[3]Frumkin Institute of Physical Chemistry and Electrochemistry RAS, Moscow, Russia

Introduction

Bi-layer ion-exchange membranes have an anisotropic structure and possess asymmetric transport properties under applying the concentration and electric field gradients. The asymmetry effects of electrotransport characteristics can be used to create membrane switches. Therefore, the progress in such materials is a very important problem, which can be solved by modifying commercial membranes with components of organic and inorganic nature.

The purpose of this paper is investigation of the current-voltage curves of hybrid perfluorinated membranes based on MF-4SK and halloysite nanotubes (HNT) in order to select samples with the most asymmetric transport properties.

Experiments and Results

A series of bi-layer membranes was prepared by casting method from perfluoropolymer solution in dimethylformamide[1] containing the modifier by placing it on the membrane surface [1]. Halloysite nanotubes and HNT with platinum nanoparticles were used as the modifier (Table 1).

Table 1: Objects of research

No	Membrane layers	Modifier
1	MF-4SK/MF-4SK+HNT	4% HNT
2	MF-4SK/MF-4SK+HNT@Pt	4% HNT + 2% Pt
3	MF-4SK+HNT/MF-4SK+HNT@Pt	4% HNT/4% HNT + 2% Pt

The current voltage curves (CVC) were measured in a cell equipped with platinum polarizing and silver chloride measuring electrodes. The orientation of bi-layer membrane in the electric field towards the flow of ions was changed as shown in Fig. 1. Parameters of CVC were found graphically: the angular slope of the ohmic section of the CVC ($(\Delta i/\Delta E)_{ohm}$), the magnitude of the limiting diffusion current (i_{lim}), the length of the limiting current plateau (Δ, V) and the angular slope of the CVC in overlimiting state ($(\Delta i/\Delta E)_{overlim}$).

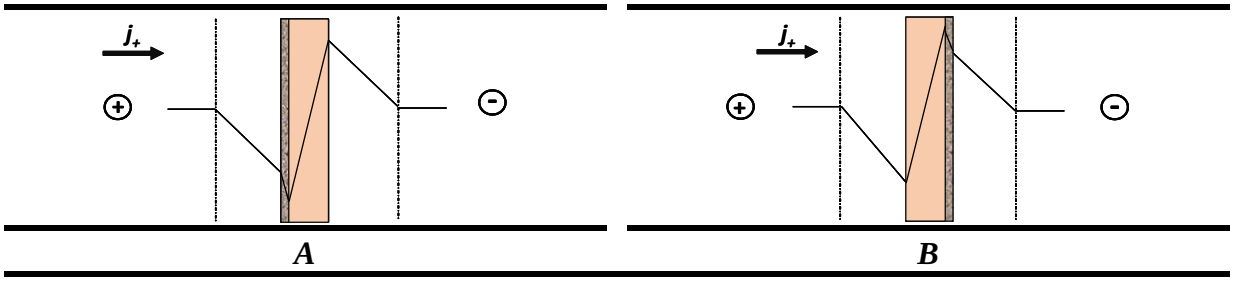

FIGURE 1. THE ORIENTATION OF BI-LAYER MEMBRANE IN THE ELECTRIC FIELD.

The results presented in Fig. 2 and Table 2 allow to reveal the impact of HNT and platinum nanoparticles, deposited on their surface, on the CVC and to find the asymmetry effect of CVC. Both the plateau length and the magnitude of the limiting current depend on orientation for MF-4SK/MF-4SK+HNT membrane. Probably in the membrane, HNT shield fixed groups which have a catalytic effect on the water dissociation process close to the membrane surface. As a result, H^+ and OH^- ions reach the modified side later than the unmodified one. The slope of the CVC in

[1] Samples were prepared by Dr. D. Petrova at Gubkin University (Moscow, Russia).

overlimiting state is 11 % higher when the limiting state occurs on the unmodified side of the membrane.

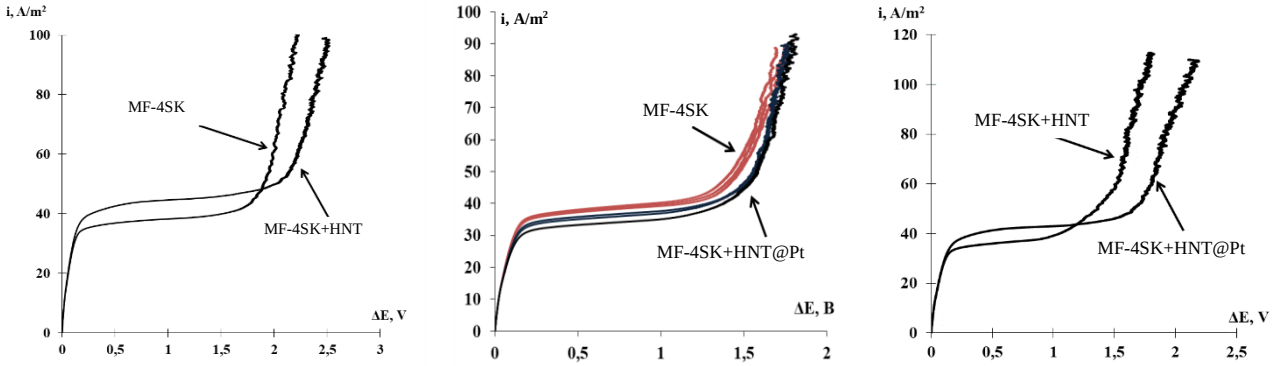

a *b* *c*

Figure 2. Current voltage curves of bi-layer membranes MF-4SK/MF-4SK+ HNT (a), MF-4SK/MF-4SK+ HNT@Pt (b) and MF-4SK+HNT/MF-4SK+HNT@Pt (c). Arrows point out the side of membrane where the limiting state occurred.

Table 2: Parameters of current-voltage characteristics of bi-layers membranes

Parameter	MF-4SK/MF-4SK + HNT		MF-4SK/MF-4SK + HNT@Pt		MF-4SK+HNT/MF-4SK + HNT@Pt	
	MF-4SK	MF-4SK+ HNT	MF-4SK	MF-4SK+ HNT@Pt	MF-4SK+ HNT	MF-4SK+ HNT@Pt
$(\Delta i/\Delta E)_{ohm}$ S/m²	314,6±0,1	337,6±0,1	357,0±0,1	382,5±0,2	318,7±0,1	317,7±0,1
i_{lim}, A/m²	36,0±0,1	42,0±0,3	35,8±0,6	34,6±0,5	34,4±0,6	40,4±0,2
Δ, V	1,75±0,01	2,02±0,02	1,35±0,01	1,42±0,04	1,27±0,04	1,57±0,04
$(\Delta i/\Delta E)_{overlim}$, S/m²	153,2±5,6	135,2±6,0	158,7±0,6	182,0±0,5	180,7±0,1	148,2±1,8

The absence of CVC asymmetry of the bi-layer membrane MF-4SK/MF-4SK+HNT@Pt is associated with simultaneous action of two factors compensating each other. These are the presence of HNT and existence of Pt nanoparticles. This means that to obtain a membrane with obviously asymmetric properties, it is necessary to synthesize a material whose layers differ only by one parameter. In fact, if both layers of bi-layer membrane contain HNT and one of them contains HNT@Pt, the asymmetry effect of the CVC is more significant. It can be seen from the Table 2, when the limiting state occurs on the side containing HNT@Pt, the limiting current increases by 8%, plateau length of the limiting current increases by 10% and the conductivity of the system in the over-limiting state decreases by 20%.

Thus, the study of the polarization behavior of bi-layer perfluorinated membranes based on MF-4SK and halloysite nanotubes shows that in order to obtain a membrane with noticeably asymmetric properties, it is necessary to synthesize a material whose layers differ only by one component: either the presence of HNT or of the metal dispersion.

The present work was supported by the Russian Foundation for Basic Research (project № 18-08-00771-a).

References

1. *Filippov A., Petrova D., Falina I., Kononenko N., Ivanov E., Lvov Y., Vinokurov V.* // Polymers. 2018. V. 10 (366). P. 1–17.

EVALUATION OF APPLICABILITY OF THE TEORELL-MEYER-SIEVERS MODEL TO DESCRIBE THE SORPTION AND KINETIC PROPERTIES OF ION-EXCHANGE MEMBRANES

Andrey Kononov, Victor Nikonenko
Kuban State University, Krasnodar, Russia, E-mail: *v_nikonenko@mail.ru*

Description of transport characteristics of ion-exchange membranes as functions of bathing solution concentration remains an actual classical problem. While the Teorell-Meyer-Sievers (TMS) theory was developed in 40s of the last century and some criticism appeared nearly immediately [1], this theory [2, 3] and some its modifications (such as the thin pores model developed by A.N. Filippov [4, 5]) are now using quite often. The aim of the present work is to asses the applicability of this model to describe the full set of sorption and kinetic properties of ion-exchange membranes as depending on the bathing solution concentration.

A numerical solution of a 1D stationary mathematical model of electrolyte diffusion into the water based on the TMS theory is developed. The adjacent diffusion layers are not taken into account. Ion transport is described by the Nernst-Planck equation, the membrane is considered as a homogenous electrically neutral medium. The Donnan equilibrium equations are applied at the membrane/solution interfaces.

For comparing the calculation with experiment, we used the data obtained by Pismenskaya et al. [6] for concentration dependencies of NaCl concentration in the membrane, its conductivity, diffusion permeability and transport numbers. The input parameters of the model are the diffusion coefficients of counter-ion and co-ion in the membrane; distribution coefficient, γ'; exchange capacity, Q, and membrane thickness. Along with the TMS model, we use the microheterogeneous model with the set of parameters determined in [2].

Note that the distribution coefficient can be related to the Donnan constant, KD:

$$K_D = (\gamma')^{-2}$$

The comparison of the calculations using the model based on the TMS theory shows that it is possible to choose a set of input parameters so that the model can adequately describe the concentration dependence of diffusion permeability and transport numbers. However, we have not succeeded to describe adequately electrolyte sorption and membrane conductivity. The reason is the presence of electroneutral solution in the center of meso- and macropores, which is not taken into account in the TMS model.

Acknowledgements

We are grateful to Russian Foundation of Basic Research (grant № 19-48-230023) for financial support of this research.

References

1. *Fetcher Jr. E. S.* A Criticism of the Teorell–Meyer–Sievers Theory of Membrane Permeability // J. Phys. Chem. 1942. V. 46. P. 570-574.
2. *Tanaka Y.* Chapter 4, Theory of Teorell, Meyer and Sievers (TMS Theory) // J. Membr. Sci. Technol. 2007. V. 12. P. 59-66.
3. *Galama A. H., Post J. W., Hamelers H. V. M., Nikonenko V., Biesheuvel M.* On the origin of the membrane potential arising across densely charged ion exchange membranes: How well does the Teorell-Meyer-Sievers theory work? // J. Membr. Sci. 2016. V. 2. P. 128-140.
4. *Filippov A. N., Safronov E. Yu., Yaroslavtsev A. B.* Theoretical and experimental investigation of diffusion permeability of hybrid MF-4SC membranes with silica nanoparticles // J.Membr. Sci. 2014. V. 471. P. 110–117.
5. *Filippov A. N., Kononenko N. A., Demina O. A.* Diffusion of electrolytes of different natures through the cation-exchange membrane // Colloid. J. 2017. V. 79(4). P. 556-566.
6. *Pismenskaya N. D., Nevakshenova E. E., Nikonenko V. V.* Using a Single Set of Structural and Kinetic Parameters of the Microheterogeneous Model to Describe the Sorption and Kinetic Properties of Ion-Exchange Membranes // Pet. Chem. 2018. V. 58(6). P. 465–473.

INFLUENCE OF ION TRANSPORT IN ION-EXCHANGE MEMBRANE BULK ON THE SHAPE OF CHRONOPOTENTIOMETRIC CURVES

Andrey Kononov, Veronika Sarapulova, Semyon Mareev
Kuban State University, Krasnodar, Russia, E-mail: *v_nikonenko@mail.ru*

Introduction

As known, the limiting current density depends on transport numbers of counter-ions in the electrolyte solution and inside the membrane [1]. Recent research showed that concentration polarization causes changes in transport numbers of ions in the ion-exchange membrane bulk [2]. However, non-stationary galvanostatic models that take into account the transfer of each type of ions in the bulk of the ion-exchange membrane do not exist.

Experiments

A 1D nonstationary mathematical galvanostatic model of binary electrolyte ion transport through a membrane was developed. The system under study consists of an ion exchange membrane and two adjacent diffusion layers. Ion transport is described by the Nernst-Planck, the Poisson and the material balance equations. The Fuji CEM Type-II cation-exchange commercial homogeneous membrane (Fujifilm, Netherlands) was selected as the object of the study. 0.1M NaCl solution was used in calculations. The values of the main parameters of the system (membrane thickness d_m, membrane exchange capacity Q, electrical conductivity κ, diffusion permselectivity P, the relation between current density and the theoretical limiting value calculated using the Leveque equation [3]) are presented in Table 1.

Table 1: Initial Values

Parameter	Value
d_m, μm	184
Q, mol/l	1.35
κ, μS/cm	3.34
P, cm^2/s	$1.6 \cdot 10^{-8}$
i/i_{lim}	0.999

Results and Discussion

Calculations for the present study were made using the Comsol Multiphysics 5.4 software. Concentration profiles of Na^+ and Cl^- ions in the membrane bulk are presented on Figure 1.

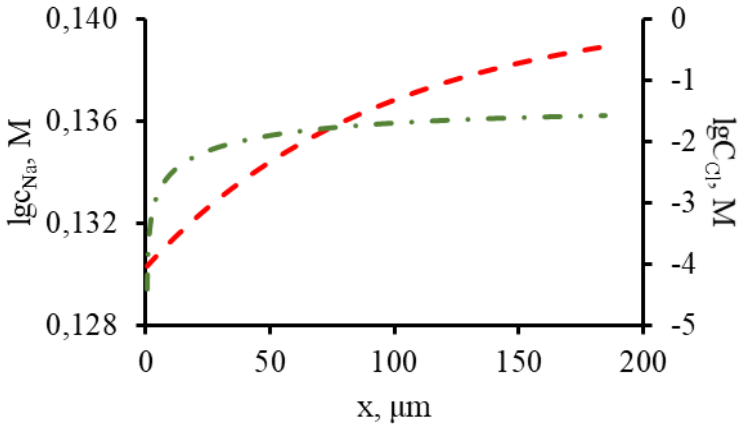

Figure 1. Concentration Profiles of Na^+ (dashed red line) and Cl^- (dash-dotted green line) Ions in the Membrane.

The developed model allows to define transport numbers of ions in a membrane system. The results of calculations and values obtained by analytical equations are presented on Figure 2.

While electrical current passes through the membrane, concentration polarization increases, which increases the transport number of co-ions, according to [2]. With the grows of transport

number of co-ions, the limiting current density decreases. This effect causes the local maximum on the chronopotentiometric curve, which is about 500 s long (Figure 3).

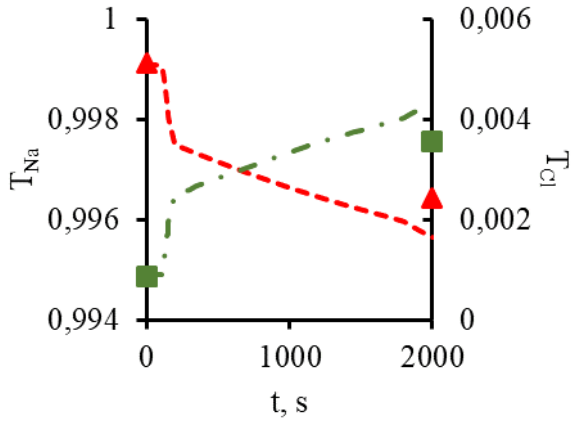

Figure 2. Time Dependence of Transport Numbers. Triangle and square dotes present transport numbers of counter-ions (Na^+) and co-ions (Cl^-), respectively, obtained by approximate analytical solution, and lines present numerical calculations (dashed red line – Na^+, dash-dotted green line – Cl^-).

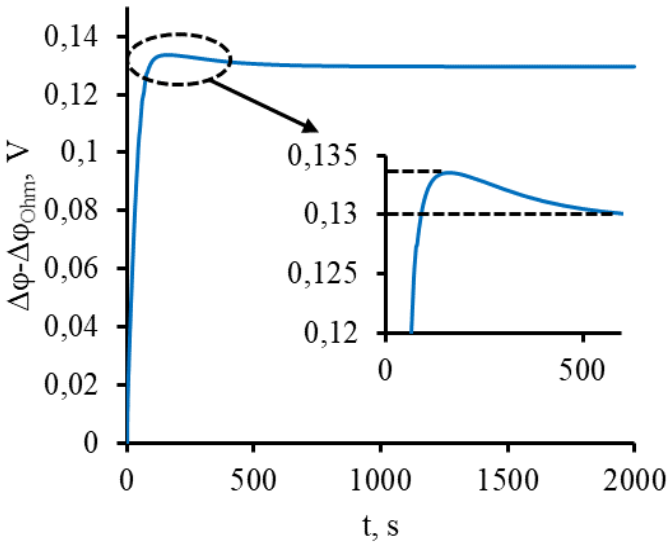

Figure 3. Chronopotentiometric Curve.

Acknowledgements

The authors are grateful to Russian Foundation of Basic Research (grant № 18-08-00397).

References

1. *Długołecki P., Anet B., Metz S. J., Nijmeijer K., Wessling M.* Transport limitations in ion exchange membranes at low salt concentrations //Journal of Membrane Science. 2010. T. 346 (1). P. 163-171.
2. *Abu-Rjal R., Chinaryan V., Bazant M. Z., Rubinstein I., Zaltzman B.* Effect of concentration polarization on permselectivity // Physical Review E. 2014. V. 89(1). P. 012302.
3. *Pis'menskaya N. D., Nikonenko V. V., Mel'nik N. A., Pourcelli G., Larchet C.* Effect of the ion-exchange-membrane/solution interfacial characteristics on the mass transfer at severe current regimes // Russ. J. Electrochem. 2012. V. 48. P. 610–628.

STUDY OF THE DECARBONIZATION PROCESS IN AN ELECTRODIALIZER WITH BIPOLAR MEMBRANES

Alexander Korzhov, Anastasia But, Viktor Zabolotskiy
Kuban State University, Krasnodar, Russia, E-mail: *nastya310392@mail.ru*

Introduction

The constant need of thermal power plants (TPPs) and boiler houses to maintain water balance is due to the presence of technological losses of water and steam, the impossibility of complete regeneration of all types of coolant, including industrial effluents, and the presence of irretrievable losses of steam and hot water. Thermal power plants (TPPs) are characterized by continuous consumption of significant amounts of high-quality water. To meet the technological requirements for the quality of water used by the TPP, a special physical and chemical treatment of natural water (softening, decarbonization of water, pH correction, desalination and deionization) is necessary. An independent task is the disposal of wastewater generated in water treatment processes [1].

The aim of the work is to study the decarbonization process of model solutions with high salinity and softened tap water of the Krasnodar water supply system.

Experiments

Studies were performed using an electrodialysis unit, a block diagram of which is shown in Figure 1.

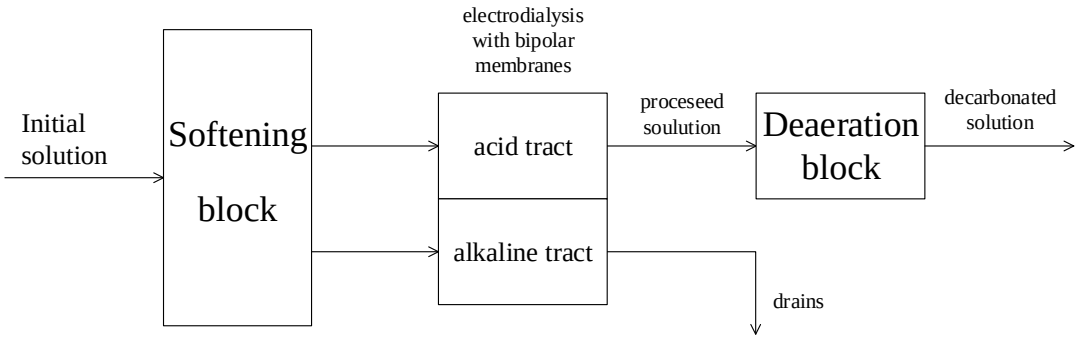

Figure 1. Schematic diagram of the installation for decarbonization of softened water.

The electrodialysis membrane package was made of 7.5 cm x 25 cm membranes, with working area of 5 cm x 20 cm = 100 cm^2, the number of elementary pair chambers is 5, the thickness of the intermembrane separator is 0.9 mm. The objects of study were an electrodialysis module with membrane pair composed of the Ralex CMH and the MB-3 membranes. This module was compared with an electrodialysis unit with the Ralex CMH and an experimental BPM membrane pair. The experimental membrane contained water-splitting catalyst.

The chemical composition and specific conductivity of the model solution and softened tap water of the Krasnodar water supply system are presented in Table 1.

Table 1: The composition of the investigated solutions

Parameter name	Softened water	Model solution
pH	8	7,9
Electrical conductivity μS/sm	704	9000
Total carbon content, mg-eq/l	5	5

Studies of the decarbonization process were carried out in a flow-through hydrodynamic mode; the flow rate of the solution was 20 L/h.

The decarbonization process was carried out in two stages. At the first stage, the acidity of the initial solutions was reduced to pH = 2.3 - 4. At the second stage, deaeration was carried out of acidified water with air purified from CO_2.

Results and Discussion

Current-voltage characteristics of the pair chamber with the investigated membrane are presented in Figure 2.

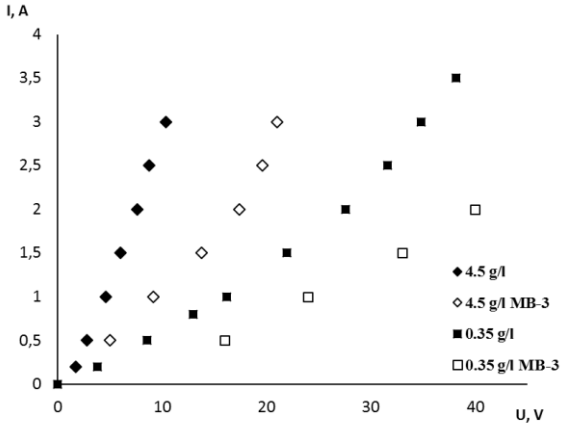

Figure 2. Current-voltage characteristics of a pair chamber, where : ♦ - model solution (salt content 4.5 g/L) with experimental bipolar membranes, ◊ - model solution (salt content 4.5 g/L) with MB-3 bipolar membranes, ■ – softened water (salt content 0.35 g/L) with experimental bipolar membranes, □ – softened water (salt content 0.35 g/L) with MB-3 bipolar membranes.

As can be seen from Figure 2, the voltage drop is lower on the pair chamber with new experimental bipolar membranes in comparison with the MB-3.

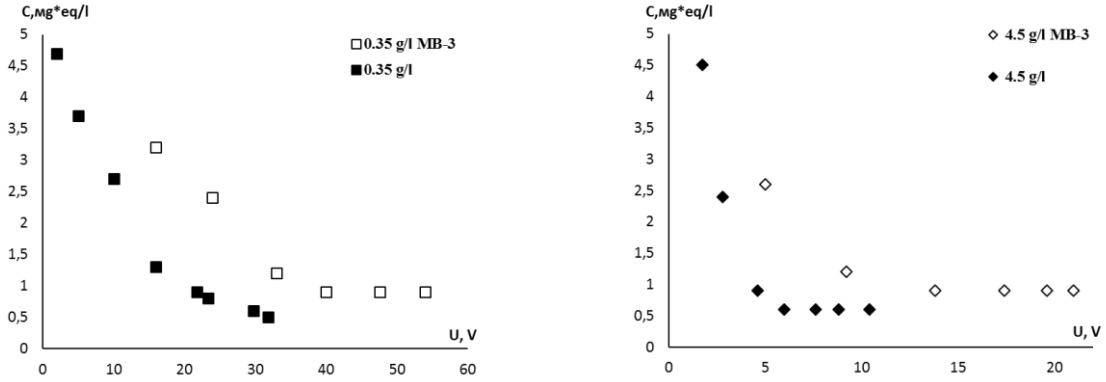

a *b*

Figure 3. The dependence of the total carbon content in the acid path from the voltage on the steam chamber after purging on softened water (a) and model solution (b).

Figure 3 shows the dependence of the total carbon content on the voltage on the electrodialysis pair chamber. Without deaeration of the solutions, the total carbon content remains almost unchanged, since the equivalent conversion of bicarbonates to carbonic acid occurs in the acid chamber. After deaeration of carbon dioxide, the content of carbonic acid is reduced to almost zero, and the content of total carbon - to 0.5-0.9 mg-eq/L.

Conclusions

As a result of the tests, it was established that in the process of electrochemical decarbonization of natural solutions of softened tap water and model solutions with high salinity, the specific energy consumption in the electrodialyzer with new experimental bipolar membranes containing the catalyst of the water-splitting reaction is lower than in the electrodialysis unit with bipolar membranes MB-3.

Acknowledgements

The present work in supported by the State Task of the Ministry of Education and Science of the Russian Federation, project № 10.3091.2017/4.6.

References

1. *Zabolotskii V.I., Utin S.V., Lebedev K.A., Vasilenko P.A., Sheldeshov N.V.//* Rus. J. of Electrochemistry. 2012. V. 48. No 7. P.767-772.

ELECTROCHEMICAL WASTEWATERS TREATMENT IN METALLURGICAL ENTERPRISES BY THE EXAMPLE ELECTRODIALYSIS OF SULPHATE-VANADIUM SOLUSION

Alexander Korzhov, Sergey Loza, Kristina Dmitrieva, Ilya Bondarenko, Victor Zabolotskiy
Kuban State University, Krasnodar, Russia, E-mail: *shtrih_ooo@mail.ru*

Introduction

Today, the problem of accumulation of technogenic toxic waste in the metallurgical industry (more than 100 m^3 of wastewater per ton of commercial product) [1] is currently the most pressing. The main goal of the national project of the Russian Federation "Ecology" 2018-2024: "Clean water - efficient handling of production and consumption wastes, including their elimination". Objectives of the project - development and effective implementation of energy-saving, environmentally friendly technologies for the purification of industrial wastewater.

In metallurgy, various methods of waste water purification are used (classical physicochemical, chemical, electrochemical, and others) [2].

Experiments

In this work, we used the electrodialysis method [3] of wastewater treatment (electrodialysis with bipolar membranes). This method is widely used in resource-saving technologies of water purification and water treatment.

As a research object, a model sulphate-vanadium solution (simulating Vanadium Production Wastewater) was used. The composition of the solution is specified in Table 1.

Table 1: Parameters of model solution

	pH	Dry residue, g/L	Content, g/l						
			V_2O_5	Mn	Si	Fe	Ca	Mg	SO_4^{2-}
Model solution	1,20	35,34	2,03	5,04	0,231	0,003	0,410	1,584	21,36

Analysis of the literature showed that the form of vanadium ions in solution varies significantly depending on the concentration and pH as shown on Figure 1.

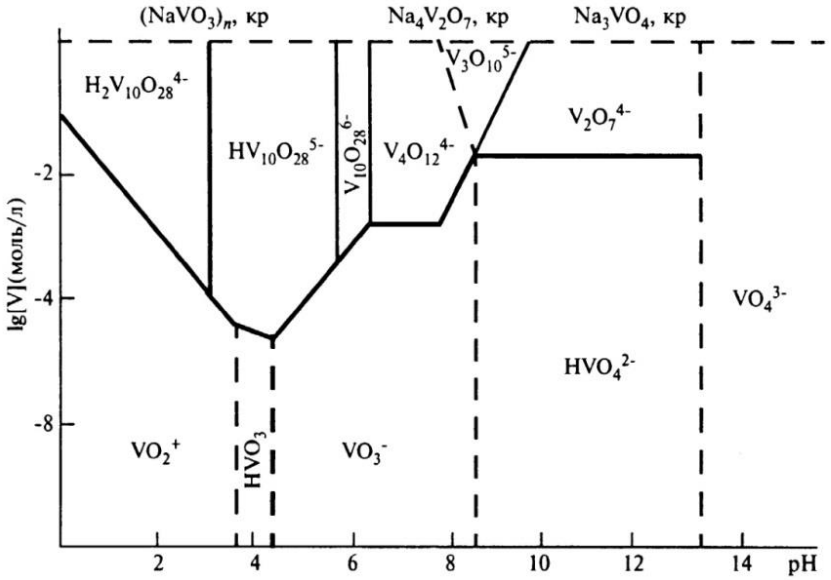

Figure 1. Various forms of vanadium-containing ions [4].

For the electrodialysis purification of the model solution, an electrodialysis cell was used, containing heterogeneous ion exchange membranes Ralex AMH / CMH (Mega a.s., Czech Republic) and experimental bipolar membranes with nanocatalyst, with a working area of membranes 5x20 cm^2.

Results and Discussion

During electrodialysis processing, it was possible to extract sulfuric acid with a concentration of 2-3% and metal ions from the initial model vanadium-containing solution. The parameters of the investigated and treated solutions are shown in Table 2.

Table 2: Parameters of solutions after electrodialysis processing

	pH	Electrical conductivity, mS/cm	Dry residue, g/l
model solution	1,20	31,0	35,34
concentrate	0,71	62,7	96,60
demineralized solution	2,25	2,30	1,30

The content of vanadium pentoxide V_2O_5 in the original and treated solutions are shown in Figure 2.

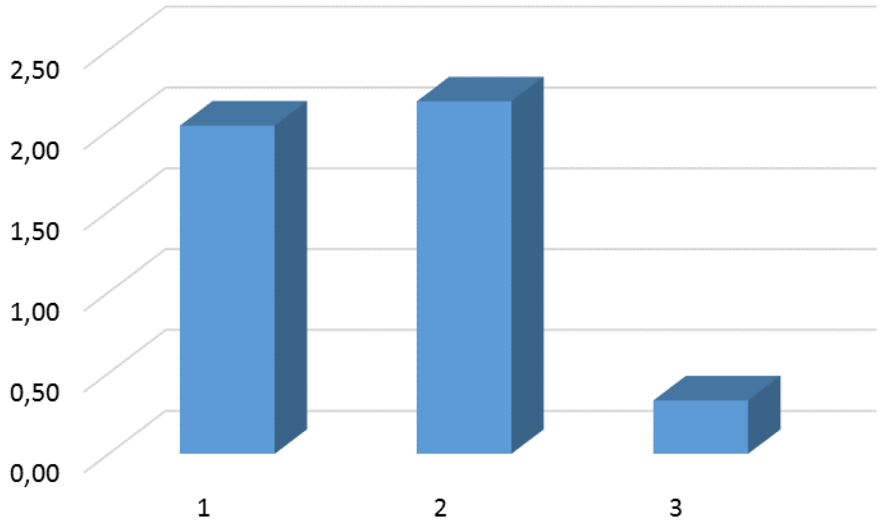

Figure 2. The content of vanadium pentoxide V_2O_5 in solutions before and after electrodialysis processing: 1 - the content of V_2O_5 in the model solution is 2.03 g/l, 2 - V_2O_5 content in the concentrat 2.18 g/l, 3 - the content of V_2O_5 in the desalting solution 0.33 g/l.

The processed solution meets the requirements for the quality of purified water for technical purposes. Further processing of the solutions is possible in order to concentrate and return the valuable components.

Conclusions

An analysis of laboratory studies shows that there is a fundamental possibility of creating a modern (non-reagent) electromembrane technology for purifying vanadium-containing sulfate effluents with a return to the production of sulfuric acid, vanadium concentrate and other metals.

Acknowledgments

The present work in supported by the State Task of the Ministry of Education and Science of the Russian Federation, project № 10.3091.2017/4.6.

References

1. *Bolshina E.P.* Ecology of metallurgical production. Novotroitsk: NF NITU "MISiS", 2012, C. 155.
2. *Sidorov. L.P.*, Industrial wastewater treatment methods. Ekaterinburg: UrFU, 2015.
3. *A. Achoh, V. Zabolotskii, S. Melnikov.* Separation and purification technology. 2019, T. 212, C. 929-940.
4. Practical manual on general and inorganic chemistry (*edited by S.F. Dunaev*). Moscow, 2003

GAS-LIQUID CONTACTORS BASED ON CELLULOSE FOR DESORPTION OF CO_2 FROM INDUSTRIAL PHYSICAL ABSORBANT

Margarita Kostyanaya, Danila Bakhtin, Viktoria Ignatenko, Stepan Bazhenov, Tatiana Anokhina

A.V. Topchiev Institute of Petrochemical Synthesis, Russian Academy of Sciences, Moscow, Russia
E-mail: *tsanokhina@ips.ac.ru*

Introduction

Recently, there have been actively developed approaches to intensify the process of releasing acid gases, first of all carbon dioxide, from gas streams (for example, flue gases, natural gas and synthesis gas) using membrane integrated systems that combine the absorption method with membrane method of separation [1, 2]. For the purification of gas mixtures at elevated pressures, the most promising is the use of "physical" absorbents because of the ease of their regeneration, since selective dissolution of acidic components proceeds without chemical reactions [3]. Such a system is a gas-liquid membrane contactor in which a selective mass transfer of components occurs between two phases separated by a membrane. The selectivity of the separation process is determined, first of all, by the difference in the solubility of gases in the absorption liquid [4].

The membrane separation method consists in the use of a gas-liquid membrane contactor in which a selective mass transfer of components occurs between two phases separated by a membrane. The prospects of using membrane contactors for gas purification processes are due to small mass-size characteristics, independent regulation of gas and liquid flows, absence of the need for vertical arrangement of the apparatus and its modularity. To separate CO_2 from the physical absorbents, the membrane used in gas-liquid contactors must have chemical stability, be impermeable to organic media, and have a high permeability for the gases emitted [5].

Therefore, cellulose can be a promising material for membranes in a gas-liquid membrane contactor. This polymer is one of the most common renewable, inexpensive and biodegradable organic materials and can be considered as an almost inexhaustible source of raw materials with increasing demand for environmentally friendly and biologically compatible products. Cellulose-based membranes are widely used for filtration processes [6 - 8], pervaporation [9], and gas separation [10]. In recent years, more and more attention has been attracted to the method of dissolving cellulose with ionic liquids (IL), considered and more environmentally friendly. To reduce the time, temperature and cost of dissolution, also co-solvents are added to the IL [7, 11] was used as co-solvent to form nanofiltration membranes from cellulose solutions in IL as a cosolvent, which made it possible to substantially reduce the viscosity of the molding mixture. Thus, the aim of this work is to produce cellulose membranes from a mixture of IL 1-ethyl-3-methylimidazolium acetate [Emim] OAc with DMSO for gas-liquid contactors.

Experiments

Commercial cellophane film with thickness of 31 μm produced according to GOST (State Standard) 7730-89 were investigatedCellulose (degree of polymerization, 600; moisture content in cellulose, no more than 8% (under equilibrium conditions); alpha-cellulose content, 92%) produced at Baikalsk Pulp and Paper Mill (Russia) was used. The [Emim]OAc IL with a density of 1.27 g/cm3 (Sigma-Aldrich) was used to dissolve cellulose. The chemical formula of this IL is shown in Fig. 2. As co-solvent was used DMSO (Sigma-Aldrich) anhydrous ≥ 99,9%. As organic liquids, tetraethylene glycol dimethyl ether (Sigma-Aldrich, 99%) simulating the industrial absorbent Genosorb (dimethyl ether of polyethylene glycols) and hexane (Chimmed, chemically pure grade) used as a model of liquid hydrocarbons. In the work the following gasses were used for membrane(s) permeability tests: Carbon Dioxide (CO_2) (99.8% purity) produced by MGPZ, Russia Methane (CH_4) (99.99% purity) produced by MGPZ, Russia.

Before dissolution, cellulose was placed in an oven at a temperature of 80°C for 16 h. The dried cellulose powder was mixed with DMSO and then with [Emim]OAc in an 1 : 1; after that, the weighing bottle was further sealed with paraffin wax. Cellulose dissolution was conducted under constant stirring at a temperature of 80°C and 100°C. Solutions with a cellulose content of 16 and

25 wt % were prepared. The solution preparation time was 24 and 72 h depending on the concentration of cellulose in the solution.

A freshly prepared solution was cooled to room temperature and then cast onto a continuous polyimide support; after that, a membrane was formed using an HLCL-1000 laminator (ChemInstruments, United States) by passing the resulting structure through the nip between the laminator rolls heated to a temperature of 80°C; the nip was calibrated to a predetermined thickness of 70 μm. Distilled water was used as the coagulation bath. The resulting composite cellulose membrane was washed in water or sustained in ethanol and hexane and then air-dried. To increase the hydrophobicity of cellulose membranes, they were treated for 30 minutes with perfluorinated acrylic copolymer Protect Guard, and then kept in air for 4 days to stabilize the properties.

Contact angle values were measured by via the conventional sessile drop technique using the LK-1 goniometer. For image capture and digital processing of the drops images, DropShape software was used providing Laplace-Young contact angle calculation. Measurement error was 2. Experiments were carried out at room temperature (23 ± 2). Membrane surface energy value was determined according to the Owens-Wendt interfacial interaction model. The relation between surface energy and equilibrium contact angle of the liquid phase placed onto solid phase is derived from the Fowkes equation. Dimethylether tetraethylene glycol was used to measure the contact angle.

The permeability of liquids through cellulose membranes were studied in dead-end cells equipped with a magnetic stirrer at a transmembrane pressure from 10 to 30atm. The entire setup was made of stainless steel; rubber rings resistant to the studied solvents were used as sealing gaskets. The active membranearea in the cells was 33.2 cm^2. Helium generated pressure in the cell.

Single gas permeation measurements were carried out at a temperature of 30.0±0.1°C and at a feed pressure of 0.2-0.8 bar using a constant volume/variable pressure experimental setup (GKSS Time-Lag Machine). Permeability coefficient P expressed in Barrer (1 Barrer = 10-10 cm^3(STP) $cm \cdot cm^{-2} \cdot s^{-1} \cdot cmHg^{-1}$) was estimated by the linear extrapolation of experimental data to zero trans-membrane pressure. Diffusion coefficient D was estimated using the time-lag method as $D=l2/6\theta$, where l is the membrane thickness, θ is the experimental time lag before the attainment of the steady state permeation regime. Solubility coefficient S was indirectly evaluated in terms of the solution-diffusion permeation model: S=P/D. Ideal selectivity of the pair of gases was calculated as the ratio of permabilities of individual gases

Results and Discussion

In the work membranes were made from cellulose solutions with different concentrations from 16 to 25 wt. % in ionic liquid [Emim] Ac with DMSO in the ratio of 1 to 1 (Fig. 1a)). After conducting experiments on filtration of dimethyl ether of tetraethylene glycol, it was found that all the membranes produced were permeable to the solvent, which indicates the formation of a porous structure in the membranes. To prevent solvent penetration through the membranes, they were treated with Protect Guard perfluorinated acrylic copolymer (Fig. 1b). Processing of cellulose membranes Protect Guard allowed to obtain membranes, barrier to dimethyl ether of tetraethylene glycol. In addition, this modification hydrophobizes the surface of cellulose membranes, due to which the value of the contact wetting angle of tetraethylene glycol dimethyl ether increases almost 3 times (Fig. 2).

A study of the gas permeability of the membranes for individual gases (CH_4 and CO_2) showed that 16% of the cellulose membrane has a minimum permeability, which after being deposited in water, its permeability coefficient for both gases is 3 orders of magnitude higher than for cellophane. The permeability coefficients for CH_4 are equal to 0.6 Barrer, for CO_2 - 1.1 Barrer.

A membrane with the same cellulose content, but sustained successively in ethanol and hexane after precipitation, has a much higher gas permeability than the membrane is soaked in water. CH_4 permeability coefficients equal to 14.5 Barrere, for CO_2 - 8.2 Barrere Since the membranes for gas-liquid contactors must be highly permeable to gases, the second approach to the post-treatment of the membranes was used for further work, namely, sequential incubation in ethanol and hexane and drying.

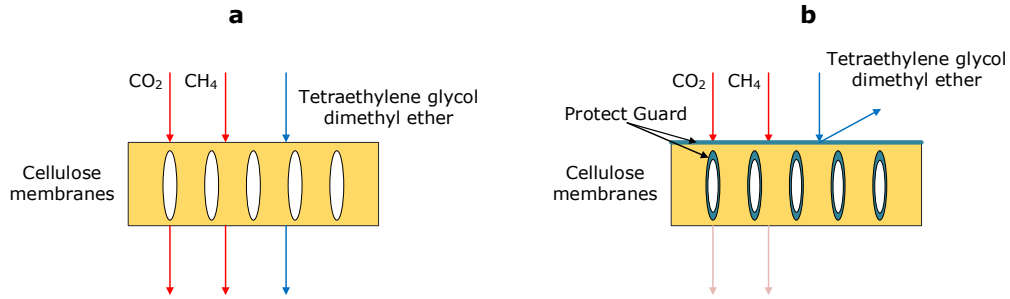

Figure 1. The effect of cellulose membrane treatment with perfluorinated acrylic copolymer Protect Guard on the permeability of the studied solvents and their gas transport characteristics: a) the original cellulose membrane; b) cellulose membrane treated with Protect Guard.

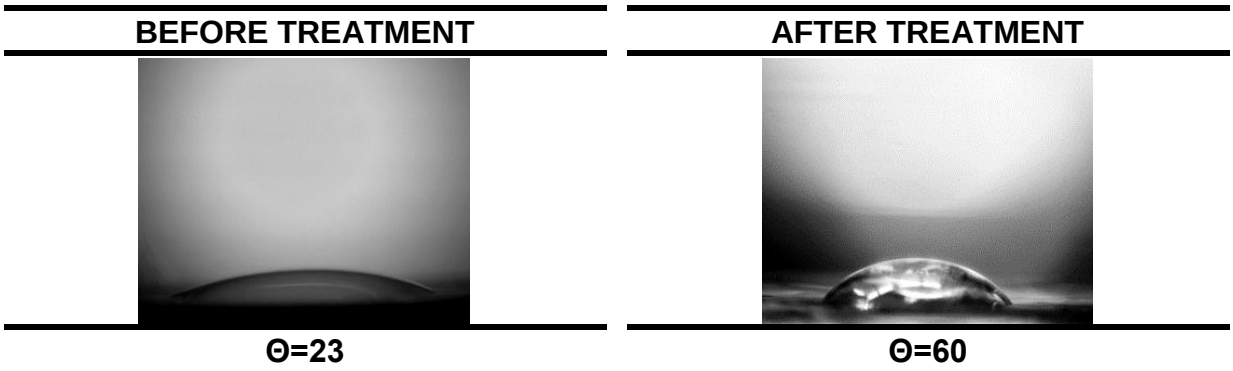

Figure 2. Images of tetraethylene glycol dimethyl ether droplets on the surface of cellophane before and after Protect Guard treatment.

The increase in cellulose concentration in the molding solution led to a decrease in gas permeability. The permeability coefficient for a membrane made from 25 wt. The% cellulose solution in the mixture of IL with DMSO and aged in ethanol and hexane on CH4 is equal to 0.7 Barrer, on CO2 - 2.4 Barrer. In addition, it was shown that the treatment of Protect Guard cellulosic membranes leads to a narrowing of the pores, as evidenced by a decrease in the values of permeability coefficients for individual gases by 2 or more times.

The reported study was funded by RFBR according to the research project № 18-38-00702 mol_a.

References

1. *Klaassen R, Feron P H M, Jansen A* E 2005 Chem. Eng. Res. Des 83 234.
2. *Bazhenov S, Bakhtin D, Volkov A* 2018 J. Membr. Sci. Res. doi: 10.22079/jmsr.2018.82177.1179
3. *Kohl A L, Nielsen R B*, Gas 1997 Gulf Professional Publishing 1395.
4. *Volkov A V, Tsarkov S E, Goetheer E L V, Volkov V V* 2015 Petr. Chem. 55(9) 716.
5. *Volkov A, Yushkin A, Grekhov A, Shutova A, Bazhenov S, Tsarkov S, Khotimsky V, Vlugt T J H, Volkov V* 2013 J. Membr. Sci. 440 98.
6. *Li H J, Cao T M, Qin J J, Jie X M, Wang T H, Liu J H, Yuan Q*, 2006 J. Membr. Sci. 279 328.
7. *Anokhina T S, Pleshivtseva T S, Ignatenko V Ya, Antonov S V, Volkov A V*, 2017 Petr. Chem. 57(6) 477.
8. *Anokhina T S, Yushkin A A, Volkov V V, Antonov S V , Volkov A V* 2015 Physics Procedia 72 171.
9. *Mao Z, Cao Y, Jie X, Kang G, Zhou M, Yuan Q*, 2010 Sep. Purif. Technol. 72 28.
10. *Wu J, Yuan Q*, 2002 J. Membr. Sci. 204 185.
11. *Sukma F M, Çulfaz-Emecen P Z* 2018 J. Membr. Sci. 545 329.

THE ROLE OF SOLVENT DURING ADSORPTION OF α - TOCOPHEROL ON CLINOPTILOLITE

Diana Kotova, Svetlana Vasil'eva, Tatiana Krysanova, Anna Sokruykina
Voronezh State University, Voronezh, Russia, E-mail: *takrys@yandex.ru*

Introduction

Clinoptilolite is one of the most interesting representatives of frame aluminosilicates, which have the potential to develop carriers of biologically active substances (BAS) and targeted delivery systems on their basis [1,2]. During modification extends the scope of its application for selective absorption of BAS the controlled change of structural and physico-chemical properties of clinoptilolite [3-5]. When an adsorption from solutions on the surface of the adsorbent should take into account solvation effects, as the physico-chemical properties of the solute, its reactivity determine solvation processes [6-8]. The mechanism of adsorption fixation of BAS on the surface is influenced by both the properties of the solvent and the hydrophilic-hydrophobic balance of the adsorbent and adsorbate. The paper presents the results of a study of the equilibrium adsorption of fat-soluble vitamin α-tocopherol from solutions of ethyl alcohol, hexane and ethyl acetate on acid-activated clinoptilolite.

Experiments

Vitamin E (α-tocopherol) manufactured by Sigma (Germany) was used in the study. The sorbent selected frame aluminosilicate clinoptilolite (field polar Ural Ugra) is recommended as enterosorbent "Klimont". Earlier it was found that vitamin E is not adsorbed on native clinoptilolite, adsorption of α-tocopherol was investigated on activated 4,0 M hydrochloric acid [5].

Sorption of α-tocopherol was carried out from solutions of ethyl alcohol, hexane and ethyl acetate. For practical convenience, the maximum value of the polarity criterion for water is taken as 100, the minimum value of the criterion for the Dean is zero. For ethanol, the pH value is 43.97, for ethyl acetate-21.84 and for hexane – 0.85 [9].

The polarity of the solvents varies in a number of ethanol > ethyl acetate > hexane. The sorption equilibrium in the system "modified clinoptilolite (fraction 0.02-0.06 mm)-α-tocopherol solution" was studied at a temperature of 295±2 K under static conditions by the method of variable concentrations. The interval used concentrations of α-tocopherol made up $1.40 \cdot 10^{-2}$ – 46.0 mmol/dm^3.

Results and Discussion

Adsorption isotherms of α-tocopherol on acid-activated clinoptilolite from solvents with different polarity (ethanol, ethyl acetate, hexane) are shown in (Fig.1).

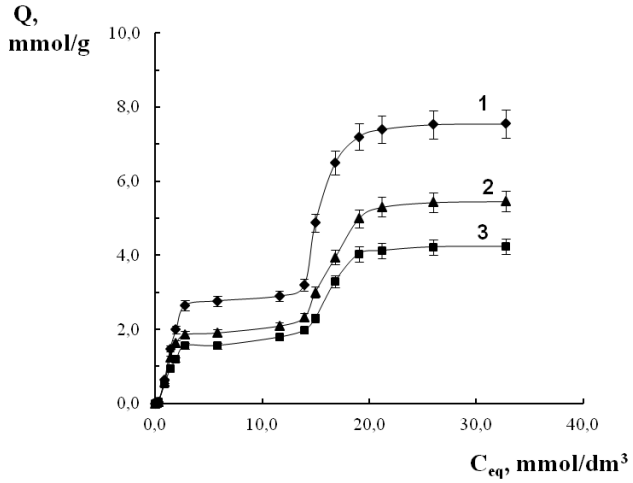

Figure 1. Adsorption Isotherms of α-tocopherol on acid-activated clinoptilolite from solution: 1- ethanol, 2- ethyl acetate, 3- hexane.

Isotherms of α-tocopherol on acid-activated aluminosilicate from different solvents have the same form and according to Giles's classification correspond to S-form. In accordance with the nomenclature of IUPAC they should be attributed to the IV type. The linear dependence of the adsorption parameter and the formation of a plateau in the region of low concentrations of the solution suggest a monolayer fixation of α - tocopherol on the active centers of the sorbent. For a quantitative description of adsorption in this area isotherm was used the equation of Langmuir. Equilibrium characteristics of α - tocopherol monolayer fixation on adsorption centers calculated using Langmuir theory are given in the table.

Table 1: Parameters of α-tocopherol sorption on acid-activated clinoptilolite from various solvents

Solvent	Q_{mono}, mmol/g, (g/g)	K_L, dm^3/mol	Q_{max}, mmol/g, (g/g)	$-\Delta G^0$, kJ/mol	R^2
Hexane	1.95 (0.84)	110	4.76 (2.05)	11.6	0.99
Ethyl acetate	2.30 (0.99)	200	5.92 (2.55)	13.1	0.97
Ethanol	3.32 (1.43)	830	7.55 (3.25)	16.5	0.98

It should be taken into account that the α-tocopherol molecule is characterized by a double reactivity due to the presence in its structure of the phenol group and oxygen of the chrome ring, which provides hydrophilic properties, and hydrophobic isoprenoid radical. The participation of an isolated Si-OH-group of acid - activated clinoptilolite in the formation of hydrogen bonds with phenolic hydroxyl and oxygen in the chromane ring is indicated by a decrease in the intensity of the maximum at 3754 cm^{-1}, for α-tocopherol there is a shift in the oscillation frequency of C-O-C bonds in the aromatic ring in the low-frequency region of the spectrum (1220 → 1120 cm^{-1}), an expansion of the maximum absorption at 3445 cm^{-1}, and a decrease in the absorption band at 3620 cm^{-1}, which correspond to the phenolic groups of vitamins. Fixing of a monomolecular α-tocopherol leads to the formation of additional sorption is energetically non-equivalent centers. Increasing the adsorption parameter with increasing concentration of α-tocopherol solution due to the formation of associates as a result of interaction between isoprenoid radicals of adsorbate molecules, which is confirmed in the IR spectra. With an increase in the content of α-tocopherol in the sorbent matrix, there is a shift in the frequency of valence vibrations of the bonds of C - H groups of the α - tocopherol molecule to the low-frequency region of the spectrum (2970 →2930 cm^{-1}, 2920→2860 cm^{-1}). Phenolic OH-groups of vitamin, carrying out antioxidant function, remain free and are reflected in the spectrum in the form of absorption band at 3620 cm^{-1}.

The change in the polarity of the solvent is manifested in the equilibrium adsorption characteristics (table). The value of vitamin adsorption on acid-activated clinoptilolite increases with increasing solvent polarity. When sorption of α-tocopherol on acid-activated clinoptilolite from ethanol solution, the maximum sorption parameter is 1.3 times higher than its value when sorption from ethyl acetate and 1.6 times from hexane. Molecules of ethyl acetate and hexane, being present in a significant excess and being guided in the solvate shell of vitamin, have a shielding effect in relation to the silanol groups of acid-activated clinoptilolite. For α–tocopherol solutions in ethyl acetate and hexane, solvophobic interactions are more pronounced. When α-tocopherol is adsorbed, the change in ΔG^0 increases with the polarity of the solvent. The results indicate a more favorable process of adsorption of α-tocopherol on acid-activated clinoptilolite from ethanol solution, which is important, since water and ethyl alcohol are recommended as a solvent for medical and food applications.

Conclusion

It was found that the adsorption of alpha-tocopherol on acid-activated clinoptilolite from dilute solutions with maximum probability is described by the Langmuir equation. Multi-molecular nature of the adsorption fixation of the vitamin determines the formation of its associates. An increase in the selectivity of acid-activated clinoptilolite to alpha-tocopherol was found to increase in a number of ethanol > ethyl acetate > hexane.

References

1. *Farıas T.* Preparation of natural zeolitic supports for potential biomedical applications // Materials Chemistry and Physics. 2009. V.118. P. 322–328.
2. *Petushrov A., Ndiege N., Salet A.K., Larsen S.C.* Toxicity of silica nanomaterials: zeolites, mesoporous silica and amorphous silica nanoparticles // Advances in Molecular Toxicology. 2010. V.4. P. 223–262.
3. *Farias T., Charles de Menorval L., Zajac J., Rivera A.* Adsolubilization of drugs onto natural clinoptilolite modified by adsorption of cationic surfactants // Colloids and Surfaces B: Bionterfaces. 2010. V. 76. P. 421–426.
4. *Rivera A., Farıas T.* Clinoptilolite – surfactant composites as drug support: A new potential application / // Microporous and Mesoporous Materials. 2005. V. 80. P. 337–346.
5. *Kotova D. L., Vasil'eva S. Yu., Krysanova T. A. [et al]*. Izmeneniye teksturnykh i fiziko-khimicheskikh kharakteristik nanoporistogo klinoptilolita pri kislotnoy modifikatsii / // Russian nanotechnologys. 2014. V. 9, № 9-10. P. 474-479.
6. *Pogorelyy V.K., Kozakova O.A., Barvinchenko V.N. [et al.]* Adsorption of cinnamic and caffeic acid on the increase of highly dispersed silica from different plants // Colloid journal. 2007. V. 69, № 2. P. 226-234.
7. *Chuev G.N., Bazilevsky M.V.* Molecular models of solvation in polar liquids // Chemistry success. 2003. V. 72, № 9. P. 827-847.
8. *Cramer Ch.J., Truhlar D.G.* Implicit solvation models: equilibria, structure, spectra, and dynamics // Chem. Rev. 1999. V. 99, №8. P.2161-2200.
9. *Rudakov O. B., Vostrov I. A., Fedorov S. V. [et al.]* Sputnik khromatografista. Metody zhidkostnoy khromatografii. Voronezh: "Vodoley", 2004. 528 p.

PROBLEMS OF SUSTAINABLE CALCULATION OF THEORETICAL CURRENT-VOLTAGE CHARACTERISTICS, CHRONOPOTENTIOGRAMS AND CHRONOGALVANOGRAMS FOR A MEMBRANE CHANNEL WITH FORCED CONVECTION, REACTIONS OF WATER DISSOCIATION/RECOMBINATION AND ELECTROCONVECTION

Anna Kovalenko, Makhamet Urtenov
Kuban State University, 149 Stavropolskaya Street, 350040, Krasnodar, Russia
E-mail: *savanna-05@mail.ru*

Introduction

Until now, the only way to study the current-voltage characteristics (CVC) was the analysis of experimental data, which shows the complex, unsteady and unstable behavior of the CVC [1-3]. For the theoretical study of such behavior of CVC, special mathematical methods and models are required. However, until now, there were no theoretical models that would allow adequately interpreting this data and understanding the processes behind the laws of change of CVC. For numerical calculation of CVC, it is necessary to have a mathematical model described by the field of study (solution), equations and boundary conditions, the algorithm for calculating CVC, as well as a formula for calculating the current density. In addition, for comparison with the experimental CVC it is important to consider the balance of currents in an electrical circuit using the charge conservation law of Gauss, which requires that in the unconfined system, the total flow of charges in the system was equal to the sum of the charges output from the system. Below, we consider the problem of the theoretical calculation of CVC for the desalting channel (DC) of electrodialysis apparatus (EA). Exactly the same arises in theoretical calculations of chronopotentiograms and chronogalvanograms [4-5].

Problem definition

Because the length of DC significantly exceeds the width, then this channel can be considered as infinitely long one, limited by an anion exchange membrane (AEM) on the left and cation exchange membrane (CEM) on the right. However, in numerical calculations, it is necessary to limit the length of DC, which depends on the capabilities of the computer system. In this regard, there are problems of accounting and balance of currents flowing in the electrical circuit, including DC [6]. These problems are not typical for real processes in industrial devices and experimental facilities, but are introduced, associated with mathematical modeling and, first of all, limited capabilities of numerical methods and modern computer systems. Below these problems are solved by modifying the mathematical models in such a way that the Gauss conservation laws are satisfied [7].

Results and Discussion

To calculate the CVC for a DC, there is a need to make an electrical circuit, namely, to determine where the measured current density, voltage drop, parallel or series connected circuit elements, etc. The electrical circuit depends on the model of DC, which is studied. In this regard, various models are considered.

1. **Short channel model.** A characteristic feature of this model is to set a uniform distribution of the ion concentration at the input and the ion flow at the output, etc. This model is designed to study the transients, both at the beginning of the channel and at the initial time.
2. **Long channel model.** This model is designed to study the process of transfer of salt ions away from the beginning of the channel, when there are no longer transients along the length of the channel, or the channel is so long that the influence of transients arising at its beginning can be neglected. However, this model allows us to study transients over time.

Suppose that the OY axis passes through AEM, and the axis perpendicular to it OX, is directed toward KEM. Let the channel width be H and the length L. The current density at any point of the channel at some point in time denote $\vec{I}(t, x, y)$.

In such a model, a region of transients is formed near the entrance. In this region, the current density is a solenoid field ($div\vec{I} = 0$), if only the process is stationary or holds true the condition of electroneutrality (in pre-limit modes). If the current density is not a solenoid field, i.e. $div\vec{I} \neq 0$, the transfer process in the transition region is characterized by unsteadiness and the formation of new carriers (i.e., the appearance of sources) of electric current [3, 8].

The main interest is the current transferred through ion-exchange membranes, which leads to desalination of the solution in the DC. The values of these currents can be calculated by the formulas:

$$i_1 = \int_0^L I_x(t,0,y)dy\,, \quad i_2 = \int_0^L I_x(t,H,y)dy$$

At the entrance to the DC currents of different nature can occur, associated with both the design and operation of the EA, so the formulation of the problem of mathematical modeling. The input current will be denoted i_{vh}. In some cases, the input current may not be available (see below).

Since the flow channel is considered, a leakage current may occur, i.e. the current flowing from the DC. The leakage current is primarily due to the convective flow of the solution. For a short channel, the leakage current can be significant. We will denote the leakage current through i_{ut}.

The currents at the inlet i_{vh} to the channel and outlet i_{ut} (leakage currents) can be calculated and estimated using formulas giving these currents by definition:

$$i_{vh} = \int_0^H I_y(t,x,0)dx\,, \qquad i_{ut} = \int_0^H I_y(t,x,L)dx$$

It is shown that the input current in absolute value is much larger than the leakage currents. The input current is due to the constant concentration at the input and serves as a source of new current carriers at the input to the DC, i.e., actually on an input there is a constant current source. For long DC it can be assumed that the output concentration of the solution is many times less than the input. Consequently, the leakage current is many times less than the current passed through the electromembrane systems (ES) $i_1 \gg i_{ut}$, $i_2 \gg i_{ut}$. Hence, the leakage current for long DC can be neglected, but then $i_1 \approx i_2$. In this case, it is convenient to consider the average current as the current in the circuit $i_{av} = \dfrac{(i_1 + i_2)}{2}$

As shown the numerical experiments of the above formulas do not allow the stable calculation of CVC. This is due to the fact that these formulas use the values of the ordinates of the current density at the boundary, which in turn depend on the derived concentrations and the potential jump over the variable x at the boundary, while the integrals are taken over the variable y.

Small errors in the calculation of these derivatives lead to large errors in the calculation. For long channels and solenoid current density we have derived the formula:

$$i_{av} = \frac{(i_1 + i_2)}{2} = \frac{1}{H}\int_0^H\int_0^L I_x(t,s,y)dyds\,,$$

allows to calculate the average current steadily with respect to rounding errors. In general, the formula looks like:

$$i_{av} = \frac{1}{HL}\int_0^H\int_0^L I_x(t,s,y)dyds - \frac{1}{2HL}\int_0^H\int_0^L (H-2x)div\vec{I}dxdy$$

Conclusion

In contrast to the original integrals in the double integral, errors in the calculation of the derivative of the variable x are compensated by the integration of the same variable, which allows you to accurately and adequately calculate the CVC.

The reported study was funded by RFBR according to the research project: 19-08-00252 a «Theoretical and experimental study of current-voltage characteristics of electromembrane systems».

References

1. *Nikonenko V.V., Mareev S.A., Pis'menskaya N.D., Kovalenko A.V., Urtenov M.K., Uzdenova A.M., Pourcelly G.* Effect of electroconvection and its use in intensifying the mass transfer in electrodialysis (review) // Russian Journal of Electrochemistry. 2017. V. 53. № 10. P. 1122-1144.
2. *Urtenov M.K., Nikonenko V.V.* Analysis of the boundary-value problem solution of the Nernst-Planck-Poisson equations, 1:1 electrolytes // Russian Electrochemistry. 1993. V. 29. P. 314.
3. *Urtenov M.Kh., Pismensky A.V., Nikonenko V.V., Kovalenko A.V.* Mathematical modeling of ion transport and water dissociation at the ion-exchange membrane/solution interface in intense current regimes // Petroleum Chemistry. 2018. V. 58. № 2. P. 121-129.
4. *Uzdenova A.M., Kovalenko A.V., Urtenov M.K., Nikonenko V.V.* Effect of electroconvection during pulsed electric field electrodialysis. Numerical experiments // Electrochemistry Communications. 2015. V. 51. P. 1-5.
5. *Mareev S.A., Nichka V.S., Butylskii D.Y., Pismenskaya N.D., Nikonenko V.V., Urtenov M.K., Apel P.Y.* Chronopotentiometric response of an electrically heterogeneous permselective surface: 3d modeling of transition time and experiment // Journal of Physical Chemistry C. 2016. V. 120. № 24. P. 13113-13119.
6. *Pismensky A.V., Urtenov M.K., Nikonenko V.V., Pismenskaya N.D., Kovalenko A.V., Sistat Ph.* Model and experimental studies of gravitational convection in an electromembrane cell // Russian Journal of Electrochemistry. 2012. V. 48. № 7. P. 756-766.
7. *Kovalenko A.V., Khromykh A.A., Urtenov M.K.* Decomposition of the two-dimensional Nernst-Planck-Poisson equations for a ternary electrolyte // Doklady Mathematics. 2014. V. 90. № 2. P. 635-636.
8. *Zabolotskii V.I., Nikonenko V.V., Korzhenko N.M., Seidov R.R., Urtenov M.Kh.* Mass transfer of salt ions in an electromembrane system with violated electroneutrality in the diffusion layer: the effect of a heterolytic dissociation of water // Russian Journal of Electrochemistry. 2002. V. 38. № 8. P. 810-818.

SOFTWARE PACKAGE FOR THE ANALYSIS OF TIME SERIES IN ELECTRO-MEMBRANE SYSTEMS

[1]Anna Kovalenko, [1] Makhamet Urtenov, [1] Alexander Pismenskiy, [1] Natalia Seidova, [1]Konstantin Sobchenko, [2] Natalja Chubyr

[1] Kuban State University, Krasnodar, Russia, E-mail: *Savanna-05@mail.ru*

[2] Kuban State Technology University, 2 Moskovskaya Street, 350042, Krasnodar, Russia

E-mail*: chubyr-natalja@mail.ru*

Introduction

Current-voltage characteristic (CVC) is the most important and common characteristic of transport in electro-membrane systems. CVC is widely used in theoretical, experimental research, and practice. However, until now, the only way to study CVC is to analyze experimental data. The study of experimental CVC using Fourier analysis, wavelet analysis and dynamic chaos shows complex, non-stationary and unstable behavior [1-5]. Special mathematical methods and models should be used for theoretical study of such behavior CVC [1]. The absence of such models does not allow to identify the relationship of the behavior of CVC with the properties of the process of transport of salt ions in the desalination channel of the electrodialyzer. For example, to interpret adequately the fluctuations and instability of the CVC, to determine the patterns of transport of salt ions in the desalination channel of the electrodialyzer, for example, the size and velocity of vortex structures, their interaction and bifurcation, etc. A similar situation develops also such important temporal characteristics of membrane systems as chronopotentiograms and chronogalvanograms. Note that from a mathematical point of view, CVC can be interpreted as a time series, where, for example, a potential jump appears as time.

Until now, theoretical models and software packages that would allow to adequately interpret and understand the processes affecting changes in the current-voltage characteristics, potentiograms, galvanograms are missing. Therefore, it is impossible to carry out engineering calculations to optimize the designs of electrodialyzers, including the optimization of their geometric and technological characteristics in order to intensify the transfer processes in electro-membrane systems.

Research results

We created a software package "Time Series Analysis" [6-7], which implements the main modern methods of calculation and analysis, based on mathematical models of time series: calculating the Hurst numbers and Lyapunov index, Fourier analysis and wavelet analysis. For the first time, the relationship between the main frequencies oscillations of the CVC, potentiograms, galvanograms, and properties of the transport of salt ions in the desalination channel was determined. The software package has an intuitive and simple interface and is designed for students, graduate students and scientists in the field of electrochemistry and does not imply knowledge of programming. The software package "Time Series Analysis" [6-7] automates the process of calculating the Fourier transform, the Daubechies wavelet transform, the Hurst indicators and Lyapunov indexes for time series and signals presented in digital form.

The software "Time Series Analysis" can be used to analyze current-voltage curves, chronopotentiograms, etc. Using it, the user can perform, for example, analysis of the frequency characteristics of the signal, perform signal cleaning from noise, compress the signal, predict time series, calculate at which a jump in potential occurs electroconvection, predict future values, etc. The user-friendly interface of the software package "Time Series Analysis" (Figure 1) allows you to display data in the form of scalable graphs, allowing you to view the smallest details of the calculation results.

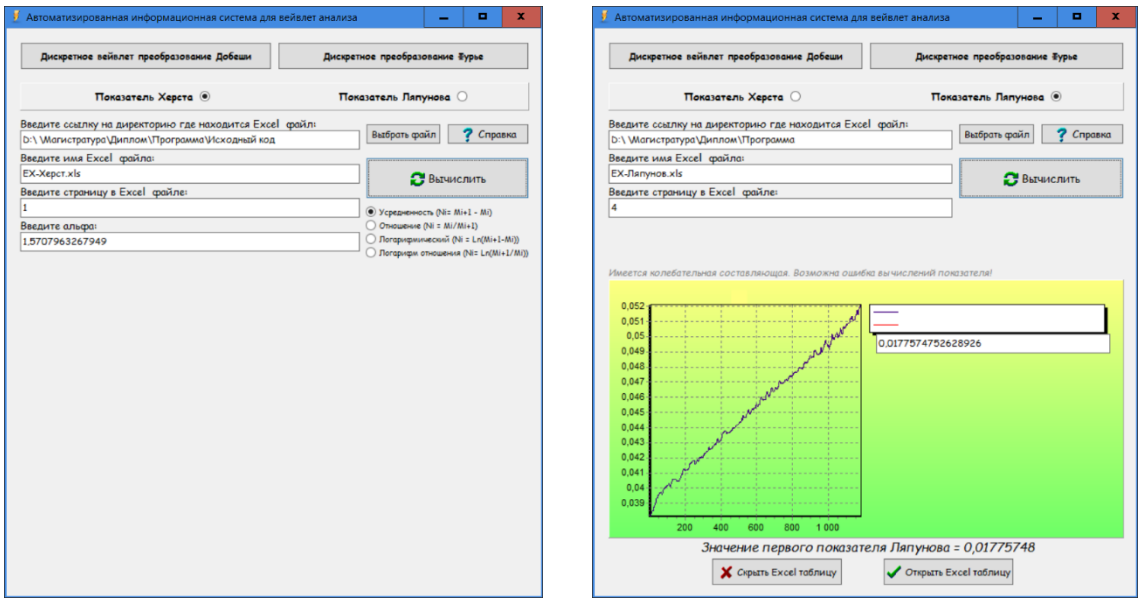

a *b*

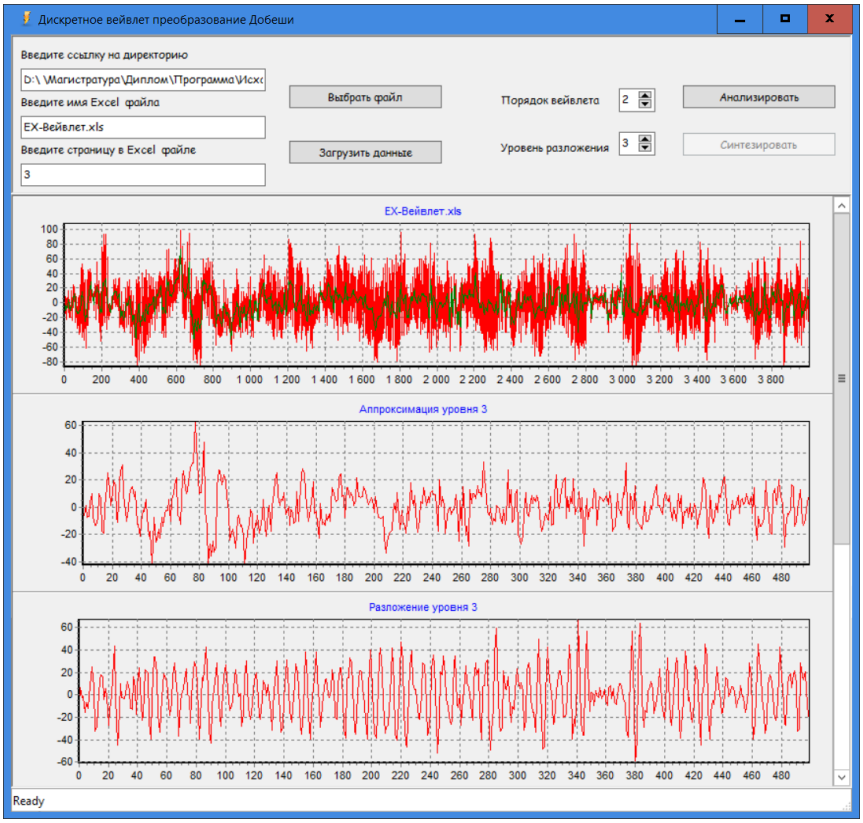

c)

Figure 1. a) interface of the software package "Time Series Analysis"; b) the calculation of the Lyapunov index; c) the results of the calculation of the Daubechies wavelet transform.

Results and Discussion

The paper describes the software package "Time Series Analysis" created by the authors [6-7], which implements the basic methods of modern time series analysis: calculating the Hurst numbers and Lyapunov index, Fourier and wavelet analysis. The software package "Time Series Analysis" can be used to analyze the current-voltage characteristics, potentiograms, galvanograms, and any other series used in membrane systems. A simple and intuitive interface, the availability of hints and assistance makes it accessible to students, graduate students and researchers in the field of electro-membrane technologies.

The reported study was funded by RFBR according to the research project № 19-08-00252 "Theoretical and experimental research of current-voltage characteristics of electromembrane systems".

References

1. *Kovalenko A.M., Evdochenko E.N., Urtenov M.Kh.* Calculation and analysis of time behavior of electroconvection in membrane systems // Scientific Journal of KubSAU, 2015. V. 05(109). http://ej.kubagro.ru/2015/05/pdf/66.pdf
2. *Rubinstein I.* Electroconvection at an Electrically Inhomogeneous Permselective Interface// Physics of Fluids A Fluid Dynamics. 1991. V. 3(10). P. 2301-2309
3. *Rubinstein I., Zaltzman B.* Equilibrium electro-osmotic instability in concentration polarization at a perfectly charge-selective interface // Physical Review Fluids V. 2(9). 2017. P. 093702
4. *Demekhin E.A., Ganchenko G., Kalaydin E. N.* Transition to electrokinetic instability near imperfect charge-selective membranes // Physics of Fluids. 2018. V. 30(8) P. 082006.
5. *Abu-Rjal R., Prigozhin L., Rubinstein I., Zaltzman B.* Equilibrium electro-convective instability in concentration polarization: The effect of non-equal ionic diffusivities and longitudinal flow // Russian Journal of Electrochemistry. 2017. V. 53(9) P. 903-918
6. *Kovalenko A.V., Urtenov M.Kh., Sobchenko K.V.* Certificate of state registration of computer programs "Calculation of Hurst indicators for current-voltage curves". №2014619390 from September 16, 2014
7. *Kovalenko A.V., Urtenov M.Kh., Sobchenko K.V.* Certificate of state registration of computer programs "Software package for Fourier and wavelet analysis" № 2017619076 of August 15, 2017

DIRECT AC/DC HEATING OF HOLLOW FIBER MEMBRANES

[1,2]Ivan Kovalev, [1]Mikhail Popov, [1]Marat Sharafutdinov, [1]Alexander Titkov, [1]Sergey Bychkov, [1]Alexander Nemudry

[1]Institute of Solid State Chemistry and Mechanochemistry SB RAS, Novosibirsk, Russia
E-mail: *popov@solid.nsc.ru*
[2]Novosibirsk State Technical University, Novosibirsk, Russia

Introduction

Oxygen-transport membranes (OTM) from oxides with mixed ionic-electronic conductivity (MIEC) are widely used in various innovative technologies. They have 100% oxygen selectivity can be easily incorporated into high-temperature processes, for example, partial oxidation of hydrocarbons (methane conversion to syngas, etc.).

In order to achieve oxygen flow rates acceptable for practical use, the OTMs must be heated to temperatures above 600°C. Since, at T>600°C, membrane materials besides ionic conductivity also have high electronic conductivity, it is possible to direct heating of OTMs by passing an electric current through it (Fig. 1). In our previous works [1,2], we show the opportunities given by the heating of OTMs by passing AC through the membranes. This way not only allows us to enhance the energy efficiency, productivity of the membranes, and gives fast-response control of the reactor temperature but also opens the access to the surface of the operating membrane and therefore makes it possible to study the mechanism of oxygen permeability *in situ* with the help of physicochemical techniques.

Experiments

It is assumed that AC is preferable instead of DC because it prevents electrode polarization due to ion migration and electrochemical decomposition of MIEC oxides with subsequent decomposition of the OTM. Nevertheless, theoretical estimates predict the negligible effect of DC used on cation migration, but the possible beneficial effects on oxygen transport.

Figure 1. Direct AC/DC heating of hollow fiber membranes.

Results and Discussion

The purpose of this study is to compare the effects of AC and DC on oxygen fluxes of promising composition $Ba_{0.5}Sr_{0.5}Co_{0.7}Fe_{0.2}Mo_{0.1}O_{3-\delta}$ (BSCFM10).

Acknowledgements

The reported research was funded by Russian Foundation for Basic Research and the government of the region of the Russian Federation, grant № 18-43-543006.

References

1. *M.P. Popov, S.F. Bychkov, A.P. Nemudry* // Solid State Ionics 312 (2017) 73–79.
2. *M.P. Popov, S.F. Bychkov, N.V. Bulina, A.P. Nemudry* // J Eur Ceram Soc, https://doi.org/10.1016/j.jeurceramsoc.2018.12.008

INFLUENCE OF TYPE OF BIPOLAR CATION-EXCHANGE AND ANION-EXCHANGE MEMBRANES ON THE CHARACTERISTICS OF THE PROCESS OF PRODUCING SULFURATE ACID AND SODIUM HYDROXIDE FROM SODIUM SULFATE

Nikita Kovalev, Tatyana Karpenko, Nikolay Sheldeshov, Victor Zabolotskiy
Kuban State University, Krasnodar, Russia

Introduction

In many chemical and biochemical technologies, acids and alkalis are used to neutralize solutions. Moreover, after neutralizing and isolating the target products, a large amount of by-products, saline solutions, is formed, which makes the technology environmentally dirty. The decision to this problem is the recovery of salt solutions into the corresponding acids and alkalis using electrodialysis with bipolar membranes and their repeated use [1-4]. This ensures recycling of acids and alkalis, the need for source acids and alkalis disappears or is significantly reduced, and highly mineralized effluents are eliminated. However, with an increase in the concentration of the resulting acids and alkalis, the non-selective transfer of salt cations to acid and salt anions into alkali through the bipolar membrane increases. The fluxes of alkali cations and acid anions and, accordingly, the transport number of these ions through the bipolar membranes strongly depend on the type of ionogenic groups contained in the cation-exchange and anion-exchange layer [5]. The largest non-selective transfer of acid anions and alkali cations is observed in the case of an industrial MB-3 bipolar membrane containing weakly acidic phosphoric acid ionic groups in the cation-exchange layer, which has the lowest voltage among industrial bipolar membranes produced in Russia. Lower transfer numbers of acid anions are observed in the case of the industrial bipolar membrane MB-1, which contains sulfonic ionic groups in the cation-exchange layer instead of the phosphoric acid groups, but the voltage on this membrane is much higher than on the membrane MB-3. The MB-2m membrane developed in recent years has the best characteristics [5], which contains sulfonic acid ionogenic groups in the cation-exchange layer, quaternary ammonium groups in the anion-exchange layer, and catalytic additive with phosphoric-acid groups in the bipolar layer. The objective of this work is to compare the characteristics of the processes of producing acid and alkali from salt using the best industrial membrane MB-3 and the developed bipolar membrane MB-2m.

Experiments

Sulfuric acid and sodium hydroxide were produced from sodium sulfate using a laboratory bipolar electrodialysis apparatus (EDA) with three-compartment elementary cells differing in the type of bipolar membrane (modified MB-2m with catalytic additive, MB-3), cation-exchange (Ralex CMX, MC-40) and anion-exchange membranes (Ralex AMH, MA-40, MA-41).

The processes were carried out in the circulation mode. Before the start of each experiment, an electrodialysis preliminary pre-launch was performed to remove salt impurities from the membranes. In the course of each experiment, the salt concentration in the tank was maintained in the range of 0.45-0.5 mol-eq/l, the volume of solution in each tank was periodically measured and samples of salt, acid and alkali solutions were taken for their subsequent analysis. The concentration of acid and alkali in the samples was determined by acid-base potentiometric titration. Impurities of salts in acids and alkalis were analyzed by ion chromatography.

Differential specific electrochemical characteristics of the device were calculated by the formulas (1)-(3)

$$\eta = \frac{F}{IN_{\text{cell}}}\left(\frac{dn}{d\tau}\right) \qquad (1) \qquad E = \frac{UF}{\eta} \qquad (2) \qquad P = \frac{\eta I}{FS_{\text{membr}}} \qquad (3)$$

where η is current efficiency acid or alkali; E is specific energy consumption upon receipt of acid or base, kW h/mol-eq; P is performance apparatus of acid or alkali, mol-eq/(h m^2); F is Faraday number; I is current, supplied to the apparatus, A; N_{cell} is number of unit cells in the membrane

stake of the apparatus; n is quantity of received acid or alkali (mol-eq); τ is time, s; U is voltage, supplied to the apparatus, V; S_{membr} is active area of each membrane, m^2.

Results and Discussion

Comparison of dependences of concentrations of sodium hydroxide and sulfuric acid in solutions on time (Figure 1a) shows that the concentrations of solutions obtained in the electrodialysis apparatus with industrial MB-3 bipolar membrane are lower than those obtained in the EDA with ~~a~~ modified bipolar membrane MB-2m.

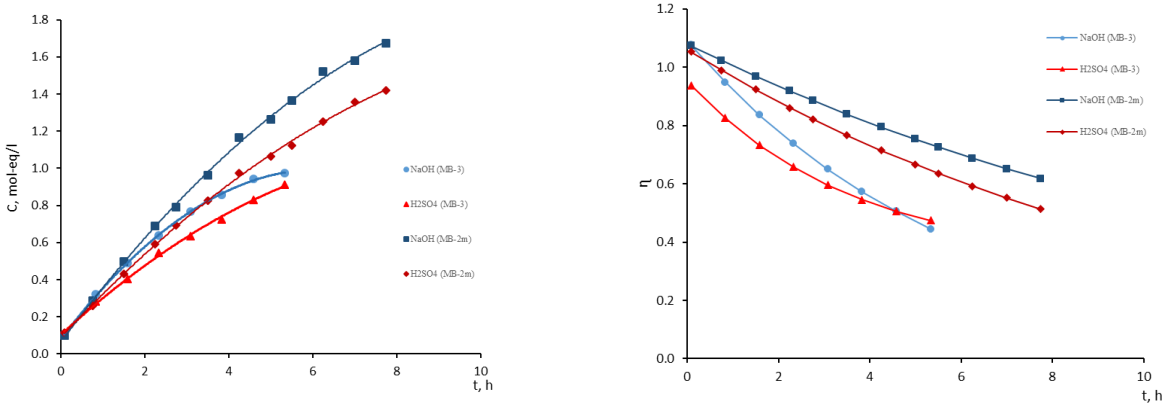

a *b*

Figure 1. Dependence of the concentrations of sodium hydroxide and sulfuric acid (a) and current efficiency of alkali and acid (b) on the operating time of EDA containing MB-3 or MB-2m bipolar membranes and Ralex CMX and Ralex AMH monopolar membranes.

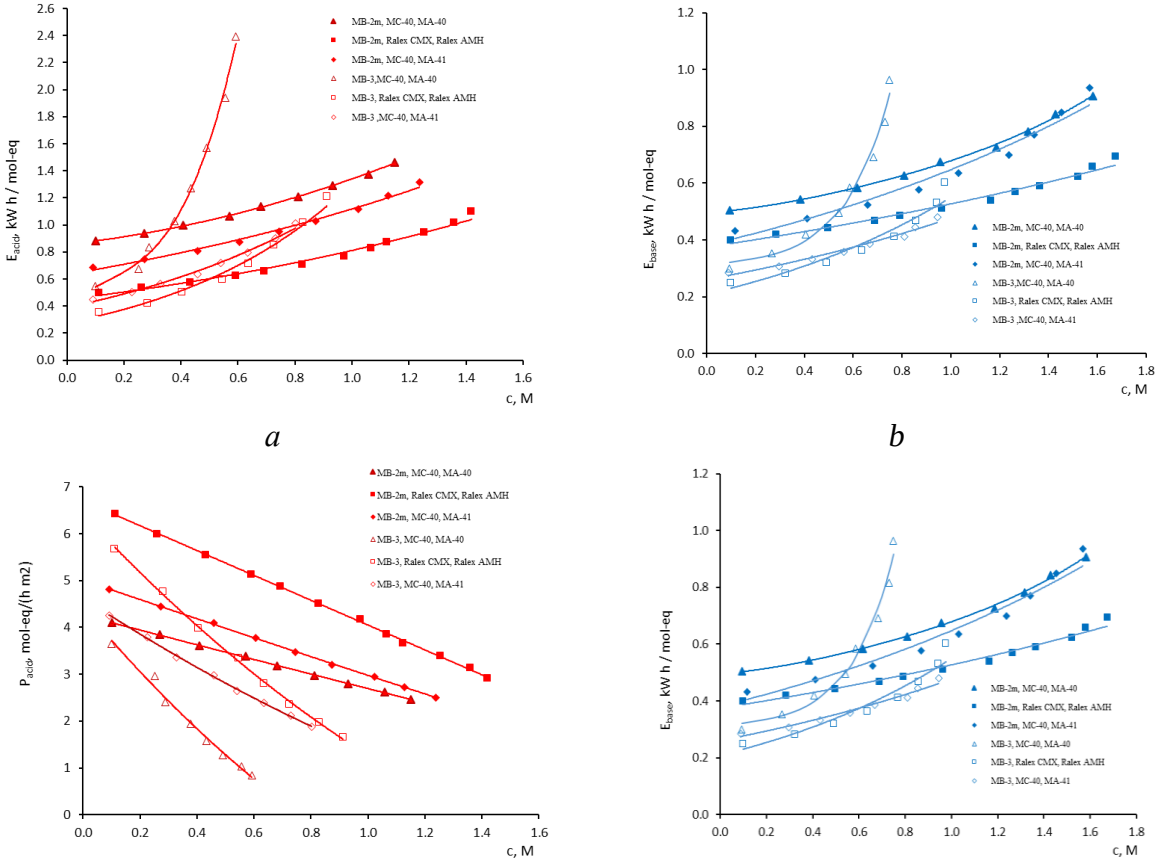

c *d*

Figure 2. Dependencies of differential specific energy consumption upon concentration of acid (a), alkali (b) and differential specific productivity of acid (b) and alkali (c) depending on the concentration of solutions and the type of bipolar and monopolar membranes.

The current efficiency of alkali and acid are higher in the case of EDA with a modified MB-2m bipolar membrane and Ralex CMX, AMH membranes (Figure 1b). The concentration of sodium ions in acid when using these membranes differ not so much. Differential energy consumption in the production of acid and alkali with a concentration above 1 M is always lower when using a MB-2m bipolar membrane, the specific productivity of the EDA under the same conditions is always higher (Figure 2). Contamination of alkali with sulphate ions is always higher in the case of the use of the industrial membrane MB-3 (Figure 3) and is very slight when using the bipolar membrane MB-2m. The reasons for these patterns are caused by the undesirable transfer of hydrogen ions and sulfuric acid through the MB-3 bipolar membrane, which contains weakly acid phosphoric acid groups in the cation-exchange layer, which in the presence of strong acids in the solution adjacent to the cation-exchange layer of the membrane are protonated and their dissociation decreases.

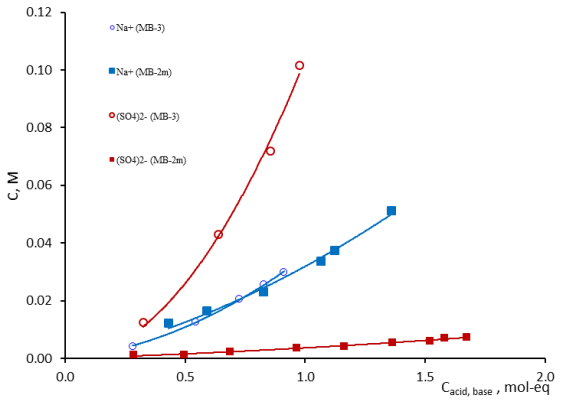

Figure 3. Depending concentration of sodium ions in solutions of acid and sulfate ions in solutions of alkali on concentration of solutions of acid or alkali, produced in EDA containing bipolar membranes MB-3 or MB-2m and monopolar membranes Ralex CMX and Ralex AMH.

This effect leads to ~~a~~ decrease in the concentration of the charged form of phosphoric acid groups, ~~a~~ decrease in the concentration of counter-ions and ~~an~~ increase in the concentration of co-ions. These undesirable processes are poorly expressed when modified MB-2m bipolar membrane is used in EDA, since its composition contains sulfonic groups, the degree of dissociation of which is not significantly reduced in the presence of sulfuric acid. Thus, the best electrochemical characteristics and higher purity of the produced acids and alkalis are provided by the EDA, the membrane package of which includes a bipolar membrane MB-2m and monopolar membranes Ralex CMX and AMH.

The present work is supported by State Task of the Ministry of Education and Science of the Russian Federation, project No. 10.3091.2017 / PCh.

References

1. *Nagasubramanian P. K., Chlanda F.P., Liu K.J.* Use of bipolar membranes for generation of acid and base - An engineering and economic analysis // J. Membr. Sci. 1977. V. 2. P. 109-124.
2. *Mani K.N., Chlanda F.P., Byszewski C.H.,* AQUATECH membrane technology for recovery of acid/base values from salt streams // Desalination. 1988.V. 68. P. 149-166.
3. *Chiao Y.C., Chlanda F.P., Mani K.N.,* Bipolar membranes for purification of acids and bases // J. Membr. Sci. 1991. V. 61. P. 239-252.
4. *Ben Ali M.A., Rakib M., Laborie S., Viers Ph., Durand G.* Coupling of bipolar membrane electrodialysis and ammonia stripping for direct treatment of wastewaters containing ammonium nitrate // J. Membr. Sci. 2004. V. 244. P. 89-96.
5. *Kovalev N., Mochalova T., Sheldeshov N., Lebedev K., Zabolotskiy V.* Influence of ionic groups of the ion exchanger on the selectivity of the bipolar membrane // Ion transport in organic and inorganic membranes 2018. P. 147-149.

SYNTHESIS OF ANION- AND CATION-EXCHANGE MEMBRANES BY CHEMICAL MODIFICATION OF FILMS-MATRIX

Tatyana Kovrigina, Tulegen Chalov, Edil Ergozhin
JSC "Institute of Chemical Sciences named after A.B. Bekturov", Almaty, Republic of Kazakhstan
E-mail: *kovriginatat@mail.ru*

Introduction

According to the concept of sustainable development of society, one of the main directions of scientific and technological progress is the introduction of resource-saving technologies. The most pressing aspect in this regard is the problem of saving clean water, widely used in industry. One of the main measures for the rational use of available water resources and their preservation from pollution by industrial effluents is the circulating water supply of enterprises and the reuse of treated wastewater [1].

It is known [2-4] that membrane processes (electro- and baromembrane, membrane-bioreactor, etc.) in combination with other methods and with the inclusion of innovative components in them, can significantly increase the efficiency and productivity of purifiers.

The role of membrane processes due to their waste-free, high efficiency and low energy costs is steadily increasing [5-6]. At the same time, the membranes themselves are the most expensive element [7]. During electrodialysis, ultrafiltration and reverse osmosis, their cost is approximately 30% of the equipment cost. Therefore, the problem of cheapening their cost becomes crucial.

Experimental part

Synthesis of anion- and cation-exchange membranes based on matrix films was carried out as follows [8]:

1. *Reception of films - matrixes*

Polyvinyl chloride (PVC) and ether (allylglycidyl ether (AGE), diglycidyl ether of resorcinol (DGER) or tetraglycidyl ether of 4,4'-diaminodiphenylmethane (THEDADPhM) were pre-dissolved in cyclohexanone (CH) in three-necked reactor equipped with a stirrer and thermometer. The reaction temperature was maintained at 70°C with two-hour stirring. Then the reaction mass was cast on a smooth surface and dried under UV light. They shot a light yellow transparent film.

2. *Amination of films*

The obtained films were modified using a 40% aqueous solution of polyethylene polyamine (PEPA) at 70°C for 3 h.

3. *Films sulfonation*

The obtained films were modified with concentrated H_2SO_4 at 70°C for 3-4 h, after which they were washed with the same acid of decreasing concentration.

Results and discussion

Inert thermoplastic films that do not contain ion exchange groups were obtained by preliminary dissolving PVC and various glycidyl ethers in a common solvent of CH. The finished matrix has the following physico-mechanical characteristics: tensile strength 40-50 kg/cm^2, elongation of 1.5-3.0%. Some physicochemical and electrochemical properties of the membranes synthesized by this method with the optimal ratio of the initial components are presented in the table.

It is seen that an increase in the sulfonation temperature for cation-exchange membranes leads to an increase in SEC and an improvement in their electrochemical properties. A further increase in temperature contributes to the deterioration of physicochemical and electrochemical characteristics due to destructive processes. The duration of the reaction practically does not affect the properties of the membranes, since complete swelling and sulfonation occurs within 3-4 h. At the same time, the SEC and electrical resistivity are 2.5-3.0 mg-eq/g and 60-80 Ohm·cm, respectively . The selectivity of the samples in the range of 96-97%.

SEC, electrochemical and physico-mechanical properties of anion-exchange membranes depend on the amination conditions of the films. With an increase in the reaction temperature, the SEC of samples increases and reaches more than 5.0 mg-eq/g.

Table: Electrochemical and physico-mechanical properties of the obtained membranes (A - SEC, mg-eq/g; B - specific electrical resistance, Ohm • cm; B - tensile strength, kg/cm^2)

The ratio of the initial components, wt.h	Cationic					Anionic				
	T, ^{0}C	τ, h	A	Б	B	T, ^{0}C	τ, h	A	Б	B
AGE : PVC										
3,0 : 1,0	60	4	2,8	53	35	60	4	4,7	73	39
	70	3	3,0	47	43	70	3	4,9	68	44
	80	2	2,7	56	31	80	2	5,2	62	36
DGER : AB : PVC										
1,5 : 1,5 : 1,0	60	4	2,2	47	42	60	4	4,1	82	41
	70	3	2,4	34	50	70	3	4,3	77	49
	80	2	1,9	49	45	80	2	4,9	84	49
THEDADPhM : AB : PVC										
1,5 : 1,5 : 1,0	60	4	2,3	43	47	60	4	3,8	89	43
	70	3	2,7	36	52	70	3	4,6	64	47
	80	2	2,0	41	42	80	2	4,5	83	45
Note: SEC - static exchange capacity, mEq/g, AB - allyl bromide										

This, in turn, leads to an increase in electrical conductivity and selectivity (98%) of membranes with a slight decrease in their strength properties. Tensile strength in the swollen state is equal to 35-50 kg/cm^2, relative elongation - 3-5%.

A study was made of the porous structure of membranes as chemically heterogeneous channel structures [9]. Studies using mercury porosimetry have shown that membranes contain mostly pores with a radius of 2.8 nm and, in a smaller amount, pores with a radius of 1.7 and 5.2 nm. The relative specific porosity of these membranes is 6.8-1.0 cm^3/g, respectively. According to literature data, the size of small pores characteristic of the gaps between polymer chains and their beams is 1.5-10 nm, and the size of large pores for polymer chains and crosslinking agent particles is more than 10 nm [10]. It has been established that the membranes obtained are not inferior, and, by some electrochemical properties, are superior to industrial membranes, which opens up great prospects for their practical application.

The figure shows the current sample of the electrodialysis apparatus and samples of ion-exchange membranes synthesized by us.

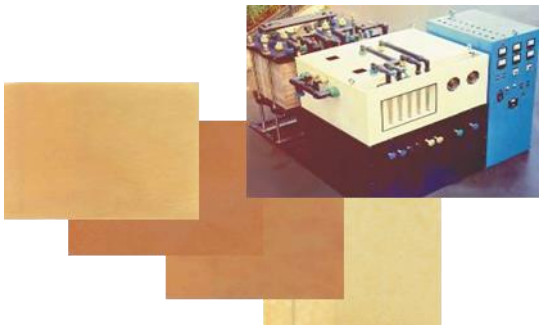

Figure. Electrodialysis unit EDA 1 - 400 × 60 and samples of synthesized anion- and cation-exchange membranes for water purification.

Thus, on the basis of the available initial monomers, promising ion-exchange membranes have been synthesized, the use of which contributes to the solution of environmental problems, the treatment of industrial wastewater, water treatment tasks and the development of membrane technologies in general.

The work was performed under the grant of the Science Committee of the Ministry of Education and Science of the Republic of Kazakhstan No. AR05131439 on the theme “Synthesis and modification of nanostructured ion-exchange membranes and the creation of innovative water treatment systems based on them”.

References

1. *Ergozhin E.E., Chalov T.K., Kovrigina T.V.* Synthetic and natural ion exchangers and sorption technologies. Almaty, 2018. 440 p.
2. *Ergozhin E.E., Chalov T.K., Kovrigina T.V., Prjatko E.Ju., Melnikov E.A.* Reagent-free wastewater treatment of petrochemical production with minimal discharge // Water: chemistry and ecology. 2018. № 7-9. P. 75-83.
3. *Jurchevskij E.B., Pervov A.G., Pichugina M.A.* Water purification from organic pollution using membrane water treatment technologies // Energy Saving and Water Treatment. 2016. № 5. P. 32-45.
4. *Balandina A.G., Hangildin R.I., Ibragimov I.G., Martjasheva V.A.* The development of membrane technologies and the possibility of their use for wastewater treatment of chemical and petrochemical enterprises // Oil and gas business. 2015. № 5. P. 336-375.
5. Membranes and membrane technologies. Ed. editor A.B. Yaroslavtsev. M.: Scientific world, 2013. 612 p.
6. *Ergozhin E.E., Chalov T.K., Khakimbolatova K.Kh.* Membranes and membrane technologies. Almaty, 2017. 260 p.
7. *Pabby A.K., Rizvi S.S.H., Sastre A.M.* Handbook of membrane separations. Francis: Taylor, 2009. 1184 p.
8. *Kovrigina T.V., Melnikov E.A., Dauletkulova N.T., Chalov T.K., Ergozhin E.E.* Synthesis and study of anion-exchange membranes based on epoxy compounds // VII All-Russia Karghin conf. "Polymers – 2017". M., 2017. P.432.
9. *Volfkovich Ju.M.* Reference Contact Porosimetry Method // Works of All-Russia scientific conference "Membranes -2007". M., 2007. P. 93.
10. *Zabolockij V.I., Nikonenko V.V.* Ion transfer in membranes. M: Science, 1996. 392 p.

ELECTRODIALYSIS OF AMMONIA-CONTAINING AQUEOUS SOLUTIONS

[1]Olga Kozaderova, [2]Oleg Kozaderov, [1]Kseniya Kim, [1]Sabukhi Niftaliev
[1]Voronezh State University of Engineering Technologies, Voronezh, Russia
[2]Voronezh State University, Voronezh, Russia
E-mail: *kozaderova-olga@mail.ru*

Introduction

In a number of industrial processes (e.g. production of mineral fertilizers, processing of nuclear fuel etc.), waste water containing ammonium ions is generated as industrial waste. Electrodialysis may be the preferred treatment for such solutions allowing the desalted and concentrated solutions to be returned to the initial steps of the process. The purpose of this work is to establish the mechanism and regularities of cations transfer during the electrodialysis of aqueous ammonium-containing solutions.

Experiments

Electrodialysis of aqueous solutions of NH_4NO_3 and KNO_3 (0.012 mol/dm^3) was carried out in a seven-section laboratory flow-type apparatus with membrane pairs MK-40/MA-41 (Shchekinoazot, Russia). The voltammetric characteristics of cation-exchange membranes and pH of the solution in the concentration chambers were measured; the intensity of generation of hydrogen ions by cation-exchange membranes was studied using the direct method of determining the ion fluxes of the medium [1]. The solution of the problem of diffusion-migration transport during electrodialysis under potentiostatic conditions was found by numerical finite element method in the Comsol Multiphysics computer package in the framework of a one-dimensional three-layer model, which considers adjacent diffusion layers along with the membrane. The process of electric mass transfer in the membrane system during the electrodialysis of an electrolyte solution containing a weak base cation was described by the Nernst-Planck and Poisson equations, without introducing electroneutrality assumption in the diffusion layers and in the membrane.

Results and Discussion

Ammonium ion fluxes through the cation-exchange membrane are shown in Fig. 1, a. Depending on the degree of polarization, two variants of the behavior of an electro-membrane system can be distinguished. When the maximum current density (1.2 mA·cm^{-2}) is exceeded, the transfer of ammonium ions can be explained using the concepts of the "barrier effect" and "facilitated migration" [2, 3]. However, an analysis of the change in the pH of the solution in the concentration channel shows that even in the pre-limiting modes of electrodialysis, the solution is acidified. This situation is not typical for electrodialysis of salts containing strong electrolyte cations. This fact makes it possible to use an approach to explain the behavior of ammonium ions in the system under consideration, developed to describe the transport of weak acids anions, taking into account hydrolysis reactions in the outer diffusion boundary layer and the inner pore solution of the membrane [4, 5]: the $NH_3{\cdot}H_2O$ particles formed during hydrolysis enter the membrane at the depleted interface and turn into NH_4^+ ions, since the interstitial solution of the membrane has a lower pH value than the external solution. Due to the influence of the Donnan elimination and under the action of direct current, the OH^- ions return to the depleted solution, where they react with NH_4^+ ions, resulting in an increase in the $NH_3{\cdot}H_2O$ concentration near the cation-exchange membrane. The ammonium cations formed in the internal solution of the membrane migrate to the opposite boundary of the membrane, pass into the enriched solution, where they capture OH^- ions from water molecules, thereby reducing the pH of the solution in the concentration chamber. Thus, pH of the depleted solution increases, and pH of the enriched solution, on the contrary, decreases, which can be considered as the transfer of H^+ ions through the cation-exchange membrane (Fig. 1, b).

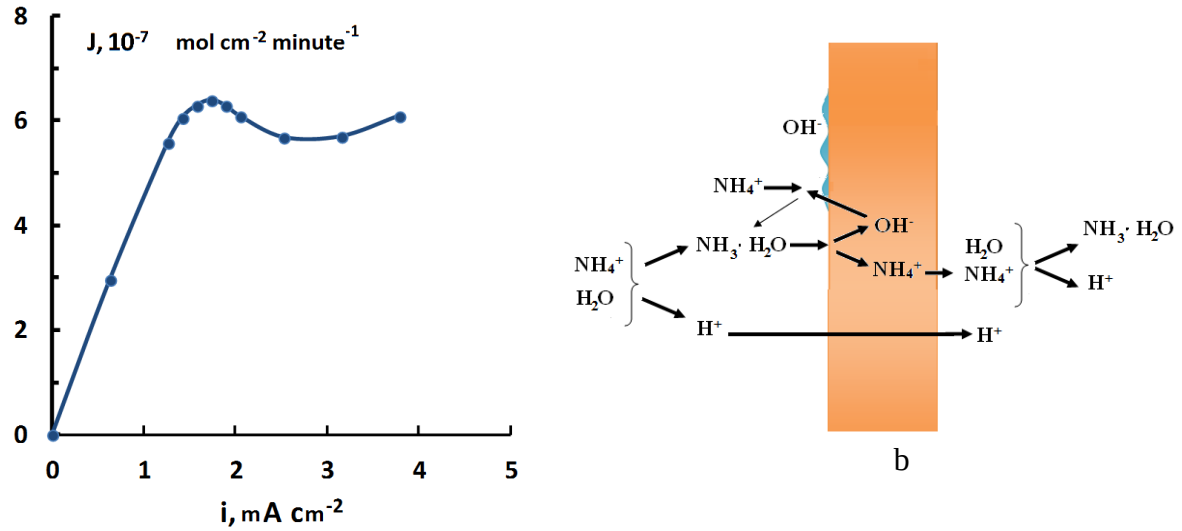

Figure 1. Ammonium ions transfer through the cation-exchange membrane: a – experimental results; b - model of the hydrolysis effect.

Numerical simulation of the average flux of hydrogen ions in the concentration section (Fig. 2, a) shows that if the salt does not undergo hydrolysis in an aqueous solution, then at pre-limiting current densities, the flux of hydrogen ions is negligible and relatively sharply increases when i_{lim} is exceeded. At the same time, if the salt is formed by a weak base, then the flux of hydrogen ions is very large, regardless of whether the limiting current density is reached or not. When the current limit is exceeded, such a decrease in pH leads to an additional increase in the hydrogen ions flux.

To test the adequacy of the mathematical model, an experiment was conducted on electrodialysis for solutions of ammonium nitrate and potassium nitrate under conditions that make it possible to measure the intensity of ion generation in the medium by cationic and anion-exchange membranes of the desalination chamber. The fluxes of hydrogen ions obtained by electrodialysis of ammonium nitrate and potassium nitrate solutions are shown in Fig. 2, b. In the case of ammonium salts, the fluxes are higher, and the result is consistent with the calculations obtained by numerical simulation. The transport mechanism of cations of a weak base through a membrane during electrodialysis is developed on the basis of analysis of experimental data on voltammetry, pH measurement for NH_4NO_3, KNO_3 alkali metal halides solutions.

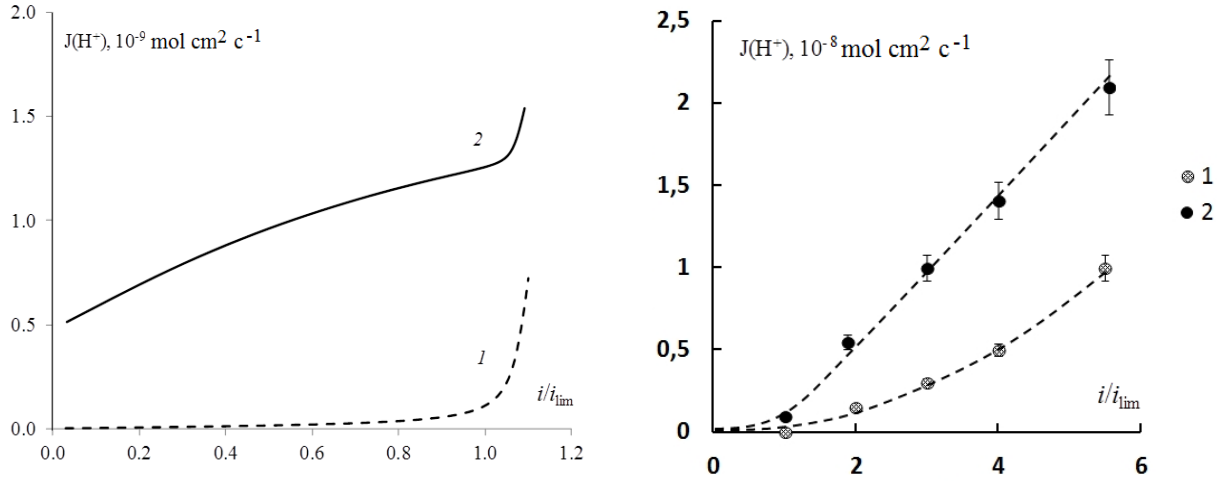

Figure 2. Hydrogen ions flux through the cation-exchange membrane vs. dimensionless current density curves: a - numerical simulation results (1 - salt is not subjected to hydrolysis in aqueous solution; 2 - salt is formed by a weak base); b – experimental results (1 - KNO_3, 2 - NH_4NO_3).

The study of the transport characteristics of heterogeneous cation-exchange membranes MK-40 in solutions of strong and weak electrolytes has been carried out. For the first time, the analysis of these parameters takes into account protonation / deprotonation reactions involving cations of a weak base and shows their significant effect on the productivity on salt ions during electrodialysis vs. current curves. The mechanism for transporting cations of a weak base in an electro-membrane cation-exchange membrane / salt solution system has been proposed.

References

1. *Shaposhnik V., Kozaderova O.* Transport of hydrogen and hydroxyl ions through ion-exchange membranes under overlimiting current densities // Russian Journal of Electrochemistry. 2012. V. 48. № 8. P. 791-796.
2. *Shaposhnik V., Eliseeva T., Tekuchev A., Lushchik I.* Assisted electromigration of bipolar ions through ion-selective membranes in glycine solutions // Russian Journal of Electrochemistry. 2001. V. 37. № 2. P. 170-175.
3. *Shaposhnik V., Eliseeva T.* Barrier effect during the electrodialysis of ampholytes // J. Membr. Sci. 1999. V.161. P. 223-228.
4. *Pismenskaya N., Nikonenko N., Volodina E., Pourcelly G.* Electrotransport of weak-acid anions through anion-exchange membranes // Desalination. 2002. V. 147. p. 345.
5. *Nikonenko V., Lebedev K., Manzanares J., Pourcelly G.* Modelling the transport of carbonic acid anions through anion-exchange membranes // Electrochimica Acta. 2003. V. 48. p. 3639.

MODELLING OF ANION-EXCHANGE MEMBRANE TRANSPORT PROPERTIES WITH TAKING INTO ACCOUNT THE CHANGE IN EXCHANGE CAPACITY AND SWELLING WHEN VARYING BATHING SOLUTION CONCENRATION AND pH

Anton Kozmai, Svetlana Zyryanova, Victor Nikonenko
Kuban State University, Krasnodar, Russia, E-mail: *kozmay@yandex.ru*

Introduction

Swelling is an important property of charged gels and membranes. The size of pores and, therefore, membrane properties such as conductivity, diffusion and hydraulic permeability, permselectivity depend on water content and degree of swelling.

In this work, the effect of pH and NaCl solution concentration on the transport characteristics of heterogeneous anion-exchange membranes (AEM) containing weakly basic functional groups is modeled. The model is based on the previously developed model [1] for equilibrium swelling of an ion-exchange membrane, as well as on the microheterogeneous model [2].

The proposed model includes Donnan equilibrium equations as well as equations for equilibrium of charged and uncharged ionogenic groups; electroneutrality condition in membrane; the Gregor [1, 3] and van't Hoff equations for the osmotic pressure in membrane and solution, respectively; the equation for the relative elongation (Hook's law); the Nernst-Plank equations and equations of microheterogeneous model [2].

To take into account the complicated porous membrane structure, for the sake of simplicity, as in microheterogeneous model, we will distinguish only two structural elements: a relatively homogeneous part of the membrane, which is microporous polyelectrolyte gel, and macropores, which include structural defects and voids. The structural element called "polyelectrolyte gel" will include, along with the ion-exchange resin particles, the polymer binder and the reinforcing fabric/net. The membrane polymer matrix is considered as ideally elastic and isotropic. The membrane contains functional groups of different nature (primary, secondary, tertiary and quaternary amines); these groups can be charged or uncharged depending on the pH. Only the protonated functional groups take part in ion-exchange, however both protonated and deprotonated groups contribute to membrane swelling [1].

In the model, the portion of intergel spaces is given as a function of the amount of "free water" in the membrane, i.e. water, located in the macropores and in the central part of the mesopores. The dependence of the diffusion coefficients of ions in the membrane on the degree of swelling is also taken into account. This dependence is described by the equation proposed by Mackie and Meares [4], using the "tortuosity coefficient" as a function of the fraction of the volume occupied by the polymer matrix impermeable to diffusion.

The input parameters of the model are the concentration and pH of bathing solution.

The fitting parameters are the portions of secondary (primary), tertiary and quaternary amines; the fraction of macropores; the structural parameter α; the equivalent volume of dry gel which contains 1 mol of functional fixed groups.

The output parameters are the concentrations of all species in the membrane, the number of free and bound water per equivalent of functional groups, the equivalent volume of the gel and that of the membrane (including macropores). It is possible to calculate the membrane exchange capacity, water content, membrane thickness, local coefficient of diffusion permeability, electric conductivity and transport numbers of ions in membrane.

Results and Discussion

A good agreement is found between the simulated curves and experimental data [5] representing the dependence of MA-40 and MA-41 membranes electric conductivity, diffusion permeability and ions transport numbers on bathing solution concentration and pH (Figure 1).

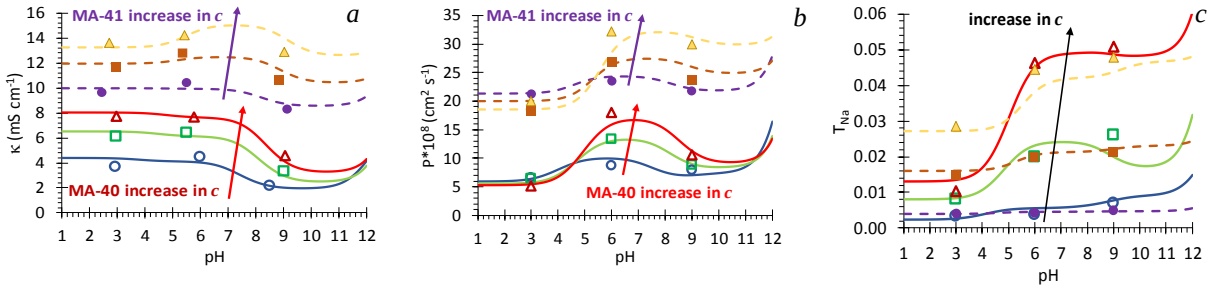

Figure 1. pH dependencies of electric conductivity (a), local coefficient of diffusion permeability (b) of MA-40 and MA-41 membranes; transport numbers (c) of Na^+ ions in MA-40 (solid lines) and MA-41 (dashed lines) membranes. Concentration of NaCl bathing solution is 0.1, 0.5 and 1 M.

The dependence of water content (Figure 2a) of the studied AEMs on the concentration of NaCl solution at a fixed pH = 3 (when the exchange capacity of the membranes is maximal) responds to the well-known concept of the effect of solution concentration on ion exchangers swelling [6]: with increasing salt concentration, swelling (and, therefore, the water content) of the membrane decreases because the osmotic pressure of the external solution increases, whereas the osmotic pressure of the internal solution in the membrane remains almost unchanged. The increase in external osmotic pressure increases the external resistance to the tendency of the matrix to stretch under the action of internal osmotic pressure.

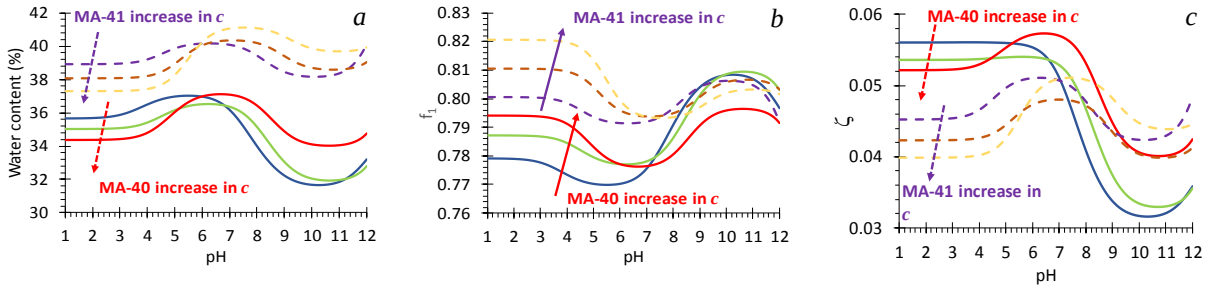

Figure 2. Water content (a), fraction of the "gel" phase (b) and the "tortuosity coefficient" in MA-40 and MA-41 membranes as functions of pH. Concentration of NaCl bathing solution is 0.1, 0.5 and 1 M.

With an increase in the pH of the external solution, deprotonation first of the tertiary amino groups, and then secondary (and primary) [1, 5, 7] ones occurs.

In the case of MA-40 membrane, where the portion of quaternary amines is up to 20% [1, 8], with an increase in pH from 3 to 6 at a given concentration, an increase in water content occurs (Figure 2a). A similar dependence is observed in the case of the MA-41 membrane. As shown in Kozmai *et al.* [1], such a dependence can be explained by a large hydration number of deprotonated tertiary amino groups as compared to their protonated forms. The greater water content of MA-41 membrane (Figure 2a), which is 38% at an external NaCl solution concentration of 0.5 M [8], is probably due to the fact that the hydration number of quaternary amino groups is higher than the hydration number of secondary (primary) and tertiary ones [1]. The MA-41 membrane may contain more than 66% of quaternary amino groups [7]. As in the MA-40 membrane, in MA-41, the maximum water content is observed within such a pH range (about 6-7), where the tertiary amino groups are completely deprotonated, and the secondary ones are not yet.

At pH over 7 there is a difference in the dependences of the water content on pH of MA-40 and MA-41 membranes. Thus, in the MA-40 membrane there is a noticeable decrease in the water content. This can be explained by the deprotonation of secondary amino groups. A significant loss of exchange capacity leads to a decrease in membrane swelling. However, with an increase in external salt concentration at low exchange capacity (the portion of which at pH 9 is about 10-20% [1, 5]), co-ions sorption occurs. Co-ions entering the membrane together with their hydration shells, causing an increase in water content.

On the contrary, in the MA-41 membrane, with an increase in pH, the water content (with the exception of the smallest concentration of the external solution) increases. This may be due to the fact that the portion of secondary amino groups in this membrane is relatively small, and at a pH = 6 and higher, strongly hydrated deprotonated tertiary amino groups are added to relatively strongly hydrated quaternary amino groups. As in the case of the MA-40 membrane, as the external concentration of salt increases, the concentration of co-ions in the MA-41 membrane increases, which causes a relatively high increase in the water content of this membrane at a pH greater than 6 and the concentration of NaCl solution of 1 M.

In the case of both membranes, a sharp increase in water content at a pH of more than 11 is due to an increase in the concentration of OH^- ions in the membranes [1].

Since the portion of intergel spaces (and, accordingly, the portion of gel) (Figure 2b) is determined as a function of free water content, and the diffusion coefficients of ions in the gel phase of the membranes depend on the tortuosity coefficient (Figure 2c), which in turn is a function of the volume of the swollen gel, then the change in the transport characteristics of the membranes with changes in the pH of the external solution (Figure 1) occurs in accordance with the change in their water content and the structural features determined in the microheterogeneous model through the parameter α.

Thus, by the influence of two opposing factors at each pH value of the external solution, namely the effective exchange capacity and the water content of the membrane, it is possible to explain the effects observed in Figure 1: a slight increase in the electrical conductivity of the MA-41 membrane at a pH of about 7 and the concentration of the external NaCl solution more than 0.1 M; a significant decrease in the electrical conductivity of the MA-40 membrane at a pH of about 8 and its sharp increase at a pH of more than 11; a slight decrease in the diffusion permeability of both membranes at a pH of about 3, its sharp growth and the presence of a maximum at a pH of about 7.

Acknowledgements

We are grateful for financial support to the RSF (grant 17-79-10166).

References

1. *Kozmai A. E., Nikonenko V. V., Zyryanova S., Pismenskaya N. D., Dammak L.* A simple model for the response of an anion-exchange membrane to variation in concentration and pH of bathing solution // J. Membr. Sci. 2018. V. 567. P. 127-138.
2. *Zabolotsky V. I., Nikonenko V. V.* Effect of structural membrane inhomogeneity on transport properties // J. Membr. Sci. 1993. V. 79. P. 181.
3. *Gregor H. P.* Gibbs-Donnan equilibria in ion exchange resin systems // J. Am. Chem. Soc. 1951. V. 73. P. 642.
4. *Mackie J. S., Meares P.* The diffusion of electrolytes in a cation-exchange resin membrane // Proc. Roy. Soc. London A. 1955. V. 232. P. 498A.
5. *Zyryanova S. V., Pismenskaya N. D., Nikonenko V. V.* The Influence of Concentration and pH of NaCl Solution on Transport Characteristics of Anione-Exchange Membranes with Different Nature of Fixed Groups // Membr. Membr. Tech. 2018. V. 8. P. 360-369.
6. *Helfferich F. G.* Ion Exchange, McGraw-Hill, New York, 1962.
7. Slavinskaya G. V., Kurenkova O. V. On the multifunctional character of strong basic anion-exchange resin // Sorp. Chromatograph. Proc. 2019. V. 19. P. 101-110.
8. *Vasil'eva V. I., Pismenskaya N. D., Akberova E. M., Nebavskaya K. A.* Effect of thermochemical treatment on the surface morphology and hydrophobicity of heterogeneous ion-exchange membranes // Russ. J. Phys. Chem. 2014. V. 88. P. 1293.

THEORY AND PRACTICE OF WATER DEOXYGENATION BY METAL-ION EXCHANGE NANOCOMPOSITES

Tamara Kravchenko, Lev Polyanskii, Dmitrii Konev, Dmitrii Vakhnin
Voronezh State University, Voronezh, Russia, E-mail: *krav280937@yandex.ru*

The most General Theory of water deoxygenation macrokinetics and dynamics by metal-ion exchange nanocomposites is constructed. Mathematical models of macrokinetics and dynamics of redox sorption processes involving nanocomposites are created, numerical solution of direct and inverse problems is performed, kinetic parameters are found, comparison with the experiment is carried out. The practical implementation is a development a new sorption-chemical and sorption-electrochemical methods of water deoxygenation.

Introduction

Water can not be considered ultrapure if dissolved oxygen presents in it. Catalytic and sorption-chemical approaches are known for deep removal of dissolved oxygen in water, based respectively on the interaction of oxygen molecules with hydrogen in the presence of catalyst nanoparticles (palladium) deposited on hollow-fiber membranes and chemically active metal nanoparticles (copper) deposited in macroporous ion-exchange matrices. This work aim is a mathematical describtion of water deoxygenation macrokinetics and dynamics.

Theory

Physico-chemical model. The formulation of the problem is based on the idea that the process of interaction of a solid porous redox sorbent (metal-ion-exchange nanocomposite, NC) placed in the liquid phase with a dissolved oxidant consists of the sorbate diffusion to the active centers followed by a successive oxidation-reduction reaction. Oxidation-reduction conversion of a homogeneous redox sorbent material occurs according to the scheme

$$\mathrm{B} \xrightarrow{k_1} \mathrm{C} \xrightarrow{k_2} \mathrm{D} \qquad (1)$$

The reaction of the oxidant with the active centers of the sorbent a localized area of the interfaces B/C, C/D are characterized by effective rate constants k_1 and k_2. The reagent diffuse through the layers of intermediate and final reaction's products with a thickness of δ_1, δ_2, with diffusion coefficients D_1 and D_2, respectively. The process is accelerated by the electric current of the cathode direction.

The macrokinetics of the redox sorption [1, 2]. We used the method of replacing the boundary with the flow of the substance on the reaction (active) layers for solving this problem. These layers have infinite diffusion permeability ($D_1', D_2' \to \infty$), finite thickness ($\delta_1', \delta_2' = \mathrm{const}$) and interact with the oxidant in whole volume. The difference upon electrochemical polarization, lies in the boundary condition of the component's balance a flow densities at the nanocomposite-solution interface, taking into account the surface electrochemical reaction

$$\mathrm{O_2} + 4\mathrm{H^+} + 4\mathrm{e^-} \to 2\mathrm{H_2O} \qquad (2)$$

$$j_2(R_0) - w_s = j(R_0). \qquad (3)$$

Here w_S is the function of the flow, which determines the disappearance of component A as a result of reaction (2) and depends of the electric current density i in the system $w_S = i/(zF)$, z is the number of electrons involved in the reaction, F is Faraday's constant.

We obtain a system of ordinary differential equations described the propagation of the boundaries of the individual stages of the sequential chemical reaction of oxidation of metal particles with oxygen during the electrochemical polarization of NC

$$\frac{d\xi_1}{d\tau} = -\left(1 - \frac{i}{i_{lim}}\right)\frac{d_{12}\xi_2}{Z_c},$$
$$\frac{d\xi_2}{d\tau} = -\left(1 - \frac{i}{i_{lim}}\right)\frac{\xi_1(\xi_2 - \xi_1) + d_{11}\xi_2}{Z_c}, \quad (4)$$

where i_{lim} is the density of the limiting diffusion current component A, $\xi_i = R_i / R_0$ is the dimensionless coordinate of i-front of the reaction, R0 is the radius of grains, dimensionless complexes kinetic constants, Di and kj are the coefficient of internal diffusion in the i-layer and the rate constant of the reaction in the j-layer, Bi is the Biot's criterion

$$Z_c = \left(1 - \xi_2\left(1 - \frac{1}{Bi}\right)\right)\left(\xi_1\xi_2\left(\xi_2 - \xi_1\right) + d_{11}\xi_2^2 + d_{12}\xi_1^2\right) - d_{22}\left(\xi_1^2 - \xi_1\xi_2 - d_{11}\xi_2\right). \quad (5)$$

The global minimum was found by the gradient descent method. Kinetic curves on a thin granular layer were calculated and compared with experimental ones using the internal parameters d_{ij}. The results suggest the adequacy of models and experiments.

Dynamics of the redox sorption. The kinetic parameters of d_{ij} were used to calculate the dynamics of oxygen uptake in a redox column with a granular layer using the material balance equation and obtained a satisfactory agreement of the calculation with experimental data. In the case of oxygen redox sorption dynamics on the cathod-polarized granular layer of nanocomposite, a current was introduced into the transport equation along the column to preserve the material balance. Columnar granular layer of NC is energized and is considered as an electrical circuit, in which each resistors $R_i(y)$ represent a general Ohmic resistance of the elementary section column layer (along the section plane) and the polarization resistance of Faraday's reactions in this section. Here y is axis coordinate directed along the layer in the direction of flow. The resistance of the i-layer of nanocomposite as oxidation is assumed to vary from a certain source $R_{NC}(\alpha=0)$ to the final R_{NC} ($\alpha=1$)

$$R_{NC}(\alpha_i) = R_{NC}(1)\cdot\alpha + R_{NC}(0)\cdot(1-\alpha_i) \quad (6)$$

where α is the degree of completeness of oxidation of NC.

Knowing the total current at the reactor I of height L, it is possible to calculate the distribution of this current in layers located at different heights,

$$I_i = I\frac{\sum_L\left[\alpha_i + \overline{R}_{NC}(1-\alpha_i)\right]}{\alpha_i + \overline{R}_{NC}(1-\alpha_i)} \quad \text{where } \overline{R}_{NC} = \frac{R_{NC}(0)}{R_{NC}(1)}. \quad (7)$$

During 100 h of experiment there is a natural decrease the dissolved oxygen obsorption rate from water at the granular layer outlet in the absence of polarization and the establishment of a constant rate of oxygen absorption concentration under the influence of an electric current. Polarization of the system allows for a long time to maintain the chemical activity of metal particles and a stationary level of oxygen redox sorption.

Experiments

Sorption-chemical method. The schematic diagram of deoxygenating electrolyzer is shown in Fig. 1. The external heating system 1, including the heating boiler 2, pipelines, radiators, is closed to an additional circuit with an oxygen-free installation. Calculation and experiment show that the concentration in the system will decrease from 8 mg/l to 10 μg/l in a short time after switching on the redox filter.

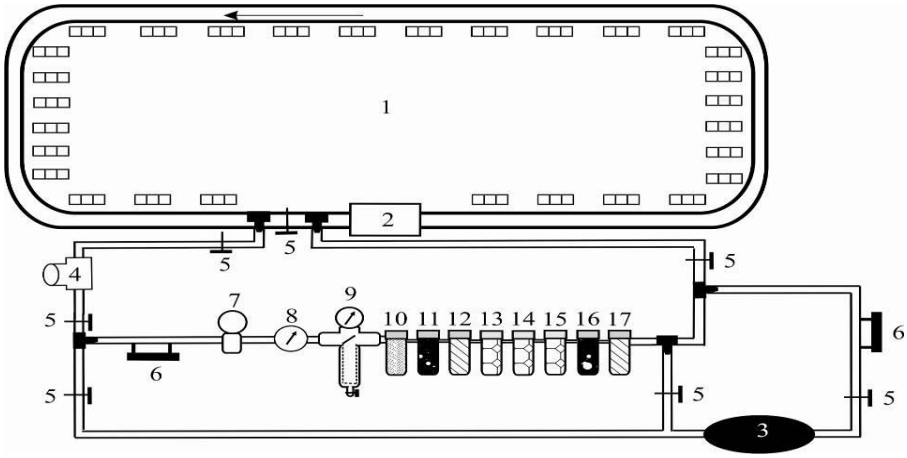

Figure 1. Diagram of the device for deoxygenating water: 1 – external closed-loop water system, 2 – boiler, 3 – oxygen, 4 – pump, 5 – control valves, 6 – rotameters, 7 – meter, 8 – thermometer, 9 – mechanical filter with pressure gauge, 10, 17 mechanical fine filters, 11 – sorption filter (coal), 12, 16 – mixed ion exchange filters, 13, 14, 15 – redox filters with granular NC.

Sorption-electrochemical method. The main processes' system occurring in sorption membrane electrolyzer can be represented as a set of electrode and ion processes (Fig. 2). Deoxygenation of water occurs without changing the pH. As a result of long-term tests, the possibility of continuous maintenance of the oxygen level at the step-polarized granular layer outlet of nanocomposite has been established. Stability is provided by simultaneous oxygen reduction due to electric current and chemical activity of copper nanodispersed particles.

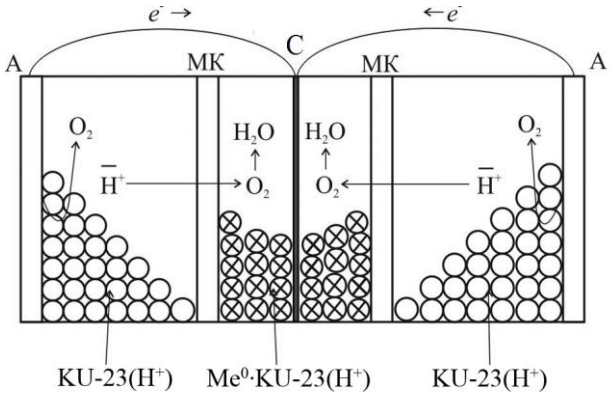

Figure 2. The scheme of processes in deoxygenator (sorption-membrane electrolyzer with the granular layer of NC): A – anode, C – cathode, MK – sulfocation-exchange membrane.

Conclusions

Proposed and implemented in production sorption-chemical method of deep water deoxygenation in closed flow systems (<10 μg/l) on copper-containing nanocomposite with optimal capacity. The theoretical calculation showed that the sorption-electrochemical process carried out in series connected multistage electrolyzers with polarization each stage in the limiting external diffusion current mode allows to obtain water in open flow systems with a given residual dissolved oxygen content.

Acknowledgments

This work was supported by the Russian Foundation for Basic Research (grant № 17-08-0426a).

References

1. *Polyanskii L.N., Korzhov E.N., Vakhnin D.D., Kravchenko T. A.* Macrokinetic model of redox sorption on metal-ion exchange nanocomposites at electrochemical polarization // Russ. J. Phys. Chem. 2016. V. 90. № 8. P. 1675-1681.
2. *Polyanskii L.N., Korzhov E.N., Vakhnin D.D., Kravchenko T. A.* Redox-sorption in metal-ion-exchanger nanocomposites upon electrochemical polarization // Russ. J. Phys. Chem. 2016. V. 90. № 9. P. 1889-1895.

STUDY OF MEMBRANE FOULING DURING ACID WHEY BIPOLAR ELECTRODIALYSIS

Vitalii Kravtsov, Irina Kulikova, Artem Bessonov, Ivan Evdokimov
North-Caucasus Federal University, Stavropol', Russia, E-mail: *craftsoe@gmail.com*

Introduction

Acid whey, a by-product of cottage cheese, casein and strained yogurts production, offers a variety of valuable nutritional constituents, including lactose and whey proteins. However, the industrial processing of acid whey is complicated due to high content of lactic acid that affects whey crystallization and drying processes significantly [1]. Nanofiltration [2] and electrodialysis [3] are considered as the promising methods to remove sufficient part of lactic acid from acid whey and thus provide a material for production of high-quality whey concentrates. Also, a sourness of acid whey hampers its application as an additive to various food products without altering of sensory characteristics. To lower whey acidity, alkaline reagents are applied, typically these are sodium or potassium hydroxide solutions. The alternative is a non-reagent alkalization of whey by means of bipolar electrodialysis (electrodialysis with bipolar membranes, EDBM) [4]. Neutralization of acid whey in EDBM occurs as the electrogenerated OH^- ions migrate from the boundary layer of bipolar ion-exchange membrane (BPM) to the whey stream during the processing. Subsequently, strong basic media is maintained at the anion-exchange side of BPM. High pH values are known to favour undesirable membrane scaling in dairy media containing Ca^{2+}, Mg^{2+} and PO_4^{3-} [5]. Moreover, the possibility of whey proteins denaturation emerges with the excessive rise of pH combined with heating both in isolates [6,7] and *in situ* [8]. In this context, membrane fouling is a subject of a thorough examination. The aim of the present work was to evaluate the problem of membrane fouling in case of acid whey EDBM processing and to suggest the origins of its formation.

Experiments

The acid whey obtained from industrial cottage cheese production was subjected to EDBM processing on a laboratory-scale circulation ED unit P EDR-Z in order to rise whey pH up to 6.5. The ED cell was equipped with heterogeneous ion-exchange membranes RALEX AM(H)-PP, CM(H)-PP and bipolar RALEX BM and configured as shown in Figure 1.

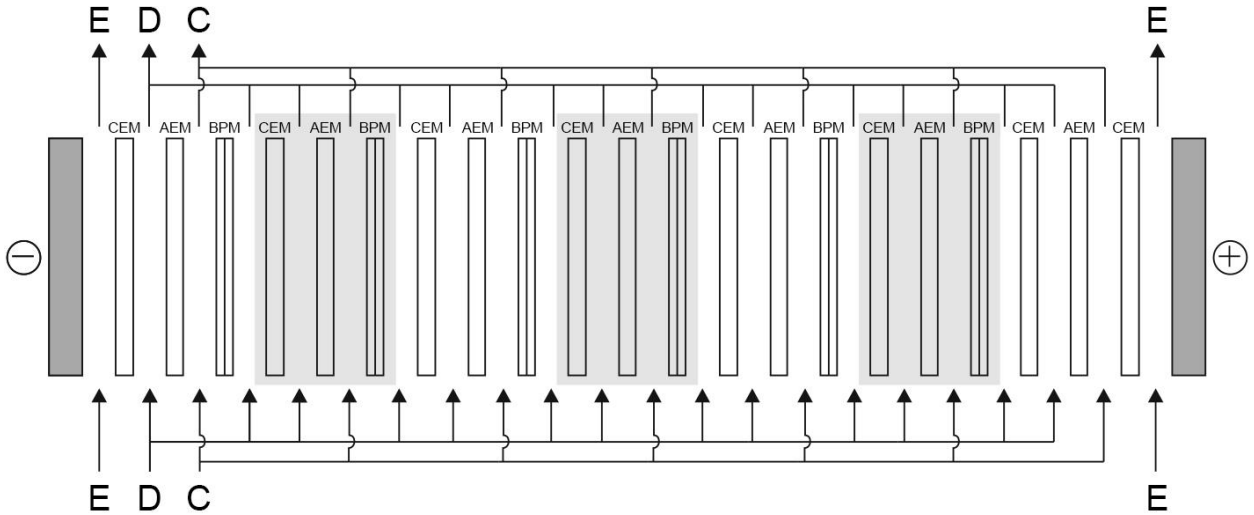

Figure 1. ED cell for acid whey treatment. E, D and C indicate electrode solution, diluate and concentrate stream, respectively; CEM, AEM and BPM are cation-exchange, anion-exchange and bipolar membranes, respectively.

The effective electrode area was 64 cm^2. The acid whey, tap water and 0.2 M sodium nitrate were utilized as diluate, concentrate and electrode solution, accordingly, with respective flow rates of 75, 75 and 100 $l \cdot h^{-1}$. The volumes of the streams were 0.30, 0.25 and 1.00 l for diluate, concentrate and electrode solution, respectively. The current density throughout EDBM treatment

was 40 to 61 $A \cdot m^{-2}$ and the constant voltage applied to the electrodes was 25 V. Temperature of bulk acid whey in the tank of ED unit was 24±1 °C throughout ED run. The duration of ED run was 30 min. The ED cell was disassembled immediately after the processing avoiding any cleaning procedure.

Results and Discussion

No visible fouling was found on the unipolar membranes after ED run. On the contrary, the surface of BPM in contact with whey stream was clogged with a large amount of white gellike deposit. (Figure 2). Although the observed fouling was located exclusively on the BPM anion-exchange surface, it was distributed unevenly on the membrane and built-up more in the area close to the inlet. This feature corroborates with the said hypothesis of pH-induced fouling. The alkalinity of the incoming whey stream is lower than that of the stream leaving diluate compartment, i.e. the pH gradient is formed in the diluate chamber adjacent to BPM. The conditions for both protein denaturation and precipitation of salts of divalent cations enhance towards the outlet.

However, the hydrodynamic characteristics of the diluate stream should be also accounted. It is important that the turbulization occurs in the ED stack compartments due to spacer design. Flow disruption makes washing of the fouling less intensive. Additionally, the fouling from the bottom of the diluate compartment (close to the inlet) is likely to be washed away and participate in deposition at the top of the compartment.

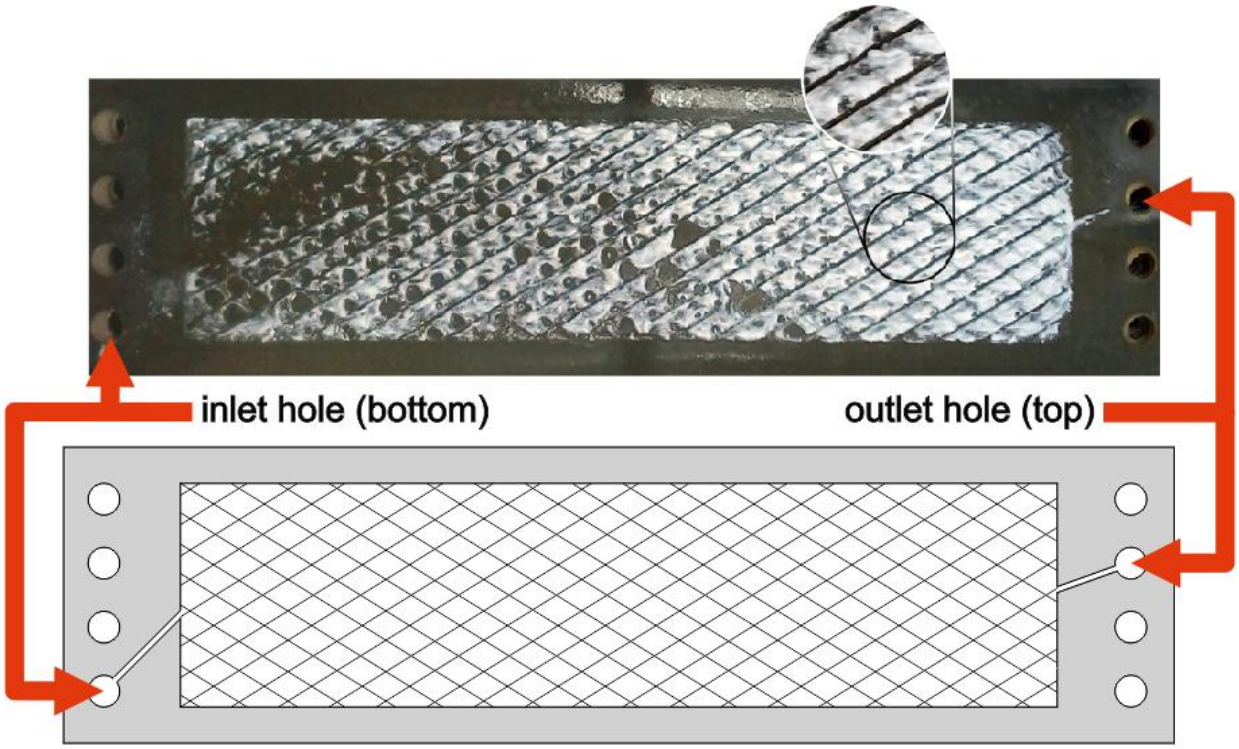

Figure 2. Image of BPM with membrane fouling after acid whey processing and membrane spacer layout. The ED cell was oriented vertically during operation.

Protein precipitation is often related to electrostatic interactions between protein molecules or thermal denaturation [9]. Sufficient temperature for whey proteins denaturation ranges from 62 to 78 °C [10]. These values are significantly higher than that maintained in diluate during EDBM run, though the alkaline reagents are known to lower the temperature threshold of whey proteins precipitation [7]. Isoelectric points of major whey proteins, β-lactoglobulin and α-lactalbumin, are in acidic medium (5.2–5.4 and 4–5, accordingly) [9,11,12]. This pH values were exceeded during the treatment, as far as pH changed from 4.5 to final 6.5. Thus, the coagulation of protein molecules in the conditions of a minimal net charge could take place. Ultimately, we consider the pH-induced

denaturation of whey proteins [6,7] as the main cause of organic fouling deposition. Yet, there are few data on whey proteins behavior in alkaline media apart from heating.

Mineral precipitates could also contribute to the observed membrane fouling. Acid whey is rich on calcium and phosphate [13] tending to form insoluble salts in alkaline media. The electrogenerated OH^- ions could therefore induce precipitation of mineral salts in the diluate stream and, particularly, on the BPM anion-exchange surface, where the concentration of OH^- is relatively high.

The revealed issue of membrane fouling is to be analyzed in detail hereafter. Chemical composition of the fouling matter should be determined to suggest possible ways of its reduction and prevention. Also, it is important to ascertain causes and mechanisms of fouling formation.

References

1. *Chandrapala J. et al.* Strategies for maximizing removal of lactic acid from acid whey – Addressing the un-processability issue // Sep. Purif. Technol. 2017. V. 172. P. 489–497.
2. *Chandrapala J. et al.* Removal of lactate from acid whey using nanofiltration // J. Food Eng. 2016. V. 177. P. 59–64.
3. *Chen G. Q. et al.* Removal of lactic acid from acid whey using electrodialysis // Sep. Purif. Technol. 2016. V. 158. P. 230–237.
4. *Bazinet L., Lamarche F., Ippersiel D.* Bipolar-membrane electrodialysis: Applications of electrodialysis in the food industry // Trends Food Sci. Technol. 1998. V. 9, № 3. P. 107–113.
5. *Mikhaylin S., Bazinet L.* Fouling on ion-exchange membranes: Classification, characterization and strategies of prevention and control // Adv. Colloid Interface Sci. Elsevier B.V., 2016. V. 229. P. 34–56.
6. *Hegg P. O.* Thermal Stability of β-Lactoglobulin as a Function of pH and the Relative Concentration of Sodium Dodecylsulphate // Acta Agric. Scand. 1980. V. 30, № 4. P. 401–404.
7. *Myra T. et al.* Gel Characteristics of B-Lactoglobulin, Whey Protein Concentrate and Whey Protein Isolate // J. Texture Stud. 1997. V. 28, № 4. P. 387–403.
8. *Chandrapala J. et al.* Properties of acid whey as a function of pH and temperature // J. Dairy Sci. 2015. V. 98. P. 4352–4363.
9. Advanced Dairy Chemistry: Volume 1A: Proteins: Basic aspects. 4th ed. / *ed. McSweeney P. L. H., Fox P. F.* 2013. 548 p.
10. Advanced Dairy Chemistry Volume 1B: Proteins: Applied aspects. 4th ed. / *ed. McSweeney P. L. H., O'Mahony J. A.* 2016. 498 p.
11. *Wong D. W. S., Camirand W. M., Pavlath A. E.* Structures and Functionalities of Milk Proteins // Critical Reviews in Food Science and Nutrition. 1996. V. 36, № 8. P. 807–844.
12. *Zydney A. L.* Protein separation using membrane filtration : new opportunities for whey fractionation // Int. Dairy J. 1998. V. 8, № 98. P. 243–250.
13. *Wong N. P., LaCroix D. E., McDonough F. E.* Minerals in Whey and Whey Fractions // J. Dairy Sci. 1978. V. 61, № 12. P. 1700–1703.

ROLE OF ION EXCHANGE MATRIX IN PROCESS OF REDUCING SORPTION OF MOLECULAR OXYGEN BY METALCONTAINING NANOCOMPOSITES

Vyacheslav Krysanov, Natalia Plotnikova, Anastasia Okushko
Voronezh State University, Voronezh, Russia, E-mail: *krysanov@chem.vsu.ru*

Introduction

Obtaining chemically pure water is an urgent problem in the modern world. The process of water purification is currently being carried out with the help of new innovative technologies that allow for deep, but at the same time unalloyed removal of oxygen. The development of ion exchange technologies and the emergence of a wide range of ion exchange resins have made them the most used in water treatment and deoxygenation processes. Lewatit K 3433 and Lewatit K 7333 (Germany), doped with palladium, are used for catalytic removal of oxygen from water. In technologies patented by Bayer (Germany), Lewatit MP 62 WS resin is used for deoxygenation of water. Patented devices and materials for deep deoxygenation of water in a closed system, the main material of which are nanocomposites based on ion exchanger KU-23 (Ukraine).

Nanocomposites based on ion exchange resins differ in capacity by counterions to the metal component, as well as in their structure (size and distribution of pores and metal particles by size and granule).

The aim of this work was to clarify the role of ion exchange matrices in the process of molecular oxygen sorption by various nanocomposites.

Experiments

Synthesis of nanocomposites Ag,Cu·КУ-23 (H^+), Cu·Lewatit SP-112H (H^+), and Ag,Cu·Lewatit K 2620 (H^+) was carried out by the known technique of ion exchange saturation and chemical deposition of metal. The metal content in the samples was regulated by the number of metal deposition cycles.

Comparison of physico-chemical characteristics monopolistic ion-exchange resins Lewatit preparesto conducted regarding ion-exchanger KU-23 (tab.1.). The size and radial distribution of copper particles in the grain were estimated from x-ray analysis (x-ray x-ray diffractometer Thermo ARL x'tra (Switzerland) and scanning electron microscopy (SEM) obtained from JSM-6380LV electron microscope (Japan). The efficiency of the created materials was evaluated based on the results of the study of the absorption rate of molecular oxygen dissolved in water at a temperature of 20±1ºC. Kinetic tests of the nanocomposite were carried out in a gasometric cell with water containing dissolved oxygen.

Table 1: Basic physical and chemical characteristics of ion exchange resins

Characteristics	CU-23	Lewatit SP-112H	Lewatit K 2620
Functional group	$R-SO_3^-H^+$	$R-SO_3^-H^+$	$R-SO_3^-H^+$
Granule size *d*, mm	0.1-0.5	0.6	0.4-0.6
Surface area, m^2/g	30-40	30	33
Porosity	Macroporous		
Pore size, nm	10-100	33	41
Ion-exchange capacity ε_{H^+}, meqv/sm^3	1.2	1.6	1.9

Results and Discussion

Comparison of kinetic curves for three samples of copper-containing nanocomposites, differing ion exchange bases, showed a sufficiently high efficiency of materials based on monodisperse matrices Lewatit SP-112H and Lewatit K 2620, not inferior, and at the initial stage for the nanocomposite Cu·Lewatit SP-112 H (H+) even superior polydisperse nanocomposite Cu·KU-23 (H+) in the rate and degree of absorption of dissolved oxygen in water (fig. 1) Analysis of the kinetics of oxygen reduction on copper – ion exchanger nanocomposites revealed that all the studied nanocomposites behave almost the same in terms of the rate and degree of oxygen

absorption. Differences in the rate and degree of absorption of oxygen do not exceed 6-8%. Some decrease in the degree of sorption during a long experiment time for Cu·Lewatit nanocomposites may also be associated with lower pore availability and a slightly higher copper content on the surface.

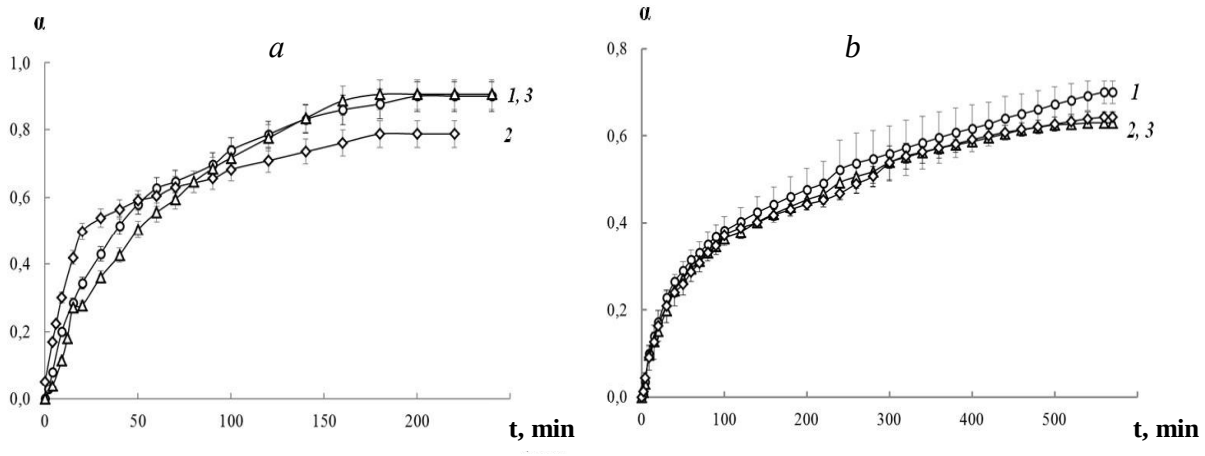

Figure 1. Kinetic curves for the degree of absorption of oxygen α from water as a function of time t by nanocomposites: 1 - Cu·КУ-23(H^+), 2 - Cu·Lewatit SP-112 H(H^+), 3 - Cu·Lewatit K 2620(H^+) with various cycles of deposition of copper; a) N=1 b) N=5.

The intensity of the process occurring on the basis of Lewatit is influenced by the high exchange capacity of composites by hydrogen ions and copper particles, as well as the smallest size of copper agglomerates in Lewatit K 2620. In addition, from a technical and economic point of view, the high metal capacity on Lewatit composites is achieved in fewer deposition cycles due to the high hydrogen exchange capacity. High-capacity nanocomposites obtained on the ion-exchange bases of Lewatit have crystallite sizes that practically coincide with the pore size of the polymer matrix (tab. 1), unlike the nanocomposite based on CU-23, whose pores are not fixed. This leads to an increase in the reproducibility of the oxygen absorption kinetics on them and a reduction in the confidence interval in comparison with the curve for Cu·KU-23 (H+) by almost two times.

The increase in the metal content from one to five deposition cycles levels differences in the kinetic properties of nanocomposites with different ion exchange matrices.

Similar patterns are observed for kinetic curves with different matrices for silver-containing nanocomposites (fig.2). It is seen that the highest degree of oxygen absorption is achieved on nanocomposites synthesized on the Lewatit K2620 matrix. Due to the monopolistic nature of the

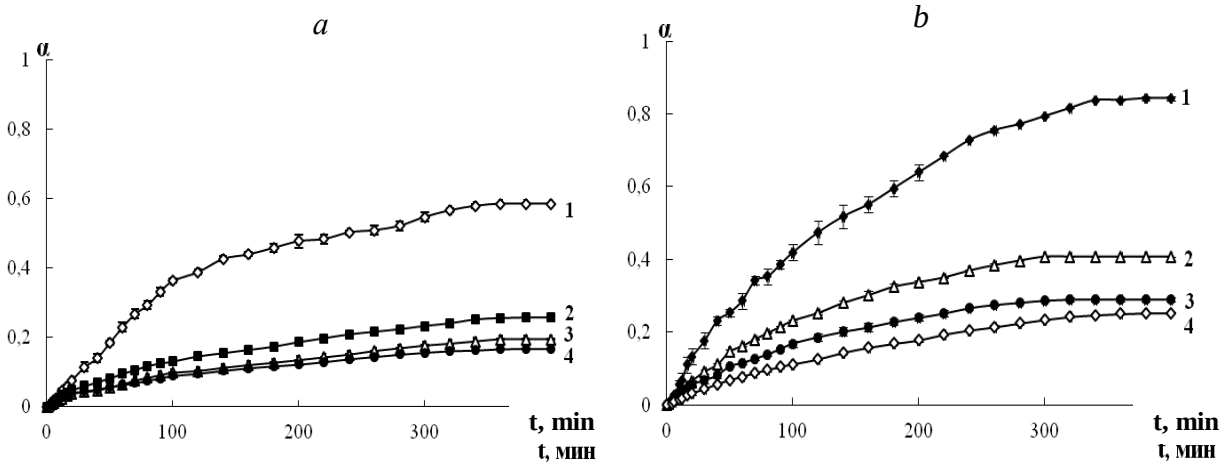

Figure 2. Kinetic curves for oxygen uptake a) Ag^0·CU-23, b) Ag^0·Lewatit K 2620 with different metal deposition cycles N: 1) N=1; 2) N=3; 3) N=5; 4) N=7.

matrix oxygen slowly diffuses to the center of the grain, a high ion exchange capacity for hydrogen ions helps to maintain the acidic environment during the process, which contributes to the formation of soluble oxidation products, and, in addition, a high amount of hydrogen cations catalyzes the process and maintains its flow until the hydrogen.

With an increase in the amount of silver in nanocomposites, differences in the kinetics of oxygen sorption are also leveled, but the nanocomposite synthesized on the Lewatit K2620 matrix shows greater efficiency in the process of oxygen removal at low capacitance values.

Conclusion

High-performance composite nanomaterials based on copper and silver and ion exchangers Lewatit K 2620 and Lewatit SP-112 H were synthesized for deep removal of oxygen from aqueous solutions. The obtained materials are characterized by a high content of the metal component, porous structure and monodisperse distribution of copper particles in size. Chemically synthesized nanocomposites show higher recovery rates of absorbed oxygen at a single copper deposition and almost the same parameters at a five-fold metal deposition, and are characterized by a higher reproducibility of the kinetics of oxygen absorption on them compared with the analog KU-23. The study of the structure of nanocomposites confirms the assumption that the previously noted regularities are associated with the monodisperse of the Lewatit K 2620 and Lewatit SP-112H matrices, which are more preferable for practical application.

The work was supported by the Russian Foundation for basic research (project code № 17-08-00426_a)

The results of microscopic studies were obtained on the equipment of the Center for collective use of scientific equipment VSU.

INFLUENCE OF STABILIZERS ON THE MORPHOLOGY OF PLATINUM DISPERSION ON THE SURFACE OF PERFLUORINATED MEMBRANE

Darya Kudashova, Irina Falina, Natalia Kononenko
Kuban State University, Krasnodar, Russia, E-mail: *pirina71@yandex.ru*

Introduction

Development of fuctional materials for hydrogen fuel cells is an important field of the material science [1-2]. The prospective route is to cover the surface of the perfluorinated membrane by platinum dispertion give the membrane catalytic properties [3]. The addition of organic substancies in working solutions during the preparation of electrocatalysts allows controlling the size of the nanoparticles formed and contributes to an increase in the active metal surface area [4-5]. The study of the possibility of using stabilizers of the platinum dispersion in the process of its deposition on the surface of perfluorinated membranes was not previously been carried out. The aim of this work is to study the influence of organic substances on the morphology of platinum deposited on the surface of perfluorinated membranes, and to evaluate the efficiency of using modified membranes in a hydrogen-air fuel cell.

Experiments

The objects of study was perfluorinated membrane MF-4SK (JSC Plastpolymer, St. Petersburg), modified with a platinum dispersion. The membranes modification was carried out in a two-chamber cell by the counter-diffusion of oxidant (H_2PtCl_6) and reducing agent ($NaBH_4$) solutions through the membrane during an hour. The oxidant solution contained ethylenglycol (EG) and polyethylenglycol (PEG) of various concentrations to stabilize the platinum nanoparticles. Modification conditions are presented in Table.

Table: Conditions of modification of the membranes MF-4SK by platinum dispersion

NO	REDUCING AGENT SOLUTION	CONCENTRATION OF ORGANIC MATTER
1	**0.05 M $NABH_4$ +0.5 M NAOH**	**–**
2	**0.05 M $NABH_4$ + 0.25 M NAOH**	**25% VOL. EG**
3	**0.025 M $NABH_4$ + 0.25 M NAOH**	**50% VOL. EG**
4	**0.05 M $NABH_4$ +0.5 M NAOH**	**5 G/L PEG**
5	**0.05 M $NABH_4$ +0.5 M NAOH**	**10 G/L PEG**
6	**0.05 M $NABH_4$ + NAOH (PH=12)**	**–**
7	**0.05 M $NABH_4$ + NAOH (PH=12)**	**25% VOL. EG**
8	**0.025 M $NABH_4$ + NAOH (PH=12)**	**50% VOL. EG**

After modification membranes were washed with distilled water to remove the sorbed solution. The study of the membranes surface morphology was performed using a JEOL JSM - 7500 scanning electron microscope. Testing of hybrid membranes in the fuel cell was carried out at a temperature of 25 °C, the feed rate of hydrogen and air was 20 and 300 L/h, respectively.

Results and Discussion

Figure 1 shows SEM-images of surfaces of the samples obtained. One can see, that addition the 25% vol. EG to the oxidizing solution results in a uniform coating of the membrane surface with a catalyst (Fig. 1b) and decrease in the aggregation of particles compared to sample 1 (Table) (Fig. 1a). This effect indicates the stabilizing action of EG. The increase in EG content to 50% vol. leads to growth of layer heterogeneity (Fig. 1c). EXD-analysis of the surfaces elemental composition shown that Pt content decreases as EG concentration rises. Similar results are observed in the case of using PEG as stabilizer: for concentration 5 g/L the platinum layer consists of individual small agglomerates (Fig. 1d); for concentration 10 g/L Pt content on the surface significantly reduces (Fig. 1e).

To study the effect of pH on the morphology of the platinum dispersion we obtained the samples using the solution of reducing agent containing an excess of alkali (pH 13.5) or with pH 12. In the

case of pH 12 a uniform dense coating is formed. Samples obtained by simultaneously adding stabilizers to the oxidant solution and adjusting the pH of the reducing agent solution contain significantly larger amounts of platinum on the membrane surface than other samples, but intense peeling and precipitation of the metal into the solution was observed (Fig. 1f).

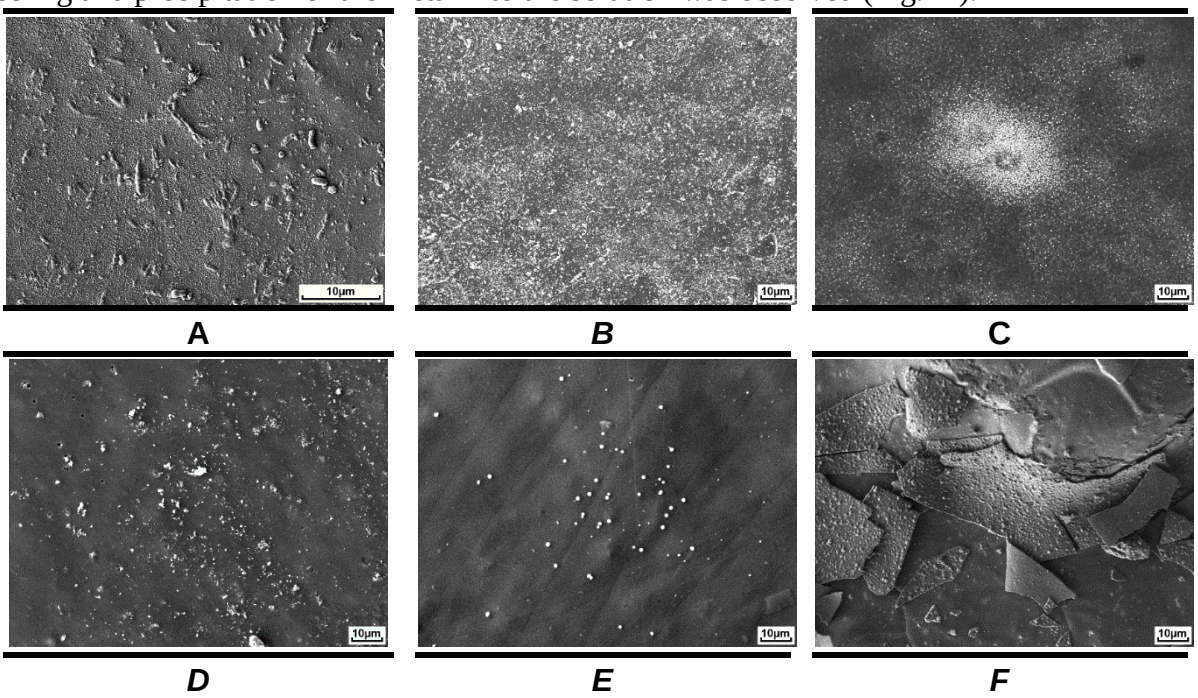

Figure 1. SEM-images of modified surface of hybrid membranes MF-4SK/Pt: a-f - samples 1-5, 7 in Table 1, respectively.

The obtained samples were tested as polymer electrolytes in the membrane-electrode assemble (MEA) of a hydrogen-air fuel cell. The characteristics of MEA with samples 1-3 is higher than with the initial membrane that indicates the catalytic activity of the platinum coated on the membrane surface. The power density of the MEA with sample obtained without stabilizers (92 mW/cm^2) is higher than with 25% vol. EG (76 mW/cm^2) and decreases with the increase in the content of EG in the oxidizer solution. It may be due to the smaller amount of platinum coated on the membrane surface. The power density of MEA with samples 4-5, obtained using PEG, is less than with the initial membrane MF-4SK. The blocking of the platinum catalytic layer and membrane transport channels by the stabilizer could cause it.

Acknowledgements

This work was financially supported by the Russian Foundation for Basic Research (project №18-08-00771), the Foundation for Assistance to the Development of Small Forms of Enterprises program U.M.N.I.K (Project №. 11075/2016).

References

1. *Peighambardoust S.J.* // International journal of hydrogen energy. – 2010. – Vol.35. – P. 9349-9384.
2. *Dobrovol'skii, Yu.A., Volkov, E.V., Pisareva, A.V., Fedotov, Yu.A., Likhachev, D.Yu., and Rusanov, A.L.//* Russ. J. General Chem., 2007, vol. 77, N. 4, p. 766.
3. *Berezina, N.P., Chernyaeva M.A., Kononenko, N.A., and Dolgopolov S.V.// Petroleum Chemistry*, 2011, vol. 51, N. 7, p. 502.
4. *Lee, W.-D., Lim, D.-H., Chun, H.-J., and Lee, H.-I.// Int. J. Hydrogen Energy*, 2012, vol. 37, p. 12629.
5. *Belenov, S.V. Gebretsadik, V.Y., Guterman, V.E., Skikina, L.M., and Lyanguzov, N.V.// Condensed Matter and Interfaces*, 2015, vol. 17, N. 1, p. 37.

FLUID FLOW THROUGH MEMBRANE: AN ANALYTICAL APPROACH FOR NAVIER-STOKES EQUATION BY LIE SYMMETRY ANALYSIS

Mukesh Kumar

Department of Mathematics, Motilal Nehru National Institute of Technology Allahabad, Prayagraj-211004, India, E-mail: *mukesh@mnnit.ac.in*

In the present work, Lie symmetry analysis has been performed to obtain symmetry reductions and group invariant solutions of unsteady viscous incompressible fluid flow through membrane. The Navier-Stokes equation is widely used in diverse physical contexts such as fluid flows, motion of suspended and dissolved solutes in pressure driven membrane processes etc. Lie symmetry transformations have been applied to generate various forms of invariant solutions of the Navier-Stokes equation. All possible vector fields and commutative relations are constructed under invariance property of Lie groups. A repetition of symmetry reductions transforms the equation into system of ordinary differential equations, which provide invariant solutions. The obtained solutions are supplemented by numerical simulation, which exhibit multisoliton profiles, soliton interaction and their annihilation on the variation of time. The nature of solutions is investigated both analytically and physically through their evolutionary profiles by considering adequate choices of arbitrary functions and constants.

Keywords: Navier-Stokes equations, similarity transformations method, symmetry reductions, invariant solutions.

PULSE ALTERNATING CURRENT SYNTHESIS OF Pd/C CATALYSTS AND THEIR APPLICATION IN PEM FUEL CELLS THECHNOLOGIES

[1]Alexandra Kuriganova, [1]Nikita Faddeev, [2]Igor Leontyev, [1]Nina Smirnova
[1]Platov South-Russian State Polytechnic University (NPI), Novocherkassk, Russia
[2]Southern Federal University, Rostov-on-Don, Russia
E-mail: *kuriganova_@mail.ru*

It is well known that platinum is the best catalyst for processes occurring in low-temperature fuel cells and, in particular, in fuel cells with direct oxidation of liquid fuels (methanol, ethanol, formic acid) [1]. An alternative to expensive platinum catalysts may be palladium, which is able to exhibit higher catalytic activity than platinum in the oxidation of alcohols, formic acid, both in acidic and alkaline media. [2].

Both Pt-based catalysts and Pd-based catalysts are often obtained by standard methods for such systems.: impregnation-reduction method [3], polyol process [4]. Electrochemical methods for the preparation of Pd-based catalysts based on the electrochemical reduction of palladium ions from a solution of its salt are presented to a lesser extent. [5].

In this paper, we showed the applicability of the pulse alternating current (PAC) method for the synthesis of a Pd/C catalyst for the proton exchange membrane (PEM) fuel cell application, which was previously successfully applied to the synthesis of Pt/C catalysts [6]. The presence of palladium complexes in the electrolyte after PAC synthesis is demonstrated by UV-vis spectroscopy, which indicates a different mechanism for the formation of Pt and Pd nanoparticles under these conditions. The microstructural characteristics and catalytic activity of synthesized Pd/C catalyst were compared with those of Pt/C catalyst which was prepared under the similar conditions. Pd NPs of Pd/C catalyst exhibited smaller average size and narrower particle size distribution. The electrochemical study highlighted that the electrochemically active surface area of Pd/C catalyst was 1.4 times higher than for Pt/C. The rate of ethanol oxidation on Pd/C catalyst exceeded the rate of ethanol oxidation on Pt/C by 2.6 times, while the rate of oxidation of formic acid was comparable on both catalysts. However, on Pd/C, there was a significant decrease in the overvoltage of the formic acid electrooxidation reaction as compared to the Pt/C sample (by 590 mV).

The authors thank the Russian Foundation for Basic Research (No 18-33-20064 mol_a_ved) for financial support of this work.

References

1. *Ong* B. C., *Kamarudin* S. K., *Basri* S. Direct liquid fuel cells: a review // Int. J. Hydrogen Energy. 2017. V. 42. P. 10142-10157
2. *Yu* X., *Pickup* P. G. Recent Advances in Direct Formic Acid Fuel Cells (DFAFC) // J. Power Sources. 2008. V. 182. P. 124-132.
3. *Moraes* L. P. R., ., et. al. Synthesis and performance of palladium-based electrocatalysts in alkaline direct ethanol fuel cell // Int. J. Hydrogen Energy. 2016. V.*41*. P. 6457-6468.
4. *Lesiak* B., et. al. Effect of the Pd/MWCNTs anode catalysts preparation methods on their morphology and activity in a direct formic acid fuel cell // Appl. Surf. Sci. 2016. V. 387. P. 929-937.
5. *Gioia* D., *Casella* I. G. Pulsed electrodeposition of palladium nano-particles on coated multi-walled carbon nanotubes/nafion composite substrates: Electrocatalytic oxidation of hydrazine and propranolol in acid conditions// Sensors and Actuators B: Chemical 2016. V. *237*. P. 400-407.
6. *Leontyev* I., *Kurihnova* A., *Kudryavtsev* Yu., *Dhil* B., *Smirnova* N. New life of a forgotten method: Electrochemical route toward highly efficient Pt/C catalysts for low-temperature fuel cells // J. Appl. Catal. A: Gen. 2012. V. 431-432. P. 120-125

TRANSPORT CHARACTERISTICS OF POROUS GLASS MEMBRANES IN ELECTROLYTE SOLUTIONS

[1,2]Anastasiia Kuznetsova, [1]Lyudmila Ermakova, [1]Anna Volkova, [2]Tatiana Antropova

[1]St. Petersburg State University, St. Petersburg, Russia, E-mail: *a_kuznetsova95@mail.ru*

[2] Grebenshchikov Institute of Silicate Chemistry, (ISC RAS), St. Petersburg, Russia

Introduction

Recently, much attention has been paid to the study of the physical properties of various materials introduced into porous matrices with a pore diameter of the order of units and tens of nanometers. Porous glassy membranes (PGs) have a number of advantages compared with other porous membrane materials: homogeneous chemical composition, low impurities, thermal, chemical and microbiological stability, transparency in the visible part of the spectrum, adjustable structural characteristics. In this work, iron-containing PGs were produced by introducing an iron (III) oxide into the batch during a melting of sodium borosilicate glass. PGs produced in this way are essentially membrane materials of new generation, important for various practical applications. Analysis of the literature data shows that in recent years the number of studies of morphology and physical characteristics (magnetization, dielectric constant, electrical conductivity, spectral characteristics, etc.) of iron-containing porous glasses has increased, while their characteristics in electrolyte solutions remain unexplored. In this regard the study and comparison of the transport characteristics (filtration coefficient, counterion transport numbers, surface conductivity, streaming potential) of iron-containing micro- and macroporous (MIP and MAP) glasses (Fe-4) in 10^{-1}-10^{-4} M solutions of an indifferent electrolyte NaCl [1,2] and of KNO_3 specific to the silica surface with the parameters of MIP and MAP glasses previously obtained from basic sodium borosilicate (8V) glass were carried out. Taking into account the fact that triply charged counterions have the maximum capacity for specific adsorption, a comparative analysis of transport characteristics of basic 8V membranes in NaCl, KNO_3 and $FeCl_3$ [2] solutions was also carried out.

Experiments

The sodium borosilicate glasses without or with iron oxide (8V or modified Fe-4 glasses) were chosen as objects of study. To obtain MIP glasses (as defined by S.P. Zhdanov [3]), two-phase 8V and Fe-4 glasses in the form of polished discs with diameter of 30 mm and thickness of about 1 mm were leached in 3M solutions of hydrochloric or nitric acid. To obtain MAP glasses (as defined by S.P. Zhdanov [3]), the MIP samples were treated with 0.5M KOH solution at 20 ^{0}C for 4 hours (porous glasses 8V), or for 1, 2.5 and 4 hours (porous glasses Fe-4). Macroporous iron-containing glasses are marked as "1", "2" and "3" in order of increasing alkaline treatment time.

X-ray phase analysis method was used to identify the magnetite phase in MIP and MAP iron-containing glasses. The iron content (averaged over 5–9 EDX spectra for each PG sample) in micro- and macroporous iron-containing membranes is shown in Table 1.

Table 1: The relative iron content in the samples of porous glass

Iron content	Membranes			
	Fe-4 MIP	Fe-4 MAP-1	Fe-4 MAP-2	Fe-4 MAP-3
weight %	2.59	6.31	6.83	10.49
atomic %	1.14	2.36	2.38	3.76

Results and Discussion

Filtration coefficients G used to calculate the through pore radius (r) were measured for MAP 8V and Fe-4 glasses in 0.1 M NaCl [1,2], KNO_3 and $FeCl_3$ [2], solutions before and after the measurements of electrosurface transport characteristics. It was found that with increasing alkaline treatment time of Fe-4 MIP membranes from 1 to 4 hours, the filtration coefficient increases in accordance with the removal of secondary silica from the pore space. During long-term contact (about 4 weeks) of iron-containing MAP glasses with KNO_3 solutions, the filtration coefficient increased 1.5–2 times, which corresponds to an increase in average pore radius from 6.3-15 nm up

to 7.0-17.7 nm. Note that the tendency of an increase in G and r values for Fe-4 MAP glasses during the contact of membranes with 1:1 electrolytes in the neutral pH region was more pronounced than for 8V MAP glasses (their r values changed from 13 up to 13.9 nm in NaCl solutions and from 15 up to 15.6 nm in KNO_3 solutions). This phenomenon can be explained by the greater dissolution of the silica skeleton of Fe-4 glasses than that of 8V. It was also obtained that the values of G and r for 8V MAP in the $FeCl_3$ solutions in the acidic pH region remained practically unchanged (15.1 and 15.6 nm for parallel samples).

The results of measurements of the specific electrical conductivity of the membranes were used to calculate the specific surface conductivity K_S, the cause of which is the excess ion density in the electrical double layer (EDL) in the pore space of the membranes and efficiency ratio α (equal to the ratio of the specific electrical conductivities of pore and free solutions). An analysis of the results shows that the specific surface conductivity in 1:1 electrolyte solutions for both PG compositions has the usual order — 10^{-10} Ω. The K_S values of MIP glasses in NaCl and KNO_3 (fig. 1) solutions are close to each other and tend to slightly increase with increasing electrolyte concentration, which is characteristic of PG, in the pore space of which secondary silica is contained. A decrease in the degree of its swelling with increasing concentration leads to an increase in the average mobility of counterions, which, along with an increase in the absolute value of the surface charge, increases the surface conductivity. Note that a decrease in the amount of secondary silica due to additional alkaline treatment of MIP glasses, leading to an increase in the size of the pore channels, leads to an increase in the average pore mobility of Na^+, K^+ ions and an increase in K_S values. This phenomenon is associated with a large surface charge of the MAP glass compared with MIP glass. The results of the study showed that the α obtained for microporous 8V and Fe-4 glasses are close in a neutral pH region and more than one both in NaCl solutions and in KNO_3 solutions, whereas both for MIP and MAP 8V membranes in the $FeCl_3$ solution there are concentration regions in which the electrical conductivity of the free solution exceeds the electrical conductivity of the pore solution (α <1). That leads to the negative K_S values in these concentration regions as a result of a sharp slowdown in the mobility of specifically adsorbed Fe^{3+}ions in a pore liquid.

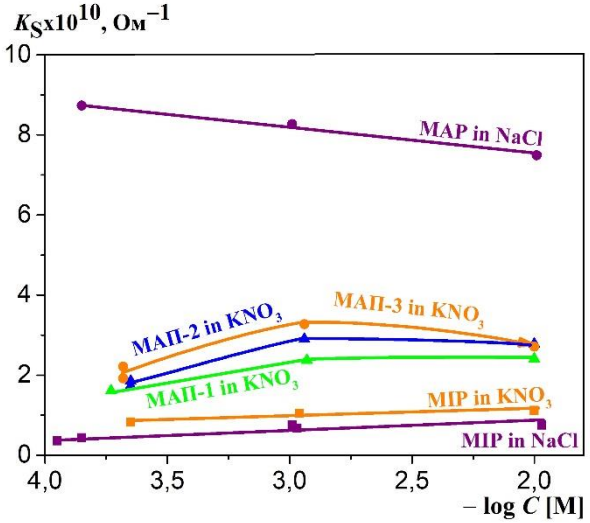

Figure 1. Dependencies of specific surface conductivity of iron-containing Fe-4 porous glasses on the concentration of NaCl[1] and KNO_3 solutions.

It was found that the values of the transport numbers of sodium and potassium counterions (n_+) practically do not depend on the composition of the MIP PGs. As the concentration of the electrolyte increases, the values of n_+ decrease in accordance with the decrease in the contribution of ions of DEL to membrane transport processes. The counterion transport numbers of MAP Fe-4 were larger than those of MAP 8V membranes due to the larger surface charge $|\sigma_o|$ of Fe-4 porous glass. With an increase in the treatment time of the Fe 4-6 MIP membranes with an alkali solution,

that is, with an increase in the pore size, the values of transport numbers K^+ decrease. Note that n_+ values of Na^+ ions are larger than those for specifically adsorbed K^+ ions at $C \leq 0.01$ M. At $C = 10^{-4}$ M all membranes have high selectivity ($n_+ = 0.87 – 1.00$).

From the measured values of the streaming potentials for all the porous membranes under study, the values of the zeta-potentials (ζ) were calculated taking into account the electrical conductivity of the pore solution and the overlapping of DEL. Comparison of the values of ζ-potentials found in NaCl and KNO_3 solutions shows that the values of |ζ| for MAP membranes with the same size of pore channels (8V MAP and Fe-4 MAP-3) decrease during the transition from NaCl to KNO_3 due to the pronounced specificity of potassium ions, resulting in a greater degree of Stern layer filling, and, therefore, to a decrease in the absolute values of the electrokinetic potential. For MAP membranes, the ratios |ζ| for basic PG 8V and a Fe-4 membrane, the same: at concentrations of $C > 10^{-3}$ M, the values of |ζ| in NaCl solutions are higher than in KNO_3 solutions, and at $C < 10^{-3}$ M, the values of |ζ| in both electrolytes converge. The observed patterns are associated both with different specificity of counterions and with the influence of secondary silica contained in the pore space of the MIP glass on all transport characteristics of PG. Electrokinetic potential is negative in the whole study area of NaCl and KNO_3 concentrations and only at very low concentrations of $FeCl_3$. As the $FeCl_3$ concentration increases, the system passes through the isoelectric point and the ζ values become positive.

Acknowledgements

This work was supported by RFBR according to the research project № 17-03-01011. This research was carried out using the equipment of the Research Park of Saint-Petersburg State University (Centre for X-ray Diffraction Studies, Interdisciplinary Resource Center in the direction "Nanotechnology", Chemical Analysis and Materials Research Centre). Authors thank to I. Anfimova (ISC RAS) for help in obtaining glass samples.

References

1. *Ermakova L.E., Grinkevich E.A., Volkova A.V., Antropova T.V.* Structural and electrosurface properties of iron-containing porous glasses in NaCl solutions. I. Structural and transport characteristics of porous glasses // Colloid J. 2018. V. 80. P. 492-500.
2. *Ermakova L.E., Volkova A.V., Kuznetsova A.S.*, E. A. *Grinkevich E.A., Antropova T.V.* Electrokinetic Characteristics of Porous Glasses in Solutions of Sodium and Iron(III) Chlorides // Colloid J. 2018. V. 80. P. 255-265.
3. *Zhdanov S.P.* Porous glasses and their structure // Wiss. Z. Friedrich-Schiller-Univ. Jena: Naturwiss. Reihe. 1987. V. 36. P. 817–830.

PROPERTIES OF INTERFERENCE PATTERNS IN THE TRANSMISSION SPECTRA OF NUCLEAR FILTERS PREPARED FROM THE POLYETHYLENEREPHTHALATE FILMS IRRADIATED BY XENON IONS

[1]Sergey Lakeev, [2]Ann Korneychuk, [3]Polina Semina, [1]Nina Kozlova, [4]Alexander Khorokhorin, [5]Alexander Smolyanskii

[1]Branch of JSC "Karpov Institute of Physical Chemistry", Moscow, Russian Federation,
E-mail: *lakeev@mail.ru*

[2]Lomonosov Moscow State University, Moscow, Russian Federation, *E-mail: anna-chuk@mail.ru*

[3]Reshetnev Siberian State University of Science and Technology, Krasnoyarsk, Russian Federation,
E-mail: *polina_semina@mail.ru*

[4]Scientific and Technological Center of Unique Instrumentation RAS, Moscow, Russian Federation,
E-mail: *sandervan@mail.ru*

[5]D. Mendeleev University of Chemical Technology of Russia, Moscow, Russian Federation,
E-mail: *assa@nifhi.ru*

Introduction

Diffraction effects associated as a rule with the interaction of light waves with micropores are considered when studying the optical properties of nuclear filters (NF) [1]. At the same time relatively little attention is paid to the study of interference patterns (IP) observed in the NF optical spectra [2].

The aim of this study was to investigate the changes in IP observed in the transmission spectra of polyethylene terephthalate (PET) films irradiated with Xenon ions due to chemical treatment and the formation of numerous micropores.

Experiments

NF samples were obtained from biaxially oriented PET films with a thickness of 10±1 μm (State Standard 24234-80); the degree of orientation is 3, the level of crystallinity is not higher than 50%, the polymer density is 1400 kg/m^3, the molecular weight is 31000. The material contained kaolin as a filler; its mass fraction is 0.2. Irradiation with a flux of heavy ions ($_{54}Xe^{129}$, energy ~ 1 MeV/nucleon, ion fluence ~3×10^8 cm^{-2}) was carried out at the Laboratory of Nuclear Reactions named after G.N. Flerov (JINR, Dubna) on the U-400 accelerator of heavy ions in vacuum conditions at room temperature. Chemical treatment of the ion-irradiated PET films was carried out for 3–60 min in aqueous solutions of 0.5–5 N NaOH in the temperature range 303–353 K. As a result an array of open micropores of approximately cylindrical shape with an average diameter of ~ 0.2 μm appeared in a PET film (Figure 1). Registration of the optical absorption spectra of PET and NF samples in the form of disks of Ø25 mm was carried out in air at room temperature using a UV-365 spectrophotometer. The size and distribution of pore size in nuclear material were determined by analyzing of electron microscopic images obtained using a Quanta 200 3D scanning electron microscope.

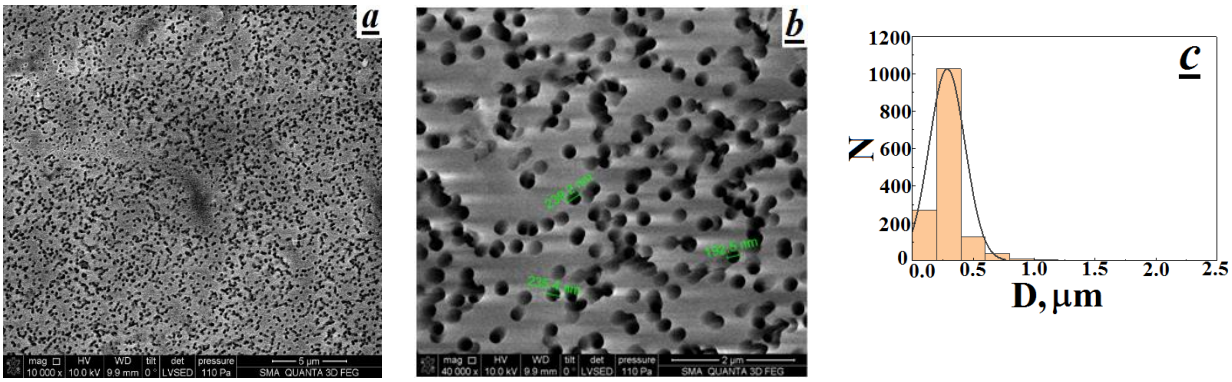

Figure 1. a, b) Electron microscopic images of the nuclear filter samples surface irridated by xenon ions with an energy of ~ 1 MeV / nucleon to ~ 3 x 10 cm-2 polyethylene terephthalate films, after chemical treatment in aqueous solutions of 5N NaOH at 343 K for three minutes; c) pore size distribution function and the result of its approximation by a lognormal distribution.

Results and Discussion

The optical absorption spectrum of a PET film irradiated with xenon ions is determined by an intense absorption band with the maximum at the wavelength region of $\lambda \leq 300$ nm. Its origin can be associated with the terephthalic groups in the PET monomeric array. Besides optical spectrum of PET film contains an interference pattern observed at the wavelengths from 300 to 2500 nm and further to the infrared (IR) region (Figure 2). The interference pattern has the form of a standing wave and includes four wave packets located in the region λ = 320–400 nm (wave packet I in Figure 2); 400-565 nm (II); 565 - 1130 nm (III); 1130 -> 2500 nm (IV). Complex form of the interference pattern is due to anisotropy of the PET refractive index. It can be explained the occurrence of birefringence of PET film as a result of orientation extension when manufacturing [3].

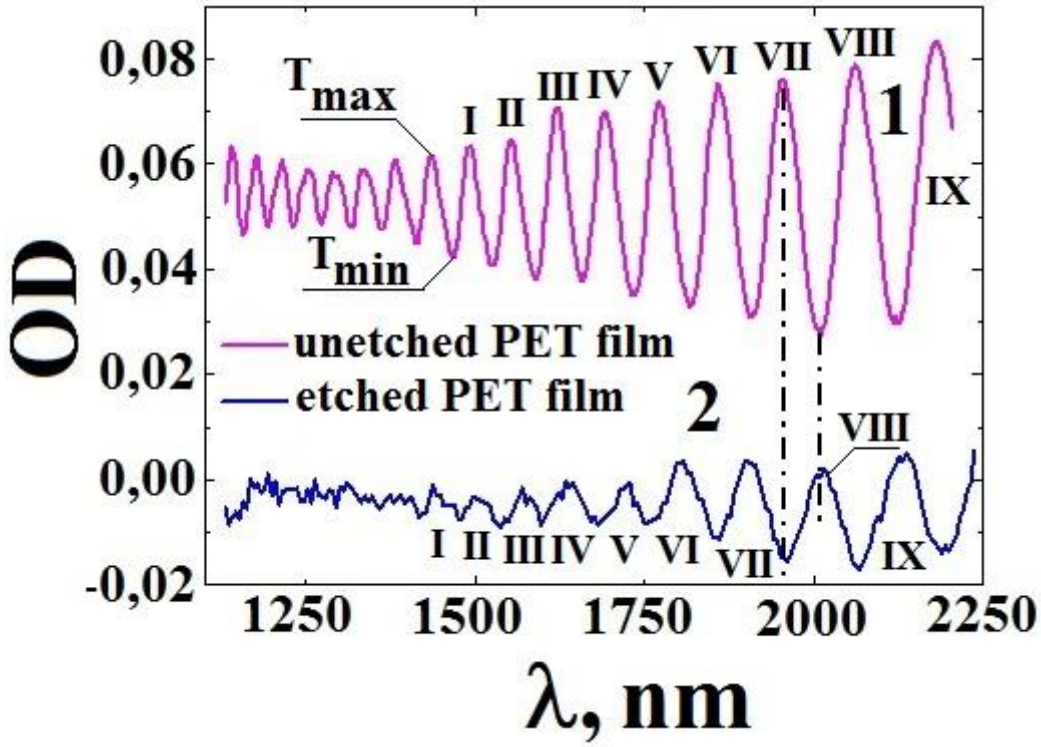

Figure 2. Interference patterns observed in the spectral range of 1250 - 2250 nm in the transmission spectra of the Xe-ion-irradiated PET films before (1) and after (2) chemical treatment in aqueous NaOH solutions at 343 K for three minutes. I - IX - numbers of interference fringes.

Formation of a micropore system significantly changes the shape of the optical absorption spectrum of PET due to the appearance of an intense diffraction background whose long-wave edge appears in the region of $\lambda \geq 1100$ nm. At the same time a low-intensity interference pattern can be observed on the decay of the diffraction background which located at the wavelengths from 1300 - 2500 nm and extending further into the IR region. It was found that the intensity of the long-wave edge of the diffraction background band varies proportionally to λ^{-2} in accordance with the Rayleigh-Gans model [4].

Numerous pores filling the NF significantly reduces the visibility of the interference pattern (Figure 2). Diffraction background "masks" the NF interference pattern in the spectral range $\lambda \leq$ 1400 nm. Interference bands begin to appear in the wavelength region from 1400 to 2250 nm and further. Comparison of interference patterns of ion-irradiated PET films in the optical absorption spectra and NF in the same spectral range shows that in both cases of interference patterns contain the same number of interference fringes of different intensity.

In this case the spectral shape of the interference fringes in the NF interference pattern is significantly deformed compared with the spectral shape of similar interference fringes in the interference pattern of the ion-irradiated PET film. Deformation of the shape of interference

fringes contained in the NF interference pattern may be associated with an increase in the surface roughness of the PET film after the formation of open pores [2].

The most significant difference is the short-wavelength shift of the NF interference pattern relative to the interference pattern for ion-irradiated PET film. The magnitude of the shift corresponds to the change in phase angle by $\pi/2$. Possibly this shift of the NF interference pattern is connected with a thickness decrease of the PET film during the alkaline hydrolysis of the ion-irradiated polymer. Analysis of the both interference patterns shows that the thickness of the PET film decreases from 11.55 to 10.97 μm as a result of chemical treatment. As noted above the visibility of interference pattern in the NF transmission spectra decreases by three times compared with the interference pattern of ion-irradiated PET film (from 0.06 to 0.02). In both cases, there is a tendency to increase the contrast of the interference pattern with increasing wavelength from 1400 to 2250 nm.

The same type of the NF and the ion-irradiated PET film interference patterns (Figure 2), the results of the evaluation of the thickness of PET films before and after etching allow us to conclude that the interference pattern observed in the transmission spectrum of NF is a part of the interference pattern that is observed in the transmission spectra of an ion-irradiated PET film. The rest of the interference pattern in the NF transmission spectrum is hidden under the diffraction background.

Thus it was shown in the present study that the interference patterns observed in the transmission spectra of NF and ion-irradiated PET films have the same origin. It is due to the interference between the probing light beam and the light reflected from the surfaces of the film. However, the formation of a pore structure and a decrease in the thickness of the PET film as a result of chemical treatment lead to a decrease in intensity and a short wavelength shift deformation of the spectral shape of the interference bands due to the appearance of distortions caused by changes in the NF surface topography.

This study was carried out with the support of the Russian Foundation for basic research (project No. 17-07-00524).

References

1. *Mitrofanov A.V., Apel P.Yu., Blonskaya I.V., Orelovich O.L.* Diffraction filters based on polyimide and polyethylene naphthalate track membranes // Journal of Technical Physics. 2006. V. 76, No 9. P. 121 – 127. (in Russian)
2. *Smolyanskii A.S., Smirnova Yu.A., Vasilenko V.G., Burukhin S.B., Briskman B.A., Milinchuk V.K.* Refractive properties of nuclear microfilters // Nuclear Instruments and Methods in Physics Research B. 1999. V. 155. P. 331 – 334.
3. *Yang Sung Mo, Hong Sera, Kim Sang Youl*. Wavelength dependent in-plane birefringence of transparent flexible films determined by using transmission ellipsometry // Japanese Journal of Applied Physics. 2018. V. 57. 05GB03. https://doi.org/10.7567/JJAP.57.05GB03
4. *Lednei M.F., Pinkevich I.P., Reshetnyak V.Yu., Sluckin T.J.* Rauleigh-Gans theory of light scattering by liquid crystals filled with cylindrical particles // Journal of Molecular Liquids. 2001. V. 92. P. 139 – 146.

PURIFICATION OF N-BUTANOL FROM AQUEOUS SOLUTIONS USING NOVEL PERVAPORATION MEMBRANES BASED ON POLYMER COMPOSITES

[1]Alyona Larkina, [1]Alexandra Pulyalina, [1,2]Galina Polotskaya, [2]Ludmila Vinogradova
[1]Saint Petersburg State University, Saint Petersburg, Russia, E-mail: *larckina2010@mail.ru*
[2]Institute of macromolecule compounds, RAS, Saint Petersburg, Russia

Introduction

Pervaporation is a membrane separation technology applying for selective removal of impurities and isolated of industrial important liquids. Comparing with conventional methods, this process has many advantages of low energy consumption, easy operation, and moderate conditions. Moreover, pervaporation is not limited by thermodynamic VLE (vapor-liquid equilibrium) and is efficient in separating azeotropic mixtures.

In order to overcome the trade-off relationship between permeability and selectivity, several attempts have been made such as modification polymer materials with different fillers, thermal annealing and chemical cross-linking. Among them, preparation of mixed matrix membranes is the most popular and effective method since it allows combining ease of fabrication and reasonable separation performance of polymer material and mechanical stability and exceptional transport properties of inorganic fillers.

This paper presents the study of membranes based on the industrial polymer poly(m-phenylene-iso-phtalamide) (PA) modified with star-shaped macromolecules (SM) with a C_{60} fullerene core containing 6 arms of polystyrene (PS) and 6 arms of poly-tret-butyl methacrylate (PTBMA) for n-butanol dehydration via pervaporation.

Experiments

The composites PA/SM were prepared by mixing solutions of PA and SM in N,N-dimethylformamide. The polymer films were obtained by pouring onto a glass plate and dried in a vacuum oven at 60 ° C to constant weight.

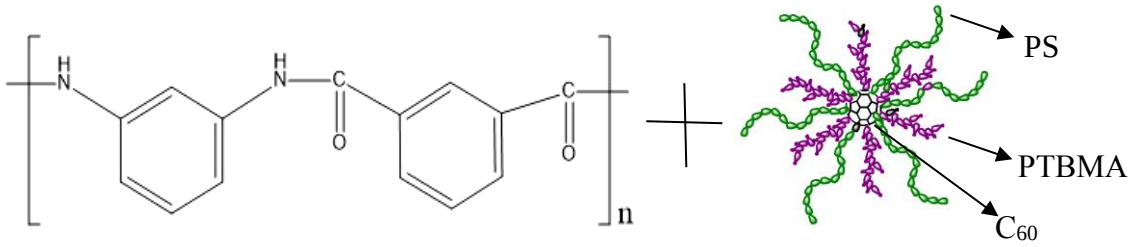

Figure 1. Structures of PA and hybrid star-shaped macromolecule.

Membranes` structures were studied by scanning electron microscopy (SEM), atomic force microscopy (AFM) and X-ray diffraction analysis. Thermal characteristics were obtained during thermogravimetric analysis (TGA) and the method of differentiating scanning calorimetry (DSC). The transport properties of the membranes were studied using pervaporation experiments on the dehydration of n-butanol.

Results and Discussion

The physical characteristics of new hybrid materials based on PA with the addition of a star-shaped fullerene-containing modifier were studied.

The effect of the star macromolecules inclusion in the PA matrix on the membrane morphology was studied by SEM. Figure 2 shows micrographs of cross-section for PA and PA/SM containing 2 and 5 wt% star filler. It is observed that significant changes occur in the internal structure of PA membrane with the inclusion of a star modifier.

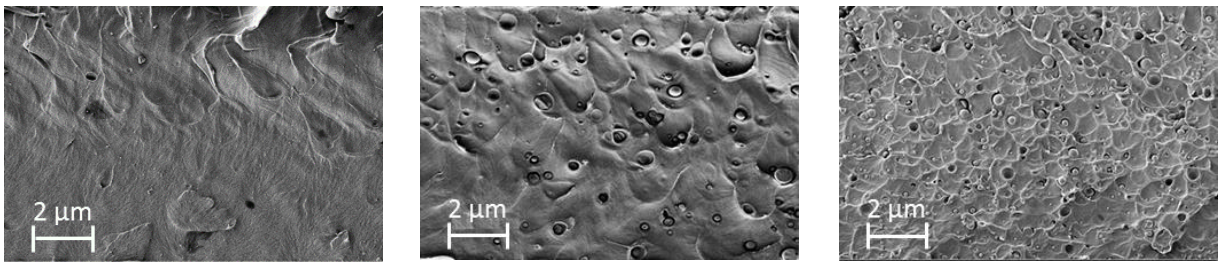

(a) PA *(b) PA/SM(2%)* *(c) PA/SM(5%)*

Figure 2. SEM micrographs of and membrane cross-section.

The table 1 presents some physical parameters of the membranes, namely density and contact angels for water and n-propanol.

Table 1: Physical parameters of membranes

Membrane	Density, g/sm^3	Contact angles	
		Water	Toluene
PA	1.312	79.2	20.6
PA/SM(2%)	1.305	82.5	16.5
PA/SM(5%)	1.299	86.7	15.6

As a result of SM inclusion, modified membranes exhibit less compact structure and lower density than that of the pure PA membrane.

Additives of SM containing nonpolar PS and PTBMA arms promote an increase the contact angle of water and decrease contact angle of n-propanol on the membrane surface (Table 1). The surface of the modified membranes becomes more hydrophobic compared to the surface of PA membrane.

The transport properties of polyamide-based membranes containing 0, 2, 5 wt.% star-shaped modifier were investigated during vacuum pervaporation for dehydration of n-butanol (experimental conditions — 50 ° C, residual pressure under the membrane — 0.2 bar, the feed — 2-12 wt% water).

Figure 3a and 3b show the main transport parameters of the membranes: the total flux and the separation factor as a function of the water concentration in the feed. Increase of water concentration in the feed leads to the increasing total flux through all the membranes. The higher SM containing the more water passes through membranes. As it is shown in Figure 3b, separation factor of all membranes decrease with an increasing the water concentration in the feed.

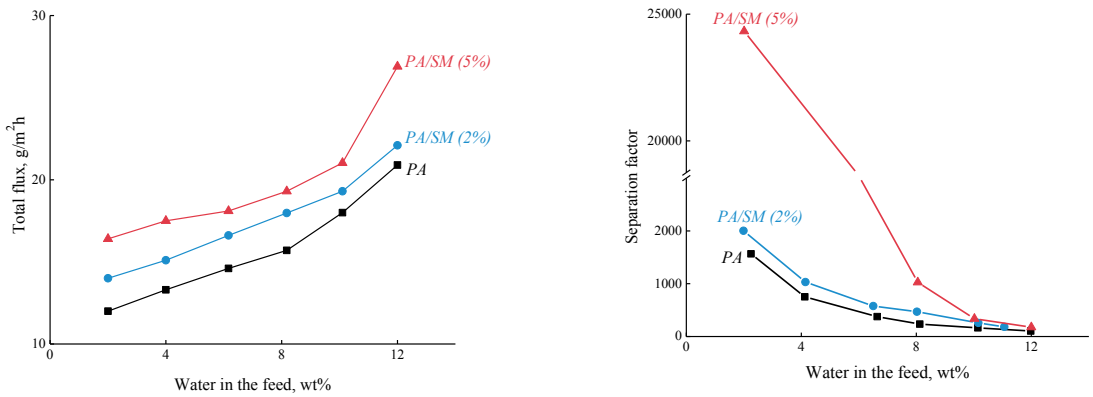

(a) *(b)*

Figure 3. Dependence of (a) total flux (water-n-butanol) on water concentration in the feed and (b) water concentration in permeate on water concentration in feed and for pervaporation water-n-butanol mixture, 50 °C.

Conclusions

Novel mixed matrix membranes with star-shaped fullerene-containing nanomodifiers for diffusion separation methods characterized by high thermal stability, mechanical strength and chemical stability have been developed. Increasing of the star-shaped modifier content up to 5 wt% SM leads to decreasing density. Furthermore, the PA/SM membrane has a relatively loose structure that is suitable for the penetration of molecules and formation of transport channels. It is shown that the mixed matrix membranes have improved transport properties and are highly efficient in the process of n-butanol dehydration. PA/SM membranes the total flux through membrane increases, and the value of separation factor increases with the growth of SM content in membranes.

Acknowledgments

The investigation was carried out by the financial support of Russian Science Foundation (RSF), grant 18-79-10116.

STUDY OF MECHANISMS OF THE IONS TRANOSPORT IN ACTIVE NANOFILTRATIONAL MEMBRANES CONTAINING GOLD NANOPARTICLES

[1]Denis Lebedev, [1]Maksim Novomlinsky, [1]Vladimir Kochemirovsky, [2]Tatiana Antropova, [2] Irina Anfimova

[1] Saint Petersburg State University, St. Petersburg, Russia, E-mail: *denis.v.lebedev@gmail.com*

[2] Grebenshchikov Institute of Silicate Chemistry RAS (ISC RAS), St. Petersburg, Russia

Introduction

Nowadays, the ion transport in nanopores and nanochannels attracts a great interest. This scientific direction is relevant and exhibits a fundamental value in various fields of science and technology, including the separation of mixtures and the production of pure substances [1], the electrochemical conversion of energy [2], the development of chemical sensors [3], the physiology, molecular biology of cells [4], etc.

Hybrid or composite membranes containing various nanoparticles have been actively studied in the last decade [5-7]. It was previously shown that the presence of different inorganic particles in the membrane structure can lead to a change in the transport and selective properties of the membrane. On the other hand, investigation of the shift of the plasmon absorption band of gold nanoparticles with the presence of various ions and molecules in their surroundings is also very important problem [8]. Thus, the combination of the transport properties of nanochannels and particles exhibiting plasmon resonance has great potential for application in many technologies.

The current work is aimed to studying of new mechanisms of selective separation of solution components in the presence of an inhomogeneous electromagnetic field inside the pores of the micro- and nanofiltration membranes.

Experiments

In this work, the method of laser-induced metal deposition is used for the formation of a new type of membrane [9]. Laser radiation is monochromatic and has a small beam divergence. Due to the possibility of focusing, the laser beam is a good source of energy for initiating chemical reactions in micron-sized regions, in turn; the irradiation parameters can be selected in such a way that the radiation power sufficient for proceeding the chemical reaction is reached only at the focal point of the laser beam. One of the most important factors of the method of laser-induced metal deposition is the possibility of the formation of the deposits on the surface of the optically transparent dielectrics.

We propose to use various porous glasses as a basis for the synthesis of membranes. Porous glass (PG) samples (in the form of plane-parallel polished plates $10 \times 10 \times 1.0$ mm^3 in size) have been prepared by chemical etching of phase-separated sodium borosilicate glass with two-frame structure [10] in HCl and KOH solutions consistently with subsequent washing in distilled water and drying at 120 ° C in an air atmosphere as described in [10, 11]. The PG's porosity and average pore diameter are 0.5 (cm^3/cm^3) and 25 nm respectively [12].

The potentiometric methods was use in order to study the selective properties of the membrane. Previously, this methodology was successfully applied for studying the transport properties of membranes [13, 14]. In this method, a potential difference between two electrolyte solutions of different concentrations separated by a membrane is measured. The main element of the setup is an electrochemical cell consisting of two half-cells divided by the test membrane. As material for production of a cell transparent plexiglas will be used optically, it is necessary to have an opportunity to light a membrane with an external light source. A double-junction Ag/AgCl reference electrode connected to the input of a P-20 X potentiostat (Elins, Russia) was placed in each of the half-cells. In this configuration, the potentiostat was used as a millivoltmeter with high input resistance (10^{12} Ω). For minimization of influence of concentration polarization pumping of solutions through half-cells will be used.

Results and Discussion

A new type of membrane containing gold nanoparticles was synthesized. A porous glass with an average pore size of 20 nm was used as the basis for these membranes. Gold nanoparticles were synthesized inside the pores. As part of the work, the selective properties of the obtained membranes in model solutions of KCl and NaCl salts were investigated. It was shown that the formation of particles inside the pores of the membranes leads to a dramatic change in their selective properties. The results obtained can be widely used in various technologies.

Acknowledgment

The reported study was funded by RFBR according to the research project № 19-08-00823.

References

1. *Strathmann, Heiner*. Ion-exchange membrane separation processes. Vol. 9. Elsevier, 2004.
2. *Cipollina, Andrea, and Giorgio Micale, eds*. Sustainable energy from salinity gradients. Woodhead Publishing, 2016.
3. *Banica, Florinel-Gabriel.* Chemical sensors and biosensors: fundamentals and applications. John Wiley & Sons, 2012.
4. *Malmivuo, Plonsey, Jaakko Malmivuo, and Robert Plonsey*. Bioelectromagnetism: principles and applications of bioelectric and biomagnetic fields. Oxford University Press, USA, 1995.
5. *A. B. Yaroslavtsev,* Correlation between the properties of hybrid ion-exchange membranes and the nature and dimensions of dopant particles. // Nanotechnologies in Russia, 2012. 7(9-10), 437-451.
6. *A.I. Sidorov, & T. V. Antropova.* Synthesis of silver nanospheroids in silver-containing nanoporous glass under the effect of nanosecond laser pulses. // Quant. Electron., 2018. 48 (10), 962-966.
7. *A.S. Pshenova, A.I. Sidorov, T.V. Antropova, & A.V. Nashchekin*. Luminescence enhancement and SERS by silver nano- and microdendrites in nanoporous silicate glasses. // Plasmonics, 2019. 14, 125-131.
8. *B. G. Ershov, V. I. Roldughin, V. M. Rudoy, et. al.* Size effect in plasmon absorption of gold nanoparticles upon adsorption of ozone. // Colloid Journal, 2012. 74(6), 686-689.
9. *V. A. Kochemirovsky, et. al.* Sorbitol as an efficient reducing agent for laser-induced copper deposition. // Applied Surface Science, 2012. 259, 55-58.
10. *T.V. Antropova, S.V. Kalinina, T. G. Kostyreva, I. A. Drozdova, & I. N. Anfimova.* Peculiarities of the Fabrication Process and the Structure of Porous Membranes Based on Two-Phase Fluorine-and Phosphorus-Containing Sodium Borosilicate Glasses. // Glass Phys. Chem., 2015. 41 (1), 14–25.
11. *A. Gutina, T. Antropova, E. Rysiakiewicz-Pasek, K. Virnik, & Yu. Feldman.* Dielectric relaxation in porous glasses. // Micropor. Mesoporous Materials, 2003. 58, 237–254.
12. *V.A. Kreisberg, T.V. Antropova* Changing the relation between micro- and mesoporosity in porous glasses: The effect of different factors. // Micropor. Mesoporous Materials, 2014. 190 (1), 128-138.
13. *D. V. Lebedev, et. al.* Preparation and ionic selectivity of carbon-coated alumina nanofiber membranes.// Petroleum Chemistry,2017. 57(4), 306-317.
14. *V. S. Solodovnichenko, D. V. Lebedev, V. V. Bykanova, et. al.* Carbon Coated Alumina Nanofiber Membranes for Selective Ion Transport. // Advanced Engineering Materials, 2017. 19(11), 1700244.

OBTAINING ELECTRIC ENERGY BY REVERSE ELECTRODIALYSIS

Sergey Loza, Kristina Dmitrieva, Alexander Korzhov, Nikita Smyshliaev, Nazar Romanyuk, Ilya Bondarenko, Natalia Loza

Kuban State University, Krasnodar, Russia, E-mail: *s_loza@mail.ru*

Introduction

This work is aimed to solve a global problem - the use of renewable energy sources, such as solar energy. Recently, the interest of direct conversion a gradient of a salt concentration between seawater and fresh water into electric power using reverse electrodialysis has sharply increased.

Reverse electrodialysis is an electromembrane process of generating electricity using a concentration gradient. This method of obtaining energy is environmentally friendly. The resulting electricity can be obtained: by mixing sea and river water; at the enterprises, dumping sewage with high salinity; on ships of the navy, to create energy-saving devices.

Experiments

The cell for reverse electrodialysis consists of alternating cationic and anion-exchange membranes, between which salt and fresh water flows. The potential difference arising on the membranes is summed up and can be used as an energy source. MK-40 and MA-40 were used as ion-exchange membranes. The number of paired chambers in the cell was 5, the working size of the membranes was 5x20 cm^2; model solution of salt water: saturated NaCl (350g/l), and fresh water: NaCl with a concentration of from 0.001 to 3.5 g/l; flow rate through all chambers – 260 ml/min; load range: 0-500 Ohms. To convert the current of ions into electric current, it is necessary to use the RedOx system. The RedOx system was used: a mixture of 0.025 M $K_4[Fe(CN)_6]$, 0.025 M $K_3[Fe(CN)_6]$, and 0.25 M NaCl. solutions. In this case, a reversible reaction proceeded:

$$[Fe(CN)_6]^{3-} + e \leftrightarrow [Fe(CN)_6]^{4-}$$

In another case, the electrode chambers were fed with a saturated solution of sodium chloride to abandon special RedOX system, while irreversible electrolysis reactions occurs:

(–)K:	$2H_2O + 2E \rightarrow H_2\uparrow + 2OH^-$
(+)A:	$4H_2O - 4E \rightarrow O_2\uparrow + 4H^+$
	$2CL^- - 2E \rightarrow CL_2\uparrow$

Dependence of power versus current density were obtained by connecting various ohmic loads.

Results and Discussion

The dependence of the received power on the current density on the cell is shown in Fig 1.

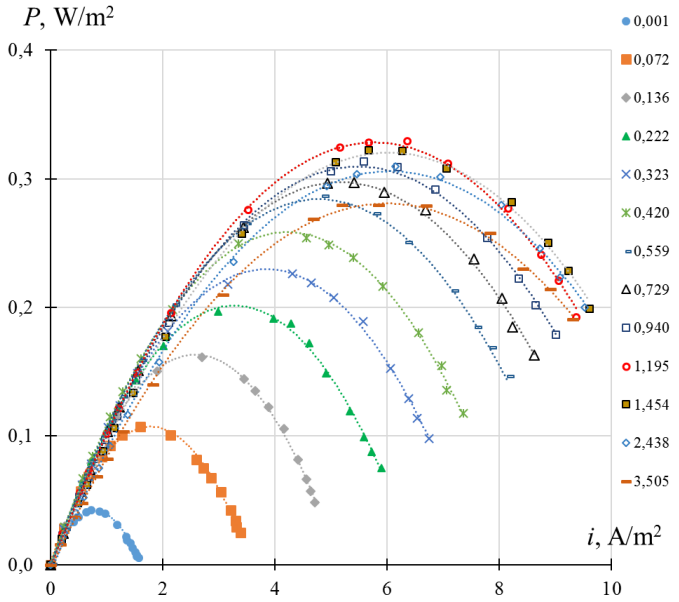

FIGURE 1. DEPENDENCE OF THE MAXIMUM SPECIFIC POWER ON THE CURRENT DENSITY FOR VARIOUS CONCENTRATIONS OF NACL IN A MODEL SOLUTION OF FRESH WATER. NUMBERS IN THE LEGEND - NACL CONCENTRATION, G/L.

The dependence of the maximum power received on the concentration of sodium chloride is shown in Fig.2. As the salt concentration in fresh water increases, the power grows due to a decrease in the ohmic resistance of the fresh water chambers. When the concentration rises, the power characteristics decrease due to a decrease in the concentration gradient.

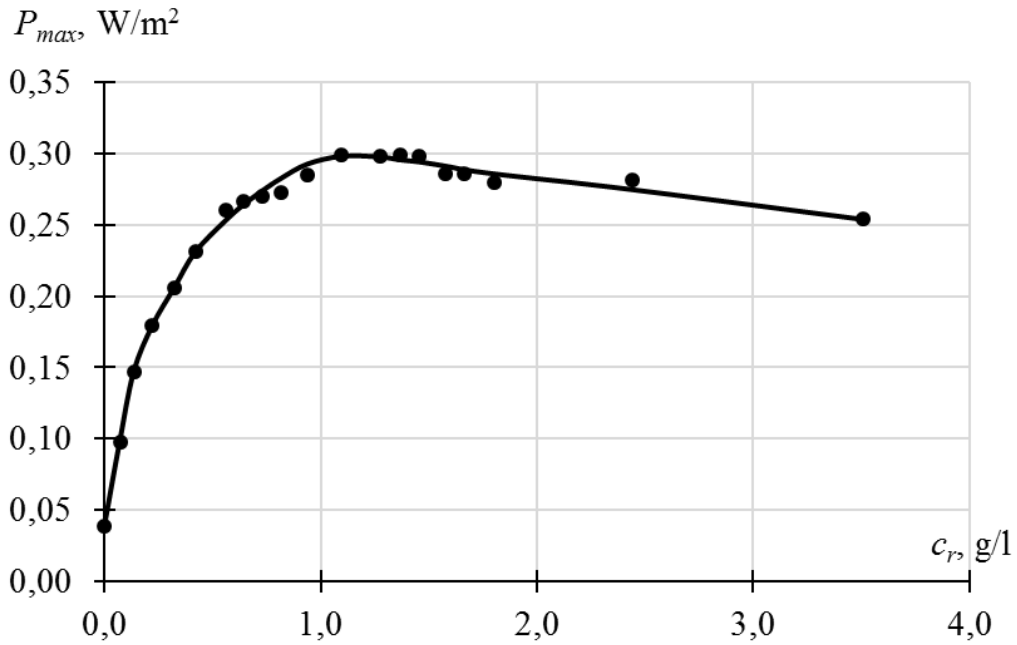

Figure 2. Dependence of the maximum specific power on the concentration of NaCl in the model solution of fresh water for various RedOx systems.

The effect of various RedOx systems on the electrical power received was then evaluated. When refusing to use ferri/ferrocyanide in electrode chambers, the received power decreases several times.

Conclusions

A laboratory setup was created to obtain the power characteristics of the reverse electrodialysis cell. The influence of salt concentration in fresh water on the output power is determined. It is shown that the presence of a special RedOx system significantly increases the power received.

Acknowledgments

The reported study was funded by RFBR and Krasnodar region according to the research project № 19-48-230047.

References

1. *Pattle, R.* Production of Electric Power by mixing Fresh and Salt Water in the Hydroelectric Pile // Nature – 1954. – 174. – 4431. – 660–660.
2. *Weinstein, J.* Electric power from differences in salinity: the dialytic battery / J. Weinstein and B. Leitz // Science, – Vol.191. – 1976. – P.557 – 559.
3. *Turek, M.* Cost-effective electrodialytic seawater desalination, Desalination// 153. – 2002. – 371. – 376.
4. *Długołęcki, P.* Current status of ion exchange membranes for power generation from salinity gradients // *P. Długołęcki, K. Nymeijer, S. Metzand M. Wessling* // Science, –319. – 2008. – P. 214 – 222.

TRASNSPORT CHARACTERISTICS OF BILAYERED PROFILED MEMBRANES MODIFIED BY SUPERBRANCHED POLYMERS

Sergey Loza, Stanislav Utin, Natalia Loza, Victor Dotsenko
Kuban State University, Krasnodar, Russia, E-mail: *s_loza@mail.ru*

Introduction

One of the promising way for the development of electro-membrane technologies is the preassigned modification of ion-exchange membranes in order to give them the necessary properties to increase the efficiency of the electrodialysis process. Promising method for such modification is profiling of membranes with their simultaneous surface modification with various modifiers, including functionalized hyperbranched polymers.

Objects and methods of research

In this work, the profiled membranes obtained by the technology, described in [1], were investigated. It is known that during hot pressing of ion-exchange membranes, their microstructure changes: the number of macro- and mesopores increases, which leads to an increase in the diffusion permeability of samples and a decrease in their selectivity [2, 3]. The application of a layer of a homogeneous cation-exchange film on the membrane surface reduces negative effects [3].

Samples of membranes were made, on the surface of which a different amount of MF-4SK solution in isopropanol mixed with functionalized hyperbranched polymer based on Boltorn H20 was applied [4]. The specific volumes of the applied modifier were 0.25, 0.5, 1.0, 1.5, and 2.0 ml/cm^2. The thickness of the samples as a result of the application of the modifier film to the membrane surface did not change within the measurement error of the micrometer.

In this work, we used the method of studying the diffusion of an electrolyte solution through a membrane into deionized water. The calculation of the diffusion flux was carried out on the basis of an experimental determination of the diffusion rate of electrolyte through the membrane in a non-flowing two-chamber cell. The cell was thermostated in an air thermostat at a temperature of 25 °C. The volume of each chamber was 100 ml. The membrane under investigation was fixed between two chambers. Control of the increase in the concentration of the electrolyte in the water chamber was carried out by the conductometric method using platinized platinum electrodes connected to an immittance meter.

Experiments

Profiled samples of heterogeneous membranes were used as initial membranes for modification. The membrane surface was pretreated with “glacial” acetic acid to increase the adhesion of the modifier according to [5]. Then a mixture consisting of a 10% solution of perfluorosulfopolymer in isopropyl alcohol, a phosphorylated hyperbranched polymer based on Boltorn H20 and glacial acetic acid was applied on a profiled surface. After evaporation of volatile solvents (isopropanol and acetic acid), the membranes were dried at 90 °C. With this method of obtaining bilayer membranes, polyethylene is interlaced with the hydrophobic part of the sulfonated polytetrafluoroethylene matrix to form a new intermediate layer, which due to the presence of the hydrophobic part has high adhesion to the hydrophobic part to sulfonated polytetrafluoroethylene, and due to the polar part - high adhesion to the substrate membrane. This method allows to obtain mechanically strong membranes with improved electrochemical characteristics that can function stably in electrodialysis cells.

Results and Discussion

The dependence of the diffusion flow of salt upon diffusion of 0.1 M NaCl into the deionized water on the amount of modifier is shown at the Figure 1. Since the membrane has one side with a smooth surface and the other is profiled, the measurements were performed with a different orientation of the membrane to the salt flux. The diffusion permeability of the profiled membrane decreases with an increase in the amount of modifier.

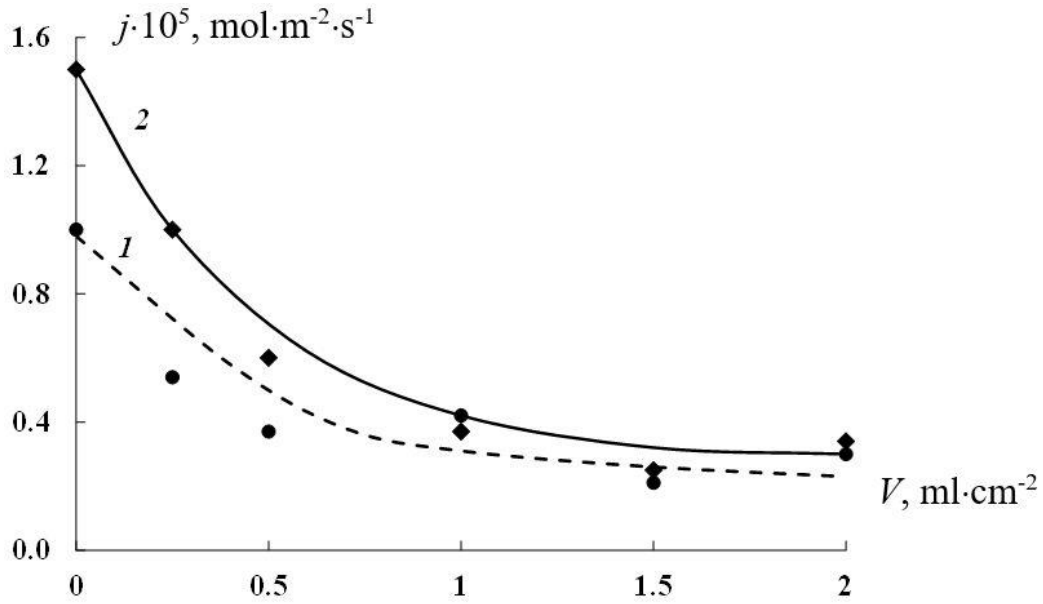

The orientation of the membranes in relation to the flux of sodium chloride: 1 - smooth surface; 2 - profiled surface.

Figure 1. Dependence of the diffusion flux density of sodium chlorided through the membranes on the specific volume of the applied modifier.

Conclusions

In present work, profiled membranes were obtained, the surface of which was modified, as well as its mixture of perfluoropolymer with functionalized phosphoric acid groups, hyperbranched polymer, the optimal amount of modifier was determined. The dependence of diffusion permeability on the amount of modifier was measured, asymmetry of diffusion permeability was found depending on the orientation of the membrane to the salt flow. The resulting membrane is a promising material for use in electrodialysis.

Acknowledgments

The present work is supported by the Ministry of Education and Science of Russia within the framework of the base part project №10.9572.2017/8.9.

References

1. *Zabolotskii V.I., Loza S.A., Sharafan M.V.* // Pat. RU № 2284851, A. № 2005101531/15, 24.01.2005; publ. 10.10.2006.
2. *Zabolotskii V.I., Loza S.A., Sharafan M.V.* // Russian Journal of Electrochemistry, Vol. 41, N. 10, 2005, pp. 1053–1060.
3. *Loza, S.A., Zabolotsky, V.I., Loza, N.V.* et al. Pet. Chem. (2016) 56: 1027.
4. *Utin, S.V., Loza, S.A., Bespalov, A.V.* et al. Pet. Chem. (2018) 58: 137.
5. *Sheldeshov N.V., Melnikov S.S., Zabolotskii V.I.* // Pat. RU № 2516160. // 2014. № 14.

SORPTION ACTIVE CARBON MEMBRANES

Aleksandr Lysenko, Olga Astashkina, Nadezhda Diankina
Saint Petersburg State University of Industrial Technologies and Desig, Saint Petersburg, Russia
E-mail: *thvikm@yandex.ru*

Introduction

In the privies publication [1, 2, 3] synthesis and properties of activated carbon fibers based on new precursor – polyoxadiazole – were discussed.

Experiments

In the present report on describe the process to obtain the adsorption active carbon-carbon composites in the form of electro conductive membranes. To produce the membranes on utilized as the filling materials or the nonwoven materials or the tissues made of activated carbon filaments. The carbonized phenolic resin acts as a matrix. The scheme employed in order to make the composite membrane is as follows: in the first step on impregnate the activated carbon fiber material by phenolic resin so on obtain the prepreg; in the same time on polymerize the plate and in the same time on polymerize the resin at the temperature of 175-180 °C. After that on carbonize the previous obtained plate the inert atmosphere by the temperature 750-800 °C.

On can obtain the carbon-carbon composite plates with various thickness.

Results and Discussion

The structure of plates first of all depends on the structure of the filling materials. The thickness and apparent density depends not only on the structure of fibrous fillers but also on the matrix quantity and the compression degree of prepreg. Typically the composite plates are the thickness 0.5-3 mm and bulk density 1,3-1,4 g/cm^3. The plates also possess the electrical conductivity. There resistivity is usually ranges from 0,02 to 0,03 Om·cm.

Regarding the adsorption capacity it can be stated that the obtained carbon-carbon composites can adsorb more of some metal ions then the precursor activated carbon fibers materials. Right for example the adsorption of Ag^+ and Cr^{6+} ions activated carbon fibrous materials was 9 mg/g and 20 mg/g respectively. In the same time the composite adsorption capacity for Ag^+ and Cr^{6+} ions under the same conditions was 18 mg/g and 40 mg/g. Adsorption conditions was: temperature – 22 °C, time of adsorption 60 min, initial concentration of metal ions 100 mg/l.

The adsorption active carbon-carbon composite plates can be utilized as a filters for metal ions removal from contaminated waters or in some electrochemical processes. Also they may be the catalysts carriers.

References

1. *Rusova N. In. Astashkina O. V., Kashirsky D. A., Myznikov L. V.* On some properties of modified polyoxadiazole fibers-precursors of carbon fiber materials. Vestnik SUTD, № 2, 2017, Pp. 69-75
2. *Lysenko A., Astashkina O., Igor Landgraf I.* Carbon-carbon gas diffusion substrates for gas diffusion layers and electrodes // International conference «Ion transport in organic and inorganic membranes» Conference Proceedings, P.162, 21 – 26 May 2018
3. *Rusova N., Astashkina O, Lysenko A.* Ion exchange and adsorption of metals on materials from activated carbon fibers // International conference «Ion transport in organic and inorganic membranes» Conference Proceedings, P.240, 21 – 26 May 2018

PROTON-CONDUCTING HYBRID MEMBRANES BASED ON POLYBENZIMIDAZOLES AND SILICA WITH IMIDAZOLINE-FUNCTIONALIZED SURFACE

Anna Lysova, Andrey Yaroslavtsev
Kurnakov Institute of General and Inorganic Chemistry RAS, Moscow, Russia
E-mail: *ailyina@yandex.ru*

Introduction

The energy production methods widely used at the present moment are drastically affecting the environment. This forces the development of environmentally-friendly and, in particular, renewable energy sources. In respect to long-term storage, the most promising technology is the hydrogen cycle based on a fuel cell (FC). About 90% of fuel cells produced currently are the low-temperature proton-exchange membrane FCs. Their main advantages are a quick start-up and simplicity of operation. At the same time, a high humidity of the supplied gas should be maintained, and a high-purity hydrogen should be used [1]. This makes it impossible to use a cheaper hydrogen produced by conversion of the natural gas, alcohols or biomass [2]. Therefore, it is necessary to develop fuel cells able to operate at 120-200°C and at relatively low humidity. In this context, considerable attention is drawn to the membranes based on polybenzimidazoles (PBIs) doped with phosphoric acid, that are able to operate at elevated temperatures, have high chemical resistance, and thermal stability.

Stabilization of phosphoric acid in the polymer matrix is one of the primary challenges in the development of PBI-based composite membranes. The main approach is associated with introduction of inorganic dopants with a high sorption activity [3]. In addition, the conductivity of PBI membranes usually correlates with the phosphoric acid content, the latter acting both as a charge carrier and conduction medium.

The aim of the present paper is to study hybrid PBI membranes containing silica particles with propyl-imidazoline groups-modified surface (SiO_2-Im).

Experiments

The phthalide-containing PBI (PBI-O-PhT) and polybenzimidazoles obtained from 2,6- or 2,5-pyridinedicarboxylic acids (PBI-2,6Py and PBI-2,5Py) were used as starting materials. Two methods were used for polymer modification: casting of a solution with the pre-synthesized silica particles (SiO_2Im-ex, the 1st method) or with a precursor for their synthesis (SiO_2Im-in, the 2nd method). In both synthesis methods, the silica content was varied from 0 to 20 wt%. All the obtained samples were kept in phosphoric acid at 25°C for 7 days. Its concentration was 75% and 60% for PBI-O-PhT and PBI-2,5Py (PBI-2,6-Py), respectively. After the treatment, the weight of the membranes increased 2.5-3 fold. Finally, the samples were dried under vacuum at 70°C for 4 h.

Results and Discussion

Incorporation of the silica with additional basic nitrogen atoms on the surface leads to an increase in the doping degree of phosphoric acid for all the studied polymers. The most pronounced increase is observed in the case of modification with SiO_2Im-in. It is probably due to a smaller particle size compared with SiO_2Im-ex or a higher sorption capacity. The interactions between 3-(2-imidazolin-1-yl)propyl group of silica and nitrogen-containing moieties of the PBI can also play a role in the packing of polymer chains. As a result, the grafted functional groups of silica and the nitrogen atoms of the PBI itself become more accessible to the acid.

With increasing relative humidity, the growth of conductivity is observed for all the PBI-based hybrid membranes (Fig. 1). For the membranes obtained by the 1st method, the highest conductivity increase is 26% for the PBI-O-PhT/SiO_2Im-ex-15 membrane (at RH = 50%) and 43% for the PBI-2,6Py/SiO_2Im-ex-10 membrane (at RH = 85%). For the membranes obtained by the 2nd method, the conductivity increases up to 32% for the PBI-2,6Py/SiO_2Im-in-10 membrane (at RH = 50%) and 40% for the PBI-O-PhT/SiO_2Im-in-10 (at RH = 50%). The reason for the

conductivity enhancement in this case is the increase in charge carrier concentration due to a larger dissociation degree of phosphoric acid in a more dilute solution within the pores. In addition, the growth of relative humidity lowers the viscosity of the "solution" within the membrane (due to an increased water uptake) thus promoting an increase in ion mobility and, consequently, an increase in conductivity.

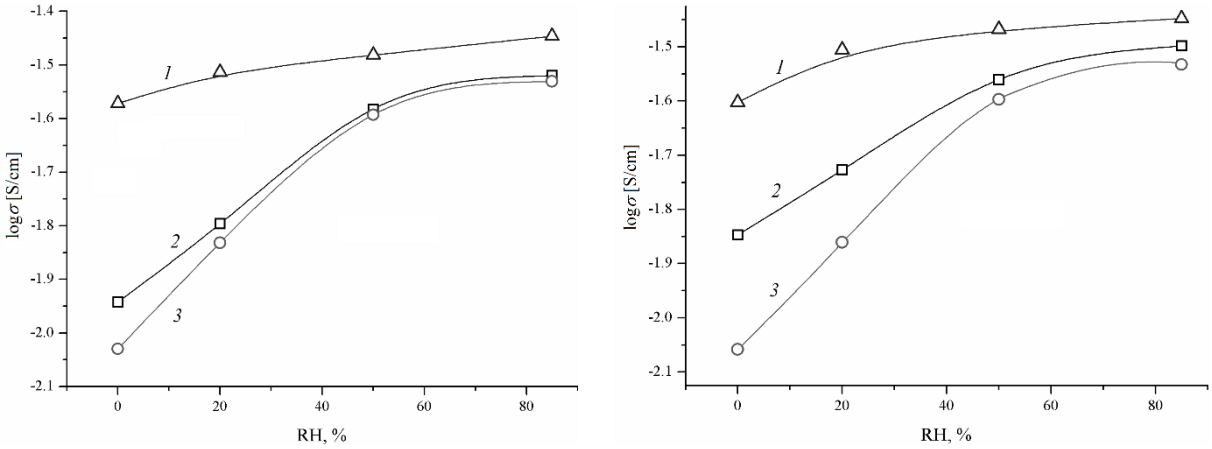

Figure 1. Plots of conductivity versus relative humidity at 90°C for the PBI-O-PhT (1), PBI-2,5Py (2), PBI-2,6Py (3) membranes containing 15 wt% of SiO_2Im-ex (a) and 15 wt% of SiO_2Im-in (b).

The temperature dependence of the conductivity in composite membranes without additional wetting revealed that incorporation of the modified silica leads to a conductivity enhancement regardless of the membrane preparation method. For the hybrid membranes obtained by the 1st method, the maximum in the conductivity-composition curves appears at 5-15 wt% of SiO_2Im-ex. Further increase in its content leads to a decrease in the hybrid membrane conductivity. For the membranes modified by the 2nd method, the highest conductivity enhancement is observed for the PBI-2,5Py-based samples. Notably, the difference in the structure of the obtained hybrid membranes (mutual positions and packing of polymer chains) has a significant impact on the observed composition effect.

Incorporation of small amounts of silica surface-modified with basic groups results in a reduction of hydrogen permeability. Yet, in the case of SiO_2Im-ex incorporation, the increase in its concentration leads to a considerable enhancement of gas permeability, whereas in the case of SiO_2Im-in, an opposite effect is observed. This effect is due to different particle sizes used in different methods.

The results suggested that the obtained hybrid membranes are promising electrolytes in high temperature proton exchange membrane fuel cells without additional moistening.

This work was financially supported by the Russian Science Foundation (project no. 17-73-10447).

References

1. *Stenina IA, Yaroslavtsev AB.* Nanomaterials for lithium-ion batteries and hydrogen energy. Pure and Appl Chem 2017;89:1185-1194.
2. *Basov NL, Ermilova MM, Orekhova NV, Yaroslavtsev AB.* Membrane catalysis in the dehydrogenation and hydrogen production processes. Russ Chem Rev 2013;82:352–368.
3. *Özdemir Y, Üregen N, Devrim Y.* Polybenzimidazole based nanocomposite membranes with enhanced proton conductivity for high temperature PEM fuel cells. Int J Hydr En 2017;42:2648-2657.

C4 HYDROCARBONS SEPORATION THROUGH THE POLYETHYLENE-GRAFT-SULFONATED POLYSTYRENE MEMBRANES

[1]Aleksandra Lytkina, [1]Natalia Zhilyaeva, [1]Natalia Orekhova, [1]Margarita Ermilova, [3]Nina Shevlyakova, [3]Vladimir Tverskoy, [1,2]Andrey Yaroslavtsev

[1] Topchiev Institute of Petrochemical Synthesis RAS, Moscow, Russia, *lytkina@ips.ac.ru*

[2] Kurnakov Institute of General and Inorganic Chemistry RAS, Moscow, Russia, *yaroslav@igic.ras.ru*

[4] Moscow Technological University, Moscow, Russia, *tverskoy@mitht.ru*

Introduction

The constant growth of the interest in the processes associated with refinery gases and their components (ethane, propane, butane) is observed [1]. These gases are known as not only a fuel, but also as a raw material for the synthesis of valuable products having olefins as the products of the first stage of the processing. The oil industry is under pressure to find replacements for the high octane blending components in gasoline which are no longer allowed. And olefins like isobutylene, butene and their oligomers (octenes), have a high potential as their blending octane values are much higher-up to 164.

One of the problems along this path is the separation of saturated and unsaturated hydrocarbons mixtures. Industrially, this separation is carried out by cryogenic distillation, which is highly energy-intensive. The membrane separation has some advantages in comparison with distillation and adsorption methods due to its low energy consumption, moderate cost and compact design [2].

However, butene/butane separation using conventional membranes has some difficulties caused by the similar structure and sizes of their molecules. This problem can be solved with the use of membranes in which the facilitated transport mechanism is realized [3]. The significant attention to such materials and processes is determined by their high efficiency. One of the examples is the process of facilitated olefin transport via the selective formation of complexes with silver and copper ions contained in the membranes. The advantages of these systems are high olefin permeability coefficients and selectivity of the gas mixture separation processes. In light of the above, the ion exchange membranes form can be suggested as the most promising solution. The membranes based on polyethylene with radiation chemically grafted sulfonated polystyrene (SPS) were chosen because of the possibility to obtain membranes with a wide range of carrier concentrations by varying the polystyrene grafting degree and its sulfonation [4].

In this paper, the dependence of the transport processes selectivity of butenes/butane mixture components on the concentration of sulfonic acid groups and the gas stream humidity in membranes based on polyethylene with radiation chemically grafted SPS.

Experiments

The sulfocathionite membranes obtained by post-radiation graft polymerization of styrene on a low density polyethylene (PE) film with a thickness of 20 μm were studied, followed by sulfonation of the grafted polystyrene (PS) by the procedure described in [4]. The membranes with different grafting degrees were studied (0-122%). The grafting degree of polystyrene (Δp) was calculated as the weight gain of the film, referred to the original film mass.

The permeability measurements of the polymeric membranes based on polyethylene grafted with sulfonated polystyrene for the butene/butane mixture separation were carried out in a stainless steel flow-through diffusion cell divided by a membrane with an area of 3.46 cm^2 into two non-communicating chambers. The studied gas mixture was introduced into one of the chambers, while helium was introduced into another chamber and acted as a carrier gas. Both gas streams were moistened by passing through the bubbler. The relative humidity level (from 30 to 80%) was created by changing the temperature of the bubblers with distilled water. Before each experiment, the membrane was pre-moistened with a stream of moistened gases for two hours. Humidity of gases was determined at the outlet from the membrane cell.

The permeability coefficients of ethylene and ethane (P) were determined as the individual gases fluxes through the membrane at room temperature and expressed in Barrers [1 Barrer =

10^{-10}·cm^3(STP) cm/(cm^2·s·cm Hg)]. The separation factor of ethylene and ethane was determined as the ratio of the permeability coefficients of these gases.

Results and Discussion

The development of test modes for C4 olefin/paraffin mixtures separation with the use of the polyethylene-graft-sulfonated polystyrene membranes in a flow-through diffusion cell with gas chromatographic analysis of the penetrated through the membrane mixtures has been occurred.

A comparative study of butenes permeability was performed on a sample with PS grafting degree of 50% and the gas humidity of 80%. The membrane was fed a mixture of butenes and isobutylene in a 1: 2 ratio, obtained during the butanol dehydration reaction. It was shown that the butene permeability 3 times exceeds the isobutylene permeability (450 versus 150 Barrer). In this regard, further permeability studies were carried out for isobutylene, having the lowest permeability in a series of isomers. The effect of the gas mixture humidity on the permeability coefficient of isobutylene was studied on a membrane with a PS grafting degree of 36%. The moistening process was performed using the thermostatic barbaters with distilled water simultaneously on the membrane both sides in order to avoid the appearance of a humidity gradient across the membrane thickness. It was shown that with a humidity increase, the permeability of isobutylene increases. The membranes permeability for isobutylene increases substantially with an increase in the relative humidity and, accordingly, in the moisture content of the membranes. However, permeability actually reaches saturation with increasing humidity.

A study of the membranes permeability with varying PS grafting degrees (36, 50%) for individual butane and isobutylene gases showed that the isobutylene permeability in all studied systems exceeds the butane permeability strongly, despite the larger effective cross section of the branched isobutylene molecule. This indicates a significant role of the facilitated transport in the penetration process (due to the formation of a isobutylene complex with a proton through a double bond). The permeability coefficient value and the separation factor decreases with the PS grafting degree increasing.

Table 1: Gas permeability coefficients and separation factors of C_4H_8/C_4H_{10} mixtures for the membrane with PS grafting degree of 36%. Relative humidity 80%

The isobutylene/butane mixture composition	Gas permeability coefficient, Barrer		Separation factor of isobutylene/butane mixture
	isobutylene	butane	
10:90	665	26	26
25:75	250	29	8,6
65:35	77	24	3,2

It was shown that butane permeability from the mixtures with a relatively low content of isobutylene is much lower than the permeability of isobutylene (Table 1). The separation factor and the permeability of isobutylene increases with a decrease in its concentration in the mixture. The highest permeability coefficients for isobutylene and separation factors are observed when using a mixture of i-C_4H_8/C_4H_{10} containing the minimal amounts of isobutylene. At the same time, the value of the permeability coefficient of butane practically does not change with an increase in the isobutylene concentration in the mixture.

The dependences obtained (Fig. 1) indicate an increase in the isobutylene permeability with an increase in the polystyrene grafting degree from 8 to 36% and a further decrease in the isobutylene permeability with an increase in the PS grafting degree, wherein butane permeability varies slightly. The gas separation factor maximum value is also observed for a membrane with a grafting degree of 36%, and its subsequent increase leads to a drop in the separation factor magnitude.

The effect of isobutylene/butane mixture humidity changes on the permeability coefficients was studied. The Isobutylene permeability increases with the relative humidity, while butane permeability gradually decreases. As a result, the factor of their separation increases with the gas mixture humidity increasing; its maximum value is achieved in the membrane with the grafting degree of of 36%.

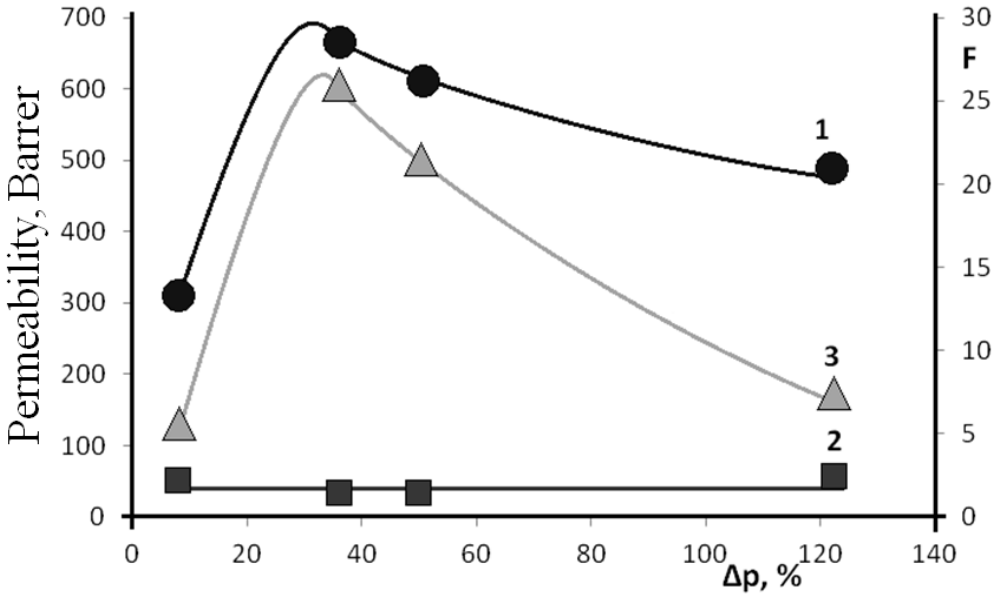

Figure 1. The permeability coefficients dependence of gases recovered from the isobutylene and butane mixtures of composition C_4H_8 / C_4H_{10} = 10:90 v / v. on the membrane PS grafting degree: 1 - isobutylene permeability, 2 - butane permeability, 3 - isobutylene - butane mixture separation factor. Relative humidity - 80%.

This work was supported by the Ministry of Education and Science of the Russian Federation (agreement no. RFMEFI58617X0053) and CNRS (France, project no. 38200SF).

References

1. *James O.O., Mandal S., Alele N., Chowdhury B., Maity S.* Lower alkanes dehydrogenation: Strategies and reaction routes to corresponding alkenes // Fuel Process. Technol. 2016. V. 149. P. 239–255.
2. *Lee J.H., Sudhager P., Cho Y., Kang S.W.* Effect of temperature on separation performance in ionic liquid/Ag nanocomposite membranes for olefin/paraffin mixtures // J. Industrial Eng. Chem. 2019. V. 74. P. 103-107.
3. *Dou H., Jiang B., Xiao X., Xu M., Wang B., Hao L., Sun Y., Zhang L.* Ultra-stable and cost-efficient protic ionic liquid based facilitated transport membranes for highly selective olefin/paraffin separation // J. Membr. Science. 2018. V. 557. P. 76-86.
4. *Zhilyaeva N.A., Mironova E.Yu., Ermilova M.M., Orekhova N.V., Bondarenko G.N., Dyakova M.G., Shevlyakova N.V., Tverskoy V.A. and Yaroslavtsev A.B.* Polyethylene-*graft*-Sulfonated Polystyrene Membranes for the Separation of Ethylene–Ethane Mixtures // Petroleum Chem. 2016. V. 56. P. 1034–1041.

UTILIZATION OF GASSEPARATION MEMBRANES BASED ON POLYELECTROLYTES

Mariia Makhonina, Kseniia Otvagina, Nail Yanbikov, Andrey Vorotyntsev, Alla Mochalova, Ilya Vorotyntsev

Laboratory of membrane and catalytic processes, Nizhny Novgorod State Technical University n.a. R.E. Alekseev, Nizhniy Novgorod, Russia, E-mail: *makhonina.m.n@nntu.ru*

Introduction

Nowadays the membrane gas separation technologies are a high-tech, energy-efficient and environmentally friendly process. The presence of possible numbers of membrane polymers usually shown on Robeson plot [1]. But in gas separation commercially there are used not many membranes. Moreover, from the economical point of view any technological process should be calculated on only with consumption of product creation, but also by membrane disposal after its usage. In the literature very a few works are devoted to the topic of membranes polymers utilization, the study of ways to recycle membranes. Despite the fact that the volume of membrane polymers relative to the volume of polymeric wastes throughout the world is not comparatively small, toxic substances are not rarely involved in their production, which, when dumping or burned, can seriously harm the environment. It is important to understand what substances polymers decompose during recycling, so the aim of the presented work is to study of the utilization of used membranes based on polyelectrolytes after gas separation. From the ecological point of view the interest to biopolymers which can easily degraded is the area of high interests. For the current study, the membranes based on natural polymer chitosan (CS), the macromolecule of which is a polyelectrolyte in the protonated form in weakly acidic aqueous solutions, as well as a stable polyelectrolyte based on the quaternized derivative of chitosan (qv- CS) were chosen due the fact its practical application in gas separation and pervaporation processes [2,3].

Experimens

Chitosan (CS, molecular weight (MW) = $1.05 \cdot 10^5$ Da, deacetylation degree (DD) = 80%) was supplied by Bioprogress CJSC (Russia). Figure 1 suggests that uaternized derivative of chitosan was obtained by the following reaction:

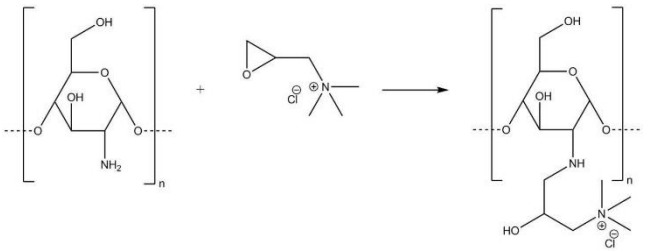

Figure 1. The reaction of CS with glyceryl-3-methylammonium chloride (GTMAC).

Quaternized derivative of chitosan was synthesized by a quaternization reaction with GTMAC in the ratio of components 5:15 in an aqueous medium for 16 hours at a temperature of 353 K. After separation of the reaction product and extraction with ethanol in the Soxelet extractor for 24 hours, the yield of the quaternized product was 70%. The formation of qv-CS was proved by IR spectroscopy. Solid polymer membranes were obtained by pouring a solution of the polymer on an inert substrate.

The fungus resistance of the obtained CS and qv-CS was evaluated in vitro *in vitro* by the strains of the fungi *Aspergillus niger, A. terreus, A. oryzae, Chaetomium globosum, Paecilomyces variotii, Penicillium funiculosum, P. chrysogenum, P. cyclopum, Trichoderma viride*. The experiments identified true destructors capable of enzymatic degradation the components of the material.

In the course of the experiments, real destructors capable of enzymatic degradation of membrane materials based on CS and qv-CS were identified. The essence of the method consists in keeping the film materials infected with spores of various fungi under optimal conditions for

development (T=302 K) on the complete nutrient medium of Chapek Doks and sucrose-depleted with a subsequent assessment of the degree of development of moldy fungi.The total aerobic biodegradation of polymers under controlled incubation conditions was conducted in the activated sludge media by measuring gravimetrically the amount of carbon dioxide emitted.

The thermophysical properties of CS and qv-CS are characterized using of evolved gases analysis (EGA) mass spectrometry during pyrrolitic decomposition in an inert medium. For direct EGA-MS measurements, a temperature-programmable Multi-Shot Pyrolyzer EGA/PY- 3030D (Frontier Laboratories, Fukushima, Japan) was used.

Results and Discussion

The results of fungus resistance showed that the studied samples of the qv-CS in comparison with the initial CS in Chapek Doks's media complete nutrient media and sucrose-depleted, have a prolonged effect. On CS films, the growth of *Aspergilus Niger* is pronounced, which uses the material as a power source in competition with *Penicillium Funiculosum* and *Trichoderma viride*, and on the fragments of qv-CS

According to the results of the study of the biodegradation of materials on the basis of CS and qv-CS, it was found that polymers are bioavailable and on the third week of testing the rate of decomposition of polyelectrolytes, in comparison with the zero day, increases by two and half times.

The results of the thermal degradation of the qv-CS correlate with the literature data, the decomposition begins at a temperature of just over 500 K (table 1.), while the thermal degradation of the original CS is initiated 40 degrees higher. It should be noted that almost all chitosan derivatives, including copolymers with vinyl monomers, have a lower decomposition temperature than the initial CS (543 K).

Table 1: Results of evolved gases analysis (EGA) mass spectrometry during pyrrolitic decomposition

Sample	m/z	Substance	Temperature of degradation, K
Chitosan	18	Water	> 543
	28	Nitrogen	
	44	Carbon dioxide	
	59	Acetamide	
	80	Butandinitrile	
	94	Dimethylpropanedinitrile	
Quaternized derivative of chitosan	18	Water	> 508.15
	17	Ammonia	
	58	N, N-Dimethylaminoethanol	
	88	1- 1-Dimethylamino-2,3-propandiol	

Conclusion

Quaternized derivative of chitosan did not affect the properties of the fungus resistance and biodegradability of the materials, the most competitive in terms of development were identified strains of *Aspergillus niger, Trichoderma viride and Penicillium funiculosum,* which are capable of enzymatic hydrolysis of CS-based membranes and qv-CS. During thermal destruction of membranes on the basis of CS and qv-CS release of toxic decomposition products was nodetected. Comparing the results of membrane utilization methods, we can say that all of them are applicable, but with respect to preserving the ecology of ecosystems, it is preferable to choose biotechnological methods for processing gas separation membranes, in which materials are destroyed due to complete aerobic biodegradation. The applicability of this method to membranes of different nature can be determined using rapid fungus resistance tests.

This work was supported by the Russian Science Foundation (grant no. 18-19-00453).

References

1. *Robeson L. M.,* The upper bound revisited // J. Membr. Sci. 2008. V. 320. P. 390-400.
2. *Otvagina, K.V., Mochalova, A.E., Sazanova, T.S., Petukhov, A.N., Moskvichev, A.A., Vorotyntsev, A.V., Afonso, C.A.M., Vorotyntsev, I.V.* Preparation and Characterization of Facilitated Transport Membranes Composed of Chitosan-Styrene and Chitosan-Acrylonitrile Copolymers Modified by Methylimidazolium Based Ionic Liquids for CO2 Separation from CH4 and N2 // Membranes. 2016, V. 6. 31.
3. *Otvagina K.V., Penkova A.V., Dmitrenko M.E., Kuzminova A.I., Sazanova T.S., Vorotyntsev A.V., Vorotyntsev I.V.* Novel Composite Membranes Based on Chitosan Copolymers with Polyacrylonitrile and Polystyrene: Physicochemical Properties and Application for Pervaporation Dehydration of Tetrahydrofuran // Membranes. 2019. V. 9(3). 38.

GAS SEPARATION IN A MEMBRANE CONTACTOR WITH A REVERSIBLE REACTION OF A GAS WITH AN ABSORBENT: EXPERIMENT AND MODEL

Alexander Malakhov, Stepan Bazhenov
A.V. Topchiev Institute of Petrochemical Synthesis, RAS, Moscow, Russia
E-mail: *sbazhenov@ips.ac.ru*

Introduction

The molecular-level separation using membrane processes are widely studied for their application in the petrochemical industry. It is attractive to combine membrane and absorption technologies for olefin/paraffin separation in gas-liquid membrane contactors. In this case, a membrane acts as interphase between gas and liquid, whereas separation results from the different solubility of saturated and unsaturated alkanes in absorption liquid [1]. The common absorbents are solutions of transition metals salts able to form π-complexes with olefins. The goals of this study were (1) the development of composite hollow fiber membrane with a thin layer made of ultra-permeable poly(1-trimethylsilyl-1-propyne) (**PTMSP**) and (2) modeling of ethylene/ethane separation in the membrane contactor with aqueous $AgNO_3$ as an absorbent.

Experimental

Asymmetrical polysulfone (**PSf**) supports were fabricated according to the well-known NIPS (nonsolvent-induced phase separation) technique. Deposition of thin PTMSP layer was performed by casting 1 wt. % PTMSP solution in *n*-hexane on the lumen surface of PSf support. The composite PSf/PTMSP membranes were characterized with pure ethylene and ethane permeance (P_A/l) by constant pressure/variable volume method. Gas-liquid membrane contactor experiment was performed on laboratory setup described elsewhere [2]. C_2H_4/C_2H_6 (20/80 mol %) gas mixture was brought to the fibers shell side. Aqueous silver nitrate solution was brought into the fibers lumen in counter-current flow mode. The gas mixture was periodically sampled, and its composition was determined by the gas chromatograph Crystallux-4000M. The concentration of $AgNO_3$ (aq) was varied from 1 to 6 M, the liquid flow rate was 4.5, 9.0, and 18.0 mL/min (linear velocities 0.05, 0.1, and 0.2 m/s). The experiment was performed under constant temperature (T = 298 K) and pressure of feed gas ($p = 10^5$ Pa).

Modeling

The experimental overall mass transfer coefficient (**MTC**) based on the gas phase K_A for component A can be calculated from the observed mass transfer flux J_A: $J_A = K_A \overline{\Delta p_A}$ where $\overline{\Delta p_A}$ is the log-mean of the partial pressure difference of component A in the gas mixture (feed) and the bulk liquid (permeate). Selectivity in the membrane contactor was defined as the ratio between ethylene and ethane MTCs or overall permeances: $\alpha = K_{C_2H_4}/K_{C_2H_6}$.

Gas mass transfer in a contactor includes three stages: diffusion from the bulk gas to gas-membrane interface with the MTC k_G, permeation through the membrane with the MTC k_M and the gas transfer from the liquid-membrane interface to the bulk liquid with the MTC k_L. According to the resistance-in-series model, the overall resistance, i.e. the reciprocal of the overall MTC, equals the sum of the gas film resistance, the membrane resistance, and the liquid film resistance is given by [3]

$$\frac{1}{K_A} = \frac{1}{k_G} + \frac{1}{k_M}\frac{d_o}{d_{ln}} + \frac{1}{k_L E_A S_A^{phys}}\frac{d_o}{d_i}, \qquad (1)$$

where S_A^{phys} is the partition coefficient of the *physically* absorbed olefin, d_o, d_i and d_{ln} are the outer, inner and log-mean diameters of the hollow fibers (in our case $d_o/d_{ln} \approx 1.3$, $d_o/d_i \approx 1.6$), E_A is the enhancement factor due to the chemical reaction of the olefin with silver ions.

The membrane contribution k_M to the overall MTC is equal to the composite membrane permeance, $k_M = P_A/l$. The liquid phase contribution to the overall MTC at physical gas absorption can be estimated using the known correlation ratios [4]. To calculate the liquid film resistance, it is necessary to find the enhancement factor E_A, which is the ratio between the olefin fluxes across the liquid boundary layer, with and without the chemical reaction.

The interaction between ethylene and silver ions to form the olefin-Ag^+ complex can be considered as an instantaneous reversible reaction taking place at the gas-liquid interface [5]. In this assumption, an equation for the enhancement factor has been derived:

$$E_A = 1 + \gamma S_A^{chem} / S_A^{phys} \approx \gamma S_A^{chem} / S_A^{phys}, \quad (2)$$

where γ is the degree of dissociation of $AgNO_3$, S_A^{chem} is the partition coefficient for *chemically* absorbed gas. The approximate equality in the Eq. (2) is obtained considering the fact that physical solubility being significantly lower than the chemical solubility. The values of γ are known from the literature. The parameter S_A^{chem} is related to the equilibrium constant K_p of the chemical absorption of gaseous C_2H_4:

$$C_2H_4\ (g) + Ag^+ \leftrightarrow C_2H_4{-}Ag^+$$

This constant was found by approximation of the experimental data of ethylene absorption in $AgNO_3$ (aq) using Langmuir-like equation. It has been obtained that the equilibrium constant decreases while the value of S_A^{chem} increase (from 8.8 to 32.3) when the $AgNO_3$ (aq) concentration increases from 1 M to 6 M. The chemical solubility of ethylene in $AgNO_3$ solution (in the limit of small partial pressures) was calculated as $S_A^{chem} = RTc_{Ag}K_p$ where c_{Ag} is the total $AgNO_3$ molarity, R denotes the gas constant, T is the temperature. Thus, we have found that the product $E_A S_A^{phys}$, which is included in Eq. (1), can be expressed in terms of known parameters:

$$E_A S_A^{phys} = \gamma RTc_{Ag}K_p \quad (3)$$

Results and Discussion

In this study, the hollow fiber membranes with a thin selective layer based on PTMSP with the thickness of 4-5 μm on porous asymmetric PSf support were fabricated. These membranes were applied for the separation of ethylene from ethane in the gas-liquid membrane contactor using aqueous $AgNO_3$ solutions.

During the process the gas mixture flows alongside the hollow fiber membranes. Some amount of gas mixture penetrates through the membrane and dissolves in the $AgNO_3$ solution. The ethylene is absorbed preferentially due to the complexation reaction with silver ions. The mole fraction of ethylene at the outlet of the contactor decreases, whereas ethane fraction increases. The ethylene recovery $\eta = 1 - x_A^{out}/x_A^{in}$ (x_A^{in} and x_A^{out} is the molar fraction of ethylene at the inlet and the outlet of the membrane contactor, respectively) reaches the value of 33% for 1 M solution and 44% for 5 M solution.

It was found that the ethylene overall permeance in the membrane module increases with the liquid flow rate and $AgNO_3$ concentration. The effect of $AgNO_3$ concentration in the absorbent is presented below (Fig. 1). The overall permeance of ethylene increases from 63 GPU for 1 M salt solution to maximum value 83 GPU for 5 M solution, and then declines to 71 GPU for 6 M solution. Ethylene/ethane selectivity reaches the maximal value of 7.1 for the 5 M silver nitrate solution. To the best of our knowledge, the realized value 83 GPU (0.22 m^3 (STP)/m^2·h·bar) is result exceeded the values for the previously studied thin film composite membranes by an order of magnitude.

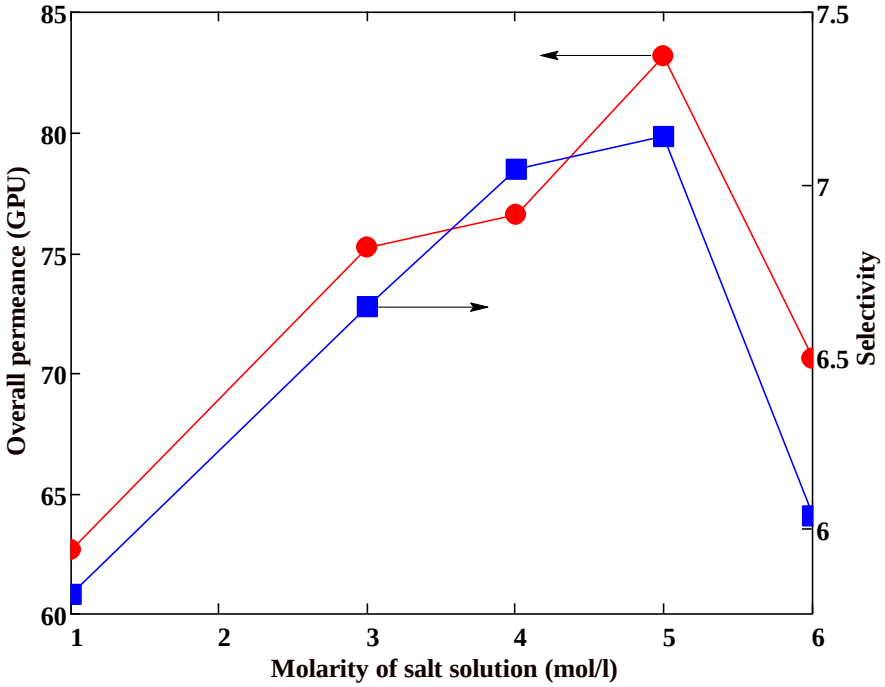

Figure 1. The overall permeance of ethylene and ethylene/ethane selectivity as a function of $AgNO_3$ concentration. The liquid velocity was 0.2 m/s; GPU denotes gas permeance unit, 1 GPU = $3.35 \cdot 10^{-10}$ mol/($m^2 \cdot s \cdot Pa$).

An important aspect of the membrane applicability is the stability of transport properties over time in the gas-liquid membrane contactor. The membranes were operated for six months under membrane contactor conditions and showed acceptable mass transfer stability confirmed by the fact that the ethylene overall permeance was decreased only by quarter from 80.7 to 61.5 GPU.

The membrane and liquid phase contributions to the overall ethylene mass transfer resistance within the resistance-in-series model was estimated using simple approximate formula for the enhancement factor which is the product of $AgNO_3$ degree of dissociation and the ratio of chemical to physical solubility of ethylene in the liquid absorbent. The resistances of membrane and liquid phase were shown to be 50 and 39 %, respectively, i.e. both resistances are significant and comparable.

Acknowledgments

The experimental research was carried out at TIPS RAS and was supported by Russian Science Foundation (project no. 14-49-00101). The modelling research was supported by the Russian Foundation for Basic Research (project no. 17-08-00619).

References

1. *Bazhenov S.D., Bildyukevich A.V., Volkov A.V.* Gas-liquid hollow fiber membrane contactors for different applications, // Fibers 2018. V. 6. Article 76 (41 pages).
2. *Ovcharova A., Vasilevsky V., Borisov I. et al.* Polysulfone porous hollow fiber membranes for ethylene-ethane separation in gas-liquid membrane contactor // Sep. Purif. Technol. 2017. V. 183. P. 162–172.
3. *Zhao S., Feron P.H.M., Deng L. et al.* Status and progress of membrane contactors in post-combustion carbon capture: A state-of-the-art review of new developments // J. Membr. Sci. 2016. V. 511. P. 180–206.
4. *Cussler E.L.* Diffusion: Mass Transfer in Fluid Systems, 3rd Ed., Cambridge University Press, 2007, p. 254.
5. *Rajabzadeh S., Teramoto M., Al-Marzouqi M. et al.* Experimental and theoretical study on propylene absorption by using PVDF hollow fiber membrane contactors with various membrane structures // J. Membr. Sci. 2010. V. 346. P. 86–97.

EFFECT OF SURFACE CHARGE OF ION-EXCHANGE MEMBRANE ON ITS ELECTROCHEMICAL CHARACTERISTICS

Semyon Mareev, Dmitrii Butylskii
Membrane Institute, Kuban State University, Krasnodar, Russia, E-mail: *dmitrybutylsky@mail.ru*

Introduction

Understanding the impact of ion exchange membrane surface charge, estimated by measuring zeta-potential (ζ), on its electrochemical properties is of great interest. According to Rubinstein and Zaltzman [1, 2] increasing ζ should lead to an increase in electroconvection (EC) rate.

Here the effect of the surface charge of ion-exchange membranes on transition time found by chronopotentiometric curves treatment is reported.

Experiments

The objects of study are Nafion 117 and Nafion 438 homogeneous ion-exchange membranes differing in surface structure and chemical composition. The studied samples consist of a perfluorosulfonic acid and polytetrafluoroethylene copolymer. Samples differ in equivalent weight that is the number of grams of dry Nafion per mole of sulfonic acid groups when the material is in the acid form, 1100 g/mol and 4300 g/mol, respectively [3].

The Nafion 438 membranes have a structure that differs from those of the Nafion 117. There is a flat reinforcing net of polytetrafluoroethylene with high strength. In addition, Nafion 117 and Nafion 438 membranes differ in surface morphology: the first is smooth on both sides, and the second has a rough relief from one side (the other is smooth).

Results and Discussion

Transition time is an important characteristic that can be determined from chronopotentiograms obtained at overlimiting current densities. This is the point in time where the mechanism of ion delivery to the membrane surface is changed from electrodiffusion to a more complex one, associated with water dissociation and convection initiated by current flow.

Figure 1 shows the experimental and theoretical chronopotentiograms calculated using the developed 2D mathematical model.

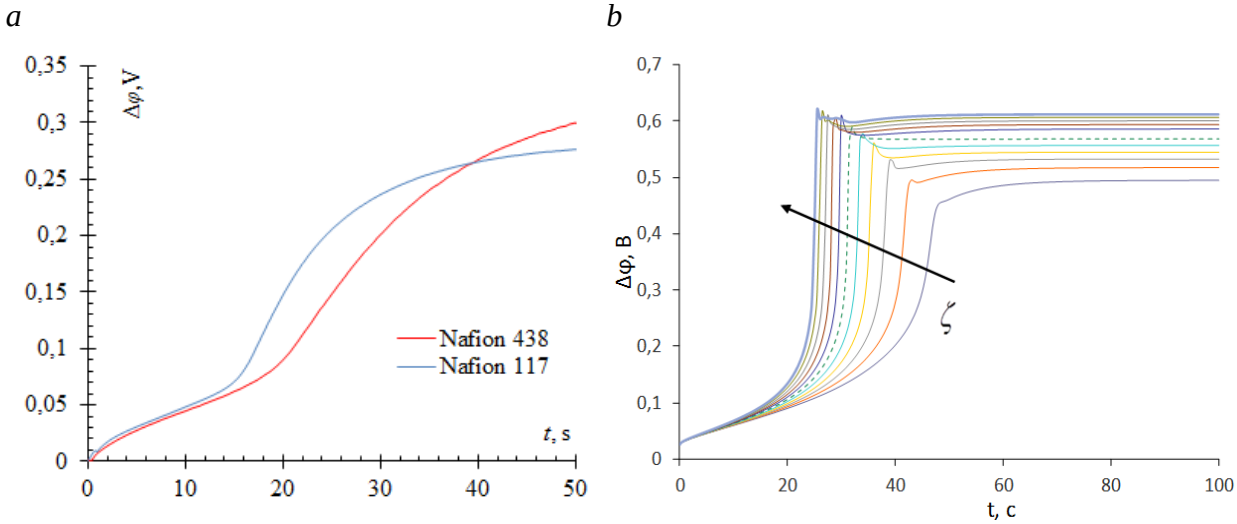

Figure 1. Experimental Chronopotentiograms for Nafion 117 and Nafion 438 Membranes (a) and Calculated Chronopotentiograms Using the Developed 2D Mathematical Model (b) (ξ-potential values were changed in the range from -0.5 to 0.5 V, the direction of increase ξ is indicated by an arrow, the dashed line indicates the chronopotentiogram for ξ = 0 V) at $j = 1.25j_{lim}$.

We have developed a 2D model based on the Nernst-Planck-Poisson-Navier-Stokes equations, where zeta-potential enters as parameter. Our computations show that the value of zeta potential

significantly affects the value of the transition time (Fig. 1b). In addition, zeta potential affects the stationary potential drop on chronopotentiograms. However, with an increase in the current density the effect of the zeta potential in both cases becomes less significant. This is due to the fact that at currents close to the limiting value, the electroconvection occuring as the electroosmosis of the first kind has the greatest influence on the behavior of an electromembrane system [4]. At currents greater than 1.4 j_{lim} electroconvection becomes dominant due to the action of the electric force on the extended space charge region. The contribution of the surface charge to the intensity of electroconvection is leveled, and differences in the behavior of the membranes associated with the chemical composition are reduced.

Acknowledgments

We are grateful to the RFBR (18-38-00600 mol_a) for financial support.

References

1. *Rubinstein I., Zaltzman B.* // Phys. Rev. Lett. 2015. V. 114. №. 11. P. 114502.
2. *Zaltzman B., Rubinstein I.* // J. Fluid Mech. 2007. V. 579. P. 173-226.
3. *Chen T. Y., Leddy J.* // Langmuir. 2000. V. 16. №. 6. P. 2866-2871.
4. *Nebavskaya K. A. et al.* // J. Membr. Sci. 2017. V. 523. P. 36-44.

CHRONOPOTENTIOMETRY OF ION-EXCHANGE MEMBRANES WITH HYDROPHOBIC AREAS ON THE SURFACE: 2D SIMULATION AND EXPERIMENT

[1]Semyon Mareev, [1]Svetlana Zyryanova, [2]Christian Larchet, [2]Lasaad Dammak, [1]Victor Nikonenko

[1]Membrane Institute, Kuban State University, Krasnodar, Russia, E-mail: *mareev-semyon@bk.ru*

[2]Institut de Chimie et des Matériaux Paris-Est, UMR 7182, 2 Rue Henri Dunant, 94320 Thiais, France

Introduction

In the recent work [1, 2], it was theoretically shown that the membranes with specified surface tailoring can possess mass transport characteristics exceeding the homogeneous membranes. The questions of precise fraction of insulating surface and other parameters affecting the mass transport, such as hydrophobicity, is required for such improvements. The aim of the work is to show the effectiveness of membrane surface hydrophobization in the mass transport improvement.

Experiment

The object of the study was the commercially available homogeneous membrane AMX (Astom, Japan), the samples of which were coated with dots of inert hydrophobic fluoroplast-42 material. Modified membranes differ in the fraction of coverage modifier.

Theory

The conventional equations system (Nernst-Planck-Poisson-Navier-Stokes) of the basic mathematical model [3] and electric current stream function [4] were applied to simulate the ion and volume transport in an electrodialysis system with a homogeneous membrane partially covered by nonconductive hydrophobic material. The model is two dimensional and nonstationary. An anion-exchange membrane whose surface consisted of alternating hydrophilic conductive and hydrophobic insulating stripes was examined.

Results and Discussion

The shape of numerically simulated and experimantal chronopotentiograms (ChPs) allows distinguishing three regions, differing in the mode of ion delivery to the membrane surface. In the first one, the dominant mechanism of ion delivery is electrodiffusion.

The second region is characterized by a steep increase of potential drop caused by depletion of the solution at the membrane surface. A low potential drop and strongly nonlinear concentration profile near the membrane show that the mechanism of ion delivery becomes mixed. However, the electroconvective mixing here is weak and occurs only close to the membrane surface near the conductive stripes.

In the third region, smooth but quite significant growth of potential drop appears due to depletion of the solution near the conductive stripes. Then the potential drop growth steeply decreases and the system reaches a stationary condition.

Acknowledgments

This study was realized in the frame of a joint French-Russian PHC Kolmogorov 2017 project of the French-Russian International Associated Laboratory “Ion-exchange membranes and related processes” with the financial support of Minobrnauki (Ref. N° RFMEFI58617X0053), Russia, and CNRS, France (project N° 38200SF).

References

1. *Davidson S. M. et al. //* Scientific Reports. 2016. V. 6. No: 22505.
2. *Urtenov M. K. et al.* // J. Membr. Sci. 2013. V. 447. P. 190.
3. *Mareev S. A. et al. //* J. Membr. Sci. 2019. V. 575. P. 179.

PECULIARITIES OF BEHAVIOR OF PERVOPORATION MEMBRANES FROM ISOTACTIC POLYPROPYLENE

Natalia Matushkina, Nadezda Strusovskaya, Eugene Ageev
Lomonosov Moscow State University, Chemistry Department, Moscow, Russia
E-mail: *ageev@phys.chem.msu.ru*

Introduction

It is known that world production of polypropylene (PP) approaches one hundred thousand tons per year, being second only to polyethylene. But after the synthesis of PP, the catalyst and other substances involved in the creation of the final product fall into the category of unnecessary and unknown impurities, and their presence may determine the properties of the material that are not inherent to PP. The presence of such impurities in the polymer is revealed by the study of transport properties – diffusion, sorption, pervaporation, which are sensitive to changes in the molecular and supramolecular structure of the polymer. The goal of this work is to investigate the interaction of such impurities contained in polypropylene membranes with hydrophobic and hydrophilic probe fluids at different temperatures using the pervaporation method.

Experiments

The objects of the study were industrial films of isotactic PP of grade 01030 with a thickness 20 μm, density 0.96 g/cm^3, melting point 160–168 °C, the volume fraction of the amorphous phase 47.5%. To study the permeability of hydrophobic isotactic PP, hydrophilic substances acetone, isopropanol and water, and hydrophobic substances hexane and dioxane were chosen. The temperature dependence of the permeability of PP films was studied by the pervaporation method. The vapor that passed through the membrane was condensed in a trap cooled with liquid nitrogen. To calculate the flux density, the mass of the condensed substance was determined.

Results and Discussion

Figure 1 shows the temperature dependences of the pervaporation flux density of the selected individual substances through films of isotactic PP. Acetone and isopropanol both contain two hydrophobic methylene groups, still remaining hydrophilic compounds due to the presence of carbonyl and hydroxyl groups with dipole moments of 2.850 and 2.660 D, respectively. Water has a dipole moment of 1.840 D, does not wet the PP film, does not dissolve in hydrocarbons and can penetrate through the films only if the hydrophobic polymer contains impurities with pronounced hydrophilic properties.

The densities of pervaporation flows of hydrophilic acetone, isopropanol and water are insignificant, practically coincide and do not depend on the direction of temperature change. The temperature dependences of the permeability of PP with respect to hydrophobic dioxane and hexane have a different appearance. In the range of 20–40 °C, the flux density of dioxane is close to the values of the flux density for hydrophilic substances, and then increases sharply and at 70 C reaches a value about 5 times higher than the initial (at 20 C), and the permeability of hexane is two orders of magnitude higher than that of hydrophilic substances. The flux densities increase apparently due to the swelling of the films in dioxane and hexane, which leads to an increase in the free volume of the polymer, to a change in its supramolecular structure, and the transmembrane flow flushes out the impregnated hydrophobic impurities.

The permeability of PP films with respect to hydrophilic substances is significantly influenced by the sorption options of hydrophobic substances. Figure 2 shows the changes in the permeability of the PP film with respect to acetone and water with different variants of the experiment. From the data it can be seen that if the modification of the film is carried out in the process of pervaporation, the so-called one-sided sorption, then the hydrophobic hexane is sorbed on the side of the film facing the liquid and modifies the supramolecular structure of the polymer not over all its thickness, since on the side of the film facing the chamber containing the vapor phase, pressure ≈ 15 Torr. It is possible to modify the structure of the PP over the entire thickness of the film, if it is previously held in liquid hexane outside the pervaporation installation, i.e., if two-sided sorption

of hexane is carried out. When replacing acetone with water, similar dependences were obtained, showing that the preliminary sorption of hydrophobic hexane due to an increase in the free volume of the polymer during its sorption leads to an increase in permeability.

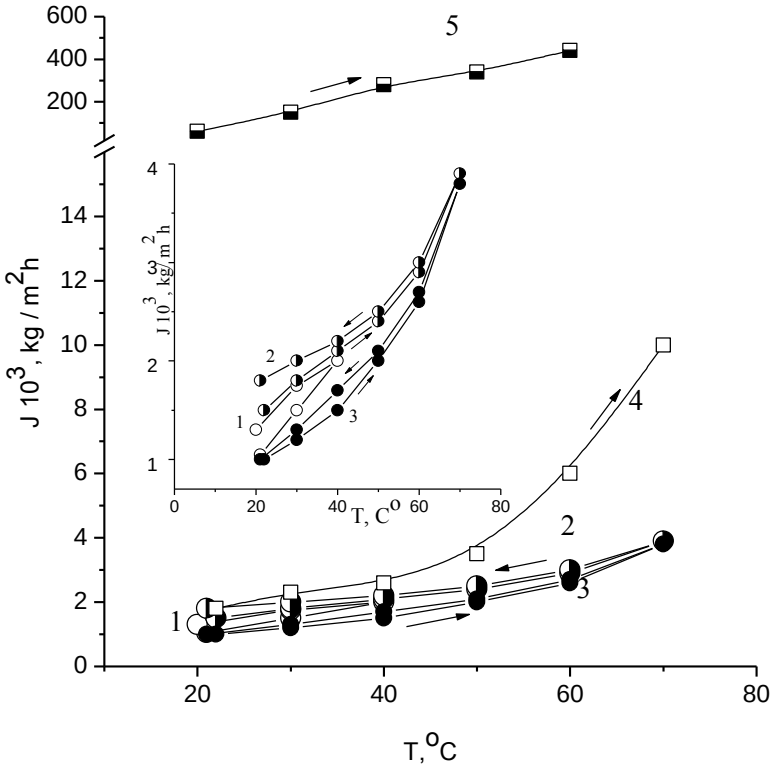

Figure 1. Temperature dependences of the pervaporation flux density of individual substances through isotactic PP films: 1 – acetone, 2 – isopropanol, 3 – water, 4 – dioxane, 5 – hexane.

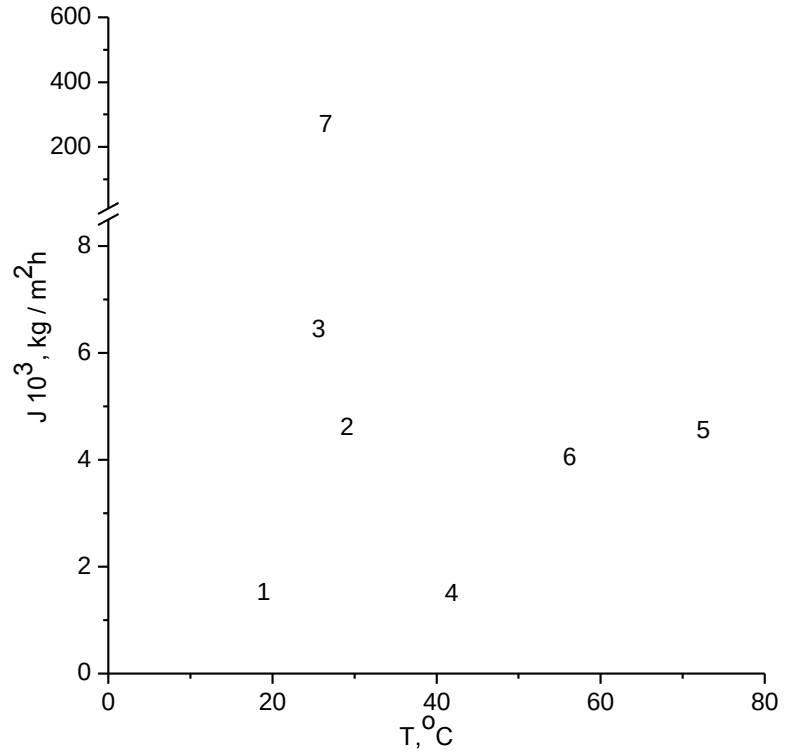

Figure 2. Temperature dependences of the pervaporation flux density of individual substances through isotactic PP films depending on the method of their modification:
1 – acetone, 2 – acetone after one-sided sorption of hexane, 3 – acetone after two-sided sorption of hexane, 4 – water, 5 – water after one-sided sorption hexane, 6 – water after two-sided sorption of hexane, 7 – hexane.

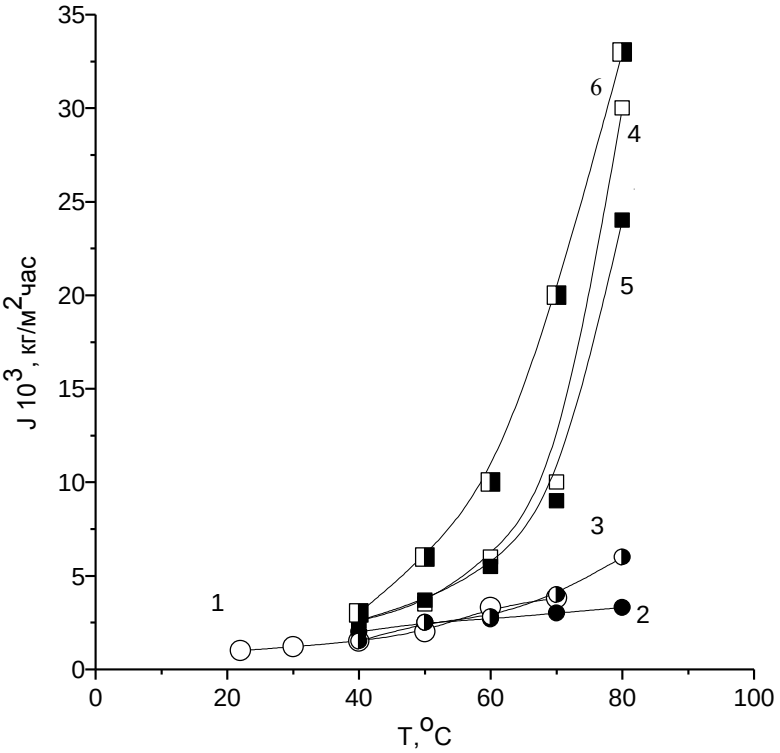

Figure 3. Temperature dependences of the pervaporation flux density of individual substances through isotactic PP films depending on the method of their modification: 1 – water, 2 – water after one-sided sorption of dioxane, 3 – water after two-sided sorption of dioxane, 4 – dioxane, 5 – dioxane after one-sided sorption of water, 6 – dioxane after two-sided sorption of dioxane.

Figure 3 shows the temperature dependences of the density of the pervaporation flow of water and dioxane through PP films, depending on the method of their modification. It can be seen that the permeability of the PP film with respect to hydrophilic water can be slightly increased if one- and two-sided sorption of hydrophobic dioxane is carried out, and the permeability of dioxane itself increases, if its two-sided sorption is first carried out.

Thus, in the work, the pervaporation properties of industrial PP films of grade 01030 with respect to model hydrophobic and hydrophilic liquids and their temperature dependences were determined for the first time. It was shown that one- and two-sided sorption of hexane and dioxane leads to a modification of the supramolecular structure of polypropylene films, making it possible to increase their permeability and partially remove the hydrophobic and hydrophilic impurities contained in them.

FORMATION, STRUCTURE AND PERFORMANCE OF POROUS MEMBRANES BASED ON ACRYLONITRILE COPOLYMERS

[1]Dmitrii Matveev, [2]Tatyana Plisko, [2]Anton Shustikov, [2]Alexander Bildyukevich, [1]Vladimir Volkov

[1]A.V.Topchiev Institute of Petrochemical Synthesis, RAS, Moscow, Russia
E-mail: *dmitriy_matveev_1994@mail.ru*
[2]Institute of Physical Organic Chemistry National Academy of Sciences of Belarus, Minsk, Belarus

Introduction

Polyacrylonitrile (PAN) features a high resistance to non-polar and low-polar solvents (alcohol, hydrocarbons) and thermal stability. [1] PAN-based membranes are widely used in the ultrafiltration process [2] and as supports for composite gas separation, pervaporation and nanofiltration membranes. However, PAN is rarely applied in the form of homopolymer, in most cases it is copolymer with itaconic acid, methylacrylate, methylmethacrylate, vinylacetate, etc. The aim of the work was to study the influence of the chemical composition and molecular weight of acrylonitrile copolymers on the structure and performance of porous membranes.

Experiments

Porous membranes based on PAN were obtained by a non-solvent induced phase inversion method. Copolymers of acrylonitrile were dissolved in N, N dimethylformamide (DMF) and dimethyl sulfoxide (DMSO) (12-16 wt.%) for the preparation of casting solutions. In this work, various acrylonitrile copolymers were used as membrane-forming polymers to obtain samples of porous flat shet membranes. The main composition, molecular weight and the degree of polydispersity of acrylonitrile polymers used in this work are listed in Table 1.

Table 1: The main properties of the used copolymers of acrylonitrile

Name	Copolymer composition	Mw, Da	Mw/Mn	Intrinsic viscosity η	Producer
PAN-1	Poly (acrylonitrile-co-methyl acrylate) (92: 8)	107126	2.31	1,414	VNIISV, Russia
PAN -2	poly (acrylonitrile-co-methyl acrylate-co-itaconic acid) (92.7: 6.0: 1.3)	61156	1.72	0,809	Open Joint Stock Company "Naftan", Belarus
PAN -3	poly (acrylonitrile-so-itaconic acid) (99: 1)	98700	2.56	1,285	European Carbon Fibers, Germany
PAN -4	poly (acrylonitrile-co-methyl acrylate) (93.6: 6.4)	75900	2.88	0,647	HAIHANG INDUSTRY CO., LTD , China
PAN -5	poly (acrylonitrile-co-methyl acrylate) (91.5: 8.5)	81000	2.35	0,955	HAIHANG INDUSTRY CO., LTD, China

The casting solution was applied onto the glass plate as a thin layer using a casting blade with a thickness of 160 μm and thereafter precipitated in distilled water to obtain porous PAN membranes. The structure of the obtained membranes from acrylonitrile copolymers was investigated by scanning electron microscopy (SEM). The intrinsic viscosity was studied using a capillary viscometer with an internal capillary diameter of 0.56 mm. Polymer solutions concentration of 0.5 wt. % in DMF was used, the system is the system was thermostatically controlled to ensure a constant temperature of 25 °C. Determination of the dynamic viscosity of the casting solutions was performed on a "Brookfield RV DV-III Ultra Programmable Rheometer" viscometer. The study of the transport properties of the membranes was carried out in cells with magnetic stirrers.

Results and Discussion

The viscosity of the casting solution, the pure water flux (Figure 1) and rejection during ultrafiltration (P=0,1 MPa, T=25°C) of 3 $g \cdot L^{-1}$ polyvinylpyrrolidone (PVP K-30, average molecular weight 40,000 g/mol) aqueous solution were determined.

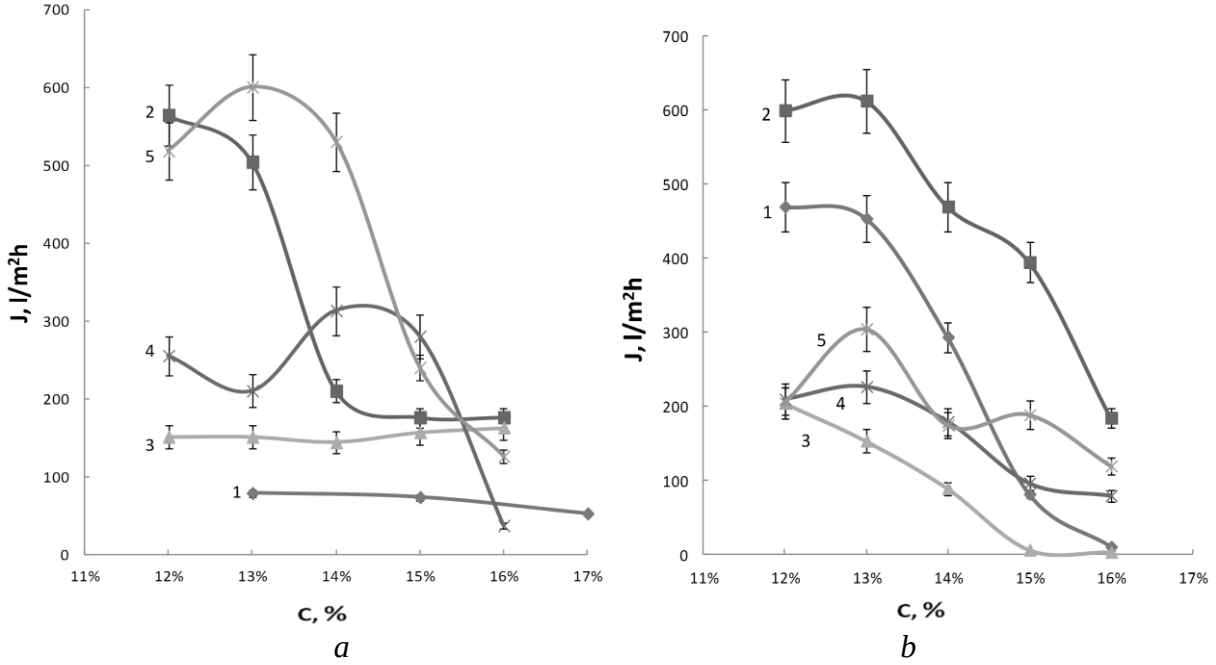

Figure 1. The pure water flux y of membranes from a) PAN-DMF, b) PAN-DMSO. Curves: 1 - PAN-1, 2 - PAN-2, 3 – PAN-3, 4 – PAN-4, 5 – PAN-5.

Figure 1 shows that the performance of flat membranes obtained from solutions of PAN-1, PAN-3 and PAN-4 (up to 15%) in DMF, on average, weakly depends on the polymer concentration in the casting solution. In the case of membranes obtained from a solution of PAN-4 in DMF, there is a sharp decrease in the pure water flux (from 250 to 37 l/(m^2h)) after reaching a concentration of 15%. On the contrary, membranes obtained from solutions of PAN-2 and PAN-5 in DMF, whose productivity is quite high, decrease with increasing polymer concentration in the casting solution. For all membranes obtained from PAN-DMSO solutions, a similar picture is observed: an increase in the concentration of the polymer in DMSO (from 12 to 16%) decreases the pure water flux. Thus, it was found that the concentration dependences of the membrane performance for all copolymers have a different character in DMF and DMSO.

It was found that with increasing of polymer concentration in the dope solution with DMSO, the structure of the resulting membrane undergoes significant changes: the number of finger-like macrovoids decreases, the thickness of the layer with a spongy-like structure and dense separation layer increases, which, in turn, leads to decrease in the membrane pure water flux. On the contrary, the structure of the membranes obtained from the dope solution with DMF slightly depends on the concentration of the polymer.

Figure 2 shows the SEM micrographs of flat membranes obtained from solutions of some acrylonitrile copolymers (PAN-1 and PAN-4) in DMSO at the same concentration of 16%. It can be seen from the Figure 2 that the membranes obtained from solutions of polymer with a higher molecular weight (therefore, with a higher viscosity of the dope solution) have a spongy-like structure, a thick selective layer. At the same time, for membranes obtained from solutions of polymer with a lower molecular weight, are characterized by the presence of large finger-like macrovoids, a thin selective layer.

The differences in membrane transport characteristics can be explained by different values of the viscosity of the dope solutions, as well as different thermodynamic affinity of DMF and DMSO for the PAN polymer. It has been established that an increase in the viscosity of the dope solutions

changes the structure of flat membranes: a spongy-like structure is formed, the number of macrovoids decreases.

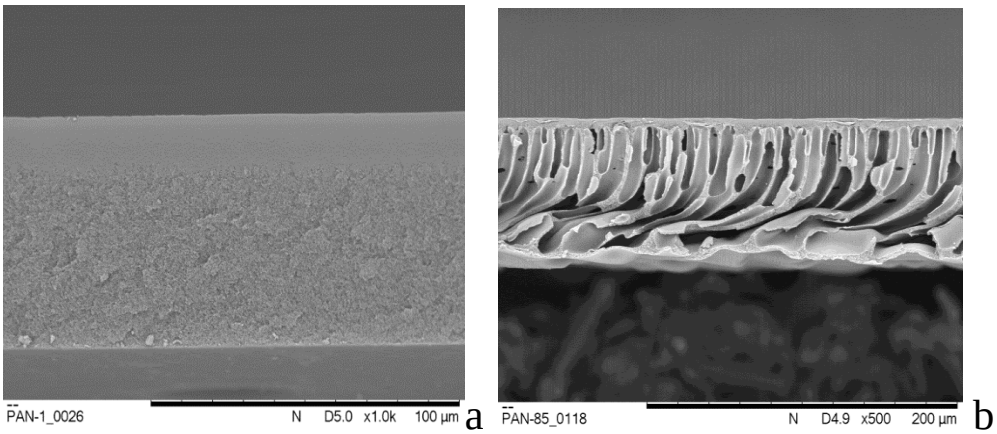

Figure 2. SEM cross-section images of flat membranes obtained from dope solution of a) PAN-1, b) PAN-4 in DMSO, 16%.

Based on the data obtained, the further task is to produce the composite porous hollow fiber membranes for gas separation.

The reported study was funded by RFBR according to the research project №18-51-00001 Bel_a and BRFFR according to the research project №X18P-083.

References

1. *Nico Scharnagl, Heinz Buschatz*. Polyacrylonitrile (PAN) membranes for ultra- and microfiltration. Desalination. 2001.V. 139. № 1. P. 191.
2. *Thi Dung Tran, Shinsuk eMori, Masaaki Suzuki*. Plasma modification of polyacrylonitrile ultrafiltration membrane. Thin Solid Films. 2007.V. 515. № 9. P. 4148.

WASTEWATER TREATMENT FROM ORGANIC COMPOUNDS BY THE EXAMPLE OF ACETIC ACID ELECTRODIALYSIS

Stanislav Melnikov, Elena Nosova, Anastasia But
Kuban State University, Krasnodar, Russia

Introduction

The problem of environmental pollution with sewage containing organic compounds is highly relevant today because organic matter is a waste of food, cosmetic, paint and varnish industry, agricultural activities and other types of industrial activity.

One of the approaches to the solution of the problem is a treatment of waste waters using electrodialysis technology [1]. The main problem preventing the use of the electrodialysis is the low electrical conductivity of solutions containing organic compounds [2].

The purpose of this work is to study the process of removal of organic substances of ionic nature by the method of electrodialysis and the search for ways to optimize the process to increase its efficiency.

Experiments

A 0.1 M solution of acetic acid was used as an object of study.

The membrane stack of an electrodialysis unit contained alternating heterogeneous anion- and cation-exchange membranes, MA-41 and MK-40, which formed 5 elementary pairs. A working area of each membrane was 5x12.5 cm^2. The tests were conducted in a batch mode. The volume of the studied solutions was 1 L for desalting and concentrating compartments and 0.5 L for electrode compartment. To prevent solutions overheating a cooler was added into the desalting compartment. The flowrate through desalting and concentrating compartments was set at a constant value of 25 L/h. The flowrate through electrode compartment was set at 20 L/h.

Scheme of the electrodialysis apparatus is shown in Figure 1.

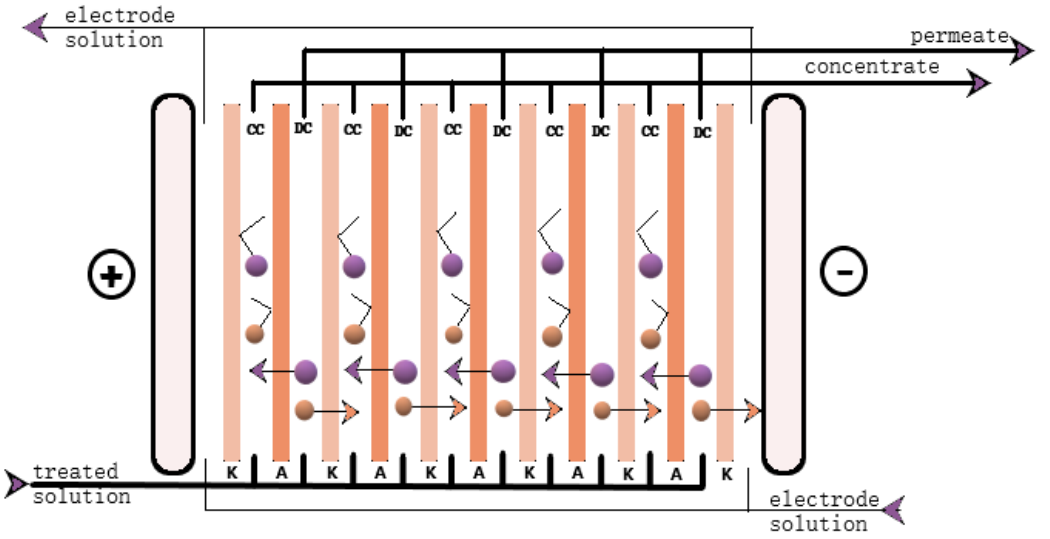

FIGURE 1. DIAGRAM OF THE PROCESS OF ELECTRODIALYSIS.

The process parameters are shown in table 1.

Table 1: Electrodialysis process parameters

SET	MEASURE	COUNT
CURRENT STRENGTH (*I*, A)	**VOLTAGE (*U*, V)**	**FLUX (*J*, MOL/ DM^2×H)**
FLOW RATE (*W*, DM^3/H)	**CHANGES IN THE CONCENTRATION IN THE DC AND CC (Δ*C*, MOL/DM^3)**	**CURRENT EFFICIENCY (*H*, %)**
WORKING MEMBRANE AREA (*S* = 0,625 DM^2)	**VOLUME CHANGE IN DC AND CC (Δ*V*, DM^3)**	**LINEAR VELOCITY (*V*, CM/S)**

CHANNEL WIDTH (*H*, MM)	TIME (*T*, H)	POWER CONSUMPTION (*E*, KWH/MOL)

To calculate the current efficiency (η), the following equation was used:

$$\eta = \frac{FJ}{IS} = \frac{F}{In}\frac{\Delta C \Delta V}{\Delta \tau} \quad (1)$$

where F is the Faraday number, equal to 26.8 (Ah/mol).

Results and Discussion

To optimize the process of electrodialysis in order to increase its effectiveness in solutions of organic compounds, a phased approach to solving the problem was chosen. At the first stage, the analysis of the behavior of MA-41 membranes in acetic acid solutions of different concentrations was carried out (Fig. 2).

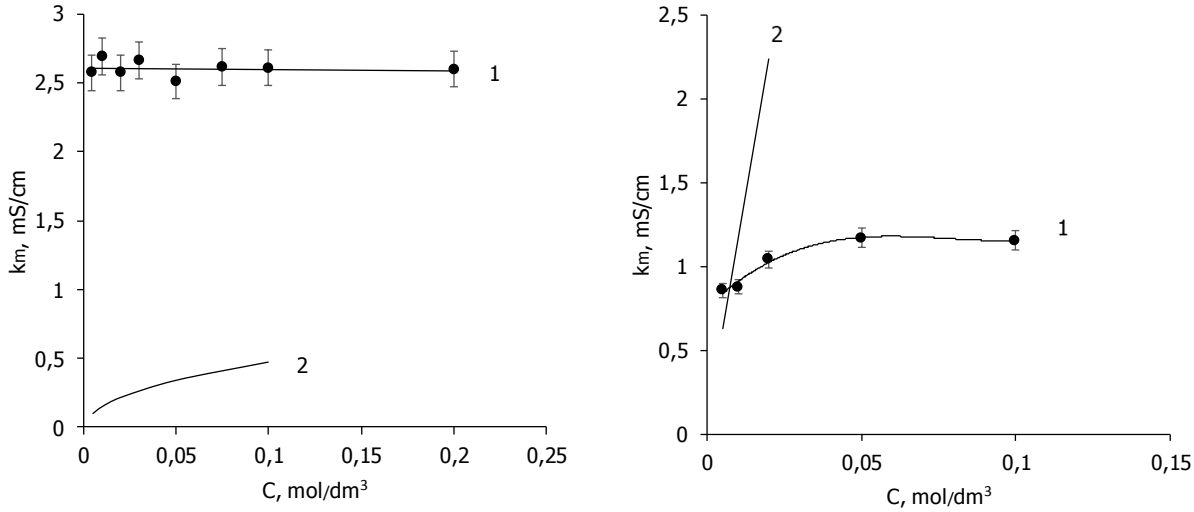

A ***B***

FIGURE 2. CONCENTRATION DEPENDENCE OF THE ELECTRICAL CONDUCTIVITY OF ION-EXCHANGE MEMBRANES IN SOLUTIONS OF ACETIC ACID (A) AND SODIUM CHLORIDE (B): 1 - MA-41; 2 - ELECTROLYTE SOLUTION.

The figure shows that for acetic acid there is no point of isoelectric conductivity, which is associated with a weak degree of dissociation of acetic acid [2]. This means that most of the molecules in the solution are in the form of neutral molecules and do not conduct electrical current. Despite this fact, experimental data showed that the electrical conductivity of the membranes in the acetic acid solution is higher than the solution itself.

It can be concluded that the limiting stage of the process of electrodialysis is not the electrical conductivity of the membranes, but the solution itself. Therefore, it is necessary to change the design of the electrodialysis apparatus.

The results show that reducing the thickness of the desalination channel should have a positive impact on the energy consumption of the process of electrodialysis. To test this assumption, the characteristics of electrodialysis apparatus with a desalination channel thickness of 1.9 mm (linear velocity 1.58 cm/s) and 0.9 mm (linear velocity 3.63 cm/s) were investigated.

The obtained dependences of current and energy output are shown in Figure 3.

It can be seen from the graphs that with decreasing thickness of the channel, the current efficiency increases (Fig. 3a). This fact can be correlated with the fact that when the thickness of the desalting channel decreases, the linear velocity of the solution increases. In turn, the linear velocity of the solution is associated with the thickness of the diffusion layer in such a way that

with increasing linear velocity the thickness of the diffusion layer decreases, which positively affects the overall mass transfer in the desalination channel.

Also, with a decrease in the thickness of the channel, the linear velocity of the solution passing through the apparatus increases, and the ohmic losses decrease. This leads to a reduction in energy consumption (Fig. 3 b, c, d). As can be seen from the graphs, with an increase in the degree of desalination, the energy consumption also increases, but with a smaller frame thickness, the costs decrease by almost 4 times.

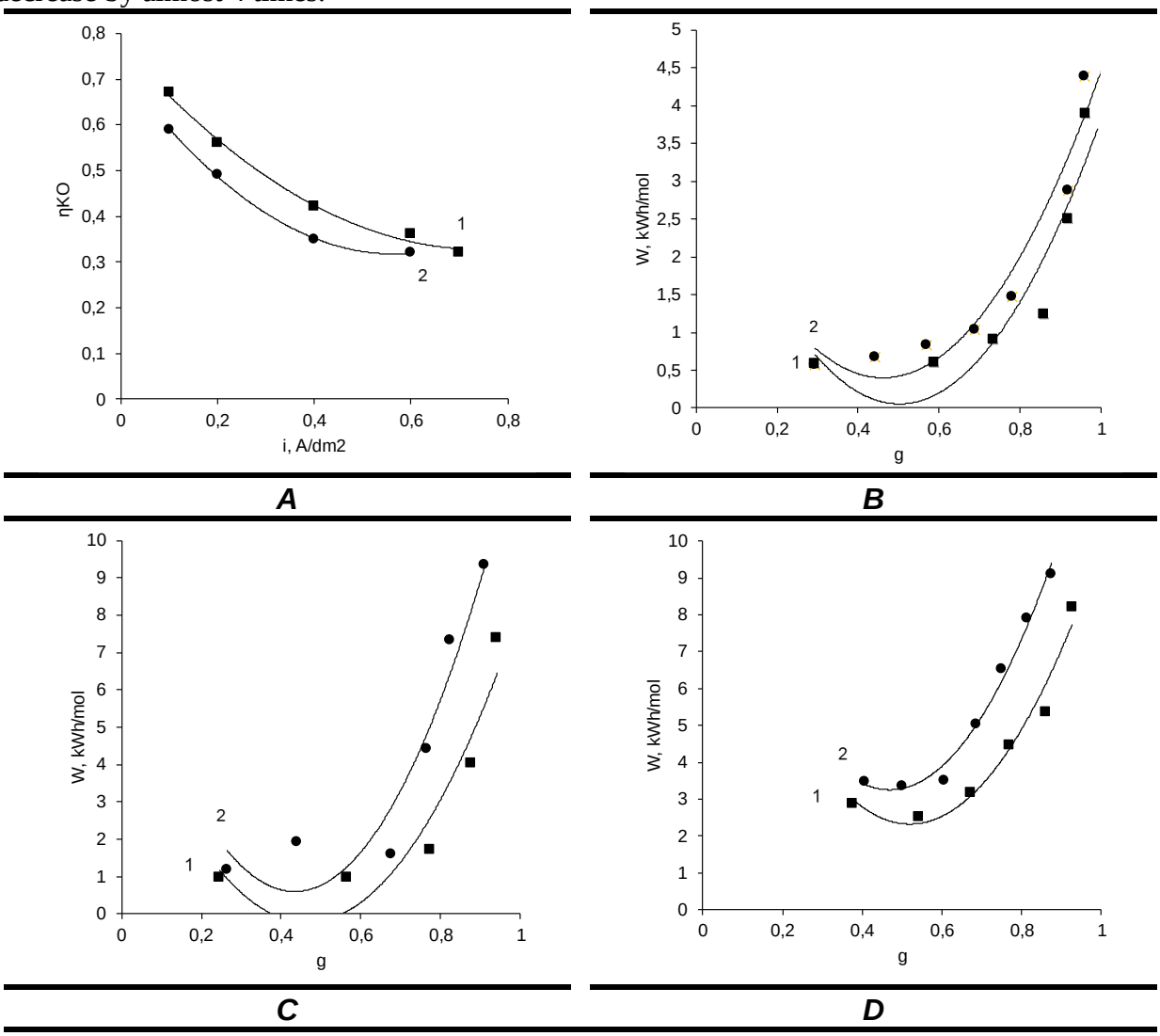

FIGURE 3. CURRENT EFFICIENCY VS CURRENT DENSITY (A)AND SPECIFIC ENERGY CONSUMPTION VS DESALTING DEGREE AT 0.32 (B), 0.64 (C), 0.96 (D) A/DM^2.
DESALINATION CHANNEL WIDTH: 1 – 0.9 MM; 2 – 1.9 MM.

Conclusions

The behavior of MA-41 membranes in acetic acid solution was studied, the design of the electrodialysis apparatus was adjusted based on the results obtained, the results of the operation of the electrodialysis apparatus were obtained for different desalination chamber channels.

It is shown that the adopted changes in the design of the device have improved important characteristics of the process such as: current efficiency and energy consumption. The advantages of the new installation are especially noticeable with a high degree of desalting, which is important when desalting water to 5 mg/L and below.

Acknowledgments

This work was supported by Russian Foundation for Basic Research, grant №-19-08-01172.

References

1. *Pourcelly G*. // Russ. J. Electrochem., 2002, vol. 38(8). p. 919-926.
2. *Melnikov S., Kolot D., Nosova E., Zabolotski V*. // J. of Membrane Science, 2018, vol 557, p. 1-12.

CURRENT-VOLTAGE CHARACTERISTICS OF BILAYERED ION-EXCHANGE MEMBRANES IN SODIUM CHLORIDE SOLUTION

Stanislav Melnikov, Svetlana Shkirskaya
Kuban State University, Krasnodar, Russia

Introduction

Today membrane technologies are widely used in various industries, and also find their application in everyday life. Further improvement of membrane technology is possible by combining two independent processes (chemical transformations and separation) in one system, which will significantly increase the efficiency of technological processes, the degree of their energy saving and environmental expediency. This is the way to improve chemical technology can ensure the sustainable development of society. Moreover, these processes can be carried out in one stage in a film, the thickness of which is tenths or even hundredths of a millimeter.

To study the characteristics of new membranes, it is convenient to use the voltammetry method, since it allows you to easily and quickly evaluate the effect of modifications on the properties of membranes in a wide range of currents.

Experiments

Four samples of ion-exchange membranes were selected for study: Ralex AMH (membrane-substrate), and the membranes on the surface of which were applied various ion-polymers MF-4SK, polyaniline, MF-4SK/polyaniline. The properties of the objects of the study are summarized in Table 1.

Table 1: Physicochemical properties of studied samples

Membrane	l, cm	Q, mmol/g	W_w, g H_2O/g_{wet}	n_m, mol H_2O/mol N^+
Ralex AMH	0.052	1.25	0.40	17.8
Ralex/MF-4SK	0.056	1.16	0.39	18.7
Ralex/PANi	0.058	1.36	0.40	17.1
Ralex/MF-4SK/PANi	0.057	1.27	0.39	16.3
Standard deviation of the value	±0.003	±0.08	±0.01	±1.0

The measurements were carried out in a four-compartment electrochemical cell (Fig. 1) with an active membrane area 2.27 cm^2. The Luggin-Haber capillaries connected to silver chloride electrodes were used to study the current-voltage characteristics and monitor the potential drop on the membrane during measurement of the transport numbers. The tips of the Luggin-Haber capillaries were located at a fixed distance from the membrane surface equal to 0.2 mm. Auxiliary membranes on both sides from the membrane under study prevent its contact with products of electrode reactions. The cell was fed with a 0.02 M NaCl. The solutions feed rate was 2 ml/min.

The solutions and the cell were kept at a constant temperature – 25±0.1°C.

A dynamic method of measuring the current-voltage characteristics was used. The test membranes were pre-conditioned for 30-40 minutes in an electrochemical cell (Fig. 1) with the pump on and without current. After that, a linearly increasing current was applied to the cell with the help of a Potentiostat/Galvanostat/EIS Analyzer Parstat 4000, and the current-voltage characteristic was recorded. Current sweep rate was set at 2×10^{-5} A/s.

When comparing the electrochemical behavior of different membranes by voltammetric measurements it is convenient to use corrected potential drop ($\Delta\varphi'$) instead of the total potential drop ($\Delta\varphi$), which can be defined as :

$$\Delta\varphi' = \Delta\varphi - iR_{\text{ef}} \quad (1)$$

where R_{ef} is the effective resistance of the membrane system at low current densities.

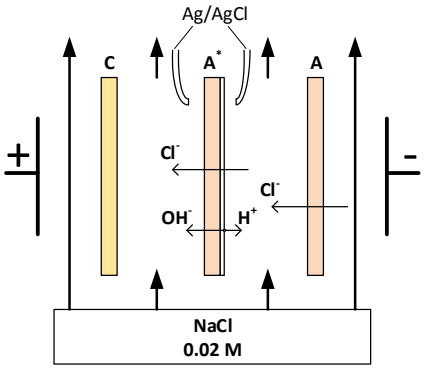

FIGURE 1. THE SCHEME OF THE EXPERIMENTAL CELL AND IONS FLUXES THROUGH THE STUDIED MEMBRANE. C – CATION-EXCHANGE MEMBRANE MF-4SC; A – ANION-EXCHANGE MEMBRANE MA-41; A* –MEMBRANE UNDER STUDY.

The same cell was used for studying the effective transport number of hydrogen ions.

The effective transport number of hydrogen or hydroxyl ions can be calculated by the formula:

$$T_W = \frac{Fc_W V}{iS\tau} \quad (2)$$

where c_W is the concentration of the hydrochloric acid at the outlet of the cell, mol/L; V is the volume of the solution, L; i is the current density, A/cm^2; S is the cell area, cm^2; τ is the sample collection time, s.

Results and Discussion

The current-voltage characteristics of the composites studied in sodium chloride solution are presented in Figure 2.

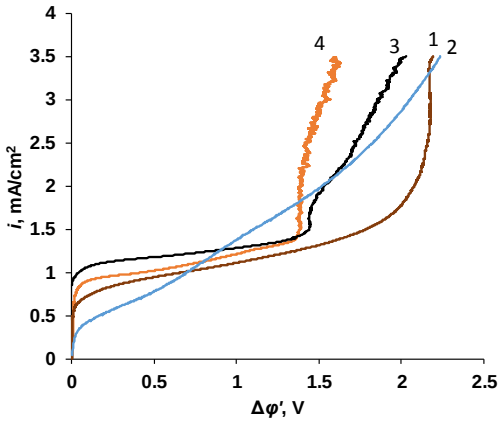

FIGURE 2. GENERAL CURRENT-VOLTAGE CHARACTERISTICS OF ION-EXCHANGE MEMBRANES IN 0.02 M NACL SOLUTION. 1 - RALEX AMH, 2 - RALEX/MF-4SK, 3 - RALEX/PANI, 4 - RALEX/MF-4SK/PANI.

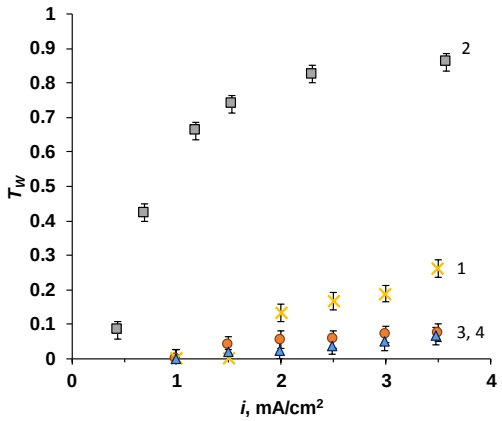

FIGURE 3. TRANSPORT NUMBERS FOR WATER DISSOCIATION PRODUCTS MEASURED IN 0.02 M NACL SOLUTION FOR MEMBRANES: 1 - RALEX AMH, 2 - RALEX/MF-4SK, 3 - RALEX/PANI, 4 - RALEX/MF-4SK/PANI.

From the obtained results it can be seen that the behavior of the investigated membranes when they are polarized by current is significantly different.

So for the original Ralex AMH membrane is characterized by a rather long plateau of the limiting current, which abruptly turns into an over-limiting current. The main mechanism of current growth for this membrane is the onset of the water-splitting reaction at the membrane/solution interface. In the work [1] the authors pointed out the substantial contribution of this mechanism of overlimitting mass transfer for this membrane. This assumption is confirmed by the measured transfer numbers of the products of water-splitting reaction (Fig. 3).

For a membrane with a thin MF-4SK film, a decrease in the value of the limiting current and the absence of a pronounced plateau of the limiting current are observed. This effect is explained by the fact that when a cation-exchange film is deposited on an anion-exchange membrane, a

bipolar boundary is formed at the interface of the cation-exchanger/anion-exchanger. As a result, for this membrane, the transfer numbers of water-splitting products approach 0.9 (Fig. 3, curve 2). Such behavior is described in detail in a number of papers in which the authors call such membranes asymmetric bipolar [2, 3]. The same effect can be obtained by sequential deposition of layers of ionpolymers with charges of different signs [4].

In contrast to the aforementioned work by Wessling et al. in our case, deposition of a layer of polyaniline (a positively charged ionpolymer) on a layer of MF-4SK (a negatively charged ionpolymer) does not significantly accelerate the dissociation of water. Apparently this is due to the fact that polyaniline is embedded in the volume of the MF-4SK film and does not form with it a sharp boundary, which is necessary for the formation of the space charge region and the water-splitting at a noticeable rate. In our case, the interfering boundary of the anion-exchanger/cation-exchanger/anion-exchanger can also serve as an interfering factor, which reduces the current efficiency of water dissociation products. At the same time, a sharp current increase is observed at the current-voltage characteristic, accompanied by significant potential oscillations at a current density above 1.2 mA/cm^2 (Fig. 2). Such a behavior of the current-voltage characteristic is currently explained by the development of non-equilibrium electroconvection, often referred as the electroosmosis of the second kind [5, 6]. Also, the electroconvective nature of this current is indicated by the fact that the measured Hittorf transport numbers of water-splitting products for this membrane do not exceed 0.07 (Fig. 3, curve 4).

An increase in the limiting electrodiffusion current can be caused by the development of a membrane surface microrelief. The appearance of geometric inhomogeneities on the membrane surface leads to the development of equilibrium electroconvection [7], which manifests itself in an increase in the value of the limiting electrodiffusion current [8].

A similar behavior is observed for the polyaniline-modified membrane (Ralex / PANi), however, for it, the potential jump oscillations are somewhat lower (Fig. 2), while the transfer numbers of water dissociation products almost coincide (Fig. 3, curve 3).

Acknowledgments

This work was supported by Russian Foundation for Basic Research, grant № 19-08-01172-a.

References

1. *Zabolotskii V.I., Bugakov V.V., Sharafan M.V., Chermit R.K.* // Russ. J. Electrochem., 2012, vol. 48. p.650.
2. *Zabolotskii V., Sheldeshov N., Melnikov S.* // J. Appl. Electrochem., 2013, vol. 47. p. 1117.
3. *Melnikov S., Zabolotskii V., Sheldeshov N., Achoh A., Bondarev D.* // Desalin. Water Treat., 2018, vol. 124. p. 30.
4. *Abdu S., Wessling M.* // Appl. Mater. Interfaces. 2014. vol. 3. p. 1843.
5. *Rubinstein I., Zaltzman B.* // Phys. Rev. E, 2000, vol. 62. p. 2238.
6. *Dukhin S.S.* // Adv. Colloid Interface Sci., 1991, vol. 35. p. 173.
7. *Larchet C., Zabolotsky V.I., Pismenskaya N.D., Nikonenko V.V., Tskhay A., Tastanov K., Pourcelly G.* // Desalination., 2008, vol. 222. p. 489.
8. *Balster J., Yildirim M.H., Stamatialis D.F., Ibanez R., Lammertink R.G.H., Jordan V., Wessling M.* // J. Phys. Chem. B., 2007, vol. 111. p. 2152.

THE ACTIVITY OF TRIMETALLIC CATALYSTS WITH DIFFERENT GOLD CONTENT FOR METHANOL ELECTROOXIDATION

Vladislav Menshikov, Sergey Belenov, Leonid Polevoj
Southen Federal University, Rostov-on-Don, Russia, E-mail: *men.vlad@mail.ru*

Introduction

The direct methanol fuel cell (DMFC) is a relatively recent development in hydrogen energy. Methanol offers several advantages over other fuel cells as fuel: it can be easily transported and stored, it is inexpensive, it can be quickly refilled into a tank, or it can be replaced with fuel cartridges. The fuel cell can be used in mobile devices due to its portability. However, the widespread commercial use of such devices makes some problems difficult. One of these problems is the poisoning of the cathode catalyst with methanol oxidation products due to its crossover through the membrane. The goal of our work was to obtain trimetallic catalysts ($Pt_xCu_yAu_z/C$) that have high activity in the oxygen reduction reaction (ORR) and the electrooxidation reaction of methanol (MOR) [1,2].

Experiments

We obtained samples containing different amounts of Au by atomic fractions (1/5, 1/10, 1/20, 1/30 atomic fractions). Catalysts were studied by X-ray diffraction to determine of the average crystallite size (Table 1); cyclic voltammetry on a disk electrode for measuring of the electrochemically active surface area (ESA), and activity in ORR and MOR.

Table 1: The average crystallite size

Materials	Average size (nm)	Pt loading (%)
$Pt_xCu_yAu_z/C$ 1/5	3.9 ± 0.5	38.6 ± 4
$Pt_xCu_yAu_z/C$ 1/10	3.7 ± 0.5	43.8 ± 4
$Pt_xCu_yAu_z/C$ 1/20	3.2 ± 0.5	34.8 ± 3
$Pt_xCu_yAu_z/C$ 1/30	2.7 ± 0.5	33.7 ± 3

Results and Discussion

The ESA of the obtained materials was determined by two methods: adsorption/desorption of hydrogen and CO-stripping. Values turned out to be lower than for commercial material (Table 2). However, the activity of some materials in ROM was higher, both in terms of mass and specific characteristics (Figure 1, 2). Also, the some materials are more active in the ORR than the commercial JM40 (Table 2), high tolerantly materials containing 1/10 and 1/20 of Au, to the intermediate products of oxidation of methanol (Figure 2a).

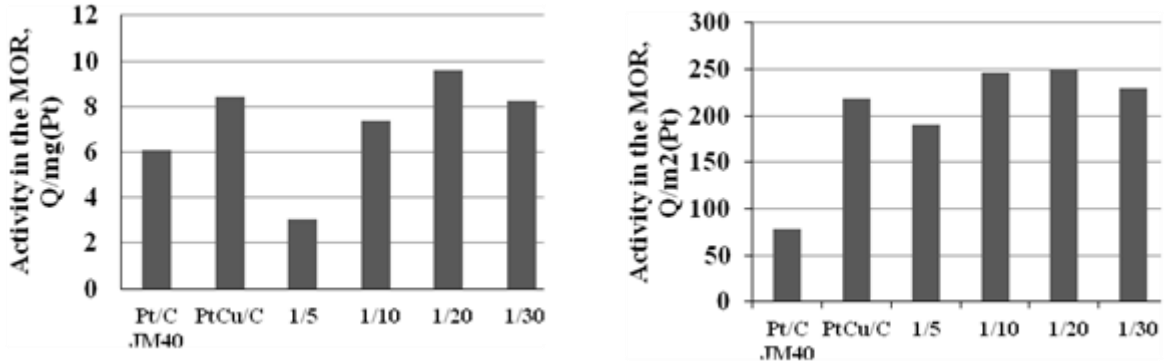

Figure 1. Histograms of activity of materials in ROM.

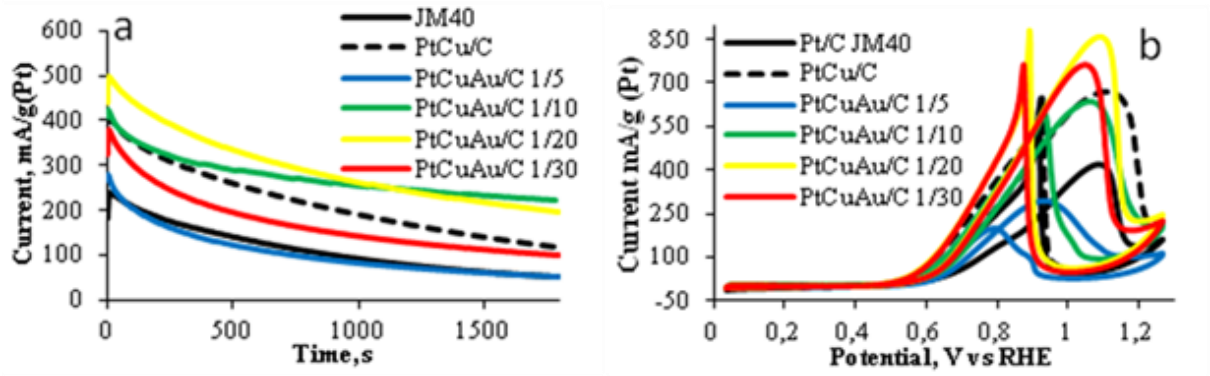

Figure 2. (a) Chronoamperogramms and (b) Cyclic voltammograms to Pt/C and PtCuAu/C catalysts, electrolyte 0.1M HClO4 + 0.5M CH3OH, saturated with argon, at atmospheric pressure; potential sweep rate 20 mV/s.

Table 2: The ESA material on two methods and activity of ORR

Materials	ESA (ad/des H_2), $m^2/g(Pt)$	ESA (CO), $m^2/g(Pt)$	n, number of ē	I_k A/g(Pt)
Pt/C	78	74	3.8	180
PtCu/C	40	38	3.9	165
PtCuAu/C 1/5	16	17	-	-
PtCuAu/C 1/10	29	30	3.7	160
PtCuAu/C 1/20	39	35	3.7	200
PtCuAu/C 1/30	36	35	3.7	114

It was found that the PtCuAu/C 1/20 catalyst show higher activity in the methanol electrooxidation reaction, because this material was demonstrated highest value of currents of methanol oxidation in compare with different studied materials.

Thus, a comparative study of Pt/C and $Pt_xCu_yAu_z$/C catalysts showed, that a small addition of Au can increase activity in the methanol electrooxidation reaction, in despite of the smaller electrochemically active surface area then JM40.

The work was carried out within the framework of the Russian Science Foundation № 18-73-00161.

References

1. *Wang X., Zhang L., Gong H., Zhu Yan., Zhao H., Fu Yu.* Dealloyed PtAuCu electrocatalyst to improve the activity and stability towards both oxygen reduction and methanol oxidation reaction // Electrochim. Acta. 2016. V. 212. P. 277-285.
2. *Chang G., Cai Z., Jia H., Zhang Z., Liu X., Liu Z., Zhu R., He Yun.* High electrocatalytic performance of a graphene-supported PtAu nanoalloy for methanol oxidation // Int. J. Hydrogen Energy. 2018. V. 43. P. 12803-12810.

AN INTEGRATED PROCESS DEVELOPED FOR WHEY DEMINERALIZATION

[1]Arthur Merkel, [2]Martin Ondrušek
MemBrain s.r.o., Stráž pod Ralskem, Czech Republic, E-mail: *arthur.merkel@membrain.cz*
Mega a.s., Stráž pod Ralskem, Czech Republic, E-mail: *edr@mega.cz*

Introduction

Membrane separation processes were used in dairy industry for many applications [1]. It has also been considered for separate the lactose and the mineral salts from the whey permeates. The concentrate stream in whey demineralization which is rich in lactose and calcium content is often treated as the waste. Furthermore, more stringent environmental regulations make its disposal more expensive. Thus, alternative applications for the lactose content are being searched. Two methods have been proposed for the concentration and separation of whey from cheese production, the nanofiltration (NF) [2, 3] and the electrodialysis (ED) [4]. Both techniques are capable of removing the high quantities of sodium, potassium and chloride ions [5]. The corresponding acids are then processed and utilized. In addition, minerals such as calcium may also be separated out and used as a supplement in existing and new products.

Processes such as precipitation, ion exchange, electrodialysis and membrane filtration may be used to remove the minerals. Membrane filtration, ion exchange and electrodialysis do not denature proteins thereby preserving protein solubility in demineralized whey produced by such methods. The exact process used will determine the mineral profile of the final product. Demineralized whey often will have a less salty flavor because of the removal of minerals.

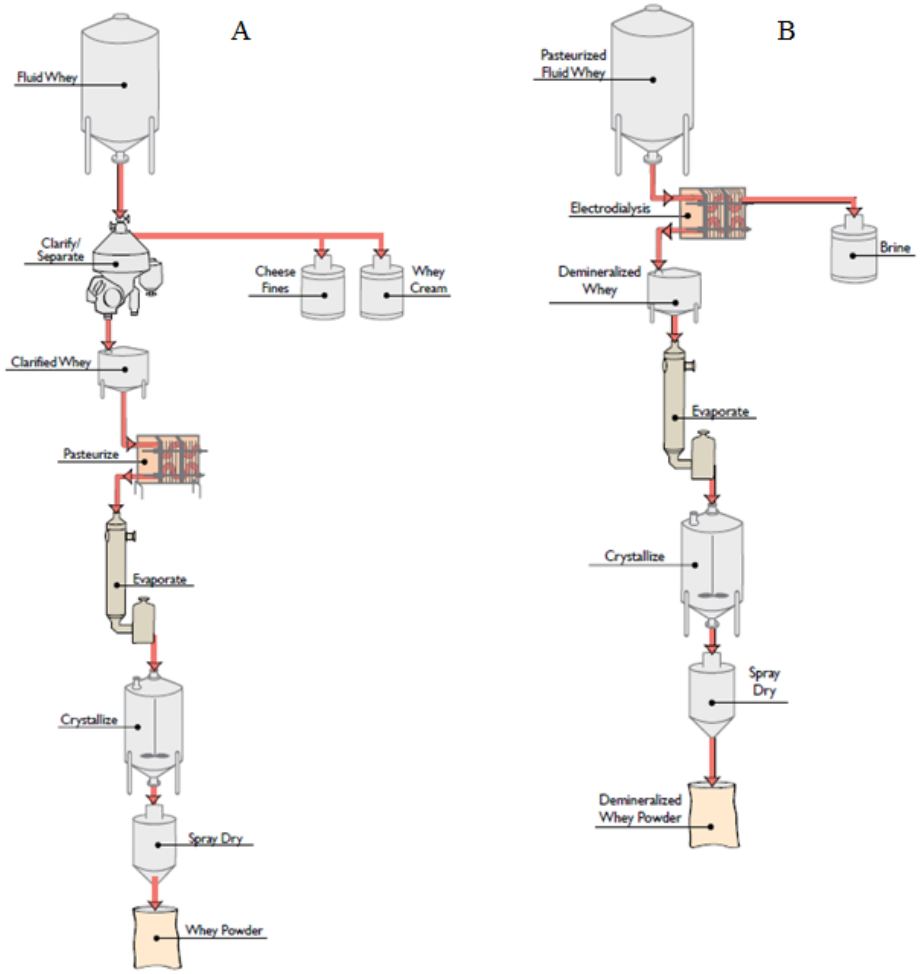

Figure 1. Manufacture of sweet or acid whey A); manufacture of demineralized whey B [6].

Experiments

A series of experiments were carried out and data were obtained in industrial conditions. The whey contains a content up to 20% total solids was processed using electrodialysis unit. The

composition of the whey treated by NF/ED is obviously dependent upon the operating conditions of the upstream stages, and the origins of the whey. Using the developed integrated process, the control of the mineral profile of the final product was possible. The flow diagram of the apparatus is presented in Figure 2.

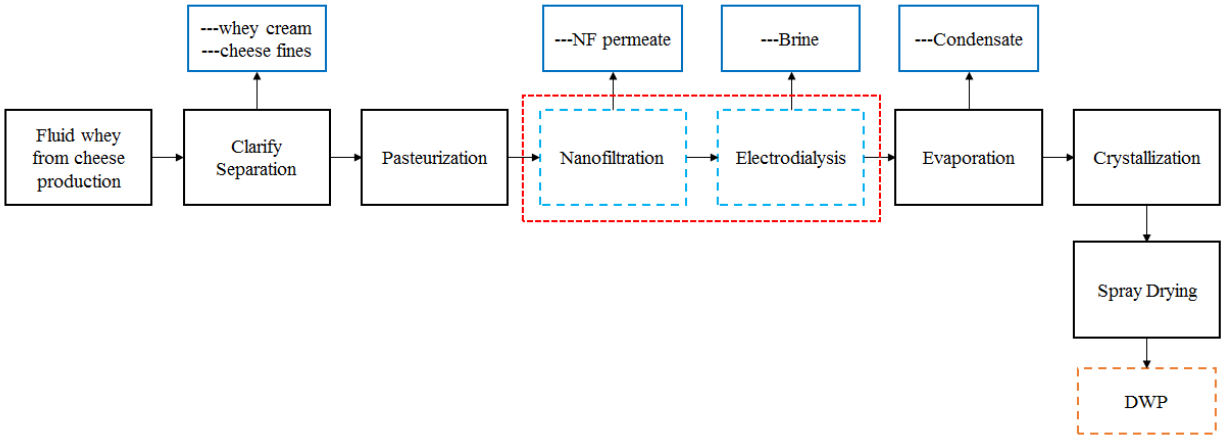

Figure 2. NF and ED flow diagram.

Results and Discussion

It can be seen that both methods are capable of partial separation of lactose and divalent salts from undesirable monovalent salts such as KCl and NaCl. Hence, to select the more efficient technology, several factors including: level of demineralisation, solids concentration, efficiency of ion separation and efficiency of lactose rejection must be taken into account. The parameters of concentrated sweet and acidic whey after nanofiltration are summarized in Table 1.

Table 1: Concentrated whey solutions (sweet and acidic) by nanofiltration

Parameter	Unit	Sweet whey	Acidic whey
pH	-	5.85	4.51
Ash	%	1.19	1.62
Ash OD	%	5.97	8.11
Total solids	%	20	20
Titratable acidity	°SH	18.9	84.7
Na^+	ppm	685	509
K^+	ppm	2415	1785
Mg^{2+}	ppm	214	353
Ca^{2+}	ppm	1248	3143
Cl^-	ppm	1057	1267
SO_4^{2-}	ppm	1291	246
PO_4^{3-}	ppm	999	1503
NO_3^-	ppm	62	9
Citrates	%	0.38	0.40
Lactose	%	15.73	13.3
Lactates	%	0.14	2.21
True protein	%	2.05	1.74
NPN	%	0.44	0.51
Fat	%	0.21	0.21

Nanofiltration can be used as the first step of the demineralization, because NF process can remove minerals and part of organic acids up 30%. Electrodialysis effectively removes salts and organic acids from whey. The results are shown in Table 2.

Table 2: Demineralized whey solutions (sweet and acidic) by electrodialysis to 70% and 90% of purity

Parameter	Unit	Sweet whey D70	Sweet whey D90	Acidic whey D70	Acidic whey D90
pH	-	5.72	5.2	4.34	4.3
Ash	%	0.44	0.19	0.45	0.17
Ash OD	%	2.3	1	2.5	1
Total solids	%	19.6	19.4	18.3	17.4
Titratable acidity	ºSH	11	8.2	37.2	19.3
Na^+	ppm	339	171	73	23
K^+	ppm	831	131	128	30
Mg^{2+}	ppm	114	58	179	65
Ca^{2+}	ppm	663	339	1116	363
Cl^-	ppm	56	6	96	75
SO_4^{2-}	ppm	549	140	14	4
PO_4^{3-}	ppm	478	271	633	422
NO_3^-	ppm	17	10	2	1
Citrates	%	0.14	0.06	0.12	0.04
Lactose	%	16.23	16.41	14.11	14.28
Lactates	%	0.06	0.03	0.88	0.33
True protein	%	2.14	2.16	1.87	1.89
NPN	%	0.40	0.37	0.48	0.45
Fat	%	0.22	0.22	0.22	0.23

One of the important goals is the production of lactose dry concentrates. By ED the result of further processes such as concentration and drying can be improved. Moreover, the product which contains the minimum amount of salts and acids can be used to standardize various food products.

Acknowledgements

This work was created under the project CZ.01.1.02 / 0.0 / 0.0 / 17_107 / 0012377 "Dairy Ingredients" with the support of the Ministry of Industry and Trade through the Agency for Entrepreneurship and Innovation. The project is co-funded by the European Union.

References

1. *G. Rice, S. Kentish, V. Vivekanand, A. Barber, A. O'Connor and G. Stevens*. Membrane-Based Dairy Separation: A Comparison of Nanofiltration and Electrodialysis. Dev. Chem. Eng. Mineral Process. I3 (1/2), pp. 43-54, 2005.
2. *Kai Pan, Qi Song, Lei Wang, Bing Cao***.** A study of demineralization of whey by nanofiltration membrane, Desalination 267 (2011) pp.217
3. *Liang Ge, Bin Wu, Qiuhua Li, Yaqin Wang, Dongbo Yu, Liang Wu, Jiefeng Pan, Jibin Miao, Tongwen Xu.* Electrodialysis with nanofiltration membrane (EDNF) for high-efficiency cations fractionation. Journal of Membrane Science, http://dx.doi.org/10.1016/j.memsci.2015.10.001
4. *Arthur Merkel, Amir M. Ashrafi, Jiří Ečer*. Bipolar membrane electrodialysis assisted pH correction of milk whey. Journal of Membrane Science. https://doi.org/10.1016/j.memsci.2018.03.035.
5. *K. Ideue*, Desalination with ion exchange membranes in food industry, Food Dev. 21 (1986) pp.54–59.
6. *Karen Smith, Ph.D.* Dried Dairy Ingredients. Book. pp. 33-35.

THE EFFECT OF POST-PROCESSING ON THE STABILITY OF PLATINUM COPPER ELECTROCATALYSTS

Elizaveta Moguchikh, Anastasia Alekseenko, Kirill Paperzh, Angelina Pavlets, Vladimir Guterman

Southern Federal University, Rostov-on-Don, Russia, E-mail: *liza.moguchix@mail.ru*

Introduction

Alternative sources of energy are widely used nowadays. Among others there are low-temperature fuel cells (FC), including platinum containing catallysts[1-2]. With platinum being an expensive metal, researchers are trying to decrease its content by means of different methods. Embedding a less noble metal into the structure of nanoparticles (NP) favorably affects electrochemically characteristics of materials. However, while in commision an alloying constiuent is being dissolved, what results in a proton exchanging membrane being poisoned and FC length of service being decreased. In order to decrease this effect, catalysts are acidly pre-processed[3-4].

This study is aiming at examining the influence of acid processing on stability of catalysts with bimetal structure of NP.

Experimental section

In the course of this research catalysts with gradient structure of NP [5] before acid processing and after it were used. For comparison the commersial sample JM 20 and Pt/C material with 40% platinum scaling PM40 were tested. Nanoparticles with gradient structure were obtained with consecutive precipitation of platinum and copper followed by decreasing amount of copper. The material was being processed in 1M of HNO3 for 60 minutes.

Before stability tests the phase of preparation is carried out and an initial value of electrochemically active surface area ESA is measured. The latter is respectively equal to 103 $m^2/g(Pt)$ – Grad; 84 $m^2/g(Pt)$ – Acid; 94 $m^2/g(Pt)$ – PM40; 96 $m^2/g(Pt)$ – JM20. Catalysts stability was examined by means of nonsingle cycling in the range of potentials between 0.6–1.0V (5000 cycles), 0.6–1.4V (1000 cycles) at the temperature of 23^0C. 1M of chlorid acid was used as an electrolyte, the involuting speed was equal to 100 mV/s. This way to evaluate stability is called "stress-test". Stability was measured regarding variations of electrochemically active surface area.

Results and Discussion

The obtained platinum-copper catalysts are characterized by an actual composition close to the calculated one: the mass fraction of metals in Alloy and Grad samples is 28% and 29% with pure platinum content of 21% and 20%, respectively (Table 1). The results of the X-ray fluorescence analysis of their composition confirmed that the ratio of metals in the samples is close to the calculated ratio of 1: 1.

Comparison of the relative stability of catalysts during long cycling makes it possible to consider the most stable sample Grad, which demonstrates high values of ESA both before and after the stress test (Table 1, Fig. 1a, b). Significantly lower is stability of Alloy and commercial Pt/C catalyst E-TEK (Figure 1a).

Table 1: Electrochemical characteristics of Pt(Cu)/C and Pt/C catalysts

Test material	ESA $m^2/g(Pt)$ after stress-test		Stability, %	
	0.6 – 1.0V	0.6 – 1.4V	0.6 – 1.0V	0.6 – 1.4V
Grad	81	71	78	69
Acid	76	60	90	72
PM40	72	39	77	42
JM20	61	>19	64	>20

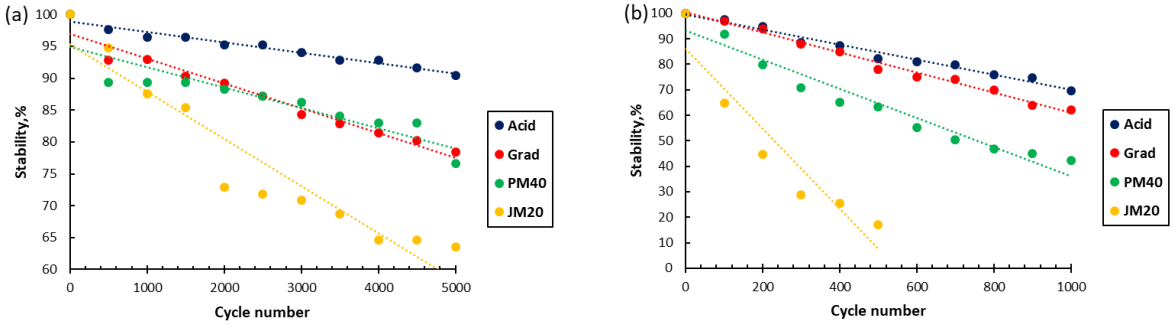

Figure 1. Stability change during voltammetry stress-test in potential range (a) 0.6 – 1.0V (b) 0.6 – 1.4V. 0.1 M $HClO_4$, Ar atmosphere.

In the narrow range of potentials the catalyst Acid manifests the biggest stability (90%). In the range of potentials between 0.6–1.4 V the material after acid processing MK is characterised by higher stability (70%), than the initial material M (63%), and the commersial catallyst JM shows stability <20% (Table 1, Fig. 1a, b). It is connected with platinum NP catalyzing the process of carrier oxidation under the given conditions with direct contact.

The ultimate analysis shows that during stress-tests an alloying constituent in the material after acid processing is practically not dissolved. This means that the obtainable copper was mostly dissolved while leaching. Perhaps, this was for reorganisaion of NP surface, which resulted in platinum producing a protecting monolayer and preventing the alloying d-metal from being dissolved. Acid processing causes the stability increase.

The research was supported by State specification (№ 13.3005.2017/PCH).

References

1. *Alekseenko A.A., Moguchikh E.A., Safronenko O.I., Guterman V.E.,* Durability of de-alloyed PtCu/C electrocatalysts // Int. J. of Hydr. Energy. 2018. V. 43. P. 22885 - 22895.
2. *Yaroslavtsev A.B., Dobrovolsky Y.A., Shaglaeva N..S, Frolova L.A., Gerasimova E.V., Sanginov E.A.* Nanostructured materials for low-temperature fuel cells // Russian Chemical Reviews. 2012. V. 81. P. 191–220.
3. *Moguchikh E.A., Alekseenko A.A., Guterman V.E., Tabachkova N.Y., Menshchikov V.S.,* Effect of the Composition and Structure of Pt(Cu)/C Electrocatalysts on Their Stability under Different Stress Test Conditions // Russian Journal of Electrochemistry. 2018, V. 54, P. 979 – 989.
4. *Pavlov, V.I., Gerasimova, E.V., Zolotukhina, E.V., Dobrovolsky, Y.A., Don, G.M., Yaroslavtsev, A.B.,* Degradation of Pt/C electrocatalysts having different morphology in low-temperature PEM fuel cells, Nanotechnologies in Russia, 2016, vol. 11, p. 743.
5. *Alekseenko, V.E. Guterman, S.V. Belenov, Moguchikh E.A.,* Pt/C electrocatalysts based on the nanoparticles with the gradient structure // Int. J. of Hydr. Energy. 2018. V. 43. P. 3676 – 3687.

VIZUALIZATION OF ELECTROCONVECTION DURING ELECTRODIALYSIS OF STRONG ELECTROLYTE AND AMPHOLYTE SOLUTIONS

Ilya Moroz, Aleksey Rogov, Dmitrii Butylskii, Semyon Mareev, Natalia Pismenskaya
Kuban State University, Krasnodar, Russia, E-mail: *ilya__moroz@mail.ru*

Introduction

In present days, the process of electrodialysis is carried out at underlimiting current densities. The use of overlimiting current modes will reduce the capital cost of ion-exchange membranes, due to the reduction of the active surface area. In such conditions, a positive effect is achieved due to the intensification of ion transfer by electroconvection [1]. This phenomenon is quite well studied for the case of strong electrolytes. In weak electrolytes, protonation-deprotonation reactions take place, which contribute to the emergence of new charge carriers at overlimiting current densities. The question of the presence of electroconvective mixing in such solutions remains open. In this work, experimental data were obtained that confirm the presence of electroconvection.

Experiments

For visualization of concentration distribution, 10 μM rhodamine 6G (R6G) were added to the solution. 0.01 and 0.1 M NaCl and NaH_2PO_4 solutions were used in the experiments. The flow rate of the solution in the chambers of the cell was controlled by the height of the liquid column. At a current six times higher than the limiting value, videos of electroconvective vortices were obtained. Dark areas correspond to a high concentration of the solution, light – low. Due to the high resolution of shooting, the shape of electroconvective vortices is clearly visible.

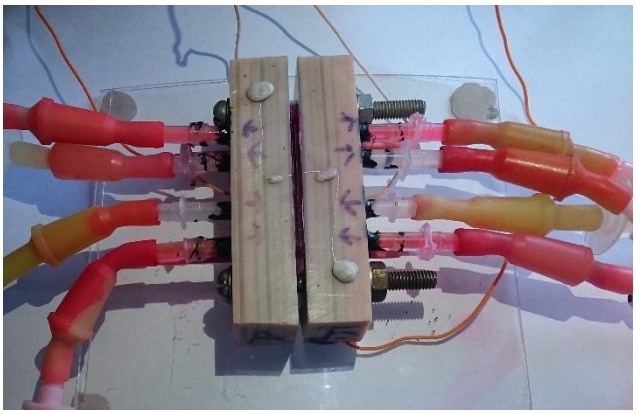

Figure 1. Image of the Electrodialysis Cell Developed for Visualization of Electroconvective Vortex.

Results and Discussion

In solutions of a binary electrolyte, intense electroconvective mixing is observed at overlimiting current densities. The size of the electroconvective mixing region increases with the decrease of the initial solution concentration. In solutions of sodium dihydrophosphate, the overlimiting mass transport is due to electroconvective vortices mixing. All the experimental results are in good qualitative agreement with the theoretical data presented in [2, 3].

With an increase in the concentration of the initial electrolyte solution, the region of electroconvective mixing decreases. This behavior is due to a decrease in the space–charge region with increasing concentration at fixed ratio of current density to its limit value. In NaH_2PO_4 solutions, the intensity of electroconvective vortices is lower than in NaCl solutions. This is due to the protonation-deprotonation reaction of dihydrophosphate anions. As a consequence of the Donnan exclusion, the split protons are quickly removed from the membrane against the movement of anions, the space charge region decreases and, therefore, the electroconvective vortices intensity decreases.

In addition, the effect of flow rate on the electroconvective vortices intensity has been studied.

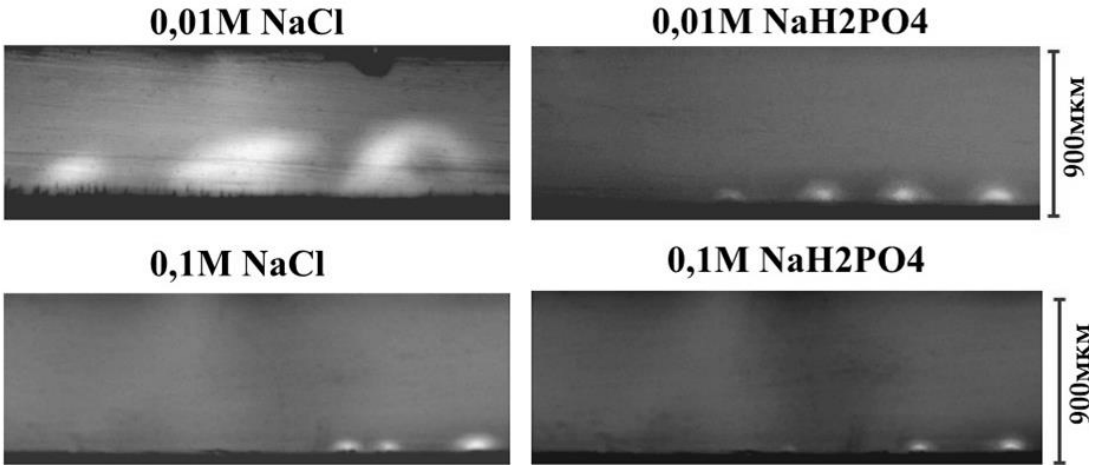

Figure 2. Images of the Electroconvective Vortices in Strong Electrolyte (left) and Ampholyte (right) Solutions at $i=6i_{lim}$.

Acknowledgments

The study is realized with the financial support of the Russian Science Foundation, project № 17-19-01486 (study in solutions of sodium dihydrophosphate) and 18-38-00600 mol_a (study of the effect of flow rate in solutions of sodium chloride).

References

1. *Kwak R., Guan G., Peng W. K., Han J.* Microscale electrodialysis: concentration profiling and vortex visualization // Desalination. 2013. V. 308. P. 138-146.
2. *Urtenov M. K., Uzdenova A. M., Kovalenko A. V., Nikonenko V. V., Pismenskaya N. D., Vasil'eva V. I., Sistat P., Pourcelly G.* Basic mathematical model of overlimiting transfer enhanced by electroconvection in flow-through electrodialysis membrane cells // J. Membr. Sci. 2013. V. 447 (15). P. 190-202.
3. *Nikonenko V. V., Mareev S. A., Pismenskaya N. D., Kovalenko A. V., Urtenov M. K., Uzdenova A. M., Pourcelly G.* Effect of electroconvection and its use in intensifying the mass transfer in electrodialysis (review) // Russ. J. Electrochem. 2017. V. 53. № 10. P. 1122-1144.

STRUCTURE – PROTON TRANSPORT CORRELATIONS IN PERFLUORINATED SULFOPOLYMER MEMBRANES WITH SHORTER SIDE CHAINS

[1,2]Kamila Mugtasimova, [2]Alexey Melnikov, [2]Alexey Kashin, [2]Vitaliy Sinitsyn

[1]IGP RAS, Vavilova 38, 119991, Moscow, Russia

[2]InEnergy Group, Elektrodnaya 12-1, 111524, Moscow, Russia

E-mail: *kamila.mugtasimova@gmail.com*

Introduction

Today the most common commercial product for the proton exchange membrane fuel cell is the membrane Nafion™ produced by the DuPont® company, but still there are a lot of attempts to make another promising membranes or modify existing. The structure of short-side chain polymer membranes, as Aquivion®, is different in comparison to traditional long side-chain polymer membranes, as Nafion™ [1-2]. This difference in structures strongly influence on the final properties of the membrane. The aim of this work is to study structure – protonic conductivity correlations in new type of proton-exchange membranes, made from new short-side chain perfluorinated sulfopolymer Inion - Russian analogue of Aquivion® [3].

Experiments

Proton-conducting membranes were obtained by solution casting method from new ionomer Inion (Russian analog of Aquivion). Obtained membranes were annealed for 20 h at different temperatures (at temperature range from 100 ° C to 220 ° C). The structures of all experimental samples were investigated by small-angle X-ray diffraction methods. . It was shown, that the ionomer peak, corresponding to the formation of cylindrical structures, could be observed only above Tan ≥ 130 ° C. With the increase of annealing temperature up to 190 ° C and higher ionomer peak shifted towards smaller angles that indicated the formation of broader cylindrical channels. Also it was shown that higher annealing temperatures led to significant increase of specific proton conductivity, measured at different temperatures (20, 30, 50 and 70 ° C) and 100% relative humidity. This increase was observed up to Tan = 170 ° C, where specific proton conductivity reached its maximum and then drastically fell down. The membranes, annealed at Tan = 170 ° C demonstrated the values of specific proton conductivity even higher, than those of commercial membrane Nafion NR212 and the activation energies, calculated from the temperature dependences conductivity were about Ea≈0.1 eV, which is much less than those of a membrane based on Nafion NR212, where Ea is about 0.25 eV.

Results and Discussion

In this case, our investigations showed that the transport characteristics and dielectric properties of water in nanopores strongly depend on the membrane morphology and its pore size. In this connection, it can be assumed that the lower activation energy Ea and higher values of specific proton conductivity of prepared polymer samples may be due to a smaller diameter of the proton transport channels in the matrix of such a polymer than the diameter of the Nafion NR212 polymer channels. The theoretical model was proposed, according to which a decrease in the dimensions of the channels leads to an increase in the concentration of bond defects and, consequently, to a decrease in the activation energy Ea of the migration process, which was observed in our investigations.

From SAXS data, which are presented on the Figure 1, it can be seen, that the ionomer peak, corresponding to the formation of cylindrical structures, could be observed only above annealing temperature ≥ 130 ° C. With the increase of annealing temperature up to 190 ° C and higher ionomer peak shifts towards smaller angles, that indicated the formation of broader cylindrical channels.

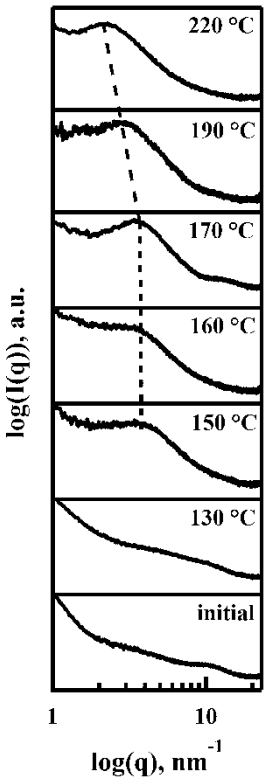

Figure 1. The ionomer peaks of membrane samples annealed at different temperatures.

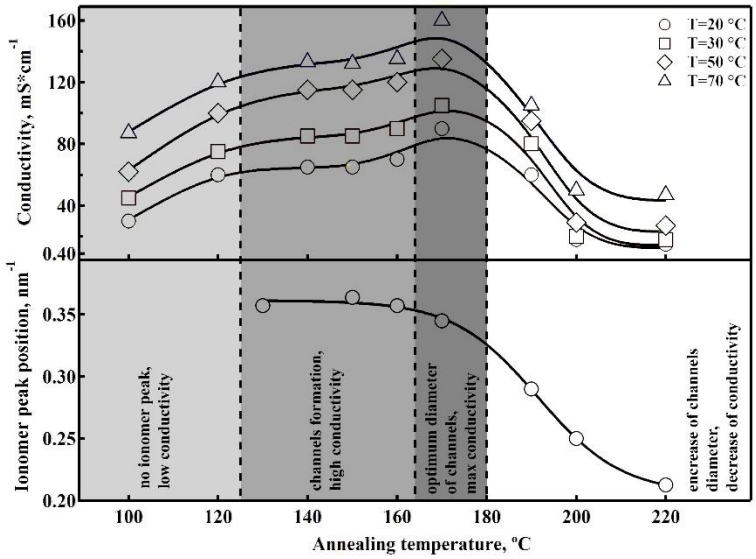

Figure 2. The structure – protonic conductivity correlation for membranes annealed at different temperatures.

On the Figure 2 it is shown that higher annealing temperatures led to significant increase of specific proton conductivity, measured at different temperatures. All this data is strongly correlated with the position of ionomer peak.

References

1. *R. Hiesgen, T. Morawietz, M. Handl, M. Corasaniti, K.A. Friedrich* // Journal of The Electrochemical Society, 161 (12), 2014, p1214-1223.
2. *K. Schmidt-Rohr, Q. Chen* // Nature materials, 7, 2008, p75-83.
3. Patent RU 2545182 C1-2013

OPTICAL VISUALIZATION OF FILTRATION PROCESS OF COLLOIDAL PARTICLES IN TRACK-ETCHED MEMBRANES AT NANO-SCALE

[1]Andrey Naumov, [2]Pavel Apel, [1]Sergey Kulik, [1]Ivan Eremchev, [3]Dmitry Zagorskiy
[1]Institute for Spectroscopy of the Russian Academy of Sciences, Troitsk, Russia
[2]Joint Institute for Nuclear Researches, FLNR, Dubna, Russia
[3]Shubnikov Institute of Crystallography, Moscow, Russia

Till now filtration process was investigated mostly in macroscopic scale. At the same time the microscopic aspects of filtration, separation absorption are of great interest. The application of new-developed optical techniques seems to be very useful for detection of individual nanoparticles during the filtration process.

Modern technologies make new demands on methods and instruments for characterizing new materials, structures, and devices based on them. Important problems include development of methods for rapid diagnostics of structure and dynamic processes with nanometer spatial resolution. Considerable potential for solving such problems is demonstrated by super-resolved far-field fluorescence microscopy methods (nanoscopy). Optical nanoscopy methods are based on the fact that the accuracy of recovery of the spatial coordinates for a point light source (molecule, nanocrystal) in detection of its fluorescent image using a far-field microscope equipped with an ultrasensitive array detector (CCD and CMOS) is determined only by the signal-to-noise ratio of the detected luminescence, the total number of collected photons,and the stability of the apparatus. Computer analysis of the fluorescent image taking into account the apparatus function for a point source in a modern experiment gives an accuracy in recovery of the lateral coordinates of the emitter within a few nanometers for detection of several thousand photons. So we have possibility to determine position of individual nanoparticle with a high accuracy and to determine movement of this particle with high time resolution.

We have used fluorescence nanoscopy for direct imaging of adsorption of individual colloidal quantum dots of diameter ~10 nm (spherical core/shell CdSeS/ZnS semiconductor nanocrystals, functionalized by organic oleic acid ligands) in nanopores of a nuclear filter (a polypropylene track membrane with pores of diameter ~500 nm). We have shown that when a colloidal toluene solution passes through the pores of the membrane, the nanoparticles are completely retained at a depth of 10 μm.

We have demonstrated the feasibility of direct imaging of ultrafiltration of semiconductor nanocrystals, functionalized by ligand shells, from a colloidal toluene solution in nanopores of a track membrane, using super-resolved fluorescence spectroscopy. Fluorescent images of individual nanocrystals (quantum dots) and their agglomerates are recorded in an epiluminescence scheme at different depths along the thickness of a track membrane, after ultrafi ltration and complete evaporation of the solvent. In the case of a propylene membrane with pore diameter ~500 nm, we imaged the adsorption of ~10 nm quantum dots all the way down to a depth of 10 μm.

Acknowledgment

Experimental work to develop methods for detecting individual semiconductor quantum dots and their agglomerates was supported by a grant of Russian Science Foundation (17-72-20266). Preparation and electron microscopy of the membranes was partially supported by the Ministry of Science and Higher Education within the State assignment FSRC «Crystallography and Photonics» RAS

SELECTIVITY OF HETEROGENEOUS CATION-EXCHANGE MEMBRANES MODIFIED BY POLYANILINE

Ekaterina Nazyrova, Svetlana Shkirskaya, Anastasiya Norenko, Ekaterina Dankovtseva
Kuban State University, Krasnodar, Russia, E-mail**:** *shkirskaya@mail.ru*

Introduction

The selectivity of ion-exchange membranes is especially important for the membranes using in electromembrane processes. The true transport number of ions is the fundamental characteristic of the selective properties of ion-exchange membranes and used for a theoretical description of transport phenomena. The purpose of this work was to estimate the true transport number of ions in the MK-40 and MK-40/PANI membranes in sodium chloride and hydrochloric acid solutions.

Experiments and theory

A heterogeneous membrane MK-40 and a modified MK-40/PANI were the objects of the study. The modification was carried out by the method of sequential diffusion of polymerizing solutions through the membrane to water [1]. The conducting properties (k_m) of initial and composite membranes were studied by the mercury contact method as an active part of the membrane impedance. Diffusion permeability was found by the diffusion rate of electrolyte from solution through the membrane to distilled water. The water transport numbers (t_w) were measured in a two-chamber cell with reversible silver chloride electrodes by the volumetric method [2]. The apparent counterion transport number (t_{+app}) in the membrane was determined by the potentiometric method using a two-compartment cell and silver–silver chloride measuring electrodes. The concentration on the two sides of the membrane differed twice [3]. The measurements were carried out for the MK-40 and MK-40/PANI membranes in NaCl and HCl solutions. Two approaches were used to estimate the true ion transport numbers that are shown schematically in Table.

Table: Schematic representation of methods for assessing the selectivity of ion-exchange membranes

By Schachard equation	Using electrodiffusion coefficients
$t_{+app} = \frac{1}{2}\left(1+\frac{\Delta E_{mb}}{\Delta E_{id}}\right)$ $\quad t_w = \frac{VF}{Si\tau M_w}$ $E_{id} = \frac{RT}{F}\ln\frac{(m\gamma_{\pm})_2}{(m\gamma_{\pm})_1}$, $t_{+app} = \psi(C)$ $\quad t_w = \psi(C)$ $t^*_+ = t_{+app} + Mm_{\pm}10^{-3}t_w$ (1)	$k_m = \psi(C)$ $\quad P^* = \psi(C)$ $L^*_+(C) = \frac{\kappa^d_m(C)}{2F^2}\left[1+\sqrt{1-\frac{2P^*(C)CF^2}{RT\kappa^d_m(C)\pi_{\pm}}}\right]$ (2) $L^*_-(C) = \frac{\kappa^d_m(C)}{2F^2}\left[1-\sqrt{1-\frac{2P^*(C)CF^2}{RT\kappa^d_m(C)\pi_{\pm}}}\right]$ (3) $t^*_+(C) = \frac{L^*_+(C)}{L^*_+(C)+L^*_-(C)}$ (4)

The first approach allows to calculate the true transport numbers of the counterions (t^*_+) using the Schachard equation (1) which takes into account the water transport numbers (tw) and the apparent transport numbers of counterions (t_{+app}). The other approach establishes a relationship

between the true transport numbers of the counterions $t^*_+(C)$ and the electrodiffusion coefficients of the counter- $L^*_+(C)$ and coions $L^*_-(C)$ according to equation (4). The concentration dependences of electrodiffusion coefficients were calculated based on concentration dependences of electrical conductivity (k_m) and diffusion permeability (P^*) of the ion-exchange membrane according to expressions (2, 3). In Eq. (2, 3), $\pi_\pm$ is the correcting coefficient taking into account solution imperfectness

$$\pi_{\pm} = 1 + \frac{d \log \gamma_{\pm}}{dC},$$

where $\gamma_\pm$ is the average activity coefficient of the electrolyte. The membrane conductivity under direct current (k_m^d) was calculated by the equation:

$$k_m^d = k_m t_+^{(1-f)}, \quad (5),$$

where t_+ is transport numbers of the counter-ions in solution; (1-f) is the parameter of the two-phase microheterogeneous model, which characterizes the volume fraction of the intergel solution in the swelled ion-exchange membrane [4].

Results and Discussion

The concentration dependences of the apparent transport numbers of counterions and water transport numbers (Fig. 1) in NaCl and HCl solutions were used to calculate the true transport numbers of counterions for the MK-40 and MK-40/PANI membranes by the Schachard equation (1). It was shown (Fig. 1) that the values of apparent ion transport numbers for both the initial and the modified membranes are less in NaCl comparison with HCl solutions.

Investigation of the water transport numbers in the initial and modified membranes in a wide range of different electrolytes concentrations showed that t_w value in HCl is 2-2.5 times lower than in NaCl solutions. It is associated with different mechanisms of transport of these ions in the electric field. In HCl solutions the water transport numbers for both membranes practically do not change with increasing concentration.

Evaluate of values $t^*_+(C)$ showed that the selectivity of the modified membranes remains fairly high in both NaCl and HCl solutions (Fig. 2).

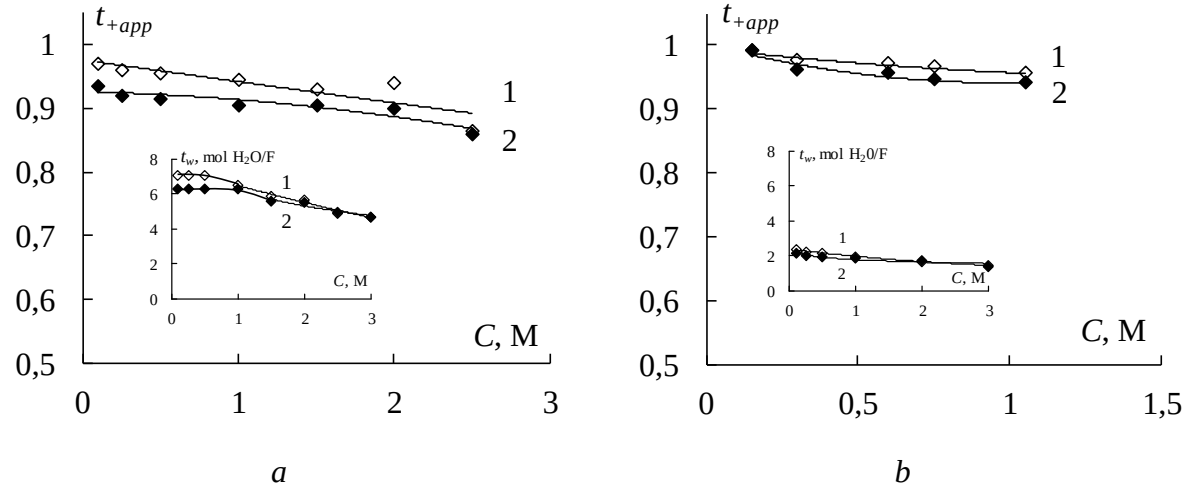

a *b*

Figure 1. Concentration dependences of apparent transport numbers counterions and water transport numbers for MK-40 (1) and MK-40/PANI (2) membranes in NaCl (a) and HCl (b) solutions.

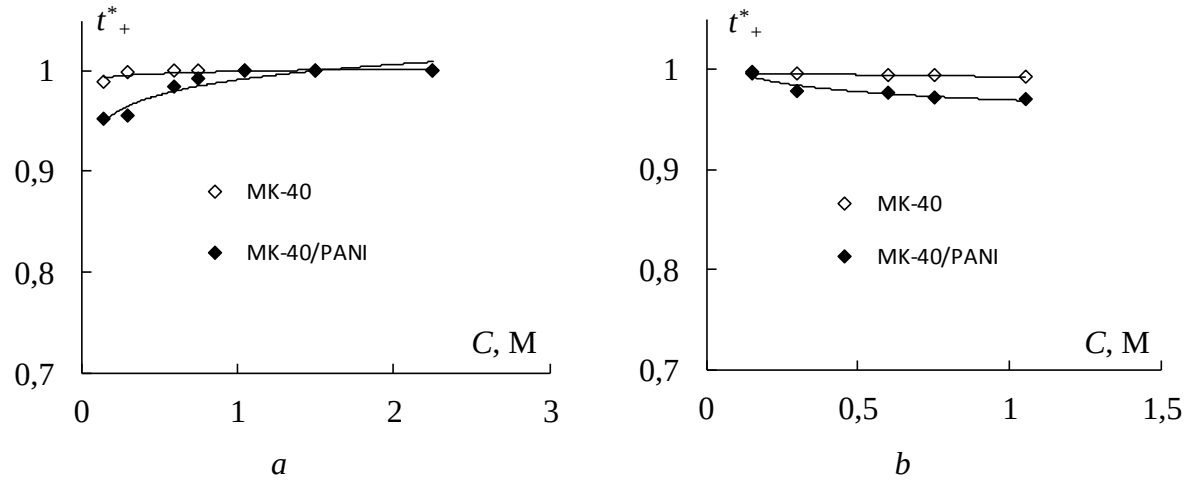

Figure 2. Concentration dependences of the true transport numbers of counterions calculated by Schachard equation for MK-40 and MK-40/PANI membranes in NaCl (a) and HCl (b) solutions.

To validate the results obtained based on the equation Schachard we additionally calculated the concentration dependences of true transport numbers of hydrogen ions for both membranes based on the electrodiffusion coefficients of counter- L^*_+ and coions L^*_-. The results of the true proton transport numbers for both membranes are close to 1 (Fig. 3).

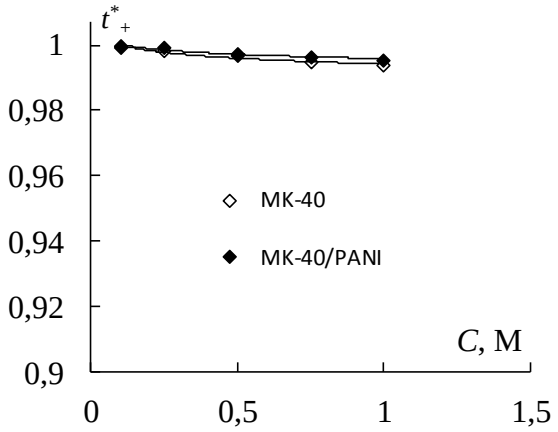

Figure 3. Concentration dependences of the true transport numbers of counterions calculated using electrodiffusion coefficients for MK-40 and MK-40/PANI membranes in HCl solutions.

Thus, all the methods used to calculate the true numbers of ion transport confirm the preservation of a sufficiently high selectivity of the MK-40 membrane after modifying with polyaniline.

The present work was supported by the Russian Foundation for Basic Research (project № 19-08-00925).

References

1. *Shkirskaya S.A., Senchikhin I.N., Kononenko N.A., Roldugin V.I. //* Russ. J. Electrochem. 2017. V. 53. P. 89-96.
2. *Berezina N.P., Shkirskaya S.A., Sycheva A.A.-R., Krishtopa M.V.* // Colloid Journal. 2008. V.70, P. 397–406.
3. Nazyrova E.V., *Shkirskaya S.A., Kononenko N.A., Dyomina O.A.* // Petroleum Chemistry. 2016. V. 56, No. 10, P. 931–935.
4. *Zabolotsky V.I., Nikonenko V.V.* Transport of ions in membranes. Nauka. 1996. 393 p.

AROMATIC POLYAMIDE MEMBRANES FOR ORGANOPHILIC PERVAPORATION

[1]Vera Nesterova, [1]Alexandra Pulyalina, [1,2]Galina Polotskaya

[1]Saint-Petersburg State University, Saint-Petersburg, Russia, E-mail: *st049110@student.spbu.ru*

[2] Institute of macromolecule compounds, Russian Academy of Sciences, Saint Petersburg, Russia

Introduction

Pervaporation (PV) has recently gained much attention as an alternative separation process for azeotropic, close-boiling and thermally unstable mixtures. Moreover, PV is an energy-saving and easy scale-up process.

Nowadays research in pervaporation is focused on finding new membrane materials with higher transport characteristic. Membranes based on polyamides are promising due to their high mechanical, thermal and chemical stability with appropriate separating properties.

The aim of the present work is an investigation of physico-chemical and transport characteristics of aromatic polyamide (PA) and complex polymer-metal PA-Cu(I) in the process of fuel desulphurization by pervaporation. Thiophene along with other sulfur-containing compounds causes environmental pollution due to sulfur dioxide emissions from fuel combustion. Thus, the reduction of sulfur level in fuels is a relevant problem in the petrochemical industry. In this paper, n-heptane was chosen to simulate gasoline, with thiophene as the representative sulfur impurity.

Experiments

PA was obtained by polycondensation reaction**.** The PA-Cu(I) complex was obtained by adding the equimolar amount of copper (I) chloride dissolved in N-methylpyrrolidone to the solution of PA. It should be emphasized that formation of metal-polymer complex is accompanied by a marked increase in viscosity of polymer solution. Dense nonporous membranes were obtained by casting polymer solution in N-methylpyrrolidone onto a glass plate. The membranes were dried at 90°C in vacuum until the constant weight was reached.

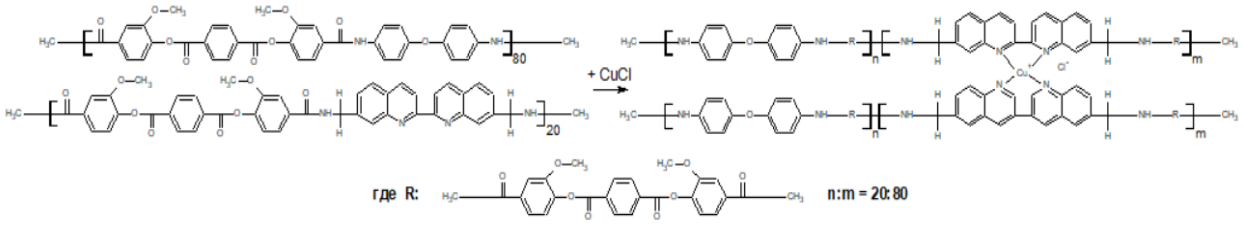

Figure 1. Scheme of PA to PA-Cu(I) transformation.

The mechanicals properties and structure of membranes were characterized using scanning electron microscopy (SEM), differential scanning calorimetry (DSC), thermogravimetric analysis, sorption experiments toward the components of the separating mixture and measurement of contact angles with water and ethanol.

The transport properties in pervaporation of the n-heptane-thiophene mixture were measured using a laboratory cell having an effective membrane area of 23.8 cm^2 at 20°C. Downstream pressure below 10^{-2} mm Hg was maintained. The composition of permeate was determined using gas chromatograph «Chromatec–Crystal 5000.2» (Chromatec, Russia) with thermal conductivity detector.

Results and Discussion

A detailed study of the internal structure of membranes was carried out by SEM. Figure 2 shows the morphology of PA and PA-Cu(I) cross-sections. The PA film cross-section exhibits comparatively smooth structure. Introduction to copper leads to changes in the polymer film.

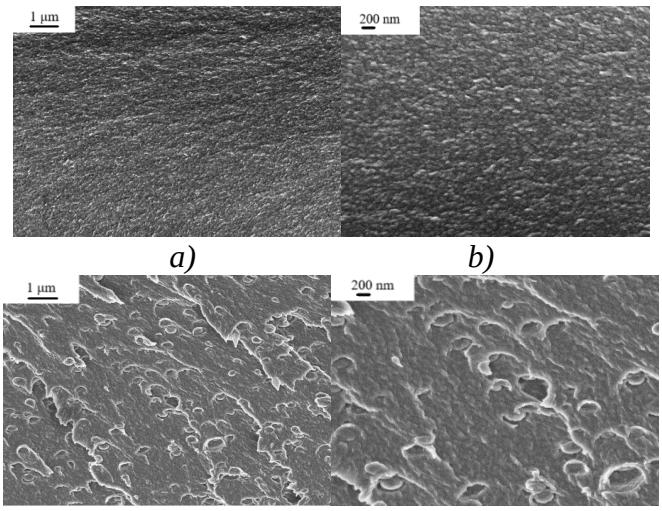

Figure 2. SEM micrographs of PA (a,b) and PA-Cu(I) (c,d) cross-section.

DSC shows that the glass transition temperature is 201°C for PA и 203°C for PA-Cu(I). According to this data, polymers are in a glassy state during separation process.

Separation of n-hepatane–tiophene mixture through PA ana PA-Cu(I) membranes was studied by pervaporation experiments in the concentration range of 0.1 — 0.2 wt% of tiophene in the feed at 20°C. Figure 3 shows the dependence of thiophene concentration in permeate on thiophene concentration in feed during the pervaporation of n-heptane-thiophene mixture through membranes. The content of thiophene in the permeate is higher than in the feed; with an increase in the amount of thiophene in the initial mixture, its content in the permeate increases. As can be seen PA-based membrane is more selective for thiophene compared to the polymer-complex membrane PA-Cu(I).

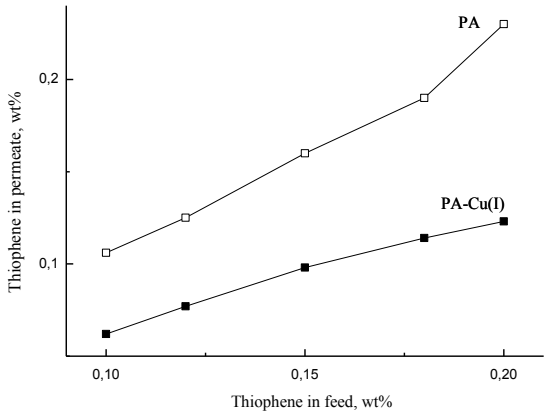

Figure 3. Dependence of thiophene concentration in permeate on thiophene concentration in feed in the pervaporation of n-heptane-thiophene for PA and PA-Cu(I) membranes.

Figure 4a and 4b show the main transport parameters of the membranes: total flux and separation factor as a function of the thiophene concentration in the feed. As shown in Figure 4b, separation factors of both membranes insignificantly decrease with an increasing the thiophene concentration in the feed. It is evident that PA membrane is more permeable and more selective to thiophene as compared to the PA-Cu(I) membrane in the separation of n-heptane-thiophene mixture. Increase of thiophene concentration in the feed leads to the decreasing total flux through PA-Cu(I) membrane and to a slight change in flux through PA membrane. Values of this parameter of PA-Cu(I) membrane exceed that of PA membrane.

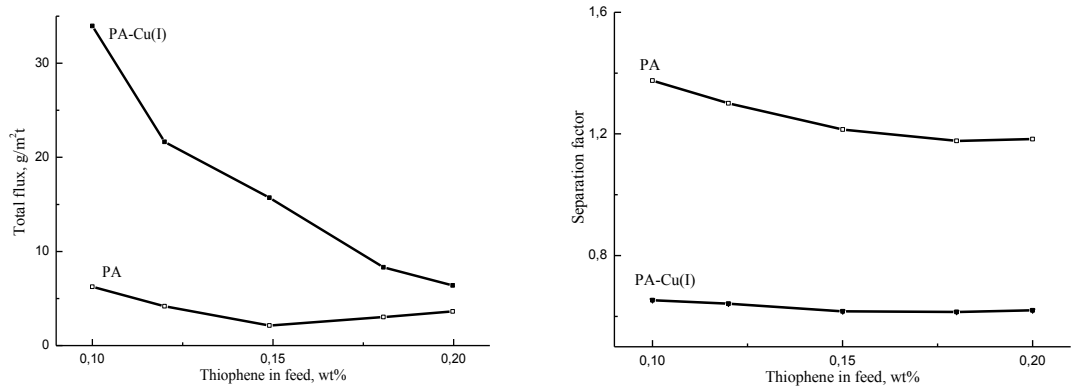

a) *b)*

Figure 4. Dependence of (a) total flux and (b) separation factor(thiophene/heptane) on thiophene concentration in the feed for pervaporation of n-heptane-thiophene mixture using membranes: PA and PA-Cu(I), 20℃.

Conclusions

Polymer–metal complex PA-Cu(I) and its prepolymer PA were successfully used for dense membranes preparation. The physical characteristics of polymers were studied. It is shown that the studied membranes are highly thermally stable and can be used as a material for pervaporation.

Mass transfer through PA and PA-Cu(I) membranes was studied by sorption and pervaporation tests toward thiophene and n-heptane. In the separation of n-heptane-thiophene mixture by pervaporation the PA membrane is less permeable but more selective to sulfur containing compounds as compared to the PA-Cu(I) membrane.

Acknowledgments

The reported study was funded by RFBR according to the research project № 18-33-01203. Equipment of Resource Centers of Saint Petersburg State University, namely, Interdisciplinary Resource Center “Nanotechnologies” and “X-ray Diffraction Studies” were used for investigation.

MODIFIED MICROHETEROGENEOUS MODEL FOR DESCRIBING THE ELECTRICAL CONDUCTIVITY OF MEMBRANES IN DILUTED ELECTROLYTE SOLUTIONS

Vladlen Nichka, Michail Porozhnyy, Svetlana Shkirskaya, Natalia Pismenskaya, Victor Nikonenko

Membrane Institute, Kuban State University, Krasnodar, Russia, E-mail: *nichkavs@mail.ru*

Introduction

The microheterogeneous model [1] makes it possible to describe many transport properties of ion-exchange membranes using a single set of parameters, but it is applicable in a limited range of concentrations of electrolyte solutions. We propose a new modification of this model, taking into account the contribution of the electric double layer (EDL) at the internal boundaries of the gel and the solution phases to describe the conductivity of the membrane in dilute electrolyte solutions.

Theory

The model takes into account that the thickness of the EDL in the internal solution phase increases with the dilution of external solution. Since the EDL is more conductive than the electroneutral part of the solution, it is possible to describe the trend of the concentration dependence of the membrane conductivity more accurately in comparison with the basic microheterogeneous model [1]. The new version of the microheterogeneous model uses an additional parameter – the effective pore radius – which was absent in the basic version of the model.

Results and Discussion

The behavior of a specially prepared homogeneous cation-exchange membrane, similar in structure and composition to commercial Nafion membrane was studied. Calculated concentration dependences of the electrical conductivity of the membrane shows a good agreement with the experimental data (Fig. 1). The larger the size of the effective pore radius, the more the electrical conductivity decreases and the lower the threshold concentration of the equilibrium salt solution.

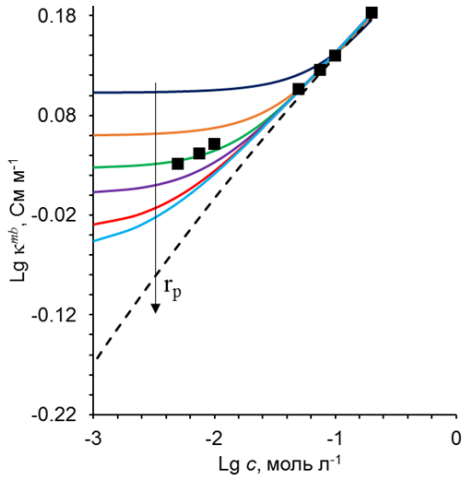

Figure 1. Experimental (dots) and Calculated (lines) Concentration Dependences of the Membrane Conductivity in NaCl Solutions. Calculations are made for pores with a flat geometry. The dashed line is the prediction of the base microheterogeneous model [1]; solid lines - prediction of the modified microheterogeneous model. The arrow shows the direction of increase r_p *= 1, 3, 6, 10, 20, 30 nm.*

Acknowledgments

The study is realized with the financial support of the Russian Science Foundation, project № 17-19-01486.

References

1. *Zabolotsky V. I., Nikonenko V. V.* Effect of structural membrane inhomogeneity in transport properties // J. Membr. Sci. 1993. V. 79. P. 181-198.

CONVERSION OF HYDROCARBONS USING HOLLOW FIBER OXYGEN-PERMEABLE MEMBRANES

Natalya Niftalieva, Mikhail Popov, Alexander Nemudry
Institute of Solid State Chemistry and Mechanochemistry, SB RAS; Novosibirsk, Russia
E-mail: *popov@solid.nsc.ru*

Introduction

Oxygen-permeable (OP) membranes from oxides with mixed oxygen and electronic conductivity are now widely used in various innovative technologies. They have 100% selectivity with respect to oxygen, are easily incorporated into high-temperature processes, for example, partial oxidation of hydrocarbons (methane conversion to synthesis gas, etc.).

In order to achieve acceptable for practical use of the values of oxygen flows, the membrane OP must be heated to a temperature above 600°C. Usually this is achieved by external heating, as well as heat generated by the exothermic chemical reactions on the membrane surface. Since, at T> 600 ° C, membrane materials, in addition to ionic, also possess high electronic conductivity, we have for the first time shown the possibility of direct / direct heating of OP membrane capacitance by passing an electric current through it [1,2]. On the one hand, this method of heating oxygen-permeable membranes allows increasing their energy efficiency, productivity and efficiency of control. On the other hand, it opens access to the surface of the working membrane, and, therefore, makes it possible to study the mechanism of oxygen permeability by various in situ physico-chemical methods. In addition, when the membrane operates in a catalytic membrane reactor mode (when gaseous reagents, for example, hydrocarbons are supplied from the permeable side), sharp temperature gradients occur in the supplied gas, which allow quenching non-equilibrium products of oxidative conversion of hydrocarbons (for example, acetylene during oxidative pyrolysis of methane). Such quenching can lead to a significant increase in the selectivity of the processing of hydrocarbons into target products (Figure 1).

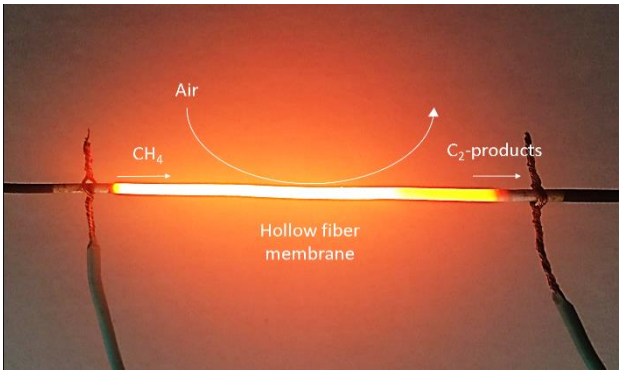

Figure 1. Conversion of hydrocarbons using hollow fiber oxygen-permeable membranes.

Results and discussion

In the work, (1) new possibilities were studied that open up to study the mechanism of oxygen permeability and (2) the features of practically important processes that occur when using direct heating of membranes with electric current.

Acknowledgements

The reported research was funded by Russian Foundation for Basic Research and the government of the region of the Russian Federation, grant № 18-43-543006.

References

1. *Mikhail P. Popov, Daniel V. Maslennikov, Igor I. Gainutdinov, Igor P. Gulyaev, Andrey N. Zagoruiko, Alexander P. Nemudry* // Catalysis Today, https://doi.org/10.1016/j.cattod.2018.11.009
2. *Mikhail P. Popov, Igor I. Gainutdinov, Sergey F. Bychkov, Alexander P. Nemudry*, New approaches for enhancement of oxygen fluxes on hollow fiber membranes // Materials Today: Proceedings 4 (2017) 11381–11384.

RELATIONSHIPS BETWEEN ELECTROCONVECTION AND WATER SPLITTING IN MEMBRANE SYSTEMS IN INTENSIVE CURRENT REGIMES

[1]Victor Nikonenko, [1]Anna Kovalenko, [1,2]Elizaveta Evdochenko, [2]Matthias Wessling, [3]Gerald Pourcelly

[1]Kuban State University, Stavropolskaya Str. 149, 350040 Krasnodar, Russia
E-mail: *v_nikonenko@mail.ru*
[2]RWTH Aachen University, Chemical Process Engineering, 52074 Aachen, Germany
E-mail: *Elizaveta.Evdochenko@avt.rwth-aachen.de*
[3]European Membrane Institute, University of Montpellier, Montpellier, France
E-mail: *Gerald.Pourcelly@umontpellier.fr*

Electroconvection (EC) and water splitting (WS) are two main phenomena causing overlimiting conductance in membrane and microfluidic systems. However, in most cases, EC is desirable effect, which increases mass transfer rate and reduces membrane fouling, while WS is undesirable, as it reduces current efficiency and provokes scaling and fouling. In this contribution, interactions between these two effects are examined.

EC is produced by the action of the electric force on the space charge region adjacent to the membrane (electroosmosis) or on the residual space charge of the stoichiometrically electroneutral macroscopic bulk solution (bulk EC). It can be shown that the ratio of the extended space charge region thickness, δ_{SCR}, to the diffusion layer thickness, δ, is approximately expressed by the following equation:

$$\delta_{SCR} / \delta = \tilde{\varepsilon}\left(C_1^0 / C_{1s}\right)^2 \quad (1)$$

where C_1^0 and C_{1s} are the counterion concentrations in the bulk solution and at the membrane surface, respectively; $\tilde{\varepsilon}$ is a small dimensionless parameter at the derivative in the Poisson equation, $\tilde{\varepsilon} = 2\left(L_D / \delta\right)^2$, L_D is the Debye length in electrolyte solution with concentration C_1^0. It is clear that more the δ_{SCR} value, the stronger EC, which therefore is a function of the C_1^0 / C_{1s} ratio. Note that the C_1^0 / C_{1s} can be considered as a measure of concentration polarization (CP) of the membrane system by the applied electric field.

In the spirit of irreversible thermodynamics, we can consider EC as a thermodynamic flux, which is caused by a driving force. EC can be quantified by the ratio of the counterion partial current density, i_1, to the theoretical value of the limiting current density, $i_{\lim}^0$. As for the driving force, in general, concentration polarization can be considered as this force. Then we arrive at the following relationship:

$$i_1 / i_{\lim}^0 = L_{EC} C_1^0 / C_{1s} \quad (2)$$

where L_{EC} may be called electroconvection effective conductance coefficient.

Eq. (2) shows that less the C_{1s} value, stronger the EC. L_{EC} depends on the membrane surface properties; the more appropriate these properties are (an optimized electric and geometric heterogeneity [1], suitable distribution of hydrophilic and hydrophobic surface areas), the stronger the EC.

Similarly, a relationship between the rate of WS (denoted as $R_{H/OH}$, in moles of H^+/OH^- generated per m^3 and per s) and the driving force (which can be measured by C_1^0 / C_{1s}, as above) can be written:

$$R_{H/OH} = L_{WS} C_1^0 / C_{1s} \quad (3)$$

where L_{WS} is the water splitting effective conductance coefficient.

Justification of Eq. (3) follows from the reason that the H^+ (OH^-) ions produced in water splitting reaction should successfully compete with the salt counterions in their transport across the membrane. If the concentration of the salt ions will be very high in comparison with that of the H^+ (OH^-) ions, the flux of the latter will be too small. It is known that within the space charge

region in the depleted solution, diffusion transport of ions is negligible. Therefore, the competition between the salt and H^+ (OH^-) ions can be evaluated by their electromigration transport numbers proportional to the product of the ion diffusion coefficient and concentration. Since the diffusion coefficient of H^+ (OH^-) ions is about ten time higher than that of salt ions, the concentration of salt ions should be no more than 100 times higher than that of H^+ (OH^-) ions to obtain a flux of water-splitting products, which is comparable with that of salt ions. When taking the characteristic concentration of the H^+ (OH^-) ions equal to 10^{-7} M, we can evaluate the threshold salt concentration, C_{1s}, as 10^{-7} M, when water splitting becomes noticeable. However, this condition of low salt concentration at the interface is necessary, but not sufficient to obtain a high rate of water splitting.

It is known that WS rate is favored (L_{WS} is high) by catalytic participation of membrane functional fixed groups and/or metallic hydroxides such as $Mg(OH)_2$ or $Fe(OH)_3$ present at the membrane/solution interface [2, 3]. The rate of water splitting can be presented as follows:

$$R_{H/OH} = B\left(k_d^* - k_r^* c_H c_{OH}\right) \tag{4}$$

where k_d^* and k_r^* are the effective dissociation and recombination rate constants for water splitting reaction, respectively; *B* depends on the basicity/acidity of membrane functional group, so that this value is a function of catalytic activity of these groups in relation to water splitting. k_d^* and k_r^* satisfy the same relationship $k_d^* / k_r^* = K_w \approx 10^{-14}$ (mol/L)^2, as in free solution. k_r^* is always very high, of the order of 10^{10} (L mol^{-1} s^{-1}) independently of the electric field, while k_d^* is a function of electric field, *E*, in the reaction layer [3]:

$$\frac{k_d^*(E)}{k_d^{*0}} = f(E) = \exp\left(\beta E\right) \tag{5}$$

where k_d^{*0} stands for the case where no external electric field is applied; β is a fitting factor.

Along with the catalytic participation of functional and/or other groups present at the interfacial layer and catalysing water splitting, there is an important feature of this reaction, which is that the reaction occurs within the entire space charge region, no matter how thick it may be. Even if the reaction rate constant is rather low in depleted SCR of solution, the large thickness of the SCR reaching several μm at high voltages can cause great fluxes of the H^+ (OH^-) ions generated in water splitting reaction [4]. The problem for the application of ED at high voltages, e.g. in shock electrodialysis [5], is in the fact that this effect cannot be mitigated by changing membrane functional groups.

When L_{EC} is high, it is possible to obtain an intensive EC in conditions of relatively low value of C_1^0 / C_{1s}. Therefore, in these conditions, the driving force of WS can be low, which reduces the WS rate. In other words, WS can be partially suppressed, if the membrane surface is optimized in a way favoring EC. Experimental evidences of this effect were obtained in [6, 7], where it was found that application of a thin Nafion film on the MK-40 membrane surface simultaneously increases EC and reduces WS. Note that in this case, there was only optimization of the surface heterogeneity without changing the chemical nature of the functional groups, because it was SO_3^- groups in both cases, hence, without changing the L_{WS} parameter.

Inversely, an increase in WS rate by changing the nature of functional groups [8] or by adding particles forming a bipolar interface (such as DNA molecules in the experiments of Slouka et al. [9]) on the membrane surface (an increase in L_{WS}) reduces EC. The cause is in the fact that the H+ (or OH^-) ions, the products of water splitting, enter the space charge region at the depleted membrane surface as co-ions and thus reduce the space charge density [10]. Thus, to increase electroconvection, it is necessary to reduce water splitting. This reduction in the case of anion-exchange membranes is possible by grafting quaternary ammonium groups in a near-surface

membrane layer [8]. These groups do not have a catalytic effect on the water dissociation reaction [3].

Another effect of WS occurs in the case of anion-exchange membranes with weakly basic functional groups. In this case, OH^- ions generated in water splitting at the depleted membrane interface deprotonate these functional groups, that is, discharge them. Due to this current-induced membrane discharge [11] reduces EC because of lower membrane surface charge.

The conclusion is that to enhance mass transfer, it is not sufficient to optimize membrane surface heterogeneity, but it is also necessary to exclude from the membrane interface the species, which are catalysts for the WS reaction.

Acknowledgments

The study is realized with the financial support of the Russian Foundation of Basic Research, project №17-08-01442 А.

References

1. *Davidson S. M., Wessling M., Mani A.* On the dynamical regimes of pattern-accelerated electroconvection // Sci. Rep. 2016. V. 6. P. 22505.
2. *Simons R.* Electric field effects on proton transfer between ionizable groups and water in ion exchange membranes // Electrochim. Acta 1984. V. 29. P. 151-158.
3. *Zabolotskii V. I., Shel'deshov N. V., Gnusin N. P.* Dissociation of water molecules in systems with ion-exchange membranes // Russ. Chem. Rev. 1988. V. 5713. P. 801-808.
4. *Urtenov M. K., Pismensky A. V., Nikonenko V. V., Kovalenko A. V.* Mathematical modeling of ion Transport and water dissociation at the ion-exchange membrane/solution interface in intense current regimes // Petroleum Chemistry 2018. V. 58. P. 121-129.
5. *Deng D., Dydek E. V., Han J. H., Schlumpberger S., Mani A., Zaltzman B., Bazant M. Z.* Overlimiting current and shock electrodialysis in porous media // Langmuir. 2013. V. 29. P. 16167-16177.
6. *Nikonenko V .V. et al.* // Adv. Colloid Interface Science. 2010. V. 160. P. 101-123.
7. *Andreeva M. A. et al.* // J. Membr. Sci. 2017. V. 540. P. 183-191.
8. *Pismenskaya N. D. et al.* // J. Membr. Sci. 2018. V. 566. P. 54-68.
9. *Slouka Z., Senapati S., Yan Y., Chang H. C.* Charge inversion, water splitting, and vortex suppression due to DNA sorption on ion-selective membranes and their ion current signatures // Langmuir. 2013. V. 29. P. 8275-8283.
10. *Mishchuk N. A.* Concentration polarization of interface and non-linear electrokinetic phenomena // Adv. Colloid Interface Sci. 2010. V. 160. P. 16-39.
11. *Andersen M. B., Van Soestbergen M., Mani A., Bruus H., Biesheuvel P. M., Bazant M. Z.* Current-induced membrane discharge // Phys. Rev. Lett. 2012. V. 109. P. 108301.

INFLUENCE OF CARBON SUPPORT ON CATALYTIC LAYER PERFORMANCE OF FUEL CELLS

[1]Ksenia Novikova, [2]Nina Smirnova, **[1]Yury Dobrovolsky**
[1]Institute of Problems of Chemical Physics of RAS, Chernogolovka, Russia, E-mail: *kcenia-4@mail.ru*
[2]Platov South-Russian State Polytechnic University (NPI), Novocherkassk, Russia

Introduction

Proton exchange membrane fuel cells (PEMFCs) are expected to find wide application as mobile, portable, and distributed stationary power sources owing to their outstanding advantages, such as high efficiency, zero or low emission, high power density, and rapid start-up. One of the basic elements of the fuel cell with a proton exchange membrane (PEM) is the membrane electrode assembly (MEA). The efficiency and performance of PEMFCs are mainly determined by the parameters of MEA, which depend to a large extent on the structural features of the catalyst layers (CLs). The CLs with a thickness around several micrometers are the critical components of PEMFCs, whose specific structure allows attaining the high rate of the electrode reactions with a minimum amount of the expensive catalyst. The overall CL performance depends on the following critical factors: (i) large three-phase interface in the CL; (ii) efficient transport of protons; (iii) easy transport of reactant and product gases and removal of condensed water; and (iv) continuous electronic current passage between the reaction sites and the current collector. Identification of the electrode structures and operation conditions is therefore essential [1]. The morphology of the carbon nanomaterial has a significant effect on the characteristics of CL.

The aim of this work was to establish the role of carbon support morphology on catalyst performance.

Experiments

Pt/C catalysts have been prepared via Pt electrochemical dispersion under the action of the AC pulse current in the presence of a carbon nanomaterial, as was described in details in [2, 3]. Various multiwalled carbon nanotubes (MWCNTs) were used as the carriers of catalysts: (i) nanotubes by the Russian branch of LG Chem Company (LGCNT), (ii) lab-made samples of carbon nanotubes acquired by the pyrolysis of a propane–butane mixture on a Cu–Ni catalyst (S-0CNT), and (iii) nanotubes produced by the catalytic pyrolysis of methane on Fe–Mo/MgO (FWCNT). Vulcan XC-72R (Cabot) carbon soot was used as the reference support. The synthesized catalysts were labeled as Pt/LGCNT, Pt/S0CNT, Pt/FWCNT, and Pt/Vulcan.

TEM images were obtained with a JEM-2100 unit (200 kV). SEM images were acquired on a Hitachi S4500. The electrochemically active surface area (ECSA) of Pt/C electrocatalysts was determined by oxidative COads desorption (CO stripping), using a standard three-electrode electrochemical cell and a PI-50-1 potentiostat (Elins, Russia), as was described in our previous papers. CO was adsorbed at the surface of the working electrode by bubbling CO through 0.5 M H_2SO_4 for 15 min, while the electrode was kept at a constant potential of 300 mV vs. RHE. After CO bubbling, the electrolyte was purged with N_2 (30 min) to remove the dissolved CO, and the CV curves were measured. The ECSA was evaluated by calculating the charge accumulated during CO adsorption after subtracting the double-layer charging current taking into account that the charge required for the desorption of a CO_{ads} monolayer was 420 μC cm^{-2} of the true surface.

Results and Discussion

According to the TEM study and the particle size distribution histograms (Figs. 1e–h), the CNT-based Pt/C catalysts are characterized by the agglomerates with the dimensions above 20 nm, unlike the Vulcan soot-based catalyst.

The variations in the ECSA values calculated from the hydrogen desorption integrals with the cycle number during the APCT are shown in Fig. 2. It can be clearly seen that the ECSA of the Pt/Vulcan catalyst reduces more than 60% after APCT. However, the ECSA of Pt/CNTs catalysts decreases by 35, 26, and 13% for Pt/FWCNT, Pt/S0CNT, and Pt/LGCNT, respectively, after the same tests, showing that the Pt/CNT catalysts are much more stable than the standard Pt/Vulcan

catalyst. These results are in agreement with the onset oxidation temperature of Pt/Vulcan and Pt/CNTs. The main reasons for degradation of the platinum are the dissolution, reprecipitation, and Pt particle separation from the carbon support [4, 5]. It is a well-known particle size effect: smaller Pt particles dissolve faster [6]. Moreover, corrosion of the carbon support is possible. The OH groups formed by the electrochemical oxidation of platinum spill over the carbon surface with the emergence of the·OH radicals adsorbed on the carbon surface.

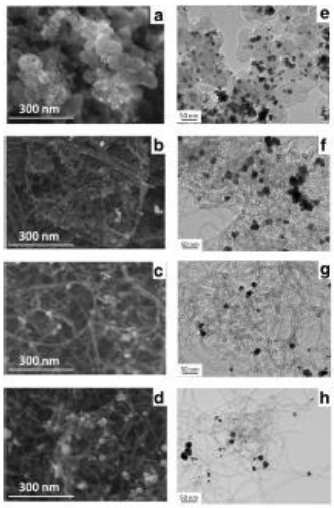

Figure 1. SEM (a–d), TEM (e–h) images, and platinum particles size distribution of Pt/Vulcan (a, e), Pt/FWCNT (b, f), Pt/S0CNT (c, g), Pt/LGCNT (d, h) catalysts.

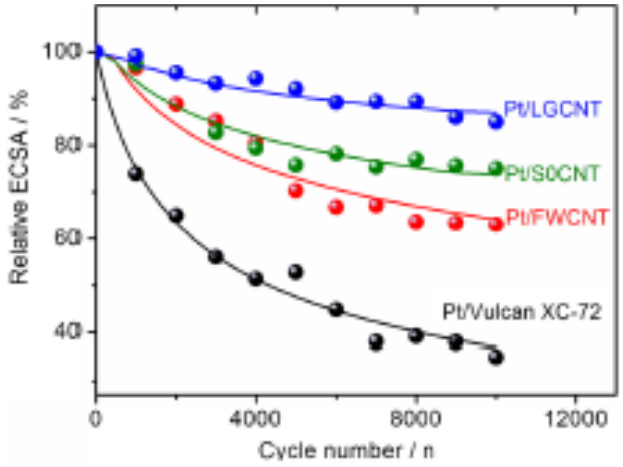

Figure 2. Relationship between the ECSA and the cycle number during the APCT.

The role of carbon support morphology on the Pt/C catalyst performance was established. It was found that formation of Pt agglomerates is more typical for Pt/C catalysts based on CNT than for carbon black. However, this causes no decrease in electrochemically active surface areas. ORR activity of the synthesized catalysts increased in the sequence Pt/Vulcan < Pt/LGCNT ≤ Pt/S0CNT < Pt/ FWCNT. The maximum power of MEA was obtained with the use of FWCNT which can be due to the difference in the value of the total pore volume of the carbon supports, causing differences in the structure of the CLs and better mass transport properties (O_2 and H^+) of MEAs based on FWCNT.

References

1. *Zhang J.*, in Fundamentals and applications. PEM fuel cell electrocatalysts and catalyst layers (Springer Publisher, New York, 2008).
2. *Leontyev I., Kuriganova A., Kudryavtsev Y., Dkhil B., Smirnova N.*, Appl. Catal A.2012. V. 120. P. 431–432.
3. *Smirnova N.V., Kuriganova A.B., Novikova K.S., Gerasimova E.V.*, Russ. J. Electrochem. 2014. V. 50. P. 899.
4. *Borup R.L., Davey J.R., Garzon F.H., Wood D.L., Inbody M.A.*, J. Power Sources. 2016. V.76. P. 163.
5. *Dubau L., Castanheira L., Berthomé G., Maillard F.,* Electrochim. Acta. 2013. V.273. P. 110.
6. *Pandy A., Yang Z., Gummalla M., Atrazhev V.V., Kuzminyh N.Y., Sultanov V.I., Burlatsky S.*, J. Electrochem. Soc. 2013. V. F972. P.160.

THE EFFECT OF ABSORBENT FEEDING CONDITIONS ON THE PARAMETERS OF REVERSE ELECTRODIALYSIS

Eduard Novitsky, Evgenia Grushevenko, Vladimir Vasilevsky, Alexey Volkov
A.V. Topchiev Institute of Petrochemical Synthesis, Moscow, Russia, E-mail: *ednov@ips.ac.ru*

Introduction

Reverse electrodialysis (RED) is a relatively new trend in the development of an electric generation. For the first time, RED was described in 1954. In [1] author assembled the electrodialysis apparatus using chambers each of which contains a pair of anion and cation exchange membranes and electrodes (anode and cathode). In contrast to a regular electrodialysis apparatus, this unit was not connected to a power source. The electrodes were connected by an external closed circuit, which included an ammeter and a voltmeter. Sea water was introduced into the desalting chambers (salt content 35 g/l) and the concentration and pre-electrode chambers were rinsed with fresh river water. In this case, the separate transfer cations and anions were transformed into an electron flux in the external network from the anode to the cathode due to redox reactions at the electrodes. Since then, this topic has become popular (more than 200 publications already in 2015). In 1980 it was shown that making the RED process viable in industrial scale could improve anion-exchange membrane properties (minimization of their thickness, stability of properties during long-term operation, reduction of their electrical resistivity), which will overcome the main economic RED disadvantages – high production cost [2]. Another direction of reducing RED electric potential losses can be realized by decreasing the inter-membrane distance in the assembly from 0.5 to 0.2 mm. Moreover, optimization of gaskets geometry also improves the performance of the system [3].

Earlier, we proposed to implement the RED process using carbonized aqueous solutions of monoethanolamine (the electrical conductivity of which is close to sea water) as a working fluid instead of sea water.

Experiments

Experiments were carried out using the laboratory apparatus described earlier [4]. Carbonized aqueous of monoethanolamine (MEA) solutions were obtained according to [5]. The specific electric conductivity of solutions was measured using conductometer MultiLine P4 (WTW, Germany). The concentration of MEA anions was determined qualitative and quantitate on ion chromatograph “Akvilon Staier-M”. Solutions with 30% and 12% concentration MEA were chosen for the purpose of this research. Scheme of RED lab-scale with three chambers is shown on Fig. 1. Anode and cathode were made of platinized titanium. Dilution chamber was formed by the anion-exchange membrane MA-41 and cation-exchange membrane MK-40 (Shchekinoazot).

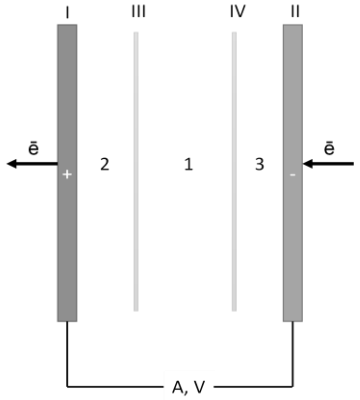

Figure 1. Scheme of RED lab-scale. I – anode, II – cathode, III – anion-exchange membrane, IV – cation-exchange membrane, A – ammeter, V – voltmeter, 1 – dilution chamber, 2 – pre-anode chamber, 3 – pre-cathode chamber.

Results and Discussion

This work is aimed at studying the effect of the circulation rate of the MEA solution in the dilution chamber and in the pre-electrode chambers on the RED parameters. Achieved carbonization degree is higher for 12 wt. % solution than 30 wt. % solution (0.70 and 0.58 mol CO_2/mol MEA respectively). The RED process was implemented in a non-stationary mode without and with forceful pumping of chambers: feed solution was filled dilution chamber and distilled water or MEA solution without CO_2 was filled pre-electrode chambers. Ion transport processes in different chambers are schematically present in Fig. 2.

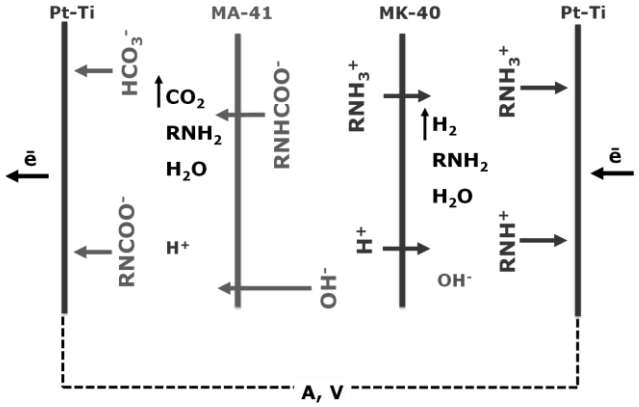

Figure 2. Ion transport in RED processes.

It was found that in the process of energy generation in the pre-electrode chambers, the MEA solution is regenerated. The quantitative value of these processes is going to be determined with experiments using RED apparatus, consisting of several dilution chambers.

Figure 3 shows the current output of RED operation at the example of 30 wt. % MEA in the case of the presence and absence of circulation of solutions for various combinations of solutions in the near-electrode chambers. The average linear velocity of solutions in electrodialysis chambers was maintained at 0.15 cm/s in circulation case.

As we can see, the circulation of the solutions in the near-electrode chambers and the desalting chamber leads to stabilize the electrical characteristics of the RED process. This allowed us to estimate the generated power of the process: in case 30 wt. % MEA in the pre-electrode chamber – 2.4 W/(h·m^2); in case distilled water in the pre-electrode chamber – 23.2 W/(h·m^2). Moreover, in the case of distilled water in the pre-electrode chamber, the amount of removed CO_2 was 43 g/l; and in case 30 wt. % MEA in the pre-electrode chamber, the amount of removed CO_2 was 21 g/l.

Thus, the use of distilled water for pumping the pre-electrode chambers allows intensifying the RED process.

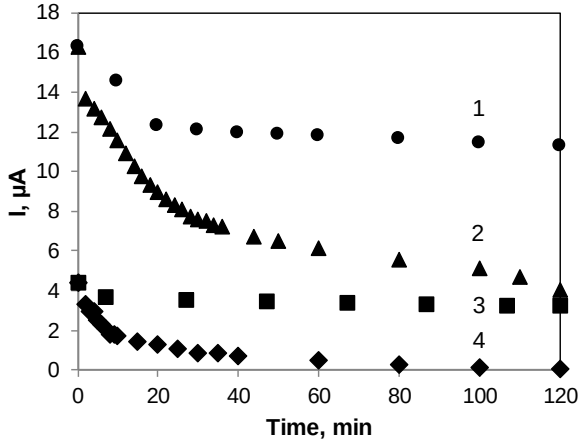

Figure 3. Current output in case 30 wt. % MEA solution. 1 – distillate water in the pre-electrode chamber with circulation, 2 – distillate water in the pre-electrode chamber without circulation, 3 – 30 wt. % MEA solution in the pre-electrode chamber with circulation, 4 – 30 wt. % MEA solution in the pre-electrode chamber without circulation.

Acknowledgments

This work was supported by the Russian Foundation for Basic Research, project no. 17-08-00312.

References

1. *R.E. Pattle*. Production of electric power by mixing fresh and salt water in the hydroelectric pile // Nature. 1954. V. 174 P. 660.
2. *R.E. Lacey*. Energy by reverse electrodialysis // Ocean Eng. 1980. V. 7. No. 1. P. 1-47.
3. *P.W. Jan, H.V.M. Hamelers, C.J.N. Buisman*. Energy recovery from controlled mixing salt and fresh water with a reverse electrodialysis system // Environ. Sci. Technol. 2008. V. 42. No. 15. P. 5785-5790.
4. *Vladimir Vasilevsky, Eduard Novitsky, Evgenii Trofimenko, Evgenia Grushevenko, Kirill Kutuzov, Alexey Volkov*. Study of reverse electrodialysis processes of an aqueous solution of carbonized monoethanolamine// International conference «Ion transport in organic and inorganic membranes». Conference Proceeding. May 2018. С. 303–305. ISBN 978-5-9906777-8-4.
5. *E. G. Novitsky, V. P. Vasilevsky, S. D. Bazhenov, E. A. Grushevenko, V. I. Vasilyeva, and A. V. Volkov*. Influence of the Composition of Concentrate Solutions on the Efficiency of Carbon Dioxide Removal from Monoethanolamine Aqueous Solution by Electrodialysis//Petroleum Chemistry, 2014, Vol. 54, No. 8, pp. 680–685.

PLATINUM ELECTROCATALYSTS BASED ON OXIDE AND OXIDE CARBON CARRIERS FOR FUEL CELL

Ivan Novomlinskiy, Irina Gerasimova, Vadim Volotchaev, Vladimir Guterman
Southern Federal University, Rostov-on-Don, Russia, *E-mail: novomlinskiy@sfedu.ru*

Introduction

At the present stage of technological development, platinum nanoparticles deposited on a porous carbon carrier are the only catalysts used in low-temperature fuel cells, since platinum has the highest activity in the oxygen reduction reaction among all pure metals [1]. Increasing the durability of the electrocatalyst and reducing platinum loading is one of the most actively developing areas of research in the field of fuel cells. Both indicators are closely related, and often the reduction of platinum loading on the electrode leads to a decrease in the life of the fuel cell. At the same time, various reasons are considered as causes of a decrease in the service life of a fuel cell: degradation of the membrane, bipolar boards and seals, moisture content of gases, the concentration of aggressive additives in gases, etc. [2]

A simple way to prevent carbon carriers at the cathode from corrosion is to replace soot with alternative materials that are less susceptible to degradation. As an alternative approach, oxides of tin, titanium and their mixtures with carbon are considered [3].

The aim of this work was to obtain platinum catalysts on oxide-carbon carriers and study their activity in the reaction of oxygen reduction and electrooxidation of alcohols.

Experiments

To obtain SnO_2-C electrocatalysts electrolysis conducted in galvanostatic conditions with stirring the carbon suspension (Vulcan XC-72), in a tin electrolyte ($SnCl_2$ solution, 0.1-1 M). The technique is described in detail in the article [3]. As the background electrolyte was used a 2M H_2SO_4. Current strength 9 A. Thus, a series of SnO_2-C materials with different mass fraction of SnO_2 was obtained. Further, the reduction of platinum with formaldehyde [4] in the liquid phase received a series of Pt/ SnO_2-C materials.

The resulting materials were investigated by gravimetry, x-ray diffraction, x-ray fluorescence analysis and cyclic voltammetry.

Results and Discussion

Platinum nanoparticles were deposited on SnO_2/C composites, the mass fraction of which was about 20%. Studies by X-ray diffraction confirmed the presence of a platinum phase in all materials, the average crystallite size of which was 1.3-2.3 nm.

The calculation of the electrochemically active area of Pt from cyclic voltammograms after surface standardization showed that the resulting catalysts have rather high area values. Most materials have an electrochemically active surface area of about 130 $m^2 \cdot g^{-1}$, which exceeds the electrochemically active surface area of the commercial Pt/C catalyst HiSPEC 3000.

The activity of electric catalysts in ORR is comparable to that of a commercial analogue, and in some cases exceeds it (fig. 1). The values of the maximum currents in the reactions of electro-oxidation of alcohols on the forward and reverse voltammograms, as well as the area under the corresponding maxima for the Pt/(SnO_2-C) catalysts were noticeably higher than for the commercial counterpart.

Apparently, this behavior of oxide-containing electrocatalysts is due to the presence of three-page structures Pt-SnO_2-C. Depending on the ratio of the sizes and the mass fraction of platinum and tin oxide, the number of such contacts will vary, which affects the characteristics of the obtained electrocatalysts. Stronger adhesion of such nanoparticles to the surface of a composite carrier can impede platinum degradation during the stress test, and the presence of a Pt/SnO_2 contact can provide a bifunctional mechanism of catalysis in the electro-oxidation reaction of methanol.

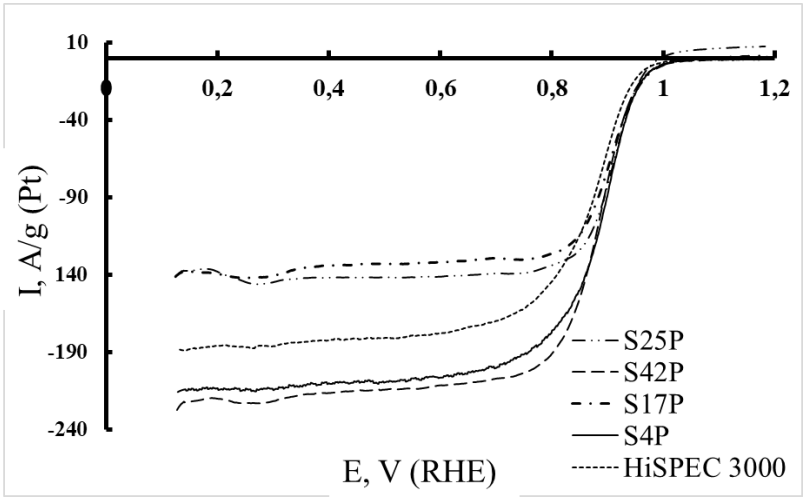

Figure 1. Voltammograms of the reaction of electroreduction of oxygen.

The work was performed in the framework of the state assignment of the Ministry of Education and Science of the Russian Federation (Topic No13.3005.2017 / 4.6).

References

1. *J. K. Norskov, J. Rossmeisl, A. Logadottir, L. Lindqvist, J. R. Kitchin, T. Bligaard, H. Jynsson* Origin of the Overpotential for Oxygen Reduction at a Fuel-Cell Cathode // Journal of Physical Chemistry B. 2004. V. 108. P. 17886 – 17892.
2. *K. Sasaki, F. Takasaki, Z. Noda, S. Hayashi, Y. Shiratori, K. Ito:* Alternative Electrocatalyst Support Materials for Polymer Electrolyte Fuel Cells // ECS Transactions. 2010. V. 33 P.473 – 480
3. *Novomlinskiy, I.N., Tabachkova, N.Y., Safronenko, O.I. Guterman V.E.*. A novel electrochemical method for the preparation of Pt/C nanostructured materials // Monatsh Chem. 2019. V. 150 P. 631–637
4. *Alekseenko A.A., Guterman V.E., Volochaev V.A., Belenov S.V.* Effect of wet synthesis conditions on the microstructure and active surface area of Pt/C catalysts. Inorganic Materials, 2015. 51. c.1258-1263

SYNTHESIS OF NANOPOROUS MEMBRANES WITH GOLD NANOPARTICLES BY LASER-INDUCED DEPOSITION

Maksim Novomlinsky, Denis Lebedev, Alena Fogel, Vladimir Kochemirovsky
Saint Petersburg State University, 7/9 Universitetskaya nab., St. Petersburg, Russia
E-mail: *ooc41hmo@mail.ru*

Introduction

The separation of media, including the purification of liquids, is extremely important for the majority of technological processes. At the same time, the unusual properties of nanostructures are well studied and are actively used to create materials with unique properties. Structuring the pore geometry of the membranes gives hight results [1,2]. The result of the application of nanostructuring in membrane technology will be an increase in productivity and selectivity of membranes.

There are a lot of methods for producing nanoparticles of noble metals (gold, platinum ...) [3]. However, most methods have a some limitations or are not applicable to achieve the goal of this work.

The purpose of this work is the deposition of gold nanoparticles on the surface of pores of membranes. Nanoparticles should have a high uniformity in size and shape, be rigidly fixed on the surface (withstand high pressures and liquid flow), and the growth of nanoparticles should occur mainly in the pores of the membranes.

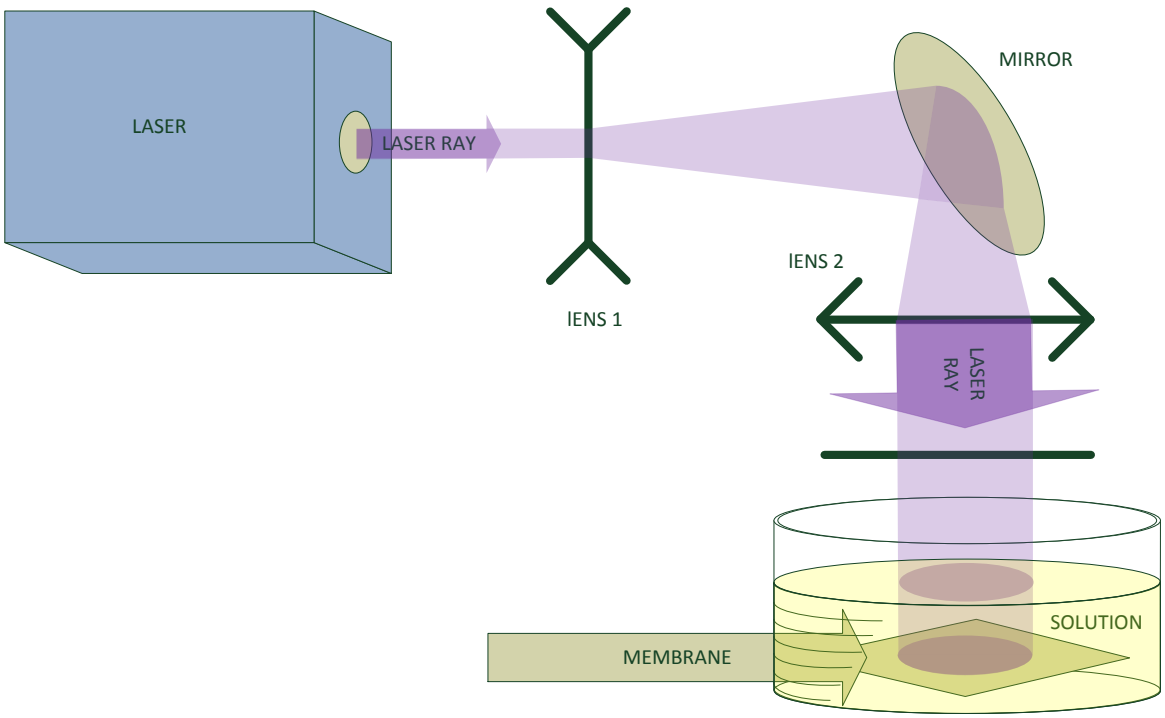

Figure 1. Installation scheme for obtaining a laser beam of the required parameters.

Experiments

The method of laser-induced deposition of metals proved to be the best method for the task [4]. This method is based on the initiation of the reaction of deposition of metals on the surface of the dielectric under the action of laser radiation [5].

As can be seen from the experiments, the growth and size distribution is determined by parameters such as laser wavelength, laser pulse power and frequency, exposure time, solvent properties and concentration. The growth of gold nanocrystals of a given shape and size occurs in a very narrow range of the indicated synthesis parameters.

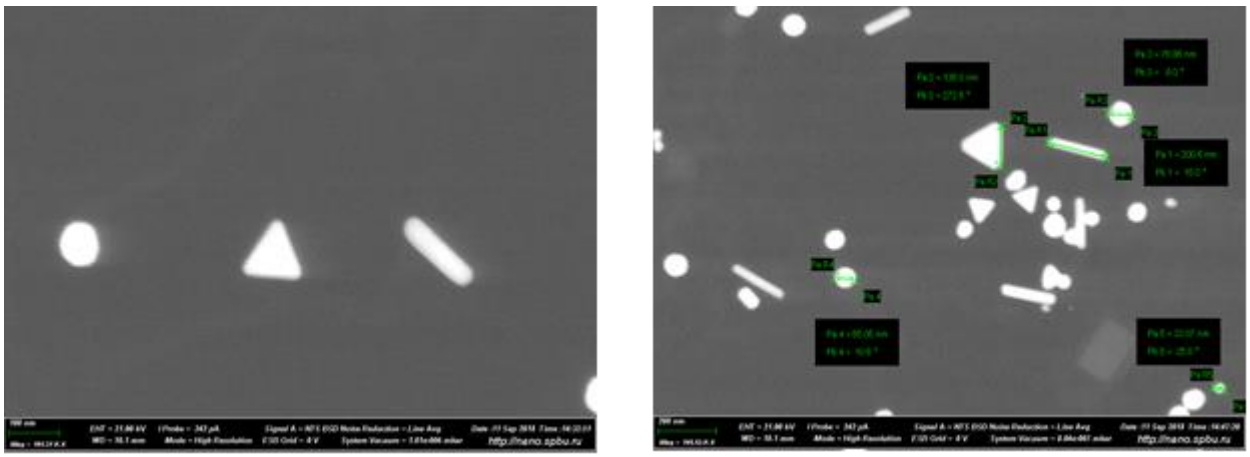

Figure 2.SEM images of gold nanoparticles on a glass substrate.

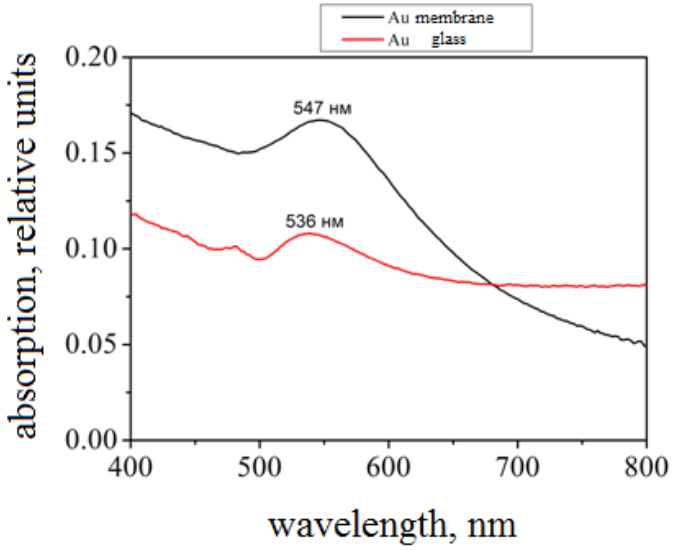

Figure 3. Au nanoparticle absorption spectra.

Results and Discussion

At the first stage, the optimal parameters of the laser (power, wavelength, number of pulses per second) were selected. At the second stage, the selection of optimal irradiation regimes was carried out (exposure time, the thickness of the solution layer).

The correlation between the modes of synthesis and the properties of the particles obtained was established by SEM, spectrometric methods, and the reliability of particle attachment to the surface. The results are presented in table 1.

Reliability of fixing was estimated on a conventional scale from 0-5 (5-particles can be removed only by the action of aqua regia; 4- preparation in an ultrasonic bath; 3-under water pressure for an hour or more; 1- washed away under water pressure in less than 1 hour; 0-separated immediately or not formed). Samples with a value of 3 and below are not suitable for use. The presence of particles of a triangular shape was determined quantitatively, by an SEM study and corresponds to: 0 - there are no particles of a triangular shape; ◊ - particles with a triangular shape of less than 10%; ◊◊ -particles with a triangular shape of 10-50%; more than 50% of particles of a triangular shape. In addition, the presence of plasma resonance was determined (the wavelength corresponding to the maximum peak). In the absence of a dash was put.

Typical SEM images of the obtained nanoparticles are shown in Fig. 2. From the presented images it can be seen that at low concentrations of the precursor (0.025 M) single-crystal gold nanoparticles of a triangular, round and oblong shape are formed. Typical particle size of 50 nm (in one direction). Typical absorption spectra of the particles obtained are shown in Fig. 3. A clear peak is observed on the absorption spectra at a wavelength of about 540 nm. According to the

literature, this absorption is typical for particles with an average diameter of 50 nm. Which confirms the data of the SEM.

Table 1: The dependence of the results on the operating parameters

Time, min	Solution layer thickness, cm					
	1	2	3	4	5	6
1	3;0;-	3;0;-	3;0;0	3;0;0	2;0;0	2;0;0
2	3;0;0	1;0;0	3;0;0	3;0;0	2;0;0	3;0;0
4	3;0;0	2;0;0	3;0;0	3; ◊;0	3;0;0	3;0;0
8	4;0;510	3;0;510	3; ◊;0	3; ◊◊;0	3; ◊;0	3;0;0
16	4; ◊;550	3; ◊;530	3; ◊;0	4, ◊◊;536	2, ◊;530	4;0;0
30	4;0;510	4;0;510	5;0;0	5, ◊;480	2, ◊;530	4;0;0

As you can see from the table, the optimal solution layer thickness is 4 cm, the exposure time is 16 minutes. Below are the size, shape and absorption spectra of nanoparticles obtained by laser-induced deposition. The above method allows you to synthesize nanoparticles of a given shape and size.

References

1. *Goh P. S., Ismail A. F., Hilal N.* Nano-enabled membranes technology: sustainable and revolutionary solutions for membrane desalination? //Desalination. 2016. V. 380. P. 100-104.
2. *Grzelczak M. et al*. Shape control in gold nanoparticle synthesis //Chemical Society Reviews. 2008. V. 37. №. 9. P. 1783-1791.
3. *Visser C. W. et al.* Toward 3D printing of pure metals by laser- induced forward transfer //Advanced materials. 2015. V. 27. №. 27. P. 4087-4092.
4. *Wang Z. et al.* Nanoparticle-templated nanofiltration membranes for ultrahigh performance desalination //Nature communications. 2018. V. 9. №. 1. P. 2004.
5. *Kochemirovsky V. A. et al*. Laser-induced chemical liquid phase deposition of metals: chemical reactions in solution and activation of dielectric surfaces //Russian Chemical Reviews. 2011. V. 80. №. 9. P. 869.
6. *Cheryan M.* Ultrafiltration and microfiltration handbook, Technomic Publishing Inc., Lancaster PA., 1998.
7. *Decarolis A., Hong J. S., Taylor J.* Fouling behavior of a pilot scale inside out hollow fiber UF membrane // J. Membr. Sci. 2001. V. 191. P. 165-178.

LITHIUM EXTRACTION BY DIFFUSION DIALYSIS USING NOVEL COMPOSITE MEMBRANES

[1]Takoua Ounissi, [2]Lasâad Dammak, [2]Christian Larchet, [2]Jean-François Fauvarque, [1]Emna Selmane Bel Hadj Hmida

[1]Laboratoire de Chimie Analytique et d'Électrochimie, Département de chimie, Faculté des Sciences de Tunis, Campus Universitaire, 2092 Tunis El Manar, Tunisie

[2]Institut de Chimie et des Matériaux Paris-Est (ICMPE), UMR 7182 CNRS, Université Paris-Est, 2 Rue Henri Dunant, 94320 Thiais, France

Introduction

In the context of fossil fuels depletion and climate change pending threats, expectations for cleaner and more sustainable transport solutions are being embodied in electric vehicles [1].

The highest redox potential value and the highest specific heat capacity of any solid element of lithium make it the hottest commodity for modern life and a key element for modern electric vehicle revolution. So, due to the rapid expansion of worldwide lithium ion batteries market, the procurement of this metal is becoming a matter of importance worldwide [2].

Therefore, the selective separation, purification and recovery of Lithium from seawater and brine water generate great attention from scientists, engineers, and industrialists [3].

Experiments

The present work consists on the synthesis of novel lithium ion-selective membranes based on Lithium Ion Conductor (LICGC) as Lithium Ion Sieves embedded in a copolymerized matrix of an Anionic Polymer (PECH-DABCO) and (NH_2-PES). A nonionic surfactant (Brij76) was also used to prevent the agglomeration of inorganic Lithium conductor in the polymer matrix. To optimize both the synthesis and the appropriate composition, several experiments have been carried out. The morphological and thermal properties of these prepared membranes were determined using SEM and TGA. Additionally, water uptake, contact angle and conductivities of these membranes were also determined. To test the performances and the selectivity of these membranes, Diffusion Dialysis experiments of Li and Na mixture solution were affected using a two compartments cell.

Results and Discussion

Morphological results confirm the homogeneity of our membranes, the good dispersion of the inorganic fillers into the polymer matrix and the compatibility between different compounds. Thermal characterization shows that these membranes are stables up to 200°C. Conductivities of these membranes are more important in Li solution then in Na media.

The performance of these composite membranes was tested in diffusion dialysis of reconstituted solutions containing a mixture of sodium (0.05 M) and lithium (0.05 M) ions. We observed a remarkable selectivity for Li^+ which we attribute to the effect of the lithium-conductor powder (see Table 1). The highest selectivity coefficient was obtained for the membrane M3 that contains 50.5 $\%^{wt.}$ of LICGC, 25.5 $\%^{wt.}$ of PECH-DABCO, 18 $\%^{wt.}$ of NH_2-PES and 6 $\%^{wt.}$ of Brij76. The main physicochemical characteristics of this membrane are: Thickness (130 μm), water content (11.3 $\%^{wt.}$), contact angle (61°), conductivity in 0.1 M LiCl solution (7.5×10^{-4} $S.cm^{-1}$) and conductivity in 0.1 M NaCl solution (3.2×10^{-4} $S.cm^{-1}$).

Table 1: Ionic flux of Li^+ and Na^+ from equimolar solution after 4 hours of dialysis

Membrane	Li^+ flux (10^{-9} mol cm^{-2} s^{-1})	Na^+ flux (10^{-9} mol cm^{-2} s^{-1})
M1	22.30	1.15
M2	20.00	0.15
M3	30.53	0.08

References

1. *Grosjean C., Miranda P. H., Perrin M., Poggi P.* Assessment of world lithium resources and consequences of their geographic distribution on the expected development of the electric vehicle industry // Renew. Sust. Energ. Rev. 2012. V.16. P. 1735– 1744.
2. *Swain B.* Recovery and recycling of lithium: A review // Sep. Purif. Technol. 2017. V. 172. P. 388–403.
3. *Swain B.* Separation and purification of lithium by solvent extraction and supported liquid membrane, analysis of their mechanism: a review // J Chem Technol Biotechnol. 2016. V. 91. P. 2549-2562.

GAS TRANSROPTATION PARAMETERS OF MEMBRANES MODIFIED BY STAR-LIKE PALLADIUM NANOCRYSTALLITES

Iliya Petriev, Ivan Lucenko, Kirill Voronin, Polina Pushankina, Mikhail Baryshev
Kuban State University, Krasnodar, Russia, E-mail: *petriev_iliya@mail.ru*

Introduction

Every year for the needs of alternative energy requires more and more high-purity hydrogen. The most common method to obtain it is reforming of organic raw materials with gas mixture formation and subsequent release of high-purity hydrogen, with the help of various types of metal membrane filters. As a basis for creation of these membrane filters palladium and its alloys are used as they have unique properties in relation to the hydrogen transmission.

The formation of nanostructured palladium layer capable for chemisorbing of hydrogen on the surface of membrane increases the actual operating surface, which leads to increase of chemisorption centers quantity, which role is most often played by crystallites angles and facets. Moreover in case of sufficiently small Pd crystal size the majority of octahedral interstices belong to the surface, that facilitates the transmission of hydrogen and reduces the probability of hydrogen atom capture by various kinds of surface defects. This modification may be effective in case of limiting the process of hydrogen transfer through the membrane by dissociative-associative absorption-elimination processes at the boundaries.

In the present work an attempt is made to create a thin palladium-silver membrane and its modification by creating a nanostructured (palladium star-like nanocrystallites) layer on its surface, which accelerates the chemisorption and dissociative processes of hydrogen transmission. The developed membrane can become the base not only for low-temperature diffusion purification of hydrogen and creation of hydrogen electrode for oxygen-hydrogen fuel element, but also for processes of hydrogen isotopes separation. Also, these membranes are integrated into methanol steam reforming plants, which allows to make compact membrane reformers effective for producing hydrogen in situ [1].

Experiments

Modification of palladium membranes according to the method of "nanostars" was carried out as follows. Pd-23% Ag alloy film – were fixed in a holder, washed by 96% ethanol, defatted by boiling for 30 min. in concentrated 6 M NaOH solution, and then transferred for mordanting to 60% HNO3 solution for 30 sec., then immediately put into a vessel with flowing distilled water for 10 minutes. Then the palladium-silver alloy film was transferred to a cell with 0.1 M HCl and anodically polarized at a current density of 10-20 mA / cm2 using a potentiostat-galvanostat P-250I, washed, cathodically polarized at 0.05 M H2SO4 at current density of 10-20 mA / cm2 , then filled with 2% H2PdCl4, tetrabutylammonium bromide 0.1 M used as a sealing surfactant. The black precipitation was carried out at current density of 2-6 mA / cm2 for 0.5 hours, after that it was washed with bidistillate and cathodically polarized in 0.05 M H2SO4.

Micrographs of the samples were obtained using a JEOL JSM-7500F scanning electron microscope. Measurement of hydrogen permeability was carried out with the help of the apparatus developed by us on the basis of a microgasovolumetric method [5].

Results and Discussion

In the course of this study, two types of surface modification of hydrogen permeable membranes were developed: “nanostars” and “nanopores”. The microphotographs of the films surface obtained by JEOL JSM-7500F scanning electron microscope are shown in Fig. 1. In Fig. 2 the data is shown on the measurement of hydrogen permeability for a palladium-silver alloy modified by coating of “nanostars” type (a) and coating of “nanopores” type (b).

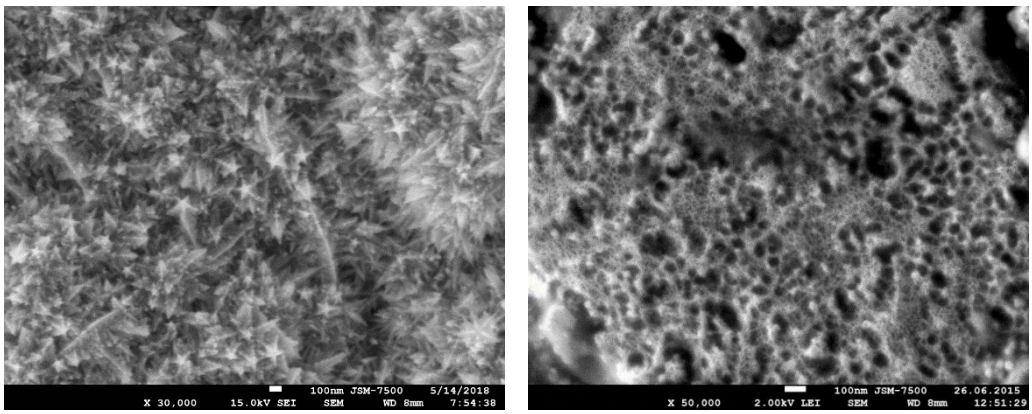

a *b*

Figure 1. Microphotographs of palladium-silver films surface with modified surface, obtained by the method of "nanostars" (a), and by the method of "nanopores" (b).

From fig. 2 it is obvious that the dependence of the flow density on hydrogen overpressure on the input side of the membrane with modified surface is well approximated by a line of the 1st order, which indicates according to [2] that hydrogen penetration velocity is limited by dissociation of hydrogen on the surface.

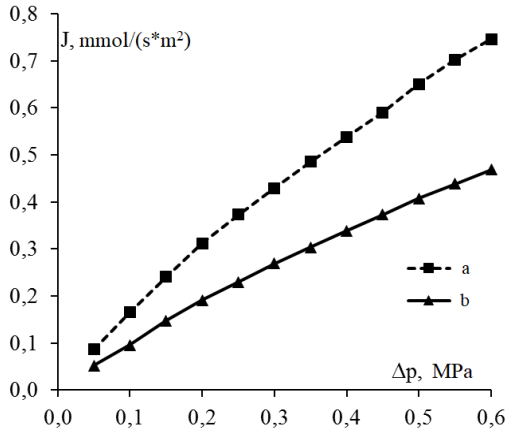

Figure 2. Dependence of the rate of fluence (the ratio of hydrogen flow to the area of a sample) on the excess pressure of hydrogen on the outer face of the membrane for the method "nanostars" (a) and the method of "nanopores" (b).

Thus it has been experimentally confirmed that the velocity of hydrogen transmission under conditions of low temperature (<90 ° C) and pressure (<0.6 MPa) through sufficiently thin palladium membranes (<10 μm), is limited by dissociative-associative processes at the boundaries, and can be significantly increased (up to order of magnitude) due to acceleration of the limiting stage by applying a superficial modifying palladium coating. Modification of membranes with "nanostars" type of coating allows achieving hydrogen flow density up to 0.76 mmol / (s*m^2) that is 1.6 times greater than with modified by "nanopores" type of coating

This work was supported by the scholarship of the President of the Russian Federation to young scientists and post-graduate students SP-1237.2018.1.

References

1. *Lytkina A. A, Orekhova N. V, Ermilova M. M. et al.* // International Journal of Hydrogen Energy. 2017. V.43 № 1. P. 198-207.
2. *Baychtok Y K, Sokolinsky Y A and Ayzenbud M B* 1976 Physical Chemistry Journal 50(6) 1543-1546

COUPLING BETWEEN MASS TRANSFER AND PROTON GENERATION DURING ELECTRODIALYSIS OF AMPHOLYTE-CONTAINING SOLUTIONS

Natalia Pismenskaya, Olesya Rybalkina, Kseniia Tsygurina, Ekaterina Melnikova
Membrane Institute, Kuban State University, Krasnodar, Russia, E-mail: *n_pismen@mail.ru*

Introduction

Electrodialysis is increasingly used for cleaning, concentrating and conditioning ampholytes (proteins, amino acids, anions of polybasic inorganic and organic acids, etc.), which are products of biochemical processing of biomass, or are contained in liquids of food and pharmaceutical industries. Similar substances (phosphates, ammonium ions) are extracted as nutrients from municipal and livestock wastewaters. The study aim is the identify regularities of mass transfer during electrodialysis of ampholyte-containing solutions in underlimiting and overlimiting current modes.

Experiments

The experiments were carried out using a laboratory scale four-chamber flow-through electrochemical cell, the membrane stack of which contains CMX cation-exchange membranes and AMX anion-exchange membranes (Astom, Japan). The active surface area of each membrane is 4 cm^2, the intermembrane distance is 0.66 cm, the flow rate of a 0.02 M NaH_2PO_4 solution is equal to 0.4 cm/s. This cell, the set-up and the method of obtaining the total and partial current-voltage characteristics (CVC) of the membranes forming a desalination channel through which a solution of a strong electrolyte (NaCl, KCl) is pumped, are described in detail in [1]. The case of NaH_2PO_4 or KH_2PO_4 solution is described in [2].

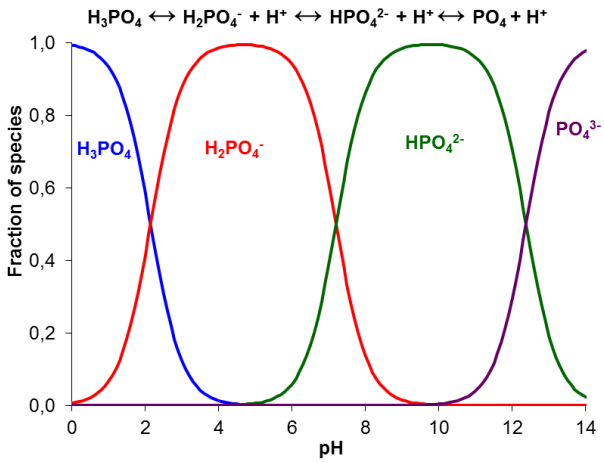

Figure 1. Distribution of the Phosphoric Acid Species (in Mole Fractions) as Functions of pH.

Distribution of the phosphoric acids species as functions of pH presented in fig. 1. It is calculated using the constants of the reactions of protonation - deprotonation of phosphoric acid in the first, second and third stages.

Theory

The calculation of the CVC, as well as the transport numbers, partial fluxes and partial currents of ions in the membrane system is carried out using a stationary 1D model described in detail in [3]. A three-layer system under direct current conditions is considered. It consists of an anion exchange membrane AMX and two adjacent diffusion boundary layers (DBL). Migration and diffusion transport of ampholyte species and the products of protonation-deprotonation reactions H^+ (OH^-) in all three layers are taken into account. The model is based on the Nernst-Planck equation under the local electroneutrality condition. It uses the assumptions of the independence of the current density and the total flux density of phosphorus-containing species from the coordinate as well as local chemical equilibrium between the ampholyte species participating in protonation-deprotonation reactions in the AEM and in the DBLs. Besides the condition of ion-exchange equilibrium at the membrane / solution boundaries is applied.

Results and Discussion

Fig. 2 shows the theoretically and experimentally obtained total and partial CVC of the AMX membrane in NaH_2PO_4 solution**.**

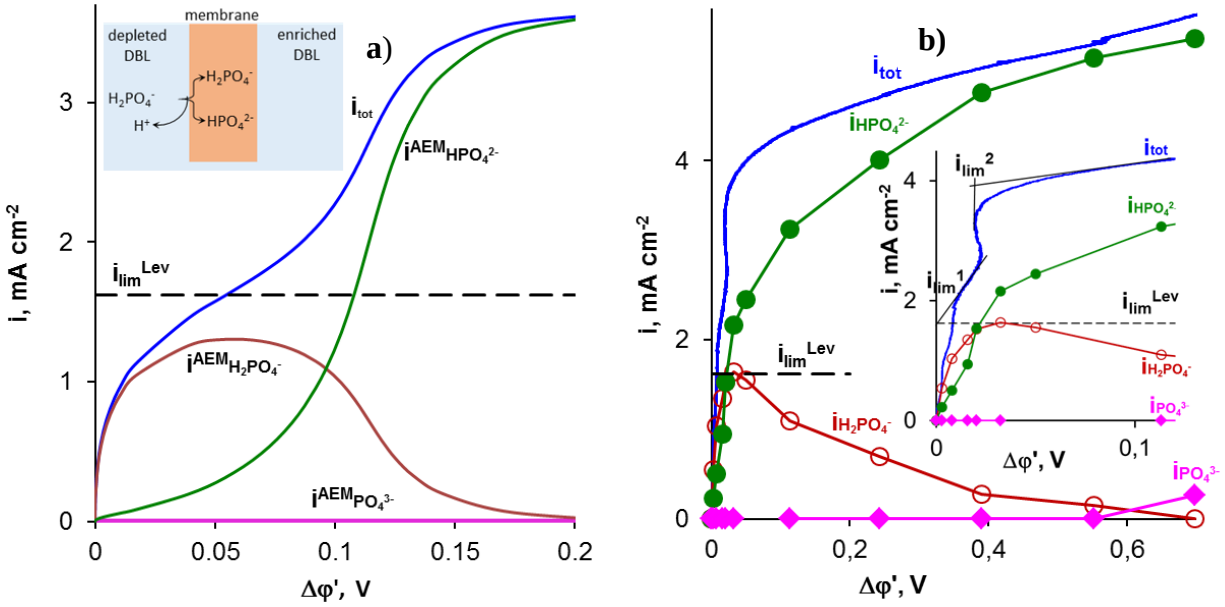

Figure 2. Total and Partial Current-Voltage Characteristics of AMX Membrane in 0.02 M NaH_2PO_4 Solution: Calculation Using Model (a), Experiment (b). The dashed line is the limiting current calculated using the Leveque equation.

Analysis of the calculation results and experimental data allows us to conclude that when a current is applied, the solution at one of the surfaces of anion-exchange membrane is desalted, that leads to an increase in the Donnan exclusion of H^+ ions and an increase in the fraction of doubly (triply) charged anions in the membrane. Due to Donnan exclusion of protons from the anion-exchange membrane (as co-ions), the pH of the internal solution in the micropores of the membrane is higher than the external solution pH. Therefore, the fraction of doubly (triply) charged anions in an anion-exchange membrane is always higher than in the external solution. For phosphates, there are two inclined plateaus, whose appearance can be related to two limiting currents. The first limiting current occurs when the NaH_2PO_4 salt diffusion to the membrane surface is saturated, the second limiting current corresponds to the saturation of the proton flux when the membrane is almost completely converted into the $H_2PO_4^-$ form. A current increase above the second limiting current in the phosphate-containing system is possible due to two mechanisms: the membrane transition into the form of triply charged phosphates and / or the water splitting. The shape of experimental and theoretical dependences i, i_i vs $\Delta\varphi'$ basically coincides. Higher experimental values $i^{AEM}_{H_2PO_4^-}$ (Fig. 2b,) and j_P (Fig. 3a) compared with those calculated by the model are mainly due to the effect of exaltation of the limiting current. They arise because the protons, which are excluded from the membrane into solution, carry a positive charge, which creates an additional electrostatic field attracting $H_2PO_4^-$ anions from the bulk solution to the depleted membrane surface. The increase in the charge of anions of orthophosphoric acid in the membrane compared with the solution is a parasitic process in relation to the transfer of the target component - phosphorus in AMX membrane. Therefore, the flux of phosphorus j_P, the transfer of which in AMX is carried out by all phosphorus containing species, is much less than that which can be expected using Eq: $j_{Plim} = i_{lim} / F$ (Fig.3a). The fact is that in the practice of electrodialysis, the limiting current is usually determined by graphic processing of CVC (Fig. 3b), represented in Cowan–Brown coordinates [4] ($i_{\lim} = i_{\lim}^{C-B}$). This current corresponds to the value $i_{\lim}^2$ (Fig.2b) at which doubly charged phosphorus-containing anions are mainly transferred in the membrane.

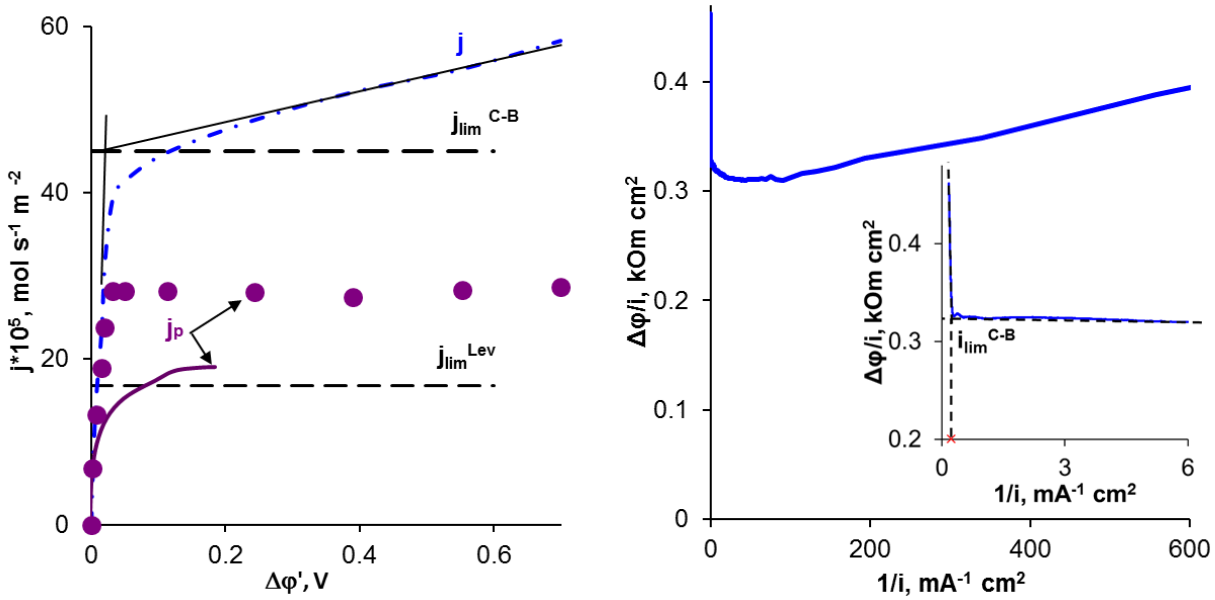

Figure 3. The Dependence of the Experimental (markers) and Theoretical (curve) Phosphorus Fluxes in the Investigated AMX Membrane Upon the reduced Potential Drop (a). The dash-dotted line is the flux defined using the Eq: $j=i_{tot}/F$. Dotted lines are fluxes determined using the limiting currents: i_{lim}^{Lev} is calculated by the Leveque equation; i_{lim}^{C-B} is determined using the current-voltage characteristic represented in the Cowan–Brown coordinates [6] (b).

The results obtained explain the reason for the unexpectedly low current efficiency of the target components or the unexpectedly high energy consumption [5,6] during electrodialysis of ampholyte-containing solutions.

Acknowledgements

The study is realized with the financial support of the Russian Science Foundation (Project No 17-19-01486).

References

1. *Rybalkina O. A., Tsygurina K. A., Melnikova E. D., Pourcelly G., Nikonenko V. V., Pismenskaya N. D.* Catalytic effect of ammonia-containing species on water splitting during electrodialysis with ion-exchange membranes // Electrochim. Acta. 2019. V. 299. P. 946-962.
2. *Tsygurina K.A., Rybalkina O.A., Melnikova E.D., Pismenskaya N.D. Total and partial current-voltage characteristics of anion-exchange membranes in NaCl and* NaH_2PO_4 solution // Kondensirovannye sredy i mezhfaznye granitsy (CONDENSED MATTER AND INTERPHASES). 2018. T. 19. № 4. C. 585-595.
3. *Belashova E. D., Pismenskaya N. D., Nikonenko V. V., Sistat P., Pourcelly G.* Current-voltage characteristic of anion-exchange membrane in monosodium phosphate solution. Modelling and experiment // J. Membr. Sci. 2017. V. 542. P. 177-185.
4. *Cowan D. Q. Brown I. W.* Effect of turbulence in limiting current in electrodialysis cell // Ind. Eng. Chem. 1959. V. 51. No 2. P.1445-1449.
5. *Chen X., Liang P., Zhang X., Huan X.* Bioelectrochemical systems-driven directional ion transport enables low-energy water desalination, pollutant removal, and resource recovery Review // Bioresource Technol. 2016. V. 215. P. 274-284.
6. *Yuan F., Wang Q., Yang P., Cong W.*. Transport properties of amino acid ions at isoelectric point in electrodialysis // Sep. Pur. Technol. 2016. V. 168. P. 257-264.

MATHEMATICAL MODELING OF MASS AND HEAT TRANSFER DURING ELECTRODIALYSIS OF SODIUM DIHYDROPHOSPHATE

Alexander Pismenskiy, Mahamet Urtenov, Anna Kovalenko
Kuban State University, Stavropolskaya 149, 350040 Krasnodar, Russia, E-mail: *pism@kubsu.ru*

Introduction

The experimental current-voltage characteristics of the anion-exchange membrane (AEM), obtained [1] in ampholyte-containing sodium dihydrogen phosphate (NaH_2PO_4) solution, indicate a significant increase of the limiting current in a vertical direction of the desalination channel (DC) of an electrodializer, compared to a horizontal one with the DC located under the membrane. This is explained by the influence of gravitational convection, which evolves in a vertical position of the DC. At the same time, this effect is much lesser observed during electrodialysis under the same conditions of solutions that do not contain ampholytes, e.g. *NaCl* solution. One of the reasons for the observed gravitational convection in ampholyte-containing systems is presumably the thermal effects arising from deprotoning-protoning reactions [2]. Here we study this phenomenon with the direct mathematical modeling.

Theory

Simulating the process of electrodialysis desalination of NaH_2PO_4 solution, we directly consider the transfer of the molecules of orthophosphoric acid (H_3PO_4) and four kinds of ions (Na^+, $H_2PO_4^-$, H^+, HPO_4^{2-}). The scheme of the compound interaction in the transverse section of the DC, are simplified in Fig. 1. Herein $x = 0$ corresponds to the interphase boundary AEM/solution, $x = h$ is the conditional boundary diffusion layer (DL) / bulk of the solution.

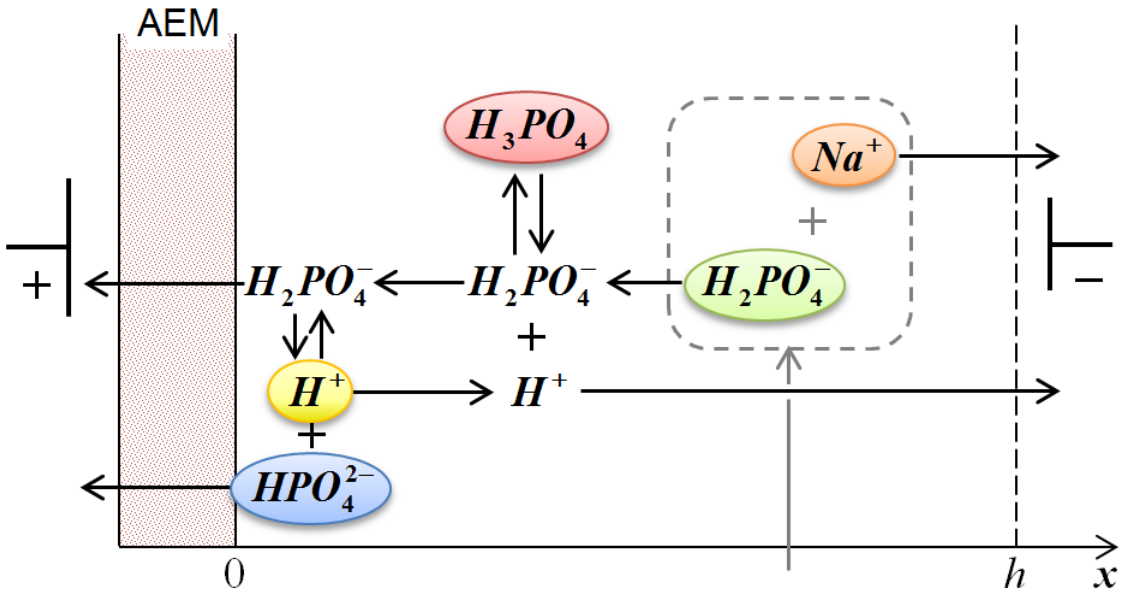

Figure 1. Scheme of the ions transport in the diffusion layer. Ellipses indicate the 5 particles taken into account in the model.

Two reactions during electrodialysis of the NaH_2PO_4 solution are considered:

$$H_2PO_4^- + Q_1 \leftrightarrow H^+ + HPO_4^{2-}, \quad (1)$$

$$H^+ + H_2PO_4^- + Q_2 \leftrightarrow H_3PO_4. \quad (2)$$

A more detailed description of the reactions is given in [2] and [3]. The 2D model for this problem for 3 types of ions and with an assumption of the electroneutrality condition fulfillment was described in detail in [4].

During the electrodialysis of solutions using intensive current modes (“over-limiting” modes), the electroneutrality condition is violated near the membrane / solution interfaces, where space charge regions (SCR) are formed that can significantly effect on electrochemical characteristics of membrane systems. So the new 1D stationary mathematical model based on Nernst-Planck, Poisson, material balance and heat transfer equations is created. It allows to compute

electrochemical and thermal components of the ampholyte electrodialysis (e.g. concentrations, fluxes, electric potential, electric field intensity, current density, space charge, temperature and heat sources). Heat sources we have considered include the Joule heating and sources Q_1 and Q_2 of chemical reactions (1),(2). Moreover, a heat transfer through the membrane is taken into account. On the second stage of the study we use the calculated 1D temperature distribution for the 2D modelling of the hydrodynamics of an ampholyte containing solutions in a desalination channel of electrodialyzer. This 2-stage method simplifies the 2D simulation in orders.

Results

The model computation results show that deprotonation of 1-charge dihydrophosphate occurs mainly in the quasi-equilibrium SCR. The flux of hydrogen reaches values of 10^{-6} mol·m^{-2}s^{-1} (Fig. 2a). Then hydrogen ions, migrating towards the cathode, enter into the protonation reaction with dihydrogen phosphate to form orthophosphoric acid. Thus, the regions of deprotonation of dihydrogen phosphate and the formation of acid are separated in space. This is indirectly indicated by concentration profiles (Fig. 2b).

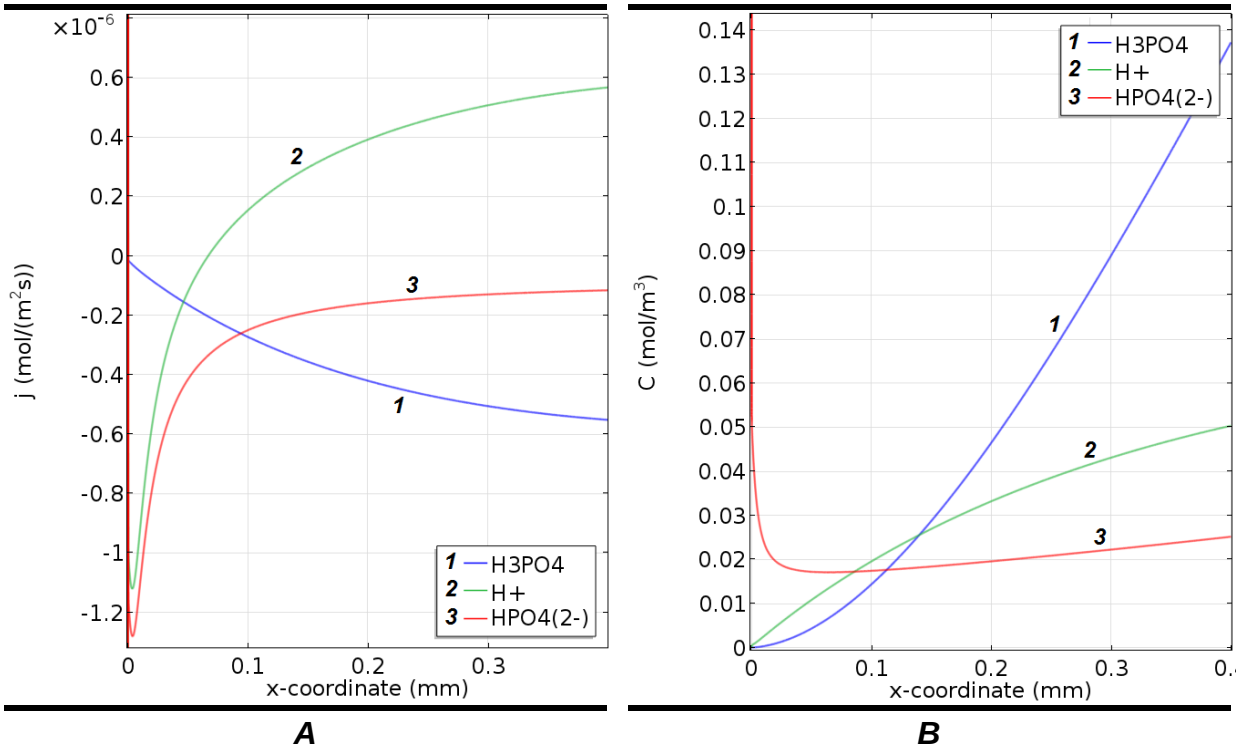

Figure 2. Fluxes (a) and concentrations (b) of H_3PO_4, H^+ and HPO_4^{2-} for NaH_2PO_4 solution with concentration 20 mol/m^3 at a given potential drop in the diffusion layer $d_\phi = -0.2V$.

Both reactions occur with the absorption of heat. The distribution of heat sources is shown in Fig. 3. It can be seen that ***heat sources due to Joule heating are at least an order of magnitude greater than the sources of both chemical reactions*** (and in the quasi-equilibrium SCR – by several orders of magnitude). This is especially noticeable in solutions with low concentrations. Therefore, even local cooling of the solution due to the deprotonation reaction of 1-charge dihydrogen phosphate (Fig. 3b, curve 3) and the acid formation reaction (Fig. 3b, curve 4) near the AEM/solution boundary does not change the overall heating trend of the solution (Fig. 3b, curve 1) caused by the Joule heating (Fig. 3b, curve 2) magnitude.

The Joule heating domination is negligible in prelimiting current modes, but in overlimiting ones the temperature increase may reach several degrees (up to +7K in our simulations). Calculations using a 2D model show that under similar conditions, even with a sufficiently high pumping rate of the solution (0.65 mm/s) a gravitational convection develops in a vertical position of the channel, which affects the physicochemical characteristics of the system, in particular, causes the behavior of the CVCs observed in the experiment [1].

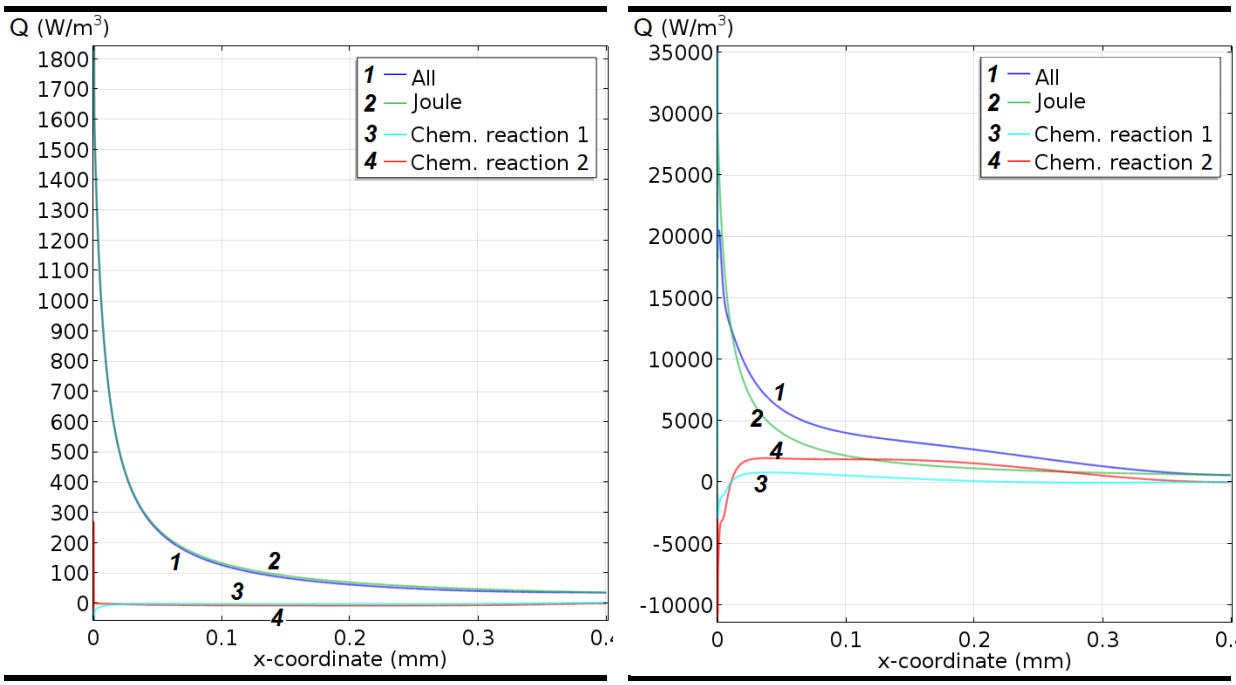

Figure 3. Heat sources for NaH_2PO_4 solution with concentration 1 mol/m^3 (a) and 20 mol/m^3 (b) at a given potential drop in the diffusion layer $d_\phi = -0.2V$.

Acknowledgements

The study is sponsored by RFBR and the administration of Krasnodar region (grant no. 16-48-230856 r_a).

References

1. *Rybalkina O.A., Melnikova E.D., Pismenskiy A.V.* Influence of gravitational convection on current–voltage characteristics of an electromembrane stack in sodium dihydrogen phosphate solution // Petroleum Chemistry, 2018, 58(2), 114–120.
2. *Pismenskiy A.V., Urtenov M. K., Kovalenko A.V., Belashova E.D.* Modeling of mass transfer processes in electrodialysis of ampholites with the account of nonisothermal deprotoningprotoning reactions // International conference «Ion transport in organic and inorganic membranes»: conference proceedings. Russian academy of sciences. Section «Membranes and membrane technologies», Sohi, Russia, 23.05.2017-28.05.2017. Krasnodar: Best Print, 2017. P. 278-280.
3. *Melnikova E.D., Pismenskaya N.D., Bazinet L., Mikhaylin S., Nikonenko V.V.* Effect of ampholyte nature on current-voltage characteristic of anion-exchange membrane // Electrochimica Acta, 2018, 285, 185–191.
4. *Pismenskiy A., Urtenov M., Kovalenko A.* 2D modeling of nonisothermal transfer of ampholytes in a desalination channel of electrodialyzer // International conference «Ion transport in organic and inorganic membranes»: conference proceedings. Russian academy of sciences. Section «Membranes and membrane technologies». Sohi, Russia, 21–26.05.2018. Krasnodar: Best Print, 2018. P. 209-211.

SELECTIVITY OF ION-EXCHANGE RESIN PARTICLES – THE FACTOR OF INTERNAL STRUCTURE

[1]Petr Polezhaev, [1]Tomáš Belloň, [1]Lucie Vobecká, [1,2]Zdeněk Slouka

[1]University of Chemistry and Technology, Prague, Technická 5, 166 28 Praha 6, Czechia

[2]University of West Bohemia, New Technologies - Research Centre Univerzitní 8, 301 00 Plzeň, Czechia

E-mail: *petr.polezhaev@vscht.cz, tomas.bellon@vscht.cz, lucie.linhartova@vscht.cz, zdenek.slouka@vscht.cz*

Introduction

Electroseparations with ion-exchange membranes are often accompanied with unwanted processes of fouling by charged organic compounds [1]. Fouling causes deterioration of membrane transport properties and brings additional expenses for membrane cleaning and replacement. The latter can make up to 50 % of the production costs for certain separations [2]. The aim of our contribution is to determine characteristic internal dimensions of the ion-exchange resins, the main functional component of the heterogeneous ion-exchange membranes, and to study mutual interactions of the resin and the large organic counterions with the size larger than the critical one. Our research brings new knowledge about the behaviour of the ion-exchange resins in the presence of possible fouling agents.

Experiments

The experiments employ electrochemical measurements (CVC, CA) and simultaneous video capture of the electrokinetics in the surface vicinity of the single ion-exchange resins in polycarbonate microcells, which are fabricated according to the in-lab developed methods. DOWEX^{TM} HCR-S/S strong base cation exchange resin particles with sulfonic R-$(SO_3)^-$ functional groups (for industrial demineralisation systems) are used in our experiments. Solutions of tetra-alkylammonium chlorides of increasing molecular weight (from $(CH_3)_4N^+Cl^-$ to $(C_6H_{13})_4N^+Cl^-$) with selected molar concentrations are used as model fouling agents.

Results and Discussion

As it can be seen from the Fig. 1, the current-voltage curves of the DOWEX^{TM} HCR-S/S in the solutions of quaternary ammonium cations display strong dependence on the molecular weights and the diameters of the organic counterions. The characteristic internal dimension of the ion-selective system corresponds to the one of tetrabutylammonium cation (green half filled hexagons), which is visible from the course of the CVC curve, whereas tetrapentylammonium cations display negligible conductivity (blue asterisks) and their transport is hindered.

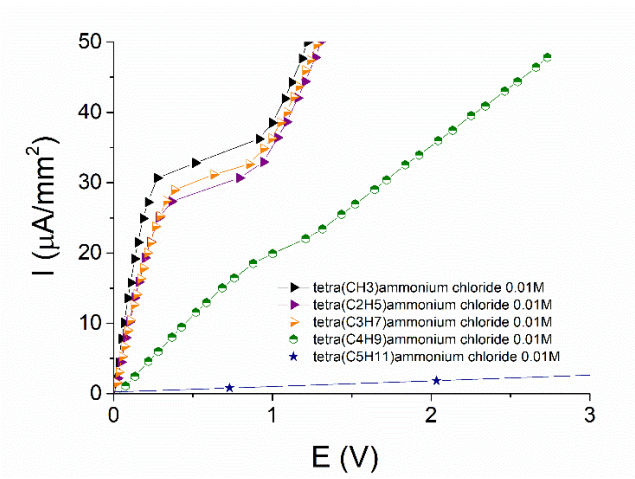

FIGURE 1. DOWEX^{TM} HCR-S/S CURRENT-VOLTAGE CURVES FOR AQUEOUS SOLUTIONS OF

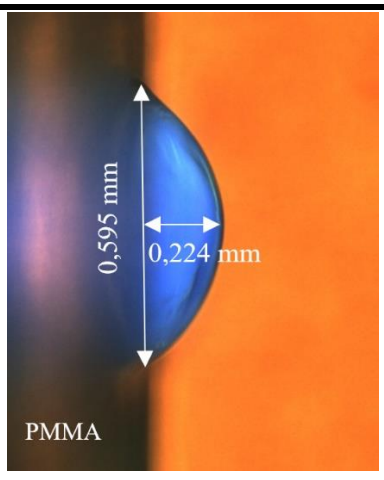

FIGURE 2. PRISTINE DOWEX^{TM} HCR-S/S PARTICLE IN A

TETRAALKYLAMMONIUM CHLORIDES OF INCREASING SIZE.

POLYCARBONATE MICROCELL BEFORE THE EXPERIMENT.

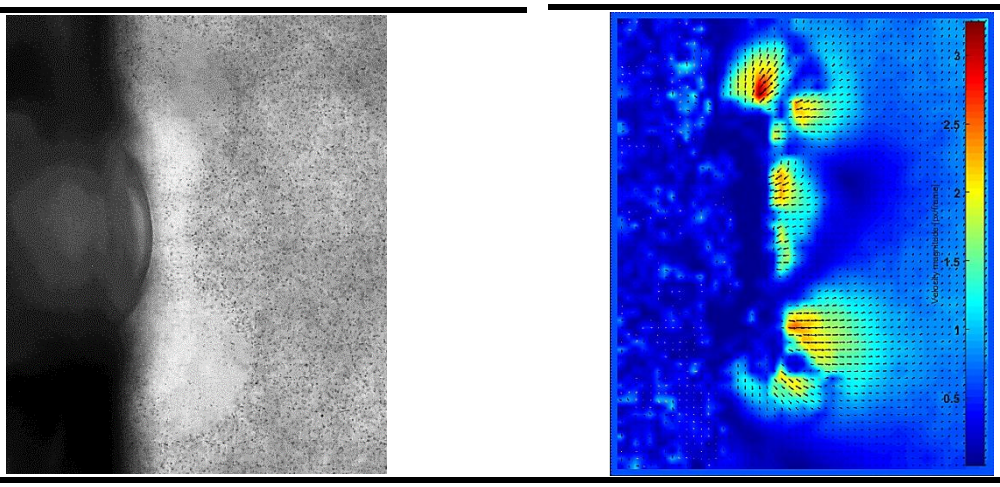

FIGURE 3.ELECTROCONVECTION VELOCITY MAGNITUDE MAP FOR DOWEX^{TM} HCR-S/S PARTICLE IN THE SOLUTION OF TERAMETHYLAMMONIUM CHLORIDE 0,01M DURING THE CVC MEASUREMENT.

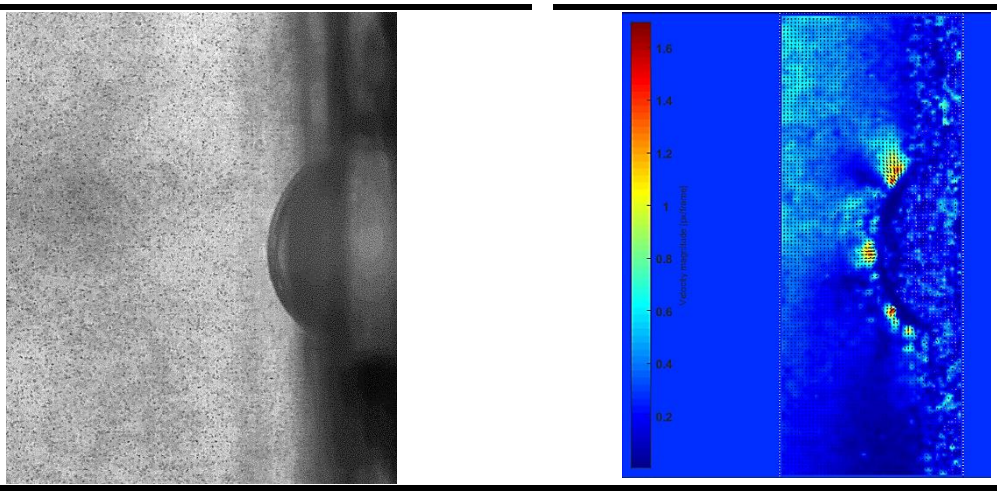

FIGURE 4.ELECTROCONVECTION VELOCITY MAGNITUDE MAP FOR DOWEX^{TM} HCR-S/S PARTICLE IN THE SOLUTION OF TERAPENTYLAMMONIUM CHLORIDE 0,01M DURING THE CVC MEASUREMENT.

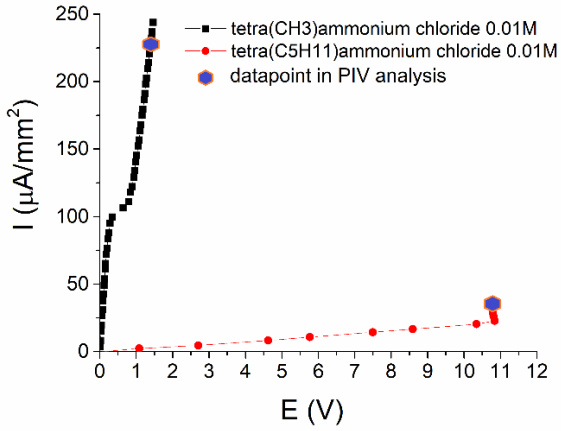

Figure 5. CVC complementary to the velocity maps for DOWEX^{TM} HCR-S/S particle in the solution of tetramethyl and terapentylammonium chlorides 0,01M.

The electrokinetics of the studied systems in tetramethylammonium and tetrapentylammonium chloride 0.01M solutions are demonstrated in Fig. 3 – 5. Significantly different vortex patterns were observed for the two solutions. Namely, two pairs of vortices with varying effective diameter (central microvortices and larger boundary ones) were observed for tetramethylammonium solution, as it is indicated in Fig. 3 and 5. The electroconvection pattern corresponding to tetrapentylammonium solution is characterized by a set of microvortices of lesser intensity.

CA measurements with PBS buffered working electrodes were conducted to evaluate pH and specific conductivity variations in the all the chambers of the PCB microcell. The pH and specific conductivity remained almost unchanged for all the 6 tetralkylammonium chloride solutions after 300 s with a final load of 6V. The results summarized in Tab. 1. Are presented to demonstrate the effect of water splitting phenomenon in the total ionic transport through the ion-exchange resins.

Table 1: pH before/after chronoamperometry (6V, 300s)

	COUNTER EL.	REFERENCE EL.	WORKING SENSE EL.	WORKING EL.
$(C_6H_{13})_4N^+CL^-$	**5.357/6.539**	**5.357/6.116**	**5.357/5.684**	**5.357/5.684**
$(C_5H_{11})_4N^+CL^-$	**5.975/6.595**	**5.975/6.257**	**5.975/6.507**	**5.975/6.466**
$(C_4H_9)_4N^+CL^-$	**6.193/6.463**	**6.193/6.193**	**6.193/6.200**	**6.193/5.439**
$(C_3H_7)_4N^+CL^-$	**6.682/6.451**	**6.682/6.356**	**6.682/6.269**	**6.682/6.517**
$(C_2H_5)_4N^+CL^-$	**6.169/6.492**	**6.169/5.983**	**6.169/6.214**	**6.169/6.370**
$(CH_3)_4N^+CL^-$	**6,396/6.372**	**6,396/6.367**	**6,396/6.250**	**6,396/6.226**

References

1. *Mikhaylin, S. and L. Bazinet*, Fouling on ion-exchange membranes: Classification, characterization and strategies of prevention and control. Advances in Colloid and Interface Science, 2016. **229**: p. 34-56.
2. *Grebenyuk, V.D., et al.*, Surface modification of anion-exchange electrodialysis membranes to enhance anti-fouling characteristics. Desalination, 1998. 115(3): p. 313-329.

STUDY OF PHASE COMPOSITION AND ELECTROTRANSPORT PROPERTIES OF SYSTEMS BASED ON MONO AND DISUBSTITUTED PHOSPHATES OF CESIUM AND RUBIDIUM

Valentina Ponomareva[1,2], Irina Bagryantseva[1,2], Anna Gaydamaka[1,2]

[1] Institute of Solid State Chemistry and Mechanochemistry SB RAS, Novosibirsk, Russia

[2] Novosibirsk State University, Novosibirsk, Russia

E-mail: *ponomareva@solid.nsc.ru*

Introduction

Acid salts of the $M_xH_y(AO_4)_z$ family (M = Cs, Rb, K, Na, Li, NH_4; A = S, Se, As, P) are characterized by superionic phases with structural disordering of hydrogen bonds network, increased proton mobility and high proton conductivity, up to $\sigma \sim 10^{-3}$–10^{-2} S/cm at 100–250°C. CsH_2PO_4 is the most conductive compound of the family and promising material for use as a proton conductive membrane for medium-temperature fuel cells and other electrochemical devices. As for the related salts based on disubstituted hydrophosphates of cesium and rubidium, until recently there were no quite correct data on the transport properties, composition of crystalline hydrates. Only recently crystalline structures were developed. At the same time, the study of $(1-x)MH_2PO_4$–$xM_2HPO_4 \cdot 2H_2O$ (M=Rb, Cs) mixed systems is of fundamental scientific interest for the relationship between the structural features of the crystal lattice and proton transfer parameters, which can serve as a basis for understanding the proton transport mechanism in acid salts, targeted regulation of the functional properties of compounds and the search for new highly conductive phases.

The aim of this work is to investigate the phase composition in the systems based on mono- and disubstituted phosphates of cesium and rubidium $(1-x)MH_2PO_4$– $xM_2HPO_4 \cdot 2H_2O$ (M=Rb, Cs) to compare the electrotransport and thermodynamic properties of the phases, to identify and characterize new compounds.

Results and Discussion

A detailed study of the phase composition, transport and thermodynamic characteristics of systems based on mono- and disubstituted cesium and rubidium phosphates $(1-x)MH_2PO_4$–$xM_2HPO_4 \cdot 2H_2O$ (M=Rb, Cs) was carried out over a wide range of compositions ($0 \le x \le 1$). The new phases $Cs_3(H_2PO_4)(HPO_4) \cdot 2H_2O$ (x=0.5) and $Rb_5H_7(PO_4)_4$ (x=0.25) were identified in the cesium and rubidium systems. $Cs_3(H_2PO_4)(HPO_4) \cdot 2H_2O$ single crystals were synthesized and their crystal structure, as well as thermodynamic characteristics and proton conductivity, were determined for the first time. The compound crystallizes in Pbca space group and forms a structure with strong hydrogen bonds connecting phosphate tetrahedra with a length 2.445 Å and 2.549 Å. The compound was shown to have no superionic phase transitions. Anhydrous $Cs_3(H_2PO_4)(HPO_4) \cdot$ is stable up to 275°C and crystallizes in a monoclinic C2 space group. In the rubidium system a monophasic region was found at x=0.25, corresponding to the $Rb_5H_7(PO_4)_4$ compound. Its electrotransport and thermodynamic properties were investigated. It is shown that $Rb_5H_7(PO_4)_4$ has a phase transition at 252°C to the high-temperature phase, which is characterized by high proton conductivity. At the other values of the mole fraction two-phase regions are realized in $(1-x)MH_2PO_4$–$xM_2HPO_4 \cdot 2H_2O$ (M=Rb, Cs) systems. Phase composition of these regions corresponds to the initial component prevailing in this region and the newly formed compound, which significantly affects the physicochemical properties of the system.

This work was carried out with a partial financial support from state assignment to ISSCM SB RAS project 0301-2019-0001.

STUDY OF NEW PROTON-CONDUCTING MATERIALS BASED ON METAL ORGANIC POLYMERS

[1]Valentina Ponomareva, [2]Konstantin Kovalenko, [1]Elena Shutova, [2]Anastasia Cheplakova, [2]Danil Dybtsev, [2]Vladimir Fedin

[1]Institute of Solid State Chemistry and Mechanochemistry SB RAS, Novosibirsk, Russia
E-mail: *Ponomareva@solid.nsc.ru*
[2]Institute of Inorganic Chemistry SB RAS, Novosibirsk, Russia

Introduction

Metal organic polymers (MOF) represent a new interesting class of compounds with crystallinity and porosity [1]. The inclusion of various compounds into the pores of the MOF with different size allows the synthesis of functional materials with desired properties. This work is aimed to the studying new proton-conducting materials based on mesoporous MOF and compounds with different acidic properties. Mesoporous $Cr_3O(H_2O)Y(bdc)yHNO_3$* nH_2O(bdc - 1,4-$C_6H_4(COO_2)_2$, Y = F, NO_3, y = 0.15, n = 13) so called Cr-MIL-101 was used as a heterogeneous matrix for the synthesis of nanocomposites, as well as CrMIL-100 and CrMIL-53 analogues. Cr-MIL-101 is characterized by high thermal stability, porous structure with a system of cavities ~ 3.8 nm and 2.9 nm and a large pore volume.

Experiments

Phosphoric acid of various concentrations with the low volatility was used as inclusion compound. A number of the acid salts of the $M_nH_m(XO_4)_p$ family such as CsH_2PO_4, $CsHSO_4$, $CsH_5(PO_4)_2$), as well as imidazolium triflate and benzimidazolium triflate were used to create new highly conductive compounds at medium temperatures (100-250°C). Hybrid materials of various compositions were studied by X-ray diffraction, DSC and TA analysis, IR, Raman, ^{1}H-NMR and impedance spectroscopy at different temperatures and different partial pressures of water vapor. The samples of H_3PO_4-CrMIL-101 hybrid compounds were synthesized in a wide range of phosphoric acid concentrations by different preparation methods.

Results and Discussion

The X-ray diffraction patterns of all compounds confirm the stability of the CrMIL-101 crystal structure after the repeated conductivity measurements and heating, as well as a long storage. This is also observed for hybrid compounds with a high concentration of H_3PO_4. The proton conductivity and thermal properties significantly depend on the synthesis conditions of hybrid compounds, H_3PO_4 content, mesoporous structure of matrix of CrMIL-101, CrMIL-100 and CrMIL-53 and relative humidity. The data of thermal analysis show that only the water molecules release from composites when heated to 250°C and H_3PO_4 are not removed from pores when heated. The transport of protons is carried out according to the Grotthuss mechanism with the effective activation energy of ~ 0.25 eV. Hybrid compounds H_3PO_4 - CrMIL-101 are characterized by high proton conductivity ($> 3 \cdot 10^{-2}$ S•cm^{-1} at T=60–80°C), which strongly depends on the acid concentration [2, 3] and atmospheric humidity. A change in relative humidity over a wide range affects both the concentration of water molecules in hybrid compounds and the network of hydrogen bonds for efficient proton transfer and proton mobility. The correlation of proton conductivity and water sorption for different relative humidity was found for H_3PO_4 - CrMIL-101 and H_3PO_4 - CrMIL-100 hybrid materials.

The significant nanocomposite effect was shown for different acid salts such as $CsHSO_4$, $CsH_5(PO_4)_2$) and imidazolium triflates or benzimidazolium triflates with high dispersed nonconducting CrMIL-101. The addition of nonconducting MOFs was shown to increase significantly the proton conductivity up to three orders of magnitude, depending on composition. The highest proton conductivity $\sigma \sim 10^{-1}$ -10^{-2} S/cm at 230°C was observed. The unusual behavior of salts in the MOFs nanospace and a significant increase in conductivity are associated with the surface interfacial interaction and the formation of a disordered amorphous state of salt in the

mesopores. Hybrid compounds with high conductivity are promising as membranes in fuel cells and supercapacitors.

This work was supported by the RFBR grant 18-29-04039.

References

1. *Taylor J.M., Mah R.K., Moudrakovski I.L.,* et.al. JACS. 2010. V. 132. P. 14055.
2. *Ponomareva V. G., Kovalenko K.A., Dybtsev, D. N. et. al.* 2012 JACS. *V. 134 P. 15640.*
3. *Dybtsev, D., Ponomareva, V., Aliev, S., at.el.* Applied Materials and Interfaces. 2014. V.6. P. 5161.

THE MAIN ROLE OF EQUIPOLAR CONTACTS ION-EXCHANGERS GRANS IN THE ELECTRODEIONIZATION

Alla Reshetnikova, Vladimir Shaposhnik
Voronezh State University, Voronezh, Russia, E-mail: *v.a.shaposhnik@gmail.com*

Introduction

Filling the electrodialyzer sections with a mixed bed of granulated ion exchangers was first used by W. Walters, D. W. Weiser, L. J. Marek for treatment of radioactive aquatic waste [1]. E. Glueckauf applied this method for water demineralization, created his theory based on dissociation of water molecules in heteropolar contacts of ion-exchange membranes and granules, ion exchange of regenerating hydrogen and hydroxyl ions with ions of electrolytes dissolved in water, but did achieve good practical results [2]. N. P. Gnusin and V. D. Grebenyuk [3] paid attention to the flow of electric current through heteropolar contacts of granules. They found that at the boundaries $\overrightarrow{C-A}$ there is a concentration of electrolytes, and at the boundaries $\overrightarrow{A-C}$ desalination, which leads to the exclusion of these contacts from mass transfer. However, they concluded that the absence of concentration changes on equipolar boundaries $\overrightarrow{C-C}$ and $\overrightarrow{A-A}$. In practice, however, the method EDI Z. Matêjka got clean water with a specific resistivity of 10 MΩ cm [4], V. A. Shaposhnik, A. K. Reshetnikova and other ultrapure water with resistivity of 20 MΩ cm, suitable for use in microelectronics [5]. The objective of this work is the proof of the decisive role of equipolar contacts the process of deep deionization.

Experiments

Experimental work was carried out in a flat electrodialyzer, in which circles of ion-exchange membranes were simulated ion exchange granules. A universal indicator was introduced into the solution, which allowed to determine the transition time by measuring the pH of ion exchangers.

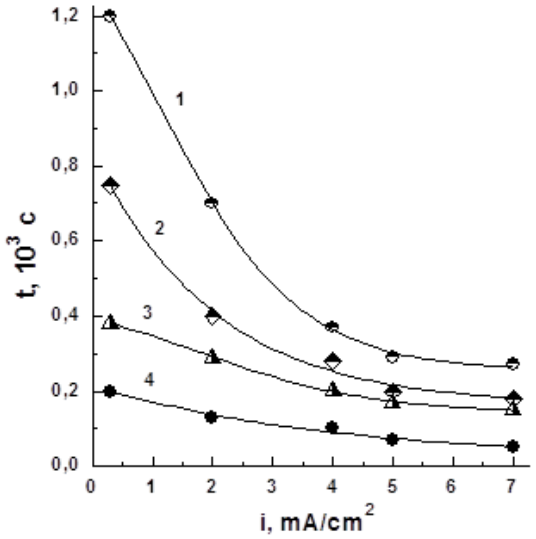

FIGURE 1. THE DEPENDENCE OF THE TRANSITION TIME AT THE BOUNDARIES OF THE ANION EXCHANGE MEMBRANE AND CATION EXCHANGER GRANULES (1), ANION EXCHANGE MEMBRANE AND SOLUTION (2), ANION EXCHANGER GRANULES (3) AND CATION EXCHANGERS (4) ON THE CURRENT DENSITY DURING ELECTRODIALYSIS OF 0.001 M SODIUM CHLORIDE SOLUTION.

Discussion

Figure. 1 shows that the transition time at the boundaries of the equipolar ion exchangers is achieved at lower current densities than at the contacts of granules with the membrane and solutions. Upon reaching the transition time in equipolar contacts on the boundary of the equipolar ion exchangers is leaking process is irreversible dissociation of water molecules, which leads to the conjugated transport of mobile hydrogen ions with the cations of the electrolyte in a chain of granules cation exchangers and hydroxyl ions and anions of the electrolyte in a chain of granules anion exchangers. The small contact surface of the granules enhances the non-equilibrium dissociation of water molecules.

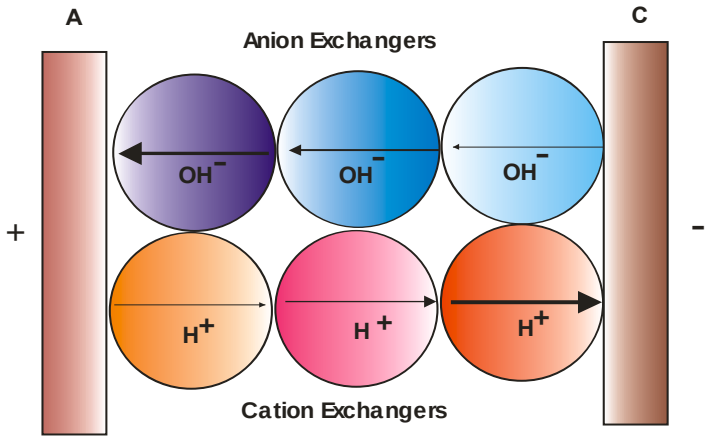

Figure 2. Scheme of ions electromigration in chains of equipolar ion exchangers by continuous electrodeionization.

This process was considered from the standpoint of nonequilibrium thermodynamics [6]. An alternative approach to the interpretation of overlimiting ion transport was developed in the work of Kharkats Yu. I. and called the effect of exaltation [7]. Processes on heterogeneous contacts neutralize each other, therefore, the main processes in which deep demineralization is achieved is the conjugated transport of mobile ions of the medium and ions of desalted electrolytes.

References

1. *Walters W.R., Weiser D.W., Marek* // Ind. Eng.Chem. 1955.Vol. 47. P. 61
2. *Glueckauf E.* // Brit. Chem. Eng. 1959. V. 4. P. 646.
3. *Gnusim N.P., Grebenyuk V.D.* Electrochemistry of ion exchangers granules. 1972, Kiev, Naukova Dumka.
4. *Matejka Z.* // J.Appl. Chem. Biotechnol. 1971. V. 21. P. 117.
5. *Shaposhnik V.*A., *Reshetnikova A.K., Zolotareva R.I., Drobysheva I.V., Isaev N.I.* // Rus. J. Appl. Chem. 1973. V. 46. No. 12. P. 2659.
6. *Shaposhnik V.A., Isaev N.I.* In: Ion exchange membranes in electrodialyse. 1970, Leningrad, 1970, p. 98.
7. *Kharkatz Ju. I.* // Russ. J. Electrochem. 1985. V. 21. No. 7. P. 974.

COMPETITIVE TRANSFER OF SODIUM AND CALCIUM IONS THROUGH ION EXCHANGE MEMBRANES MODIFIED BY POLYANILINE

Nazar Romanyuk, Sergey Loza, Natalia Loza
Kuban State University, Krasnodar, Russia, E-mail: *romanyuknazar@mail.ru*

Introduction

Ion exchange membranes are widely used in industry and technology. They are mainly used to process solutions containing several components by different processes such as electrodialysis demineralization of salty water [1], extraction of acid from wastewater [2] and desalination of whey solutions [3, 4]. The selective separation of single and multiple charged ions is not only important for industrial use, but also an interesting fundamental problem. The actual problem is the modification of ion-exchange membranes in order to make they selective to definite charge of ions to increase the efficiency of the separation of the mixture. Therefore, the aim of this work is to study the competitive transfer of sodium and calcium cations through ion-exchange membranes modified with polyaniline.

Experiments

The competitive mass transfer of ions was studied in a laboratory electrodialysis cell (Fig.1), consisting of alternating 5 cation-exchange and 6 anion-exchange membranes. Heterogeneous electrodialysis membranes MA-41 were used as anion-exchange membranes, cation-exchange membrane were MK-40. The experiments were carried out in a potentiostatic mode at voltages of 0.75, 1.0, 1.25, 1.5, 2.0 and 4.0 V on a pair chamber ($U_{p.c.}$) consisting of one concentration chamber (*CC*) and desalination chamber (*DC*).

To study the charge selectivity of cation-exchange membranes, a mixture of 0.1 M sodium chloride and 0.05 M calcium chloride solutions was used. The volume of solutions in the feed of desalting and concentration chambers varies depending on the applied voltage, and was chosen in such a way as to ensure a constant rate of desalting during all experiments.

To measure the concentration of sodium and calcium cations, solution samples were taken from *CC* and *DC* at the inlet of the apparatus at fixed intervals. The concentration of ions was determined by ion chromatography using an ion chromatograph “Stayer” manufactured by Aquilon.

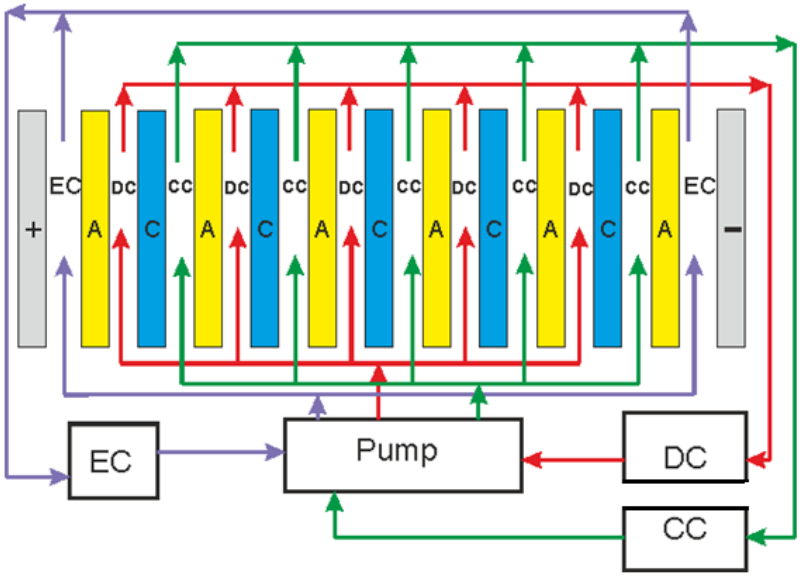

A – anion-exchange membrane; C – cation-exchange membrane;
DC – desalting chamber; CC – concentration chamber; EC – electrode chamber
Figure 1. Experimenal setup to study the competitive electromass transfer of sodium and calcium cations.

Results and Discussion

During the experiments, the mass transfer characteristics of the MK-40 membranes in the $Ca^{2+}/Na^{+}/Cl^{-}$ system were studied at voltage drops 0.75 - 4.0 V per pair chamber. The dependences of changes in the concentration of calcium and sodium chlorides in the *DC* and *CC* on the time of electrodialysis were obtained. Ion flux densities were calculated by equation:

$$J_i = \frac{\Delta C_i V}{tSN}$$

where *Ji* is the integral ion flux, mol-eq·m^{-2}·s^{-1}; *ΔCi* is the change in the concentration of the i^{th} ion during the experiment, mol-eq/m^3; *V* is the volume of the desalting chamber, m^3; *t* is time, s; *N* is the number of cation-exchange membranes; *S* - membrane area, m^2.

Analysis of the data shows that at low voltage drops ($U_{p.c.}$ = 0.75-2), calcium is more preferably transferred through the MK-40 membranes. As the voltage drop rises, the flux density increases for both ions. At higher voltages ($U_{p.c.}$ = 2-4), the fluxes reach the plateau and remain almost unchanged. This is probably due to the onset of an overlimiting state on cation-ion exchange membranes. The onset of the overlimiting state also confirms a sharp change in the electrical conductivity and pH of the solutions, due to the dissociation of water at the border of the ion-exchange membrane/solution, from neutral to acidic in *CC* and *DC* at voltages of 2 and 4 V.

To change the specific selectivity of cation-exchange membranes MK-40, they were modified by polyaniline. Modification was carried out directly in the electrodialysis apparatus, according to the method described in the patent [5]. For this purpose, an electrodialysis cell was assembled as shown at the Fig. 2. The appearance of the modified membrane is shown at the Fig. 3.

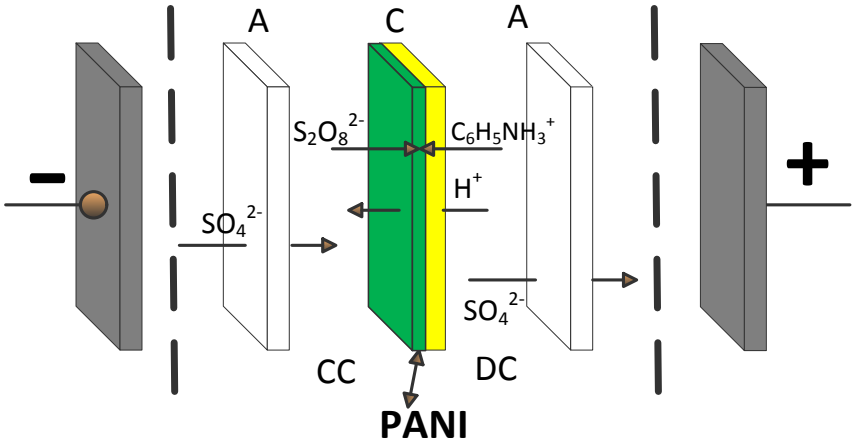

A – anion-exchange membrane; C – cation-exchange membrane; DC – desalting chamber; CC – concentration chamber; EC – electrode chamber; PANI –polyaniline layer

Figure 2. Scheme of MK-40 membrane modification by polyaniline.

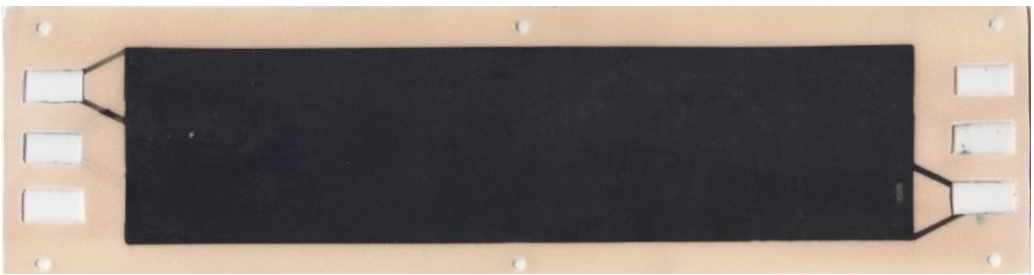

Figure 3. Image of the membrane MK-40 modified by polyaniline (active area 5x20 cm^2).

After the modification, the electrodialysis apparatus shown at the Fig. 1 was assembled from the obtained membranes, so that the layer modified with polyaniline was facing the desalination chamber. Experiments on processing a mixture of solutions 0.1 M sodium chloride and 0.05 M

calcium chloride were carried out under the same conditions as the experiments with the initial membranes.

Analysis of the data obtained shows that a layer of polyaniline deposited on the surface of the cation-exchange membrane retards doubly charged calcium ions. Their total flux decreases on average by 2 times, while the flux density for sodium ions decreases by 25%.

Conclusions

Thus, an electrodialysis desalination study was performed on a mixture of solutions 0.1 M sodium chloride and 0.05 M calcium chloride using MK-40 and MK-40 membranes modified with polyaniline. It was shown that membranes modified by polyaniline are capable of retaining calcium ions, as compared with the original membranes.

Acknowledgments

The present work is supported by the Russian Foundation for Basic Research (project № 18-38-20069 mol_a_ved).

References

1. *Xu X., He Q., Ma G., Wang H., Nirmalakhandan N., Xu P.* // Desalination. – 2018. – Vol. 428. – P. 146-160.
2. *Wang, L., Zhang F., Li Z., Liao J., Huang Y., Lei Y., Li N.* // J. Membrane Sci. – 2018. - Vol. 549. – P. 543-549.
3. *Rice, G., Kentish S., Vivekanand V., Barber A., O'Connor A., Stevens G.* // Developments in chemical engineering and mineral processing. 2005. – Vol. 13. – P. 43-54.
4. *Zolotareva M.S., Volodin D.N., Bessonov A.S., Topalov V.K.* // Rus. J. Dairy industry. – 2014. – № 3. – P. 37-38.
5. *Kononenko N.A., Loza S.A., Loza N.V.* // Pat. RU № 2566415, № 2014129703/05, 18.07.2014; publ. 27.10.2015.

STUDY OF PROTONATION-DEPROTONATION REACTIONS IN THE SYSTEM ANION-EXCHANGE MEMBRANE / KHT SOLUTION USING IMPEDANCE SPECTROSCOPY

Olesya Rybalkina, Kseniia Tsygurina, Ekaterina Melnikova, Anton Kozmai, Natalia Pismenskaya

Membrane Institute, Kuban State University, Krasnodar, Russia, E-mail: *olesia93rus@mail.ru*

Introduction

The transfer of ampholytes in systems with ion-exchange membranes is associated with the chemical reactions of protonation-deprotonation. A large number of substances (including nutrients or valuable components of food) possess the ability to be involved in these reactions. A feature of electrodialysis processing of ampholyte-containing solutions is that these species transform from one form to another not only in the solution, but also inside the ion-exchange membrane. This research is aimed at studying the chemical reactions at the anion-exchange membrane/ampholyte solution interface using impedance spectroscopy.

Experiments

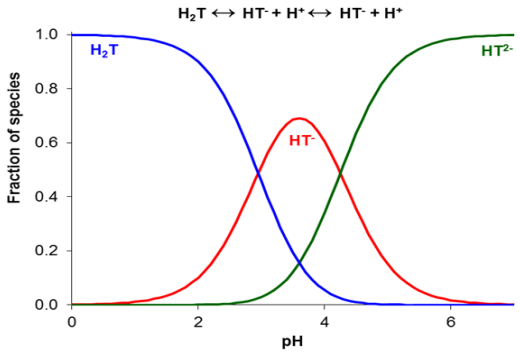

Figure 1. Distribution of Tartaric Acid Species (in Mole Fraction) as a Function of pH.

The experiments were carried out in a flow-through desalination channel of an electrodialysis cell. This channel is formed by the auxiliary cation-exchange membrane CMX and the AMX anion-exchange membrane under study. Both membranes are made by the paste method (manufacturer ASTOM, Japan). The membranes underwent standard salt treatment before the experiment [1]. The electrodialysis cell and setup for the research are described in detail elsewhere [2]. Electrochemical impedance spectra were obtained using the FRA2 module for Autolab-100n in the frequency range 0.03-30000 Hz. The studies were carried out in 0.02 M solutions of KCl and potassium hydrotartrate (KHT). KCl is a typical strong electrolyte that does not participate in protonation-deprotonation reactions with water. KHT is involved in protonation-deprotonation reactions. The result of these reactions is a change in the chemical structure and charge of this tartaric acid species depending on the pH of the medium (Fig. 1).

Results and Discussion

Some of the electrochemical impedance spectra of the AMX membrane in 0.02 M KCl and KHT solutions are presented in Fig. 2 and Fig. 3. Dependencies of the effective rate constant of water splitting reaction (χ) upon current density (i) normalized to the limiting current ($i/i_{\lim}^{Lev}$), which is calculated by Leveque equation, are presented in Fig. 4. These constants are calculated from the value of frequency at the maximum point of the Gerischer arch using the equation [4]:

$$f_{III} = \frac{\chi\sqrt{3}}{2\pi}$$

It is established that in the KCl solution water splitting with the involvement of fixed secondary and tertiary amino-groups of AMX membrane is registered if $i/i_{\lim}^{Lev} \geq 1$. The χ values of this reaction increase with increasing current density. These data are in agreement with the known concepts of water splitting in the case of strong electrolytes [4].

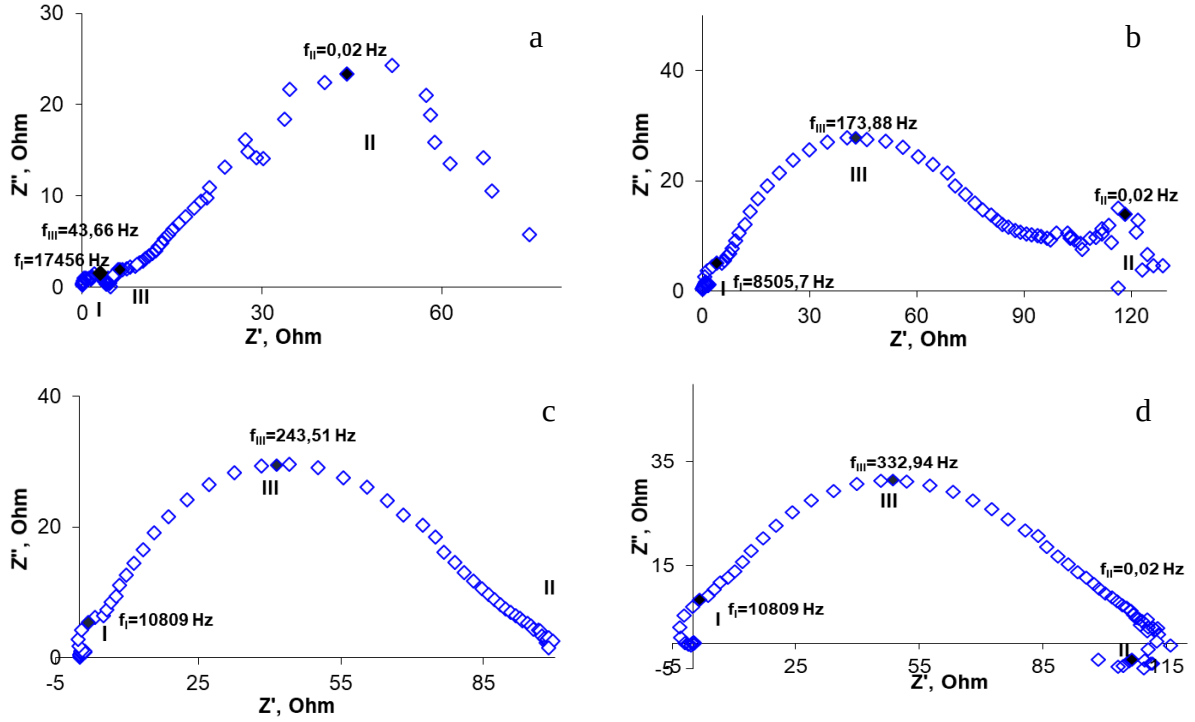

Figure 2. Electrochemical Impedance Spectra Obtained for the AMX Membrane in 0.02M KCl at i/i_{lim}^{Lev}: 1.0 (a); 1.2 (b); 1.4 (c); 1.6 (d).

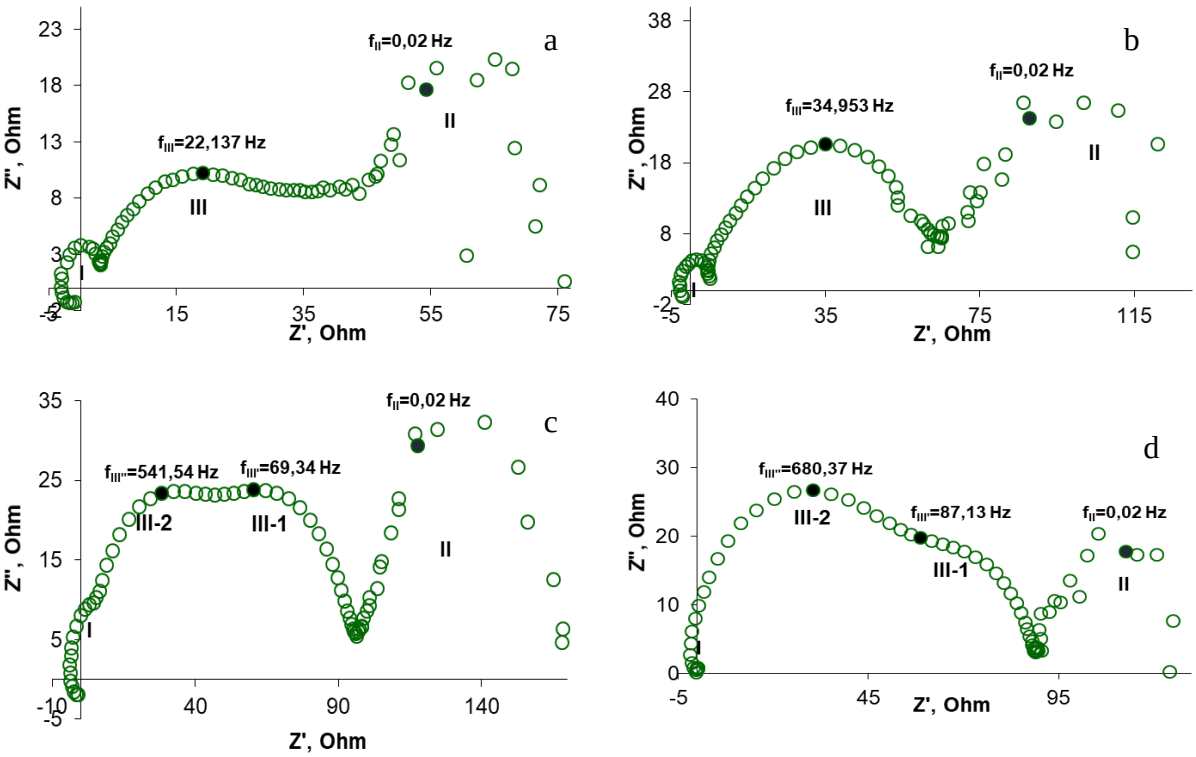

Figure 3. Electrochemical Impedance Spectra Obtained for the AMX Membrane in 0.02M KHT at i/i_{lim}^{Lev}: 1.5 (a); 1.6 (b); 2.0 (c); 2.3 (d).

It is well-known that the reaction zone is located within the interfacial electrical double layer where there is a strong electric field (about 10^8 V m^{-1} [5]), which produces several effects on the water splitting reaction. First, under the action of a strong electric field, the H – OH bond in the water molecule is stretched, which weakens it and leads to an increase in the dissociation rate constant (the second Wien effect) [5,6]. Second, in a strong electric field, the rotational mobility of water molecules increases [7], and the orientation of the water molecules is more favorable for

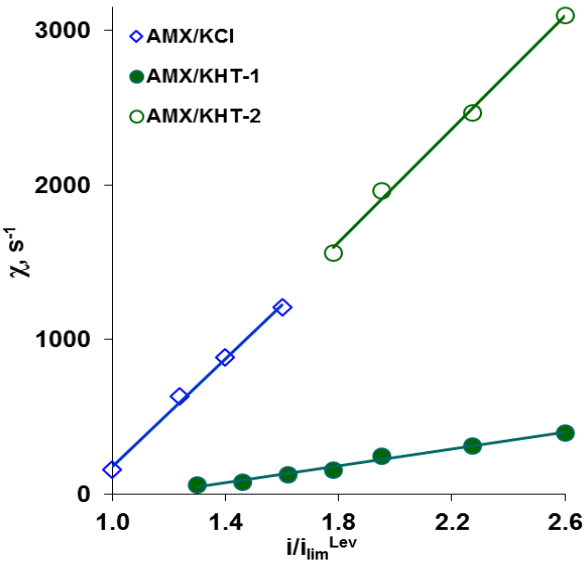

Figure 4. Values of the Effective Rate Constant of Water Splitting Reaction at the Membrane/Solution Interface vs i / i_{lim}^{Lev}

the proton transfer [8]. Third, a strong electric field promotes faster removal of products (H^+ and OH^- ions) from the reaction zone, for example, from the vicinity of the fixed groups located at the membrane/solution interface [9]. In the system AMX/KHT solution, two chemical reactions occur. Based on the determined values of the effective constants, we can assume that one of these reactions is water splitting with the involvement of fixed secondary and tertiary amino-groups of the membrane (AMX / KHT-2, Fig. 4). The second reaction: $HT^- \rightarrow T^{2-} + H^+$ (AMX / KHT-1, Fig. 4) occurs when a single-charged tartaric anion from the solution gets into the membrane. This reaction is irreversible due to the Donnan exclusion of the proton from the membrane into the solution. The electric field helps to remove the protons from the reaction zone (membrane). Therefore, the effective constant of this reaction growth with increasing i / i_{lim}^{Lev}.

Acknowledgements

This study was supported by the Russian Science Foundation (Project no 17-19-01486).

References

1. *Berezina N. P., Timofeev S. V., Kononenko N. A.* Effect of conditioning techniques of perfluorinated sulphocationic membranes on their hydrophylic and electrotransport properties // J. Membr. Sci. 2002. V. 209. № 2. P. 509-518.
2. *Rybalkina O. A., Tsygurina K. A., Melnikova E. D., Pourcelly G., Nikonenko V. V., Pismenskaya N. D.* Catalytic effect of ammonia-containing species on water splitting during electrodialysis with ion-exchange membranes // Electrochimica Acta. 2019. V. 299. P. 946-962.
3. *Kniaginicheva E., Pismenskaya N., Melnikov S., Belashova E., Sistat P., Cretin M., Nikonenko V.* Water splitting at an anion-exchange membrane as studied by impedance spectroscopy // J. Membr. Sci. 2015. V. 496. P. 78-83.
4. *Zabolotskii V. I., Shel'deshov N. V., Gnusin N. P.* Dissociation of water molecules in systems with ion-exchange membranes // Russ. Chem. Rev. 1988. V. 57. P. 801-808.
5. *Simons R.* Strong electric field effects on proton transfer between membrane-bound amines and water // Nature. 1979. V. 280. P. 824-826.
6. *Timashev S. F., Kirganova E. V.* On the mechanism of electrolytic decomposition of water molecules in bipolar membranes // Russ. J. Electrochem. 1981. V. 17. № 3. P. 440-443.
7. *Eigen M., De Maeyer L.* Self-dissociation and protonic charge transport in water // Proc. R. Soc. Lond. A. 1958. V. 247. № 1251. P. 505-533.
8. *Mafé S., Ramírez P., Alcaraz A.* Electric field-assisted proton transfer and water dissociation at the junction of a fixed-charge bipolar membrane // Chem. Phys. Lett. 1998. V. 294. № 4/5. P. 406-412.
9. *Urtenov M. Kh., Pismensky A. V., Nikonenko V. V., Kovalenko A. V.* Mathematical modeling of ion transport and water dissociation at the ion-exchange membrane/solution interface in intense current regimes // Petrol. Chem. 2018. V. 58. № 2. P. 121-129.

SWITCHABLE IONIC SELECTIVITY IN CONDUCTIVE NANOPOROUS MEMBRANES: 1D AND 2D MATHEMATICAL MODELS VS EXPERIMENTAL DATA

[1,2]Ilya Ryzhkov, [1,2]Anton Vyatkin, [2]Anastasia Bortsova, [2]Mikhail Simunin, [1]Sofia Kozlova, [1]Valerij Kucheryavyj

[1]Institute of Computational Modeling, Federal Research Center KSC SB RAS, Krasnoyarsk, Russia
[2]Siberian Federal University, Krasnoyarsk, Russia
E-mail: *rii@icm.krasn.ru*

Introduction

Over the last two decades, the development of nanopores and nanochannels with controlled ion transport has attracted a lot of research attention. The applications of such structures include separation and purification processes, water treatment, chemical sensors, and synthetic analogues of biological ion channels and pumps [1, 2]. Tunable ion transport can be realized via the interaction of pore geometry and surface physicochemical properties with external stimuli, such as electric field, radiation, temperature, solution pH, etc [3].

The use of electric field for switching the ionic selectivity of a nanoporous membrane was first demonstrated in [4]. The membrane was prepared by electroless plating of gold on the pore walls of track-etched polymeric support. It was shown that its selectivity can be continuously and reversibly switched from cation to anion by applying the prescribed potential to the conductive membrane surface. The modulation of membrane potential at zero current by the external electric field in solid-state channels was also demonstrated in [5].

Recently, a new type of highly porous ceramic membranes (C-Nafen) with a conductive coating was suggested [6]. The membranes were prepared by vacuum filtration of a colloidal solution of Nafen alumina fibers with a diameter of about 10 nm through a porous substrate and subsequent drying and annealing. The deposition of a thin carbon layer on the nanofibers by chemical vapor deposition (CVD) provided the formation of an electrically conductive membrane surface. The preliminary experimental results on controlling the membrane potential at zero current and ionic conductivity by externally applied potential were reported in [7].

In this work, we develop one- and two-dimensional mathematical models for describing the variation of membrane potential by application of a prescribed potential to the membrane surface. An extensive comparison between theoretical predictions and experimental data obtained by the authors as well as other researchers is performed.

Theoretical

The membrane is modelled as an array of cylindrical pores of radius R and length L. The Navier-Stokes, Nernst-Planck, and Poisson equations are used to describe the ion transport in a single nanopore. The two-dimensional (2D) model is based on the extension of Space-Charge model [8] to the case of nanopores with conductive surface [9, 10]. In the present work, it is further generalized by including the Stern layer next to the nanopore surface, which is characterized by thickness δ and relative permittivity ε. The latter is significantly reduced near the nanopore surface in comparison with its central part due to preferential orientation of water molecules under high electric field.

One-dimensional (1D) model is derived from two-dimensional one by assuming that the potential, ion concentrations, and pressure do not depend on the radial coordinate. It is a valid approximation when the pore radius is smaller than the Debye length. The Stern layer capacitance used in 1D model is calculated on the basis of cylindrical Stern layer thickness δ and its relative permittivity ε according to the formula

$$C_S = \frac{\varepsilon\varepsilon_0}{(R-\delta)\ln\left(R/(R-\delta)\right)}, \qquad (1)$$

where ε_0 is the vacuum permittivity.

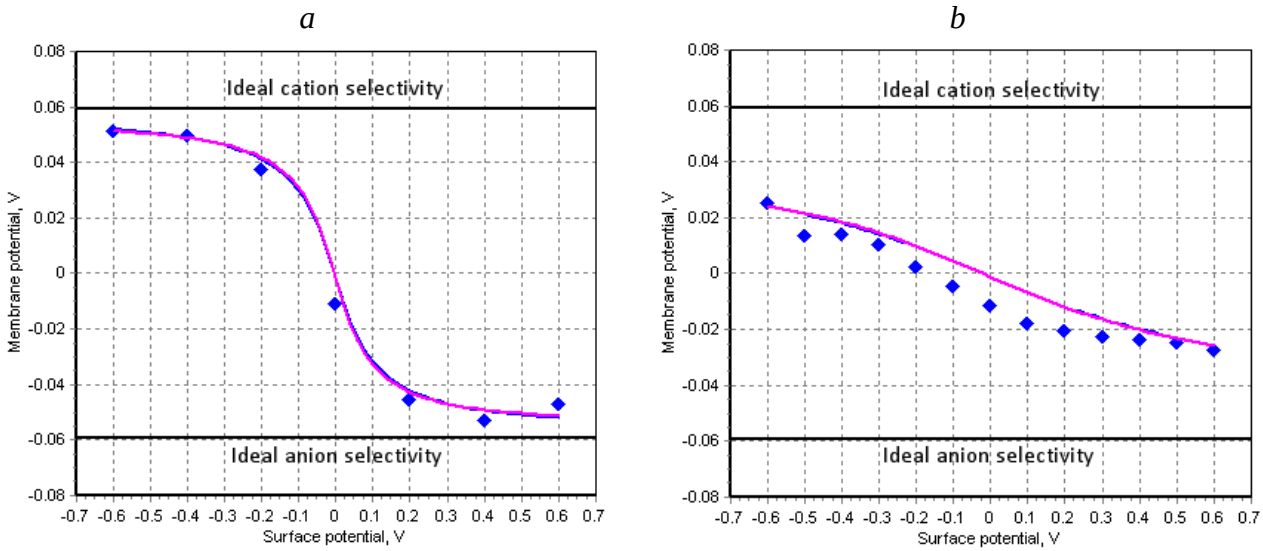

Figure 1. The dependence of membrane potential on the surface potential for KCl aqueous electrolyte with C_L=10 mM, C_R=1 mM (a) and C_L=100 mM, C_R=10 mM (b). Experiment (dots) and theoretical models (blue curves – 2D, magenta curves – 1D). The fitted value of pore radius is 12.9 nm (a) and 11.0 nm (b), pore lengths is 400 μm.

The 1D model reduces to the system of ordinary differential equations, which are integrated along the pore under conditions of equal pressures and different constant concentrations in the reservoirs, which are separated by the membrane. All models are realized as a software tool with graphical user interface, which allows not only calculation, but also fitting experimental curves to experimental data and determining model parameters (pore radius, Stern layer thickness, dielectric permittivity, etc).

Experimental

To investigate the switchable ionic selectivity, we measure the membrane potential at zero current of C-Nafen membranes under different surface potentials. The experimental setup [7] consists of two half-cells, between which the membrane is clamped. The half-cells are filled with aqueous KCl or NaCl electrolyte of different concentrations (C_L and C_R). To minimize the concentration polarization, the solutions in both half–cells are stirred by a closed loop pumping system based on Lead fluid BT601L peristaltic pump. The potentiostat P-20X (Elins, Russia) is used for applying a prescribed potential to the conductive membrane surface with respect to 4.2. Ag/AgCl reference electrode. The membrane serves as a working electrode, while the two platinum wires (counter-electrodes) are placed in both half-cells. The second potentiostat Pi-50Pro is used for measurement of zero current voltage between the half-cells. The measurements are performed at different surface potentials in the range –600 … + 600 mV.

Results and discussion

The dependence of membrane potential on the applied surface potential is presented in Fig. 1 (a) for aqueous KCl electrolyte with C_L=10 mM, C_R=1 mM. The experimental results are shown by dots. It can be seen that when the applied potential is changing from +600 mV to –600 mV, the membrane potential continuously varies from approximately –50 mV to +50 mV. It indicates that at high positive applied potentials (> 400 mV), the membrane is anion selective, while for high negative applied potentials (< –400 mV), it is cation selective. In these cases, the values of membrane potential approach the Nernst potential, which corresponds to ideal selectivity. In the intermediate range, the continuous change from anion- to cation-selective state is observed. Theoretical results based on 2D model are shown by continuous blue curve. The curve was fitted to the experimental data by varying the pore radius. The Stern layer thickness was taken as 0.33 nm, while the relative permittivity in the Stern layer was taken as ε=1. The fitted value of R=12.9 nm correlates with the pore size distribution of C-Nafen membrane [9]. The 1D model gives almost

the same results as the 2D model. The Stern layer capacitance in 1D model C_S=0.027 F/m^2 was calculated according to (1).

Figure 4 (b) shows the dependence of membrane potential on the applied potential for C_L=100 mM, C_R=10 mM. The increase of concentration leads to the decrease of Debye length, which in turn reduces the membrane selectivity. It results in significant reduction of membrane potential variation. The predictions of 1D and 2D models agree with the experimental data quite well.

Conclusion

In this work, we have demonstrated both experimentally and theoretically with the help of 1D and 2D models that the variation of potential applied to nanoporous membrane surface can provide a continuous change of membrane selectivity from anion to cation. The selectivity becomes stronger with decreasing the electrolyte concentration.

The reported study was funded by Russian Foundation for Basic Research, Government of Krasnoyarsk Territory, Krasnoyarsk Regional Fund of Science, to the research project 18–48–242011 "Mathematical modelling of synthesis and ionic transport properties of conductive nanoporous membranes".

References

1. *Tagliazucchi M., Szleifer I.* Transport mechanisms in nanopores and nanochannels: can we mimic nature? Mater. Today, 2015. V. 18, 131.
2. *Siwy Z.S., Howorka S.* Engineered voltage-responsive nanopores. Chem. Soc. Rev., 2010. V. 39, 1115.
3. *Hou X., Guo W., Jiang L.* Biomimetic smart nanopores and nanochannels. Chem. Soc. Rev., 2011. V. 40, 2385.
4. *Martin C.R., Nishizawa M., Jirage K., Kang M., Lee S.B.* Controlling ion-transport selectivity in gold nanotubule membranes. Adv. Mater. 13, 1351 (2001).
5. W. Guan, M.A. Reed, Electric field modulation of the membrane potential in solid-state ion channels, Nano Lett. 2012, V. 12, P. 6441–6447.
6. *Solodovnichenko V.S., Lebedev D.V., Bykanova V.V., Shiverskiy A.V., Simunin M.M., Parfenov V.A., Ryzhkov I.I.* Carbon coated alumina nanofiber membranes for selective ion transport. Advanced Engineering Materials, 2017, V. 19, 1700244.
7. *Lebedev D.V., Solodovnichenko V.S., Simunin M.M., Ryzhkov I.I.* The influence of electric field on the ion transport on nanoporous membranes with conductive surface. Petroleum Chemistry, 2018. V. 58. Issue 6. P. 474–481.
8. *Peters B.B., Van Roij R., Bazant M.Z., Biesheuvel P.M.* Analysis of electrolyte transport through charged nanopores, Phys. Rev. E, 2016. V. 93, 053108.
9. *Ryzhkov I.I., Lebedev D.V., Solodovnichenko V.S., Minakov A.V., Simunin M.M.* On the origin of membrane potential in membranes with polarizable nanopores. Journal of Membrane Science, 2018. V. 549. P. 616-630.
10. *Ryzhkov I.I., Lebedev D.V., Solodovnichenko V.S., Shiverskiy A.V., Simunin M.M.* Induced-charge enhancement of diffusion potential in membranes with polarizable nanopores. Physical Review Letters, 2017. V. 119, 226001.

RESEARCH OF KINETIC TRANSFORMATIONS OF THE CHEMICAL SUPREMOLECULAR STRUCTURE IN THE SYSTEM: THE ORIGINAL RAW MATERIAL - FORMING SOLUTION - FILTER MEMBRANE

Valentin Sedelkin, Larisa Potekhina, Olga Lebedeva, Marina Schneider, Elmira Ulyanova
Engels Technological Institute (branch) of the Saratov State Technical University named after Yuri Gagarin, Engels, Russia. E-mail: *sedelkinvm@mail.ru*

Introduction

Chitosan is a linear half-stranded crystallizing polymer and has a good balance of hydrophobic and hydrophilic properties, solubility in dilute acids, high ability to physico-chemical modification and film formation, availability and renewability of raw materials for its production, full biodegradability in natural conditions. Therefore, chitosan is perspective as a raw material for the production of film materials of various physicochemical modifications, including for the manufacture of filtration membranes [1].

The complex of physico-chemical properties of the initial powdered chitosan raw material is determined by molecular and supramolecular levels of structural organization. At the same time, the functional characteristics of chitosan film products depend mainly on the supramolecular structure of the initial chitosan, which has not been studied sufficiently.

The processing of powdered chitosan into films and filtration membranes is carried out through its solutions. In solutions, chitosan from the basic chemical form, in which it is found in the feedstock, is converted to the salt chemical form. The type of chitosan salt in solution depends on the type of acid used to prepare the polymer solvent. In the process of preparing the molding solution, the supramolecular structure of the initial chitosan, which is characterized by a complex of amorphous-crystalline parameters (the angular position of the diffraction crystal reflexes and the corresponding interplanar distances, the type and parameters of the elementary crystallographic cells, the dimensions of the crystallized and amorphous regions of the polymer matrix, the integral degree of crystallinity, etc.) will undergo kinetic changes.

Getting chitosan membranes occurs by casting a solution on a solid substrate with the subsequent transfer of the solution (sol) to the gel. In the process of gelation, prerequisites are created for the formation of new supramolecular structures that reflect the kinetic features of the sol - gel processes in the preparation of film materials from chitosan salts.

Salt chitosan films have antibacterial activity, however, they dissolve in water. To obtain water-insoluble and durable filtration membranes, salt chitosan films are treated with alkali solutions, which leads to the transition of chitosan from the polysol form to the polybase form. At the same time, due to the chemical reaction of modification, the supramolecular structure of chitosan in the film material may again undergo changes.

Thus, the supramolecular structure of chitosan filtration membranes, on which their deformation-strength and other performance characteristics mainly depend, will be determined by kinetic transformations along the entire technological process of processing the initial chitosan raw materials into finished products. The study of these kinetic transformations of the supramolecular structures of chitosan was the task of this work.

Experiments

In this work, the most demanded for the manufacture of film materials of various physicochemical modifications and functional purposes of powdered crab chitosan, obtained from chitin by the method of alkaline deacetylation, was used as a raw material. The viscosity average molecular weight of chitosan was 420 ± 10 kDa, the degree of deacetylation - 80 ± 2 mol.%.

Chitosan membranes were obtained from 2% solutions of the feedstock in 2% acetic acid by pouring onto a glass substrate, followed by drying the castings under room conditions for three days. The conversion of chitosan in the membranes from the salt form to the main form was carried out by treating them with a 10% aqueous solution of NaOH, followed by washing with water until neutral.

To study the supramolecular structure of chitosan and membrane materials obtained from it, we used the methods of full-profile X-ray diffraction analysis (PAP), which were experimentally implemented using the computer-based diffractometer DRON-3.

The figure shows the experimental diffraction patterns, as well as the results of their full-profile analysis for the initial chitosan (a), membranes with chitosan in salt form (b) and membranes with chitosan in the basic form (c).

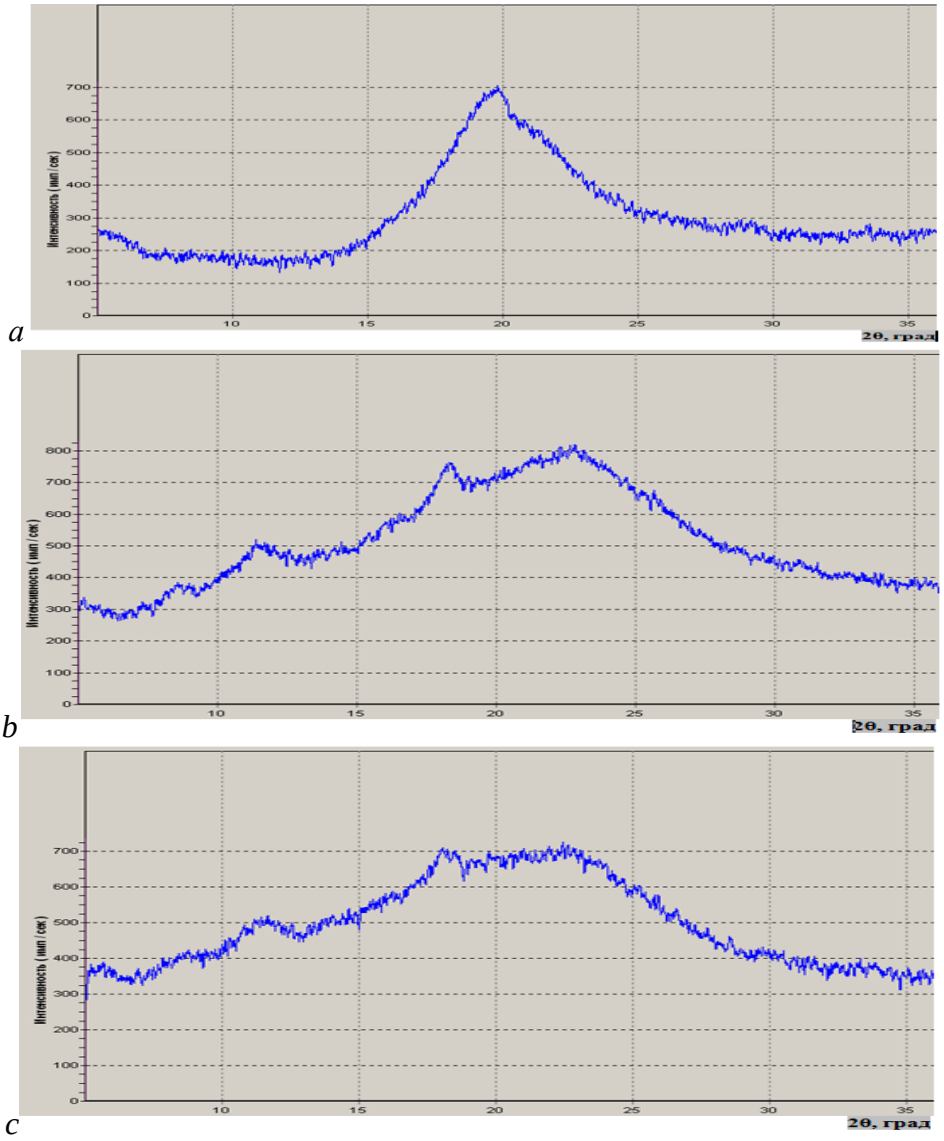

Figure 1. Graphical interpretation of the results of full-profile analysis (PPA) of experimental diffractograms for chitosan and chitosan membranes: a - initial chitosan, b - membrane with chitosan in salt form, c - membrane with chitosan in basic form.

A bimodal Gauss function was used to approximate the crystal reflections and diffuse scattering of the amorphous structures of chitosan and membranes. The resulting approximation curves served as the basis for calculating such parameters of supramolecular structures as the size of the coherent radiation scattering region in the crystalline (Lcr.) And amorphous (Lam) parts of the polymer matrix, as well as the interplanar spacings (d) characterizing the modification of the elementary crystallographic cells of the polymer.

The calculated values of the parameters of the supramolecular structure of chitosan and membranes are given in the table.

The analysis of the results showed that high-molecular crab chitosan used for the manufacture of filtration membranes of various functional purposes, contains both crystalline and amorphous areas. The degree of crystallinity of chitosan was 50%, salt films -14%, basic membranes - 17%.

Table 1: Calculated values of the parameters of the supramolecular structure of chitosan and membranes

STRUCTURE PARAMETERS		CHITOSAN							
CALCULATED ANGLE 2Θ, HAIL		**10,3**	**17,1**	**18,0**	**18,4**	**20,0**	**35,3**	**38,5**	
INTEGRAL INTENSITY J, PULSE / SECOND		**40,0**	**377,3**	**214,1**	**3188,6**	**116,6**	**2446,9**	**121,5**	
PEAK WIDTH B, RADIAN		**7,0**	**2,14**	**0,54**	**10,4**	**1,45**	**55,0**	**21,5**	
INTERPLANAR DISTANCE D, Å		**8,55**	**5,2**	**4,93**	**4,81**	**4,45**	**2,53**	**2,36**	
SIZES OF COHERENT SCATTERING REGIONS	L_{KP}, Å	**2,2**	**7,3**	**30,0**	**-**	**18,0**	**-**	**-**	
	L_{AM}, Å	**-**	**-**	**-**	**15,0**	**-**	**3,0**	**20,3**	
		MEMBRANES WITH SALT FORM OF CHITOSAN							
CALCULATED ANGLE 2Θ, HAIL		**8,58**	**11,56**	**13,7**	**16,2**	**18,25**	**20,31**	**22,89**	**25,68**
INTEGRAL INTENSITY J, PULSE / SECOND		**22,2**	**538,6**	**121,6**	**340**	**410**	**1400**	**2023,5**	**1106,6**
PEAK WIDTH B, RADIAN		**0,36**	**2,51**	**2,10**	**5,15**	**1,32**	**4,37**	**4,32**	**4,68**
INTERPLANAR DISTANCE D, Å		**10,35**	**7,71**	**7,0**	**5,51**	**4,86**	**4,38**	**3,89**	**3,47**
SIZES OF COHERENT SCATTERING REGIONS	L_{KP}, Å	**24,56**	**32,9**	**-**	**16,3**	**33,8**	**-**	**19,7**	**-**
	L_{AM}, Å	**-**	**-**	**7,2**	**-**	**-**	**19,4**	**-**	**18,1**
		MEMBRANES WITH THE MAIN FORM OF CHITOSAN							
CALCULATED ANGLE 2Θ, HAIL		**8,7**	**11,43**	**13,6**	**15,44**	**18,1**	**20,34**	**22,9**	**33,5**
INTEGRAL INTENSITY J, PULSE / SECOND		**20,66**	**353,8**	**21,5**	**914,8**	**618,0**	**1024**	**1414,1**	**17,1**
PEAK WIDTH B, RADIAN		**0,49**	**2,19**	**0,75**	**4,72**	**2,32**	**3,67**	**4,02**	**0,3**
INTERPLANAR DISTANCE D, Å		**10,28**	**7,75**	**7,2**	**5,75**	**4,91**	**4,34**	**3,88**	**2,75**
SIZES OF COHERENT SCATTERING REGIONS	L_{KP}, Å	**18,1**	**38,1**	**16,0**	**17,9**	**37,1**	**-**	**-**	**16,5**
	L_{AM}, Å	**-**	**-**	**-**	**-**	**-**	**23,0**	**21,1**	**-**

During the processing of chitosan through solutions into membrane products, a radical reorganization of its amorphous-crystalline structure occurs. The report describes the kinetic mechanism of this rearrangement in successive processes of chitosan swelling in distilled water, dissolving the polymer by solvating its individual functional groups with dissociation and forming salt (chitosan acetate), including NH3 + and CH3COO- ions, producing a solid chitosan acetate membrane through the stage of transition of the solution into the gel casting, the treatment of the salt membrane with alkali and its final drying.

Results and Discussion

It was established that when chitosan is dissolved, its initial amorphous-crystalline structure is "disassembled". In the process of gelation and the production of salt and base membranes, a new amorphous-crystalline structure is formed, as evidenced by the appearance of new crystalline reflexes that were not observed on the diffractogram of the initial chitosan.

The change in such amorphous-crystalline parameters, such as the angular position of the diffraction crystal reflections and their corresponding interplanar distances, the sizes of crystallites and ordered amorphous formations, the integral degree of crystallinity (see table).

The obtained Lcr values indicate that the crystallized regions of the initial chitosan, salt and basic chitosan membranes have a microcrystalline structure with crystallite sizes less than 40Å. For comparison, it can be noted that the size of "mature" polymer crystals can reach 106Å [2].

References

1. *Galbrahih L.S.* Chitin and chitosan: structure, properties, application / LS. Galbraich // Soros Educational Journal. - 2001. - T.7, №1. - 51-56 p.
2. *Tager A.A.* Physical chemistry of polymers //A.A. Tager - M: Scientific world. - 2007. - 576 p.

VAPOR-PHASE MEMBRANE METHOD FOR RECOVERY AND CONCENTRATION OF BIOALCOHOLS FROM FERMENTATION BROTHS

[1]Maxim Shalygin, [1]Alina Kozlova, [2,1]Alexander Netrusov, [1]Vladimir Teplyakov

[1]Topchiev Institute of Petrochemical Synthesis RAS, Moscow, Russia, E-mail: *mshalygin@ips.ac.ru*

[2]Faculty of Biology, Moscow State University, Moscow, Russia

Introduction

Various types of biofuels such as biomethane, biohydrogen, biodiesel and bioalcohols are currently produced more and more widely. There is a significant production of bioalcohols as alternative fuels due to the possibility of their utilization as directly as additives to gasoline. The production of bioalcohols formed diluted water-alcohol mixture with typical ethanol concentration of about 10 wt.% (after ethanol fermentation) and butanol concentration of about 1.5 wt.% (after ABE fermentation). In the case of subsequent alcohols use as renewable energy carriers the recovery and further concentration steps should be highly effective in order to provide maximum overall utilization of energy.

Vapor-phase membrane method (VPMM) was proposed previously for alcohols concentration from dilute water-alcohol solutions. This method combines stripping and subsequent membrane separation of vapors. Stripping provides recovery of alcohols from liquid and preconcentration. Membrane separation of vapors provides further concentration of alcohols in vapor phase and allows to achieve high final concentration of organic components. Alcohol-selective or water-selective membranes can be applied at this step in contrast to pervaporation which demands alcohol-selective membranes for such purpose. Application of water-selective membranes seems to be much more promising first of all due to the considerably higher membrane selectivity and secondly due to the benefits of concentration of target component in retentate that allows to achieve low content of water in the product.

Experiment

Experimental study was performed in semi-batch mode of operation: recovery and concentration of organic components from fermentation broths after ethanol and ABE fermentation by VPMM was continuous with progressive decrease of alcohols concentration in initial solution. Membrane module with water-selective membrane was applied in the process. Initial concentrations of ethanol and butanol in fermentation broths were 9 and 2 wt.% respectively. ABE fermentation broth also contained acetone and ethanol with concentrations around 1 and 0.2 wt.% respectively.

Results

It was found that VPMM provides effective concentration of organic components even in semi-batch mode of operation. Achieved ethanol concentration varied from 76 to 81 wt.% at the level of ethanol extraction degree from fermentation broth from 99 to 90 % respectively and productivity of 0.8-1 kg/(m^2·h). Achieved butanol concentration varied from 49 to 59 wt.% at the level of butanol extraction degree from 99 to 94 % respectively and productivity of 0.2 kg/(m^2·h). The overall ABE concentration varied from 76 to 92 wt.% at the level of the extraction degree from 99 to 90 % respectively and productivity of 0.3 kg/(m^2·h).

The productivity of the system and purity of organic components can be significantly improved keeping the same level of alcohol extraction degree in case of addition of stripping column. The modeling of the process with stripping column shows the improvement of productivity from several times to one order. The estimation of appropriate energy consumptions was carried out.

Acknowledgements

This work is supported by the Russian Science Foundation under Grant No. 16-14-00098.

CONJUGATE TRANSPORT OF MASS AND ENERGY IN ION EXCHANGE MEMBRANES BY ELECTRODIALYSE

Vladimir Shaposhnik
Voronezh State University, Voronezh, Russia, E-mail:v.a.shaposhnik@gmail.com

Thermoelectric effect in membranes

For electrodialysis with highly selective membranes, if the diffusion contributions and pressure drop between the sections are neglected, the linear Onsager law for mass and energy flows can be written in the form

$$J_1 = L_{11} X_1 + L_{12} X_2 = u_i c_i \left(-z_i \frac{d\varphi}{dx} \right) + \frac{\lambda}{R} \left(-\frac{1}{T} \frac{dT}{dx} \right) \quad (1)$$

(L is the phenomenological coefficient of the fluxes of mass and energy, X is the generalized thermodynamic force causing the flow of mass and energy, u – electric mobility, φ is the electric potential, λ - coefficient of thermal conductivity). In 1821, T. Seebeck discovered the thermoelectric effect in conductors of the 1st kind, when at $X_1 = 0$ the temperature gradient causes the flow of electricity. This effect is used thermocouples. The thermoelectric effect in the conductors of the second kind (membranes, solutions) can be measured by electrodialysis in potentiostatic regime, if the ion flow when applying the electric potential gradient is constant, and only the temperature varies. Fig. 1 shows the linear dependence of cation transport through the cation exchange membrane during electrodialysis of the suspension of slightly soluble strontium and barium sulphates, which allows to maintain a constant concentration in the desalination section. The linear increase of strontium and barium cation fluxes as a function of temperature at a constant electric potential gradient proves the coupling of mass and energy fluxes during electrodialysis with ion-exchange membranes.

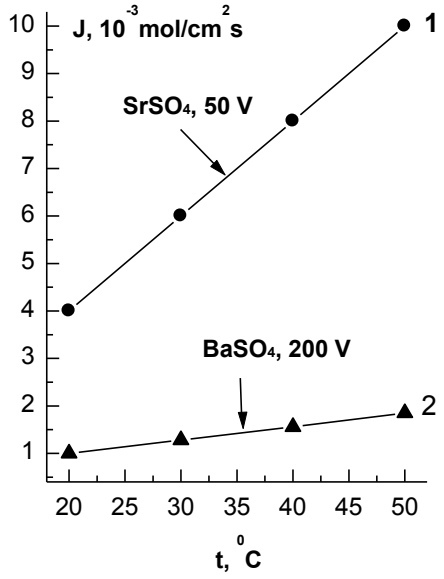

FIGURE. 1. THE DEPENDENCE OF THE FUXES OF IONS OF STRONTIUM (1) AND BARIUM (2) IN ELECTRODIALYSIS OF SULPHATE SUSPENSIONS ON THE TEMPERATURE AT A VOLTAGE OF 50 (1) AND 200 (2) WITH ALTERNATING ANION EXCHANGE AND CATION EXCHANGE MEMBRANES MA-40 AND MK-40.

For electrodialysis in galvanostatic mode to more efficiently apply the theory of the Arrhenius, which allows to write for the electric mobility of ions

$$\frac{u_2}{u_1} = \frac{T_1}{T_2} \exp \frac{E_a (T_2 - T_1)}{R T_1 T_2} \quad (2)$$

(E_a is the energy of activation and R is the universal gas constant). Equation (2) allows describing not only linear but also nonlinear processes. We obtained an exponential dependence of the limiting current density and temperature consistent with the experimental data [1].

Joule heat and recombination of hydrogen and hydroxyl ions as internal sources of energy during electrodialysis.

Sources of heat during electrodialysis can be external and internal. External sources are hot or preheated before it enters the section solutions. The particular interest are the internal sources of energy. Dissipation of electrical energy leads to the release of Joule heat

$$\sigma_q = i^2 \rho \tag{3}$$

(i is the current density, ρ is the electrical resistivity). In [2] the linear dependence of the temperature increment as a function of the square of the current density was obtained, which corresponds to equation (3). In accordance with equation (2), the electrodialysis temperature should be higher in the desalting section solution. However, this occurs only up to densities not exceeding the limit diffusion. At extreme current densities, the temperature in the concentration sections is higher (Fig.2). The reason is the release of heat of recombination of hydrogen and hydroxyl ions formed during irreversible dissociation of water on the interfacial surfaces of membranes and solution into water molecules. The heat of recombination is highlighted in sections desalting and concentrating sections, however in sections of desalting heat is absorbed by irreversible dissociation.

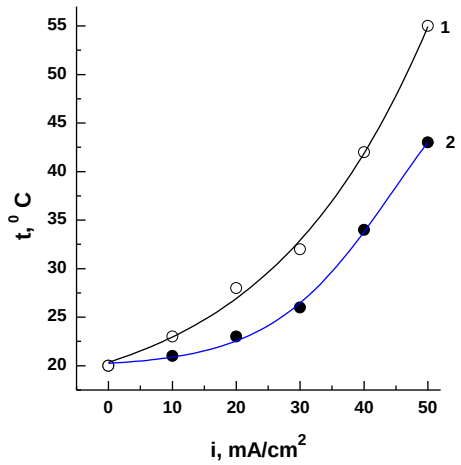

FIGURE 2. THE DEPENDENCE OF THE INCREMENT OF TEMPERATURE ON TIME AT A CURRENT DENSITY OF AT ELECTRODIALYSIS 0.05 M SOLUTION OF POTASSIUM CHLORIDE (SOLID CIRCLES SHOW THE INCREMENT OF TEMPERATURE IN THE SECTIONS OF DESALINATION AND HOLLOW CIRCLES SECTIONS CONCENTRATING).

The presence of endothermic and exothermic effects causes self-oscillating process and the phenomenon of thermo-electroconvection, which lead to dynamic chaos [3], increased convection and mass transfer through the membranes, which can be effectively used for deep purification of solutions during electrodialysis.

References

1. *Shaposhnik V.A., Zolotareva R.I.* // Russ. J. Electrochem. 1979, V.15, P. 1545.
2. *Gnusin N.P., Shaposhnik V.A., Sheldeshev N.V.* Russ. J. Appl. Chem., 1975, V. 43, P. 2641.
3. *Shaposhnik V.A., Vasil'eva V.I., Grigorchuk O.V.* // Adv. Colloid and Interface Sci., 2008, V. 139, P. 74.

TRANSFER PROCESSES IN MEMBRANE SYSTEMS USED FOR PRODUCTION ACIDS AND BASES FROM THEIR SALTS BY BIPOLAR ELECTRODIALYSIS

Nikolay Sheldeshov, Victor Zabolotskiy, Konstantin Lebedev
Kuban State University, Krasnodar, Russia, E-mail: *sheld_nv@mail.ru*

During creating electrodialyzers, the need arises to select the type of ion-exchange membranes that provide its best performance. One of the main characteristics of ion-exchange membranes, which determines the current efficiency of a substance, the specific energy consumption and productivity of the process, is the ion transport numbers through the membrane. Among the known types of ion transport numbers across membranes, only effective transport numbers that reflect all the ion transport mechanisms in membrane systems are suitable for calculating the main characteristics of electrodialyzers. In the case, such as in bipolar electrodialysis, when chemical substances in solutions are capable of undergoing protonation and deprotonation reactions, the task of measuring transfer numbers becomes much more complicated. The reason is the complex multicomponent composition of solutions surrounding the membranes in such electrodialyzers. Among the known methods for measuring the effective transport numbers through membranes in such systems, the method proposed in [1] is most applicable. However, the well-known method [1] does not allow to determine the ion transport numbers through the membrane in systems that coincide with membrane systems of electrodialyzers, since they require the use of auxiliary solutions.

For experimental measurement of ion transport through bipolar, cation-exchange and anion-exchange membranes in the systems "organic acid solution and its salt – alkali solution" and "amine solution and its salt – sulfuric acid solution" more general method of measuring fluxes through the individual membrane under investigation was developed on the basis of the hydrodynamic isolation method [1]. The developed method makes it possible to determine the fluxes of all ions and molecules of organic acids and bases through the investigated membrane. The proposed method can be used to measure the transport numbers of inorganic ions and molecules across membranes. The advantage of this method is the ability to determine transport numbers of those ions and molecules that can be oxidized, or reduced at the electrodes.

Mathematical model of a membrane system consisting of bipolar membrane and two diffusion layers on both sides containing solution of organic acid and it's salt near the cation exchange layer of bipolar membrane and alkali solution with organic base salt near the anion-exchange membrane layer is developed. The model takes into account the reaction layers in which the recombination of ions and molecules takes place: recombination of hydroxyl ions generated by the space-charge region of the membrane and acid molecules diffusing through the cation-exchange layer to the bipolar boundary, and recombination of hydrogen ions generated by the space-charge region of the membrane with anions of organic acid. In determining the relationships between the ion and molecular fluxes in the layers of the membrane system, the generation of hydrogen and hydroxyl ions in the space-charge region of the bipolar membrane is also taken into account. The transport of ions and molecules is described by the Nernst – Planck equations. The system of equations of the mathematical model is solved by numerical method. The model makes possible to calculate the fluxes and concentration profiles of ions and molecules, the electrical potential difference across all layers of the membrane system.

Study was supported by Russian Foundation for Basic Research, research project № 17-08-01689.

References

1. *Zabolotskii V.I., Shel'deshov N.V., Orel I.V., Lebedev K.A.* Determining the ion transference numbers through a membrane by its hydrodynamic isolation // Rus. J. Electrochem. 1997. V. 33. P. 1066-1071.

ON THE FEATURES OF ELECTROPHORESIS OF CHARGE-SELECTIVE PARTICLES

[1]Vladimir Shelistov, [1,2]Elizaveta Frants, [1]Georgy Ganchenko
[1]Financial University, Krasnodar, Russia, E-mail: *shelistov_v@mail.ru*
[2]Kuban State University, Krasnodar, Russia

Introduction

Electrophoresis is a fundamental phenomenon in theoretical physics with ever-increasing applications in microfluidics and bio-analysis. The behavior of a charge-selective particle was for the first time investigated only recently [1] for a small Debye layer and weak external field, using asymptotic methods. We extend this study by performing numerical simulations.

Simulation

We consider a solid spherical microparticle with an ideal cation-selective surface that moves in a certain direction in an electrolyte solution. Such a particle can be treated as a sophisticated type of electric membrane. Once a proper hydrodynamic condition for the particle's movement is imposed, the electroosmotic effects that occur near the particle's surface can be investigated with the same methods as those applied to planar membrane systems [2]. In this study, we assume a zero-force condition. Since the statement has an axial symmetry, we can reduce it to a two-dimensional one. Some analysis of such statement is presented in [3].

Results and Discussion

For a not very large external field, a steady-state solution was achieved eventually. Three boundary layers that are nested inside each other are formed: the EDL region, the SCR, and the thin diffusion layer (Figure 1). At the external electric field above the critical value, the steady-state solution loses its stability, which is justified by linear stability analysis. For very large external fields, our numerical analysis fails, and a sophisticated semi-analytical solution is obtained instead. Both simulated and semi-analytical solutions are in a reasonable good agreement with the available experimental data.

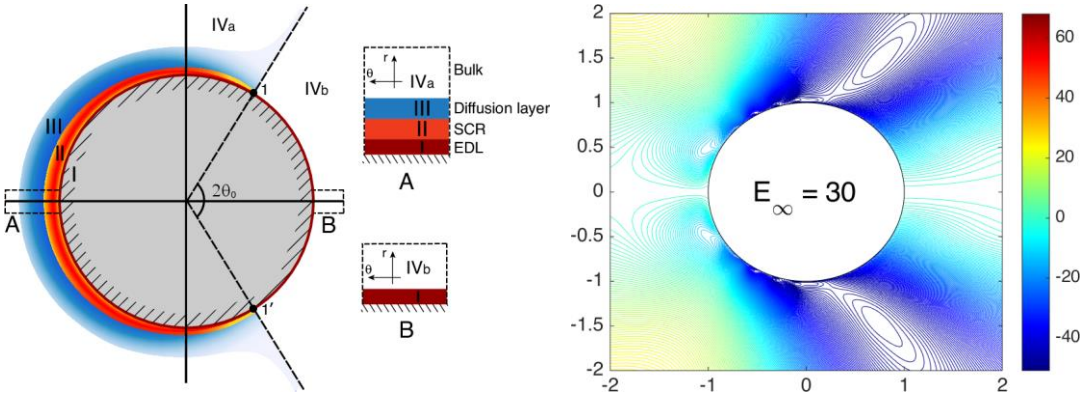

Figure 1. Boundary layer structure (left) and electroosmotic vortex formation (right) near a charge-selective particle.

The study has been supported by RSF project 17-79-10343 and joint RFBR+Ministry of Education and Science for Krasnodar region project 19-48-233010.

References

1. *Yariv E.* Migration of ion-exchange particles driven by a uniform electric field // J. Fluid Mech. 2001. V. 655. Pp. 105-121.
2. *Demekhin E. A., Nikitin N. V., Shelistov V. S.* Direct numerical simulation of electrokinetic instability and transition to chaotic motion // Phys. Fluids. 2013. V. 25. 122001.
3. *Frants E. A., Ganchenko G. S., Shelistov V. S. et al.* Nonequilibrium electrophoresis of an ion-selective microgranule for weak and moderate external electric fields // Phys. Fluids. 2018. Vol. 30. 022001.

WATER TRANSPORT IN MODIFIED ION EXCHANGE MEMBRANES

Svetlana Shkirskaya, Viktoria Soloshko
Kuban State University, Krasnodar, Russia, E-mail: *shkirskaya@mail.ru*

Introduction

Among membrane methods, electrolyte solution concentration by electrodialysis occupies an exclusive position since it makes it possible to obtain solutions with high salt concentrations [1]. It is well known that the concentration process by electrodialysis is influenced by a variety of technological and physicochemical factors. Physicochemical factors include properties of the membranes forming the membrane packet. It is established that the dominant influence on salt solution concentration have the electroosmotic and osmotic flux of water transport while the diffusion component of the salt flux has a negligibly small influence [1]. One of the promising methods for increasing of work of the electrodialyzer–concentrator is the development of a new type of membrane, which makes it possible to increase the level of salt solution concentration. Such membranes must be characterized by low electroosmotic permeability for decreasing the volume of water entering the concentration chambers in the structure of counterion hydration shells and by low osmotic permeability for decreasing free water transport. Therefore, the purpose of this work is to evaluate changes osmotic and electroosmotic water flux in MF-4SK membrane and composite with polyaniline based on it (MF-4SK/PANI) in NaCl solutions.

Experiments

A homogeneous sulphocathionite membrane on perfluorinated matrix MF-4SK and MF-4SK/PANI were the objects of the study. The modification was carried out by the method of successive diffusion of polymerizing solutions through the membrane to water [2]. The electroosmotic flux (m^2/s) was measured by the volumetric method in a two-chamber cell with reversible silver chloride electrodes and measuring capillaries under the application of electric current [3]. The osmotic water flux (m^2/s) was measured at the same cell by measuring changes of solution volume under concentration gradient 10 times. In this work the total water flux was also determined by measuring changes of solution volume in measuring capillaries under both concentration and electric potential gradient according to equation (1).

$$j_w = \frac{V}{S \cdot \tau \cdot M_w}$$

where V – volume of water flux passing through surface membrane area S per unit time τ; M_w – is the volume of a mole water.

Results and Discussion

The real electromembrane processes of concentrating electrolytes are carried out under both concentration and electric fields. As a result there are different fluxes appear in electromembrane cells such as diffusional, electroosmotic, osmotic. The total water flux (j_w(total)) transfers through membrane by electroosmotic and osmotic mechanism as presented in Figure 1. So during the electrodialysis concentration the osmotic (j_w(OS)) and electroosmotic (j_w(EO)) fluxes of water coincide and transport to concentration chamber of electrodialysis cell:

$$j_w(\text{total}) = j_w(\text{OS}) + j_w(\text{EO})$$

This makes it possible to calculate the contribution of electroosmotic and osmotic mechanisms to the total water transport. Figure 2*a* shows that the total water flux through cation-exchange membrane MF-4SK in NaCl solution while maintaining a constant concentration difference of 10 times does not change with increasing absolute values of concentrations (from 1/0.1 till 3/0.3). However, it was found that the contribution of osmotic and electroosmotic fluxes in the total water transport changed. It was shown that increasing concentration leads to decrease of the electroosmotic flux contribution. This is due to a decrease of the water amount in the hydration shell of the Na^+-ion with increasing concentration.

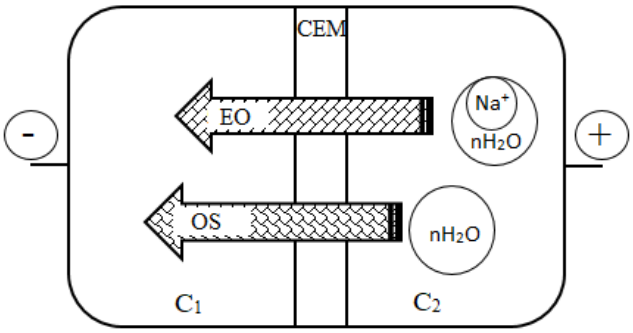

Figure 1. Schematic representation of the electroosmotic and osmotic mechanisms of water flux through cation-exchange membrane in NaCl solution (C_1>C_2).

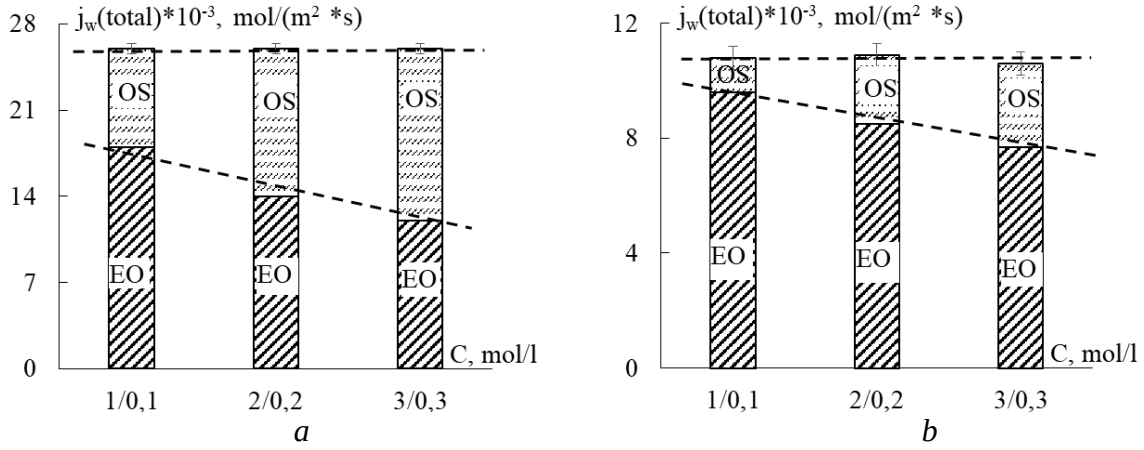

Figure 2. The total water flux through MF-4SK (a) and MF-4SK/PANI (b) membranes in NaCl solutions: OS and EO - the contribution of osmotic and electroosmotic mechanism of water transport correspondently.

It was found that the modified membrane MF-4SK/PANI reduces the total water flux by 2.5 times (Fig. 2*b*). It corresponds to our earlier data on the determination of the water transport numbers for the same composites during the investigation of their electroosmotic permeability [2]. It should be noted that the contribution of osmotic water flux is reduced more significantly – 5-6 times compared to the original membrane, while the electroosmotic transfer is reduced only 1.5 times. This is due to the barrier effect of the polyaniline layer to the water transport through the composite membrane, as a result only water of close hydration is transported. The decrease of osmotic flux through MF-4SK/PANI membrane is related to a reduce of the membrane water content [2], therefore the transport of free water through modified membrane essential decrease. Thus, the contributions of electroosmotic and osmotic fluxes to the total water transport through individual membranes were first time experimentally determined.

The present work was supported by the Russian Foundation for Basic Research (project № 19-08-00925).

References

1. *Protasov K.V., Shkirskaya S.A., Berezina N.P., Zabolotskii V.I.* // Russ. J. Electrochem. 2010. V. 46. P. 1131-1140.
2. *Berezina N.P., Shkirskaya S.A., Kolechko M.V., Popova O.V., Senchikhin I.N., Roldugin V.I.* // Russ. J. Electrochem. 2011. V. 47. P. 995-1005.
3. *Berezina N.P., Shkirskaya S.A., Sycheva A.A.-R., Krishtopa M.V.* // Colloid Journal. 2008. V.70. P. 397–406.

STUDY OF ELECTROCHEMICAL CHARACTERISTICS OF FUJI TYPE – X ANION EXCHANGE MEMBRANES PRODUCED VIA ELECTROSPINNING METHOD

Inna Shkorkina, Veronika Sarapulova, Olesya Rybalkina
Kuban State University, Krasnodar, Russia, E-mail: *shkorkina_inna@mail.ru*

Introduction

In recent years, manufacture began to produce ion-exchange membranes the structure of which is fundamentally different from those widely used in electrodialysis and dialysis. The basis of this membranes consist of three-dimensional structure of thin fibers made by the method of electrospinning. This work is aimed at studying the electrochemical characteristics of one of these membranes as well as it surface structure before and after a long operation in electric field.

Experiments

The homogeneous aliphatic anion exchange membrane (AEM) Type – X was investigated (Fujifilm, Netherlands). This membrane is made using electrospinning method. The homogeneous aromatic membrane AMX (Astom, Japan) produced by the paste method was studied for comparison [1]. The experiments were carried out in NaCl solutions at 25 ° C in a flow-through four-chamber electrochemical cell using the AutolabPGStat-100 electrochemical complex. This cell and technique to determine partial current voltage characteristics were described in [2].

Results and Discussion

Figure 1 shows the partial current-voltage characteristics of the AEM Type-X and AMX membrane.

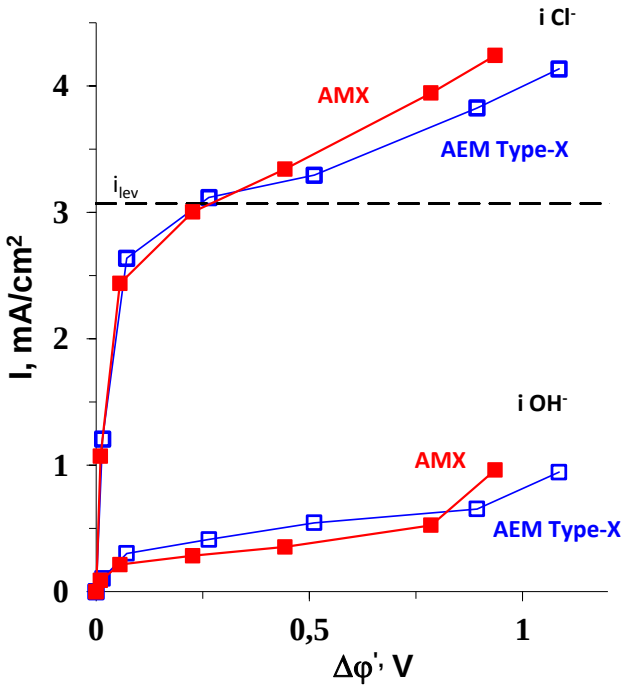

Figure 1. Partial current-voltage characteristics of AMX and AEM Type-X membranes obtained in a 0.02 M NaCl solution. The dashed line is the limiting current calculated using the Leveque equation.

It is shown that partial current-voltage characteristics of both membranes are almost identical. The partial currents of Cl^- ions increase in the overlimiting current mode. Apparently, the geometrically inhomogeneous surface of both membranes stimulates the development of electroconvection. Water splitting at the surface of the investigated membranes is insignificant. The transfer of OH^- ions in both membranes under study does not exceed 20% over the entire

range of reduced potential drops. We can concluded based on the results of the work that AEM Type-X can be effectively used for the electrodialysis of dilute solutions.

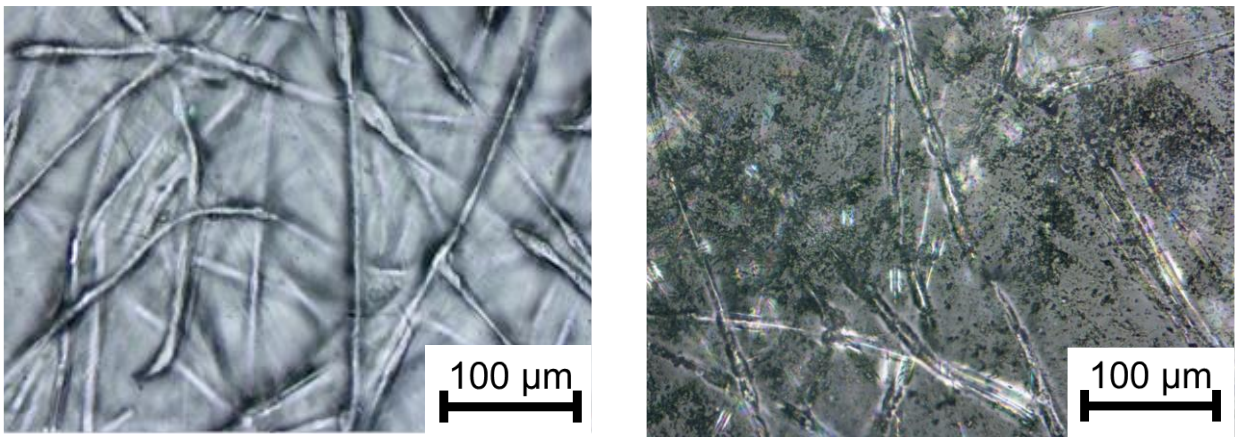

a *b*

Figure 2. Optic images of the AEM Type – X surface before (a) and after (b) it long-term operation in the electric field.

Unfortunately long-term operation of the AEM Type-X in the electric field leads to the degradation of the ion-exchange polymer. The result of this degradation is the formation of cavities, which are visible on optical images of the membrane (Fig.2b). A similar process was observed in the case of AMX membranes [2]. In the future, we will study the influence of this electrochemical degradation on the efficiency of the AEM Type-X operation in electrodialysis process.

Acknowledgment

This investigation was realized with the financial support of Russian Foundation of Basic Researches, grant № 18-38-00521mol_a.

References

1. *Mizutani Y.* Studies of ion exchange membranes. XVI. The preparation of ion exchange membranes by the “paste method” / Y. Mizutani, R. Yamane, H. Ihara, H. Motomura // Bull. Chem. Soc. Jpn. 1963. V. 36, №. 4. P. 361-366.
2. *Rybalkina O.A., Tsygurina K.A., Sarapulova V.V., Mareev S.A., Nikonenko V.V., Pismenskaya N.D.* Evolution of Current–Voltage Characteristics and Surface Morphology of Homogeneous Anion-Exchange Membranes during the Electrodialysis Desalination of Alkali Metal Salt Solutions. // Membr. Membrane Technologies. 2019. V.1. № 2. C. 107–119.

APPLICABILITY OF APPROXIMATE EQUATIONS FOR CALCULATION OF THE CHRONOPOTENTIOMETRIC TRANSITION TIME IN MEMBRANE SYSTEMS WITH A DIFFUSION LAYER OF FINITE LENGTH

[1]Ekaterina Skolotneva, [1]Daria Mareeva, [1]Semyon Mareev, [2]Christian Larchet, [2] Lasâad Dammak, [1]Victor Nikonenko

[1]Kuban State University, 149 Stavropolskaya St., 350040 Krasnodar, Russia
E-mail: *mareev-semyon@bk.ru*
[2]Institut de Chimie et des Matériaux Paris-Est, UMR7182 CNRS – Université Paris-Est, 2 Rue Henri Dunant, 94320 Thiais, France. E-mail: *dammak@u-pec.fr*

Introduction

The Sand equation commonly used for determination of chronopotentiometric transition time was deduced for the case of infinitely large diffusion layer (DL). However, in the real systems the influence of finite-length DL of ion exchange membrane (IEM) system on its behavior is observed using different electrochemical technics such as chonopotentiometry, impedance spectroscopy, voltammetry or chronoamperometry. In the present paper, we specify the range of currents, at which the Sand equation is applicable for the systems with diffusion layer of finite length. For other current densities, we adapted the approximate equation, which was proposed by Soestbergen and coauthors for the case of electrode systems [1].

Experiments

The experimental setup consists of an electrodialysis cell, hydraulic and measuring systems already used for voltammetric studies of IEM and described in detail in [2]. A Neosepta CMX homogeneous cation-exchange membrane and the commercial homogeneous cation exchange Fujifilm CEM Type I membrane were investigated.

Theory

The system under study is considered as a plane one-layer system involving a depleted diffusion layer restricted by the bulk solution at the left side and the IEM at right side. 1D electrodiffusion of a binary electrolyte is studied. The dependence between spatial and time concentration variations is described by the second Fick's law.

The value of steady-state limiting current density, i_{lim}, may be calculated using the Peers equation. This problem was solved analytically. Taking into account that at $\tau=\tau_{tr}$ the electrolyte concentration reaches zero at the depleted DL/membrane interface (at position $x=\delta$) we get:

$$\sum_{n=1}^{\infty}(-1)^{n-1}\frac{\sin\left[(2n-1)\frac{\pi}{2}\right]}{(2n-1)^2}\times\exp\left[\frac{-(2n-1)^2\pi^2\tau_{tr}D}{4\delta^2}\right]=\frac{\pi^2}{8}\left(1-\left|\frac{i_{\lim}}{i}\right|\right) \quad (1)$$

here the transition time τ_{tr} is an implicit function of the current density.

Results and Discussions

In the first order approximation (i.e. n=1) the transition time is explicitly related to the current as:

$$\tau_{app}=-\frac{4\delta^2}{\pi^2 D}\ln\left[\frac{\pi^2}{8}\left(1-\left|\frac{i_{\lim}}{i}\right|\right)\right] \quad (2)$$

Eq.(2) is valid for small applied currents, and for the current densities 1.92 times higher than i_{lim} this equation starts to deviate from the analytical solution as shown at Fig. 1a. For the first time it was derived by Soestbergen and coauthors in [1].

For large applied currents (more than $1{,}92i_{\lim}$) the transition time is well described by the classical Sand equation (Fig. 1a):

$$\tau_{Sand}=\left(\frac{\pi D}{4}\right)\left(\frac{c_{k0}z_kF}{T_k-t_k}\right)^2\frac{1}{i^2} \quad (3)$$

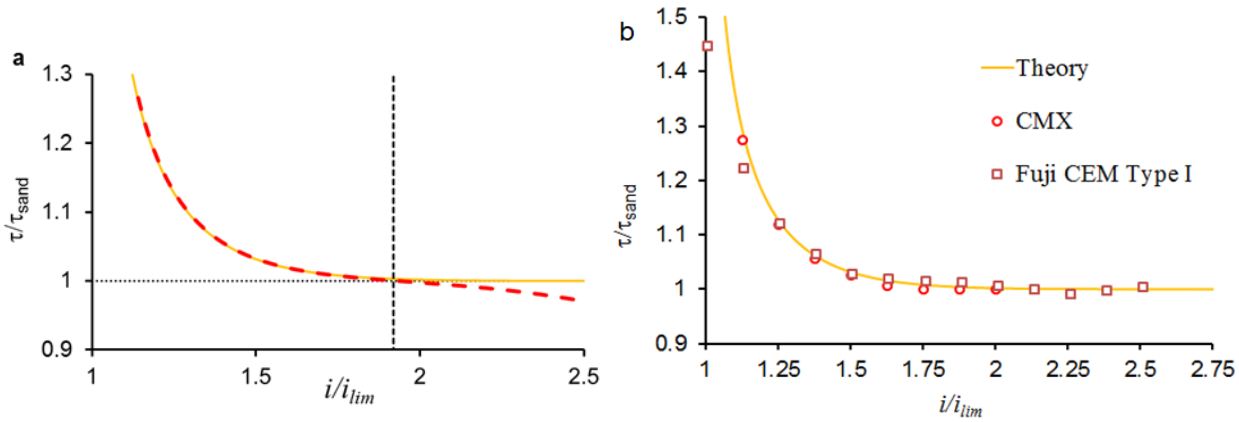

Figure 1. Dependence of normalized by τ_{Sand} on i/i_{lim}. The solid curve is the exact analytical solution. a) The doted horizontal line is the τ_{Sand} (Eq.(2)), the dashed line is the τ_{app} (Eq. (3)). b) Points are the experimental data of Fuji CEM Type I and Neosepta CMX adapted from [2].

There are two partial analytical solutions each of which represents precisely the dependence of transition time on current density for two non-overlapping ranges of current. Since the inaccuracy of the partial solutions is less than 0.3% and it appears only in the thin range of current densities near the $1.92i_{lim}$, it is mostly convenient to apply them separately: Eq. (1) suits at the current densities less than $1.92i_{lim}$ and the Eq. (2) suits at the current densities more than $1.92i_{lim}$.

The transition time calculated using 1D model is in good agreement with experimental data at wide range of current densities as shown in Fig. 1b. It should be mentioned that the experimental data of Neosepta CMX membrane, presented in [2], are closer to the theoretical ones. We suppose that the higher deviation of transition time of Fuji CEM Type I is due to the lower transport number of counterions in its volume and higher surface heterogeneity, than in the case of CMX.

Acknowledgments

The study is realized with the financial support of the Russian Science Foundation, project № 19-19-00381.

References

1. *Van Soestbergen M., Biesheuvel P. M., Bazant M. Z.* Diffuse-charge effects on the transient response of electrochemical cells // Phys. Rev. E. 2010. V. 81. P. 1-13.
2. *Mareev S. A., Butylskii D. Y., Pismenskaya N. D., Nikonenko V. V.* Chronopotentiometry of ion-exchange membranes in the overlimiting current range. Transition time for a finite-length diffusion layer: modeling and experiment // J. Memb. Sci. 2016. V. 500. P. 171-179.
3. *Sistat P., Pourcelly G.* Chronopotentiometric response of an ion-exchange membrane in the underlimiting current-range. Transport phenomena within the diffusion layers // J. Memb. Sci. V. 123. P. 121-131.

INFLUENCE OF THE FIBER FILLER ON THE SORPTION CHARACTERISTICS OF POLYMER COMPOSITES "POLIKON A"

[1]Ilya Strylets, [1,2]Denis Terin, [1]Marina Kardash, [3]Tamara Druzhinina
[1]Yuri Gagarin State Technical University of Saratov
E-mail: *ilya.strilets@gmail.com, m_kardash@mail.ru*
[2]Saratov State University, Saratov, Russia, E-mail: terinden@mail.ru
[3]Moscow State University of Design and Technology, Moscow, Russia, E-mail: *druzhininiv@gmail.com*

Introduction

Over the past 60 years, ion exchange membranes have evolved from a laboratory tool in the commercial product a significant technical and commercial potential. Membranes for the desalination of sea and brackish water, the treatment of industrial effluents, the purification of food and pharmaceuticals are successfully used, as well as for the production of basic chemical products. [1]. Recently, membranes with a poly(ethylbenzene-1,4-dicarboxylate) (in russian – lavsan (*лавсан*)) reinforcing component, obtained by the polycondensation filling method, are very promising, since interest in reinforced polymer membranes based on thermosetting matrices and high-temperature fibers is growing [2]. Research "structure, formation and properties of membranes" on the basis of thermosets (polyester, phenolic and epoxy) which were reinforced with chemical fibers (polypropylene poly(propene) - (PP), viscose, polyacrylonitrilepoly(1-acrylonitrile) (PAN), novoloid phenol-aldehyde fibers with phenol-formaldehyde (NPF) and others) were previously carried out by us. The main regularity of the reinforcement process is the mutual influence of the polymer components of the membranes on their structure and properties, which we have discovered. The study of the effect of fibrous fillers and comparison of the sorption characteristics of "Polikon A" membranes based on them with "Polikon A" membranes obtained on poly(ethylbenzene-1,4-dicarboxylate) was the aim of this work.

Experiments

The membrane was synthesized by polycondensation of polyethylene polyamines with epichlorohydrin (EDE-40P) and fibrous filler (poly (ethyl benzene-1,4-dicarboxylate)) in a ratio of 70% to 30%. The prepared fiber was impregnated with the composition of the impregnation bath at a temperature of 20-30^{o}C for 15 min. The synthesis was carried out at a temperature of 57^{o}C for 30 min. The obtained prepreg was dried for 30 min at a temperature of 70^{o}C. Curing was carried out at a temperature of 90-100^{o}C for 24 hours. The morphology and elemental composition of the finished membrane structures were studied on an electronic analytical complex (Figs. 1 and 2).

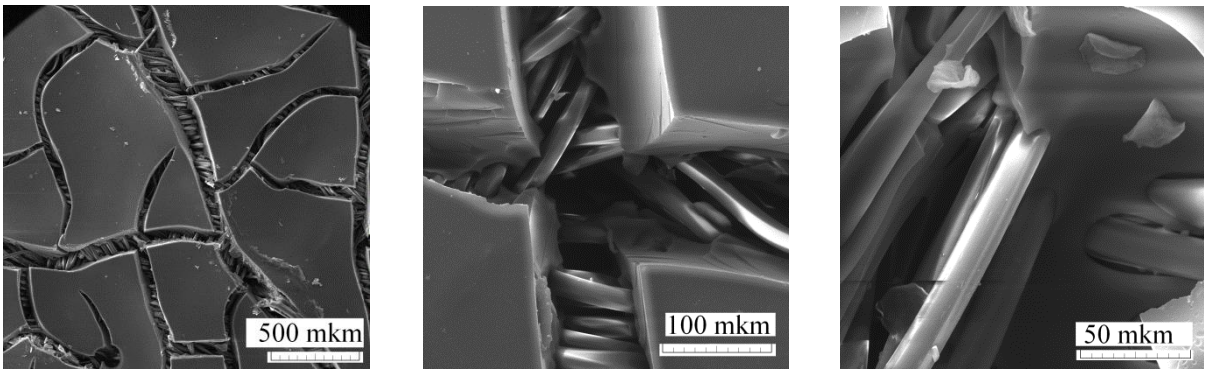

a) *b)* *c)*

Figure 1. SEM image membrane "Polikon A" on the base of poly(ethylbenzene-1,4-dicarboxylate).

Results and Discussion

The research data on the influence of the choice of fibrous base on the sorption characteristics of anion-exchange membrane structures are presented in table 1. From a comparison of experimental data (table 1), we see that the anion-exchange membrane structure "Polykon A" on

the base of poly(ethylbenzene-1,4-dicarboxylate) has sorption characteristics 20% higher than those of materials based on PAN, NPF fibers and 40% higher than on viscose and PP fillers.

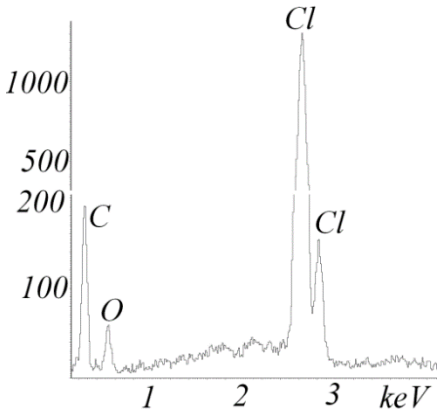

Figure 2. EDX spectra membrane "Polikon A" on the base of poly(ethylbenzene-1,4-dicarboxylate).

Table 1: Sorption properties of composite chemisorption fibrous materials "Polikon A"

Polikon A	anion-exchange capacity, mg-eq/g	water-absorbing capacity, %
poly(ethylbenzene-1,4-dicarboxylate)	2,6	54
NPF	2,0	64
PAN	2,0	55
viscose	1,8	43
PP	1,5	35

Curing processes at poly(ethylbenzene-1,4-dicarboxylate) are much slower that we had seen. The change in kinetic curing conditions depends on the composition of the binder at the fiber surface and the molding pressure. The magnitude of the equilibrium moisture capacity directly depends on the concentration of the fiber (in terms of the polymer matrix) and determines the optimal porosity of the entire membrane. Thus, the influence of fibrous filler on the membrane structure is ambiguous: - the choice of fiber affects the speed and depth of curing of the binder, as well as the nature of its supramolecular formations; - the fibers in the polymer matrix form their own fibrous structures with their own deformability under load; - thin surface layers are formed on the surface of the fibers, differing in structure and properties from the polymer in volume and interlayers. It is the structure and properties of these layers that determine the porosity of "Polikon A" membranes.

The reported study was funded by RFBR according to the research project №19-08-00721 A.

References

1. *Tewari P.K.* Nanocomposite. Membrane. Technology. Fundamentals and applications. BocaRaton.London. New York. CRC Precc, 2016, 326 p.
2. *Tsyplyaev S., Terin D., Kardash M., Druzhinina T., Strilets I.* Physicochemical and structurial characteristics of anion exchange material "Polikon A" based on novolac phenol-formaldehyde fibers// Ion transport in organic and inorganic membranes: Proc. Int. Conf., Krasnodar, 2018. P.284-285.

DIFFUSION PEARMABILITY OF COMMERCIAL HOMOGENEOUS AND HETEROGENEOUS ION-EXCHANGE MEMBRANES IN NaCl, $CaCl_2$ AND Na_2SO_4 SOLUTIONS

Valentina Titorova, Veronika Sarapulova, Natalia Pismenskaya, Victor Nikonenko
Kuban State University, Krasnodar, Russia, *E-mail: valentina.titorova@mail.ru*

Introduction

Present wastewater treatment methods include various technologies, such as combination of classical and electro-membrane separation methods. One of the promising methods for water purification is electrodialysis metathesis. Basically, the main idea of it is that in one of the two concentration chambers, singly charged cations and all anions are collected, and in the other, singly charged anions and all cations are collected. Thus, the possibility of precipitation is excluded. The membranes used in such processes must meet rather high requirements. Consequently, the study of the transport of multiply charged ions through them is a very topical problem.

Experiments

Heterogeneous MK-40 cation exchange membrane and MA-41 anion exchange membrane (Shchekinoazot, Russia) as well as homogeneous Neosepta CMX cation exchange membrane and Neosepta AMX anion exchange membrane (Astom, Japan) were chosen as the objects of the study. Such a choice of objects for the study is due to the fact that the ion-exchange matrix of all membranes is made of a copolymer of styrene and divinylbenzene, and the fixed groups are sulfonic groups for cation-exchange membranes and quaternary ammonium bases (with a small number of tertiary and secondary ones) for anion-exchange.

For experiments we used the laboratory-made distilled water (electrical conductivity 0.5 μS/cm at t=25 °C, pH=5.5), and solid NaCl, $CaCl_2$ and Na_2SO_4 (Vekton, Russia). The diffusion permeability coefficients for each membrane were obtained using flow cell with controlled thickness of diffusion layer [1] in NaCl, $CaCl_2$ and Na_2SO_4 solutions.

Results and Discussion

Concentration dependences of the integral diffusion permeability coefficient of ion-exchange membranes in binary solutions (NaCl) and ternary ($CaCl_2$, Na_2SO_4) electrolytes are presented on Fig. 1.

In general, the obtained dependences of the diffusion permeability of heterogeneous membranes in the studied electrolyte solutions are higher than ones of homogeneous membranes. These data are consistent with the results obtained earlier for the membranes MK-40 [2] and can be explained by the diffusion of electrolyte through macropores present in the structure of heterogeneous membranes and absent in homogeneous ones. Replacing a single-charged co-ion with a double-charged (Cl^- to SO_4^{2-} for CMX and MK-40; Na^+ to Ca^{2+} for AMX and MA-41) significantly reduces the integral diffusion permeability coefficient. Apparently, this can be explained by a stronger Donnan exclusion of doubly charged co-ions, which reduces the diffusion of the electrolyte solution through the ion-exchange membrane.

On the contrary, the replacement of a single-charge counter-ion (Na^+ to Ca^{2+} for CMX and MK-40; Cl^- to SO_4^{2-} for AMX and MA-41) leads to an increase in the integral diffusion permeability coefficient. This may be through the fact that the sorption of electrolyte in the presence of a double-charged counter-ion is enhanced due to an increase in the force of attraction between the ion and the counter-ion. Because of the fact that the limiting factor in the process of electrolyte diffusion is the concentration of co-ions, the transition to a doubly charged counter-ion leads to an increase in diffusion through the membrane. In addition, more complex interactions of ions with functional groups and the membrane matrix are quite possible.

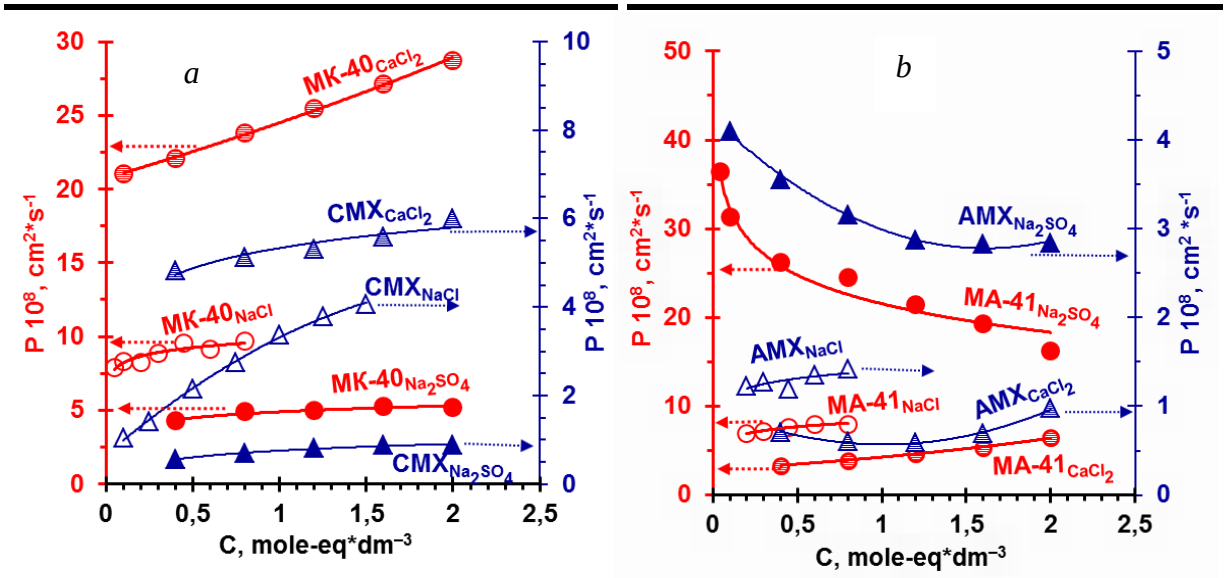

Figure 1. Concentration Dependences of Diffusion Permeability of Cation-Exchange Membranes CMX and MK-40 (a), Anion-Exchange Membranes AMX and MA-41 (b) in NaCl, $CaCl_2$ and Na_2SO_4 Solutions.

A comparison of cation- and anion-exchange membranes among themselves shows that if for the first, with an increase in the concentration of the electrolyte solution with which the membrane contacts, there is a regular increase in the integral diffusion permeability coefficient, then for the second in a solution of sodium sulfate, it decreases. The latter phenomenon can probably be explained by the fact that the diffusion coefficient Na_2SO_4 in solution decreases more strongly with increasing concentration compared to other electrolytes (NaCl and $CaCl_2$) (Fig. 2).

This phenomenon is explained by the high ability of sulfate ions to water structuring [3] or the formation of ion associates [4]. With increasing electrolyte concentration, the proportion of such associates increases, resulting in a sharp drop in diffusion coefficients of Na_2SO_4.

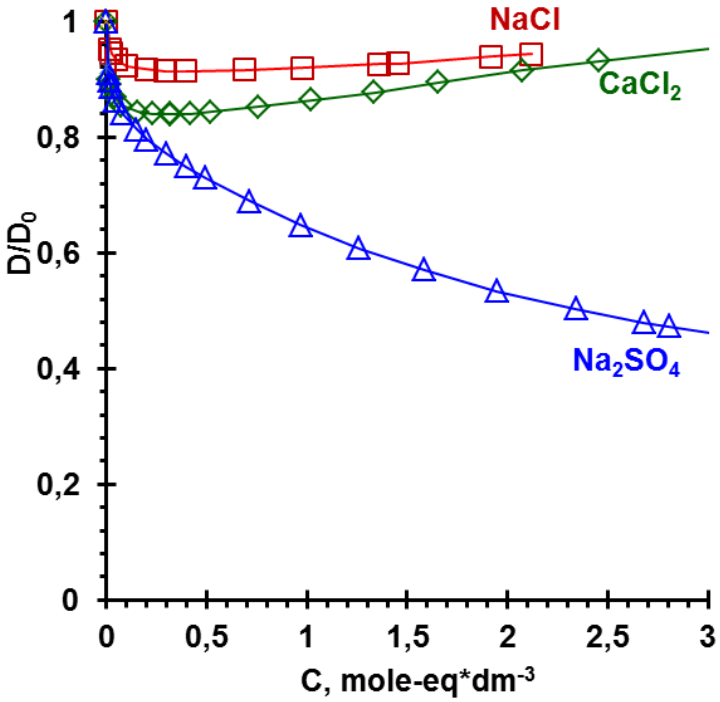

Figure 2. The Concentration Dependence of the Diffusion Coefficient of the Electrolyte D at the Temperature 25°C. Values of D normalized to the diffusion coefficient corresponding to each electrolyte at infinite dilution of the solution, D_0). The curves are plotted from experimental data taken from [5,6].

Acknowledgement

The study is realized with the financial support of the RFBR, project № 18-08-00397 A.

References

1. Pat. 100275 RF, IPC51 G01N27/40 (2006.01). Device for measurements of diffusion characteristics of membrane / *Nikonenko V. V., Vedernikova E. E., Pismenskaya N. D.* (Krasnodar, RF); the applicant and the patent owner: GFO HPE Kuban State University (RF); №2010121195/28; Claimed 25.05.2010; Published 10.12.2010.
2. *Filippov A. N., Kononenko N. A., Demina O. A.* Diffusion of electrolytes of different natures through the cation-exchange membrane // Colloid J. 2017. V. 79. № 4. P. 556.
3. *Zhu S., Kingsbury R. S., Call D. F., Coronell O.* Impact of solution composition on the resistance of ion exchange membranes // J. Membr. Sci. 2018. V. 554. P. 39.
4. *Leaist D. G., Goldik J.* Diffusion and Ion Association in Concentrated Solutions of Aqueous Lithium, Sodium, and Potassium Sulfates // J. Solution Chem. 2001. V. 30. № 2. P. 103.
5. *Robinson R. A., Stokes R. H.* Electrolyte solutions. L.: Butterworths Scientific Pub., 1955. 512 p.
6. *Rard J. A., Miller D. G.* The mutual diffusion coefficients of NaCl-H_2O and $CaCl_2$-H_2O at 25°C from Rayleigh interferometry // J. Solution Chem. 1979. V. 8. № 10. P. 701.

THE EFFECT OF CATALYST COMPOSITION ON CHARACTERISTICS OF MEMBRANE-ELECTRODE ASSEMBLE OF HYDROGEN-AIR FUEL CELL

[1]Ekaterina Titskaya, [1]Maria Timchenko, [1]Irina Falina, [2]Anastasia Alekseenko
[1]Kuban State University, Krasnodar, Russia, E-mail: *irina_falina@mail.ru*
[2]Southern Federal University, Rostov-on-Don, Russia

Introduction

The development of alternative energy sources, including hydrogen-air fuel cells, is an important task of modern electrochemistry. The high cost of catalysts for electrode reactions is one of the main factors limiting the development of this equipment [1]. Bimetallic alloys containing platinum and d-elements are currently being developed to increase the specific characteristics and reduce the cost of the catalyst. However, selective dissolution of the alloying component can lead to poisoning of perfluorosulfonic acid, which is part of the catalytic layer, and the membrane.

The aim of this work was to study the process of poisoning the perfluoropolymer with copper cations during the degradation of bimetallic catalysts based on platinum and copper nanoparticles.

Experimental

The Table presents the set of investigated catalysts, which included commercial platinum catalyst E-TEC and experimental samples of copper and bimetallic catalysts, which were prepared by the scientific group from the Southern Federal University. The bimetallic catalyst has the alloy-type structure with "loosely bound" copper [2].

Table: Objects of research

Catalyst	Weight fraction Pt, %	Weight fraction Cu, %
E-TEK C1-40	40	-
Cu/C	-	14
$PtCu_{2.8}$/C	18	16

The membrane-electrode assemble (MEA) is obtained by hot pressing of gas diffusion layers and proton exchange membrane. It consists of electrodes, which are carbon paper with catalytic ink, and the membrane MF-4SK. The composition of the catalytic ink includes water, isopropyl alcohol, solution of the polymer Nafion (12.5 % wt. of catalyst) and the catalyst (Pt loading of electrodes was 0.4 mg/cm^2).

MEA tests were carried out by its holding for ten hours under the potential drop of 500 mV; every two hours we measured the electrochemical impedance spectrum of the MEA.

Preparation of membranes in mixed ionic form H^+/Cu^{2+} was carried out by immersion of MF-4SK in H^+-form in a copper sulfate solutions of different concentrations. The content of copper ions in the copper sulfate solution was determined by copper-selective electrode vs standard silver-silver chloride electrode. Spectrophotometry was used to estimate the degree of membranes saturation with copper ions (Θ). Conductivity (κ, S/m) of the membranes in H^+/Cu^{2+}-form was measured by the mercury-contact method as the active part of the cell impedance.

Results and Discussion

Figure 1a shows the changes of the current density produced by MEA on the testing time. It is seen that for the MEA with platinum catalyst, an increase in the current density is observed. Current densities for MEA with copper and bimetallic catalysts are significantly lower than with platinum one. Fig. 1b shows the conductivity of the membrane calculated according to the ohmic resistance of the MEA. The dependence of the membrane conductivity on test time for bimetallic catalyst is similar to the dependence for the platinum catalyst. The conductivity of the MEA with the copper catalyst is significantly lower and reduces during the testing.

We studied the dependence of the conductive properties of perfluorinated membrane on its saturation degree with copper ions. The saturation degree of the membranes with copper ions was calculated according to eq. taking into account the exchange capacity of the membrane (Q), its

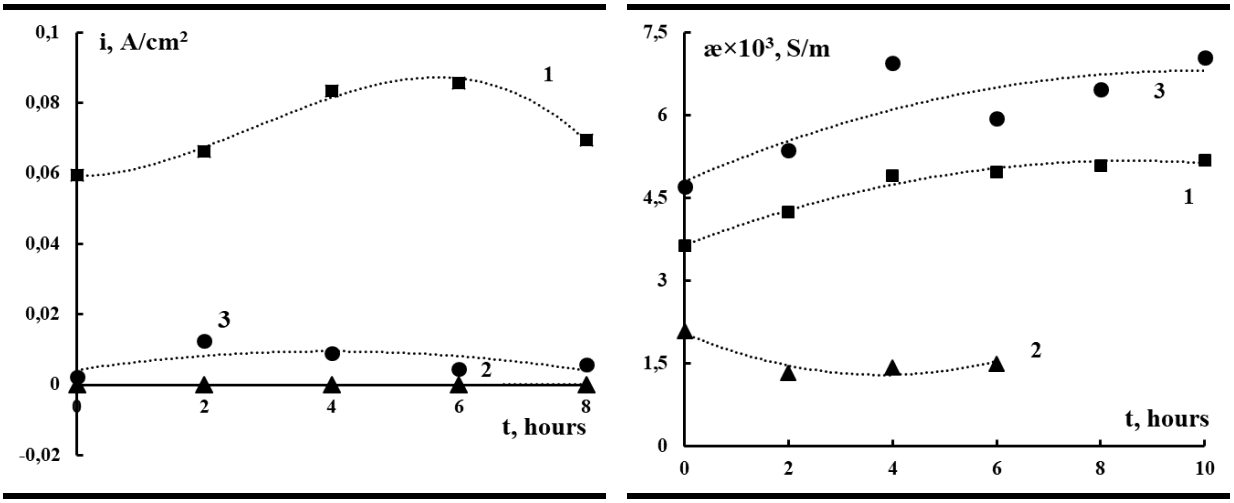

FIGURE 1. THE TIME DEPENDENCE OF CURRENT DENSITY(A) AND DEPENDENCE OF THE ELECTRICAL CONDUCTIVITY OF THE MEA ON TIME AT A POTENTIAL DIFFERENCE OF 0.5 V (B); 1.E-TEK-C1-40 (PT); 2.CU/C; 3.PTCU$_{2.8}$/C.

weight (m), quantity of copper ions in initial solution (n_0), after sorption (n_1) and desorbed in water (n_2).

$$\theta = \frac{(n_0 - n_1 - n_2)}{mQ} \quad .$$

The sorption isotherm is presented on Fig. 2. The shape of the isotherm indicates the selectivity of the sulfocationic membrane towards the double-charged cations. One can see that the saturation degree of the samples by Cu^{2+}-ions in the most concentrated solutions exceeds unit. This may be due to the over-equivalent donnan sorption or experimental error in determining the composition of the solutions. Figure 3 shows the dependence of membrane conductivity on saturation degree with Cu^{2+}-ions. As can be seen, the electrical conductivity decreases significantly with increasing saturation of the membrane with copper ions. This is caused by the replacement of highly mobile hydrogen cations by less mobile copper ions.

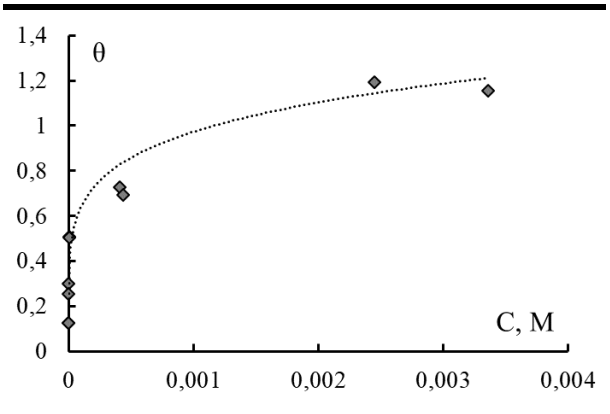

FIGURE 2. THE DEPENDENCE OF THE DEGREE OF SATURATION OF THE MEMBRANE WITH COPPER IONS FROM THE EQUILIBRIUM CONCENTRATION.

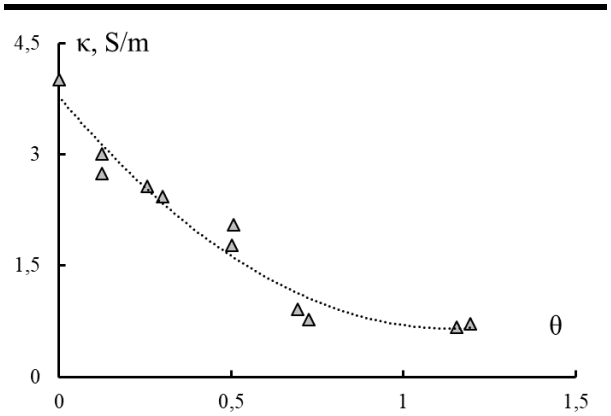

FIGURE 3. DEPENDENCE OF THE MEMBRANES CONDUCTIVITY ON THE SATURATION DEGREE OF THE MEMBRANE WITH COPPER IONS IN SOLUTIONS OF COPPER SULFATE.

It can be assumed that the main reason for the decrease in the characteristics of the MEA with bimetallic catalyst is the poisoning of the perfluorosulfonic acid that is part of the catalytic ink,

and with copper catalyst, both the perfluoropolymer and the perfluorinated membrane are poisoned.

So the preliminary acid treatment of electrocatalysts containing PtCu nanoparticles is the essential step in their synthesis to remove the "loosely bound" copper and to prevent the reduction of MEA characteristics. The catalysts based on bimetallic nanoparticles with a special structure ("shell-core", "gradient") are interesting for the study.

The work was funded by the Ministry of Education and Science of the Russian Federation (project No 13.3005.2017/4.6)

References

1. *A. El-kharouf, A. Chandan, M. Hattenberger, B. G. Pollet* // Journal of the Energy Institute. 2012 Vol. 85, No 4. P. 188-200.
2. *A.A. Alekseenko, V.E. Guterman, S.V. Belenov, V.S. Menshikov, N.Yu. Tabachkova, O.I. Safronenko, E.A. Moguchikh* // Int. J. of Hydrogen Energy. 2018. Vol. 43. P. 3676–3687.

THE INVESTIGATIONS OF THE STRUCTURE AND PROPERTIES OF ION-EXCHANGE MATERIALS "POLIKON CA" WITH MOSAIC-LATERAL MORPHOLOGY

[1]Sergey Tsipliaev, [1,2]Denis Terin, [1]Marina Kardash, [2]Igor Galushka, [3]Larisa Karpenko-Jereb, [1]Timur Turaev

[1]Yuri Gagarin State Technical University of Saratov
E-mail: *ilya.strilets@gmail.com, m_kardash@mail.ru*
[2]Saratov State University, Saratov, E-mail: *terinden@mail.ru*
[3] Graz University of Technology, Graz, Austria, E-mail: *larisa.karpenko@gmail.com*

Introduction

Polymeric ion exchange membranes are nanoporous structures are widely used in various industries, and one of the most technologically advanced types of materials [1]. The aim of this work was to expand the range of already widely studied "Polikon" membrane structures [2], namely, membranes with mosaic-lateral morphology.

Computing experiment

The computational experiment is based on elementary units involved in chemical synthesis of substances (figure 1). Simulation at the atomic level, taking into account the bond length and / or Van der Waals interatomic interaction forces, and quantum chemical calculations were carried out using the Atomistix Toolkit QuantumWise software package. The geometry was optimized using the quasi-Newtonian method.

The results of the computational experiment are presented by calculating the energy dependence of the density of states and analyzing the elemental contribution of the chemical elements included in the molecular model, which makes it possible to judge the most probable type of chemical interaction of polycondensation synthesis.

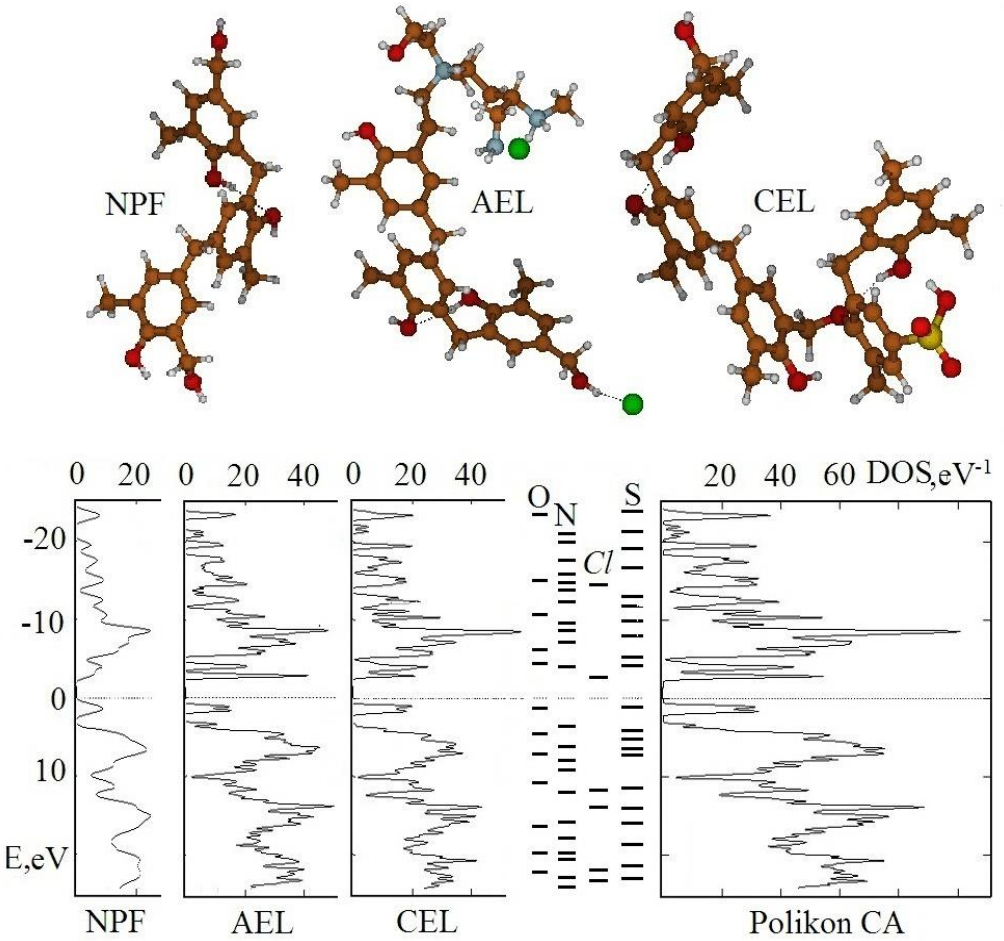

Figure 1. Computing Experimental Data.

Table 1: Energy characteristics of the model “Polikon CA”

interaction type	Polykon CA, eV	NPF, eV	AEL, eV	CEL, eV
exchange-correlation	-6475.09106	-1948.74737	-3062.70814	-3407.15077
kinetic	13190.40742	4134.59890	6089.40089	7101.00653
electrostatic	-28053.87016	-8691.65423	-13005.66935	-15047.22729
total energy system	-21338.55380	-6505.80270	-9981.97687	-11353.37153

Experiments

Striped membrane "Polikon CA" was obtained based on «Kynol» novolac phenol-formaldehyde fibrous matrix (KYNOL EUROPA GmbH, Germany) - NPF. Ion exchange constituents were synthesized directly inside fibrous matrices. As a filler of the cation-exchange layer (strip), the analogue of KU-1 strongly acidic resin containing -SO3H groups was used. In order to obtain an anion exchange layer (strip), the analogue of EDE-10P anion exchange resin was synthesized in the matrix. This analogue contains secondary, tertiary and quaternary aminogroups The mentioned ion-exchangers are produced by the United Chemical Company "Schekinoazot" LTD, Russia. The stripes (4 mm of a width) were formed successively on the surface and in the bulk of the fibrous matrix. The formation was carried out according to the developed methods of synthesis and curing of ion exchanges resins directly in fibrous matrices. First of all, cation exchange stripes were formed leaving loose strips for the subsequent formation of anion exchange matrix. The thickness "Polikon CA" of the was 0.6 mm.

The surface morphology and elementary chemical elemental composition of the samples of laminar-mosaic membranes were studied on an optical microscope and a scanning MIRA II LMU scanning microscope with an attachment of energy dispersive analysis. Mechanical properties (tensile strength) were investigated on a tensile testing machine Unimat 052, the magnitude of the mechanical load was recorded on the Physimeter 906 MC. Dry samples measuring 90x90 mm were cut into strips 10 mm wide and 90 mm long along the deposited portions of ion exchangers so that the test sample had both cation-exchange and anion-exchange sections in a 50/50 ratio.

Results and Discussion

Morphology and developed surface of the obtained membrane are shown in Figure 1 a, b. Figure 1c shows a typical end section perpendicular to the membrane surface.

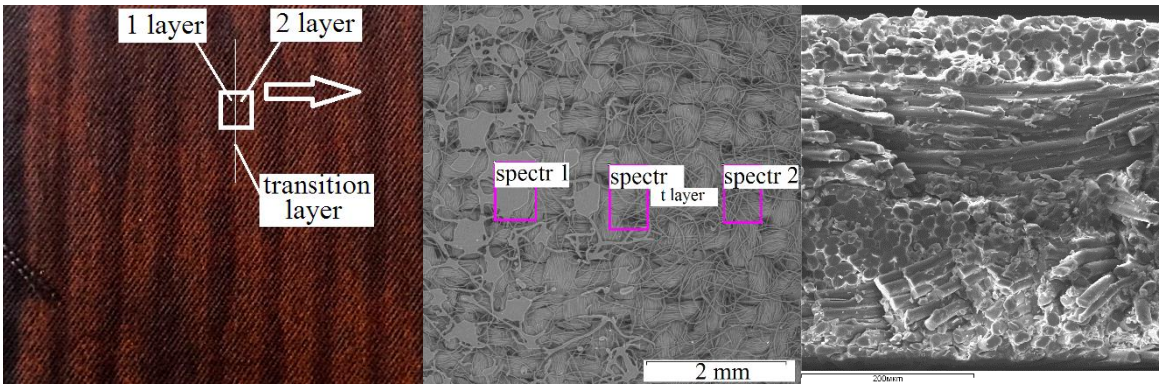

a *b* *c*

Figure 2. Morphological and structural features: optical image “Polikon CA” (a); SEM image of fragment “Polikon CA”: from the left side – cation-exchange layer, on the right side – anion-exchange layer (b); cross-section of the sample structure (c).

The data of elemental analysis of the analyzed cation-exchange, anion-exchange and transition sites (in accordance with Fig. 1 b) are presented in Table 2.

Elemental analysis and the results of a computational experiment make it possible to characterize the resulting membranes as membranes with a pronounced cationic asymmetry.

Table 2: Data EDX analysis of the elementary chemical composition of the membrane "Polikon CA"

EDX Spectra	C	O	S	Cl	Total
cationite layer	70.84	25.36	2.79	1.01	100.00
anionite layer	74.20	24.64	0.73	0.42	100.00
transition layer	72.95	25.82	0.81	0.41	100.00
mean value	72.66	25.28	1.45	0.62	100.00
standard deviation	1.70	0.60	1.17	0.34	
max	74.20	25.82	2.79	1.01	
min	70.84	24.64	0.73	0.41	

The physicomechanical properties under investigation are the tensile test results of the obtained membrane with the movement speed of the clamps 50 mm / min presented in Table 3.

Table 3: Physicomechanical properties of the membrane "Polikon CA"

Polikon CA	tensile stress, N	tearing strength, MPa
Sample 1	40	5,71
Sample 2	37	5,29
Sample 3	46	6,57
Sample 4	34	4,86
	mean value	5,61

We calculated the maximum possible theoretical level of static exchange capacity for the anion-exchange and cation-exchange layer (the dimensions of the elementary models from Figure 1 were used in the calculation) to study the prospects of development of this laminar-mosaic modification of membranes. The length, width and thickness (in angstroms) for anion exchange resin are 11.63, 6.86, 17.83 and for cation-exchanger (8.82, 6.75, 12.84), respectively 5.2 mg-eq/g and 7.2 mg-eq/g. The experimentally obtained exchange capacity does not reach the maximum possible theoretical value, which suggests that it is possible to further improve the material being developed.

The reported study was funded by RFBR according to the research project №19-08-00721 A.

References

1. *Kardash M.M., Vol'fkovich Yu.M., Tyurin I.A., Kononenko N.A., Oleinik D.V., Chernyaeva M.A.*, Effect of Process Parameters of Manufacturing of Composite Fibrous Membranes on Their Structure and Ion Selectivity. Petroleum Chemistry 53 (2013) 482–488.
2. *Kardash M.M., Terin D.V.,* Search for a Technological Invariant and Evolution of the Structure – Property Relation for Polikon Materials, Petroleum Chemistry, 56 (2016) 413–422.

COMBINED ELECTRIC BAROMEMBRANE TECHNOLOGY FOR DESALINATION OF THE CASPIAN SEA WATER

Alexandr Tskhay, Yelena Pryatko, Konstantin Kudelya
Membrane Technologies S.A. LLP, Almaty, Republic of Kazakhstan, E-mail: *info@mtca.kz*

The deficiency of fresh water constrains the development of industry, agriculture and tourism in the Caspian Sea region of the Republic of Kazakhstan. The Astrakhan-Mangyshlak water pipeline built in the middle of the 20th century does not cover the requirements of the rapidly growing needs of the area. A technical and economic study of the distillation and reverse osmosis units currently operated in the area showed that the former is very expensive in terms of price and maintenance and the latter does not ensure the stable operation during the year due to the seasonal fluctuations in temperature and salinity.

A combined seawater desalination scheme was developed: the first stage includes the electrodialysis reversal process, and the second stage includes reverse osmosis (Fig.1).

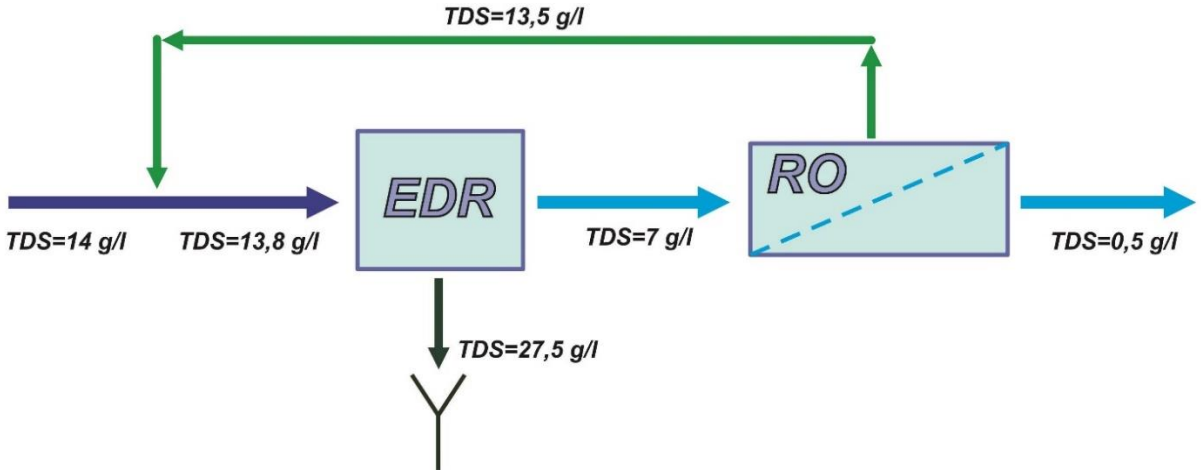

Figure 1. Desalination process flow diagram.

The proposed scheme allows reducing capital costs, improving the efficiency of the treatment and desalination process, increasing the reliability and service life of equipment and minimising the amount and consumption of reagents.

A project for a pilot plant with a capacity of 2 m³/hour and feasibility study on the design of a desalination plant with a capacity of 3,000 m³/day was developed. In the future, it is planned to create a research and production division together with a service centre in the region for the prompt solution of emerging problems with the introduction of membrane technologies in various areas of the industrial and agricultural sectors.

The long-term experience of operating membrane systems allows concluding that the combined process flow diagram will more flexibly respond to changes in external factors and ensure high quality of desalinated fresh water during the entire period of operation.

INFLUENCE OF THE «FACILITATED» DIFFUSION NH_3 THROUGH THE ANION-EXCHANGE MEMBRANE ON THE RATE OF WATER SPLITTING IN ELECTRODIALYSIS PROCESS

[1]Kseniia Tsygurina, [1]Olesya Rybalkina, [1]Ekaterina Melnikova, [2]Gerald Pourcelly, [1]Natalia Pismenskaya

[1]Membrane Institute, Kuban State University, Krasnodar, Russia, *E-mail:kseniya_alx@mail.ru*

[2]European Membrane Institute, University of Montpellier, France

E-mail: *gerald.pourcelly@umontpellier.fr*

Introduction

The composition of municipal wastewater contains large amounts of nutrients, such as potassium ions, phosphates and nitrogen in the form of ammonium ions. Nutrients are biologically active substances involved in the vital activity of the body. Electrodialysis is one of the most effective methods for the simultaneous extraction of potassium, ammonium and phosphate ions [1]. Some researchers note that in intensive current modes, the current outputs of phosphates and ammonium ions are lower than in solutions of strong electrolytes, for example, NaCl. In particular, it has been shown that one of the reasons for the decrease in current efficiency is the increase of water splitting in ammonium-containing solutions [2]. The purpose of the work was to clarify the nature of this phenomenon.

Experiment

A desalination compartment formed by the homogeneous ion-exchange membranes AMX and CMX from Astom (Japan) was investigated. The experiment was carried out using a four-compartment electrodialysis cell [3], through which a 0.02 M KCl or NH_4Cl solution was pumped. The color indication of the pH of the internal solution of the AMX membrane was determined using anthocyanins, the structure and color of which depend on the pH of the medium [4]. The integral diffusion permeability coefficient, P, of the membranes was determined using a flow-through two-compartment cell [5].

Results and Discussion

An analysis the effective chemical reaction constants [6] (table 1) found using Gerischer archs of the electrochemical impedance spectra shows that the generation of H^+ and OH^- ions at the interface of the CMX cation-exchange membrane/solution is extremely small and almost the same in the case of KCl and NH_4Cl solutions. It only slightly increases with sufficiently high currents.

Table 1: Values of the Effective Rate Constant of Water Splitting Reaction at the Membrane/Solution Interface

MEMBRANE	$I/I_{LIM}^{THEOR} = 1.00$		$I/I_{LIM}^{THEOR} = 1.24$		$I/I_{LIM}^{THEOR} = 1.60$	
	KCL	*NH_4CL*	*KCL*	*NH_4CL*	*KCL*	*NH_4CL*
CMX	***-***	***-***	***-***	***-***	***1.6***	***77***
AMX	***158***	***325***	***667***	***847***	***1077***	***1233***

In the case of the AMX anion-exchange membrane (AEM) in the NH_4Cl solution, the Gerischer arch on the impedance spectrum is clearly recorded already at a current equal to the limiting one. The difference in AMX behavior in KCl and NH_4Cl solution is reduced with increasing current density (table 1). These data are in good agreement with the results of measurements of the partial currents of Cl^- and OH^- ions, with electrodialysis desalination of the same solutions using MA-41 membranes [2]. Thus In electrodialysis, the presence of NH_4^+ ions in the feed solution causes a significant increase in the rate of the water splitting reaction at the depleted boundary of the AMX membrane, while the increase in the rate of this reaction on the CMX membrane is not significant.

According to our hypothesis, this is due to the fact that in the case of KCl the rate of diffusion is limited by the diffusion of the salt co-ion (K^+), while the transport of NH_4Cl across the membrane is "facilitated" by the diffusion of NH_3 molecules, whose concentration in the membrane should be higher than that of the salt co-ions. Data of diffusion permeability confirm this hypothesis. Indeed, the experimental integral diffusion coefficients are equal to $2.27\ 10^{-8}$ cm^2 s^{-1} and $1.70\ 10^{-8}$ cm^2 s^{-1} in the case of 0.5 M NH_4Cl and KCl solutions.

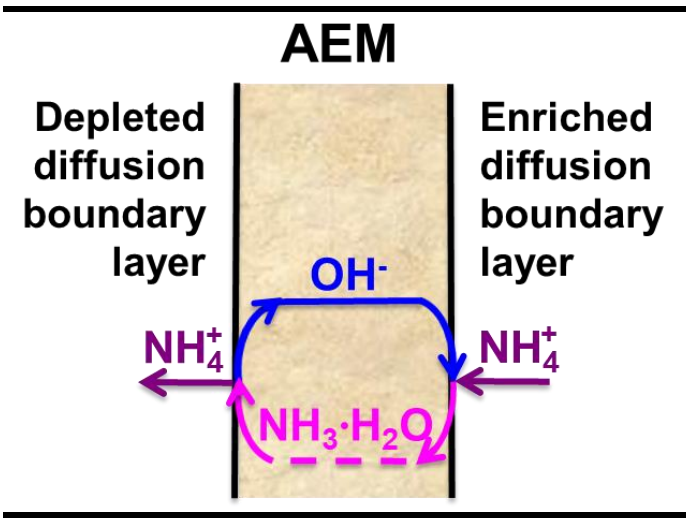

FIGURE 1. SCHEMATIC REPRESENTATION OF THE TRANSPORT OF NITROGEN-CONTAINING SPECIES THROUGH AN ANION-EXCHANGE MEMBRANE.

The "facilitated" diffusion of NH_3 molecules through the AEM (fig. 1) allows to maintain a sufficiently elevated concentration of the NH_4^+ and NH_3 species at the depleted solution/AMX boundary to assure the protonation and deprotonation reactions of these species with water. As a result of these reactions, there is generation of H^+ and OH^- ions at this boundary by a mechanism similar earlier to that described by Simons [7]. As for the "facilitated" diffusion, this phenomenon is possible due to the shift of the pH of the internal solution of the AEM to the alkaline region compared to the external solution; the latter is explained by the Donnan exclusion of H^+ ions from the membrane as co-ions (fig. 2). An additional pH shift in the alkaline region is due to the appearance in the membrane of OH^- ions generated at the depleted membrane boundary by the protonation-deprotonation mechanism with the participation of fixed secondary and tertiary amino groups present in a small amount in AMX membranes. The pH of the internal membrane solution in this case can be at the level of 11-12. The elevated pH of the internal solution in the AEM causes an almost complete conversion of the NH_4^+ ions, located in the enriched solution adjoining the AEM in the concentration compartment, into the NH_3 molecules inside the membrane at this boundary. The NH_3 molecules formed at this boundary diffuse to the opposite boundary of the membrane, where they again transform in NH_4^+ with the release of OH^- ions, which return to the boundary with the concentration compartment.

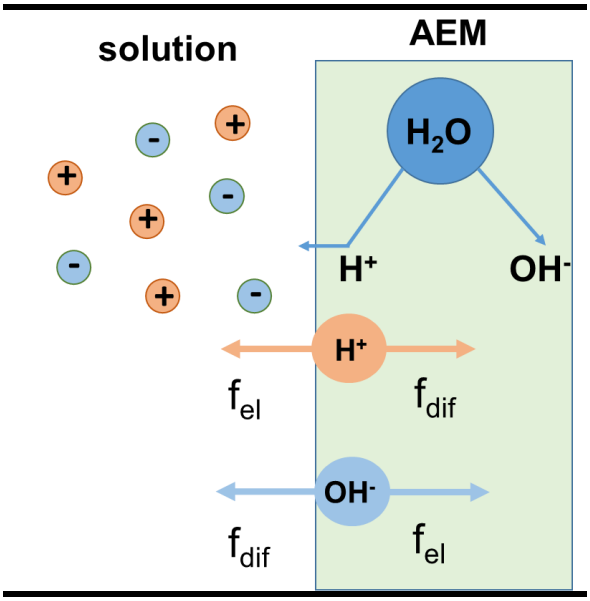

FIGURE 2. SCHEME OF PH SHIFT IN AN ANION-EXCHANGE MEMBRANE.

The data of color indication of the internal solution and the results of measurements of diffusion permeability as well as the shape of chronopotentiograms that were obtained in the AMX/KCl and AMX/NH_4Cl systems confirm the above hypothesis.

Protonation-deprotonation reactions between NH_4^+, NH_3 and water in the system with a cation-exchange membrane do not play such a noticeable role as in the case of AEM. This is explained by a very small concentration of the molecular form of NH_3 in the CEM internal solution due to

the shift of pH inside this membrane to the acid region as a result of Donnan exclusion of hydroxyl ions. On the other hand, electric current flow causes concentration polarization, which results in a very low concentration of NH_4^+ ions at the depleted boundary of the membrane.

Acknowledgements

This research was supported by the Russian Scientific Foundation (project № 17-19-01486).

References

1. *Ippersiel D., Mondor M., Lamarche F., Tremblay F., Dubreuil J., Masse L.* Nitrogen potential recovery and concentration of ammonia from swine manure using electrodialysis coupled with air stripping // J. Environ. Manage. 2012. V. 95. P. 165-169.
2. *Kozaderova O. A., Niftaliev S. I., Kim K. B.* Ionic transport in electrodialysis of ammonium nitrate // Russ. J. Electrochem. 2018. V. 54. № 4. P. 416-422.
3. *Pismenskaya N. D., Nikonenko V. V., Belova E. I., Lopatkova G. Y., Sistat F., Pourcelly G., Larshe K.* Coupled convection of solution near the surface of ion-exchange membranes in intensive current regimes // Russ. J. Electrochem. 2007. V. 43. № 3. P. 307-327.
4. *Ribereau-Gayon P., Glories Y., Maujean A., Dubourdieu D.* Phenolic Compounds // Handbook of Enology. 2006. V. 2. P. 141-203.
5. *Pismenskaya N. D., Nevakshenova E. E., Nikonenko V. V.* Using a single set of structural and kinetic parameters of the microheterogeneous model to describe the sorption and kinetic properties of ion-exchange membranes // Petrol. Chem. 2018. V. 58. № 6. P. 465-473.
6. *Kniaginicheva E., Pismenskaya N., Melnikov S., Belashova E., Sistat P., Cretin M., Nikonenko V.* Water splitting at an anion-exchange membrane as studied by impedance spectroscopy // J. Membr. Sci. 2015. V. 496. P. 78-83.
7. *Simons R.* Electric field effects on proton transfer between ionizable groups and water in ion exchange membranes // Electrochim. Acta. 1984. V. 29. P. 151-158.

GAS DIFFUSION THROUGH STRUCTURALLY INHOMOGENEOUS BILAYER MEMBRANE

Valery Ugrozov
Financial university under the Government of the Russian Federation, Moscow, 123995, Russia,
E-mail: *vugr@rambler.ru*

Introduction

Traditionally, when describing gas transfer in a membrane, it is assumed that it is structurally homogeneous and characterized by a constant diffusion coefficient. However, for polymeric materials with structural heterogeneity, this assumption is incorrect. At present, the Fokker – Planck equation in one of the three most well-known representations: Ito, Stratonovich or Khangi – Klimontovich (the generalized Fick equation) is used to describe transport in structurally inhomogeneous media. However, when studying gas transfer in a non-uniform membrane, this approach has hardly been applied.

The purpose of this work was to study of gas diffusive through a dense membrane consisting of two structurally inhomogeneous layers, by help the Fokker – Planck equationin the framework of representation the Khanggi – Klimontovich.

Model of gas diffusion through inhomogeneous bilayer membrane

Consider the diffusion of gas through a bilayer membrane, when the surface of the first layer - i = 1 is in contact with a diffusible gas (diffusant) at a pressure p_{in} , and the surface of the second layer - i = 2 is in contact with a permeate at a pressure p_{out} (Figure 1a), with $p_{\text{in}} > p_{\text{out}}$.

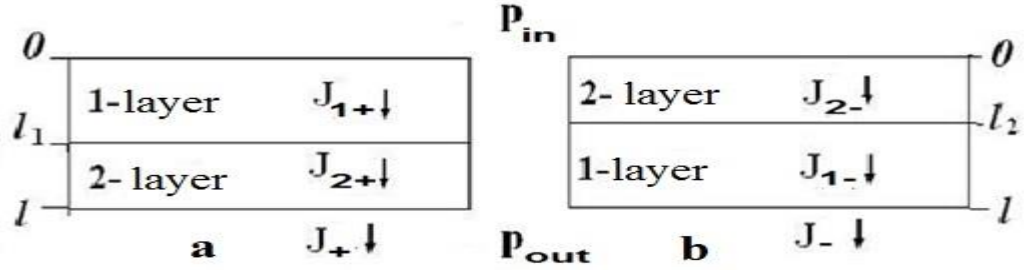

Figure 1. The scheme of gas diffusion through inhomogeneous bilayer membrane.

Assume that gas diffusion in membrane layers is stationary and thermodynamic equilibrium has been established at the external and internal interfaces of the membrane.

Then in the representation of Khanggi – Klimontovich, diffusion flows through the membrane layers are described by expressions of the form

$$J_{1+} = -D_1(x)\frac{dc_1}{dx}\ , \qquad J_{2+} = -D_2(x)\frac{dc_2}{dx}\,, \tag{1}$$

where J_{i+} **,** c_i и $D_i(x)$ – diffusion flow, concentration and diffusion coefficient of gas in the i-th layer. Accordingly, on the outer and inner interfaces of the membrane thermodynamic equilibrium is described by the following relations

$$c_1(0) = S_1 p_{\text{in}},\ \ c_2(l) = S_2 p_{\text{out}}\,,\ c_1(l_1)/c_2(l_1) = S_1/S_2 = K \tag{2}$$

where l_i – the thickness of the i-th layer, $l = l_1 + l_2$ – membrane thickness, $c_1(0), c_2(l)$ – concentrations of the diffusant at the outer interfaces of the first and second layers, respectively, S_i – the solubility coefficient (Henry) of the gas in the i-th layer, $c_1(l_1), c_2(l_1)$ - concentrations of the diffusant in the first and second layers at the inner interface.

By taking into account the assumed assumptions, gas transfer in the opposite direction (Fig. 1b) is described by the following equations

$$J_{1-} = -D_1(x)\frac{dc_1}{dx}\ , \qquad J_{2-} = -D_2(x)\frac{dc_2}{dx}\,, \tag{4}$$

and the thermodynamic equilibrium at the corresponding boundaries is described by the relations

$$c_2(0) = S_2 p_{\text{in}},\ \ c_1(l) = S_1 p_{\text{out}}\ ,\ \ c_2(l_2)/c_1(l_2) = S_2/S_1 = 1/K \tag{5}$$

The structural inhomogeneity of the membrane was modeled by the dependence of the diffusion coefficients in the layers on the spatial variable - x

$$D_i(x) = D_{0i} f_i(x) \tag{6}$$

where $f_i(x)$ – function simulating the structural inhomogeneity of the i-th layer, D_{0i} – constant diffusion in the i-th layer.

Taking into account relations (1) - (6), expressions were obtained for gas flows - J_+, J_- and gas permeability coefficients for two opposite directions of gas diffusion - P_+, P_- for arbitrary dependences of gas diffusion coefficients in layers

$$\frac{l}{P_+} = \frac{F_{1+}}{D_{10}S_1} + \frac{F_{2+}}{D_{20}S_2} \quad \text{and} \quad \frac{l}{P_-} = \frac{F_{1-}}{D_{10}S_1} + \frac{F_{2-}}{D_{20}S_2}, \tag{7}$$

where $F_{1+} = \int_0^{l_1} \frac{dx}{f_1(x)}$, $F_{2+} = \int_{l_1}^{l} \frac{dx}{f_2(x)}$, $F_{2-} = \int_0^{l_2} \frac{dx}{f_2(x)}$, $F_{1-} = \int_{l_2}^{l} \frac{dx}{f_1(x)}$.

In this paper, we considered the case when the structural heterogeneity of the membrane layers was modeled by functions

$$f_1(x) = exp(a_1 x/l_1),\ f_2(x) = exp(a_2 x/l_2), \tag{8}$$

where a_i – parameter characterizing the degree of structural heterogeneity of the i -th layer.

In this case, expressions (7) take the forms

$$\frac{l}{P_+} = \frac{l_1}{P_{e1}} + \frac{l_2}{P_{e2}} exp(-a_2 \frac{l_1}{l_2}), \qquad \frac{l}{P_-} = \frac{l_2}{P_{e2}} + \frac{l_1}{P_{e1}} exp(-a_1 \frac{l_2}{l_1}), \tag{9}$$

where $P_{e1} = \frac{D_{10}S_1 a_1}{(1-exp(-a_1))}$, $P_{e2} = \frac{D_{20}S_2 a_2}{(1-exp(-a_2))}$ – effective permeability coefficients of the corresponding structurally inhomogeneous layers.

Results and Discussion

From the analysis of expressions (9) it follows that the structural heterogeneity of the membrane layers initiates the dependence of the value of the gas permeability coefficient on the direction of transfer (i.e. the effect transfer asymmetry - **EAT**).

For a quantitative assessment and analysis of the intensity of **EAT**, we have proposed the coefficient of asymmetry intensity

$$\chi = \frac{P_+ - P_-}{P_+ + P_-} \tag{10}$$

Using the Mathcad15 package, expression (9), and the asymmetry coefficient χ, we performed an analysis of the dependence of the intensity **EAT** on the parameters of the structural heterogeneity of the layers.

It was established that the intensity of **EAT** is significantly influenced by the degree of structural heterogeneity of the layers, which are determined by the values of the parameters -a_1, a_2.

It has been found that **EAT** can occur even if only one of the membrane layers is structurally heterogeneous.

It is shown that the intensity of **EAT** also depends on the ratio between the thicknesses of the membrane layers.

The study was supported by a grant from the Russian Science Foundation (project No. 18-19-00738).

NANOCOMPOSITES BASED ON LITHIUM PERCHLORATE IN THE METAL-ORGANIC FRAMEWORK MATRIX

[1]Artem Ulihin, [1,2,3]Nikolay Uvarov, [1,2]Valentina Ponomareva, [4]Konstantin Kovalenko, [4]Vladimir Fedin

[1] Institute of Solid State Chemistry and Mechanochemistry SB RAS, Novosibirsk, Russia
[2] Novosibirsk State University, Novosibirsk, Russia
[3] Novosibirsk State Technical University, Novosibirsk, Russia
[4] Nikolaev Institute of Inorganic Chemistry SB RAS, Novosibirsk, Russia
E-mail: *ponomareva@solid.nsc.ru*

Introduction

Solid electrolytes with high lithium-ion conductivity are important materials for solid state lithium batteries. Among the solid electrolytes composite systems are of special interest as their physical properties may be easily adapted to a particular application by variation of the type and concentration of the components. Metal-organic frameworks (MOFs) are excellent porous matrices for preparation of nanocomposites with unusual physical and chemical properties.

Results and Discussion

In the present work nanocomposite solid electrolytes $LiClO_4$ – CrMIL101 were prepared and their electrical properties were investigated at the temperature range of 300-450 K. It was demonstrated that lithium perchlorate easily penetrates into the pores of MOF with formation of nanocomposites. Reproducible heating-cooling cycles of conductivity were observed in vacuum. The concentration dependence of the conductivity goes through the maximum and reaches ~10^{-3} S/cm at 430 K (Fig.1), the activation energy for conductivity changes from 0.93 eV for pure lithium perchlorate to 0.62 eV in the nanocomposites. The value of electrochemical decomposition was determined as 3 V at 500K. It suggests that the ionic conductivity is caused by lithium cations rather that protons or electrons. The results were interpreted in terms of the model of the composite in which the lithium salt uniformly covers surfaces of the MOFs pores. According to the model with the increase in the concentration of the MOF the thickness of the salt layer may decrease to a single layer level with the changing the salt properties due to size effect.

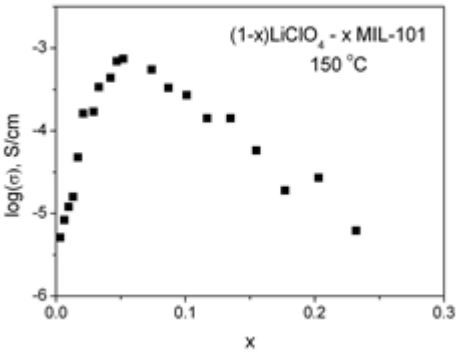

Figure 1. Concentration dependence of conductivity of the (1-x)$LiClO_4$ - xCrMIL-101 composites.

The work is supported by the Russian Fund of Basic Research, grant No.18-29-04039.

ANALYSIS OF THE THEORETICAL CURRENT-VOLTAGE CHARACTERISTICS OF A MEMBRANE CHANNEL

Makhamet Urtenov, Victor Nikonenko, Anna Kovalenko, Elizaveta Evdochenko
Kuban State University, 149 Stavropolskaya Street, 350040, Krasnodar, Russia
E-mail: *urtenovmax@mail.ru*

Introduction

In this paper, for the first time we carry out a theoretical analysis of current-voltage characteristics (CVC) taking into account the oscillations of electric current where the applied voltage increases linearly with a sufficiently low rate.

Problem definition

For the convenience of the analysis, the CVC chart was divided into sections selected on the basis of physical meaning. Namely, the first section $i \in [0, i_{\lim})$ corresponds to the change in the current density from zero to the limiting current density, $i_{\lim}$. The second section $i \in [i_{\lim}, i_{km})$ - from $i_{\lim}$ to the current density where the first electroconvective vortices at the cation-exchange membrane (CEM) appear. The third section $i \in [i_{km}, i_{am})$ corresponds to the range of current densities, where there are electroconvective vortices at the CEM, but they are not at the anion-exchange membrane (AEM). The fourth section $i \in [i_{am}, 2.7 i_{\lim}]$ corresponds to the range of current density, where there are electroconvective vortices at both CEM and AEM, but they still do not interact with each other [1-3].

As an example, we present the analysis of CVC in the fourth section:

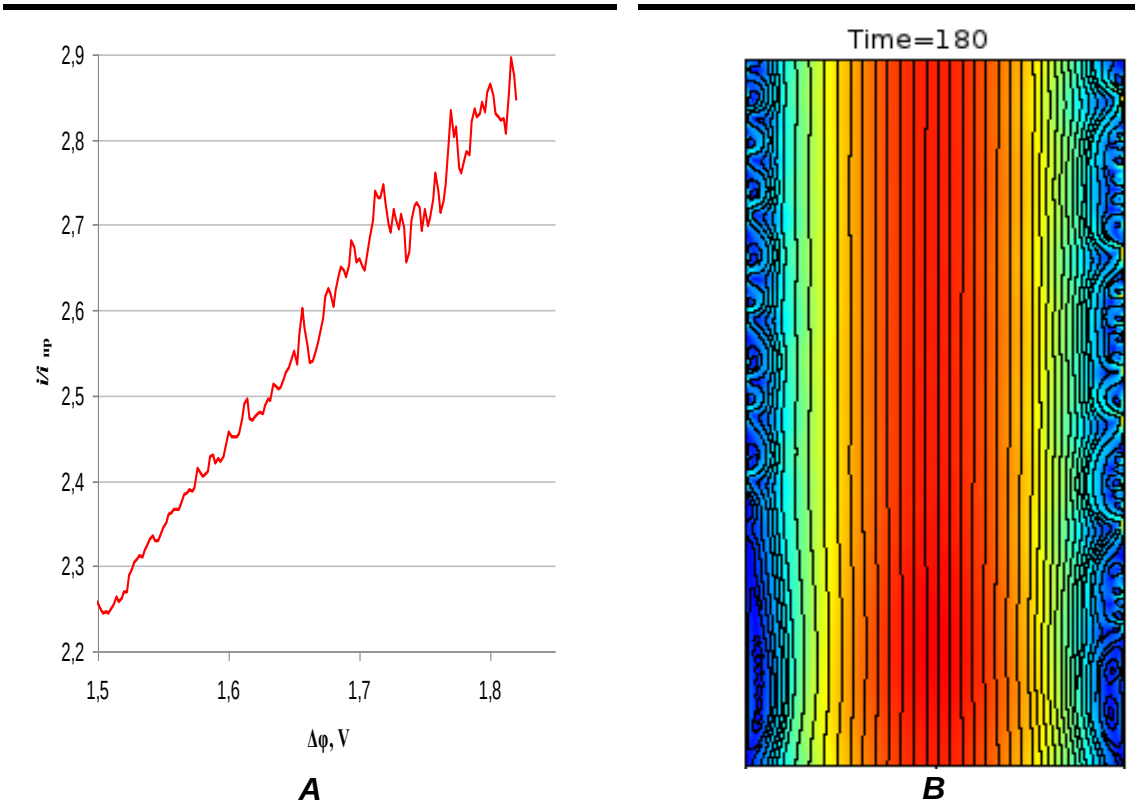

Figure 1. The fourth phase of CVC: a) CVC plot, b) streamlines of the solution. It is seen that electroconvective vortices at the CEM do not interact with electroconvective vortices at the AEM.

Results and Discussion

Figure 2 shows the results of Fourier analysis of the fourth phase of CVC at a sampling rate (the number of samples per unit of time) equal to 16.

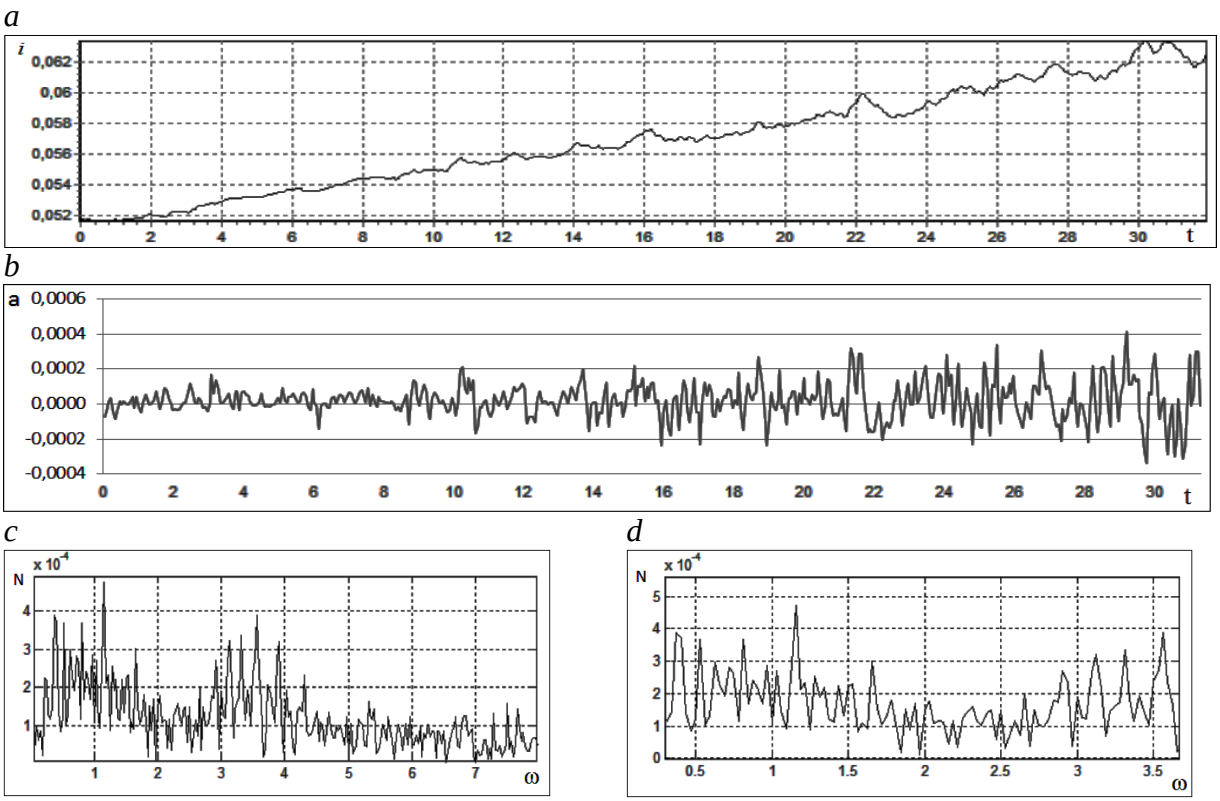

Figure 2. a) graph of the fourth section of the CVC at a sampling rate of 16; b) Plot with a remote trend; c) power spectrum CVC; d) the main and accompanying frequency CVC.

The equation of the trend line is as follows: $y = 0.00002x + 0.05164$. The value of the accuracy of the approximation $R^2 = 0.985$, $R^2 \approx 1$, the dispersion is $\sigma^2 \approx 1.8 \cdot 10^{-5}$.

Consequently, the trend line accurately approximates the physical process in the area of CVC. Figure 2 (b) shows that the main energy of the signal is concentrated in the vicinity of the frequency equal to 1 Hz. It follows that the frequencies concentrated in the vicinity of the frequency equal to 1 Hz are predominant in the section 4 of the signal under consideration. After filtering, we obtain that the main frequency is ≈ 1.15 Hz.

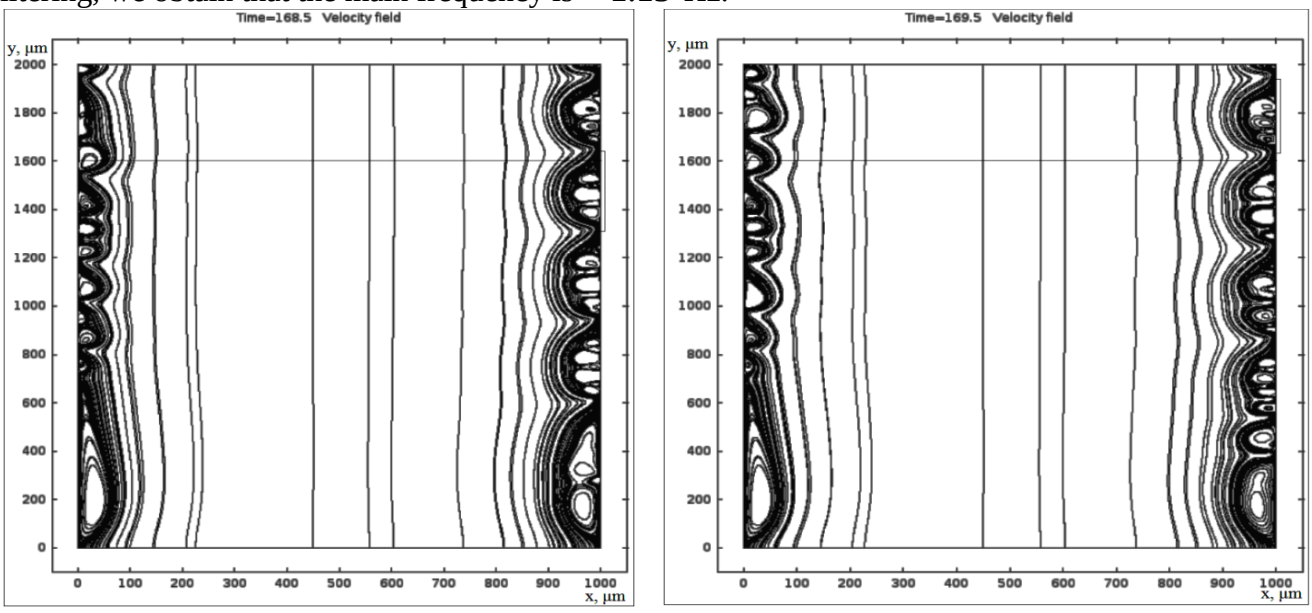

a *b*

Figure 3. Solution flow lines: a) the position of the vortex cluster under study before passing through the cross section; b) -the position of the vortex cluster under study after passing through the cross section.

From figures 3 a) and b), it is seen that the time of passage of the vortex complex through the cross section of the channel is approximately 1 s, i.e. the frequency is 1 Hz.

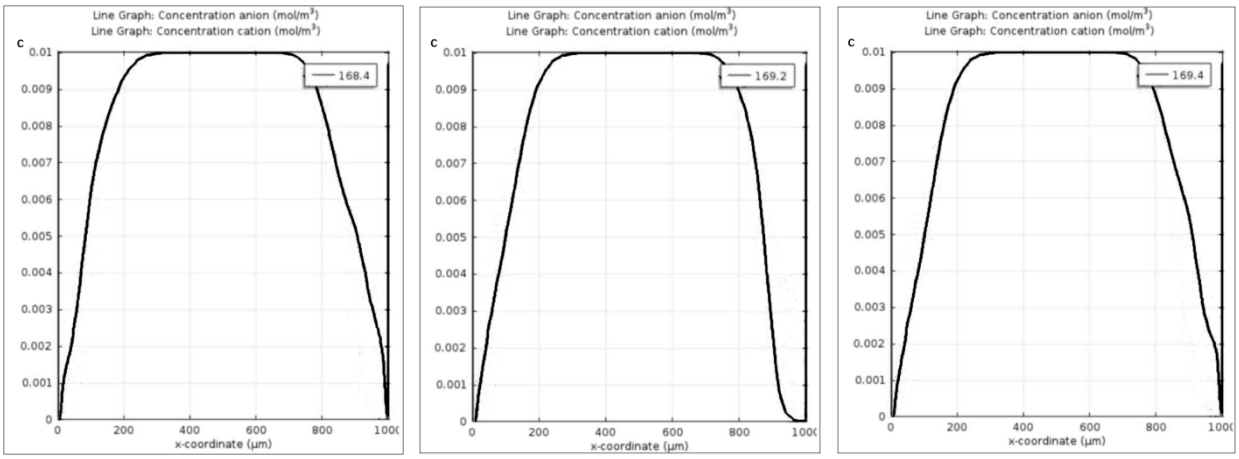

a) b) c)

Figure 4. a) the initial position of the profile in the period of oscillation (168.4 s); b) the maximum deviation of the plot (169.2 s); c) the final position of the profile (169.4 s).

As follows from figures 4 (a)-(c), the period of oscillation of the concentration profile in the fourth section of the VAC is equal to 1 s. The frequency of oscillation of the concentration profile is 1 Hz, and coincides with the frequency of passage of vortex clusters.

Conclusion

It is shown that the main oscillation frequency of CVC at each site of its change corresponds to the frequency of passage of vortex clusters through the cross section of desalination channel (DC) of electrodialysis apparatus (EA). In addition, the oscillation frequency of the concentration profile also coincides with the frequency of passage of vortex clusters through the cross section of the DC of EA. Consequently, the oscillations of CVC are caused by changes in conductivity and resistance due to changes in concentration during the passage of vortex clusters.

The reported study was funded by RFBR according to the research project: 19-08-00252 a «Theoretical and experimental study of current-voltage characteristics of electromembrane systems»

References

1. *Nikonenko V.V., Mareev S.A., Pis'menskaya N.D., Kovalenko A.V., Urtenov M.K., Uzdenova A.M., Pourcelly G.* Effect of electroconvection and its use in intensifying the mass transfer in electrodialysis (review) // Russian Journal of Electrochemistry. 2017. V. 53. № 10. P. 1122-1144.
2. *Urtenov M.Kh., Pismensky A.V., Nikonenko V.V., Kovalenko A.V.* Mathematical modeling of ion transport and water dissociation at the ion-exchange membrane/solution interface in intense current regimes // Petroleum Chemistry. 2018. V. 58. № 2. P. 121-129.
3. *Urtenov M.K., Nikonenko V.V.* Analysis of the boundary-value problem solution of the Nernst-Planck-Poisson equations, 1:1 electrolytes // Russian Electrochemistry. 1993. V. 29. P. 314.
4. *Mareev S.A., Nichka V.S., Butylskii D.Y., Pismenskaya N.D., Nikonenko V.V., Urtenov M.K., Apel P.Y.* Chronopotentiometric response of an electrically heterogeneous permselective surface: 3d modeling of transition time and experiment // Journal of Physical Chemistry C. 2016. V. 120. № 24. P. 13113-13119.
4. *Pismensky A.V., Urtenov M.K., Nikonenko V.V., Pismenskaya N.D., Kovalenko A.V., Sistat Ph.* Model and experimental studies of gravitational convection in an electromembrane cell // Russian Journal of Electrochemistry. 2012. V. 48. № 7. P. 756-766.

EFFECT OF POTENTIAL OF PULSED ELECTRIC FIELD ON AVERAGE CURRENT DENSITY IN ELECTRODIALYSIS CELL: NUMERICAL EXPERIMENT

[1]Aminat Uzdenova, [2]Makhamet Urtenov, [2]Victor Nikonenko

[1] Umar Aliev Karachai-Cherkess State University, Lenina Str., 29, 369200 Karachaevsk, Russia
E-mail: *uzd_am@mail.ru*

[2]Kuban State University, Stavropolskya Str. 149, 350040 Krasnodar, Russia

Introduction

One of the ways of improving electrodialysis (ED) and some microfluidic processes is the optimization of current regime. It is recognised now that the use of pulsed electric fields (PEF) in ED allows enhancement of mass transfer and mitigation of fouling [1]. In this study, the effect of the potential of a pulsed electric field (PEF) on the average current density in the ED cell is studied. For this purpose, calculations of the average current density dependence on time in the PEF regime were performed using the 2D mathematical model of overlimiting transfer in the ED cell [2].

Mathematical model

The system under consideration is half of a flow-through ED desalination channel at the cation-exchange membrane (CEM), Fig. 1. Let x and y be the transverse and longitudinal coordinates, respectively; $x = 0$ relates to the middle of the ED channel, $x = h$ is the electrolyte solution/CEM interface; $y = 0$ corresponds to the inlet and $y = l$ to the outlet of the channel.

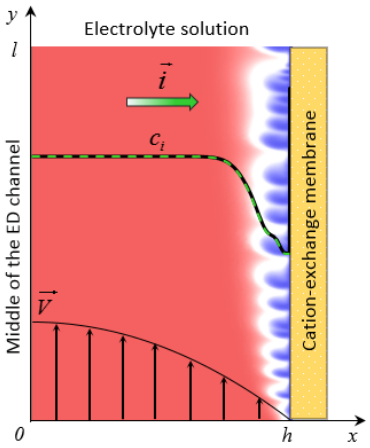

Figure 1. Scheme of the system under consideration: half of the ED cell adjacent to the CEM. Schematic concentration profiles of cations (c_1, solid line) and anions (c_2, dashed line), direction of the electric current $\vec{i}$, forced flow velocity $\vec{V}$, electroconvection vortices (blue color) are shown.

The non-stationary process of transfer of binary electrolyte ions in membrane systems in the absence of chemical reactions, taking into account electroconvection, is written as follows:

$$\frac{\partial \vec{V}}{\partial t} + (\vec{V}\nabla)\vec{V} = -\frac{1}{\rho_0}\nabla P + \nu\Delta\vec{V} - \frac{1}{\rho_0}F(z_1c_1 + z_2c_2)\nabla\varphi, \quad \mathrm{div}\,\vec{V} = 0, \tag{1}$$

$$\frac{\partial c_i}{\partial t} = -div\left(-\frac{F}{RT}z_iD_i\,c_i\nabla\varphi - D_i\nabla c_i + c_i\vec{V}\right), \quad i = 1,2, \tag{2}$$

$$\Delta\varphi = -\frac{F}{\varepsilon}(z_1c_1 + z_2c_2), \tag{3}$$

$$\vec{i} = F\sum_{i=1}^{2} z_i\left(-\frac{F}{RT}z_iD_i\,c_i\nabla\varphi - D_i\nabla c_i + c_i\vec{V}\right). \tag{4}$$

Here $\vec{V}$ is the velocity; D_i, z_i and c_i are individual ion diffusion coefficients, charge number and concentration of the i-th ion; P is pressure; t is time; F is the Faraday constant; R is the gas constant; T is the absolute temperature; φ is electric potential; ε_0 is the dielectric constant; ε_r is

the solution relative permittivity; ρ_0 is the solution density, ν is the kinematic viscosity; $\vec{i}$ – current density. $\vec{V}$, p, c_1, c_2, φ, $\vec{i}$ are unknown function of t, x and y.

The Navier–Stokes equations, Eqs. (1), describe the velocity field under the action of the forced flow and the electric body force. The equations of Nernst–Planck, Eqs. (2), and Poisson, Eq. (3), describe the ion concentration and potential fields. Equation (4) is a formula for the current density.

At the channel inlet ($x \in [0, h]$, $y = 0$), the velocity profile is parabolic and satisfies Poiseuille's law; the concentration is uniformly distributed along x; the condition for the electric potential sets the zero tangential current density:

$$V_x(x,0,t) = 0\,,\ V_y(x,0,t) = 1.5V_0(1-(x/h)^2)\,, \tag{5}$$

$$c_i(x,0,t) = c_0,\quad i = 1,2\,, \tag{6}$$

$$\frac{\partial\varphi}{\partial y}(x,0,t) = -\frac{RT}{F(z_1^2 D_1 + z_2^2 D_2)c_0}\left(z_1 D_1 \frac{\partial c_1}{\partial y} + z_2 D_2 \frac{\partial c_2}{\partial y}\right). \tag{7}$$

At the channel outlet ($x \in [0, h]$, $y = l$) the velocity profile is again parabolic; the sum of diffusion and migration tangential components of the cation ($i = 1$) and anion ($i = 2$) fluxes is zero; the tangential derivative of the potential is set to be zero:

$$V_x(x,l,t) = 0\,,\ V_y(x,l,t) = 1.5V_0(1-(x/h)^2)\,, \tag{8}$$

$$\left(-\frac{\partial c_i}{\partial y} - z_i c_i \frac{\partial\varphi}{\partial y}\right)(x,l,t) = 0,\quad i = 1,2\,, \tag{9}$$

$$\frac{\partial\varphi}{\partial y}(x,l,t) = 0\,. \tag{10}$$

At $x = 0$, $y \in [0, l]$ (middle of the ED channel) the following conditions are applied:

$$V_x(0,y,t) = 0\,,\ V_y(0,y,t) = 1.5V_0\,, \tag{11}$$

$$c_i(0,y,t) = c_0,\quad i = 1, 2\,, \tag{12}$$

$$\varphi(0,y,t) = 0. \tag{13}$$

At $x = h$, $y \in [0, l]$ (the solution/membrane interface), the no-slip condition is applied; the counterion concentration, c_1, is set as a constant value N_c greater than the bulk solution concentration, c_0; continuous flow of co-ions; the normal to the membrane surface component of the electric field strength is specified as function of the electric current density:

$$V_x(h,y,t) = 0\,,\ V_y(h,y,t) = 0\,, \tag{14}$$

$$c_1(h,y,t) = N_c c_0\,, \tag{15}$$

$$\left(-D_2\frac{\partial c_2}{\partial x} - z_2 D_2 \frac{F}{RT} c_2 \frac{\partial\varphi}{\partial x}\right)(h,y,t) = \frac{(1-T_1)}{Fz_2} i_x(h,y,t), \tag{16}$$

$$\varphi(h,y,t) = \Delta\varphi\,. \tag{17}$$

Here, V_0 is the average velocity of the forced solution flow, c_0 is the concentration in the solution bulk, $\Delta\varphi$ is the potential drop.

Calculation were made for the following system parameters: thickness of the considered region $h = 0.25\cdot10^{-3}$ m; channel length $l = 10^{-3}$ m; average velocity of forced flow $V_0 = 3.8\cdot10^{-3}$ m/s; input concentration of the electrolyte solution of NaCl $c_0 = 0.1$ mol/m^3.

Results and Discussion

Figure 2 shows the current-voltage curve (CVC) calculated by setting the potential drop in Eq. (17) to $\Delta\varphi = \alpha t$, $\alpha = 0.01$ V/s. The value of α is chosen sufficiently small so that the electric regime can be considered quasi-stationary. The CVC has a linear initial part. Then, after an intermediary non-linear underlimiting region, the current density grows over the limiting value, i_{lim}. There is a sloping plateau where the PD smoothly increases with increasing current density. Then the plateau is replaced by a more rapidly increasing region in which oscillations of the PD appear.

Calculations of the current density in the PEF regime were performed for average potential drop values corresponding to both the underlimiting and overlimiting currents: $U_{av} = 0.05, 0.1, ..., 0.7$ V (Fig. 3). The duty cycle of the PEF $\alpha = T_{on}/(T_{on} + T_{off}) = 0.5$, where T_{on} and T_{off} are the pulse and

pause durations, respectively. Thus, $T_{on} = T_{off} = 0.5$ s; the potential drop during a pause T_{on} is $\Delta\varphi = 0$; the potential drop during a pulse T_{off} is $\Delta\varphi = U_{av}/\alpha = 2U_{av}$. In Fig. 2, the values of the average current density for the period in PEF are identified with markers.

From Fig. 2, it can be seen that in the initial linear part of the CVC ($U_{av} \leq 0.1$V), the use of the PEF insignificantly affects the current density (differs less than 4%). At 0.1 V < U_{av} < 0.45 V, the average current density for the period in PEF regime is less than in a quasi-stationary one (Fig. 2, 3b). When U_{av} > 0.45 V, the value of the potential drop during the pulse, $\Delta\varphi = 2U_{av}$, is sufficiently large for the development of intensive electroconvection. Electroconvective mixing of the electrolyte solution in the area near the membrane surface increases the efficiency of mass transfer. Therefore, the average current density in PEF regime is higher than in quasi-stationary (Fig. 2, 3c). The maximum effect of the PEF regime is observed when the average potential drop equals $U_{av} = 0.65$ V, which corresponds to the rise of the CVC due to the development of electroconvection. This fact is confirmed by experimental study [3].

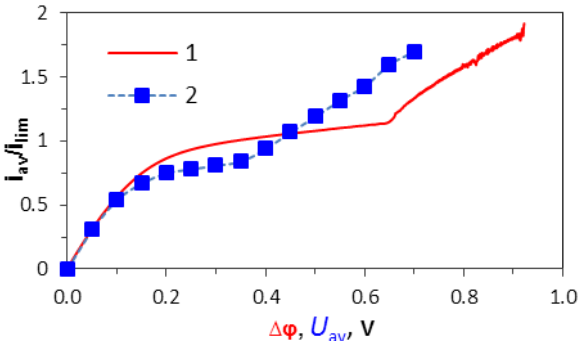

Figure 2. CVC (1) and dependence of the average current density on potential of the PEF (2).

Here $i_{\lim} = \frac{Dc_0F}{h(T_1 - t_1)}\left[1.47\left(\frac{h^2V_0}{lD}\right)^{1/3} - 0.2\right]$ *is the limiting current density [1].*

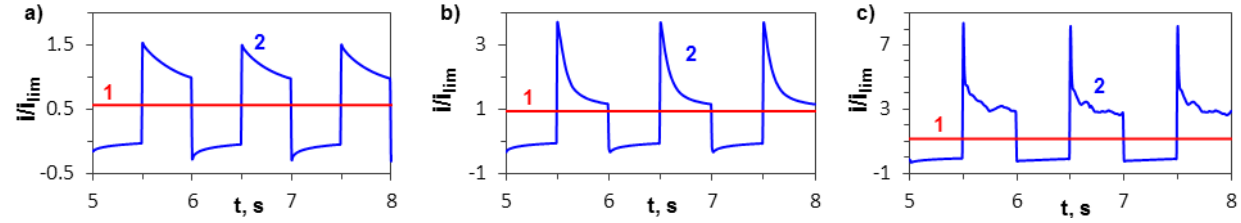

Figure 3. Dependences of the current density on time at the quasi-stationary (1) and PEF (2) regimes for the average potential drop equals U_{av} = 0.1V (a), 0.45 V (b), 0.65 V (c).

Acknowledgments

The reported study was funded by RFBR according to the research project №18-38-00572.

References

1. *Nikonenko, V.V., Mareev, S.A., Pis'menskaya, N.D., Uzdenova, A.M., Kovalenko, A.V.,Urtenov, M.K., Pourcelly, G.* Effect of Electroconvection and Its Use in Intensifying the Mass Transfer in Electrodialysis (Review) // Russ. J. Electrochem. 2017. 53. P. 1122–1144.
2. *Urtenov M. K., Uzdenova A. M., Kovalenko A. V., Nikonenko V. V., Pismenskaya N. D., Vasil'eva V. I., Sistat P., Pourcelly G.* Basic mathematical model of overlimiting transfer enhanced by electroconvection in flow-through electrodialysis membrane cells // J. Membr. Sci. 2013. V. 447. P. 190-202.
3. *Zyryanova S.V., Butyl'skii D.Yu., Mareev S.A., Pis'menskaya N.D., Nikonenko V.V., Pourcelly G.* Effect of parameters of pulsed electric field on average current density through nafion 438 membrane in electrodialysis cell // Russ. J. Electrochem. 2018. 54. P. 775–781.

OXYGEN ELECTROREDOX – SORPTION BY METAL ION-EXCHANGE NANOCOMPOSITES. THE CURRENT EFFECT

Dmitrii Vakhnin, Natalya Zheltoukhova, Alina Tregubova, Tamara Kravchenko
Voronezh State University, Voronezh, Russia, E-mail: *vakhnin.dima@rambler.ru*

Introduction

Dissolved oxygen removal from water is the main task in various industries, such as semiconductor industry, pharmaceuticals, biotechnology etc. It is known that dissolved oxygen removal can be carried out using physical and chemical methods [1]. The most effective method is catalytic reduction, which allows to achieve an oxygen concentration at least 10 ppb [2].

Experiments

Molecular oxygen electroreduction from flowing distilled water was carried out in a single-stage three-chamber electrolyzer, the scheme of which is shown in fig. 1 on thin and granular layers copper-sulfocationites nanocomposites (NC). The metal was deposited into granules of macroporous high-acid ion exchanger Lewatit K2620 (Germany) by chemical method [3]. The capacity of the synthesized metal nanocomposites was ε_{Me} = 9.6 mEq/cm^3. The installation consisted of two anode compartments with platinum anodes and a central cathode compartment separated by MK-40 membranes. The cathode was a granular layer of porous copper-ion exchange nanocomposite with a current supply of thin copper wire. Anode compartments contained a granular ion exchanger in required ionic form. Cation-exchange membrane provided the continuity and the directional migration ions from anode to cathode chambers. Polarization was carried out by the power source B5-47 (Russia) by direct current *I*, which is a certain proportion of the limiting current I_{lim} on the granular NC layer with height *l*.

The processes occurring during the electrochemical polarization can be represented as follows:
- on platinum anodes:

$$2H_2O \xrightarrow{I} O_2 + 4\bar{H}^+ + 4e^-; \quad (1)$$

- ions $\bar{H}^+$ transfer through the cation exchange membrane from anodes to the cathode;
- electrochemical oxygen reduction at the composite cathode:

$$O_2 + 4\bar{H}^+ + 4e^- \xrightarrow{I} 2H_2O; \quad (2)$$

- oxygen chemical reduction due to copper nanoparticles self-dissolution and reverse copper reduction from oxides:

$$Cu^0 \underset{e^-}{\overset{O_2,H_2O}{\rightleftarrows}} Cu_2O \underset{e^-}{\overset{O_2,H_2O}{\rightleftarrows}} CuO. \quad (3)$$

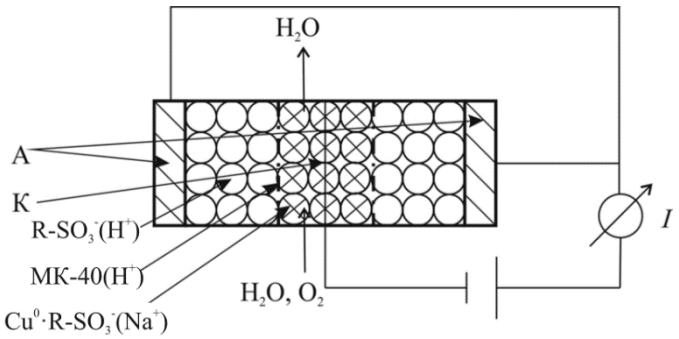

Figure 1. Sorption-membrane electrolytic cell scheme.

Results and Discussion

The experiment was carried out at different current forces, which corresponded to the relative currents I/I_{lim} within 0 to 1. The external polarizing current value has a significant effect on oxygen

concentration in water. The oxygen concentration is falling with increasing current. It is necessary to pay attention to a significant decreasing concentration at high currents. The minimum value is reached at the relative current I/I_{lim} = 0.8. At a higher current, the side hydrogen release becomes significant and dissolved oxygen concentration at the outlet of granular layer increases.

The dependence of the consumed oxygen amount from water from time on Cu^0·Lewatit K2620 (Na^+) composite is shown on fig 2. Based on the fact that oxygen can be restored only through a chemical reaction with metal nanoparticles in current-free conditions, so the electrochemical reaction is added during the polarization.

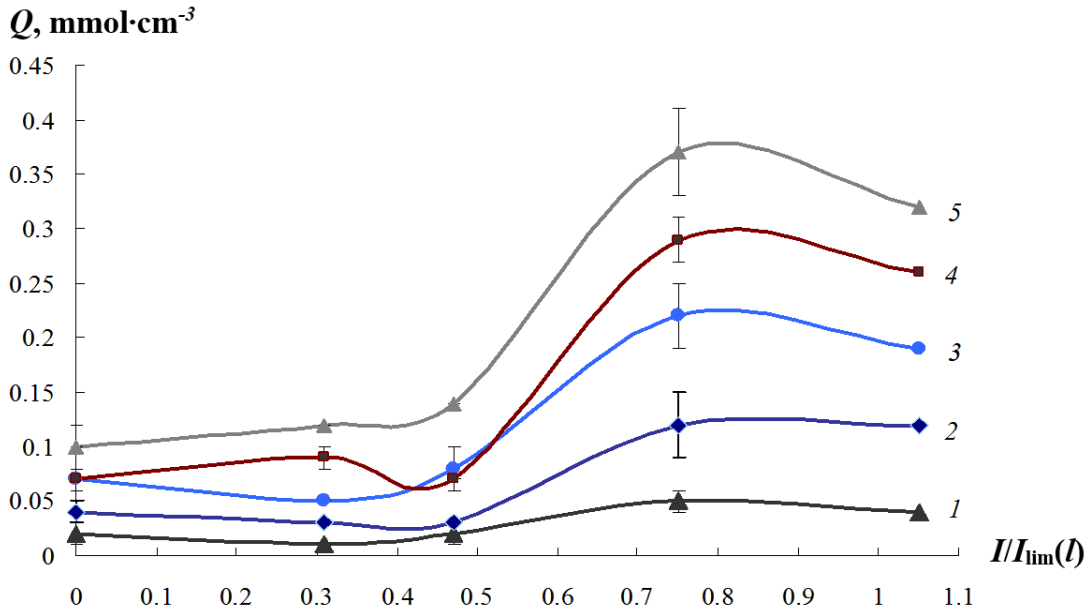

Figure 2. Reduction oxygen quantity on Cu^0·Lewatit K2620(Na^+) nanocomposite at the time t, h: 1 – 1; 2 – 2; 3 –3; 4 – 4; 5 – 5. Experiment conditions: l= 1·10^{-2} m, u=0.23 cm/sec, $I_{lim}(l)$ =2.9 mA. Experiment time is 5 h.

For a relatively short time (5 h) of the nanocomposite's metal interaction with the oxidizer, electric reduction of oxygen prevails (97-100 %) at a whole (table 1).

Table 1: Chemical ω_{ch} and electrochemical ω_{elch} components' depositions of oxygen reduction process and current efficiency of oxygen $\eta_C(O_2)$ and copper oxides η_C(ox) on *Cu^0·Lewatit K2620(Na^+)*. c_0=(8.2±0.2) mg/l

Polarazing current intensity *I*, mA	I/I_{lim}	ω_{ch}, %	ω_{elch}, %	*q*, Cl	$q(O_2)$, Cl	$\eta_c(O_2)$, %	η_c(ox), %
I = 1·10^{-2} m, $I_{lim}(I)$ =2.9 mA. Experiment time is 5 h.							
0	0	100	-	-	-	-	-
1.0	0.3	58.3	41.7	18.0	19.3	100	0
1.5	0.5	56.3	43.7	27.0	27.0	100	0
2.4	0.8	70.3	29.7	43.2	42.5	98.4	1.6
3.1	1.1	56.3	43.7	55.8	54.0	96.8	3.2
I =6·10^{-2} m, $I_{lim}(I)$ =12.3 mA. Experiment time is 100 h.							
3.7	0.3	54.1	45.9	1332	1154	86.64	13.36
6.2	0.5	36.1	63.9	2232	3690	-	-
8.6	0.7	25.5	75.5	3096	2686	86.76	13.24
11.1	0.9	40.3	59.7	3996	2049	51.28	48.72

In a long-term experiment (100 h) there is an increase electrochemical stage contribution of oxygen reduction in comparison with its consumption in chemical stages due to copper nanoparticles oxidation. The current efficiency of electrochemical stage increases as a result of oxidized copper reduction.

The dependence of absorbed oxygen amount from polarizing current value is particularly interesting (fig.3). It has an extreme form, and over time the maximum is more pronounced. It is shown that with increasing of superimposed current density, the amount of oxygen absorbed by the nanocomposite increases. As well as a thin granular layer, at high currents the side hydrogen electroreduction is shown.

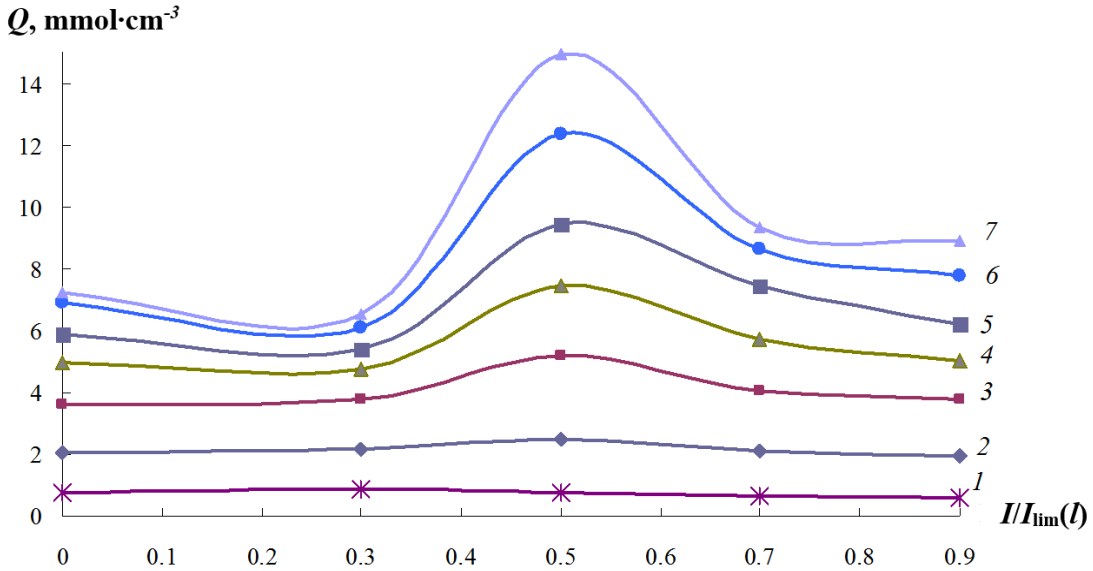

Figure 3. Reduction oxygen quantity on Cu^0·Lewatit K2620(Na^+) nanocomposite at the time t, h: 1 – 5; 2 – 15; 3 – 30; 4 – 45; 5 – 60, 6 – 80; 7- 100. Experiment conditions: l= $6 \cdot 10^{-2}$ m u=0.23 cm/sec, c_0=8.1±0.2 mg/l, $I_{lim}(l)$=12.3 mA.

Conclusions

The feature of redox-sorption process is the simultaneous consideration of electrochemical due to current and chemical due to metal nanoparticles oxygen reduction on the granular layer of metal-ion exchange nanocomposite. The main consumption of electricity for electrical recovery of oxygen is obvious.

Acknowledgments

This work was supported by the Russian Foundation for Basic Research (grant № 17-08-0426a).

References

1. *W. Shi*. Removal of dissolved oxygen from water using a Pd – resin based catalytic reactor / W. Shi, C. Cui, L. Zhao et al. // Frontiers of Chemical Engineering in China. – 2009. – Vol. 3. – P. 107 – 111.
2. *M.S.Gross*. Catalytic Deoxygenation of Water: Preparation, Deactivation, and a Resin Catalyst / M.S.Gross, M.L. Pisarello, K.A. Pierpauli et al. // Industrial and Engineering Chemistry Research. - 2010. – Vol. 49. – P. 81 – 88.
3. *Kravchenko T.A*. Electrochemistry of Metal-Ion Exchangers / T.A. Kravchenko, E.V. Zolotukhina, M.Yu Chaika., A.B. Yaroslavtsev – Moscow: Nauka, 2013. – 365 p.

ELECTROCONVECTIVE INSTABILITY IN SYSTEMS WITH HETEROGENEOUS MEMBRANES RALEX WITH DIFFERENT CONTENT OF ION-EXCHANGER

Vera Vasil'eva, Elmara Akberova
Voronezh State University, Voronezh, Russia, E-mail: *elmara_09@inbox.ru*

Introduction

The aim of the present work is to experimentally assess the effect of changes in fractions of the sulfocation-exchanger on the current-voltage characteristics (CVC) and on the sizes of electroconvective instability region in solution at the interface with heterogeneous ion-exchange membranes Ralex.

Experiments

In the study there was evaluated the structure and CVCs of experimental samples of heterogeneous membranes Ralex CM Pes (MEGA a.s., Czech Republic) with fraction of cation-exchanger from 45 to 70%. The membranes were obtained by rolling the homogenized mixture of milled ion-exchanger and polyethylene.

Experiments were carried out in a horizontally oriented electrodialysis cell at a concentration-temperature stable stratification. The height of membrane channel L was of $4.1 \cdot 10^{-2}$ m, width was of $1.4 \cdot 10^{-2}$ m, intermembrane distance was $h = 2.0 \cdot 10^{-3}$ m. Sodium chloride solutions with the initial concentration of $2.0 \cdot 10^{-2}$ M were supplied with the rate of $1.3 \cdot 10^{-3}$ m/s, that corresponds to laminar flow (Re=3). The CVC of the test membrane were measured using two silver–chloride probes placed on each side of the membrane at a distance of 1.3 mm from its surfaces.

Visualization of a hydrodynamic picture of interphases was carried out by using of Mach – Zender type interferometric set up. Thickness of convective instability region at the interphase membrane-solution d was determined as the distance from membrane surface where the interference band and concentration profile, respectively, are of unstable, oscillation character.

The experimental studies of surface morphology of swollen membranes were conducted using the method of scanning electron microscopy at JSM-6380 LV microscope (Japan) equipped with regulated pressure. Microphase fractions and sizes were estimated by means of an original software system.

Results and Discussion

There is a comparison of current-voltage characteristics of samples of heterogeneous Ralex CM Pes membranes with different volume ratio of conductive (ion-exchanger) and non-conductive (polyethylene) phases in Fig. 1a. The CVCs have a traditional shape with three regions that have a different slope to the potential axis. A comparative analysis of the characteristics of the current-voltage curves of the membranes shows that they are determined by the fraction of the ion-exchanger in the membrane composition. With an increase in the content of the ion-exchanger in the membrane, an increase in the limiting diffusion current density, a reduction in the length of the limiting current plateau of the current-voltage curve was established. The reduction in the plateau length indicates that electroconvection in the unstable regime, which is accompanied by the appearance of nonstationary vortices, begins at a smaller potential drop. The results of measuring the thickness of the electroconvective instability region (Fig. 1b) are direct evidence of a more intensive mixing of the solution at the interface with the membrane with an ion-exchanger content of 70%.

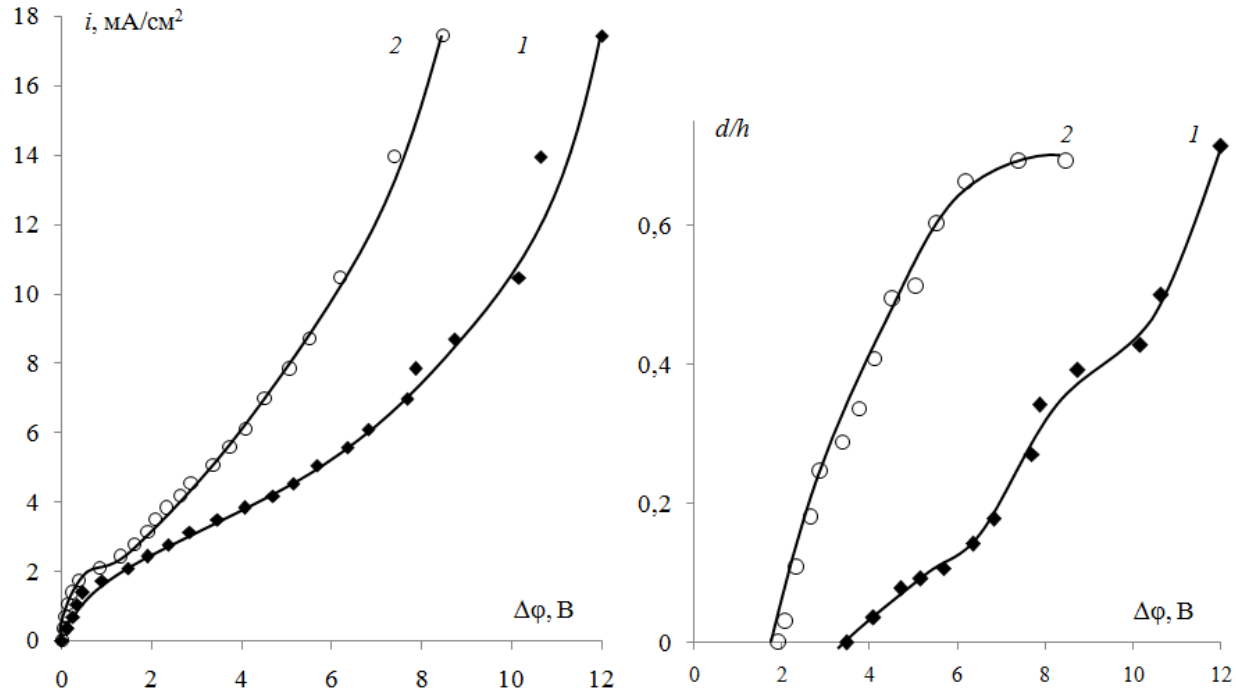

a *b*

Figure 1. Current-voltage curves (a) and thickness of the convective instability region normalized to the intermembrane distance h (b) in solution at the boundary with cation-exchange membranes with the sulfocation-exchanger fraction of 45 % (1) and 70% (2).

The changes in the microstructure of membranes with different content of the ion-exchanger determine their electrochemical behavior at overlimiting currents. It was established that the fraction of the conductive areas and the porosity on the swollen membrane surface increase but the radii of microphases remained constant with the increase in the ion-exchanger content and the distances between them decreased (Table 1).

Table 1: Surface characteristics of heterogeneous CM Pes membranes

Ion-exchanger content	*S*, %	$\overline{R}$, μm	$R_{min} - R_{max}$, μm	*P*, %	$\overline{r}$, μm	$r_{min} - r_{max}$, μm	$\overline{l}$, μm
45	20	2.3	0.5 – 18	2,2	1.5	0.4 – 8	4.9
70	38	2.1	0.5 – 17	3,6	1.4	0.4 – 6	2.5

where *S* is the proportion of the ion-exchanger; *P* is the porosity; $\overline{R}$ and $\overline{r}$ are the radii of the ion exchangers and macropores, respectively; $\overline{l}$ is the distance between conductive areas.

Thus, the parameters of current-voltage characteristics and the sizes of electroconvective instability region depend on the properties of the membrane surface that determine the intensity of electroconvection under intensive current regimes.

Acknowledgements

The work is supported by the grant of the President of the Russian Federation MK-925.2018.3.

Microphotographs of the membrane surface and cross-section were obtained on the equipment of the Collective Use Center of Voronezh State University. URL: http://ckp.vsu.ru.

The authors are grateful to the «MEGA» a.s. company (Czech Republic) and its owner Mr. L. Novak for providing experimental samples of membranes.

A COMPARATIVE ANALYSIS OF THE EFFECT OF PHENYLALANINE ON PHYSICOCHEMICAL, STRUCTURAL AND TRANSPORT CHARACTERISTICS OF PROFILED HETEROGENEOUS ION-EXCHANGE MEMBRANES MK-40 AND MA-40

Vera Vasil'eva, Mikhail Smagin, Elena Goleva
Voronezh State University, Voronezh, Russia, E-mail: *viv155@mail.ru*

Introduction

The study of the causes for organic contamination of ion-exchange membranes in solutions is a topical problem [1]. The effect of amino acids can diminish the performance properties of membranes and decrease the efficiency of membrane processes [2-4]. Low mobility of amino acids, their ability to manifest the acidic and basic properties, the presence in the amino acid structure of both positive and negative charges result in the deterioration of the transport properties of ion-exchange membranes in amino acid solutions [5,6] .

The goal of the present work is to make a comparative analysis of the effect of the aromatic amino acid on the physicochemical, structural and transport characteristics of the profiled heterogeneous ion-exchange membranes.

Experiments

Heterogeneous cation-exchange membranes MK-40 and anion-exchange membranes MA-40 with geometrically inhomogeneous (profiled) surface were selected as the test objects. The experimental membrane samples with a profiled surface were manufactured by the innovative company OOO "Membrane Technology" (Krasnodar). The membrane profiling technology is described in [7, 8]. The method for profiling consists in the method of hot pressing of swollen commercially produced membranes (manufactured by OOO OKhK Shchekinoazot, Russia) to obtain a given geometric surface relief. Before the experiments were carried out, the membranes were subjected to salt pretreatment [9] and then transferred to the hydrogen and hydroxyl ionic form.

Aqueous solutions of the neutral alkylaromatic amino acid phenylalanine $NH_2CH(CH_2C_6H_5)COOH$ (99% PS ,"Panreac") were chosen as the test solutions. Phenylalanine is an ampholyte, i.e. a substance that enters with water into the protolysis reactions with the formation of H_3O^+ and OH^- ions and changes its charge depending on the pH of the solution. Phenylalanine is a hydrophobic amino acid having a non-polar side substituent (a benzene ring) in its structure. It does not bear a partial charge and is not noticeably solvated by water. In model solutions, phenylalanine was mainly in the form of bipolar ions at pH 5.60 ± 0.05 (pI = 5.91).

To assess the effect of the amino acid on the physicochemical characteristics of the membrane, we used relative changes in the measured values (Δ A, %), which were calculated using the formula: $\Delta A, \% = 100\cdot(A_t-A_0)/A_0$, where A_t is the value of the physicochemical characteristic of the membrane after contact with the amino acid, A_0 is the corresponding parameter of the conditioned membrane sample. The total static exchange capacity of the membrane (Q_0, mmol/g_{sw}) was found by the method of acid-base titration; the moisture content (W,%) was established by the method of air-heat drying [9]. The thickness of the swollen membrane was measured with Schut Digital micrometers (accuracy 0.001 mm). The thickness of the membrane with a profiled surface was measured along the sample length of 5×5 cm^2 with an interval of 15 mm [8]. The result was taken as the arithmetic mean value. The diffusion properties (the integral coefficient of diffusion permeability) of the membranes were determined by measuring the amount of amino acid transferred from the phenylalanine solution of a given concentration under the influence of diffusion forces through the investigated membrane into water. The analytical control of the amino acid concentration was performed using the method of absorption spectroscopy with an SF-2000 spectrometer at a wavelength λ = 257nm (the detection limit of phenylalanine is $5.8\cdot10^{-6}$mol/dm^3).

The microstructure of the swollen membranes was investigated by scanning electron microscopy technique (SEM) in the low-vacuum mode with JSM-6380 LV microscope (Japan). The information on the share of macropores (P) and the share of the ion-exchange parts (S) of membranes was obtained by using of the author software package [10]. The morphology of the membrane surface was visualized using atomic force microscopy (AFM) with NT-MDT Corporation's scanning probe microscope of the SolverP47 Pro model (Zelenograd, Russia) in semi-contact mode on air-dry samples.

Results and Discussion

Figure 1 shows the kinetic curves of the relative changes in the physicochemical characteristics of the investigated profiled membranes after contact with the phenylalanine solution of concentration C_0=0.15mol/dm^3.

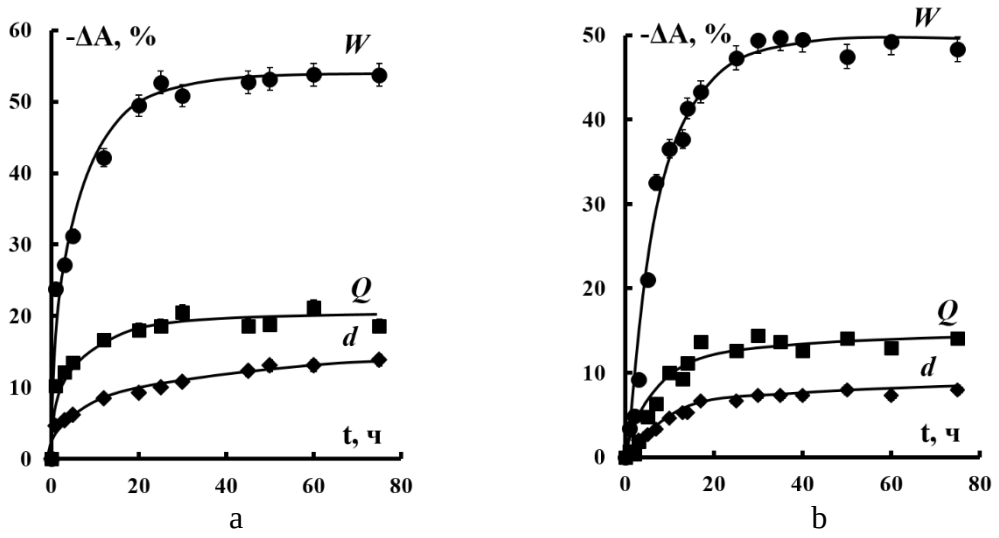

Figure 1. The kinetic dependences of the relative changes in moisture content (W), total exchange capacity (Q) and thickness (d) of the membranes MK-40$_{pr}$ (a) and MA-40$_{pr}$ (b) after contact with the phenylalanine solution of concentration C_0=0.15mol /dm^3.

In the first 5-10 hours, there is a sharp decrease in the values of the total exchange capacity, moisture content and thickness compared with the corresponding parameters of the conditioned samples. After that, the rate of change in characteristics drops and after 40-50 hours the membrane parameters remain almost unchanged (Table 1).

Table 1: Physicochemical characteristics of the membranes MK-40$_{pr}$ and MA-40$_{pr}$ before and after contact with phenylalanine aqueous solutions of concentration C_0=0.15 mol/dm ^{3} during 80 hours

Characteristics	MK-40$_{pr}$	MA-40$_{pr}$	MK-40$_{pr}$+Phe	MA-40$_{pr}$+Phe
Ion exchange capacity, Q, mmol/g$_{sw}$	1.56±0,1	2.70±0,1	1.27±0.1	2.32±0,1
Water content, *W*, %	45.5±1	44.6±1	21.0±1	23.0±1
Thickness in the swollen state, *d*, μm	650±10	755±10	560±10	695±10

The estimation of the total exchange membrane capacity with respect to mineral ions shows that contact with the phenylalanine solution during 80 hours resulted in the decrease in the total content of active functional groups by 2 2.8% in the MK-40 membrane and by 6 .4% in the MA-40 membrane.

To a greater extent, the phenylalanine solutions have an effect on the moisture content of the membranes. After contact with the amino acid solution during 80 hours, the moisture content of the membranes is halved. The decrease in the moisture content and thickness of the membrane is caused by the elastic compression of the ion-exchange matrix due to the introduction of the aromatic amino acid into micro- and macropores of the hydrophobic ions.

A significant effect of phenylalanine on the physicochemical characteristics of the sulfo cation-exchange membrane compared with the anion exchange membrane is caused by the higher sorption of phenylalanine due to the structural similarity of a side aromatic amino acid radical with the polystyrene cation-exchange matrix.

The decrease in the moisture content in the membrane MK-40_{pr} leads to a compacting of its structure (reducing the height and radius of the surface profile elements, as well as the share and size of macropores both on the surface and in the volume of the membrane) and to a smoother surface microrelief (reducing all the amplitude parameters of the initial membrane surface).

The concentration dependences of the integral coefficients of diffusion permeability of the membranes MK-40_{pr} and MA-40_{pr} in the phenylalanine solutions are presented in Figure 2.

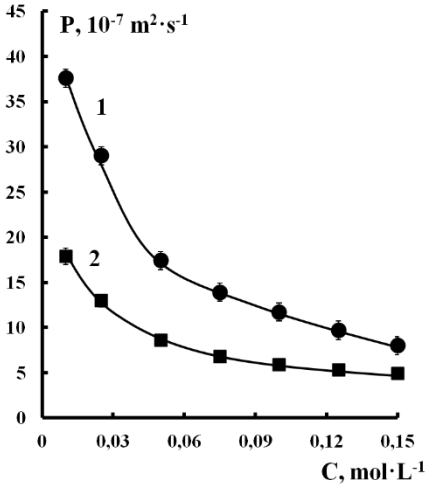

Figure 2. Dependences of the integral coefficients for the diffusion permeability of the membranes MK-40_{pr} (1) and MA-40_{pr} (2) on the concentration of the phenylalanine solutions.

The decrease in the diffusion permeability of the membranes MK-40_{pr} and MA-40_{pr} with the increase in the concentration of the contacting phenylalanine aqueous solution is connected with the pore compression, the drop in moisture content and the decrease in the number of the active functional groups in the membranes due to the formation of complex associative structures of the amino acid in external and internal solutions.

Acknowledgements

The work was supported by the RFBR (project No 18-08-01260).

We are grateful to Prof. V.I. Zabolotskiy for providing the samples of the profiled ion-exchange membranes.

References

1. *Mikhaylin S., Bazinet L.* // Adv. Colloid Interface Sci. 2016. V. 229. P. 34.
2. *Bukhovets A., Eliseeva T., Oren Y.* // J. Membr. Sci. 2010. V. 364. P. 339.
3. *Suwal S., Doyen A., Bazinet L.* // Ibid. 2015. V. 496. P. 267.
4. *Langevin M.-E., Bazinet L.* // J. Membr. Sci. 2011. V. 369. P. 359.
5. *Vasil'eva V., Goleva E., Pismenskaya N., Kozmai A., Nikonenko V.* // Separation and Purification Technology. 2019. V. 210. P. 48.
6. *Goleva E., Vasil'eva V. //* Proceedings of Voronezh State University. Series: Chemistry. Biology. Pharmacy. 2012. № 1. P. 33.
7. *Zabolotsky V.I., Loza S.A., Sharafan M.V.* Pat. RF 2284851. Published 10.10.2006. Bulletin № 28.
8. *Zabolotsky V.I., Loza S.A., Sharafan M.V.* // Russ. J. Electrochem. 2005. V. 41. No 10. P. 1053.
9. *Berezina N.P., Kononenko N.A., Dyomina O.A., Gnusin N.P.* // Adv. Colloid Interface Sci. 2008. V. 139. P. 3.
10. *Vasileva V.I., Kranina N.A., Malykhin M.D., Akberova E.M., Zhiltsova A.V.* // J. Surf. Invest.: X-Ray, Synchrotron and Neutron Techniques. 2013. V. 7. No 2. P. 144.

WATER SPLITTING AT ION-EXCHNAGE RESIN PARTICLES AND THE HETEROGENEOUS ION-EXCHANGE MEMBRANES

[1]Lucie Vobecká, [1]Zdeněk Slouka

[1]University of Chemistry and Technology, Dept. of Chemical Engineering, Prague, 16628, Czech Republic, E-mail: *lucie.vobecka@vscht.cz, sloukaz @vscht.cz*

Introduction

Heterogeneous ion-exchange membranes are often used in the electrodialysis and electrodeionization units operated in separation industry. Although they are usually characterized by worse electrochemical properties such as resistivity or selectivity, they outperform homogeneous ion-exchange membrane in their mechanical and chemical stability.

Heterogeneous ion-exchange membranes usually consist of (i) finally ground ion-exchange resin, (ii) plastic binder and (iii) polymeric mesh laminated on both sides of the membrane [1]. While the binder and the polymeric mesh are passive components of the membrane regarding the functionality of the membrane, the resin provides the membrane with the property of ion selectivity which is then responsible for selective ion transport in DC electric field [2]. It is thus reasonable to assume that the properties of the resin will largely affect the functional properties of the final heterogeneous membrane. Quantitative properties such as overall resistance of the membrane are influenced by the amount of the resin within the membrane and also its distribution in the binder. Qualitative properties of the membranes are influenced by the properties of the pristine resin.

Here we investigate the ability of selected ion-exchange resin to split water in low concentrated electrolytes. Water splitting occurs on depletion side of monopolar membranes when overlimiting current [3] passes through the system. The extent of water splitting depends on the type of the membrane and is strongly affected by the functional groups forming the fixed charge in the membrane [4]. In bipolar membranes the water splitting is facilitated by localizing the depletion region in between two monopolar membranes which make them suitable for applications involving production of H^+ and OH^- ions [5].

The main aim of the presented research is to answer the question whether the properties of ion-exchange resin is reflected in heterogeneous ion-exchange membranes containing the same resin, in this case it is the ability of the monopolar systems to split water.

Experiments

The experiments are carried out in a specific fluidic cell that allows to insert and study single ion-exchange resin particles (see Figure 1a) or small pieces of ion-exchange membranes (Figure 1b).

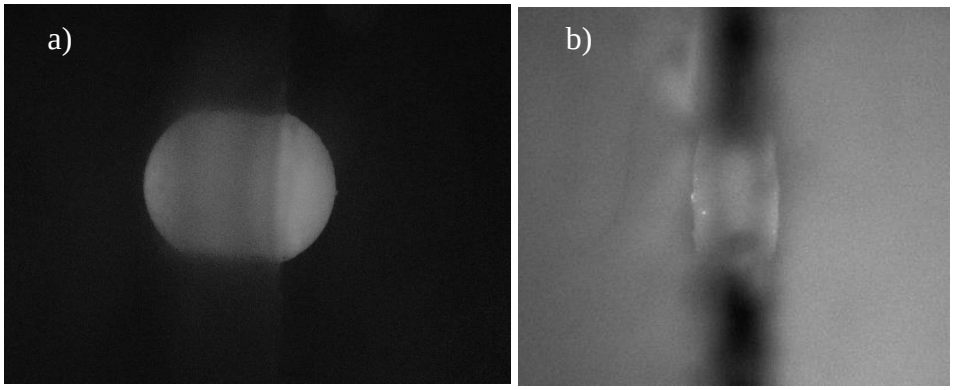

Figure 1. a) single ion-exchange resin particle, b) small piece of ion-exchange membrane used for experimental studies.

The fluidic system consists of four chambers, two of them serving as desalination and concentration chambers and two others as electrodes compartments [6]. We used frits filled with strong buffer as electrode compartments. The buffer prevents changes in pH caused by electrochemical reaction on the electrodes to influence measurement of pH values in the system. The actual measurement proceeds in the following way. The four compartments are filled with a

given KCl buffer whose pH is measured. Then constant voltage is applied on the studied system and the current passing through the system is measured for five minutes. After five minutes the solution in all chambers in the chip is well mixed and its pH is measured. We carried out the same experiments on three systems for each studied ion-exchange particle and membrane.

Results and Discussion

Figure 2 depicts the pH changes in the KCl solution adjacent to the studied ion-exchange systems, namely cation exchange particle Suqing 001×4 in sodium form (Figure 2a), heterogeneous cation-exchange membrane (Figure 2b), anion-exchange resin particle Suqing 201×4 in chloride form (Figure 2c) and heterogeneous anion exchange membrane (Figure 2d).

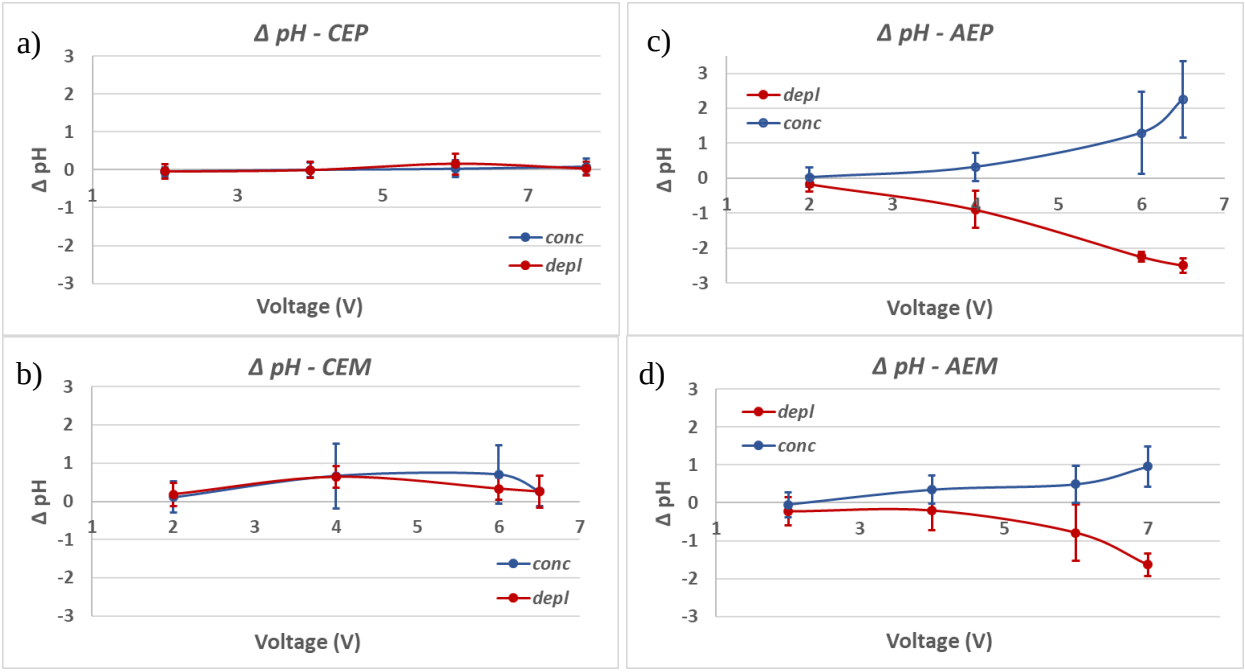

Figure 2. a) pH changes of the cation-exchange particles, b) pH changes of the corresponding cation-exchange membranes, c) pH changes of the anion-exchange particles, and d) pH changes of the anion-exchange membranes. The red and blue lines correspond to the depletion and concentration sides of the given ion-exchange systems. The error bars represent 65% confidence interval form experiments on three systems with a give ion-exchange material.

Based on the theoretical analysis of the ion exchange systems, the depletion and the concentration sides of anion exchange systems should be characterized by the decrease and increase in pH, respectively, and the opposite should be true for the cation-exchange systems if the water splitting reaction occurs. The pH of the original solution was 5.8 on average, which means that the changes in pH in positive and negative direction are symmetrical in terms of concentration changes of H^+ and OH^- ions. Since the ion-exchange systems has certain capacity in terms of accumulating H^+ or OH^- ion, it is better to evaluate the extent of water splitting reaction on the depletion side of the membrane. In our experimental arrangement, we also measured pH changes in the electrode reservoirs to make sure that there are no pH changes that could affect the measurement in the solutions on the depletion and concentration sides of the studied ion-exchange systems. Our experimental study shows that: (i) cation exchange particles tested in this work do not split water, at least under the applied voltage, (ii) cation-exchange membrane made of the same cation exchange particles do not split water either, (iii) anion-exchange particles split water very efficiently and is detectable for voltages as low as 4V, and (iv) anion exchange membrane made of the same anion-exchange particle also tends to split water although to a much lesser degree. The presented study is part of larger study looking at the possibility to predict the properties of heterogeneous ion-exchange membranes from the behavior of ion-exchange resin particles.

References

1. *Svoboda, M., et al.,* Swelling induced structural changes of a heterogeneous cation-exchange membrane analyzed by micro-computed tomography. Journal of Membrane Science, 2017. 525: p. 195-201.
2. *Slouka, Z., S. Senapati, and H.C. Chang*, Microfluidic Systems with Ion-Selective Membranes. Annual Review of Analytical Chemistry, Vol 7, 2014. 7: p. 317-335.
3. *Tomáš Belloň, P.P., Lucie Vobecká, Miloš Svoboda, Zdeněk Slouka*. Experimental observation of phenomena developing on ion-exchange systems during current-voltage curve measurement. Journal of Membrane Science 2019 [cited 572; 607-618].
4. *Nikonenko, V.V., et al.*, Desalination at overlimiting currents: State-of-the-art and perspectives. Desalination, 2014. 342: p. 85-106.
5. *Slouka, Z., et al.*, Charge Inversion, Water Splitting, and Vortex Suppression Due to DNA Sorption on Ion-Selective Membranes and Their Ion-Current Signatures. Langmuir, 2013. 29(26): p. 8275-8283.
6. *Vobecka, L., et al.*, Heterogeneity of heterogeneous ion-exchange membranes investigated by chronopotentiometry and X-ray computed microtomography. Journal of Membrane Science, 2018. 559: p. 127-137.

ACTIVATED CARBONS AS NANOPOROUS ELECTRON-ION EXCHANGERS WITH HYDROPHILIC - HYDROPHOBIC PROPERTIES

Yury Volfkovich
A.N. Frumkin Institute of Physical Chemistry and Electrochemistry, Moscow, Russian Federation
E-mail: *yuvolf40@mail.ru*

Introduction

The importance for electrochemistry of the science of activated carbon (AC) is evidenced by the fact that A.N. Frumkin received his first government award in 1931 for research on AC. It is known that ACs have the following unique properties: high specific surface area ~ 50 - 2500 m^2/g, high adsorption capacity, electronic conductivity and the presence of a large number of surface groups (SG), for example:

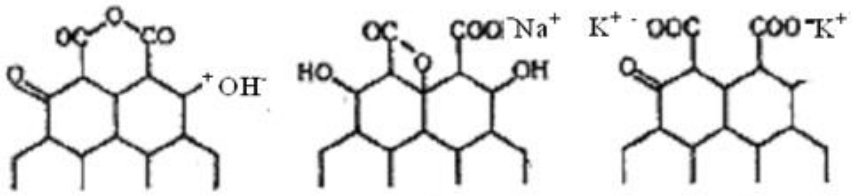

Experiments and Discussion

The porous structure and hydrophilic-hydrophobic properties of a number of ACs were studied in the widest range of pore radii ~ from 1 to 10^5 nm by the method of standard contact porosimetry (MSCP) developed by us [1,2]. It was found that ACs are unique materials because they have both hydrophilic and hydrophobic pores (see Fig.1 and Table). The dependences of the wetting angle with water on the pore radius, which largely depend on the distribution of SG in pores of different sizes (fig.2) [2], were measured.

Table: Cation and anion exchange capacity and porosimetric characteristics of AC electrodes

ACTIVATED CARBON	CATION EXCHANGE CAPACITY	ANION EXCHANGE CAPACITY	HYDRO-PHILIC POROSITY	HYDRO-PHOBIC POROSITY	TOTAL SPECIFIC SURFACE AREA	HYDROPHILIC SPECIFIC SURFACE AREA	AVERAGE WETTING ANGLE
	MMOL G^{-1}	MMOL G^{-1}	CM^3G^{-1}	CM^3G^{-1}	M^2G^{-1}	M^2G^{-1}	DEGREE
NORIT	**0.56**	**0.20**	**0.60**	**1.05**	**1260**	**570**	**89**
CH900	**0.06**	**0.70**	**2.95**	**0.61**	**1520**	**870**	**77**

It turned out that the studied ACs have sufficiently high values of both cation-exchange and anion-exchange capacities, comparable to the corresponding values of known ion-exchange membranes, for example, Nafion (see Table). For the first time surface conductivity (SC) of AC electrodes was obtained. The dependence of the ion conductivity on the concentration of dilute KCl solutions in the pores of the AC electrodes was measured in a specially designed 5-electrodes and 6-cells cell. When extrapolating to zero concentration, the values of SC are obtained, which are due to the presence of a large number of ionogenic surface groups (SG) in AC (Fig. 3) [3].

The presence of sufficient value of SC made it possible to use these AC electrodes to obtain clean drinking water by the method of capacitive deionization of water (CDI). The total ionic conductivity in the pores of the AC electrode is equal to the sum of the conductivity of the solution in the pores and the surface conductivity. After the clean water remains in the pores as a result of the deionization process, then these electrodes remain ion-conducting due to the SC. To obtain pure drinking water by CDI instead of the usual porous glass separator, we first used a cation – anion – exchange membrane with a mosaic structure that has surface conductivity in pure water due to the presence of ionogenic groups [2].

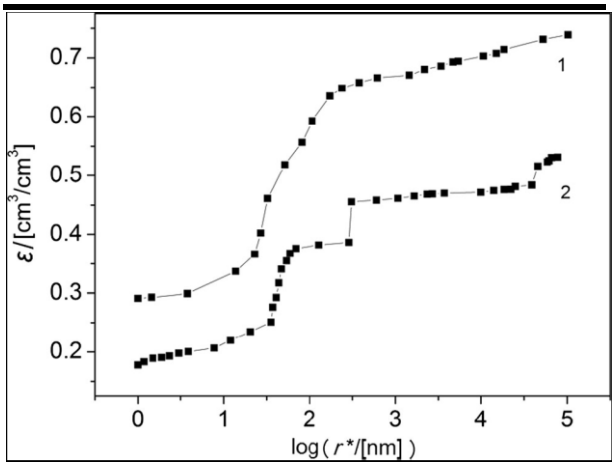

FIGURE 1 INTEGRAL PORE SIZE DISTRIBUTIONS FOR THE ELECTRODE BASED ON NORIT CARBON. THE CURVES ARE PLOTTED AS PORE VOLUME VS EFFECTIVE PORE RADIUS.WORKING LIQUIDS: OCTANE (1) AND WATER (2).

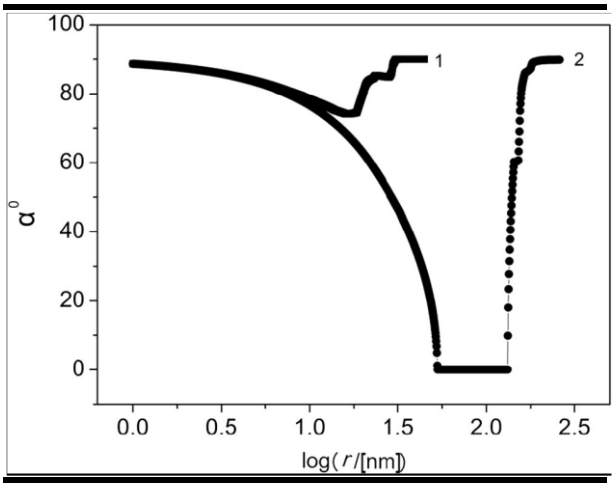

FIGURE 2 WETTING ANGLE FOR WATER AS A FUNCTION OF PORE RADIUS. MATERIALS ARE THE NORIT CARBON POWDER (1) AND THE ELECTRODE BASED ON CARBON NORIT (2).

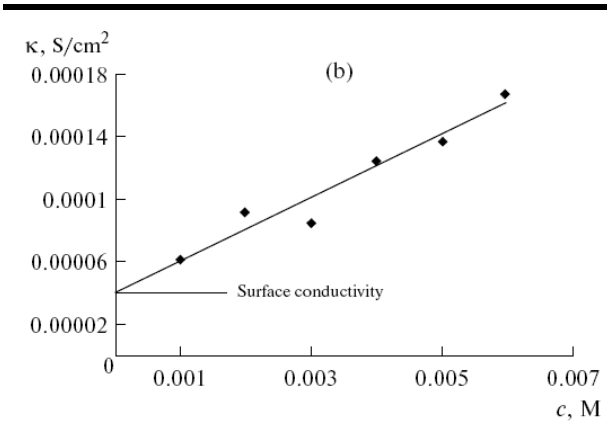

FIGURE 3. DEPENDENCES OF THE ELECTRIC CONDUCTIVITY OF (B) SAIT CARBON ELECTRODES ON THE VOLUME CONCENTRATION OF KCL. ILLUSTRATION OF EXTRAPOLATION TO OBTAIN.

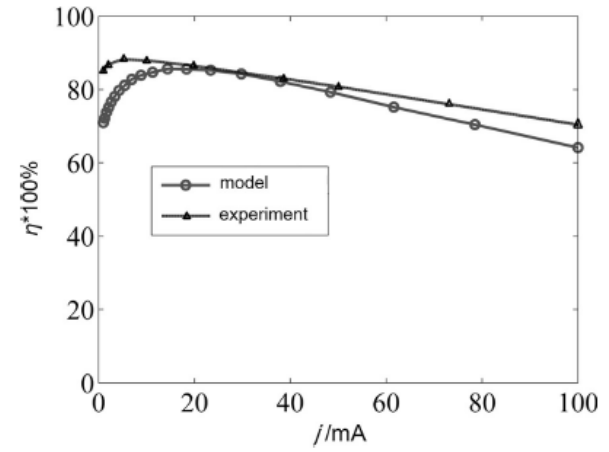

FIGURE 6. THEORETICAL AND EXPERIMENTAL 4VALUES OF EFFICIENCY AS FUNCTIONS OF CURRENT FOR ECSC BASED ON NORIT AC.

Fig. 4 shows the CVA curves obtained in an electrochemical cell with two AC electrodes separated by a mosaic membrane (MM) and impregnated with pure water. Rather high specific capacitances of 56–66 F/g for AC electrodes were obtained with a minimum scan rate. This is due to the presence of surface conductivity in the AC and MM. Fig. 5 shows the CVA curves for the same cell, measured at concentrations C= 0; 0.01 and 0.05 M KCl. As you can see, the maximum values of capacity do not depend on the salt concentration. This can be explained by the fact that this capacitance is determined by the concentration of surface groups in AC electrodes, and not by the capacitance of a conventional electrostatic electric double layer (EDL). As a result we have shown that using of AC electrodes and MM in CDI to obtain pure water is the way to solve the problem of its efficiency and minimize energy costs.

AC electrodes is widely used in supercapacitors (SC) due to its high specific surface area. We measured the energy efficiency as a function of current for SC. These dependences have maxima,

which are caused by the occurrence of two processes: charging — discharge of DEL and redox reactions of SG in AC, as well as ohmic losses (Fig. 6) [4]. This property allows to optimize the SC' design for smoothing peak loads of electrical networks.

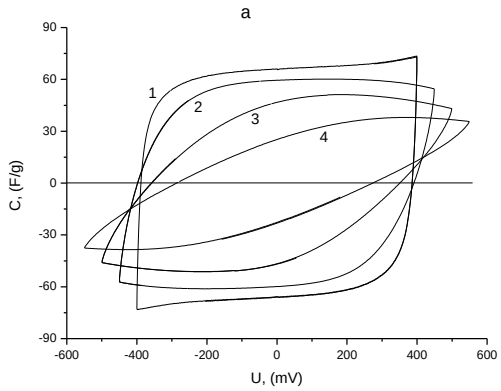

FIGURE 4. CAPACITANCE OF STATIC CELL WITH PURE WATER AS A FUNCTION OF VOLTAGE AT DIFFERENT SCAN RATE: 1 - 0.1 MV / S; 2 - 0.5 MV / S; 3 - 2 MV / S; 4–5 MV / S.. PURE WATER, AC NORIT , MOSAIC FILM MEMBRANE.

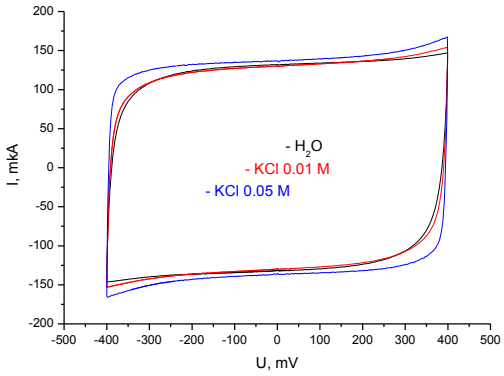

FIGURE 5. CAPACITANCE OF STATIC CELL AS A FUNCTION OF VOLTAGE FOR SCAN RATE 0.1 MV S-1 FOR DIFFERENT KCL CONCENTRATION. PURE WATER, AC NORIT , STRIPED MOSAIC MEMBRANE.

We have developed a mathematical model of capacitive processes for SCs with AC -electrodes, which well describes the experimental results (see Fig. 6). As a result of the deep cathode charging of AC-electrodes in concentrated acids, we for the first time obtained a record capacity value of 1000 F/g. This new phenomenon is due to the intercalation of hydrogen into carbon until the formation of a new compound C_6H. As a result of using MSCP for KJEC 600 carbon black and carbon nanofibrous material, a new phenomenon of superhydrophilicity was discovered, which is caused by the SG swelling.

Conclusion

Due to the remarkable properties of activated carbons they are excellent electrode materials for capacitive deionization and supercapacitors.

The work was supported by Russian Foundation of Basic Research (Grant no. 17-03-00092).

References

1. *Yu.M. Volfkovich, V.S. Bagotzky*. J. Power Sources 48 (1994) 339-348.
2. *Yu.M. Volfkovich, A. Yu. Rychagov, A.A. Mikhalin , M.M. Kardash , N.A. Kononenko , D.V. Ainetdinov , S.A. Shkirskaya , V.E. Sosenkin*. Desalination. 426 (2018) 1–10.
3. *Yu. M. Vol'fkovich, A. A. Mikhalin, A. Yu. Rychagov*. Russ. J. Electrochem. 2013, Vol. 49, No. 6, pp. 594–598.
4. *Yu.M. Volfkovich, D A. Bograchev, A.Yu. Rychagov, V.E. Sosenkin , M.Yu. Chaika*. J Solid State Electrochem (2015) 19:2771–2779.

INFLUENCE OF THE MANUFACTURING METHOD OF MOSAIC CATION – ANION - EXCHANGE MEMBRANES ON THE CHARACTERISTICS OF CAPACITIVE DEIONIZATION OF WATER

Yury Volfkovich[1], Alexey Mikhalin[1], Alexey Rychagov[1], Valentin Sosenkin[1], Marina Kardash[2], Natalya Kononenko[3], Sergei Tsipliaev[2], Svetlana Shkirskaya[3]

[1]A.N. Frumkin Institute of Physical Chemistry and Electrochemistry, Moscow, Russia, E-mail: *yuvolf40@mail.ru*

[2] Engels State Tehnology University, Engels, Saratov region, Russia

[3] Kuban State University, Stavropol'skaya Str., 149, Krasnodar, Russia

Introduction

Capacitive deionization (CDI) is a promising electrochemical method of water desalination. Economically, it is the most attractive technique in comparison with reverse osmosis (3 times cheaper), distillation, and electromembrane separation due to lower energy consumptions. CDI involves the passage of aqueous solution through the electrochemical cell between two highly dispersive carbon electrodes, often from activated carbon (AC) with high specific surface area (500 – 2500 m^2 g^{-1}). Low potential difference ($\geq$ 1.2 V) is applied providing a high safety level. Deep water purification requires high energy consumptions also in the case of CDI because of high ohmic losses caused by huge electrical resistance of pure water. At the same time, ionic conductivity of AC electrodes is rather high even in pure water [1] due to surface conductivity (SC) caused by large amount of ion exchange groups on the surface of carbon materials. Therefore, at the final stage of the deionization process, energy consumptions are determined by practically zero conductivity of water, which fills pores of the spacer between the electrodes. In this connection, a new membrane - electrode assembly (MEA) was developed and investigated in [2] for CDI processes to obtain pure water. The MEA design provides specially manufactured membrane of mosaic structure (mosaic membrane, MM) instead of inert porous spacer in order to decrease energy consumptions as much as possible. The membrane contained both cation and anion exchange groups. It was also necessary to use ACs that are characterized by highly developed surface and contain oppositely charged surface groups. The energy losses for the MEA , containing MM, were much less than those for the cell containing a conventional porous spacer. This is due to high ionic conductivity of MM that is caused by ion exchange groups. Both film and fibrous MM were used in [2].Porous structure of the membranes was researched with MSCP in [3]. As shown, the fibrous MM is characterized by higher total porosity and larger volume of macropores in comparison with the film membrane. Thus, hydrodynamic permittivity of the fibrous MM is higher. This gives a possibility to use this membrane for CDI processes under dynamic conditions. The film MM is not suitable for use in CDI due to the fact that macropores occupy only a small fraction of its porous structure, which does not provide the necessary hydrodynamic permeability. Therefore, the purpose of this study was to examine the effect of the manufacturing technique (and design) of fibrous mosaic cation-anion-exchange membranes on CDI characteristics.

Experiments and Discussion

Pressed fibrous MM "Polycon" was manufactured with the method developed in the Engels Technological Institute (Engels, Russia). The technique involves polycondensation filling of polymeric composite materials. "Polycon" MM is the composite material containing both strongly acidic cation exchange constituent and weakly basic anion exchange component. Synthesis of ion exchangers was performed on the outer surface and inside fibrous phenol-formaldehyde matrix. The cationite and anionite membranes were hot-pressed into each other. Analysis of micrographs, obtained by SEM, showed that using such manufacturing technique of mosaic membrane causes its nonsimilarity structure.

Striped mosaic membrane. 4 mm wide strips of weakly basic anion exchanger [4] and strongly acidic sulfonic exchanger were sequentially formed on the surface and in the structure of novolac phenol-formaldehyde fibrous matrix in accordance with the developed methods of synthesis and

curing of ion-exchange matrices directly on the fibrous base. In contrast to a pressed mosaic membrane, the striped membrane is completely similarity in chemical composition and structure across the thickness of the samples. The objects of study were samples obtained by the method of polycondensation filling on a fibrous basis (FB).

Composite carbon electrodes based on Norit DLC Supra 30 activated carbon (Norit The Netherlands BV) have been obtained with thickness of 150 μm. The other electrode was made of AC CH900 textile (Kuraray Company, Japan).

The values of cation and anion exchange capacity were determined both for the AC electrodes and MMs. As seen, membranes and electrodes possess both cation and anion exchange ability. This is fundamentally important for the CDI method to obtain pure water. The presence of cation-exchange and anion-exchange capacity in the AC is associated with the presence of a large number of surface groups.

The MSCP [3] was used to study the membranes. Water was used as working liquid for porosimetric investigations of MMs. It is known that the main flow of the aqueous solution through the membrane at CDI is carried out through macropores. From porosimetric data was obtained that the macroporous values of both membranes are quite large, which is good for using them in CDI.

It was measured the dependence of specific electrical conductivity of pressed and striped

MMs on concentration of equilibrium solution NaCl. Extrapolation of the curves to zero concentration gives the value of membrane conductivity in deionized water (surface conductivity), which depends on the presence of functional groups that is similar to conventional ion exchange membranes. It was shown, both MM studied possess significant surface conductivity, which leads to their possible use for CDI in obtaining pure water.

A static cell (without liquid flow) was applied to study electrochemical characteristics of the MEA that was preliminarily impregnated with deionized water. The cell contained two electrodes from Norit AC and MM between their. Preliminarily the electrodes and MM were penetrated be pure deionized water. Fig.1 illustrates cyclic Volt - Farad CVF) curves for a cell with a striped membrane (a) and with a pressed membrane (b) at different voltage sweep rates

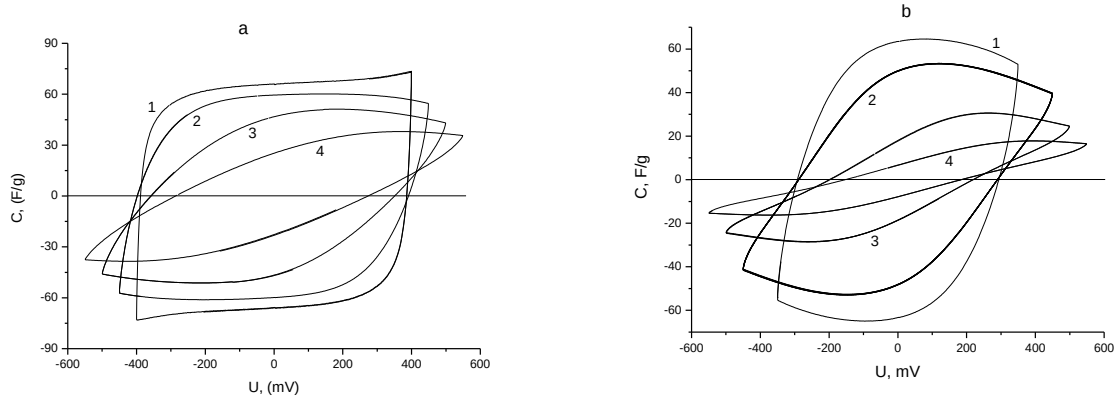

Figure 1. Cyclic Volt Farad curves for a cell with a striped membrane (a) and with a pressed membrane (b) at different voltage sweep rates: 1 - 0.1 mV/s; 2 - 0.5 mV/s; 3 - 2 mV/s; 4 – 5 mV/s.

These CVF curves for striped MM have the form of classical CVF curves for charging the double electric layer as for double-layer capacitors (DSC) with concentrated electrolytes, despite the fact that the curves in Fig. 1a were measured in pure water. This is due to the high concentration of cation-exchange and anion-exchange groups in both the AC Norit electrodes and the mosaic membrane. From fig. 1a, and fig. 1b it can be seen that the maximum values of specific capacitance (C) for striped MM and for pressed MM C = 66 F/g, and C = 60 F/g correspondingly. The higher characteristics of the CVF curves for MEA with a striped membrane as compared to MEA with a pressed membrane can be explained by the similarity of the structure across the thickness of the striped membrane as compared to the substantial nonsimilarity of the structure of the pressed membrane.

In a dynamic cell (with liquid flow), comparative studies of CDI operation were performed for two electrochemical cells with different mosaic membranes. The aim of the work was to obtain clean drinking water. As the initial salt, the KCl salt was taken with a concentration of 0.004 M. The following constant values of cell voltage were set: 1.2 V, 1.4 V, 1.6 V, 1.8 V and 2.0 V at liquid flow rates of 2.5 ml / min, 5 ml / min, 10 ml / min and 15 ml / min. The dependence of the electrical conductivity of an aqueous solution with time were measured during the stages of deionization (charging) and concentrating (discharging). From these data, the dependences of the concentration on the deionization time and concentrating time for different flow rates and voltages were calculated (Fig. 2), as well as the degree of deionization

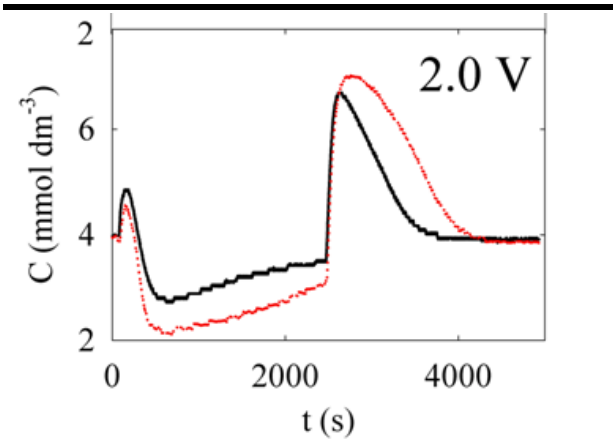

FIGURE 2. DEPENDENCE OF KCL CONCENTRATION ON DEIONIZATION TIME AND CONCENTRATION FOR A FLOW OF 15 CM³ / MIN AND VOLTAGE 2 V FOR PRESSED (BLACK) AND STRIPED (RED) MEMBRANES.

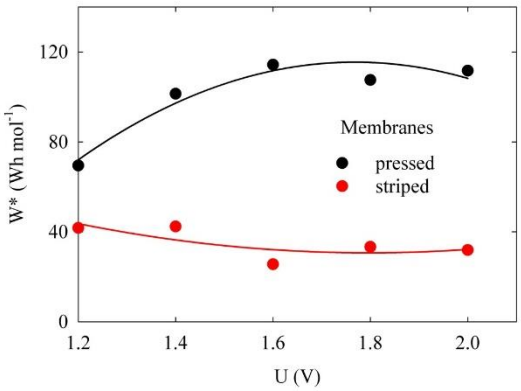

FIGURE 3. DEPENDENCE OF SPECIFIC ENERGY COSTS ON VOLTAGE FOR CDI WITH PRESSED AND WITH STRIPED MEMBRANES AT A FLOW RATE OF 15 CM³/MIN.

It was found that at a low flow rate (2.5 ml / min), the specific energy consumption per mole of absorbed salt is less for a pressed membrane, while for high flow rates (10–15 ml / min) the specific energy consumption is less for striped membrane. The degree of deionization at low flow rates is greater for a pressed membrane, and for high flow rates it is more for a striped membrane (Fig. 3). The specific energy consumption for deionization for the striped MM is 32 Wh / mol of salt, and for the pressed MM 112 Wh /mol at a flow rate of 15 ml / min and a voltage of 2.0 V. The degree of deionization under the same conditions is 0.47 for the striped MM, and for pressed MM is 0.32.

Conclusion

In order to obtain clean drinking water, taking into account the performance of the CDI installation, it is much preferable to use a striped membrane. In this case, there are large values of the deionization degree and smaller values of the specific energy consumption.

The work was supported by Russian Foundation of Basic Research (Grant no. 17-03-00092).

References

1. *Yu.M. Volfkovich, A.A. Mikhalin, A.Y. Rychagov.* Russ. J. Electrochem. 49 (2013) 594–598.
2. *Yu.M. Volfkovich, A. Yu. Rychagov, A.A. Mikhalin, M.M. Kardash , N.A. Kononenko, D.V. Ainetdinov, S.A. Shkirskaya, V.E. Sosenkin.* Desalination. 426 (2018) 1–10 .
3. *Yu.M. Volfkovich, V.S. Bagotzky.* J. Power Sources 48 (1994) 339-348.
4. *M.M. Kardash, N.B. Fedorchenko, O.V. Epancheva.* Fibre Chem. 34 (2002) 466–469.

HYDRATION AND IONIC TRANSPORT IN ION EXCHANGE MEMBRANES ON NMR DATA

[1,2] Vitaly Volkov, [1,2]Alexander Chernyak, [1]Olga Yarmolenko, [3] Vladimir Tverskoy, [4]Daniel Golubenko

[1]Institute of Problems of Chemical Physics RAS, 142432, Chernogolovka, Acad. N.N.Semenov av., 1, Russia

[2]Science Center in Chernogolovka RAS, 142432, Chernogolovka, Lesnaya str, 9, Russia

[3] Educational Institution of Higher Education "MIREA – Russian Technological University". Institute of Fine Chemical Technology named after M.V. Lomonosov, 119571, Moscow, pr. Vernadskogo, 86

[4] Kurnakov Institute of General and Inorganic Chemistry of RAS, Leninsky pr-t 31, 119991, Moscow, Russia

E-mail: *vitwolf@mail.ru*

Introduction

Hydration processes control ionic transport in ion exchangers. Nafion membrane is the more used and investigated among the rather wide ion exchange systems set. Membranes MSC, based on polyethylene and grafted sulfonated polystyrene show a good selectivity for alkaline metal cation separation Our presentation devotes to reveal the interconnection of cation hydration, water and ionic translational mobility. For this goal attainment NMR is applied as the main technique for direct hydration, ionic and water mobility in spatial scales from 10^{-10} to^{-4} m. The brief reviewer and novel experimental results are presented.

Experiments

Sulfonic cation-exchange MSC membrane of 20 micron thickness was synthesized by post radiation styrene grafted polymerization on peroxide low density polyethylene film following sulfonating by 96% sulfuric acid. Sulfonated group concentration, ion-exchange capacity, was 2.5 mg-eq/g. Nafion 117 membrane was also investigated as model system. ^{1}H,^{7}Li, ^{23}Na and ^{133}Cs high resolution spectra were recorded on AVANCE-III-500 Bruker NMR spectrometer. Self-diffusion coefficients of water molecules and H^+, Li^+, Na^+ and Cs^+ were measured by pulsed field gradient NMR on ^{1}H,^{7}Li, ^{23}Na and ^{133}Cs nuclei on AVANCE-III-400 Bruker NMR spectrometer with diff. 60 unit. Ionic conductivity was measured by impedance spectroscopy.

Results and Discussion

The main particularities of sulfonate groups hydration, water molecule and alkaline metal cation translational mobility and ionic conductivity were revealed by high resolution NMR, pulsed field gradient NMR and impedance spectroscopy techniques in membrane MSC, based on polyethylene and grafted sulfonated polystyrene and in Nafion 117 membrane as model system.

It was determined that at low water content in MSC and Nafion membrane counter ion H^+ forms hydroxonium ion $H_5O_2^+$, but with humidity increasing cation $H_9O_4^+$ is also arisen [1]. Hydration number of Li^+ cation in Nafion is about 3-4 water molecules per cation, some more details of cation hydration in perfluorinated sulfocation membranes MF-4SC are given in [2]. The hydration numbers are 4, 6 and 3 for Li+, Na+ and Cs+ correspondingly. Self-diffusion coefficients of water molecules and cation Li^+, Na^+, Cs^+ (for the first time in ion-exchangers) were measured by pulsed field gradient NMR on ^{1}H, ^{7}Li, ^{23}Na, ^{133}Cs nuclei. The dependences of water molecule and Li^+, Na^+ and Cs^+ self-diffusion coefficients on relative humidity RH are shown in Fig. 1,2. As it is shown in Fig.1 water self-diffusion humidity dependence is similar to the Li^+ self-diffusion coefficient humidity dependence. It means that lithium cation translational mobility and water molecule mobility are correlated.

Self-diffusion coefficient temperature dependences are shown in Fig. 3 for MSC membrane, as example. The main self-diffusion coefficients temperature dependence features is the increasing curve slopes in low temperature regions. High and low temperature dependence parts were approximated by Arrhenius equitation. At high water content the activation energies are close to bulk water activation energy. At low water content activation energies increase and became closer to each other.

Self diffusion coefficients of alkaline metal cation increase in the row $Li^+<Na^+<Cs^+$ in MSC membrane equilibrated with water as it is shown in Fig. 2 and Table 1. Cation conductivities were also measured by impedance spectroscopy. It was shown that conductivity of H^+ counter ion is essentially more compare to alkaline metal cations Fig.2). The conductivity values are the next row $Li^+<Na^+<Cs^+<H$ (Table 2), which is agreed with self-diffusion data. Proton conductivity humidity and temperature dependences calculated from Nernst-Einstein equation (1) and experimentally measured conductivities are in symbasis.

$$\sigma = ne^2 \frac{D}{kT} \tag{1}$$

where n is the number of charge carriers (H^+ cation) per unit volume; e is the electron charge (1.9 10^{-19} C); D is the self-diffusion coefficient; k is the Boltzmann constant (1.38 10^{-23} J/K); T – absolute temperature.

Ionic conductivities conductivities calculated from (1) are one order of magnitude more than experimental values in MSC membrane (Fig. 1,2 and Table1). The conductivities of H^+ and Li^+ cations calculated from self-diffusion coefficients are also essentially more compare with experimental conductivities in Nafion membrane. Evidently this fact is fundamental and more deep theoretical and experimental investigation is necessary which may proposal task in future.

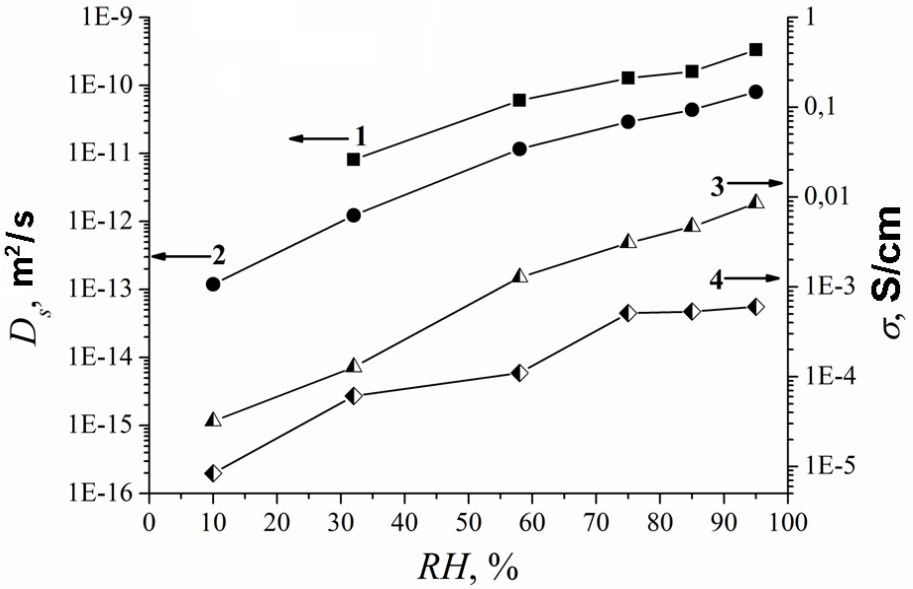

Figure 1. Humidity dependence of water molecule self-diffusion coefficients (curve 1); Li^+ self-diffusion coefficients (curve 2): ionic conductivity calculated from Nernst-Einstein equation (curve 3) and experimentally measured (curve 4) in Li^+ form of Nafion.

Table 1: Self-diffusion coefficients of water molecules D_s^{H2O}, Li^+, Na^+, Cs^+ cations D_s^{Me+}; ionic conductivities calculated from Nernst-Einstein equation σ_{calc} and experimentally measured conductivities σ_{exp} in MSC membrane in water

Ionic form	D_s^{H2O}, m²/c	D_s^{Me+}, m²/c	σ_{calc}, S/cm	σ_{exp}, S/cm
Li^+	$5\cdot10^{-10}$	$3.7\cdot10^{-10}$	$5\cdot10^{-2}$	$1.8\cdot10^{-3}$
Na^+	$7.8\cdot10^{-10}$	$4.6\cdot10^{-10}$	$6\cdot10^{-2}$	$3.1\cdot10^{-3}$
Cs^+	$8\cdot10^{-10}$	$7.7\cdot10^{-6}$	$1\cdot10^{-1}$	$5\cdot10^{-3}$

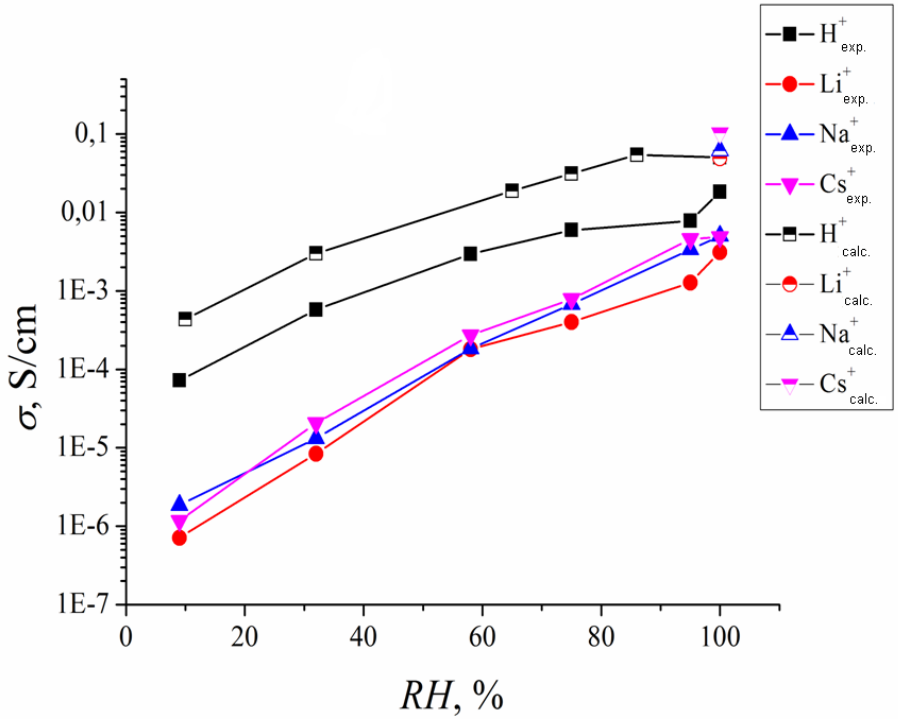

Figure 2. Humidity dependence of ionic conductivities in MSC membrane in H^+ and in Li^+, Na^+, Cs^+ forms.

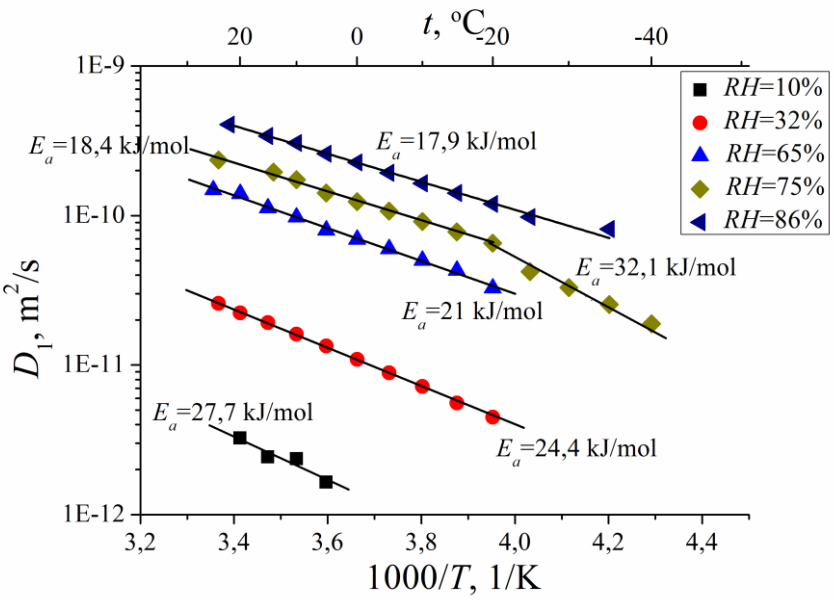

Figure3. Temperature dependence of self-diffusion coefficients in acid form MSC membranes at different water content.

This work was supported by Russian Foundation for Basic Research (projects No. 18-08-00423 A).

References

1. *A.V.Chernyak, S.V.Vasil'ev, I.A.Avilova and V.I.Volkov* Hydration and Water Molecules Mobility in Acid Form of Nafion Membrane Studied by 1H NMR Techniques, Applied Magnetic Resonance (Feb. 2019), DOI: 10.1007/s00723-019-1111-9
2. *V.I. Volkov, A.A. Marinin.* NMR methods for studying ion and molecular transport in polymer electrolytes // Russian Chemical Reviews 2013. V.82. p.248-272.

STUDY OF OXYGEN TRANSPORT IN GROSSLY NONSTOICHIOMETRIC OXIDES VIA OXYGEN PARTIAL PRESSURE RELAXATION TECHIQUE

[1,2]Bogdan Voloshin, [1]Sergey Bychkov, [1,2]Stanislav Chizhik, [1]Alexander Nemudry

[1]Institute of Solid State Chemistry and Mechanochemistry SB RAS, Novosibirsk, Russia

[2]Novosibirsk State University, Novosibirsk, Russia, E-mail: *csagbox@gmail.com*

Introduction

Nonstoichiometric oxides are characterized by high mixed (oxygen and electronic) conductivity, which makes them promising for development of solid oxide fuel cells, membranes for oxygen separation and oxygen sensors [1-4].

An important trend for such materials is the rate of oxygen exchange with the gas phase. To study the kinetics of oxygen exchange, a new method of oxygen partial pressure relaxation has been proposed. This technique is based on measuring the amount of oxygen, as a result of which a sample is obtained with a sharp change in the partial pressure of oxygen in the gas.

The purpose of this work is to determine the rate constant of surface oxygen exchange *k* for $La_{0.6}Sr_{0.4}CoO_{3-\delta}$ oxide (hereinafter LSC).

Experiments

LSC was synthesized by standard ceramic method. The obtained LSC cylinders were tableted from the fraction 56-64 microns. The sieved fraction was washed with alcohol to remove fines. The resulting powder was pressed and sintered at a temperature of 900°C. As a result, a sample with an open porosity of 25% was obtained.

Kinetic curves were recorded at a temperature of 600–800°C with a step of 50 degrees. Kinetic curves measured at oxygen partial pressure (used oxygen partial pressures: 0.001, 0.002, 0.003, 0.005, 0.007, 0.010, 0.015, 0.020 atm).

Results and discussion

From the obtained relaxation curves, we calculated the rate constant of surface exchange reaction *k* for LSC sample. The values of the constants: $k_{600} = 4.1\times10^{-4}$, $k_{650} = 3.9\times10^{-4}$, $k_{700} = 3.5\times10^{-4}$, $k_{750} = 3.7\times10^{-4}$, $k_{800} = 2.2\times10^{-4}$ см/с (error of determination of constants within 10%). The obtained data are consistent with literature data obtained by other methods.

Acknowledgements

The research was funded within the state assignment to ISSCM SB RAS (project No. AAAA-A17-117030310277-6).

References

1. *X. Tan, Z. Wang, B. Meng, X. Meng, K. Li*, Pilot-scale production of oxygen from air using perovskite hollow fiber membranes, J. Membr. Sci. 352 (2010) 189–196.
2. *Z. Rui, J. Ding, Y. Li, Y.S. Lin*, $SrCo_{0.8}Fe_{0.2}O_{3-\delta}$ sorbent for high-temperature production of oxygen-enriched carbon dioxide stream, Fuel. 89 (2010) 1429–1434.
3. *H.H. Wang, C. Tablet, T. Schiestel, S. Werth, J. Caro*, Partial oxidation of methane to syngas in a perovskite hollow fiber membrane reactor, Catal. Commun. 7 (2006) 907–912.
4. *M. Mori, Y.Itagaki, Y.Sadaoka*, Effect of VOC on ozone detection using semiconducting sensor with SmFe1-xCoxO3 perovskite-type oxides, Sensor. Actuat.B-Chem.163 (2012) 44–50.

ANALYSIS OF KINETIC AND THERMODYNAMIC PROPERTIES OF NON-STOICHIOMETRIC OXIDES IN REACTION WITH OXYGEN USING THE CONCEPTION OF CONTINUOUS HOMOLOGUOS SERIES

[1,2]Bogdan Voloshin, [1]Mikhail Popov, [1]Sergey Bychkov, [1,2]Stanislav Chizhik, [1]Alexander Nemudry

[1]Institute of Solid State Chemistry and Mechanochemistry SB RAS, Novosibirsk, Russia
[2]Novosibirsk State University, Novosibirsk, Russia, E-mail: *csagbox@gmail.com*

Introduction

Numerous studies of mechanism of oxygen exchange of mixed ionic-electronic conducting (MIEC) perovskites ($ABO_{3-\delta}$) with gas phase done in the last few decades [1-3] still leave many blind spots in this field that do not allow formulating general principles and stages of processes that determine the reaction on the oxide surface [4]. The interpretation of the kinetic data is complicated by the strong dependence of the oxides properties on widely varying oxygen nonstoichiometry δ [5]. A new fruitful approach, in which non-stoichiometric oxides are considered as continuous δ-homologous series [6] proposed for solving this problem, requires the development of a new methodology for the collection and analysis of kinetic data.

Experiments

$Ba_{0.5}Sr_{0.5}Co_{0.75}Fe_{0.2}Mo_{0.05}O_{3-\delta}$ (BSCFM5) δ-homologues were used as examples to demonstrate the novel methodology for studying the kinetics of oxygen exchange by oxygen partial pressure relaxation technique. It includes analyze of the kinetic data in an isostoichiometric cross-section, a nonlinear model of relaxation kinetics, a detailed consideration of the mass balance in the reactor, accounting the distribution of particle sizes in the sample and the response time of the experimental setup.

Results and Discussion

For the continuous series of BSCFM5 δ-homologues, the Brønsted-Evans-Polanyi relationship is established: the linear correlation of the Gibbs activation energy with the chemical potential of the oxide, as well as the compensation effect between the activation parameters of the equilibrium oxygen exchange rate.

Acknowledgements

The research was supported by RSF (project No. 18-13-00059).

References

1. *B. C. H. Steele and A. Heinzel*, Nature, 2001, 414, 345.
2. *W. Yang, H. Wang, X. Zhu, L. Lin*, Topics Catal., 2005, 35 (1–2), 155.
3. *H. J. M. Bouwmeester, A. J. Burggraaf*, In CRC Handbook of Solid State Electrochemistry; Gellings, P. J.; Bouwmeester, H. J. M., Eds.; CRS Press: Boca Raton., 1997, 501.
4. *G. Kim, S. Wang, A. J. Jacobson, L. Reimus, P. Brodersen, C. A. Mims*, J. Mater. Chem., 2007, 17, 2500.
5. *S. F. Bychkov, I. I. Gainutdinov, S. A. Chizhik, A. P. Nemudry*, Solid State Ionics, 2018, 320, 297-304
6. *S. A. Chizhik, A. P. Nemudry*, PCCP, 2018. 20(27), 18447-18454

PLASTISIZED POLYMER ELECTROLYTES BASED ON SULFONATED POLYSTYRENE: SOLVATION AND Li^+/Na^+ CONDUCTIVITY

[1,2]Daria Voropaeva, [1,2]Daniel Golubenko, [2]Ardalion Ponomarev, [1,2]Andrey Yaroslavtsev

[1]Kurnakov Institute of General and Inorganic Chemistry of the Russian Academy of Sciences, Moscow, Russia

[2]Institute of Problems of Chemical Physics of the Russian Academy of Sciences, Moscow, Russia

E-mail: *voropaeva-dd@yandex.ru*

Introduction

Searching for the new materials for lithium and sodium-ion batteries (LIBs and SIBs) is one of the most important tasks of alternative energy nowadays. Electrolyte, which provides ion transfer between electrodes, largely determines the performance of the batteries. Most of ion batteries are based on liquid electrolyte which are presented by the solution of some salts such as $MClO_4$, $MAsF_6$, MBF_6, MTf, MPF_6 and others ($M=Li^+$, Na^+) in different nonaqueos organic solvents. But using this electrolytes is unsafe and can leads to degradation of cathode and anode materials. Rejection of the most common liquid electrolytes and using the alternative types of electrolytes can provide greater safety, better stability, as well as a more convenient battery geometry. One of the most promising types of electrolytes are unipolar polymer electrolytes, containing low-molecular aprotic plasticizers.

This work is devoted to the synthesis and investigation of properties of Li^+ and Na^+ conducting polymer electrolytes with pores and channels filled with different aprotic organic solvents and study of transport properties. Polymers based on sulfonated polystyrene: sulfonated block copolymer of poly(styrene-ethylene-buthylene-styrene) (SSEBS), cross-linked sulfonated polystyrene and polymethylpentene (PMP+SPS) with different grafting and crosslinking degree, stretched polytetrafluoroethylene–sulfonated polystyrene (strPTFE+PS) were studied. The relationships between nature of solvents and polymer matrices, swelling, ionic form and conductivity were studied.

Experiments

PMP + sPS and strPTFE+PS films were synthesized according to a procedures described in [1] and [2], respectively. SSEBS and PMP+sPS films were sulfonated in 3 vol % solution of chlorosulfonic acid in dichloroethane at room temperature for 30 min. The reaction was terminated by methanol addition. strPTFE+sPS and SSEBS films were converted to Li^+ and Na^+ forms by ion exchange in a 2M MCl solution ($M = Li^+, Na^+$). Ion exchange in the PMP+sPS polymer was carried out in 1M solutions of MOH ($M = Li^+$, Na^+) in methanol in the temperature range 50 - 70 °C for 2 hours. To remove solvents from membrane pores, they were dried under vacuum at 70 °C for 4 h. To obtain plasticized polymer electrolyte prepared samples were placed in glove argon-filled box (with a moisture level <10 ppm) and placed in individual solvents dimethylformamide (DMF), dimethyl sulfoxide (DMSO), dimethyl acetamide (DMA), and also in a mixture of solvents: ethylene carbonate and propylene carbonate (EC-PC); ethylene carbonate and dimethylacetamide (EC-DMA) and ethylene carbonate, propylene carbonate, dimethylacetamide, tetrahydrofuran (EC-PC-DMA-THF). The membranes were kept in these solutions over activated molecular sieves 3 Å for 2 days.

Ion-exchange capacity (IEC) was determined using acid-base titration method.

The solvation degree was determined as the ratio of the amount of sorbed solvent to the number of sulfo-groups of the membrane. The amount of sorbed solvent was calculated based on the increase in the mass of the membrane during swelling.◦

Conductivity of obtained membranes was determined by impedance spectroscopy by two probe method in a frequency range from 2 MHz to 10 kHz using carbon sheets electrodes in the temperature range of -20 ^{0}C to 50 ^{0}C under Ar atmosphere.

Results and Discussion

The process of membrane swollen is observed after the previously dried membranes were put into the organic solvents. During this process, organic solvents fill the system of pores and channels of obtained membranes. In general, ionic conductivity of obtained membranes increases with the increase of solvation degree and for the membranes under study, sorption of the organic solvents is shown to decrease in the following order DMSO>DMA>DMF>EC-DMA>EC-PC-DMA-THF>EC-PC. DMSO-containing membranes are characterized by the highest solvation degree and ionic conductivity due to the high dielectric permittivity (ε=45) and dipole moment (μ=3.96 D) and rather low viscosity (η=2.0 mPa·s) of DMSO.

Polymer electrolytes based on strPTFE+sPS membrane are characterized by the lowest solvation degree and ionic conductivity among studied polymers (Figure 1a) and this values do not exceed $5 \cdot 10^{-5}$ S/cm at 25 °C and 6 molecules per 1 sulfo-group for membrane in Li^+ form, containing DMSO. Obtained electrolytes have higher Li^+, than Na^+ conductivity (Figure 1a) due to the small size of Li^+ and it's greater mobility.

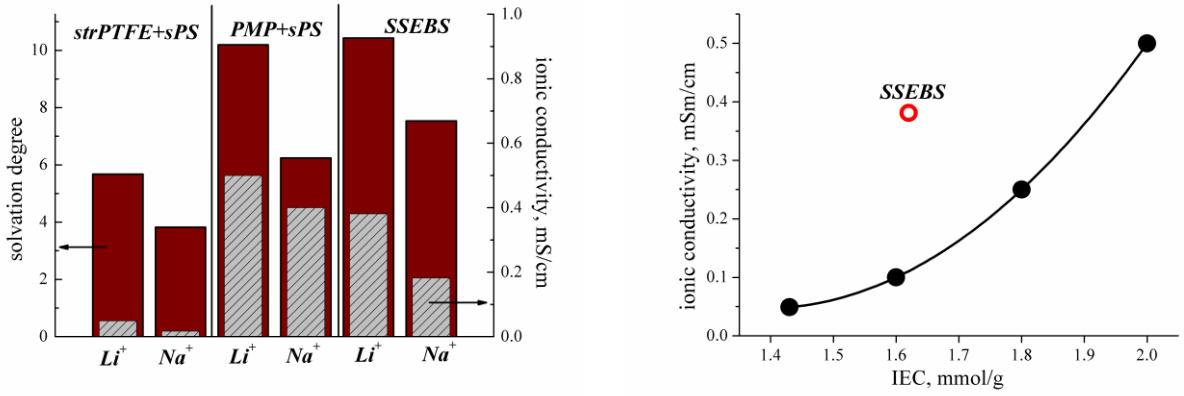

a *b*

Figure 1. Ionic conductivity at 25 °C and solvation degree of DMSO-swelling membranes (a), ionic conductivity at 25 °C of DMSO-swelling membranes in Li^+ form versus their IEC (b).

In general, the ionic conductivity increases with the increasing of IEC of the membranes. The exception is the SSEBS polymer (Figure 1b). This fact may be explained by the more flexible nonpolar polymer chain of SSEBS, which contributes to the formation of long ion-conducting channels.

DMSO-containing membranes are characterized by the highest ionic conductivity only at temperature above 5 – 15 °C, which is caused by the freezing of DMSO in the pores of the membranes. Membrane intercalated by DMF and a mixture of EC-PC-DMA-THF are characterized by a constant phase composition in a broad temperature range and the highest ionic conductivity at low temperature.

This work was financially supported by the Russian Science Foundation (project No 17-79-30054)

References

1. *D.V. Golubenko, A.B. Yaroslavtsev.* New approach to the preparation of grafted ion exchange membranes based on UV-oxidized polymer films and sulfonated polystyrene // Mendeleev Commun. 2017. V. 27. P. 572-573.
2. *E.F. Abdrashitov, D.A. Kritskaya, V.C. Bokun , A.N. Ponomarev , K.S. Novikova, E.A. Sanginov , Yu.A. Dobrovolsky.* Synthesis and properties of stretched polytetrafluoroethylene–sulfonated polystyrene nanocomposite membranes // Solid State Ionics 2016. 286. P.135-140.

SURPRISING DEPENDENCE OF THE CURRENT DENSITY OF BROMATE ELECTROREDUCTION ON THE MICROELECTRODE RADIUS

[1,2,3,4]Mikhail Vorotyntsev, [1,2,3]Anatoly Antipov, [1,2,3]Dmitry Konev

[1] D. I. Mendeleev University of Chemical Technology of Russia, Moscow, Russia
[2] M. V. Lomonosov Moscow State University, Moscow, Russia
[3] Institute for Problems of Chemical Physics, Russian Academy of Sciences, Chernogolovka, Russia
[4] ICMUB, UMR 6302 CNRS-Université de Bourgogne-Franche-Comté, Dijon, France
Email: *mivo2010@yandex.com*

Introduction

Bromate anion, BrO_3^-, has recently been proposed as a prospective oxidant for redox flow cells [1] since its 6-electron transformation into bromide anion, Br^-, in combination with a high saturation concentration of $LiBrO_3$, about 9 M, means a very high value of its redox capacity (redox-charge density), about 800 A h/kg and 1400 A h/dm^3 [2]. Earlier this system had not attracted attention for such application since bromate anions are not electroactive at all known electrode surfaces because of the multi-electron character of the process accompanied by rearrangement of several covalent bonds. As a way to overcome this problem it was proposed [1] to use a mediator redox cycle composed of two steps: reversible transformation at the electrode surface:

$$Br_2 + 2\ e^- \rightleftarrows 2\ Br^- \qquad (1)$$

and comproportionation reaction inside the solution phase:

$$BrO_3^- + 5\ Br^- + 6\ H^+ \rightarrow 3\ Br_2 + 3\ H_2O \qquad (2)$$

to regenerate Br_2 species.

Set of transport equations for the components of the system coupled with chemical step (2) in solution and electrochemical step (1) as boundary condition for the bromate process at the rotating disk electrode (RDE) was solved under steady-state conditions for various descriptions of the convective mass transfer [2-5]. It was assumed that the bulk solution contains dominantly a bromate salt and a strong acid, with a very small addition of the electroactive component, Br_2.

Paradoxical results of this analysis for the maximal current density, j^{max} (corresponding to a sufficiently high cathodic over potential) as a function of the RDE rotation frequency are shown in Figures 1a and 1b.

Figure 1a demonstrates that an ***intensive convection*** (high rotation frequencies) leads to ***very weak currents***. Diminution of the convection intensity results in a drastic increase of the current by several orders of magnitude, with passage of j^{max} via a ***maximum*** followed by a progressive decrease of j^{max} for even lower rotation frequencies.

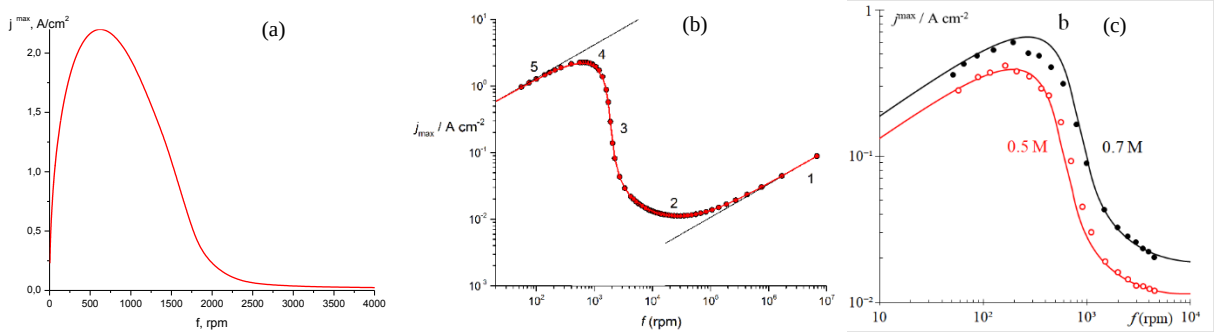

Figure 1. Dependence of the maximal current density of the bromate reduction for RDE under steady-state conditions on the electrode rotation frequency. Theoretical predictions (a) and (b). Bulk solution composition: 1 M BrO_3^- + 1 mM Br_2 + 5 M H^+. Left: linear scale for both coordinates. Right: bilogarithmic coordinates. Comparison of predictions (solid lines) with experimental data (points) in bilogarithmic coordinates: (c). Bulk solution composition: x M BrO_3^- + 1 mM Br_2 + 2 M H_2SO_4; x = 0.5 M or 0.7 M.

Figure 1b shows more distinctly quantitative features of this dependence. Its ***anomalous branch*** (segment 3) where ***diminution*** of the rotation frequency leads to ***enormous increase*** of the current separates two regions possessing quite different properties. Currents within the high-frequency range (segments 1 and 2) are very weak and are of the order of the diffusion-limited current of Br_2 so that they are proportional to the bulk-solution concentration of Br_2. On the contrary, the low-frequency range (segments 4 and 5) corresponds to very strong currents that are ***comparable to (and even exceed) the diffusion-limited current density for the non-electroactive BrO_3^- species***. Moreover, j^{max} within this frequency region is ***independent of the bulk-solution concentration of the catalytic species, Br_2***.

All these results are directly related to the ***autocatalytic*** property of the redox cycle, Eqs. (1) and (2): 5 Br^{-+} ions consumed by one act of comproportionation step (2) produce 3 Br_2 molecules which generate 6 Br^- ions so that passage of the cycle results in progressive accumulation of the components of the catalytic redox couple, Br_2/Br^-, up to the level needed for the complete consumption of BrO_3^- species diffusing from the bulk solution into the kinetic layer near the electrode surface.

All these surprising predictions of the theory were confirmed by experimental data (Figure 1c). This result represents a direct proof of both the autocatalytic reaction mechanism given by Eqs. (1) and (2) and our analysis based on this reaction scheme.

Bromate reduction at microelectrode: theory [7] and experiments [8]

Studies of electrochemical reactions with the use of microelectrodes have recently become an active area. Among their advantages one may note a much simpler equipment (no need in such a complicated device as RDE) and rapidity of measurements (short relaxation period). For the bromate process a very important merit is due to a small amount of the passing charge since this charge changes easily the bulk-solution concentration of the catalytic species, Br_2, in view of its very low value (at the millimolar or even micromolar level).

In ref. [7] we have derived approximate analytical solutions of the same transport equations based on Eqs (1) and (2) for the bromate process taking place at the surface of (hemi)spherical microelectrode of a radius, r_0.

Graphical illustrations of these solutions for the maximal current density, j^{max}, as a function of the electrode radius are given in Figure 2a. One should keep in mind that j^{max} is proportional to r_0^{-1} for a simple redox reaction, i.e. the current density is ***increasing monotonously for smaller electrode radii***. On the contrary, the same dependence predicted for the bromate process is given by a complicated graph. The current density is very low for the range of smaller electrode radii. For larger radii the current density increases drastically to reach a maximum followed by a slow decrease for even larger radii.

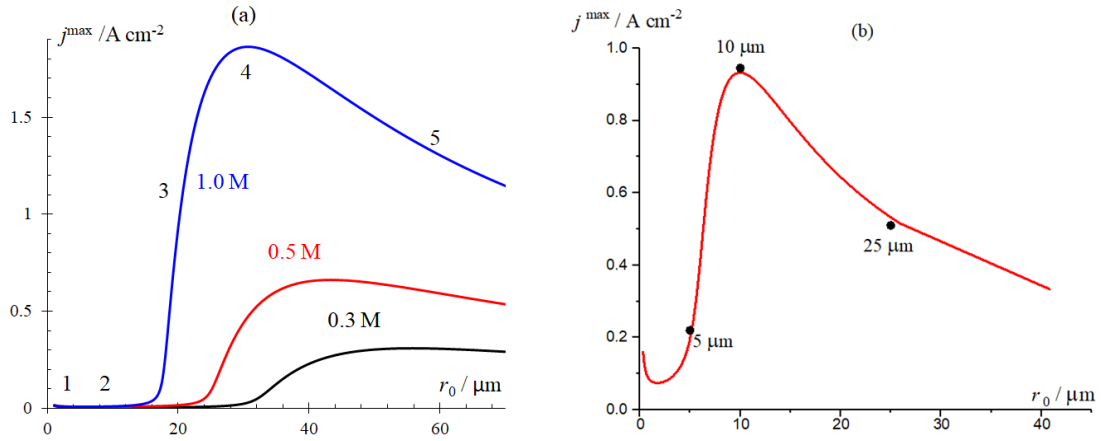

Figure 2. Dependence of the maximal current density, j^{max}, of a microelectrode on: (a),(b) its radius or (c) on its inverse radius, r_0^{-1}. Graphs (a) theoretical predictions for various bulk-solution concentration of BrO_3^-; (b), (c) experimental data for 0.2M $NaBrO_3$ + 4M H_2SO_4 (points) vs. theoretical line.

This behavior may be interpreted again in terms of the ***autocatalytic*** character of the bromate process.

If the radius is smaller than the kinetic layer thickness (where Br^- ion generated at the electrode are consumed by comproportionation reaction (2)), then the spatial area where Br_2 species are generated by step (2) is located outside the diffusion layer near the microelectrode surface so that they do not return to the electrode surface to participate again in step (1). As a result there is ***no catalysis of the bromate transformation by the Br_2/Br^- redox couple*** and the current is solely due to the reduction of Br_2 molecules from the bulk solution.

For sufficiently large microelectrode radii the diffusion layer is much thicker than the kinetic layer. As a result, step (2) takes place deeply inside the diffusion layer and Br_2 molecules generated by this step return mostly to the electrode surface. Then, the mediator redox cycle becomes very efficient and the Br_2 and Br^- concentrations grows strongly inside the kinetic layer, thus inducing a rapid transformation of BrO_3^- ions via step (2) inside the solution phase, thus leading to a strong current density.

For even larger radii the maximal current density is decreasing parallel to a lower diffusion-limited flux of bromate ion from the bulk solution into the kinetic layer.

Figure 2b provides experimental data points for the maximal current density of three microelectrodes of various radii, 5 μm, 10 μm and 25 μm. It increases for the 10 μm electrode, compared to the larger (25 μm) one but the further decrease of the radius to 5 μm leads to a ***decrease*** of the current density.

One can also see from Figure 2b that the theoretical predictions (solid line) agrees well with these experimental data.

Acknowledgements

The reported study was funded by RFBR according to the research project № 18-03-00574.

References

1. *Y. V. Tolmachev, A. Pyatkivskiy, V. V. Ryzhov, D. V Konev, M. A. Vorotyntsev*. Energy cycle based on a high specific energy aqueous flow battery and its potential use for fully electric vehicles and for direct solar-to-chemical energy conversion. J. Solid State Electrochem. 2015. V. 19. P. 2711-2722.
2. *M. A. Vorotyntsev, A. E. Antipov, D. V. Konev*. Bromate anion reduction: novel autocatalytic (EC") mechanism of electrochemical processes. Its implication for redox flow batteries of high energy and power densities. Pure Applied Chemistry. 2017. V. 89. P. 1429–1448
3. *M. A. Vorotyntsev, D. V. Konev, Y. V. Tolmachev*. Electroreduction of halogen oxoanions via autocatalytic redox mediation by halide anions: novel EC" mechanism. Theory for stationary 1D regime. Electrochim. Acta. 2015. V. 173. P. 779-795
4. *M. A. Vorotyntsev, A. E. Antipov*. Reduction of bromate anion via autocatalytic redox-mediation by Br_2/Br^- redox couple. Theory for stationary 1D regime. Effect of different Nernst layer thicknesses for reactants. J. Electroanal. Chem. 2016. V. 779. P. 146-155.
5. *M. A. Vorotyntsev, A. E. Antipov*. Bromate electroreduction from acidic solution at rotating disk electrode. Theory of steady-state convective-diffusion transport. Electrochim. Acta. 2017. V. 246. P. 1217-1229
6. *A. D. Modestov, D. V. Konev, A. E. Antipov, M. M. Petrov, R. D, Pichugov, M. A. Vorotyntsev*. Bromate electroreduction from sulfuric acid solution at rotating disk electrode: experimental study. Electrochim. Acta. 2018. V. 259. P. 655-663
7. *M. A. Vorotyntsev, A. E. Antipov*. Bromate electroreduction from acidic solution at spherical microelectrode under steady-state conditions: theory for the redox-mediator autocatalytic (EC") mechanism. Electrochim. Acta. 2017. V. 258. P. 544-553
8. *D. V. Konev, A. E. Antipov, M. M. Petrov, M. A. Shamraeva, M. A. Vorotyntsev*. Surprising dependence of the current density of bromate electroreduction on the microelectrode radius as manifestation of the autocatalytic redox-cycle (EC″) reaction mechanism. Electrochem. Comm. 2018. V. 86. P. 76-79.

EXPERIMENTAL STUDY OF SWITCHABLE ION TRANSPORT IN CARBON COATED NANOPOROUS ALUMINA MEMBRANES

[1,2]Anton Vyatkin, [2]Anastasia Bortsova, [2]Mikhail Simunin, [2]Maksim Mishnev, [1,2]Ilya Ryzhkov

[1]Institute of Computational Modeling, Federal Research Center KSC SB RAS, Krasnoyarsk, Russia
[2]Siberian Federal University, Krasnoyarsk, Russia
E-mail: *v_anton_s@icm.krasn.ru*

Introduction

In recent years, the studies of ion transport in nanopores and nanochannels have attracted increasing interest. These studies are of fundamental importance in various fields of science and technology, such as the separation of mixtures and production of pure substances [1], the electrochemical conversion of energy [2], the development of chemical sensors [3], and physiology and molecular biology of cells [4].

An important parameter in the characterization of membrane ionic permselectivity is the membrane potential at zero current [5]. It appears between two electrolyte solutions with different concentrations separated by a charged membrane. In this case, the Donnan equilibrium between diffusion and electric forces results in the corresponding potential jumps at membrane/solution interfaces, which both contribute to the value of membrane potential.

Earlier, it was shown that the ionic selectivity of a nanoporous track-etched membrane with electrically conductive surface can be continuously switched from anion to cation by varying the surface potential externally from positive to negative direction with respect to potential of zero charge [6]. The selectivity was assessed by measuring the membrane potential at zero current. Later, the possibility of controlling diffusion fluxes of ions by means of an external electric field was demonstrated [7]. Preliminary experimental results on controlling the membrane potential at zero current and ionic conductivity by externally applied potential were reported in [8]. The authors used highly porous ceramic membranes (C-Nafen) made from alumina nanofibers (10–15 nm in diameter) covered by a conductive carbon coating [9, 10].

In this work, a detailed experimental study of switchable ion transport in nanoporous C-Nafen membranes is performed. The variation of membrane potential by changing the potential applied to conductive membrane surface is investigated for different electrolyte concentrations.

Experimental

To study the transport properties of the C-Nafen membranes, an experimental setup was constructed (Fig. 1). The setup includes a fluoroplastic cell, which is divided into two halves by a membrane, and two electrical measuring circuits. To minimize the concentration polarization, the solutions in both half–cells are stirred by a closed loop pumping system based on Lead fluid BT601L peristaltic pump with Masterflex L/S Easy–Load II Head (USA). The setup comprises a P-20X potentiostat (Elins, Russia), which is referred to as Potentiostat A (Fig. 1). This device operates in accordance with a two-electrode circuit in the voltmeter mode and measures the membrane potential, which characterizes the ion-selective properties of membrane. The setup also includes Pi-50Pro potentiostat (Elins, Russia) referred to Potentiostat B. It operates in accordance with a three-electrode circuit. The working electrode is a conductive membrane; the counter electrode is a platinum wire. Potentiostat B is used to provide the polarization of the conductive membrane. Predetermined electric field is generated inside the pores by setting the potential of the conductive membrane surface relative to a 4.2 M Ag/AgCl reference electrode.

Results and discussion

The dependence of membrane potential on the applied surface potential is shown in Fig.2. The concentrations of aqueous KCl electrolyte in the half-cells are kept at constant but different values: C_L*=10 mM,* C_R*=1 mM.* The variation of the external potential in the range from

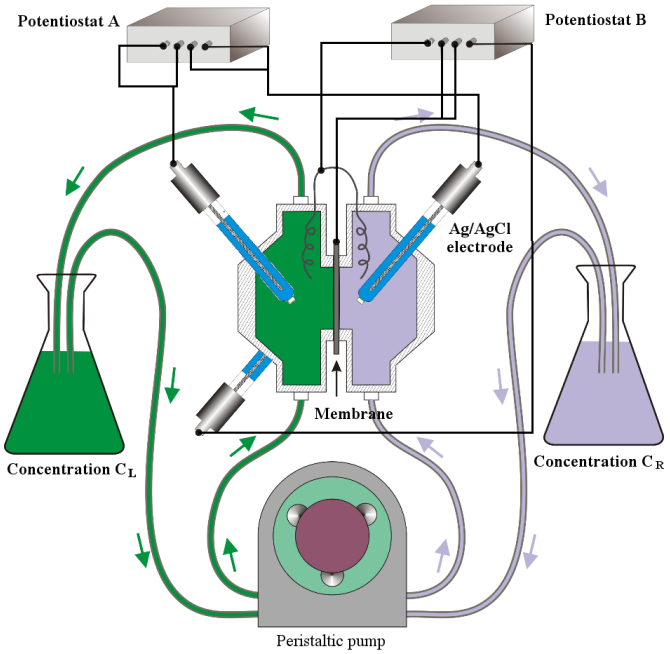

Figure 1. The experimental setup.

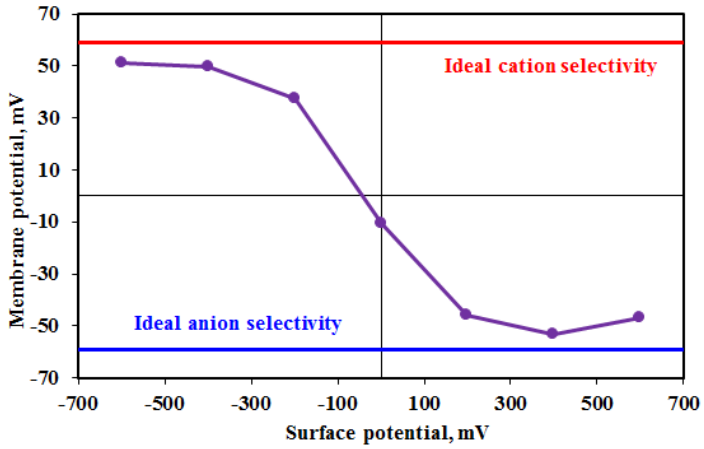

Figure 2. The dependence of membrane potential on the potential applied to the membrane surface. C_L=10 mM, C_R=1 mM. The lines correspond to ideal cation and anion selectivity.

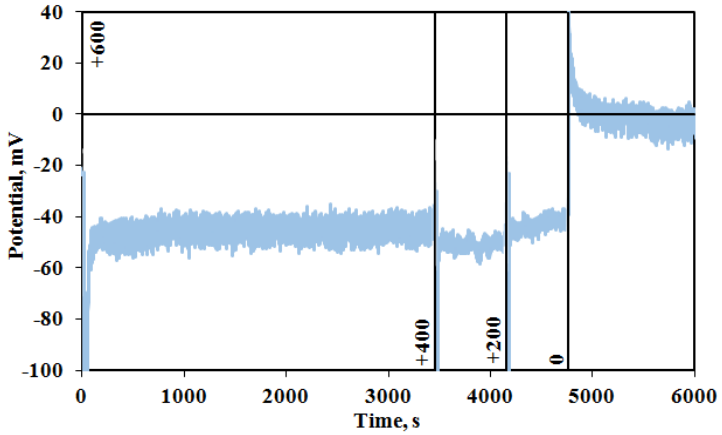

Figure 3. Variation of membrane potential during transient state. C_L=10 mM, C_R=1 mM. The applied surface potentials are +600, +400, +200, 0 mV.

–600 to +600 mV leads to a change in the membrane potential from approximately +50 to –50 mV, respectively. This behavior can be interpreted as follows: in the case of the negative polarization of the membrane, the pore surface is charged negatively; this effect leads to an increase in the cation concentration in the pores (cation-selective membrane). In the case of positive polarization, anions accumulate in the pores; as a consequence, the membrane becomes anion-selective. For large applied potentials (< –400 mV and > +400 mV), the values of membrane potential approach the Nernst potential, which corresponds to the ideal anion (or cation) selectivity.

The transient behavior of membrane potential measured by Potentiostat A (see Fig. 1) is shown in Fig. 3. During the transient time, the membrane is charged by the potentiostat B until the charging current becomes close to zero. It can be seen that the membrane potential approaches some stationary value at each applied potential. The points presented in Fig. 2 correspond to time averaging of the signal shown in Fig. 3 when the stationary state is reached.

Conclusion

In this work, we have experimentally investigated the switchable ionic selectivity of C-Nafen membranes. It is shown that the variation of potential applied to nanoporous membrane surface can provide a continuous change of membrane selectivity from anion to cation.

The work is supported by the Russian Foundation for Basic Research Grant № 18-38-20046.

References

1. *Strathmann H.* Introduction to membrane science. Wiley–VCH, Weinheim, Germany, 2011.
2. *Cipollina A., Micale G.* Sustainable Energy from Salinity Gradients. Elsevier/Woodhead Publishing, 2016.
3. *Bobacka J., Ivaska A., Lewenstam A.* Potentiometric ion sensors, Chem. Rev. 108, 329 (2008).
4. *Tagliazucchi M., Szleifer I.* Transport mechanisms in nanopores and nanochannels: can we mimic nature? Mater. Today, 2015. V. 18, 131.
5. *Tanaka Y.* Ion exchange membranes: fundamentals and applications. Elsevier, Amsterdam, 2015.
6. *Nishizawa M., Menon V.P., Martin C.R.* Metal nanotubule membranes with electrochemically switchable ion-transport selectivity. Science 1995, V. 268, 700.
7. *Martin C.R., Nishizawa M., Jirage K., Kang M., Lee S.B.* Controlling ion-transport selectivity in gold nanotubule membranes. Adv. Mater. 2001, V. 13, 1351.
8. *Lebedev D.V., Solodovnichenko V.S., Simunin M.M., Ryzhkov I.I.* The influence of electric field on the ion transport on nanoporous membranes with conductive surface. Petroleum Chemistry, 2018. V. 58. Issue 6. P. 474–481.
9. *Solodovnichenko V.S., Lebedev D.V., Bykanova V.V., Shiverskiy A.V., Simunin M.M., Parfenov V.A., Ryzhkov I.I.* Carbon coated alumina nanofiber membranes for selective ion transport. Advanced Engineering Materials, 2017, V. 19, 1700244.
10. *Solodovnichenko V.S., Simunin M.M., Lebedev D.V., Voronin A.S., Emelianov A.V., Mikhlin Y.L., Parfenov V.A., Ryzhkov I.I.* Coupled thermal analysis of carbon layers deposited on alumina nanofibers. Thermochimica Acta, 2019, V. 675, Accepted, in press.

MOTION THROUGH NON-HOMOGENEOUS POROUS MEDIUM: HYDRODYNAMIC PERMEABILITY OF MEMBRANE COMPOSED BY CYLINDRICAL PARTICLES

Pramod Kumar Yadav

Department of Mathematics, Motilal Nehru National Institute of Technology Allahabad, Prayagraj-211004 (U.P.), India, E-mail: *pramodky@mnnit.ac.in*

Abstract: The present problem concern with the flow of viscous steady incompressible fluid through non-homogeneous porous medium. Here, non-homogeneous porous medium is a membrane built up by cylindrical particles. The flow outside the membrane is governed by Stokes equation and the flow through non-homogeneous porous membrane composed by cylindrical particles is governed by Darcy's law. In this work, we discussed the effect of various fluid parameters like permeability parameter k_0, discontinuity coefficient at fluid-non homogeneous porous interface, viscosity ratio of viscous incompressible fluid region and non-homogeneous porous region, etc. on hydrodynamic permeability of a membrane, stress and on velocity profile. The comparative study for hydrodynamic permeability of membrane built up by non-homogeneous porous cylindrical particles and porous cylindrical shell enclosing a cylindrical cavity has been studied. The effects of various fluid parameters on the streamlines flow patterns are also discussed.

Keywords: Stokes equation; Darcy's equation; Stream function; Hydrodynamic Drag force, Hydrodynamic permeability.

GAS SEPARATION PROPERTIES OF SILICA-ORGANIC POLYMER MEMBRANES MODIFIED BY PLASMA AND OZONE EXPOSURE

Nail Yanbikov, Kseniia Otvagina, Tatyana Sazanova, Alexandr Logunov, Ilya Vorotyntsev

Laboratory of membrane and catalytic processes, Nizhny Novgorod State Technical University n.a. R.E. Alekseev, Nizhniy Novgorod, Russia, E-mail: *nailyanbikov@gmail.com*

Introduction

Nodaway the membrane technologies for a gas separation are rapidly developing and considered one of the most cost effective and environmentally friendly ways to extract targeted gas substances. However, the efficiency of gas separation to the great extent correlate with physico-chemical properties of the material chosen as a membrane material. In this regard, a huge demand for new efficient, low-cost and stable materials for gas separation exists and promotes further research in this field.

Silicon-based membranes, such as polydimethylsiloxane (PDMS) or poly (vinyltrimethylsilane) (PVTMS) are commercially available. Thus they are widely used for gas separation due to its high permeability and stability. Their main disadvantage of these materials is comparatively low values of its selectivity. Ultrathin selective layer casted onto the PDMS or PVTMS support can, to some extent, improve membrane selectivity and lead to the minor reduce in permeability. Composite membranes have some unique advantages: they can be applied for various separation techniques, show optimum combination of transport properties, as well as rational use of custom-made functional polymer forming a selective layer. However, a production of composite membranes is usually complicated by low adhesion of the selective layer to the porous support due to the surface properties of the substrate – topography, surface free energy and the presence of functional groups. Low adhesion lead to the defected selective layer, which cannot be used for membrane applications. Modification of obtained polymers by exposure in O_3 or by plasma treatment can significantly improves surface adhesion through changes in surface energy. Secondary advantage of this process, it could be enhanced selectivity of the modified membranes due to the firs step of the gas separation process occurs on the surface of a membrane.

Experiments

PVTMS and PDMS membranes are commercial composite membranes supplied by Vladipor JSC (Russia). Surface treatment was conducted in O_3 flow (1 ml/sec) or in nonequilibrium radiofrequency low temperature argon plasma at 10W or 40W under low pressure. Surface modification was characterized by diffuse reflectance infrared Fourier transform IR-spectroscopy (DRIFTS), atomic force microscopy (AFM) and wettability measurements. Roughness parameters (R_a, R_z) and surface energies (γ, γ^d, γ^p) were calculated based on AFM analysis and contact angle measurmetns. Transport properties such as permeability coefficient (P, Barrer) and ideal selectivity (α) were estimated for individual gases: N_2, CH_4, CO_2, H_2S.

Results and Discussion

Spectroscopy results revealed carbonyl band formation on the surface of both PDMS and PVTMS membranes after O_3 treatment. In case of plasma treatment, the formation of Si-H functionality was observed. AFM showed significant changes in bought PVTMA and PDMS membranes topography after ozonation. In the case of plasma treatment, at 10W the topography of membranes remained the same, while a slight decrease in roughness parameters. At 40W in the case of PDMS the tendency to decrease roughness parameters is preserved and in the case of PVTMS the decrease in roughness parameters was observed as well, however the membrane topography has also changed. The results of wettability tests and surface energy calculation supported the AFM conclusions. Ozonation has noticeably changed dispersive component of the PVTMS surface energy, and polar component of the PDMS surface energy. In general, surface modification by both ozonation and plasma treatment increased total surface energy in comparison with initial membranes. The changes in surface topography, roughness and energies influenced

membranes' transport properties. The results of the gas separation experiments for PVTMS membranes are presented in Figures 1 and for PDMS are presented at Figure 2.

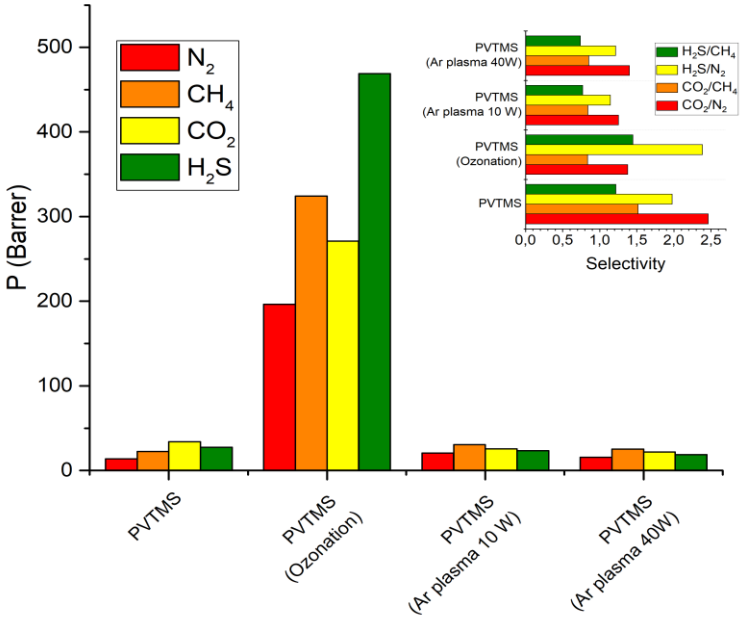

Figure 1. Permeability coefficient and ideal selectivity of the initial and modified PVTMS membranes.

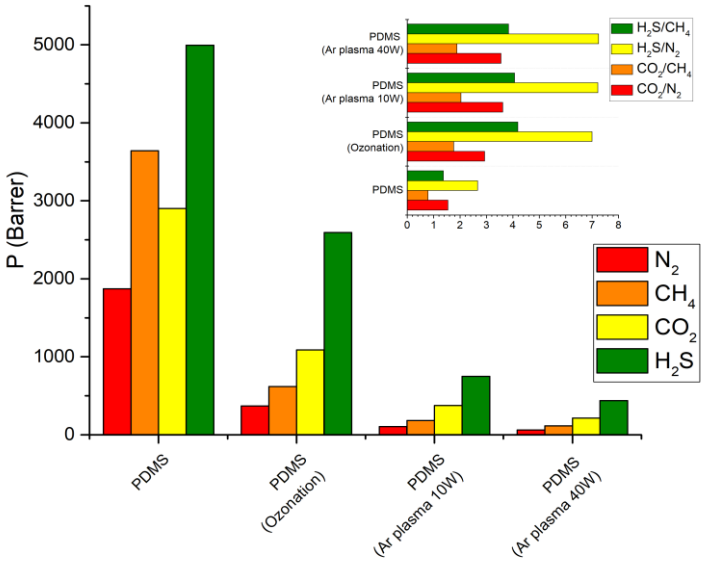

Figure 2. Permeability coefficient and ideal selectivity of the initial and modified PVTMS membranes.

Conclusion

According to the results, obtained from these experiments it is possible to conclude that polymers modification by exposure in O3 or by plasma treatment can significantly improves surface adhesion through changes in surface energy.

Acknowledgments

This work was supported by the Russian Science Foundation (grant no. 18-19-00453).

MEMBRANE MATERIALS IN MODERN ENERGY

[1-3]Andrey Yaroslavtsev

[1]N.S. Kurnakov Institute of General and Inorganic Chemistry, Russian Academy of Sciences, 119991 Moscow, Russian Federation, E-mail: *yaroslav@igic.ras.ru*

[2]Institute of Problems of Chemical Physics, Russian Academy of Sciences, 142432 Chernogolovka, Moscow Region, Russian Federation

[3]National Research University Higher School of Economics, Myasnitskaya str. 20, 101000 Moscow, Russian Federation

Energy is becoming an increasingly important product in the modern world. No modern technology can work without it. Statistics evidence that energy consumption doubles every 30 years. At the same time energy production it is not clean and safe process. So, thermal power plants keep throwing huge amounts of carbon, nitrogen and sulfur oxides into the Earth's atmosphere. No smaller problems are caused by modern vehicles. Like thermal power plants, they provide a large amount of oxide emissions into the atmosphere. The greatest harm is caused to the atmosphere of megalopolises. Issues of environmental pollution make the humanity develop ecologically safe and, primarily, renewable energy sources, including the energy of the sun, wind, tides. However, it is obvious that all these sources work irregularly. Therefore, we need electrical energy storage units to store and use it when the need for it exceeds its production. The most promising among energy storage systems are batteries, fuel cells, and supercapacitors [1].

This report is devoted to the consideration of the possibilities of using different types of membranes in modern energy.

Fuel cells are considered as one of the most promising ways of energy sources for mobile, stationary and portable devices due to high efficiency (up to 90%), low level of environmental pollution and noise. The problem is that hydrogen does not exist in nature in its pure form. Hydrogen produced by the conversion of hydrocarbons or coal is the cheapest one. However, in both cases, its production requires high temperatures and is accompanied by the formation of by-products, the main one being CO. The stream reforming of alcohols can substantially reduce its amount. Moreover, it proceeds at a much lower temperature and is much more selective. However, operation of the low-temperature fuel cells requires high-purity hydrogen, since even CO traces irreversibly poison the catalyst at temperatures below 120°C. Pure hydrogen can be produced by filtration through palladium alloys-based membranes, which have 100% selectivity for hydrogen. In the last years, composite membranes such as thin Pd and Pd/alloy layers deposited on porous substrates have attracted considerable attention due to their characteristics of higher mechanical resistance, reduced cost and higher H_2 permeance [2]. A lot of works have been selected for the use of both polymeric and inorganic (such as silica, carbon) membranes for H_2 purification [3]. The hydrogen synthesis can be carried out in a single reactor, combining the processes of its production and filtration, which increases the process efficiency [4]. Another way to produce pure hydrogen is water electrolysis.

The most common membranes used in low-temperature fuel cells are perfluorinated sulfonic acid membranes. They present a tetrafluoroethylene backbone with perfluorinated branches terminated with functional ion-exchange $-SO_3H$ groups. One of the main advantages of these membranes is their thermal and chemical stability which is due to the high C-F bond strength. In addition, they have excellent plasticity, strength and high ionic conductivity. One of the modern trends is the use of membranes with a shortened side chain. The advantages of such membranes include better performance at low humidity. Such membranes are currently manufactured under the name Aquion (Russian analogue Inion).

Much attention is paid to membranes based on polybenzimidazole doped with phosphoric acid. They exhibit high thermostability (up to 160-200°C), conductivity up to 0.13 $S*cm^{-1}$ at 160°C and low methanol permeability. Such membranes showed high efficiency in high-temperature fuel cells (up to 200°C) and were commercialized by PEMEAS and Celanese. Increasing the operating temperature significantly reduces the requirements for hydrogen purity, high humidity and cooling the system.

A promising approach is the preparation of hybrid membranes containing inorganic nanoparticles. High interest in hybrid membranes is determined by an increase in their ionic conductivity, a decrease in gas permeability, and in some cases by increased thermal stability [5]. The increase in the pore size after nanoparticles incorporation leads to an increase in the size of the connecting channels, which limit the conductivity of the membrane. Obviously, the nature of dopant surface should affect the transport properties of the hybrid membranes. An important factor is the hydrophilicity of the nanoparticles surface, which contributes to an increase in the membrane water uptake. But the acid-base properties of dopant surface are even more important. In the case of higher dopant acidity (through modification of its surface with strong acids), the carrier concentration may increase due to protons of the dopant.

In the case of solid oxide FCs, oxygen-conducting membranes are employed. The O^{2-} ion transfer has high activation energy, because this ion has a charge of 2-, large radius, and poorly deformable electron shell. Therefore, their high conductivity is usually manifested at temperatures above 700^{o}C. In solid-oxide FCs (SOFCs), ceramic membranes are used: zirconium dioxide stabilized by yttrium or scandium oxide, lanthanum gallate, and doped cerium oxides. Numerous attempts have been made to obtain materials that would allow reducing the working temperature of SOFCs and thus would markedly increase their efficiency and nanomaterials with a pronounced contribution of the transfer at grain boundaries [6].

One of the important approaches to lowering the operation temperature of high-temperature fuel cells is the transition to proton-conducting oxides. It is believed that this may allow to reduce the temperature of the SOFCs by 200 degrees. Proton conductivity of such systems take place due to the sorption of water molecules by an oxide structure containing a high concentration of oxygen vacancies. In this case, the carriers are protons moving along the interstices of such structures.

At lower temperatures, anhydrous acid salts are most often used. Researches in this area were triggered by the discovery of a phase transition in $CsHSO_4$. Above 141°C, its proton conductivity increases by more than three orders of magnitude. The conductivity of alkali metal and ammonium hydrogen salts with tetrahedral anions, $M_nH_m(XO_4)_p$, approaches 10^{-1} $S*cm^{-1}$ [7]. It is somewhat surprising that alkali metal salts rather than polyvalent metal salts (as in low-temperature systems) are used for this temperature range. This is due to the fact that the proton transfer takes place in this case along a chain of hydrogen bonds between the $H_m(XO_4)_p^{n-}$ anions rather than between water molecules. For the transfer cycle to be completed, not only proton hopping is required, but also the anion rotation. This is the rate-controlling step, which takes place much more easily for alkali metal salts in which the coordination bonds are much weaker. The formation of proton-conducting composites based on cesium hydrogen sulfates (phosphates) and nanosized polyvalent element oxides makes it possible to reduce the phase transition temperature and increase the proton conductivity in the low-temperature range [8].

Another interesting application could be the use of membranes in lithium-ion batteries. At present, their electrolytes are most often represented by solutions of lithium salts in organic aprotic solvents. At the same time, the desire to make their work more secure determines the tendency to use solid electrolytes in them. In particular, the use of proton-conducting membranes in lithium form intercalated with aprotic solvents can be one of the most interesting approaches [9].

This work was financially supported by the Russian Scientific Foundation (project № 17-79-30054).

References

1. *Yaroslavtsev A.B. Stenina I.A., Kulova T.L., Skundin A.M., Desyatov A.V.* Nanomaterials for Electrical Energy Storage.// in Comprehensive nanoscience and nanotechnology. Second edition. Ed. Andrews D.L., Lipson R.H., Nann T. V.5 Application of nanoscience. Ed. Bradshaw D.S. Elsevier. Academic. Press. Amsterdam, Boston, Heidelberg, London, New York, Oxford, Paris, San Diego, San Francisco, Singapore, Sydney, Tokio. 2019. P. 165.
2. *Fernandez E., Helmi A., Medrano J.A., Coenen K., Arratibel A., Melendez J., de Nooijer N.C.A., Spallina V., Viviente J.L., Zuniga J., van Sint Annaland M., Pacheco Tanaka D.A., Gallucci F.*

Palladium based membranes and membrane reactors for hydrogen production and purification: An overview of research activities at Tecnalia and TU/e.// Intern. J. hydrogen energy 2017. V. 42. P.13763.
3. *Gallucci F., Fernandez E., Corengia P., van Sint Annaland M.* Recent advances on membranes and membrane reactors for hydrogen production.// Chem. Eng. Sci. 2013. V. 92. P. 40.
4. *Mironova E.Yu., Ermilova M.M., Orekhova N.V., Muraviev D.N., Yaroslavtsev A.B.* Production of high purity hydrogen by ethanol steam reforming in membrane reactor.// Catal. Today 2014. V.236. P.64.
5. *Apel P.Yu., Bobreshova O.V., Volkov A.V., Volkov V.V., Nikonenko V.V., Stenina I.A., Filippov A.N., Yampolsky Yu.P., Yaroslavtsev A.B.* Prospects of Membrane Science Development.// Membranes Membrane Technologies. 2019. V. 1. P. 45.
6. *Fan L., Zhu B., Su P.-C., He C.* Nanomaterials and technologies for low temperature solid oxide fuel cells: Recent advances, challenges and opportunities.// Nano Energy 2018. V.45. P. 148.
7. *Makarova, I.P.* Superprotonics – crystals with rearranging hydrogen bonds.// Physics of the Solid State 2015. V.57. P. 442.
8. *Lavrova G.V., Ponomareva V.G., Ponomarenko I.V., Kirik S.D., Uvarov N.F.* Nanocomposite proton conductors containing mesoporous oxides as the promising fuel cell membranes.// Russ J Electrochem. 2014. V.50. P. 603.
9. *Voropaeva D.Y., Novikova S.A., Kulova T.L., Yaroslavtsev A.B.* Conductivity of Nafion-117 membranes intercalated by polar aprotonic solvents.// Ionics. 2018. V.24. P.1685.

HOMOGENEOUS CATION EXCHANGE MEMBRANES MODIFIED BY PEDOT: SYNTHESIS AND PROPERTIES

Polina Yurova, Irina Stenina, Andrey Yaroslavtsev
Kurnakov Institute of General and Inorganic Chemistry RAS, Moscow, Russia
E-mail: *polina31415@mail.ru*

Introduction

In recent years, the interest for eco-friendly ways of energy generation has grown. One of these methods is to produce energy using proton exchange membrane fuel cells (PEMFCs). The principle of PEMFC operation is based on the electrochemical hydrogen oxidation with the electrical energy generation. To ensure the high performance membrane must have high proton conductivity, low gas permeability, including high conductivity under low humidity. In this regard, a primary aim is both the search for new membrane materials and the modification of commercially available membranes. Among the modifying agents, conductive polymers - polypyrrol, poly(3,4-ethylenedioxythiophene) (PEDOT), polyaniline can be noted. The polyaniline introduction into the system of pores and membrane channels leads to an increase in the ionic conductivity, selectivity of cation transfer [1] and, as a result, the fuel cell power [2]. There are few studies of the modification effects of other conductive polymers on the transport properties of proton-exchange membranes. The purpose of this work was the synthesis and investigation of the transport properties of homogeneous perfluorinated Nafion membranes modified by PEDOT.

Experiments

Poly (3,4-ethylenedioxythiophene) was obtained by in situ polymerization in the Nafion matrix, varying the concentrations and the reagent ratio, as well as the order of their mixing.

Results and Discussion

The highest conductivity in contact with water was found for composite materials obtained by the membrane treatment with a monomer solution first and then by the oxidizer solution with a low monomer/oxidizer ratio (Figure).

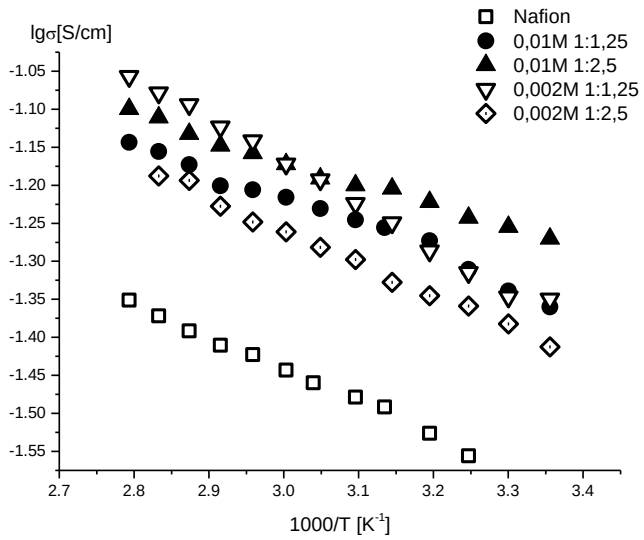

Figure. The dependence of conductivity on temperature for the obtained composite membranes. The monomer concentrations used and the monomer/oxidizer ratio are denoted in the Figure.

The PEDOT introduction leads to a decrease in the water uptake of the composite membranes, which is determined by the partial water displacement from the membrane system of pores and channels due to polymer incorporation. Based on the data on diffusion permeability and diffusion of sodium/hydrogen cations, an increase in the rate of both cationic and anionic transport in the acidic medium is shown.

For samples, prepared by the membrane treatment by an oxidizing solution, and after be the monomer, the study of the hydrogen permeability was carried out (Table). It is shown that hydrogen permeability decreases for all modified membranes at 30 °C and for the most at 50 °C, which suggests the prospect of their use in fuel cells.

Table: Hydrogen permeability (P, cm^2/s) of the obtained membranes at different temperatures and 30% relative humidity

Monomer concentration / monomer:oxidizer ratio	$P(H_2)$, 30°C	$P(H_2)$, 50°C
0 (Nafion)	$1{,}48 \cdot 10^{-7}$	$1{,}79 \cdot 10^{-7}$
0,01 / 1:1,25	$1{,}26 \cdot 10^{-7}$	$1{,}68 \cdot 10^{-7}$
0,01 / 1:2,5	$1{,}32 \cdot 10^{-7}$	$1{,}77 \cdot 10^{-7}$
0,002 / 1:1,25	$1{,}03 \cdot 10^{-7}$	$1{,}48 \cdot 10^{-7}$
0,002 / 1:2,5	$0{,}92 \cdot 10^{-7}$	$1{,}24 \cdot 10^{-7}$

This work was supported by IGIC RAS state assignment.

References

1. *Yaroslavtsev A.B., Stenina I.A., Voropaeva E.Yu., Ilyina A.A.* Ion transfer in composite membranes based on MF-4SC incorporating nanoparticles of silica, zirconia and polyaniline. // Polym. Adv. Technol. 2009. V. 20. P. 566-570.
2. *Escudero-Cid R., Montiel M., Sotomayor L., Loureiro B., Fatas E., Ocon P.* Evaluation of polyaniline-Nafion® composite membranes for direct methanol fuel cells durability tests. // Int. J. Hydr. En. 2015. V. 40. P. 8182-8192.

APPLICATION OF CONTINUOUS-FLOW ELECTROPHORESIS TO SEPARATE B-LACTOGLOBULIN HYDROLISATE

[1]Yana Yutskevich, [2]Sergey Mikhaylin, [1]Anton Kozmai, [1]Natalia Pismenskaya
[1]Kuban State University, Krasnodar, Russia, E-mail: *yana.yutskevich@gmail.com*
[2]Université Laval, Québec, Canada, E-mail: *sergey.mikhaylin@fsaa.ulaval.ca*

Introduction

Whey is a by-product in the production of dairy products, such as cheese, yogurt and casein [1]. At the moment, it is reliably known that the volume of world production of whey is about 180 million tons [2], which draws attention to possible ways of processing this product.

In whey there is not only a variety of lipids, vitamins, minerals and lactose, but also a number of proteins (β-lactoglobulin, α-lactalbumin, serum albumin, immunoglobulins, lactoferrin). These proteins have an important effect on the body – from cancer prevention to improvement digestive function [3].

The main protein of whey fraction is β-lactoglobulin. It is known that peptides obtained from it by hydrolysis have a wide range of biological activities [4]. Therefore, their production is very important for food, nutraceutical and pharmaceutical industries and obtaining them from a by-product of dairy industry such as whey solves both the problem of co-products disposal and the search for sources to obtain these peptides.

However, the separation of such valuable biologically active peptides raises the problem of choosing the optimal method, allowing to obtain the maximum possible amount of peptides, without negative impact on their biological properties. Moreover, in the light of sustainable development strategies adopted by United Nations and large numbers of governments including Russia, the peptide production should have the least negative impact on the environment. A number of well-known methods, such as membrane filtration or chromatography, have such significant drawbacks as, for example, low selectivity, high cost, or low productivity on an industrial scale [5]. However, there is a separate direction in the field of methodology – electrochemical separation, whose methods have several important advantages, such as reducing the risk of contamination of the analyzed object with foreign substances introduced with reagents, selectivity, high sensitivity and the possibility of automation. In this case, special attention is attracted by the method of continuous-flow electrophoresis (CFE), since it provides a continuous separation of the feed substances at a relatively high speed [6]. This method was used for food proteins, but it has never been tested before for peptides, so the study of this method is very important.

Experiments

In this study, a CFE cell is studied. The cell configuration was based on the principles outlined in the article Afonso J.-L. and Clifton M.J. [6]

The object of the study was hydrolysate solution obtained by enzymatic hydrolysis of 1% β-lactoglobulin with α-chymotrypsin. 0.1M H_3PO_4 was injected to the anode chamber and 0.05M NaOH to the cathode chamber. The "Clark & Lubs solution" buffer (boric acid / sodium hydroxide with KCl), pH 10.0, was injected to the separation chamber. The injection flow rate of the acid and alkali solutions into the electrode chambers was 15 mL/min, and the flow rate of the buffer and the hydrolysate sample was 1.5 mL/min. The temperature in the cooling chamber is 4°C, the temperature of the fractions and solutions obtained after passing through the electrode chambers was 24-25°C. The current source (PowerPac 3000, Bio-Rad, USA) supplied an electric current of 400 mA. The hydrolysate (10 mL) was supplied by using a peristaltic pump in 30 minutes after formation of stable pH gradient of the carrier buffer; at the same time every 10 minutes pH measurement was performed. Then the hydrolysate flow was stopped, but the separation was continued during 5 minutes for a more complete output of the hydrolysate to the resulting fractions.

Reverse-Phase Ultra Performance Liquid Chromatography couled Mass Spectrometry (RP-UPLC-MS) was performed for peptide identification using a 1290 Infinity II UPLC (Agilent Technologies, Santa Clara, CA, USA). The column was operated at a flow rate of 400μL/min at

45°C. The gradient consisted of solvent A (LC-MS grade water with 0.1% formic acid) and solvent B (LC-MS grade ACN with 0.1% formic acid) starting at 2% B and ramping to 35% B in 40 min, then ramping to 85% B to 40 min 50 s, holding until 42 min, then back to initial conditions until 45 min. A hybrid ion mobility quadrupole TOF mass spectrometer (6560 high definition mass spectrometry (IM-Q-TOF), Agilent, Santa Clara, USA) was used to identify and quantify the relative abundances of the chymotryptic peptides. The whey protein database was used to search for peptides from the hydrolysate. The databases "Uniprot", "ExPASy" and "MBPDB Search" was used for the identification of peptide bioactivities presented on the Figure 1.

Results and Discussion

In the hydrolysate, a mixture of diverse peptides was obtained. After identifying the peptides of the obtained hydrolysate by mass spectrometry, it was shown that 22.17% of the total number of all peptides in the hydrolysate were bioactive.

The distribution of biologically active peptides in fractions was unequal. Indeed, the greatest amount of bioactive peptides was concentrated in the cathode (pH 12.56), the middle/cathode (pH 12.4026) and the middle (pH 12.40) fractions, while the smallest amount was registered in the anode fraction (pH 1.6) (Fig. 1). This fact could be related to the design of the CFE cell itself, in which inlet for the peptide mixture was situated closer to the cathode. Thus, taking into account the relatively high flow rate, most of the peptides were retained in the fractions closer to cathode. However, peptides having substantial negative charge and high electrophoretic mobility were able to migrate towards the fractions, closer to the positively charged anode.

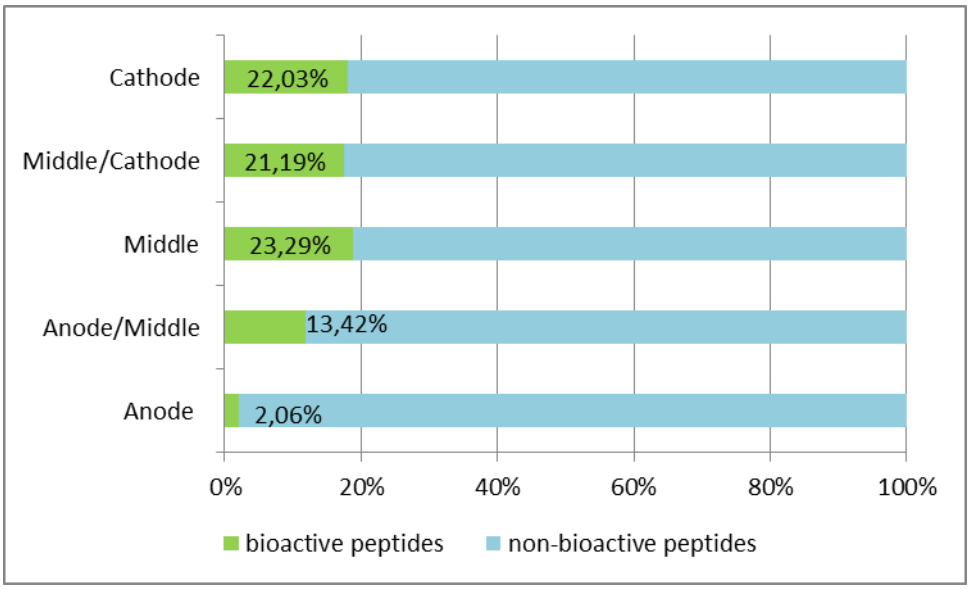

Figure 1. Percentage of Bioactive Peptides in Fractions after Continuous-flow Electrophoresis.

Only one of the obtained peptides, HIRL, possessed an anxiolytic, opioid, analgesic and antinociceptive effect. High separation efficiency of this peptide by CFE method was observed. Most of it was concentrated in the middle fraction with pH 12.26. This can be explained by the fact that the initial pH of the carrier buffer was 9.74, and pI of the peptide HIRL was 9.76, i.e. the peptide immediately entered the zone of its isoelectric point, where it remained. However, due to the flow rate and high electrophoretic mobility, a small part of these peptides, at the beginning passing the zone of its isoelectric point, moved further in partially changing pH buffer. Due to the presence of such positively charged amino acids as arginine (R) and histidine (H), the peptide carried a positive charge, as a result of which it moved to the "Cathode" fractions.

High separation was observed after analyzing the distribution of peptides with antimicrobial activity. If in most fractions their content relative to other bioactive peptides was about 40-45%, then in the "Anode" fraction their percentage was 75% (Fig. 2). Three peptides with antimicrobial activity were detected in the hydrolysate. In this case, two of them were obtained in the anodic fraction. All three peptides had an average molecular weight, a high aliphatic index, and positive

GRAVY values, indicating their relatively low electrophoretic mobility, which meant that these peptides spent more time in the separation chamber and the separation went better. However, the relatively high flow rate made worse the separation.

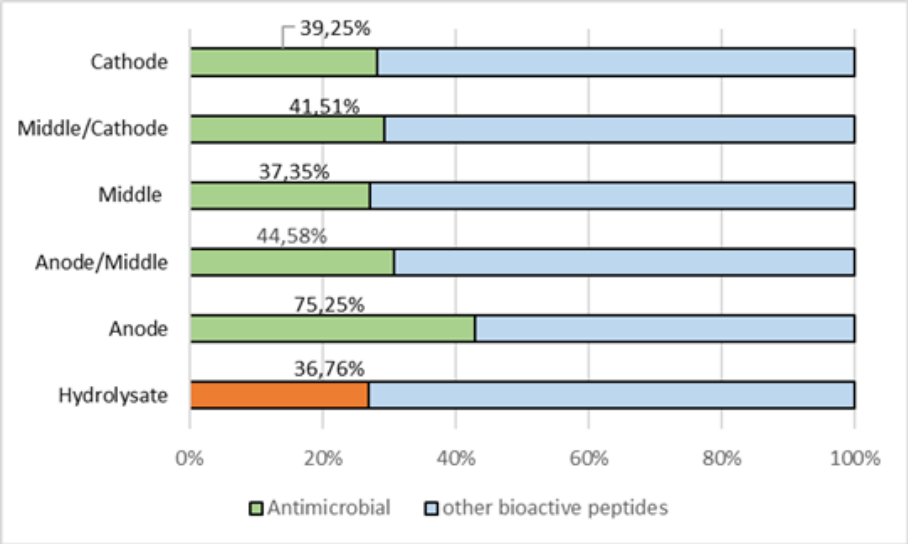

Figure 2. Percentage of peptide with antibacterial activity in all fractions after CFE relative to the total content of all bioactive peptides in each fraction.

It was noted that this method allows the separation of peptides with specific biological activity (antimicrobial, sedative, opioid, analgesic and antinociceptive using the example of HIRL peptide), even though the separation time wais short. However, for improvement the separating properties, it is necessary to optimize the process of CFE peptide separation.

Acknowledgements

The study is realized with the financial support of the Russian Science Foundation (Project No 17-19-01486).

References

1. *Bozanic V.* Protein stability in a proteomic perspective. Dissertation presented to obtain the Ph.D degree in biochemistry. Instituto de Tecnologia Química e Biológica // Universidade Nova de Lisboa. Oeiras, January, 2013.
2. *Macwan S. R., Dabhi B. K., Parmar S. C., Aparnathi K. D.* Whey and its utilization // Int. J. Curr. Microbi Appl. Sci. 2016. V.5. № 8. P.134-155.
3. *McIntosh G. H., Royle P. J., Leu R. K. L., Regester G. O., Johnson M. A., Grinsted R. L., Kenward R. S., Smithers G. W.* Whey Proteins as Functional Food Ingredients? // Int. Dairy J. 1998. V.8. I.5-6. P.425-434.
4. *Korhonen H.* Milk-derived bioactive peptides: From science to applications // J. Funct. Food. 2009. V.1. I.2. P.177-187.
5. *Doyen A., Saucier L., Beaulieu L., Pouliot Y., Bazinet L.* Electroseparation of an antibacterial peptide fraction from snow crab by-products hydrolysate by electrodialysis with ultrafiltration membranes // Food Chem. 2012. V.132. I.3. P.1177-1184.
6. *Afonso J.-L., Clifton M. J.* Coupling between transfer phenomena in continuous-flow electrophoresis: effect on the steadiness of the carrier flow // Chem. Eng. Sci. 2001. V.56. P.3053-3064.

FEATURES OF GALVANIC DEPOSITION OF MULTICOMPONENT METALLIC NANOWIRES IN POROUS OF TRACK ETCHED MEMBRANES

[1]Dmitry Zagorskiy, [2]Sergei Kruglikov, [1,3]Sergei Bedin, [1,4]Ilia Doludenko, [1]Alexandr Shatalov, [1]Dmitry Cherkasov, [1,4]Dmitry Panov

[1]Shubnikov Institute of Crystallography of Federal Scientific Research Centre "Crystallography and Photonics" of Russian Academy of Sciences", Leninskiy Prospekt 59, 119333, Moscow, Russia
[2]Mendeleev University of Chemical Technology of Russia, Miusskaya sq. 9, 125047 Moscow, Russia
[3]Moscow State Pedagogical University, Moscow, 119991 Russia
[4]National Research University Higher School of Economics (HSE), Moscow, 101000 Russia

Introduction

Nanowires (NW) is one of the types of nanoscale materials, which attracts increasing attention of researchers in recent years in studying their unique characteristics, and in terms of their practical application. An elegant way to obtain NW is matrix synthesis, the essence of which is to fill the pores of a special matrix with the required substance [1,2,3]. There are several types of porous matrices and many "filler" substances that are "loaded" into the pores in several ways. In the present work polymeric track etched membranes are used, the pores which are filling of metal via the method of electrodeposition. This process is multistage, and varying its various stages it is possible to change parameters of the received NW in a wide range. It is necessary to focus on two main issues – the preparation of the matrix and the choice of galvanic process mode.

In our work, a polymer track etched membrane is used as a matrix. The pores in the latter are formed by irradiating a thin polymer film with high-energy ions, followed by chemical etching of the latent tracks formed. Traditionally, such membranes are used for fine filtration [Brock]; nevertheless, for tasks of matrix synthesis, special irradiation and etching are often necessary – for example, to obtain pores strictly perpendicular to the surface and/or with a small surface density. Giving the pores a special shape – cigar-shaped or (more often) cone-shaped can also be a task. Further preparation of the matrix includes the processing of the pore walls to give them hydrophilic properties, changes in their roughness.

A wide range of possibilities is presented at the next stage - galvanic filling of pore channels with metal (metals). Note that in most cases two types of metals are used. The first - with high electrical conductivity (copper, silver) – NW of which have prospects of use in electronics and optics. The second - metals of the iron group (Nickel, Cobalt, Iron)- are promising for obtaining NW with unique magnetic characteristics. Note that electrochemistry makes it possible to obtain several types of NW [Vack, Lupu, Davydov]. So, the simplest NW – homogeneous, from one metal (one-component) – are obtained by electrodeposition from a solution containing the salt of the corresponding metal. It is obvious that in this case the process occurs when the growth voltage exceeds the equilibrium deposition potential of the metal. In the study of this type of process, several features are found: we note the nonlinear nature of the growth associated with diffusion restrictions on the movement of metal ions in a narrow pore channel [We-???]. Two-component (in General - multicomponent) NW can be both homogeneous and heterogeneous - consisting of alternating layers with different metal concentrations.

Experiments

Homogeneous NW are synthesized when applied to the growth bath (cell) voltage exceeds the deposition potentials of both metals. The analysis of NW synthesized under these conditions allowed to establish that the ratio of concentrations in the composition of NW differs from the ratio of concentrations in the growth electrolyte [We]. (Note that if one of the metals is iron, it often occurs because of its "abnormal" co-deposition, in which iron, despite its greater equilibrium potential, precipitates faster than the second metal). It was also revealed that the ratio of the concentrations varies along the length of the NW - which is obviously related to the change of the deposition conditions in the process of filling of the pore channels.

The two – component heterogeneous structures-NW, consisting of alternating layers of different concentrations, are obviously of the greatest interest at present. Obtaining such structures

is possible in two ways. First, the process is carried out in series in two cells with electrolytes containing ions of different metals (the so-called "two-bath method"). Secondly, it is a process in one electrolyte containing ions of both metals (the so-called "single-band method"). In the second case, the deposition using the so-called pulse voltage supply mode. During the application of a low voltage pulse, a metal layer with a lower equilibrium deposition potential is deposited. When a sufficiently high voltage is applied, a layer of another metal is deposited. (Strictly speaking, both metals are deposited – i.e. the alloy, but if necessary, the amount of the first metal in this alloy can be significantly reduced –by reducing it in the original electrolyte). In our works it was shown that in many cases during growth there is a change in the thickness of the layers and/or their composition [Ilya]. It is determined under what conditions it is possible to align the layers in thickness: the transition from the mode of pulses of the same duration to pulses with the same leaked charge. To avoid changes in concentration may be due to the slowing down of the growth process, the use of cells with a large volume and mixing of the solution during growth.

Another promising direction is to obtain so-called gradient structures. In this case, the concentration of NW smoothly changes in length. This can be achieved by a controlled change in composition, by changing the growth potential. Another way is to use growth matrices with variable cross-section channels – for example, conical. Changing the pore diameter will make it possible to obtain NW with a variable diameter along the length.

Discussion

All the above mentioned structures may have wide practical application in the future. Alloy NWs are promising for obtaining microstructures with variable magnetic properties. Layered NWs are promising as sensors, structures with giant magnetoresistance, structures for magnetic recording with high density ("in depth" record).

Acknowledgment

This work was supported by the Ministry of Science and Higher Education within the State assignment FSRC «Crystallography and Photonics» RAS. Some Chemical measurements weresupported by RFBR grant No.18-32-01066. Authors thank Prof.P.Yu.Apel (JINR, Dubna) for providing of Track Membrane samples.

References

1. *Martin, C.R.* Nanomaterials: A membrane based synthetic approach, Science. – 1994. – Vol. 266. – P. 1961 – 1966.
2. *S.K. Chakarvarti, J. Vetter* Morphology of etched pores and microstructures fabricated from nuclear track filters, Nucl. Instr. Meth. Phys. Res. 62(1) (1991) 109–115.
3. *J. Vetter, R. Spohr* Application of ion track membranes for preparation of metallic microstructures, Nucl. Instr. Meth. Phys. Res.79(1-4) (1993) 691–694
4. *Brok T.* Membrane Filtration, Springer, 1983, 397 P.
5. *Ed. M.V´azquez* Magnetic nano- and microwires: design, synthesis, properties and applications, Woodhead Publishing, Amsterdam: Elsevier, – 2005. – P. 847
6. *Ohgai T., Ed. N. Lupu.* Electrodeposited nanowires and their applications, Croatia: InTech, – 2010. – P. 61 – 85.
7. *A.A. Davydov, V.M. Volgin* Template Electrodeposition of Metals, Electrochemistry 52(9) (2016) 905-933 (In Russian)
8. *K. V. Frolov, D. L. Zagorskii, I. S. Lyubutin, V. V. Korotkov,S.A.Bedin, S.N.Sylianov, V.V. Artemov, B.V.Mchedlishvili* Synthesis, Phase Composition, and Magnetic Properties of Iron Nanowires Prepared in the Pores of Polymer Track-Etched Membranes, JETP Letters, 2014, Vol. 99, No. 10, pp. 570–576

9. *D. L. Zagorskiy, K. V. Frolov, S. A. Bedin, I. V. Perunov, M. A. Chuev, A. A. Lomov, I. M. Doludenko* Structure and Magnetic Properties of Nanowires of Iron Group Metals Produced by Matrix Synthesis, Physics of the Solid State, 2018, Vol. 60, No. 11, pp. 2115–2126.
10. *K. V. Frolova, D. L. Zagorskii, I. S. Lyubutina, M. A. Chuev, I. V. Perunova, S. A. Bedin, A. A. Lomov, V. V. Artemova, S. N. Sulyanov* Magnetic and Structural Properties of Fe–Co Nanowires Fabricated by Matrix Synthesis in the Pores of Track Membranes, JETP Letters, 2017, Vol. 105, No. 5, pp. 319–326.
11. *O. M. Zhigalina, I. M. Doludenko, D. N. Khmelenin, D. L. Zagorskiy, S. A. Bedin, I. M. Ivanov* Structure of Cu/Ni Nanowires Obtained by Matrix Synthesis, Crystallography Reports, 2018, Vol. 63, No. 3, pp. 480–484.
12. *Zhigalina O.M., Khmelenin D.N., Ivanov I.M., Zagorskiy D.L., Bedin S.A., Doludenko I.M.* Electron microscopy of nanostructures formed by Cu–Ni layer nanowires, Nanomaterialsand Nanostructures - XXI Century № 2, т. 9, 2018

EFFECT OF SURFACE DIFFUSION ON SEPARATION OF GAS MIXTURES IN NANOSIZED POROUS MEMBRANES

[1]Vladimir Zhdanov, [2]Alexander Larin

[1] National Research Nuclear University MEPhI (Moscow Engineering Physics Institute), Moscow, Russia
[2]Frumkin Institute of Physical Chemistry and Electrochemistry, Russian Academy of Sciences, Moscow, Russia

Introduction

In recent years, the great interest has been demonstrated in the study of transport processes in thin channels and nanoscale porous media, which has a direct relationship to development of membrane technologies applied for the separation of gas mixtures. Theoretical studies of flow and diffusion of a gas mixture in such media are either based on the capillary model of a porous body or the "dusty- gas" model. The latest model was developed in [1,2] and has been widely used in the analysis of gas mixture diffusion in a porous media in the intermediate regime of gas flow between the free-molecular $(Kn >> 1)$ and viscous flow with a slip $(Kn \le 0.1)$, where $Kn = \lambda / d_g$ is the Knudsen number (λ is the mean free path of molecules, d_g is the characteristic pore diameter).

A generalization of the capillary model of a porous medium on the basis of the momentum balance method has been considered in [3] for the case of a flow of a binary gas flow under conditions, when one of the gases adsorbed in a mobile phase on the surface of the capillary. The appropriate system of transport equations was derived in [4] in the framework of the "extended dusty-gas model", when the porous medium is presented as a mixture of two dust species. Accounting for one of them describes the collision of gas molecules with the wall surface free of the adsorbed molecules. Taking into account the other component corresponds to the interaction of gas molecules with the molecules adsorbed in a mobile phase.

In the present work, the model mentioned above is used to describe the flow and diffusion of a binary gas mixture in a porous medium driven by the gradients of the species partial pressures accompanied by the adsorption of molecules on the inner surface of pores and by surface diffusion of one of the gas mixture components .The expressions for the mean fluxes of the mixture species in a membrane obtained on the basis of this model for the free-molecular regime of flow in combination with information about the adsorption isotherm and the surface diffusion coefficients are used to derive the expressions for the difference in concentration of species (separation effect) in a porous membrane for a given value of the pressure drop.

Initial system of equations

For the extended dusty-gas model, the initial system of transport equations for the mixture species in a porous membrane can be written as

$$-\frac{dp_1}{dx} = \frac{kT}{D_{1k}} n_1^g u_1^g \left(1-\alpha_{11}\right) + \frac{kT}{D_{1k}} \frac{\mu_{11}}{m_1} n_1^g \left(u_1^g - u_1^s\right)\alpha_{11} \tag{1}$$

$$-\frac{dp_2}{dx} = \frac{kT}{D_{2k}} n_2^g u_2^g \left(1-\alpha_{12}\right) + \frac{kT}{D_{2k}} \frac{\mu_{12}}{m_2} n_2^g \left(u_2^g - u_1^s\right)\alpha_{12} \tag{2}$$

Here $p_1 = pc_1$ and $p_2 = p\left(1-c_1\right)$ are the partial pressure of species 1 and 2 (the first component is only adsorbed). n_i^g and u_i^g are the number density and the mean macroscopic velocity of species i, u_1^s is the mean velocity of the adsorbed molecules of species 1, T is the temperature, $\mu_{12} = m_1 m_2 \Big/ \left(m_1 + m_2\right)$ is the reduced mass of the particles 1 and 2, α_{11} and α_{12} are the mean probabilities of collisions of the incident molecules of species 1 and 2 with the adsorbed molecules of species 1, $D_{iK} = (4/3) K_0 \bar{v}_i$ is the Knudsen diffusion coefficient, $\bar{v}_i = \left(8kT/\pi m_i\right)$ is the mean

thermal velocity of the molecules of species i in gas phase , K_0 is the permeability coefficient of a porous body.

Let us define the fluxes of species in a gas phase and on the inner surface of a porous body as

$$G_i^g = n_i^g u_i^g \ (i=1,2) \quad , \quad G_1^s = n_1^s u_1^s$$

The flux G_1^s (surface diffusion) is defined by the Fick's law

$$G_1^s = -D_1^s \frac{dn_1^s}{dx} \quad , \qquad D_1^s = \frac{\left(D_1^s\right)_0}{1-\theta_1} \ , \qquad \theta_1 = \frac{n_1^s}{n_{1m}^s} \quad , \tag{3}$$

where θ_1 is the degree of adsorption for species 1, n_1^s is the surface density of particles in adsorbed phase (per unit volume of media), n_{1m}^s is the maximum density of the particles in the adsorbed phase for the given values p and T. To determine the value of θ_1 the Langmuir adsorption isotherm $\theta_1 = K_1 p_1 / (1 + K_1 p_1)$ can be used.

The expression (3) can be simplified in the situation when the degree of adsorption is very small $(\theta_1 << 1)$. In this case $(K_1 p_1 << 1)$ we have

$$G_1^s = n_1^s u_1^s = -\left(D_1^s\right)_0 K_1 n_{1m}^s \frac{dp_1}{dx} \tag{4}$$

When $\theta_1 << 1$ gas molecules interact with the adsorbate molecules located far from each other. Using of the hard sphere model for the interaction between molecules in this case leads to the result [3]: $\alpha_{12} = (3\pi/8) d_{12}^2 n_1^s d_g$, where $d_{12} = (d_1 + d_2)/2$ and d_g is the characteristic pore diameter. We have the analogous result for α_{11} when d_{12} is substituted with d_{11}. Let us define the mean free path of molecules of species 1 as $\lambda = 1/n\pi d_1^2$. As a result, we have: $\alpha_{12} \sim \alpha_{11} \sim (1/Kn)(n_{1s}/n) << 1$, since $Kn >> 1$. The estimates of contributions of the terms with $n_1^g u_1^s$ in the Eq. (1) lead to the result: $(kT/D_{1k}) n_1^g u_1^s \alpha_{11} \sim (1/Kn)\left(D_1^s / D_{1k}\right)\left(n_1^s / n\right) dp_1/dx$.

A similar estimate is valid for Eq. (2). It is evident that for the case when $Kn >> 1$ we can neglect the contribution of these terms in comparison with the left hand side of Eqs. (1)-(2). As a result, we arrive at the conclusion that for the case of freee-molecular flow of a gas mixture in pores under the condition $\theta_1 << 1$ the adsorption and surface diffusion have no effect on the transport of the species in the gas phase. In this case, the expressions for G_1^g and G_2^g following from Eqs. (1)-(2) have the familiar form [5]

$$G_1^g = -D_{1k} \frac{1}{kT} \frac{dp_1}{dx} \quad , \quad G_2^g = -D_{2k} \frac{1}{kT} \frac{dp_2}{dx} \tag{5}$$

Separation effect

In case of a stationary flow of a gas mixture in a porous membrane driven by a pressures drop $\Delta p = p_0 - p'$, the difference in the concentratons $\Delta c_1 = c_1' - c_1^0$ (the separation effect) arises between the inlet and outlet surfaces of the membrane. The magnitude of this effect can be found from the condition that the species fluxes are a constant in an arbitrary cross section of a porous body. On the outlet side of the membrane where the fluxes are convective we have $G_1 = G c_1'$, $G_2 = G\left(1 - c_1'\right)$, where G is the total molar flux of the gas mixture, $G_1 = G_1^g + G_1^s$, $G_2 = G_2^g$ and

c_1' is the concenration of the component 1 on the outlet surface of the membrane. The initial equation for the mixture separation is derived from the condition

$$G_1/G_2 = c_1' \Big/ \left(1 - c_1'\right) \tag{6}$$

Substituting the expressions for G_1 and G_2 following from Eqs. (4),(5) into the condition (6) we obtain the differential equation in the form

$$M\left(c_1'\right) p \frac{dc_1}{dp} = \left[c_1' - M\left(c_1'\right) c_1 \right], \tag{7}$$

where

$$M\left(c_1'\right) = c_1' + f^+ \left(1 - c_1'\right) \quad ,$$

$$f^+ = \left(D_{1k}/D_{2k}\right)\left(1 + a_1\right) = \left(m_2/m_1\right)^{1/2}\left(1 + a_1\right) \quad , \qquad a_1 = K_1 n_{1m}^s kTD_1^s \Big/ D_{1k} \tag{8}$$

The solution of the Eq.(7) leads to the following expression for the difference in the species oncentrations

$$\Delta c_1 = c_1' - c_1^0 = \frac{f^+ - 1}{M\left(c_1'\right)} c_1' \left(1 - c_1'\right)\left(1 - \frac{p'}{p_0}\right) \tag{9}$$

The influence of the adsorption and the surface diffusion on the separation effect is determined by the contribution of the coefficient a_1 in the expression for the coefficient f^+. When the adsorption is absent $\left(a_1 = 0\right)$ we have $f^+ = \left(m_2/m_1\right)^{1/2}$, which is consistent with well-known result [5]. To calculate a_1 we must know the parameters of adsorption isotherm for adsorbed gas and the relationship between the surface diffusion coefficient and Knudsen diffusion coefficient.

The work supported by the Russian Foundation for Basic Researches under the Grant № 17-08-00315)

References

1. *Mason E.A., Malinauskas A.P., Evans R.B.III.* Flow and diffusion of gases in porous media, //J. Chem. Phys.1967. V.46. P.3199-3216.
2. *Mason E.A., Malinauskas A.P*. Gas transport in porous media: the dusty-gas model. Elsevier, Amsterdam-New York. 1983
3. *Bell W.K., Brown L.F*. Kinetic theory approach to simultaneous gas and surface diffusion in capjllaries// J. Chem. Phys.1974.V.61.P.609-618
4. *Zhdanov V.M., Roldughin V.I.* Flow and diffusion of gas mixtures in nanosized porous bodies. Generalized dusty- gas model accounting the adsorption and diffusion . Ion transport in organic membranes, Conference Proceedings, Kuban State University, 2016, P.334-336
5. *Zhdanov V.M*. Flow and diffusion of gases in capillaries and porous media // Adv. Colloid Interface Sci. 2011.V.66.P. 1-22

SORPTION OF TOXIC COMPOUNDS OF IRON AND COBALT FROM SOLUTIONS OF HUMINE SUBSTANCES

Umirzak Zhusipbekov, Gulzipa Nurgalieva, Zamira Bayakhmetova, Aynur Shakirova, Dulat Duysenbay

JSC "Institute of Chemical Sciences after named A. B. Bekturov", Almaty, Kazakhstan

E-mail: *N_gulzipa@mail.ru*

Introduction

Humic substances belong to complex high-molecular organic compounds of natural origin, the presence in the macromolecule of humic substances of many atomic groups and different functional groups allows them to participate in various reactions. As a result, humic substances can be used as biologically active substances, flocculants, ion exchangers, complexing agents, protectors, sorbents, etc. Special interest causes their ability to bind toxic inorganic and organic compounds [1-4]. Therefore, humic substances are used as effective natural sorbents, they are non-toxic, stable in various environments and also easily regenerated.

Experiments

In this research as a sorbent was used modified sodium humate with the content of 78.02% free humic acid, as well as nitrates of iron (III) and cobalt (II). Modification of humate sodium was carried out by using ethylene diamine in the ratio of 1:3, at a temperature of 30°C for 48 h. The sorption process was carried out under static conditions at temperature of 20°C for 15-120 minutes with concentration of metal ions of 50-5000 mg/l and norm of sorbent of 0.1-1.0 g and pH in the range from 2 to 8. IR spectra were taken on an IR Fourier spectrophotometer model Nicolet 5700 "Thermo Electron" (USA) in the region of 200-4000 cm^{-1}. Samples for the study were prepared by the standard method of pressing in with KBr. The assignment of the absorption bands in the IR spectra was carried out in accordance with the literature data [5]. Electron microscopic images of the samples were taken on REM by using JXOL (Japan) electron probe microanalyzer "JXA-8230" with an accelerating voltage of 25 kV, an electron beam current less than 1 nA. Metal contents were determined using AAS mark AA240 manufactured by Varian Optical Spectros copy Instruments (Australia). The pH was measured by pH meter pH-150MI (Measuring Equipment, Russia), which is equipped with a universal glass electrode.

Results and Discussion

The obtained experimental data (figure 1) indicated that the highest sorption degree of cobalt and iron ions by the modified humate is observed at pH 4, reaching 84.6 and 96.4%, respectively. A further increase in pH leads to a decrease in the degree of sorption of cobalt to 77.5% and iron to 91.4% with the formation of precipitates of basic salts and hydroxides which apparently delayed on the surface of the sorbent and prevent more complete cleaning of the solution from iron and cobalt ions. Therefore, further experiments were performed at pH 4.

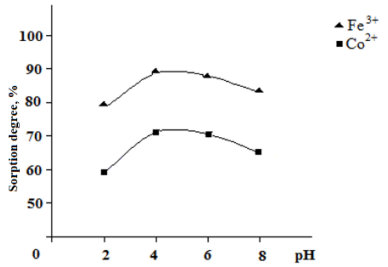

Figure 1. The dependence of the sorption degree of ions iron and cobalt on the pH.

The data obtained from the analysis (figure 2a), a growth in the concentration ions of iron and cobalt from 50 to 1000 mg/l leads to expansion in the sorption degree of these metals, and a further increase in their concentration to 5000 mg/l leads to reduced the sorption degree. Probably, an increase in the concentration of iron and cobalt ions leads to enhancement of the processes of their

structural and molecular transformation into humates of iron and cobalt, and starting with the concentration of 5000 mg/l, iron and cobalt ions desorption were occured. For example, 0.5 g of modified humate norm after 60 minutes of the process, the sorption degree of cobalt ions at the concentration of 1000 mg/l is 84.6% and iron - 96.4%, and further increase in their concentrations to 5000 mg/l, the sorption degree of cobalt ions is reduced to 77.8%, and iron ions - to 90.4%. In the study of the sorption of iron and cobalt ions with modified humate depending on the sorbent norm (figure 2b) was found that with growing mass of the sorbent regardless of metal ion concentrations and time the sorption degree of ions iron and cobalt rised.

Studying of the sorption of ions iron and cobalt with modified humate depending on the sorbent mass was revealed (figure 2b), by the increasing sorbent mass, regardless of metal ion concentrations and time, the sorption degree of iron and cobalt ions are increased. However, this dependence is non-linear and if the amount of sorbent growth to certain value, the magnitude of sorption remains constant. Thus, an increase in the sorbent rate above 0.7-1.0 g almost does not lead to rise the degree of sorption, and at the 1.0 g sorbent mass, the sorption degree of cobalt ions is 86.7% and iron is 97.5%.

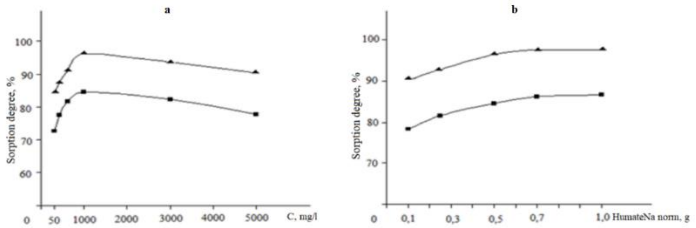

Figure 2. The effect of the concentration of metal ions (a) and the sorbent norm (b) on the sorption degree of iron and cobalt ions.

In the course of the research (figure 3) found that with an increase in the process time from 15 to 60 min, the sorption degree of iron and cobalt ions extend, then, with an increase in time to 120 minutes due to the desorption of cobalt and iron ions, the sorption degree decreased respectively, to 78.3 and 89.0%.

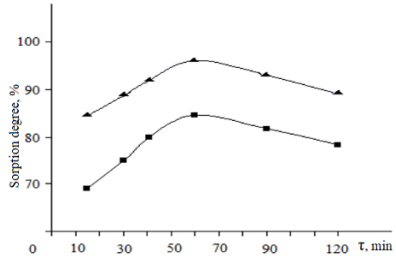

Figure 3. Dependence of the sorption degree of iron and cobalt ions on time.

Humic substances represents polyfunctional aromatic structure, alicyclic and heterocyclic nature, substituted alkyl chains with different functional groups than belong to polydentate ligands. In structure humic substances also have electron-donor functional groups in various combinations and free orbitals of metal cations promote the formation of complex compounds in the interaction of humic substances with heavy metals. From the date of IR-spectrum (figure 4) was found that modified sodium humate interacted by nitrates of iron and cobalt the formation of complex substances. This conclusion is confirmed absorption of valent oscillations groupof carboxyl, phenolic and quinoid in the field of 995-475 cm^{-1}, which identified formation of Me-O connections in the complex of humats. In the spectrum also detected absorption of valent oscillations carboxylate–ions at 1640-1620 and 1410-1390 cm^{-1}, OH- primary alcohol groups at 1060-1050 cm^{-1} [5].

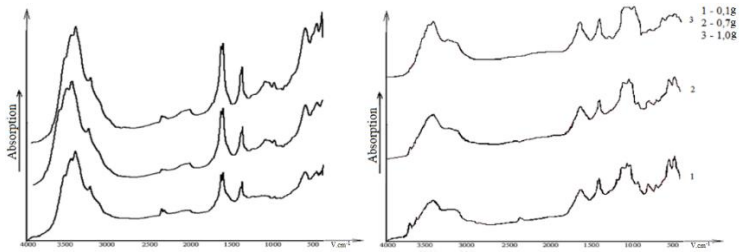

Figure 4. IR-spectra of the studied samples obtained by sorption of iron ions (a) and cobalt (b) at different sorbent norm.

Electron microscopic images of samples (figure 5) shows that the structure of the samples is inhomogeneous, consists of various particles fastened sufficiently tightly and evenly distributed by the structureand and between the particles there are slit pores. Micrographs show bright particles of iron and cobalt, sorbed on the pores of the modified humate.

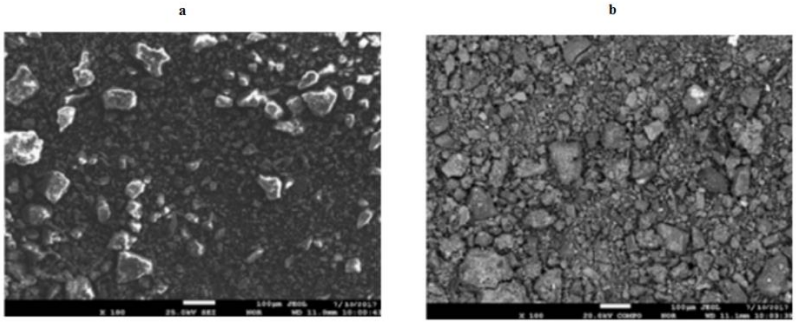

Figure 5. Electron microscopic image of samples obtained by sorption ions of iron (a) and cobalt (b).

Thus, on the basis of conducted research in laboratory conditions established patterns of influence of concentrations ions of iron and cobalt, norm of sorbent, pH and time for the sorption process of ions of iron and cobalt with modified humates. It was revealed that if pH higher than 4, modified humate norms of 0.5–0.7 g when process time one hour in the obtained sorption degree do not have a significant change. Under these conditions, the sorption degree of cobalt ions reaches 86.2% and iron ions — 97.5%. The formation of complex compounds of iron and cobalt with modified humate was established by methods of chemical and physicochemical analysis.

The work was financial supported by the Ministry of Education and Science RK, project G.2015

References

1. *Wu M., Liu Z., Zhu R., Dai X.* Adsorption of copper on soil humic // J. Tongji Univ. Natur. Sci. 2013. V.41. №2. P.240-246.
2. *Janos P., Kormunda M., Novak F., Zivotsky O., Fuotova J., Pilarova V.* Multifunctional humate-based magnetic sorbent: Preparation, properties and sorption of Cu (II), phosphates and selected pesticides// React. and Funct. Polym. 2013. V.73. №1. P.46-52.
3. *Zhernakova Z.M., Deeva N.N., Pecherskiy EG, Polyakov E.V.* Humic substances, their interaction with metals. Ekaterinburg: USTU-UPI, 2009. 20 p.
4. *Perminova I., Hatfield K.* Use of humic substances to remediate polluted environments: from theory to practice. Springer, 2005. P. 3–36.
5. *Orlov D.S., Grishina L.A.* Workshop on the chemistry of humus. Moscow: Moscow State University, 1981. 271.

EFFECT OF SURFACE MORPHOLOGY ON ELECTROCHEMICAL CHARACTERISTICS OF A HOMOGENEOUS ANION-EXCHANGE MEMBRANE AMX MODIFIED WITH AN INERT HYDROPHOBIC MATERIAL

[1]Svetlana Zyryanova, [1]Natalya Terikhova, [2] Lasâad Dammak, [1]Victor Nikonenko

[1]Membrane Institute, Kuban State University, 149, Stavropolskaya str.,350040 Krasnodar, Russia

E-mail: *zyryanova.s.v@yandex.ru*

[2]Institut de Chimie et des Matériaux Paris-Est, UMR 7182, 2 Rue Henri Dunant, 94320 Thiais, France

Introduction

Electroconvection is considered as a promising phenomenon for increasing mass transfer and combating fouling in electrodialysis. It is known that an electrical and/or geometrical surface heterogeneity can contribute to the development of electroconvection [1,2].

Experiments

In this paper, we study a Neosepta AMX anion-exchange membrane whose surface is modified by spreading a fluoropolymer. The polymer forms hydrophobic spots on the surface (Figure 1), so that the fraction of the conductive surface reduces from 100% (the case of non-modified AMX membrane) to 81, 72 and 62%. The fraction of non-conductive surface was determined using CorelDraw software.

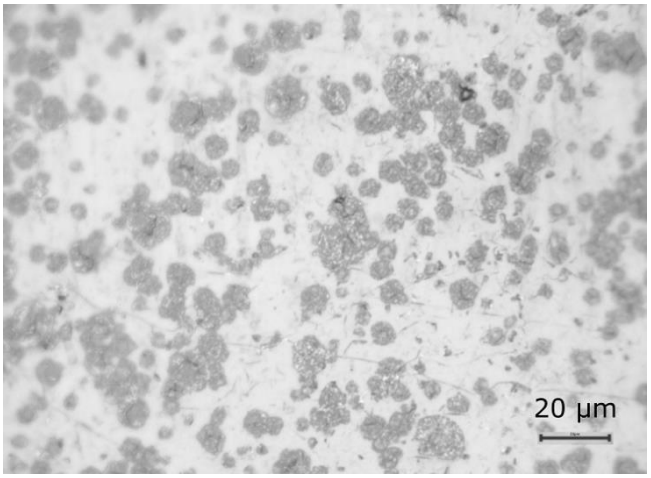

Figure 1. Optical Image of Modified Membrane.

Results and Discussion

The conductivity and contact angle of all samples are shown in the following graph (Figure 2).

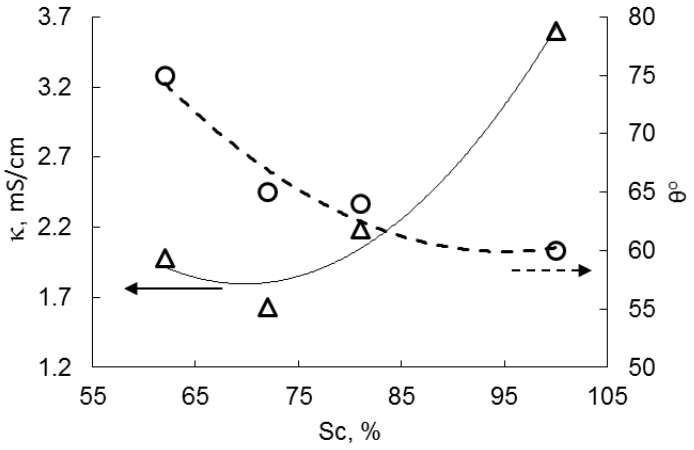

Figure 2. Contact Angle (θ^0) and Membrane Electrical Conductivity (κ, mS/cm) as Functions of the Fraction of Conductive Surface Area (Sc, %).

It can be seen that the less the fraction of the conductive surface, the higher the contact angle (because the modifier is hydrophobic). The electrical conductivity of the membranes decreases with an increase in the fraction of the non-conductive surface, which indicates that the modifier forms a low conductive layer on the membrane surface. Figs. 3 show that surface modification of AMX membrane results in increasing limiting and overlimiting current density (Figure 3a) and appearance of two transition times (Figure 3b). These phenomena are apparently due to electroconvection developing as equilibrium electroosmosis recently theoretically described by Rubinstein and Zaltzman [3].

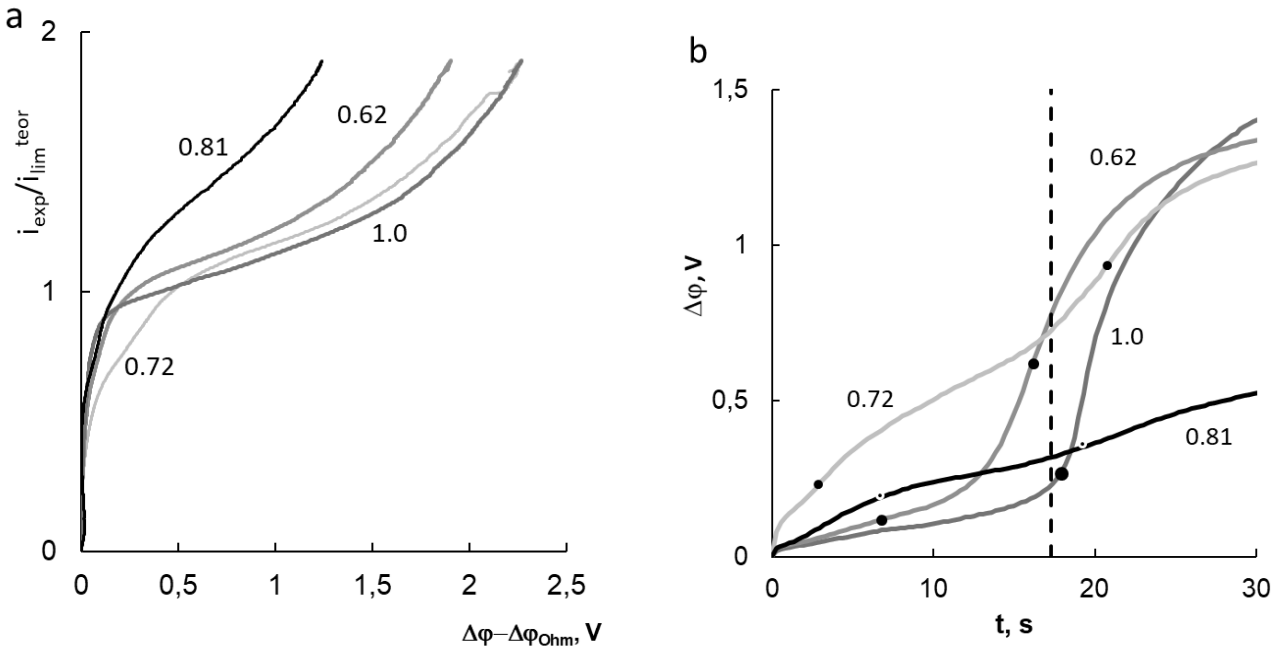

Figure 3. Current-Voltage Curves (a) and Chronopotentiogramms at i=1.4 $i_{\lim}^{theor}$ *(where* $i_{\lim}^{theor}$ *=2.9 mA cm*$^{-2}$ *is the limiting current density calculated using the Leveque equation) (b) of an AMX Membrane and Three Samples Obtained by its Modification. The numbers near the curves show the fraction of the conductive surface; the dashed straight line in (b) indiquates the Sand transition time; the markers show experimental transition times. The measurements were carried out in a 0.02 M NaCl solution.*

Acknowledgement

The study was realized in the frame of a joint French-Russian PHC Kolmogorov 2017 project of the French-Russian International Associated Laboratory "Ion-exchange membranes and related processes" with the financial support of Minobrnauki (Ref. N° RFMEFI58617X0053), Russia, and CNRS, France (project N° 38200SF).

References

1. *Nikonenko V. V., Mareev S. A., Pis'menskaya N. D., Uzdenova A. M., Kovalenko A. V., Urtenov M. Kh., Pourcelly G.* Effect of electroconvection and its use in intensifying the mass transfer in electrodialysis (review) // Russ. J. Electrochem. 2017. V. 53. № 10. P. 1122-1144.
2. *Korzhova E., Pismenskaya N., Lopatin D., Baranov O., Dammak L., Nikonenko V.* Effect of surface hydrophobization on chronopotentiometric behavior of an AMX anion-exchange membrane at overlimiting currents // J. Membr. Sci. 2016. V. 500. P. 161-170.
3. *Rubinstein I., Zaltzman B.* Equilibrium Electroconvective Instability // Phys. Rev. Lett. 2015. V. 114: 114502.

HEAVY METAL SULPHATE SALTS REMOVAL FROM SULPHURIC ACID SOLUTION VIA DIFFUSION DIALYSIS: PILOT SCALE VALIDATION

Libor Šeda, Ladislav Čopák
MemBrain s.r.o., Stráž pod Ralskem, Czech Republic, E-mail: *libor.seda@membrain.cz*

Introduction

In recent years in the European Union more and more strict regulations on release of industrial waste water are applied [1]. The process industry companies are forced to prevent the waste release into the environment by usage of the best available technologies (BAT) on the market. BATs are employed for prevention of the waste formation or for prevention of the waste release, e.g., by its recycling. The regulations among other things aim at the content of total dissolved solids (TDS) in the disposed waste water streams. Because the dissolved salts cannot be removed by the standard municipal waste water treatment plants, they are further released into rivers and can thus affect the environment. In some regions the problem with high TDS in water can be even magnified by long lasting drought. Usually, high TDS content is problematic where concentrated acid or base solutions are employed in the production process. As it is necessary to dispose water with neutral pH the TDS can rise significantly due to neutralization. Between classical industrial fields, where acids are intensively used and high TDS concentrations in the waste water are achieved, belong, for example,

- surface treatment applications, e.g., aluminum oxidizing, stainless steel pickling, modification of plastic or other types of surfaces by acids,
- leaching and processing of ores,
- recycling of batteries, etc.

In the above applications there is significant portion of free acid left in the depleted solution. Recently, such depleted solution is usually neutralized and disposed into waste water (or is handled as a dangerous waste based on pollutants and then disposed accordingly). In such applications, where free acid is present, diffusion dialysis (DD) can be taken into consideration for the free acid recovery [2,3]. In the case where the regenerated acid can be utilized repeatedly in the production or sold to other customers the benefits are obvious:

- lower costs for fresh acid,
- lower costs for neutralization chemicals, typically NaOH, Na_2CO_3,
- ecological benefits due to correspondingly lower TDS level in waste water. If TDS in the waste water is a limiting factor for production or some penalty for too high TDS has to be paid, there is also economical benefit due to acid recovery.

Based on the streams' compositions further processing, e.g., water recovery and salt concentration or recovery of acids and bases (reverse osmosis, electrodialysis, electrodialysis with bipolar membranes), can be taken into consideration. In this work we tested the performance of diffusion dialysis in pilot scale for purification of sulphuric acid from its heavy metal salts.

Experiments

For the pilot testing we utilized a pilot unit DS-AR-DB-20 equipped with two innovative spiral wound modules WD-AR-10 of the producer Spiraltec GmbH., (Germany). The modules utilize membrane FAD from the producer Fumatech (Germany) and can be easily stacked in parallel to increase DD unit capacity. The feed was approx. 20 % (w/w) waste sulphuric acid solution contaminated by heavy metal sulphates. As the second feed reverse osmosis (RO) water with conductivity 5 μS/cm was used. The goal of the experiments was to check the possibility of significant reduction of salt concentration in the acid. Therefore, purification took place in two stages to test the decrease of the heavy metal concentrations by two orders of magnitude. The basic PFD of the experimental setup is visualized in Fig. 1. The waste acid (feed) was firstly filtered by 10 μm cartridge filter to remove suspended solid particles according to the product data sheet of the membrane manufacturer. The filtered feed and RO water flowrates into each module were kept by flow restrictors at ca. 9 $l.h^{-1}$. The product streams (purified diffusate and dialysate containing

majority of salts) had similar flowrates. The chemical analysis of metal ions in the solutions were carried out with the ICP-OES method.

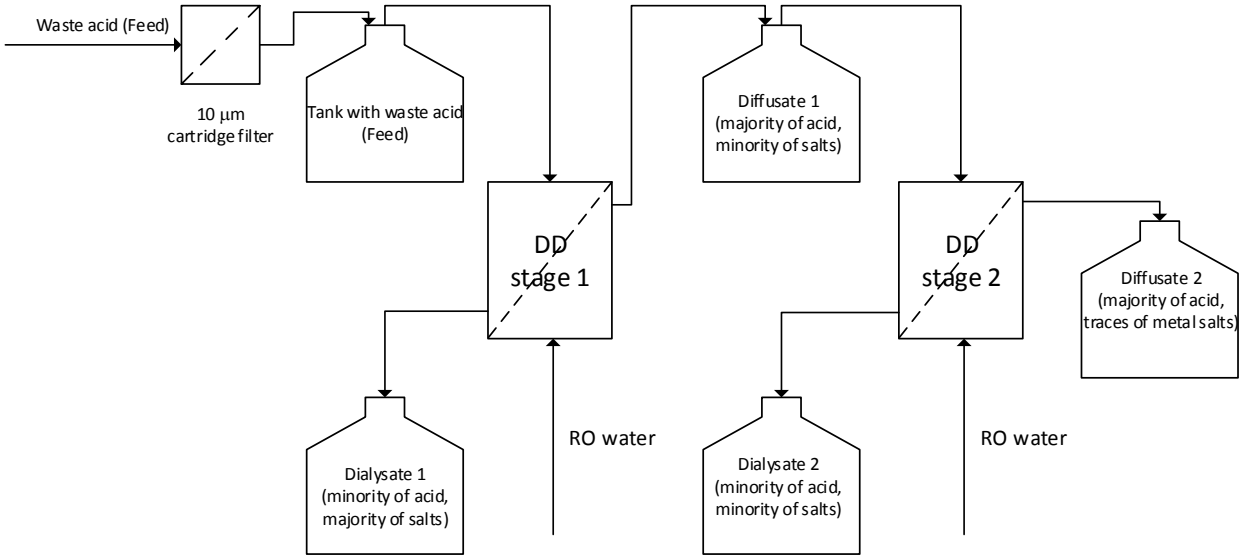

Fig.1. PFD of the pilot testing setup

Results and Discussion

The waste acid (feed) was processed according to the above PFD in two DD stages. The analysis of species in the streams are listed in Table 1 and Table 2. The acid yield *Y* and rejection *R* of the species *i* were calculated according to Eqs. (1) and (2).

$$Y = \frac{\dot{m}_{\mathrm{H_2SO_4,DIF}}}{\dot{m}_{\mathrm{H_2SO_4,FEED}}} = \frac{\dot{m}_{\mathrm{DIF}} x_{\mathrm{H_2SO_4,DIF}}}{\dot{m}_{\mathrm{FEED}} x_{\mathrm{H_2SO_4,FEED}}} \quad (1)$$

$$R = 1 - \frac{\dot{m}_{i,\mathrm{DIF}}}{\dot{m}_{i,\mathrm{FEED}}} = 1 - \frac{\dot{m}_{\mathrm{DIF}} c_{i,\mathrm{DIF}}}{\dot{m}_{\mathrm{FEED}} c_{i,\mathrm{FEED}}} \quad (2)$$

Here *x* denotes the mass fraction, subscripts DIF and FEED refer to diffusate and feed, respectively. Due to already very low concentrations and limited analytical method accuracy there were not all rejection factors evaluated for the second stage. From the obtained results we can see that for the given flowrates the rejection of the metals ranges from 86 % to 98 % for one stage. The achieved acid yields were 91 % and 83 %. That means we can save approx. 90 % of the acid containing approx. 5 % to 10 % of original amount of metal ions (salts). For some processes such decrease of salt amount can be sufficient and no other treatment is needed. In particular applications, e.g., in stainless steel pickling, it is even desired to keep certain concentration level of the metal ions in the solution, because the pickling process proceeds better than with pure acid solution without metal salts.

Let us now assume some average rejection and yield values to make some generalisations. If we consider 90 % salt rejection and evaluate the overall salt rejection for two stage DD system we obtain total rejection $R = (1 - 0.1 \times 0.1) \times 100\ \% = 99\ \%$. The overall acid yield $Y = 0.91 \times 0.83 \times 100\ \% = 76\ \%$. That means under applied conditions we can save 76 % of acid and approximately 100× lower salt concentrations. Here we took conservative values for rejection in our considerations. If we compare concentrations in the feed and in diffusate 2, we can see decrease of concentrations more than 100× (Al >560×, Zn 388×, Cd >124×, Fe 115×, Cu 164×).

The DD pilot plant was kept in continuous operation for ca. one month without issues.

We showed that it is possible to purify the waste sulphuric acid from its salts with significant efficiency (ca. 90 % recovery, ca. 90 % to 95 % salt rejection in one stage). The possibility of application of DD is limited by the possibility of reuse or disposal of the gained solutions. Ideally, the obtained diffusate can be mixed with fresh acid and directly reused in the production process.

Table 1. Analytical results of solutions processed in the first stage.

Parameter	Units	Feed	Dial_1	Dif_1	rej_1	yield_1
Al	$mg.l^{-1}$	56	66.1	0.76	98%	
Cd	$mg.l^{-1}$	6.22	6.89	0.43	91%	
Cr	$mg.l^{-1}$	2.35	2.34	0.12	94%	
Cu	$mg.l^{-1}$	14.8	15.3	1.1	91%	
Fe	$mg.l^{-1}$	297	274	32.5	86%	
Ni	$mg.l^{-1}$	5.98	6.8	0.31	94%	
Zn	$mg.l^{-1}$	96.2	107	5.05	94%	
H_2SO_4	$g.l^{-1}$	224.86	16.31	166.22		91%
w_{H2SO4}	$kg.kg^{-1}$	19.66	1.61	15.08		
Density	$g.cm^{-3}$	1.14	1.02	1.10		
Temperature	°C	22.6	22.7	22.6		
Flowrate	$l.min^{-1}$	0.126	0.122	0.156		

Table 2. Analytical results of solutions processed in the second stage.

Parameter	Units	Feed (Dif_1)	Dial_2	Dif_2	rej_2	yield_2
Al	$mg.l^{-1}$	0.773	1.12	<0.1	-	
Cd	$mg.l^{-1}$	0.417	0.543	<0.05	-	
Cr	$mg.l^{-1}$	0.103	0.126	<0.05	-	
Cu	$mg.l^{-1}$	0.963	1.19	0.09	90%	
Fe	$mg.l^{-1}$	28.6	28.6	2.58	90%	
Ni	$mg.l^{-1}$	0.314	0.412	<0.05	-	
Zn	$mg.l^{-1}$	4.56	5.79	0.248	94%	
H_2SO_4	$g.l^{-1}$	176.1	33.07	136.28		83%
w_{H2SO4}	$kg.kg^{-1}$	15.90	3.24	12.58		
Density	$g.cm^{-3}$	1.1075	1.022	1.0832		
Temperature	°C	22.7	22.9	22.6		
Flowrate	$l.min^{-1}$	0.141	0.118	0.152		

This can be different from one to another application and production site capabilities/possibilities and these factors should be evaluated individually. There can exist possibilities of further processing of the obtained streams. For example, steps for water recovery could be made, e.g., implementation of RO or electrodialysis. But this will always depend on the above mentioned process possibilities.

If we consider processing of the above feed solution with the obtained parameters, we can evaluate the savings on chemicals (fresh H_2SO_4, NaOH for neutralization). From 1 ton of the feed with 19.66 % (w/w) H_2SO_4 (196.6 kg) we can save 76 % of the acid (149 kg). That means for the neutralization we need 77 kg NaOH (50 %) instead of 321 kg. Just savings on the fresh chemicals are considerable. The overview is given in Table 3. From the table we can also see that from each ton of waste sulphuric acid we can save 217 kg of TDS in the form of sodium sulphate which will not be formed because of acid regeneration. This can bring not only significant environmental but also financial benefits considering the regulations on the waste water release. The financial impact coming from the TDS savings (due to penalties, production limitations, etc.) should be evaluated individually by each company. This item can have significant impact on the return on investment of the DD technology.

Table 3. Overview about savings of chemicals for the investigated case

	Waste acid	Waste	Recycled acid	Neutralization	Na2SO4 by neutralization	Price of chemicals	Savings chemicals
	(kg/t_{feed})	(kg/t_{feed})	(kg/t_{feed})	(kg/t_{feed})	(kg/t_{feed})	($/t)	($/t_{feed}$)
Balance of H_2SO_4							
Present process	197	197	0			40	
Recycling process	197	47	149				
Savings			149				6
Balance of NaOH (50%)							
Present process	-	-	-	321		200	
Recycling process	-	-	-	77			
Savings				244			49
Balance of Na_2SO_4							
Present process					285		
Recycling process					68		
Savings					217		

Acknowledgements

This work was carried out in the frame of the IP project (Decision Nr. 6/2018) supported by the Czech Ministry of industry and trade and in the frame of project LO1418 supported by the Czech Ministry of education, youth and sports. The project utilizes Membrane innovation center infrastructure.

References

1. https://ec.europa.eu/jrc/en/science-update/new-waste-water-emission-standards-european-chemical-industry
2. *K. Wang, Y. Zhang, J. Huang, T. Liu, J. Wang,* Recovery of sulfuric acid from a stone coal acid leaching solution by diffusion dialysis. Hydrometallurgy, 173, 9–14 (2017).
3. *A. Elmidaoui, A. T. Cherif,, J. Molenat, C. Gavach*, Transfer of H_2SO_4, Na_2SO_4 and $ZnSO_4$ by dialysis through an anion exchange membrane. Desalination, 101, 39–46 (1995).

Index of authors

A

Abdrashitov E. 21, 24
Achoh A. 27, 149
Ageev E. 229
Akberova E. 30, 342
Alekseenko A. 246, 320
Andreeva M. 34, 36
Anfimova I. 208
Anokhina T. 161
Antipov A. 38, 128, 362
Antropova T. 199, 208
Apel P. 252
Astashkina O. 214

B

Bagishev A. 41
Bagryantseva I. 42, 287
Bakhtin D. 161
Baryshev M. 276
Bayakhmetova Z. 386
Bayandin V. 43
Bazhenov S. 45, 48, 110, 161, 223
Bdiri M. 51
Bedin S. 61, 380
Bel Hadj Hmida E. S. 33, 274
Belhadj Ammar R. 33
Belenov S. 241
Belloň T. 53, 54, 55, 56, 284
Belobrovaya O. 59
Ben Sghaier A. 51
Berezkin V. 61
Bespalov A. 64
Bessonov A. 189
Bildyukevich A. 66, 123, 130, 232
Bobreshova O. 148
Bocharova A. 76
Bokun V. 21, 24
Bondarenko I. 159, 210
Bondarev D. 64
Borisov I. 107, 110, 120
Bortsova A. 298, 366
Boyarishcheva A. 125
Burts K. 66
But A. 69, 157, 235
Butylskii D. 72, 74, 226, 248
Bychkov S. 75, 173, 359, 360

C

Chaabane L. 51
Chalov T. 177
Cheplakova A. 288
Cherkasov D. 380
Chernyak A. 356
Chizhik S. 75, 359, 360
Chubyr N. 116, 170
Chukanov P. 128
Chuprynina D. 74
Čopák L. 76, 398

D

Dammak L. 33, 51, 72, 228, 274, 313, 389
Dankovtseva E. 79, 253
Demekhin E. 98
Demina O. 86
Diankina N. 214
Dmitrieva K. 159, 210
Dobrovolsky Y. 21, 24, 132, 264
Dolgopolov S. 152
Doludenko I. 380
Dotsenko V. 212
Druzhinina T. 315
Duysenbay D. 386
Dybtsev D. 288
Dzyazko Y. 81, 123

E

Eliseeva T. 138
Eremchev I. 252
Eremeev I. 107
Ergozhin E. 177
Ermakova L. 199
Ermilova M. 217
Eterevskova S. 64
Evdochenko E. 261, 333
Evdokimov I. 189

F

Faddeev N. 198

Falina I. 79, 84, 86, 195, 320
Fauvarque J.-F. 274
Faykov I. 88
Fedin V. 288, 332
Filippov A. 91, 94, 135, 152
Fogel A. 271
Frants E. 308

G
Gainutdinov I. 97
Galushka I. 59, 323
Galushka V. 59
Ganchenko G. 98, 308
Ganchenko N. 98, 100
Gaydamaka A. 42, 287
Gerasimova I. 269
Gil V. 102
Goleva E. 30, 344
Golubenko D. 105, 356, 361
Golubev G. 107, 110
Goncharova O. 128
Gor'kov K. 144
Gorobchenko A. 113
Grigoriev Yu. 61
Grushevenko E. 120, 266
Gudza V. 116
Gursky V. 119
Guterman V. 246, 269

H
Hliavitskaya T. 123

I
Ignatenko V. 161

K
Karagaichev A. 59
Kardash M. 315, 323, 353
Karelin A. 132
Karpenko T. 125, 174
Karpenko-Jereb L. 323
Kartashova N. 128
Kashin A. 250
Kasperchik V. 130
Kayumov R. 132
Khanukaeva D. 135
Kharina A. 138
Khorokhorin A. 202
Kim K. 140, 180
Kirillova E. 141
Kleinikova S. 144
Klevtsova A. 146
Knyazeva A. 120
Kochemirovsky V. 208, 271
Kolenkevich V. 84
Kolganova T. 148
Kolobkova K. 128
Kolot D. 149
Konev D. 128, 186, 363
Kononenko N. 36, 152, 195, 353
Kononov A. 154, 155
Korneychuk A. 202
Korzhov A. 157, 159, 210
Kostyanaya M. 45, 48, 161
Kostylev D. 30
Kotova D. 164
Kovalenko A. 69, 116, 141, 167, 170, 261, 281, 333
Kovalenko K. 288, 332
Kovalev I. 41, 173
Kovalev N. 125, 174
Kovrigina T. 177
Kozaderov O. 180
Kozaderova O. 140, 180
Kozlova A. 304
Kozlova N. 202
Kozlova S. 298
Kozmai A. 183, 295, 377
Kravchenko T. 186, 339
Kravtsov V. 189
Kritskaya D. 21, 24
Kruglikov S. 380
Krysanov V. 192
Krysanova T. 164
Kucheryavyj V. 298
Kudashova D. 195
Kudelko K. 81
Kudelya K. 326
Kujawa J. 66
Kujawski W. 66
Kulik S. 252
Kulikova I. 189
Kumar M. 197
Kuriganova A. 198
Kutenko N. 34

Kuznetsova A. 199

L

Lakeev S. 202
Lapshina E. 148
Larchet C. 51, 72, 228, 274, 313
Larin A. 383
Larkina A. 205
Lebedev D. 208, 271
Lebedev K. 27, 307
Lebedeva O. 301
Leontyev I. 198
Li G. 66
Logunov A. 370
Loktionov P. 128
Loza N. 34, 36, 84, 210, 212, 292
Loza S. 159, 210, 212, 292
Lucenko I. 276
Lysenko A. 214
Lysova A. 215
Lytkina A. 217

M

Madumarova M. 48
Makhonina M. 220
Malakhov A. 223
Mantsurov A. 59
Mareev S. 72, 113, 155, 226, 228, 248, 313
Mareeva D. 313
Matushkina N. 229
Matveev D. 232
Melnikov A. 250
Melnikov S. 27, 235, 238
Melnikova E. 278, 295, 327
Menshikov V. 241
Merkel A. 243
Mikhalin A. 353
Mikhaylin S. 377
Mishnev M. 366
Mochalova A. 220
Moguchikh E. 246
Moroz I. 248
Mugtasimova K. 250
Myakinchenko I. 86

N

Naumov A. 252
Nazmov V. 61
Nazyrova E. 253
Nemudry A. 41, 75, 97, 173, 260, 359, 360
Nesterova V. 88, 256
Netrusov A. 304
Nichka V. 259
Niftaliev S. 140, 180
Niftalieva N. 260
Nikitin A. 45
Nikonenko V. 72, 154, 183, 228, 259, 261, 313, 317, 333, 336, 389
Norenko A. 253
Nosova E. 235
Novikova K. 21, 24, 264
Novitsky E. 48, 266
Novomlinskiy I. 269
Novomlinsky M. 208, 271
Nurgalieva G. 386

O

Ogenko V. 81
Oksuz'an D. 100
Okushko A. 192
Ondrušek M. 243
Orekhova N. 217
Otvagina K. 220, 369
Ounissi T. 33, 274

P

Panov D. 380
Paperzh K. 246
Parshina A. 148
Pavlets A. 246
Petriev I. 276
Philippova T. 91
Pismenskaya N. 74, 146, 248, 259, 278, 295, 317, 327, 377
Pismenskiy A. 170, 281
Plisko T. 66, 232
Plotnikova N. 192
Podeshvo I. 88
Podtynnikov I. 110, 120
Polevoj L. 241

Polezhaev P. 53, 54, 55, 56, 284
Polotskaya G. 88, 205, 256
Polyanskaya V. 59
Polyanskii L. 186
Ponomarev A. 21, 24, 361
Ponomareva V. 42, 287, 288, 332
Popov M. 41, 75, 173, 260, 360
Porozhnyy M. 102, 259
Potekhina L. 301
Pourcelly G. 261, 327
Pryatko Y. 326
Pulyalina A. 88, 205, 256
Pushankina P. 276

R
Repina M. 100
Reshetnikova A. 290
Rogov A. 248
Romanyuk N. 210, 292
Rozhdestvenska L. 123
Rybalkina O. 278, 295, 311, 327
Rychagov A. 353
Ryzhkov I. 298, 366

S
Safronova E. 148
Salaschenko M. 152
Sanginov E. 21, 24, 132
Sarapulova V. 155, 311, 317
Sazanova T. 370
Scharova O. 120
Schneider M. 301
Sedelkin V. 301
Šeda L. 398
Sedov I. 45
Seidova N. 170
Semina P. 202
Shaglaeva N. 43
Shakirova A. 386
Shalygin M. 304
Shaposhnik V. 290, 305
Sharafutdinov M. 173
Shatalov A. 380
Sheldeshov N. 125, 174, 307
Shelistov V. 308
Shevlyakova N. 217
Shkirskaya S. 94, 238, 253, 259, 309, 353
Shkorkina I. 311
Shpak A. 125
Shubnikova E. 75
Shustikov A. 232
Shutova E. 288
Simunin M. 298, 366
Sinitsyn V. 250
Skolotneva E. 313
Slouka Z. 53, 54, 55, 56, 284, 347
Smagin M. 344
Smirnova N. 198, 264
Smolyanskii A. 202
Smyshliaev N. 210
Sobchenko K. 170
Sokruykina A. 164
Soloshko V. 309
Sosenkin V. 81, 353
Stenina I. 375
Strusovskaya N. 229
Strylets I. 315

T
Teplyakov V. 304
Terikhova N. 389
Terin D. 59, 315, 323
Tikhaya A. 138
Timchenko M. 320
Timofeev S. 36, 119
Titkov A. 173
Titorova V. 317
Titskaya E. 320
Tiwari A. 135
Tregubova A. 339
Tsipliaev S. 323, 353
Tskhay A. 326
Tsygurina K. 278, 295, 327
Turaev T. 323
Tverskoy V. 217, 356

U
Ugrozov V. 330
Ulihin A. 332
Ulyanova E. 301
Urtenov M. 69, 116, 167, 170, 281, 333, 336

Utin S. 212
Uvarov N. 332
Uzdenova A. 336

V
Vakhnin D. 186, 339
Vasil'eva S. 164
Vasil'eva V. 30, 69, 342, 344
Vasilevsky V. 45, 107, 266
Vasiliev A. 61
Vinogradova L. 205
Vobecká L. 56, 284, 347
Volfkovich Yu. 81, 350, 353
Volkov A. 45, 107, 266
Volkov V.I. 356
Volkov V.V. 232
Volkova A. 199
Voloshin B. 359, 360
Volotchaev V. 269
Voronin K. 276
Voropaeva D. 361
Vorotyntsev A. 220
Vorotyntsev I. 220, 370
Vorotyntsev M. 38, 128, 363
Vyatkin A. 297, 366

W
Wessling M. 261

X
Xu T. 74

Y
Yadav P.K. 135, 369
Yakovleva Y. 146
Yanbikov N. 220, 370
Yarmolenko O. 356
Yaroslavtsev A. 105, 215, 217, 361, 372, 375
Yaskevich A. 130
Yatsenko T. 81
Yelnikova A. 148
Yurova P. 375
Yutskevich Y. 377

Z
Zabolotskiy V. 27, 64, 69, 125, 157, 159, 174, 307
Zagorskiy D. 252, 380
Zhdanov V. 383
Zheltoukhova N. 339
Zhilyaeva N. 217
Zhusipbekov U. 386
Zilberberg I. 97
Zolotukhina E. 144
Zyryanova S. 183, 228, 389

ISBN 978-5-6042418-2-0

Подписано в печать 13.05.2019г. Гарнитура Таймс.
Печать цифровая. Бумага офсетная.
Заказ № 735 Тираж 100 экз.

Отпечатано в типографии «Best Print».
г. Краснодар. ул. Селезнева, 4/А, оф.49-50. Тел.: +7 (861) 210-20-16
www.bestprint.info; office@bestprint.info; kapirka@mail.ru;
@best_print_krd

ISBN 978-5-6042418-2-0